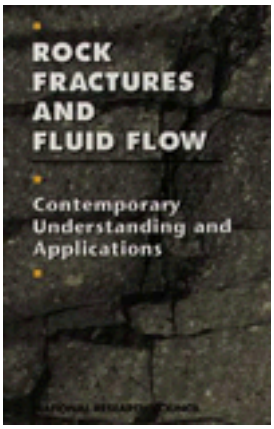

Rock Fractures and Fluid Flow: Contemporary Understanding and Applications

Committee on Fracture Characterization and Fluid Flow, National Research Council

ISBN: 0-309-56348-8, 568 pages, 6 x 9, (1996)

Rock Fractures And Fluid Flow

Contemporary Understanding and Applications

Committee on Fracture Characterization and Fluid Flow
U.S. National Committee for Rock Mechanics
Geotechnical Board
Board on Energy and Environmental Systems
Commission on Engineering and Technical Systems
National Research Council

NATIONAL ACADEMY PRESS
Washington, D.C.1996

NATIONAL ACADEMY PRESS 2101 Constitution Avenue, N.W. Washington, D.C. 20418

NOTICE: The project that is the subject of this report was approved by the Governing Board of the National Research Council, whose members are drawn from the councils of the National Academy of Sciences, the National Academy of Engineering, and the Institute of Medicine. The members of the committee responsible for the report were chosen for their special competences and with regard for appropriate balance.

This report has been reviewed by a group other than the authors according to procedures approved by a Report Review Committee consisting of members of the National Academy of Sciences, the National Academy of Engineering, and the Institute of Medicine.

This report was prepared with the support of the U.S. Department of Energy (DOE), Grant Nos. DE-AC01-89DP48070, DE-FG22-91BC14837, DE-FG05-91ER40668, and DE-FG08-92NV11227 and Contract No. DE-FG01-92CE31021, and the Nuclear Regulatory Commission (NRC), Grant Nos. NRC-G-04-91-089 and NRC-04-91-089. Any opinions, findings, conclusions, and recommendations expressed herein are those of the authors and do not necessarily reflect the views of DOE or NRC.

SPONSORS: This project was sponsored by the following federal agencies: Department of Defense (Air Force Office of Scientific Research, Defense Nuclear Agency); Department of Energy (Office of Energy Research, Office of Environmental Restoration and Waste Management, Office of Fossil Energy, Geothermal Division of the Office of Conservation and Renewable Energy, Office of the Superconducting Super Collider, Yucca Mountain Site Characterization Project Office); Department of the Interior (Bureau of Land Management, Bureau of Mines, Bureau of Reclamation); Environmental Protection Agency (Robert S. Kerr Environmental Research Laboratory, Environmental Monitoring Systems Laboratory); Federal Transit Administration; National Science Foundation; and the Nuclear Regulatory Commission. In addition, the Gas Research Institute and Dowell-Schlumberger, Inc., provided support for this project. The National Research Council, through its Day Fund, extended financial support for the publication and dissemination of the report.

Library of Congress Cataloging-in-Publication Data

Rock fractures and fluid flow : contemporary understanding and applications / Committee on Fracture Characterization and Fluid Flow … [et al.].

p. cm.

Includes bibliographical references and index.

ISBN 0-309-04996-2 (alk. paper)

1. Rocks—Fracture. 2. Rock mechanics. 3. Fluid dynamics. 4. Hydrogeology. I. National Research Council (U.S.). Committee on Fracture Characterization and Fluid Flow.

TA706.R525 1996 96-14613

624.1`5132—dc20 CIP

Committee On Fracture Characterization And Fluid Flow

Jane C. S. Long (*Chair*), Ernest Orlando Lawrence Berkeley National Laboratory, Berkeley, California
Atilla Aydin,Stanford University, Stanford, California
Stephen R. Brown, Sandia National Laboratories, Albuquerque, New Mexico
Herbert H. Einstein, Massachusetts Institute of Technology, Cambridge
Kevin Hestir, Utah State University, Logan
Paul A. Hsieh, U.S. Geological Survey, Menlo Park, California
Larry R. Myer, Ernest Orlando Lawrence Berkeley National Laboratory, Berkeley, California
Kenneth G. Nolte, Dowell-Schlumberger, Tulsa, Oklahoma
Denis L. Norton, University of Arizona, Tucson (until October 13, 1993)
Olle L. Olsson, Conterra AB, Uppsala, Sweden
Frederick L. Paillet,U.S. Geological Survey, Denver, Colorado
J. Leslie Smith, University of British Columbia, Vancouver, Canada
Leon Thomsen, Amoco Production, Tulsa, Oklahoma

Staff

Duncan Brown, Study Director
Kevin Crowley, Technical Editor
Amelia B. Mathis, Senior Secretary/Project Assistant
Wendy Lewallen, Project Assistant (from November 1994)
Peter H. Smeallie, Study Director (to May 1994)
Jennifer T. Estep, Administrative Assistant (to May 1994)
Helen Johnson, Administrative Associate (from November 1994 to July 1995)
Susanna Clarendon, Administrative Assistant (from November 1995)
Theron Feist, Project Assistant (from November 1994 to June 1995)
Beth Shevitz, Research Assistant (from December 1994 through February 1995)

U.S. National Committee For Rock Mechanics

Geotechnical Board

Liaison Members from the Commission on Engineering and Technical Systems

Former Members Active During the Course of the Study

Staff

Board On Energy And Environmental Systems

Liaison Members from the Commission on Engineering and Technical Systems

Richard A. Conway, NAE, Senior Corporate Fellow, Union Carbide Corporation, South Charleston, West Virginia

Trevor O. Jones, NAE, Chairman of the Board (Retired), Libbey-Owens-Ford Company, Cleveland, Ohio

Staff

Mahadevan Mani, Director
James Zucchetto, Senior Program Officer
Tracy Wilson, Senior Program Officer
Jill Wilson, Program Officer
Helen Johnson, Administrative Associate
Susanna Clarendon, Administrative Assistant
Amelia Mathis, Senior Secretary/Project Assistant
Wendy Lewallen, Administrative Assistant
Theron Feist, Project Assistant

THE NATIONAL ACADEMIES

National Academy of Sciences
National Academy of Engineering
Institute of Medicine
National Research Council

The **National Academy of Sciences** is a private, nonprofit, self-perpetuating society of distinguished scholars engaged in scientific and engineering research, dedicated to the furtherance of science and technology and to their use for the general welfare. On the authority of the charter granted to it by the Congress in 1863, the Academy has a mandate that requires it to advise the federal government on scientific and technical matters. Dr. Bruce M. Alberts is president of the National Academy of Sciences.

The **National Academy of Engineering** was established in 1964, under the charter of the National Academy of Sciences, as a parallel organization of out-standing engineers. It is autonomous in its administration and in the selection of its members, sharing with the National Academy of Sciences the responsibility for advising the federal government. The National Academy of Engineering also sponsors engineering programs aimed at meeting national needs, encourages education and research, and recognizes the superior achievements of engineers. Dr. William A. Wulf is interim president of the National Academy of Engineering.

The **Institute of Medicine** was established in 1970 by the National Academy of Sciences to secure the services of eminent members of appropriate professions in the examination of policy matters pertaining to the health of the public. The Institute acts under the responsibility given to the National Academy of Sciences by its congressional charter to be an adviser to the federal government and, upon its own initiative, to identify issues of medical care, research, and education. Dr. Kenneth I. Shine is president of the Institute of Medicine.

The **National Research Council** was organized by the National Academy of Sciences in 1916 to associate the broad community of science and technology with the Academy's purposes of furthering knowledge and advising the federal government. Functioning in accordance with general policies determined by the Academy, the Council has become the principal operating agency of both the National Academy of Sciences and the National Academy of Engineering in providing services to the government, the public, and the scientific and engineering communities. The Council is administered jointly by both Academies and the Institute of Medicine. Dr. Bruce M. Alberts and Dr. William A. Wulf are chairman and interim vice-chairman, respectively, of the National Research Council.

www.national-academies.org

Preface

At its meeting in June 1990, the U.S. National Committee for Rock Mechanics (USNCRM), a standing committee of the National Research Council (NRC), identified rock fractures as a subject of great concern to the rock mechanics community. The USNCRM proposed that the NRC undertake a study to review characterization and fluid flow in rock fractures. The Committee on Fracture Characterization and Fluid Flow was appointed by the NRC in April 1991 and met for the first time in May 1991. The committee membership represents many of the disciplines concerned with rock fractures and fluid flow, including rock mechanics, hydrogeology, hydrofractures, geophysics, geology, geostatistics, civil engineering, and seismology. The committee met six times over the course of this study to debate, define, and develop this report.

Interest in fluid flow in fractured rock has grown rapidly in the past two decades, as a tool in recovering water and hydrocarbon supplies and geothermal energy, in predicting the flow of pollutants underground, and in engineering structures. Practitioners have recognized that progress in this field can be made only by drawing information from a number of different disciplines. However, a person trained in hydrology may have a limited understanding of what geology, geophysics, or geomechanics can do to help solve a problem in fluid flow. As a result, hydrological modelers often disregard geological or geophysical information that they do not know how to use. Similarly, those trained in geology, geophysics, or geomechanics may fail to understand aspects of fractures that are relevant to fluid flow. Studies produced under these conditions may be fascinating, but peripheral or even irrelevant to the real problems they are intended to address. These attitudes are self-propagating and lead to dead ends.

This report is intended to promote a new, interdependent approach. It discusses the varied approaches used to solve problems of fluid flow in fractured rock, so that students, faculty, and practitioners may understand the strengths and limitations, as well as the interdependencies, of the available tools. It also contains recommendations for interdisciplinary research on problems that are not well understood, for the use of policy makers and research program managers.

This report has limitations. Its breadth has prohibited a comprehensive treatment of any single disciplinary area, although it does communicate a basic understanding of each area. Experts are unlikely to learn much from the chapters devoted to their fields, but should find much of interest in the other chapters.

The report is neither a review of the state of the art nor a literature survey, and does not include references to much important work. However, although the references are not all-inclusive, they are designed to be an entrance to the literature.

Committee members served the NRC as volunteers for more than three years to complete this study despite busy schedules and conflicting demands. Committee members responded to the chairman's unending demands and the critiques of their colleagues and of the NRC's staff and reviewers.

The committee was supported by an impressive list of outside contributors who responded with enthusiasm to calls such as "Could you write a brief treatment of the importance of diagenesis?" or "Tell us what you know about two-phase flow in fractures." These individuals made a great difference in the quality of the final report. Steve Martel of the University of Hawaii merits special thanks. He contributed a significant effort to Chapter 2 as well as helping organize a field trip for the committee to look at fracture patterns in crystalline and volcanic rocks. Chris Dyke of British Petroleum wrote an account of diagenesis. Steve Laubach of the Texas Bureau of Economic Geology wrote one about joint systems. Marcelo Lippmann contributed sections on the role of fractures in geothermal energy development. Kenzi Karasaki of Ernest Orlando Lawrence Berkeley National Laboratory contributed a treatment of well test analysis. Bill Foxall of Ernest Orlando Lawrence Berkeley National Laboratory wrote about the San Andreas Fault system. Ernie Majer of Ernest Orlando Lawrence Berkeley National Laboratory gave advice about cross-hole seismic methods. Tom Daley, also of Ernest Orlando Lawrence Berkeley National Laboratory, contributed a treatment of shear-wave anisotropy. Richard Everitt of Atomic Energy of Canada Limited contributed a description of the hydrology of fault zones at the Underground Research Laboratory. Bob Glass of Sandia National Laboratory wrote about two-phase flow in fractures in Chapter 3. Norm Warpinski of Sandia National Laboratory contributed an account of the Multiwell Experiment. Duayne Chesnut of Lawrence Livermore Laboratory and Deborah Hopkins, Robert Zimmerman, and Jahan Noorishad of Ernest Orlando Lawrence Berkeley National Laboratory put time and effort into helping us with the difficulties of Chapter 7. Ki Ha Lee

and Karstin Pruess of Lawrence Berkeley National Laboratory also made essential contributions. To all of these people we are grateful.

Several individuals were critical to the development and conduct of this study and must be mentioned explicitly. Wolfgang Wawersik, chaired the USNCRM when that committee developed the idea for this study, provided enthusiasm and moral support that sustained the project, and particularly the chairman. Peter Smeallie, as study director, developed the financial support, steered the work through the required procedures of the NRC, and guided the committee with skill, intelligence and tact. Jennifer Estep dealt with the committee's trips, its manuscripts, and its unending trivial requests—all with consistent cheerfulness, intelligence and know-how—and in addition had two beautiful babies during the study! Amelia Mathis doggedly yet cheerfully prepared numerous versions of the manuscript. Kevin Crowley edited the entire document, written by scores of people; he made it a readable and coherent document. Dev Mani became coordinator of the project near its completion and deserves our thanks for his efforts. The end game of this report was skillfully handled by Duncan Brown with help from Wendy Lewallen and Beth Shevitz. Jim Mitchell served as report review coordinator on behalf of the NRC, performing that demanding job with insight and good cheer. Nine anonymous reviewers went through the extensive text and provided comments that significantly improved the product.

The study received direct support from a number of federal government agencies concerned with research, resource development, environmental regulation and remediation, and civil infrastructure systems. These agencies were the Department of Energy's Office of Environmental Restoration and Waste Management, Office of Energy Research, Office of Fossil Energy, Geothermal Energy Division, Office of the Super conducting Super Collider, and Yucca Mountain Site Characterization Project Office; the Environmental Protection Agency's Robert S. Kerr Environmental Research Laboratory and the Environmental Monitoring Systems Laboratory; the Nuclear Regulatory Commission; the Department of the Interior's Bureau of Mines, Bureau of Reclamation, and Bureau of Land Management; the Department of Defense's Air Force Office of Scientific Research and the Defense Nuclear Agency; Federal Transit Administration; and the National Science Foundation. In addition, two private-sector organizations contributed to the support of the study: the Gas Research Institute and Dowell-Schlumberger, Inc. The National Research Council, through its Day Fund, extended financial support for the publication and dissemination of the report. The committee and staff gratefully acknowledge the support of each of these agencies and organizations.

A number of individuals from the various federal agencies and other organizations that sponsored the study helped the committee by serving as liaisons to the committee and providing data, information, and materials. The committee wishes specifically to acknowledge the contributions of the following: Max Blanchard and Robert Levich, Yucca Mountain Site Characterization Project Office, U.S.

Department of Energy; Barry H. G. Brady, Dowell-Schlumberger, Inc.; James Carney, Office of the Superconducting Super Collider, U.S. Department of Energy; Peter G. Chamberlain, F. Michael Jenkins, and Robert D. Schmidt, U.S. Bureau of Mines, U.S. Department of the Interior; Alex Crawley and Robert Lemmon, Bartlesville Project Office, U.S. Department of Energy; George Stosur, Office of Fossil Energy, U.S. Department of Energy; Joseph Dlugosz, Environmental Monitoring Systems Laboratory, U.S. Environmental Protection Agency; Allan Jelacic and Marshall J. Reed, Geothermal Energy Division, U.S. Department of Energy; Stephen Kraemer and Steven G. Schmelling, Robert S. Kerr Environmental Research Laboratory, U.S. Environmental Protection Agency; Eric Lightner and Caroline B. Purdy, Office of Environmental Management, U.S. Department of Energy; Jacob Philip and Thomas Nicholson, Office of Nuclear Regulatory Research, U.S. Nuclear Regulatory Commission; Hillary A. Oden, Bureau of Land Management, U.S. Department of the Interior; Kent F. Perry, Gas Research Institute; Byron L. Ristvet, Nevada Operations Office, U.S. Department of Energy; Greg A. Scott, Bureau of Reclamation, U.S. Department of the Interior.

This study has been an odyssey, albeit a rewarding one. We hope our readers find equivalent rewards in it.

Jane C. S. Long

Chairman, Committee on Fracture

Characterization and Fluid Flow

Contents

Executive Summary

All rocks in the earth's crust are fractured to some extent. Fractures form in response to stress. The origin of stress can be lithostatic (arising from the weight of the earth's crust), high fluid pressure, tectonic forces, or thermal loading. Fractures occur at a variety of scales, from microscopic to continental.

Fractures are important in engineering, geotechnical, and hydrogeological practice. They can act as hydraulic conductors, providing pathways for fluid flow or barriers that prevent flow across them. Many petroleum, gas, geothermal, and water supply reservoirs form in fractured rocks. Fractures exert a strong influence on the formation of ore bodies because they act as conduits for ore-forming fluids. Fractures can control the transport of chemical contaminants into and through the subsurface. They also affect the stability of engineered structures and excavations.

The application of fracture characterization and fluid flow analysis in engineering, geotechnical, and hydrogeological practice involves addressing three key questions: How can fractures that are significant hydraulic conductors or barriers be identified, located, and characterized? How do flow and transport occur in fracture systems? How can changes in fracture systems be predicted and controlled? These questions are discussed in turn below.

1. How can fractures that are significant hydraulic conductors or barriers be identified, located, and characterized?

A fundamental step in understanding and predicting the behavior of fractures involves the identification and location of hydraulically significant fractures. Such

fractures are conduits for fluid flow and are connected to other hydraulically conductive fractures to form systems or networks. Conductive fracture networks may include a large number of interconnected hydraulically active features or may be limited to a very small proportion of the total fractures in the rock mass. Sometimes it is necessary to locate the hydraulically active fractures explicitly. In other cases it may be sufficient to determine the types of patterns (i.e., regularly repeating geometrical arrangements of fractures) that the fractures form or their statistical properties (e.g., orientation and density) or to locate only the major fractures explicitly. The requirements vary from site to site and from application to application.

Chapters 2 through 5 address methods for locating and characterizing hydraulically conductive fractures through a combination of geological mapping, geomechanical analysis, and geophysical and hydrological measurements. It may be possible to predict the location of fractures at depth through an understanding of the processes that form fractures and the nature of the resulting fracture patterns. Chapter 2 addresses the development of fractures from a geological and geomechanical perspective and addresses the origin of fracture patterns as well as common fracture patterns found in various geological environments.

Fractures represent concentrations of void space in rocks. The geometry of the void space affects both the flow properties and the physical properties of the rock mass, such as the elastic and electric properties. An understanding of how the void space geometry controls the fluid flow and geophysical properties of the rock forms the foundation of geophysical methods used to detect fractures in the subsurface. These hydraulic and geophysical properties of fractures are reviewed in Chapter 3.

Geophysical techniques can be used to locate and measure the properties of fractures in the subsurface. There have been significant recent improvements in subsurface fracture detection techniques. Geophysical methods are particularly useful for identifying large individual fractures as well as groups of closely spaced and interconnected fractures or fracture zones. These methods can be used to image large fractures and fracture zones, as discussed in Chapter 4. For example, seismic propagation is slower through fractures than through intact rock. This fact can be used to locate regions that have higher fracture density and consequently regions that might also have higher hydraulic permeability.

Because the relationship between geophysical properties of a rock mass and the hydrological parameters of fractures is not unique, it is usually necessary to make direct measurements. The flow properties of fracture systems can be tested and characterized directly with wells drilled into the subsurface, as discussed in Chapter 5. Well tests and tracer tests can be used to characterize flow system geometry, including the size, density, orientation, and interconnectedness of hydraulically conductive fractures. Flow systems developed in fractures can have quite complex geometries. Special techniques have evolved to interpret test data from these systems. These techniques are discussed in Chapter 5. These flow

properties are used in mathematical models of the flow system, as described in Chapter 6.

2. How do flow and transport occur in fracture systems?

Numerical models are used to obtain quantitative estimates of flow and transport behavior in fracture systems. The first step in the development of a numerical model is the construction of an appropriate conceptual model of the fracture flow system. The conceptual model describes the main features of the geology and hydrology of the system that controls the flow and transport behavior of interest. A conceptual model incorporates an interpretation or schematization of reality that is the basis of mathematical calculations of behavior. Chapter 6 addresses the development of conceptual models from the information collected using the tools described in Chapters 2 through 5.

Conceptual model development in fracture systems is an important but frequently undervalued step in numerical modeling. Particular difficulties arise in the determination of fracture geometry and flow physics because, as noted previously, fracture systems have complex geometries. In many cases more than one conceptual model can be constructed with available data. Indeed, most of the error involved in predicting flow behavior with a numerical model is usually due to deficiencies in the underlying conceptual models.

A numerical model provides quantitative estimates of flow and transport behavior of the system described by the conceptual model. The mathematical formulation of the numerical model is determined by the flow geometry specified in the conceptual model. A wide variety of fluid flow models have been developed to address the prediction of flow and transport in fracture systems. All methods discretize the medium into conductive elements. The methods differ mainly in the way the conductive elements are defined (e.g., representing single fractures, groups of fractures, or equivalent continue) and in the way the models are parameterized (e.g., based on statistical analysis of small-scale data or on interpretation of large-scale hydraulic tests). Several classes of numerical models, their relationships to conceptual models, and their applications to fracture flow systems are described in Chapter 6. Emphasis is on models that deal with the heterogeneous nature of fracture systems.

Model parameterization, that is, the estimation of unknown parameters in the numerical models (e.g., porosity and conductance) through field tests, also is addressed in Chapter 6. There is a strong dependence between field test design and model parameterization. For example, a numerical model of the distribution of fractures at a site requires the field collection of spatial statistics for parameters such as fracture density orientation, size, and conductivity. A numerical model that explicitly specifies hydrogeological units such as fracture zones requires well tests to measure the hydrological properties of those zones.

Numerical models are usually developed to aid in management and design decisions. Two basic questions must be addressed before these models can be used effectively as management or design tools. First, does the conceptual model provide an adequate characterization of the flow system? If not, it must be revised and reevaluated. Second, is the data base adequate to estimate the parameters in the numerical model with sufficient precision to produce reliable predictions for the intended application? If not, additional field data must be collected.

Development of a numerical model should be an iterative process. It begins with the development of a conceptual model, which, in turn, is used to formulate a numerical model of the flow system. The parameters of the numerical model are determined through the collection and interpretation of field data, and the numerical model is used to predict the behavior of the flow system. The predicted behavior is compared to the actual behavior of the flow system as determined from field observations. If the predicted and observed behaviors do not match, the conceptual model is reevaluated and updated, and the process is repeated.

3. How can changes in fracture systems be predicted and controlled?

The flow and transport behavior of fracture systems can be perturbed by natural processes or by the activities of people. For example, extraction of fluids from a fracture system can lower the fluid pressure, which will increase the effective stress in the rock, thereby causing the fractures to close. Temperature-induced stresses can have similar effects. Changes in fluid chemistry can lead to either mineral precipitation in fractures or mineral dissolution. In general, any change in the void geometry of a fracture system will alter the flow and transport behavior. Tools for predicting and controlling these changes are addressed in Chapter 7.

In the final analysis, there is no prescribed procedure that can be followed to address flow and transport in fracture systems. This report describes tools that can be used in the process of characterization, model building, prediction, and refinement. These tools must be applied iteratively to determine if a flow and transport system has been characterized correctly. This iterative process must be designed to test improvements in the predictive capabilities of a numerical model. If the predictions improve with each iteration, confidence in the conceptual model as an accurate representation of the flow and transport system is enhanced. If the predictions do not improve, the conceptual model must be reexamined.

Iterative procedures can be applied to many problems in the earth sciences. The tools associated with each step of this iterative process, as applied to fractures, are described in this report, but the report should not be viewed as a "cookbook." Rather, the tools described here can be applied only in a manner appropriate to the specific geology and application under consideration. Case examples of the application of these tools are given in Chapter 8.

RECOMMENDATIONS

The recommendations developed in the technical chapters of this report (Chapters 2 through 8) are presented in Chapter 9 (Technical Summary). These recommendations are summarized below, and their application to a variety of important practical problems is provided. The committee made no attempt to assign relative priorities to its recommendations. As a group, however, the recommendations represent the committee's assessment of high-priority research needs.

The committee believes that concerned federal agencies as well as other research-sponsoring organizations should carefully consider the recommendations in this report. The following eight recommendations are cross-cutting; they do not fit neatly within the mission of any single agency or organization. The committee encourages those agencies and organizations concerned with the shallow subsurface of the earth to implement these recommendations through research partnerships and other joint-venture consortia. Among the federal agencies and other groups that would benefit from such research are the U.S. Army Corps of Engineers; Yucca Mountain Site Characterization Project Office; Department of Energy, Office of Conservation and Renewable Energy and Office of Fossil Energy; Environmental Protection Agency, Environmental Monitoring Systems Laboratory; U.S. Geological Survey; U.S. Department of the Interior, Bureau of Land Management, Bureau of Mines, and Bureau of Reclamation; Defense Nuclear Agency; and Nuclear Regulatory Commission, Office of Nuclear Regulatory Research.

1. Additional in situ research facilities should be developed in fractured rocks in a variety of geological environments.

Advances in modeling methodologies require repeated sequences of characterization, prediction, comparison, and refinement. Research facilities provide the opportunity to move freely between these stages. The tools, approaches, and conceptualizations developed at these facilities can be applied to sites in similar geological environments. In situ research facilities are especially valuable for assessing the usefulness of various characterization tools and methodologies and for learning how to jointly interpret data obtained with different tools.

Heavily characterized sites are ideal for experiments in fluid flow and chemical transport and for investigating the coupling between flow, stress, and temperature because the interpretation of such an experiment is much more certain when the site is well understood. Such experiments are needed because existing numerical models for predicting the effects of stress, flow, temperature, and multiple flow phases do not provide reliable long-term predictions of flow and transport. In situ experiments, particularly at regional scales, should be supported to develop reliable numerical models for predicting these effects.

In situ research facilities help in the development of successful testing strategies and provide critical information for extrapolating measurements from one time and one distance scale to others. Research programs at these facilities should be designed to address data requirements for evaluating various flow and transport modeling approaches. These programs should also address the practicality of collecting these data in routine hydrogeological practice.

In situ facilities should be developed in a variety of rock types with different styles of fracturing. A number of excellent facilities already exist in crystalline rocks, but there is a dearth of in situ research facilities in bedded rocks, especially where more than one fluid phase is present. Consequently, less is known about how to effectively characterize flow and transport in bedded rocks. Research at facilities in bedded rocks would have a significant impact on understanding enhanced oil and gas recovery processes in fractured reservoirs.

An example of such a facility is the Exploratory Studies Facility currently under construction at Yucca Mountain, Nevada, the site of a potential nuclear waste repository. The Yucca Mountain site is a bedded tuff that contains a variety of fracture types. The proposed repository is above the water table and, when filled with high-level nuclear waste, is expected to produce significant quantities of heat. A thorough characterization of this site is required before the behavior of fluid flow in the vicinity of the potential repository can be predicted.

2. The development of conceptual models for fluid flow and transport in fractured rock should be a focus of research.

A conceptual model describes the main features of the geology and hydrology of the system that controls the flow and transport behavior of interest. A conceptual model incorporates an interpretation or schematization of reality that is the basis of mathematical calculations of behavior. Conceptualizations used for models of fluid flow in granular media (e.g., sand) are usually inadequate for models of fluid flow in fracture systems. For example, single fractures are commonly conceptualized as the space between two parallel plates separated by a constant aperture (distance), which is too simple for many applications, especially those involving mass transport. However, it is usually impractical to completely specify complex fracture geometries for single fractures, not to mention fully three-dimensional fracture network. Consequently, simple models should be developed to describe the salient features of fractures that account for the flow and transport behavior of interest.

Numerical models developed from inappropriate conceptual models can have large uncertainties that are difficult to quantify. In many applications, errors in flow and transport predictions could be dangerous or costly. Research should be supported to develop realistic conceptual models for fracture systems. This research should identify commonly applicable relationships between rock type, stress, structure, fracture style, and flow and transport behavior. These studies

should be undertaken in a variety of geological environments and should address a variety of mass and heat transport phenomena.

Theoretical investigations and experimental work should be supported to develop appropriate and practical conceptual models for transport. These are needed to predict the fate of contaminants underground and the behavior of complex petroleum recovery schemes. Theoretical investigations and experimental work should be supported to link hydrogeological and geochemical processes in transport models for reactive solutes that take account of the unique properties of fluid pathways in fractured rock. Research is needed to determine how the geometry of fractures determines the relative importance of preferential flow paths and the surface area affecting matrix diffusion and reactive transport.

Development of realistic conceptual models for multiphase fluid flow (flow involving more than one fluid phase, e.g., water and steam) in fractures is an important research problem for nuclear waste repository siting, enhanced oil recovery, and subsurface contamination by nonaqueous phase liquids. New theoretical and laboratory work should be undertaken to relate multiphase flow in fractures to fracture geometry, rock matrix properties, and stress. Fracture network models involving two fluid phases can reveal how network geometry controls flow. Efforts to develop these models should be continued. There is a critical need for experimentation and observation of two-phase flow in natural systems. Laboratory and in situ experiments should be carried out to determine if the behavior of two-phase flow in fractures is chaotic and consequently difficult to predict in a deterministic sense.

Confidence in a conceptual model is developed through the iterative process of characterization, model building, prediction, and refinement, as described in numerous places in this report. Such "confidence building" should become the standard approach for addressing regulatory requirements. A field investigation that has multiple repetitions of the same simple experiment may serve to build confidence better than one complex, all-encompassing experiment.

3. Research on the origin and development of fracture systems should be undertaken to provide an appropriate foundation for fluid flow studies.

Understanding the origin and development of distinctive fracture patterns and void geometries in various geological environments and how these patterns affect fluid flow is extremely helpful in solving fracture flow problems. Numerical fluid flow models that account for the origin and development of fracture systems include more physical reality. This realism may provide a basis for extrapolating predictions of hydrological behavior to regions where there are few measurements. The origin and development of fracture systems should be studied in three dimensions because most natural flow problems are inherently three dimensional. The processes that determine how hydrologically important fractures form should be a priority for research. Understanding these processes will allow preliminary

conceptual models to be constructed for sites that have not yet been highly characterized. Such work will help in the exploration for resources such as petroleum, ore minerals, heat, and water and will aid in the design of optimal extraction or isolation schemes. For waste storage or contamination problems, this work will provide a physical basis for scaling up observed flow behavior to longer time and distance scales and will facilitate the design of schemes for in situ isolation of waste. A better understanding of fracture formation will also aid in the design of engineered structures in rock.

4. Efforts to develop and improve fracture detection methods should continue.

Fracture detection methods and instrumentation have improved greatly in recent years. Several detection methods are now in common use, and there is a general understanding of their strengths and limitations. However, there is still a need for theoretical research on detection methods, new instrumentation, and improved algorithms for data interpretation. Geophysical imaging methods based on differencing concepts (i.e., based on measurements before and after a perturbation to the flow system) have great potential for imaging flow systems in fractured rock. These methods should be developed and improved. Techniques that combine different geophysical methods (e.g., seismic and electrical methods) also should be developed. Methods for identifying fracture zones based on multiple geological, geophysical, and hydrological measurements should be developed and validated at in situ research facilities. This effort should include research to relate various geophysical properties of fractures to flow properties.

The effect of fractures on the propagation of shear waves (waves that cause particle motions perpendicular to the direction of wave propagation through the rock) is an important area of research for fracture detection, particularly for resource recovery. Acquisition and interpretation techniques should be developed to take advantage of recently discovered interactions between shear waves and fractures. Borehole shear-wave sources of significant strength should be developed for use in fracture imaging.

There is a need to develop methods for detecting fractures some distance from a single borehole. For example, it would be useful to develop single-hole seismic reflection methods similar to the borehole radar reflection methods.

Methods to produce three-dimensional subsurface images from seismic surveys conducted at the surface (3D seismic methods) are now relatively common in the petroleum industry. The technique is very expensive because it requires a large number of source-receiver pairs. Efforts should be made to reduce the cost of this method and to adapt it to shallower and smaller-scale environmental applications.

Geophysical technologies should be promoted for routine use in the field. This effort should include both new technology and the transfer of technology

developed in the petroleum and nuclear waste disposal industries to other applications. In many cases the state of the art in geophysical methods is far more advanced than the state of practice. Programs should be developed to facilitate technology transfer to improve the state of practice.

5. Efforts to develop realistic and efficient numerical models of fluid flow and transport should continue.

Research into efficient numerical models will facilitate practical applications of fracture flow and transport models and should be supported. These applications include resource extraction, contaminant transport and isolation, and structural integrity. Numerical models that provide simplified but adequate representations of complex fracture networks should be developed. Studies that identify appropriate ways to group features of the fracture network into simpler equivalent features are needed. Such models will expand the number of problems that can be treated numerically and will improve the treatment of problems where present data requirements are impractical.

Simple but sufficient mathematical models of fracture networks are particularly important for inverse methods, which are used to estimate fracture system parameters from field observations of hydraulic behavior. Models that incorporate hierarchical relationships among fractures or account for the origin and development of fractures hold promise in this regard. These inverse methods should be developed further. Many inverse methods produce nonunique results owing to deficiencies in the quality or quantity of field data. Nevertheless, these methods can be used to obtain distributions of possible outcomes and to determine what constraints the data actually place on predicted behavior.

6. Research should be undertaken to better understand and predict the effects of coupling between stress and flow.

Although much has been done to study the relationship between stress and flow in the laboratory, research is needed to evaluate the relationship for a range of practical field-scale problems. This research should identify threshold and scale effects and evaluate the influence of lithology and fracture history. This work should also relate the heterogeneity in stress to fracture permeability and flow. Research should be undertaken to relate temperature and effective stress changes to changes in flow properties through in situ experiments in well-characterized fracture systems. This work has important applications in geothermal reservoirs and nuclear waste repositories (e.g., the proposed Yucca Mountain repository), which are expected to generate significant quantities of heat.

The effects of shear deformation on fracture permeability should be a focus for new research. This work has important implications for the stability of engi

neered structures in fractured rock and for understanding the nature of fracture permeability in natural shear zones.

Better methods are needed to predict the geometry of fractures produced by the hydrofracture process (which creates fractures by increasing fluid pressure in the rock). Research to predict fracture geometry in complex geologies, particularly in rocks that contain preexisting fractures, should be supported. An objective of this work should be to predict the effects of hydrofracturing on the local fluid flow regime. Programs should be developed to facilitate the transfer of hydrofracture technology from the petroleum industry to the water supply industry.

7. Research should be undertaken to understand and predict coupling between chemical processes and stress, flow, and temperature in rocks.

Research to understand coupling between chemical processes and stress, flow, and temperature in rocks should be undertaken. The primary objective should be to develop techniques to predict coupling effects in engineered systems. These effects should be evaluated through field studies and augmented with laboratory tests. Part of the research effort should be directed toward understanding how to scale up the laboratory results in time. This scaling work has important applications in evaluating engineering projects with long design lives such as nuclear waste repositories and dams, where slow changes may be hard to predict based on short-term testing and evaluation schemes. It also has applications in engineering projects and petroleum and geothermal reservoirs, where extreme changes in pressure, temperature, and chemistry can lead to large changes in coupled behavior.

8. Additional work should be undertaken to develop and test waste isolation and in situ treatment technologies specifically for fractured rock.

Given the large amount of waste in the subsurface and the extreme difficulty associated with removing it, in situ remediation and isolation technologies should be developed for fractured rock. Grouting (i.e., injection of cement slurries into fractures in the rock) as an isolation technique in fractured rock deserves much more attention. Research should couple in situ waste treatment and waste isolation techniques with characterization and flow modeling of the fracture system. Efficient, reliable, and economic methods should be developed to address contamination problems.

1

Rock Fractures and Fluid Flow: Practical Problems

Fractures are mechanical breaks in rocks; they originate from strains that arise from stress concentrations around flaws, heterogeneities, and physical discontinuities. They form in response to lithostatic, tectonic, and thermal stresses and high fluid pressures. They occur at a variety of scales, from microscopic to continental.

Fractures are important in engineering, geotechnical, and hydrogeological practice because they provide pathways for fluid flow. Many economically significant petroleum, geothermal, and water supply reservoirs form in fractured rocks. Fracture systems control the dispersion of chemical contaminants into and through the subsurface. They also affect the stability of engineered structures and excavations.

The application of fracture characterization and fluid flow analysis in engineering, geotechnical, and hydrogeological practice involves addressing three key questions: How can fractures that are significant hydraulic conductors or barriers be identified, located, and characterized? How do flow and transport occur in fracture systems? How can changes in fracture systems be predicted and controlled? These questions are discussed in turn below.

1. *How can fractures that are significant hydraulic conductors or barriers be identified, located, and characterized?* A fundamental step in understanding and predicting the behavior of fractures involves the identification and location of hydraulically significant fractures. Such fractures are conduits for fluid flow and are connected to other hydraulically conductive fractures to form systems or networks. Conductive fracture networks may include a large number of inter

connected hydraulically active features or may be limited to a very small proportion of the total fractures in the rock mass. Sometimes it is necessary to locate the hydraulically active fractures explicitly. In other cases it may be sufficient to determine the types of patterns (i.e., regularly repeating geometrical arrangements of fractures) that the fractures form or their statistical properties (e.g., orientation and density) or to locate only the major fractures explicitly. The requirements vary from site to site and from application to application.

Chapters 2 through 5 address methods for locating and characterizing hydraulically conductive fractures through a combination of geological mapping, geomechanical analysis, and geophysical and hydrological measurements. For instance, it may be possible to predict the locations of fractures at depth through an understanding of the processes that form fractures and the nature of the resulting fracture patterns. Chapter 2 addresses the development of fractures from a geological and geomechanical perspective and addresses the origin of fracture patterns as well as common fracture patterns found in various geological environments.

Fractures represent concentrations of void space in rocks. The geometry of the void space affects both the flow properties and the physical properties of the rock mass, such as the elastic and electric properties. An understanding of how the void space geometry controls the fluid flow and geophysical properties of rock forms the foundation of geophysical methods used to detect fractures in the subsurface. These hydraulic and geophysical properties of fractures are reviewed in Chapter 3.

Geophysical techniques can be used to locate and measure the properties of fractures in the subsurface. There have been tremendous recent improvements in subsurface fracture detection techniques. Geophysical methods are particularly useful for identifying large individual fractures as well as groups of closely spaced and interconnected fractures, sometimes referred to as fracture zones. These methods can be used to image large fractures and fracture zones, as discussed in Chapter 4. For example, seismic propagation is slower through fractures than through intact rock. This fact can be used to locate regions that have higher fracture densities and consequently regions that might also have higher hydraulic permeabilities.

Because the relationship between geophysical properties of a rock mass and the hydrological properties of the fractures is not unique, it is usually necessary to make direct measurements of flow properties from wells drilled into the subsurface, as discussed in Chapter 5. Well tests and tracer tests can be used to characterize flow system geometry, including the size, density, orientation, and interconnectedness of hydraulically conductive fractures. Flow systems developed in fractures can have quite complex geometries. Special techniques have evolved to interpret test data from these systems. These techniques are discussed in Chapter 5. These flow properties are used in mathematical models of the flow system, as described in Chapter 6.

2. *How do flow and transport occur in fracture systems?* Numerical models are used to obtain quantitative estimates of flow and transport behavior in fracture systems. The first step in the development of a numerical model is the construction of an appropriate conceptual model of the fracture system. The conceptual model is a physical model of the system that describes the main features of the geology and hydrology that control the flow and transport behavior of interest. A conceptual model incorporates an interpretation or schematization of reality that is the basis of mathematical calculations of behavior. Chapter 6 addresses the development of conceptual models from the information collected using the tools described in Chapters 2 through 5.

   Conceptual model development in fracture systems is an important but frequently undervalued step in numerical modeling. Particular difficulties arise in the determination of fracture geometry and flow physics because, as noted previously, fracture systems have complex geometries. In many cases more than one conceptual model can be constructed with available data. Indeed, most of the errors involved in predicting flow behavior with numerical models usually reflect deficiencies in the underlying conceptual models.

   A numerical model provides quantitative estimates of the flow and transport behavior of the system described by the conceptual model. The mathematical formulation of the numerical model is determined by the flow geometry specified in the conceptual model. A wide variety of fluid flow models have been developed to address the prediction of flow and transport in fracture systems. All methods subdivide the medium into a set of discrete conductive elements. The methods differ mainly in the way the conductive elements are defined (e.g., whether they represent single fractures or groups of fractures) and in the way the models are parameterized, that is, how the unknown parameters are estimated through field tests (e.g., whether unknown parameters are estimated based on statistical analysis of small-scale data or on interpretation of large-scale hydraulic tests). Several classes of numerical models, their relationships to conceptual models, and their applications to fracture flow systems are described in Chapter 6. Emphasis is on models that deal with the heterogeneous nature of fracture systems.

   Model parameterization also is addressed in Chapter 6. There is a strong dependence between field test design and model parameterization. For example, a numerical model of the distribution of fractures at a site requires the field collection of spatial statistics for parameters such as fracture density, orientation, size, and conductivity. A numerical model that explicitly specifies hydrogeological units such as fracture zones requires well tests to measure the hydraulic properties of those zones.

   Numerical models are usually developed to aid in management and design decisions. Two basic questions must be addressed before these models can be used effectively as a management or design tool. First, does the conceptual model provide an adequate characterization of the flow system? If not, it must be revised and reevaluated. Second, is the data base adequate to estimate the parameters in

the numerical model with sufficient precision to produce reliable predictions for the intended application? If not, additional field data must be collected. Development of a numerical model should be an iterative process. It begins with development of a conceptual model, which, in turn, is used to formulate a numerical model of the flow system. The parameters of the numerical model are determined through the collection and interpretation of field data, and the numerical model is used to predict the behavior of the flow system. The predicted behavior is compared to the actual behavior of the flow system as determined from field observations. If the predicted and observed behaviors do not match, the conceptual model is reevaluated and updated, and the process is repeated.

3. *How can changes in fracture systems be predicted and controlled?* The flow and transport behavior of fracture systems can be perturbed by natural processes or by the activities of people. For example, extraction of fluids from a fracture system can lower the fluid pressure, which will increase the effective stress (the stress transmitted directly from particle to particle) in the rock, thereby causing the fractures to close. Temperature-induced stresses can have similar effects. Changes in fluid chemistry can lead to either mineral precipitation or mineral dissolution on the fracture walls. In general, any change in the void geometry of a fracture system will alter the flow and transport behavior. Tools for predicting and controlling these changes are addressed in Chapter 7.

In the final analysis there is no prescribed procedure that can be followed to address flow and transport in fracture systems. This report describes tools that can be used in the process of characterization, model building, prediction, and model refinement. These tools must be applied iteratively to determine if a flow and transport system has been characterized correctly. This iterative process must be designed to test improvements in the predictive capabilities of a numerical model. If the predictions improve with each iteration, confidence in the conceptual model as an accurate representation of the flow and transport system is enhanced. If the predictions do not improve, the conceptual model must be reexamined.

Iterative procedures can be applied to many problems in the earth sciences. The tools associated with each step of this iterative process, as applied to fractures, are described in this report, but the report should not be viewed as a "cookbook." Rather, the tools described here can be applied only in a manner appropriate to the specific geology and application under consideration. Case examples of the application of these tools are given in Chapter 8.

PROBLEMS INVOLVING FRACTURES IN ENGINEERING PRACTICE

The following section describe problems associated with the occurrence of fractures in underground reservoirs, in the isolation of hazardous wastes, in mining, and in rock excavations such as tunnels or caverns. In each of these

areas fluid flow in fractures represents opportunities or difficulties. Important resources (oil, gas, water) are produced through fractures. Waste and toxic substances can leak through fractures. Fluid flow in fractures can affect the structural stability of tunnels, mines, and dams. The discussions below give an overview of the applications that are most concerned with fluid flow in fractures.

Reservoirs

Important underground reservoirs include petroleum (oil and gas), geothermal, and water supply. In these reservoirs, fluids are frequently produced through fracture networks in rocks.

Petroleum Reservoirs

Fractures present both problems and opportunities for exploration and production from petroleum reservoirs. Many petroleum reservoirs form in highly fractured rocks, where fracture properties such as density and orientation are crucial to reservoir economics. In these cases the fractures are usually important because of permeability rather than porosity. Matrix porosity stores the hydrocarbons, and fractures provide permeable pathways for the transport of hydrocarbons to producing wells.

The objective of hydrocarbon exploration in fractured reservoirs is to find areas of intense fracturing, or "sweet spots." These areas usually do not have a visible surface expression and must therefore be located by using remote sensing methods. Once the sweet spot is located, a second objective is to assess its size. Production can quickly exhaust hydrocarbons stored in the fractures themselves, so significant matrix porosity is necessary for favorable economics. It is important to know fracture orientation because orientation controls reservoir anisotropy. Subparallel fractures, for example, do not intersect; consequently, they form poorly interconnected networks. These fractures can be connected with directionally drilled boreholes oriented perpendicular to their traces. Oriented boreholes can greatly increase the efficiency of production from the reservoir.

Even relatively small numbers of fractures can affect the propagation of seismic energy. Hence, seismic methods can be used to locate fracture zones in rocks that may act as reservoirs.

Fractures can penetrate shale layers that otherwise act as hydrological barriers. These fractures can establish hydraulic continuity and, consequently, a near-hydrostatic pore pressure gradient across otherwise impermeable horizons. Fracture-controlled hydraulic connections can affect the development of a reservoir, even though the reservoir itself may not involve fractures in an important way.

When producing from fracture-dominated reservoirs, it is important to understand fracture permeability and its dependence on pore pressure. Production of

fluids at economic rates from fractured reservoirs can lower in situ pore pressures, leading to closure of the fractures and a significant reduction in the effective permeability of the system.

Artificial fractures can be created by hydrofracturing (fracturing by pumping water or other fluids and sand into a well at high pressure) in order to improve reservoir flow characteristics. Hydrofracture operations can consume a significant fraction (~25 percent) of the production budget of a well. Induced fractures can breach cap rocks or cause short-circuiting of fluids used to flood the reservoirs. Consequently, it is important to control and monitor hydrofracturing operations.

Geothermal Reservoirs and Hot Dry Rock

Most hydrothermal-geothermal systems are found in fractured rock masses. The success of field exploration and development efforts depends largely on locating major fractures, faults, or fracture zones that control subsurface fluid circulation. In contrast to petroleum reservoirs, geothermal systems are often located in low-porosity rock. Fractures provide conduits for fluid flow through the rock. These fluids extract the heat stored in the rock matrix. This heat can be "mined" by pumping these fluids to the surface through boreholes. Despite the importance of fractures to geothermal reservoir development, the technology for locating and characterizing fractures in hostile geothermal environments is not well developed.

In hydrothermal reservoirs the rates at which steam can be produced or fluids can be reinjected are contingent on fractures that are both open and hydraulically connected. If fracture transmissivity (the rate at which fluid is transmitted through a fracture under a unit hydraulic gradient) is low, commercial operation may be uneconomical because of low fluid production or high costs of injecting waste fluids into the reservoir at high pressure. On the other hand, high fracture transmissivities from large, highly connected fractures can provide short circuits for recharge; in such cases, reinjected fluids will bypass the hot matrix rocks and will not absorb much heat.

Fractures are very important for the successful exploitation of geothermal hot dry rock systems, which lack fluid plumbing systems like hydrothermal systems. Reservoirs in these systems are developed by creating fracture networks or extending existing networks to provide pathways for fluid circulation between wells. Reservoirs can be created by hydrofracturing, which requires knowledge of subsurface stresses, lithology, and the locations of natural fractures.

Fracture properties can change during operation of the reservoir owing to fluid pressure changes, thermal cooling, and precipitation of minerals. Decreases in pressure during fluid extraction from the reservoir can cause fractures to close. Fluid injection into the reservoir, on the other hand, can produce pressure increases, causing fractures to open. Fracture behavior is hard to predict because the relationship between stress and permeability is complex and highly dependent

on temperature. Scaling, or precipitation of minerals in fractures, can occur if the fluid boils or cools during extraction. These precipitates plug and ultimately seal the fractures, preventing further operation of the reservoir. Thermal shrinkage during extraction of heat from the system, on the other hand, can lead to substantial increases in the conductance of the fracture network over the lifetime of the project.

Fluid extraction also affects fractures on the periphery of the reservoir. Pressure increases or mineral precipitation can close or seal fractures at depth beneath the reservoir. Fractures on the periphery of the reservoir can be plugged by mineral precipitates as the reservoir cools during fluid extraction. These pressure and temperature effects can combine to make the reservoir self-sealing.

Water Supply Reservoirs

Water supply problems in fractured rocks are similar to those in petroleum or geothermal reservoirs. However, water supply projects usually do not command the financial resources available for petroleum or geothermal extraction. Water supply wells are frequently located by trial and error by drilling into fractures or fracture zones. Several wells may be drilled until a water-producing fracture or fracture zone is located. There is little cost-effective technology available for siting wells for optimum production. It is now more common for hydrofracture to be used as a method for stimulating water supply.

Prediction of sustainable yields in fractured aquifers must account for the effect of fractures on the flow system. Calculation of sustainable yields requires an understanding of the water balance for the aquifer. Fractures may play an important role in this balance because they can control recharge and discharge from the aquifer. For example, subvertical fracture zones that outcrop in topographic lows may provide major recharge to the aquifer.

Groundwater Contamination

In relatively impermeable rock, fractures can form pathways for the migration of contaminants (toxic chemical or radioactive wastes) that are emplaced in or released to the subsurface environment. It is important to understand and predict where contaminants will migrate and if they will reenter the surface or near-surface environment.

Toxic and Hazardous Wastes

There will continue to be a need for the land disposal of toxic wastes, and fractured rock sites will be considered for disposal facilities. Improperly designed land disposal facilities can release contaminants into the subsurface through fractured rocks. Fracture networks control the dispersion of these contaminants

in the subsurface. Cost-effective site characterization is required to prevent subsurface contamination. However, such characterization is difficult, owing to the difficulty in determining the location of subsurface fractures and predicting the transport of contaminants through fracture systems. These characterization problems make it difficult to design monitoring and cleanup strategies.

Some contaminants are injected into the subsurface through disposal wells. Typically, wastes are injected below an impermeable confining layer that provides a barrier to upward waste migration. Fractures in these confining layers can provide conduits for upward contaminant migration, potentially compromising the disposal system. The injection of waste into the subsurface at high pressure can artificially fracture the confining layer. These artificial fractures can also provide pathways for the upward migration of contaminants.

The migration of acid mine drainage water through and out of underground mines is a related issue of concern. Acid mine drainage is produced by the interaction of water with sulfur, which is present as pyrite in mine wastes, to form sulfuric acid. Bacteria speed up the process. Acid mine drainage is a significant problem in eastern U.S. coal mining districts and in some western U.S. base metal mines. The migration of acid mine water in the subsurface is frequently controlled by fractures. A good understanding of fracture flow conditions is needed to limit the formation of acid mine water and to intercept it once it has formed.

Aquifers, which are rock bodies that contain economically significant quantities of water, are particularly sensitive to contamination owing to the rapid and somewhat unpredictable movement of contaminants through fractures. Strategies designed to protect water supply wells usually employ a capture zone, the outer boundary of which is monitored for contamination. The boundary of the capture zone is usually defined as a surface from which the travel time to the well is a constant, for example, 10 years. In a relatively homogeneous porous medium, capture zone boundaries can be estimated by using numerical fluid flow models. In fractured systems the shape of the capture zone depends on the geometry of the fracture network. The shape may be very irregular and difficult to predict using numerical models.

Usually, only modest resources are available for water well protection. Few field techniques are available for cost-effective site characterization in fractured rock. Numerical techniques used to model flow in porous rocks (i.e., equivalent continuum models; see Chapter 6) may be inadequate to predict the behavior of flow through fracture systems. Indeed, modeling techniques for demarcating capture zones in fracture systems are not in common use. Numerical techniques to model dilution, dispersion, adsorption, and decay of contaminants in the capture zone are not readily available for fractured rock.

High-Level Nuclear Waste

The term *high-level nuclear waste* refers to highly toxic and highly radioactive waste such as spent fuel from nuclear reactors. Throughout the world, geological

media are being considered as storage sites or repositories for the long-term or permanent disposal of high-level nuclear waste. Permanent repositories must isolate this waste for tens of thousands of years because of the very long half-lives of the radionuclides. The most commonly pursued repository design is a subsurface facility, in any of a variety of rock types, that contains waste stored, for example, in steel or concrete canisters.

Other than human intrusion, groundwater is the only important mechanism for escape of radioactive waste from a repository. Fractures could play a key role in the movement of groundwater into a repository (see, e.g., National Research Council, 1992). If waste canisters are breached, fractures could control the transport of waste in groundwater from the repository into the environment.

Several countries are considering construction of repositories in crystalline rock below the water table. These rocks generally have extremely low permeabilities, except where they are fractured. Fractures control fluid flow in these rocks. A series of experimental facilities have been established in crystalline rocks to study the feasibility of storing nuclear waste (see Chapter 8). At these facilities, it has been observed that a relatively small number of fracture zones or faults account for the majority of fluid flow. Consequently, the general concept for waste storage is to develop repositories in relatively unfractured rock in order to isolate the waste from conductive fracture zones. A key problem is to locate and characterize the major fracture zones without drilling exploratory holes, which are potential leakage pathways. Safety considerations usually require that canisters be located hundreds of meters from major fractures. Consequently, it is important to identify all major fractures or fracture zones in the vicinity of a repository.

The relatively unfractured rock between fracture zones can have extremely low permeabilities. Although low permeability is attractive from a safety point of view, it makes the rock difficult to characterize in reasonable time periods. Depending on the particular design of a repository (e.g., how long the waste is allowed to cool before emplacement), the flow in fractures around the repository may be affected by heat generated by the waste or by two-phase flow owing to radiolysis (radiation-induced chemical decomposition), corrosion, or degassing of the groundwater entering the mined-out facility.

For any rock type, fractures at depth must be studied and characterized from excavations in order to infer the nature of the rock mass around the potential repository. However, the excavation itself causes changes to the rock, including changes in stress state, saturation, and chemical conditions. To understand the fracture system based on information from excavations, it is also necessary to understand how the excavation changes the fractures.

The United States is evaluating a potential repository above the water table in bedded volcanic tuffs at Yucca Mountain in southwestern Nevada (Figure 1.1). The tuffs contain cooling fractures (fractures formed by contraction of the rock during cooling), that tend to be confined to individual beds. A series of

larger faults cut through these beds. The role of fractures in recharge, either as conduits or barriers to flow, is critical to understanding repository performance. Above the water table, larger fractures may be filled with gas, providing an effective barrier to fluid flow. On the other hand, fracture zones or faults may be the primary conduits for transport of water from the surface to the water table below the repository. Prediction of the behavior of the flow system around a repository requires conceptual models for flow in variably saturated, fractured rocks. Such understanding is as yet incomplete.

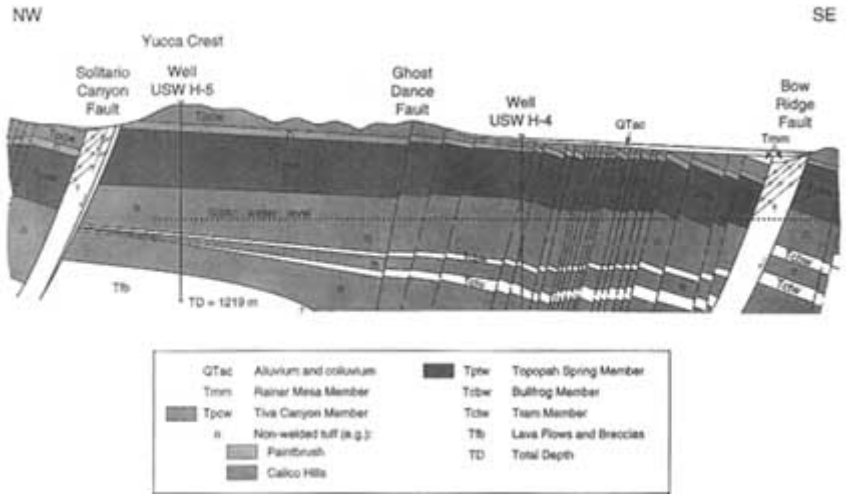

FIGURE 1.1 Cross section through a potential repository site at Yucca Mountain, Nevada, showing geology and structure. From U.S. Department of Energy (1988).

Bedded salt formations are also under consideration as waste repositories. The Waste Isolation Pilot Project site in New Mexico has been studied extensively to assess its suitability as a repository for radioactive wastes generated from defense-related activities. The salt formations themselves are thought to be very impermeable, but there is concern that leakage could occur to overlying strata if the repository is breached. If this occurred, fractures in the overlying strata could control the subsequent transport of dissolved radionuclides. Consequently, it is important to understand the flow regime in these fractures. Fractures may also exist in the salt interbeds. Radiolysis and corrosion of the waste package could generate a significant amount of gas, producing pressure buildups that might open these fractures and establish leakage pathways.

The Canadian program to develop a geological repository is focused at present on crystalline rocks at a site (yet to be determined) in the Canadian Shield, an area composed of crystalline rocks where the water table is at or close to the ground surface (Figure 1.2). The nuclear fuel waste is to be placed and sealed in engineered excavations 500 to 1,000 meters deep. Several engineered

and natural barriers will contribute to the isolation of the waste from the biosphere, including the properties of the waste; corrosion-resistant containers; engineered sealing systems for emplacement holes, excavations, and boreholes; and the properties of the surrounding rock and groundwater. It is expected that low rates of groundwater flow and geochemical retardation in a sparsely fractured repository will contribute to the overall containment design as required by existing regulatory standards.

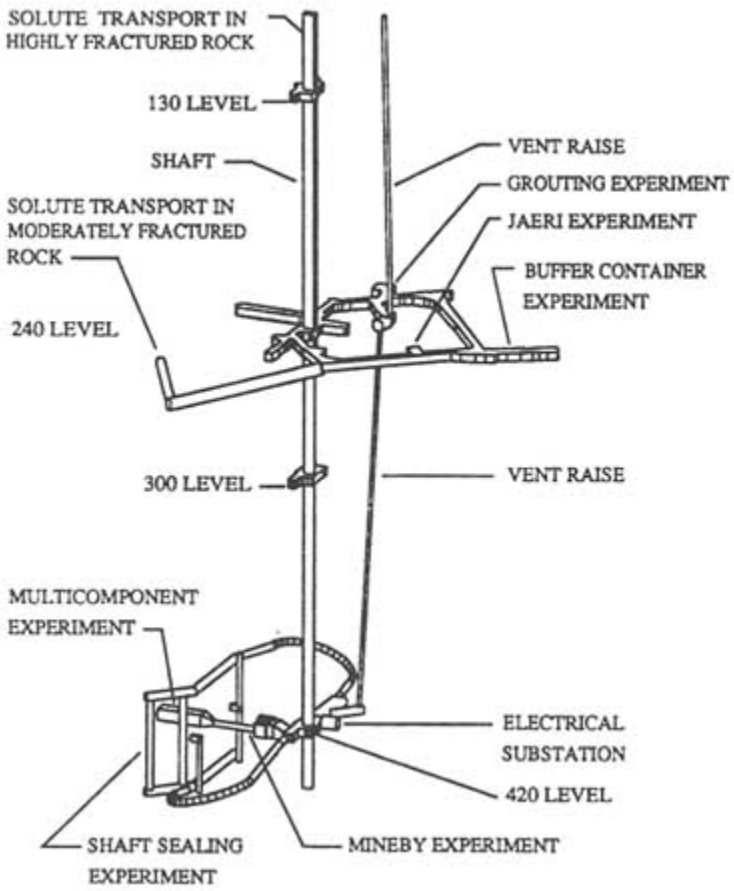

FIGURE 1.2 Facility design at Atomic Energy of Canada Ltd.'s Underground Research Laboratory near Pinawa, Manitoba. From Everitt et al. (1994).

Fractures provide the most probable pathway to the biosphere for nuclear waste buried at depth. It is important to know, at least in a statistical sense, where these fractures are located and how they might provide fluid pathways over the life of the repository.

Mining

Many problems in the mining industry relate directly to the flow of fluids through fractures in rock. A lack of understanding of fracture flow and the changes in flow conditions induced by mining (and, conversely, changes in mining conditions caused by altered fracture flow) can seriously impede mining operations. Mining activities most influenced by fracture flow include in situ leaching, mine waste disposal, underground mine dewatering, and structural stability.

Mining by in situ leaching involves the circulation of dilute chemical solvents through an ore deposit to dissolve target metals. The solvents may be applied to the top of the ore body and allowed to seep through it by gravity. Alternatively, the solvents may be forced through the ore between a series of injection and recovery wells. The recovery wells pump the solutions containing dissolved metals to the surface.

Fractures affect leaching operations in several ways. Fractures are important for developing and maintaining adequate capacity for the injection and recovery of leach solutions. New fractures may be induced by hydraulic fracturing to improve hydraulic conductivity. Fractures are also largely responsible for distributing leach solutions in the ore body. Flow through fractures may not leach effectively because it does not contact a high percentage of the target minerals. Changes in fracture geometry during leaching can profoundly change the effectiveness of leaching operations; a major concern is to prevent reprecipitation of minerals in the fractures, which seals them from further leaching action. Fractures may control the migration of leaching solutions to regions outside the leaching zone. Fracture flow may be important in restoring aquifers after leaching is completed, to satisfy environmental regulations.

Structures

Natural and Artificially Cut Slopes

Fractures and fracture zones govern the stability of rock slopes. Most types of rock slope failures, such as translational/rotational sliding failures, toppling failures, and rock falls, can usually be associated with isolated fractures or fracture zones. Fractures represent zones of weakness and are therefore less resistant than intact rock to deformation and failure by shear and tensile stresses. The presence of water in the rock mass promotes failure by lowering effective stresses and increasing static hydraulic forces on potentially sliding blocks. This effect is somewhat more pronounced under transient conditions, when changes in seepage stresses occur. Transient conditions can occur during cutting of slopes. Most open-pit mine slope failures are caused by a combination of increasing water pressure and slope height. Water-induced pore pressures may also increase if the

fractures are blocked by ice, swelling of intact rock, or precipitation of minerals. Stress levels may also rise because of rainfall, and failure may follow heavy rain.

Fractures in rock slopes have an increased susceptibility to weathering, which reduces shear and tensile resistance and may lead to blockage of water flow. Weathering of fractures may account for flatter slopes in fault zones than in the adjacent, less fractured rock.

Dams and Surface Storage Reservoirs

Fractures cause both foundation and slope problems that can affect the stability of dams, foundations, and surface storage reservoirs. Slope stability along reservoirs is affected by a rise in the water table level during the first reservoir filling and by subsequent water level changes during reservoir operations. Reservoir filling may also destabilize slopes downstream of the dam, owing to differences in water levels between the reservoir and the water table downstream. Slope instability or large deformations near the dam abutment can lead to dam failure.

The load of a dam involves the actual foundation below the dam and the lateral abutments. In the case of an arch dam the abutments can carry loads similar in magnitude to those in the foundation. Hydraulic reservoir pressures exert significant loads parallel to the ground surface that can lead to opening of fractures upstream of the dam and closure of fractures downstream. This response produces shorter seepage pathways and higher water pressures near the ground surface downstream of the dam. These high water pressures lower the effective stresses, which can produce large ground deformations and lead to collapse of the dam.

Fractures in dam foundations and abutments can also cause significant loss of water from the reservoir owing to increased permeability of the rock mass. Erosion of fault and fracture-filling materials under hydraulic gradients can cause leakage and possibly dam failure. Similarly, erosion of embankment soils into rock fractures can promote piping (formation of subsurface erosional conduits) in embankments.

Underground Structures

Water-filled fault zones and major fracture systems play an important role in the structural stability of underground openings such as tunnels and caverns. Most effects related to fractures concern the construction of underground openings and, to a lesser but not insignificant extent, its performance during operations. Fractures affect stability, deformation, and fluid flow into underground structures.

Many underground sites must be dewatered before excavation can proceed. Water is pumped from wells arranged around the periphery of an underground opening or from interceptor wells above. Problems occur in fractured formations

because water influx is often dominated by high-conductivity fracture zones. Locating these fracture zones and positioning wells to dewater them is difficult. Even more difficult is the problem of predicting the ability of dewatering wells to lower the water table in fractured formations. Well placements are usually based on conditions of uniform flow, which may be inappropriate in fractured rock. Controlling water inflow can be a significant economic factor.

Flow into tunnels through fractures can slow or delay construction. Construction conditions are often made more difficult by the flow of hot and/or chemically aggressive water into the tunnel. For example, during construction of the Simplon Tunnel through the Swiss-Italian Alps, inflows of cold water as high as about 18,000 liters per minute were encountered in fractured marble units. At another location in the same tunnel, hot water (46° C) discharged from fracture zones at rates up to about 6,300 liters per minute. Fractures may also serve as conduits for toxic (noxious) and explosive gases into tunnels and mines.

Elevated water pressures reduce effective stresses around underground excavations, which can lead to rock deformation and instability. Particularly problematical are rock masses composed of alternating impermeable and permeable (fractured) zones. The impermeable zones act as dams, which can suddenly breach if they are excavated. Thus, tunneling through a fault zone can produce a sudden inrush of water and loss of support for the face. Occasionally, such inrushing can stop the tunneling work for a significant period of time.

Fractures also have an effect on the support structure (lining) of underground excavations, which must accommodate both the rock load and water pressure. Support structures are usually designed to be watertight, which increases loads induced by water pressure. Many structures must be drained to reduce water pressure. The effects of drainage on support structures and on their interaction with the rock mass are not well understood. Drainage may induce mineral precipitation in fractures and artificial drainage conduits, which may lead to a blockage of flow and buildup of water pressures.

Underground Fluid Storage and Transport Structures

Tunnels and caverns may be used to store and transport gases and liquids. These stored fluids exert large internal pressures on the perimeters of underground structures. If the support structures fail or if no support exists, it is likely that the stored fluids will escape through fractures in the rock.

Intensely fractured rocks, and rocks containing fractures with large apertures between the fracture walls (openings), are susceptible to deformation, producing large stresses that induce cracking in excavation linings. Stored fluids can escape through these cracks, and new fractures may be induced in surrounding rock masses through hydraulic fracturing. Hydraulic fracturing may also occur if no artificial support exists. Large induced pressures from groundwater lower the effective stresses in surrounding rock masses, which lowers their stability. If an

underground structure is near a slope at the surface, such conditions may destabilize the slope. Problems with fluid loss, lining, and slope stability can be largely avoided if positive pressure gradients are maintained from the groundwater outside these underground facilities.

CONCLUSION

Fractures are a significant component in many engineering problems, including reservoirs, contamination, and structures. A wide variety of tools are now in use and under development for characterizing, analyzing, and engineering fractures in rock.

Appendix 1.A

Fractures In The Geysers Field

The Geysers geothermal field in northern California produces more power than any other geothermal energy field in the world. The economics of The Geysers geothermal field are strongly affected by reservoir fractures. Steam productivity and drilling costs depend significantly on the number and characteristics of fractures in the producing wells. A good knowledge of the subsurface fracture network in the reservoir would increase the rate of success and reduce the cost of drilling.

In The Geysers wells the steam feed zones correspond essentially to individual fractures or fracture zones in the so-called main graywacke and felsite units that compose the geothermal reservoir (Beall and Box, 1992; Thompson and Gunderson, 1992; Walters et al., 1992). Only a minor amount of steam is contributed by the rock matrix. The Geysers is a vapor-dominated geothermal system with low formation pressures. Like other vapor-dominated systems, the reservoir pressure is below hydrostatic (Carson and Lin, 1982; Evanoff et al., 1988).

Wells at The Geysers are designed to intersect as many fractures in the reservoir as possible. In some cases, wells must be abandoned because they do not intersect a sufficient number of steam-producing fractures. For these wells, low production rates make it uneconomical to install and maintain the surface equipment needed to collect and transport steam to a power plant. The location and design of new production and injection wells at The Geysers could be optimized if the reservoir fracture network were better understood.

In this and other geothermal fields it has been found that a costly and routinely encountered problem is lost circulation during drilling (Glowka et al., 1992). Lost circulation of drilling fluids occurs when the drillhole intersects a low-pressure fracture or fracture zone, which provides a pathway for flow of drilling fluid from the well. Lost circulation complicates and delays the drilling operation. The materials used to plug these low-pressure zones can damage the productivity of other feed zones. Prediction of the location and characteristics of the fractures in the reservoir would improve the design and construction of the wells and reduce the number of lost circulation zones.

Appendix 1.B

Superfund Site: Byron Salvage Yard

During the 1960s, the Byron Salvage Yard, located in north-central Illinois, accepted industrial wastes and debris, including drums of electroplating solutions, oil sludges, cutting wheels, solvents, and scrap metal. The upper aquifer at this site consists of a fractured Paleozoic dolomite, overlain by Quaternary loess and till, with a somewhat noncontinuous shale aquitard that defines the aquifer base (Kay et al., 1989). Beneath the shale is a sandstone aquifer. Regional groundwater flow is toward the Rock River, approximately half a mile to the west and northwest. The upper dolomite aquifer contains elevated levels of volatile organics, metals, and cyanide. The U.S. Environmental Protection Agency, in cooperation with the Illinois Environmental Protection Agency and the U.S. Geological Survey, initiated a series of remedial investigations and feasibility studies starting in 1983.

An integrated multiscale hydrogeological investigation has been conducted to characterize the nature of contaminant transport in the fractured dolomite (Paillet et al., 1993). There were three scales of investigation: (1) small-scale (borehole geophysical logs, natural gamma, acoustic televiewer, and caliper); (2) intermediate-scale (cross-correlated geophysical logs, electrical conductivity after fluid replacement, straddle-packer isolated slug tests, and high-resolution flowmeter logs); and (3) large-scale (topographic analysis, aerial photo lineament analysis, observation of water levels, and long-term pumping tests). These investigations indicate that the aquifer is behaving as a heterogeneous (stratified) anisotropic system. Near-vertical fractures connect with horizontal bedding planes to provide discrete flow zones. The greatest difficulty in the investigation was characterization of large-scale features such as major fractures, local faults, and caverns that are known to influence flow patterns, and ultimately contaminant transport, at the site.

Several actions were taken to clean up the contamination at this site (U.S. Environmental Protection Agency, 1989). All waste sources were removed, and abandoned monitoring wells were plugged. The site was covered by a 30-cm-thick soil cover, that was graded and revegetated. An alternative drinking water supply was provided to the affected residences.

REFERENCES

Beall, J. J., and J. T. Box, Jr. 1992. The nature of steam-bearing fractures in the south Geysers Reservoir. Special Report No. 17, Geothermal Resources Council. Davis, Calif., pp. 69–75.

Carson, C. C., and Y. T. Lin. 1982. The impact of common problems in geothermal drilling and completion. Geothermal Resources Council Transactions, 6:195–198.

Evanoff, J. I., S. W. Dunkle, and R. J. Crook. 1988. Field cementing practices help control lost circulation at The Geysers. Geothermal Resources Council Transactions, 12:37–40.

Everitt, R. A., C. D. Martin, and P. M. Thompson. 1994. An approach to the underground characterization of a disposal vault in granite. Report No. AECL-10560. Atomic Energy of Canada Ltd., Whiteshell Laboratories, Pinawa, Manitoba, Canada.

Glowka, D. A., D. M. Schafer, G. E. Loeppke, D. D. Scott, M. D. Wernig, and E. K. Wright. 1992. Lost circulation technology development status. Pp. 81–88 in Proceedings of DOE Geothermal Program Review X, March 24–26, San Francisco. CONF/920378. Washington, D.C.: U.S. Department of Energy.

Kay, R. T., D. N. Olson, and B. J. Ryan. 1989. Hydrogeology and Results of Aquifer Tests in the Vicinity of a Hazardous Waste Disposal Site, Near Byron, Illinois. USGS Water Resources Investigation Report 98-4081, U.S. Geological Survey, Urbana, Ill .

National Research Council. 1992. Groundwater at Yucca Mountain: How High Can It Rise? Washington, D.C.: National Academy Press.

Paillet, F. L., R. T. Kay, D. Yeskis, and W. Pedler. 1993. Integrating well logs into a multiple-scale investigation of a fractured sedimentary aquifer. The Log Analyst, 34:41–57.

Thompson, R. C., and R. P. Gunderson. 1992. The Orientation of Steam-bearing Fractures at The Geysers Geothermal Field. Special Report No. 17, Geothermal Resources Council. Davis, Calif., pp. 65–68.

U.S. Department of Energy. 1988. Site Characteristics Plan Overview: Yucca Mountain Site. Washington, D.C.: U.S. Department of Energy.

U.S. Environmental Protection Agency. 1989. Superfund Record of Decision, Byron Salvage Yard, Illinois, Third Remedial Action. EPA/ROD/RO5-89/-89, June, Washington, D.C.

Walters, M., J. Sternfeld, J. R. Haizlip, A. Drenik, and J. Combs. 1992. A Vapor-Dominated High-Temperature Reservoir at The Geysers, California. Special Report No. 17, Geothermal Resources Council, Davis, Calif., pp. 77–86.

2

Physical Characteristics of Fractures and Fracture Patterns

The purpose of this chapter is to provide a geological and geomechanical understanding of fracture formation, characteristics of various fracture types, network patterns, and internal structure. The geometry of fractures, their internal architecture, and present-day state of stress control fluid flow in fractured rocks. A geomechanical understanding of these properties provides an intellectual platform for making sensible inferences and predictions about the nature and location of fractures in the subsurface and underlies the interpretation of data collected through other indirect characterization techniques.

The theme that underlies rock fracture mechanics is the notion of stress heterogeneities over a broad range of scales. This includes stress concentration around material flaws and other physical discontinuities as well as broad variations in the stress field. It is this heterogeneity of stress that controls the initiation and propagation of individual fractures and the localization and clustering of the fracture systems.

Rock properties also play an important role in the formation of fractures and in the structure of fracture zones. There are marked differences in the internal structures of fractures and fracture zones in different lithologic units.

This chapter will describe some of the most prominent modes of fracturing and fracture structures for common rock lithologies. The first section deals with the definition and classification of fractures to provide a common language for a multidisciplinary readership. A following section addresses mechanisms of fracture initiation and propagation based on the concept of stress concentration. Examples of fracture formation are given for a few common rock types. The geometric characteristics of fracture networks and fracture zones and their varia

tions in terms of geological regimes and rock lithology are briefly discussed. These fracture network patterns are compared with those commonly used in reservoir simulations.

DEFINITION AND CLASSIFICATION

Fractures are mechanical breaks in rocks involving discontinuities in displacement across surfaces or narrow zones. *Fracture* is a term used for all types of generic discontinuities. This usage is common among scientists inside and outside the earth sciences and is used in other chapters of this report. However, different kinds of fractures exist, with different geometries, mechanical effects, and flow properties. Based on the nature of the displacement discontinuity, commonly encountered fractures can be classified into three geologically based major groups: (1) dilating fractures/joints, (2) shearing fractures/faults, and (3) closing fractures/pressure solution surfaces. (Pressure solution surfaces are fractures in sedimentary rock that are welded together by solution that occurs at the contact surfaces of grains [Bates and Jackson, 1980].) This chapter is concerned with the first two of these groups, joints and faults, illustrated schematically in Figure 2.1. Dilating fractures, which are also referred to as joints, can be idealized as two rough surfaces with normal displacement discontinuity; that is, the surfaces have moved away from each other in a direction perpendicular to the surfaces (Figure 2.1b). (They are also called mode I fractures in engineering fracture mechanics [Lawn and Wilshaw, 1975].) Shear fractures, which are also referred to as faults, are shear displacement discontinuities where the fracture surfaces move predominantly parallel to each other. This relative movement is either perpendicular (mode II) or parallel (mode III) to the fracture front (Figure 2.1b). Pressure solution surfaces, also referred to as stylolites, are known as anticracks in which the sense of the displacement discontinuity is opposite that of dilating fractures or mode I fractures (Fletcher and Pollard, 1981). For a review of pressure solution surfaces and their hydraulic properties, the reader is referred to Nelson (1985).

Fractures with a combination of these modes (mixed-mode fractures) also are possible. Rock masses with complex deformational histories have fractures produced by two or more of these modes in a sequential manner (Figure 2.2 a–d). This yields fractures with overprinted displacement discontinuities (Barton, 1983; Dyer, 1983; Segall and Pollard, 1983a,b; Zhao and Johnson, 1992). All combinations of displacement discontinuities may occur in nature, but the most common ones are faulted joints and jointed faults. Although these two types of fractures are kinematically similar to faults and joints, which were defined previously, their total displacement discontinuities, geometries, and internal structures may be very different because of the overprinting of two different modes of deformation.

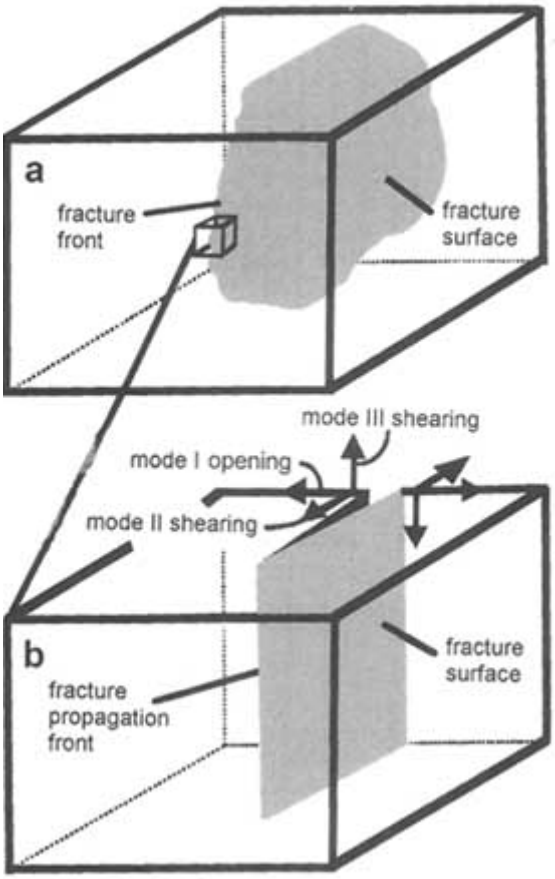

FIGURE 2.1 (a) Block diagram showing a fracture and its propagation front. (b) Three fundamental modes of fractures corresponding to joints (mode I) and faults (mode II or mode III). From Pollard and Aydin (1988).

Joints, faults, and pressure solution surfaces filled by minerals are known as veins, seams, and filled pull-aparts. The mineral fillings have important consequences for fluid flow because they may alter the flow properties of the fractured rock. The mineral fillings may have different permeabilities than the host rock, and vein bridges may keep fractures open. The mineral fillings also provide information about the nature of the fluids flowing in the fractures, the original apertures of the fractures, and the physical and chemical conditions during precipitation.

Joints and faults can be identified by distinctive surface features; joint surfaces are ornamented by the so-called plumose texture (Figure 2.3a), whereas through

going fault surfaces are polished and are marked by linear features known as grooves and striations or slickensides (Figure 2.3b). Plumose patterns record fracture propagation directions and may be radial or axisymmetric or may have a more complex geometry (Kulander et al., 1979; Pollard and Aydin, 1988; Bahat, 1988). Grooves and striations on fault surfaces record slip directions (e.g., Patterson, 1958; Suppe, 1985). Subsequent motions different from the original movements along faults may cause mismatches between opposite faces of the fracture. This mismatch may produce open channels that are potential pathways for fluid flow.

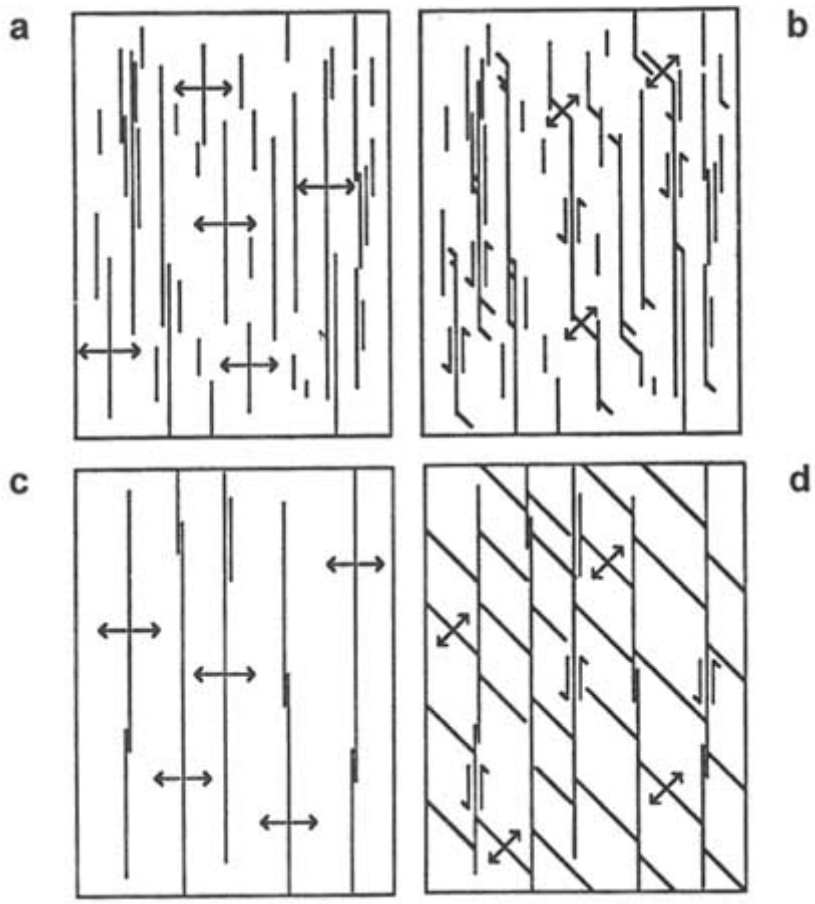

FIGURE 2.2 Development of faulted joints. Parts a and c are original joint patterns, and b and d are faulted joints with dilantant fractures in the overlap regions (b) and in between faulted joints (d). From Pollard and Aydin (1988).

Joints and faults are fundamentally different in terms of their associated stress fields (Pollard and Segall, 1987). These differences provide a basis for

understanding the initiation, propagation, interaction, and termination of joints and faults and the nature and distributions of the associated structures around them.

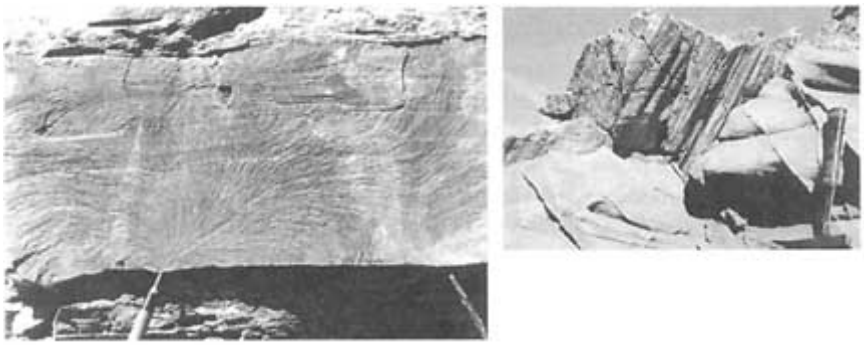

FIGURE 2.3 Left, a joint surface ornament known as plumose structure. From Pollard and Aydin (1988). Right, a normal fault surface with striations. From Aydin and Johnson (1978).

GENESIS OF FRACTURES

In general, fractures initiate and propagate when the stresses become equal to the strength of rock (a more precise propagation criterion is discussed later in this chapter, under "Fracture Propagation and Internal Structures"). Several possible sources or mechanisms that are capable of producing high stresses in the earth's crust can be identified. Among these are (1) lithostatic (changes in the weight of overburden either by burial or removal caused by uplift and erosion); (2) fluid pressure; (3) tectonic forces associated with the movement of lithospheric plates; (4) thermal (cooling of intrusive and extrusive rocks, and cooling caused by uplift and erosion of the crust); (5) impact by extraterrestrial objects; and (6) other geological processes such as folding, volcanic activity, and salt intrusion.

The relationship between fracture formation and a particular causal mechanism is obvious in some cases. For example, fractures that form a polygonal geometry (polygonal fractures) in volcanic rocks can be linked directly to thermal stresses produced during cooling of the rocks. In this case the patterns and systematic development of the fracture system can be understood in terms of the thermal history of the magma and rock fracture mechanics (Ryan and Sammis, 1978; DeGraff and Aydin, 1993).

Igneous rocks that crystallize at depth may also fracture during cooling. For example, Segall et al. (1990) dated mineralized fracture fillings in a granitic body from the Sierra Nevada in California. This analysis showed that the fractures formed as the granite was emplaced or shortly thereafter, suggesting that they formed as the granite cooled. The Sierran fractures are nearly parallel to one another, quite unlike the polygonal fracture patterns that develop as a lava flow

cools. This difference in fracture geometry may reflect the fact that the granites cooled at depth when they were subjected to other lithostatic or tectonic forces, whereas the lavas cooled under approximately homogeneous stresses at the surface.

Mechanical analyses can help relate fracture patterns to the causative geological processes when direct information on the timing of fracturing is absent. For example, Delaney et al. (1986) investigated dikes (tabular igneous intrusions) and adjacent clusters of dike-parallel joints. By representing a dike as a pressurized crack and modeling the stress field around it, these investigators showed that dike-parallel joints could open ahead of a dike. Such joints would be juxtaposed along the dike if the dike front advanced.

The task of relating a fracture system to a specific process is more difficult, however, for rocks and regions that have undergone multiple deformational events (Spencer, 1959; Wise, 1964). To establish a relationship between a particular fracture system and the mechanism responsible for its formation, it is necessary to establish the temporal and spatial relationship between the observed fracture system and the proposed process. When geological ages are not available or are uncertain, additional supporting arguments can be used. These are usually in the form of plausibility arguments based on geological and mechanical concepts or models.

The sketch in Figure 2.4 illustrates a system of joints in which the mechanism of fracture formation can be discerned through such an analysis. The joints are perpendicular to the layer and are confined primarily in the convex part of the layer. This pattern is consistent with the distribution and orientation of the axial stresses for a buckled plate. Thus, a strong case can be made that buckling or bending is the origin of these joints. In a buckled layer, dilating fractures occur initially above and perpendicular to the neutral plane, which is consistent with the geometry and distribution of the joints in the layer (Figure 2.4). In laboratory compression tests, conjugate shear fractures and opening fractures both formed, with the opening fractures forming perpendicular to the least compressive stress and bisecting the acute angle between the shear fractures (e.g., Peng and Johnson,

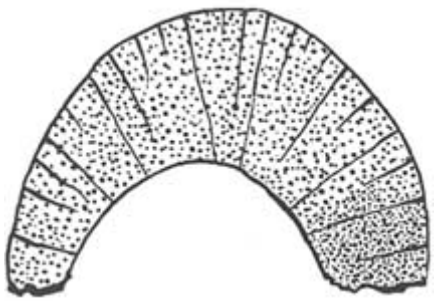

FIGURE 2.4 Sketch of a distorted layer and associated fractures. From Van Hise (1896).

1972). Stearns and Friedman (1972) used these relationships to infer the stresses responsible for natural fracture patterns in folded rock layers.

In some cases, regional distributions of joint and fault patterns mimic the trends of mountain belts, suggesting a causative relationship between the formation of fracture systems and a particular tectonic event responsible for the mountain belt. Nickelsen and Hough (1967) and Engelder and Geiser (1980) have made a case for such a correspondence between the Appalachian Mountains belt and the joints that are parallel and perpendicular to the strike of the belt. Additional examples for the genesis of fractures will be given after introduction of the basic concepts of rock fracture. For the time being it is sufficient to note that some regional or local fracture systems can be linked to one of the mechanisms listed above but that others cannot. There is a need to establish relationships between the common stress production mechanisms in the earth's crust and the resulting fracture patterns. This can be done most efficiently by case studies at the surface of the earth that take advantage of the availability of abundant direct information. Once the nature of the relationship between a process and a fracture system is established, it can be used for subsurface predictions and inferences.

FLAWS, STRESS CONCENTRATION, AND FRACTURE INITIATION

The concepts of stress concentration, amplification, and energy balance, which go back to Inglis (1913) and Griffith (1921), are essential to understanding rock fracture initiation as well as fracture propagation and distribution. Griffith showed experimentally that glass samples fractured at an applied stress level much lower than their theoretical strengths. He attributed this to the amplification of stresses around flaws in the glass, which is known as stress concentration. Most flaws in natural materials are slitlike. However, the stress distribution around a circular hole in a plate subjected to uniaxial tension (Figure 2.5) demonstrates the concept of stress concentration quite well. Because of symmetry, it is sufficient to consider the stresses on one quadrant of the hole (e.g., segments AB in Figure 2.5a). The part of the curve from A to B in Figure 2.5b shows the variation of normalized tangential stress from A to B along the perimeter of the circular hole. At a point on the circle diameter perpendicular to the direction of the applied remote stress (point A in Figure 2.5a), the tensile stress has increased threefold. The stress decreases gradually along the circular hole from point A to point B, changes its sign near point B, and finally becomes equal in magnitude but opposite in sign to the applied stress at point B. The stress concentration falls off rapidly away from the hole, as shown by curve segment BC in Figure 2.5b.

Tensile stresses can be induced even under compressive remote loading systems (Pollard and Aydin, 1988; Einstein and Dershowitz, 1990). Figure 2.6b illustrates the tangential stresses on points from A to B at the perimeter of a circular hole in a plate subjected to uniaxial compression, as shown in Figure 2.6a. A tensile stress equal to the remote (measured at some distance from

the hole) uniaxial compressive stress (σ_0) in magnitude is induced at point B. Furthermore, tensile stresses can be produced even under hydrostatically compressive loading systems (Figure 2.7a, b) if the internal fluid pressure, P, is greater than twice the applied hydrostatic compression ($P > 2\sigma_0$).

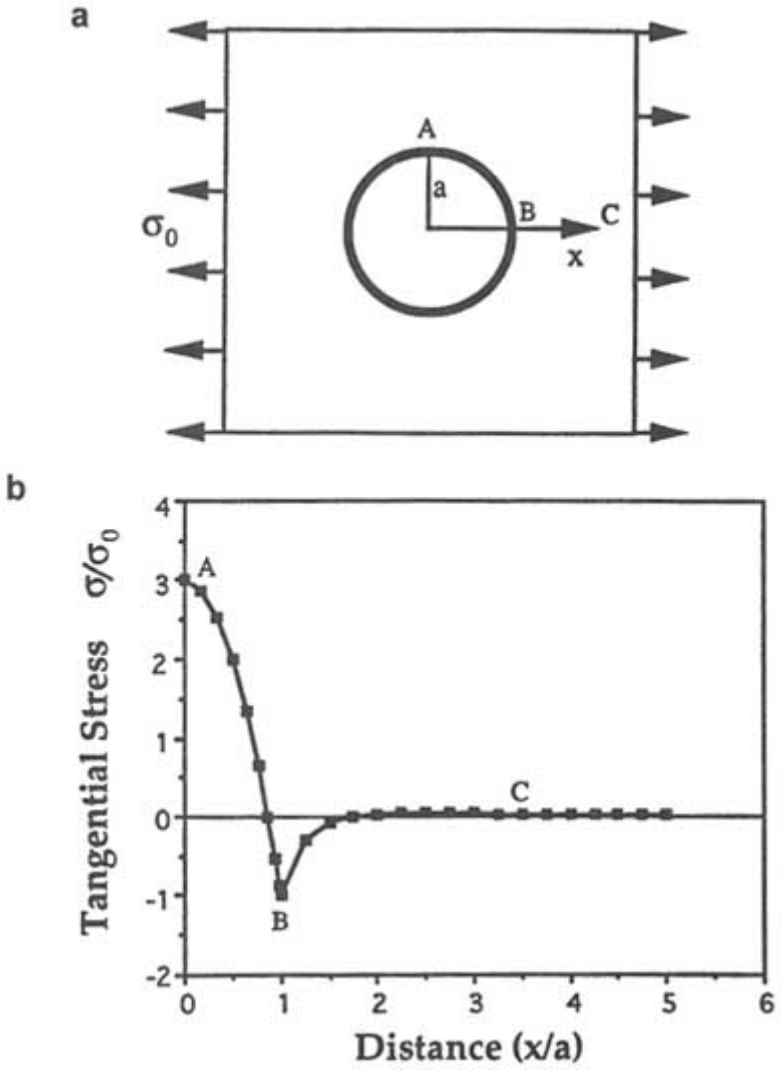

FIGURE 2.5 (a) Circular hole of radius a in a plate subjected to uniaxial tension (σ_0). (b) Stress distribution (tangential stress normalized by the remote stress around the hole). Because of the symmetry, only a quadrant of the hole (from A to B) is considered. Courtesy of Y. Du.

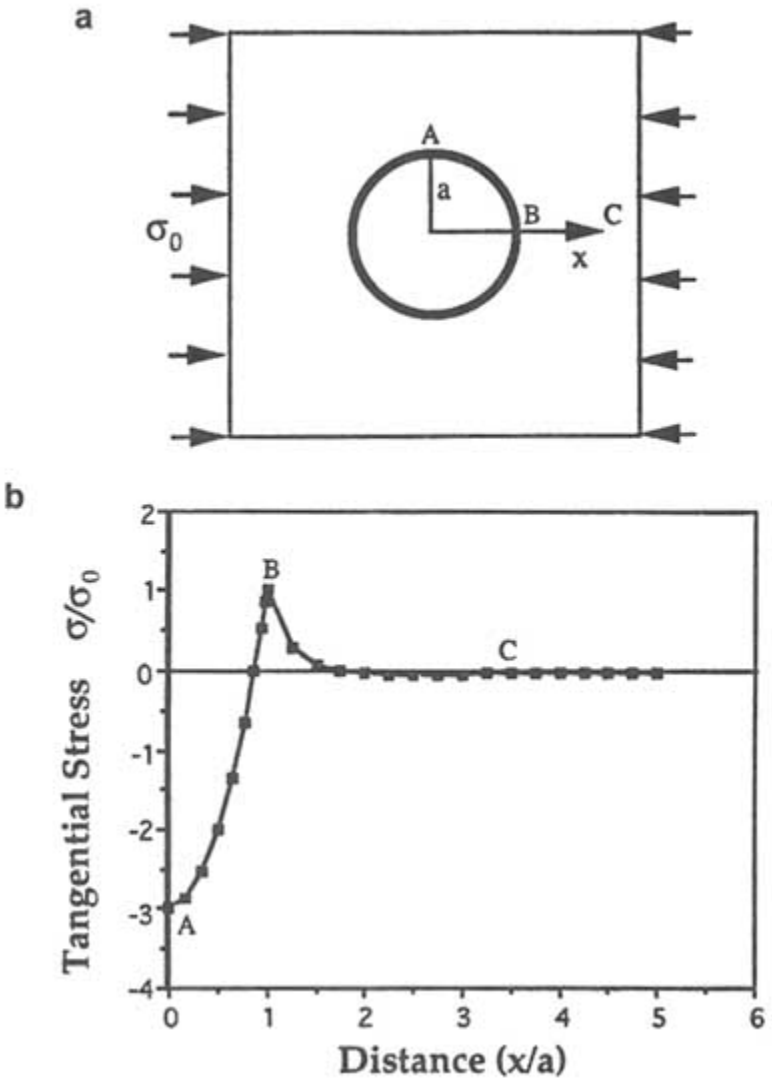

FIGURE 2.6 (a) A circular hole of radius a in a plate subjected to uniaxial compression (σ_0). (b) Stress distribution around the hole.

The amplification of stresses around holes is related to the curvature of the aspect ratio (a/b) of the opening. For an elliptical hole in a plate subjected to a uniaxial stress, the amplification of the stress at the tips is $(2a/b) + 1$, where a and b are the longest and shortest axes, respectively. Consequently, the magnitude of the stress at one of the tips of a long and thin discontinuity (Figure 2.8) can

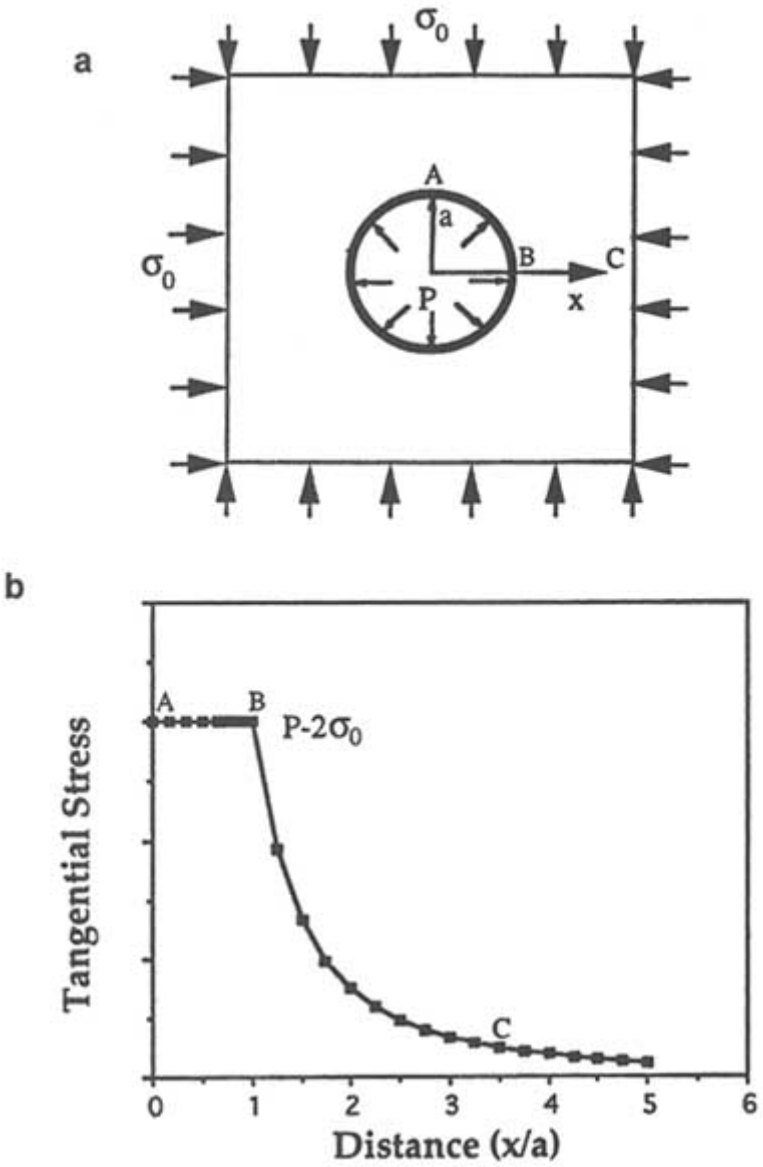

FIGURE 2.7 (a) A circular hole of a radius of *a* in a plate subjected to hydrostatic compression (σ_0) and an internal fluid pressure (*P*). (b) Stress distribution around the hole. Note that the stresses at points A and B are equal and will be negative if *P* is greater than twice the hydrostatic stress.

be many times that of the applied remote stress. For this case the expression for stress in a region immediately surrounding the tip based on the assumption of linear elasticity is given by (Lawn and Wilshaw, 1975):

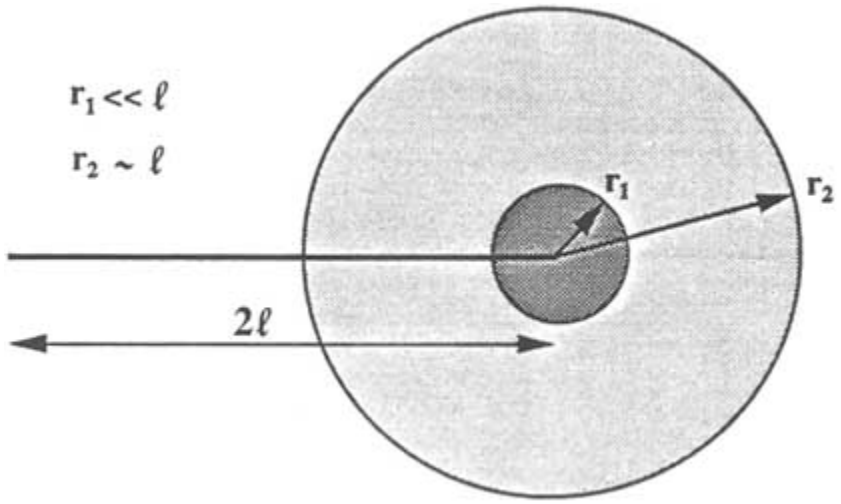

FIGURE 2.8 Regions of stress around a fracture tip. Two regions are defined: one region immediately surrounding the tip ($r_1 << l$) and one region extending to a distance roughly equal to the half-length ($r_2 \sim l$).

$$\sigma_{ij} = K_m(2\pi r)^{-1/2} f_{ij}(\theta), \text{ for } r << \qquad (2.1)$$

fracture half-length, l, and m = I, II, and III.

Here, K_m is the stress intensity factor, that is, a measure of the intensity of the stress concentration, which depends on the applied load and fracture geometry, and is known as K_I, K_{II}, and K_{III}, for modes I, II, and III, respectively. The symbols r and l are defined in Figure 2.8. For the case of a uniformly loaded fracture of half-length l, the stress intensity factor is

$$K_m = \sigma_m(\pi l)^{-1/2}. \qquad (2.2)$$

The term σ_m is the stress driving the relative displacement of the fracture walls for a particular mode of fracture (Lawn and Wilshaw, 1975). This equation, together with the previous one, shows that stresses increase near a fracture tip as the fracture lengthens. The remaining terms depend on the geometric factors about the fracture tip; r is the radial and θ is the angular component (Figure 2.8). Some of the characteristic properties of the fracture tip stress field can be seen from this expression, for example, the dependence on $r^{-1/2}$, and the singularity as r goes to zero. For larger r this relationship breaks down. For example, for $r > l$, the distance dependence of the stress is r^{-2} on average. Recall that

the preceding is based on the assumption of linear elasticity. In reality, stress concentrations at the crack tip cause inelastic behavior (e.g., in the form of microcracking). However, if the inelastic zone is small, the above-mentioned expressions from linear elastic fracture mechanics can be used to analyze the fracturing process (Rice, 1968).

Regional stress fields are generally insufficient to initiate fractures. As a result, heterogeneous stress concentrations are generally necessary for fracture propagation. Such concentrations are abundant in the earth's crust. The heterogeneity and textures in rocks can cause pervasive heterogeneities in the stress field. In detrital sedimentary rocks, for example, grains are stress concentrators (Figure 2.9a; Borg and Maxwell, 1956; Gallagher et al., 1974). In porous sandstone, fracturing on the grain scale is controlled primarily by stress concentration at the contact points between adjacent grains, as shown by Figure 2.9b. In crystalline rocks, structural defects and mismatches between adjacent grains may be the source of stress heterogeneities. Perhaps the most important source of heterogeneities in the stress field is due to geological structures induced by previous deformation at all scales.

Once initiated, fractures themselves significantly alter the stress field in adjacent rock. To illustrate this process, consider the two-dimensional theoretical mean stress fields about a joint (Figure 2.10a) and fault (Figure 2.10b). The mean stress is the average of the in-plane principal stresses (i.e., $[\sigma_1 + \sigma_2]/2$). Both fractures are of arbitrary length $2l$ and are subject to a unit driving stress. Uniaxial tension is applied to the joint, and simple shear is applied to the fault. Although the stress fields are different in each case, they are highly heterogeneous and show large stress concentrations near the fracture ends. For the case of the fault, regions of enhanced tension and enhanced compression are arranged antisymmetrically about the fault. The locations and orientations of dilational structures (e.g.,

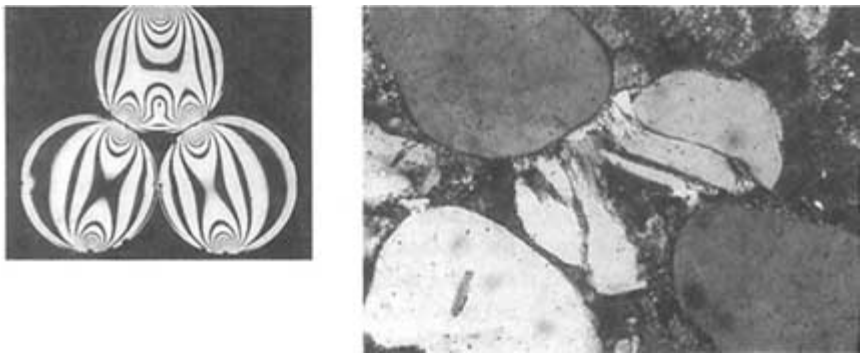

FIGURE 2.9 Left, contact stress between spherical disks made up of Columbia Resin (CR-39). From Gallagher et al. (1974). Right, thin section of Entrada sandstone showing fracturing controlled by contacts between the grains. From Aydin (1978).

veins) and constructional structures (e.g., solution surfaces) near the ends of natural faults (Figure 2.11) are remarkably consistent with the theoretical stress field of Figure 2.10b (Rispoli, 1981). Such a correspondence encourages the use of mechanical analyses as a predictive tool in geological research.

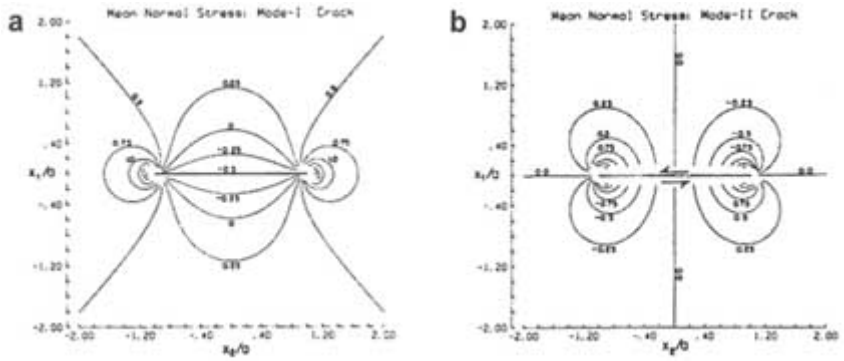

FIGURE 2.10 Mean stress distributions around (a) a joint (mode I fracture) and (b) a fault (mode II fracture). From Pollard and Segall (1987).

The global-scale inhomogeneity in the stress field is evident from a plate tectonic map of the earth showing the distributions of earthquakes, active volcanoes, and mountain chains. Stresses are high enough to cause active deformation in the interiors of some continents, but the higher intensity of deformation along relatively narrow plate boundaries is evidence for higher stress concentrations in these regions.

In many cases the geometry and mechanics of large structures allow the characteristics and spatial distribution of smaller structures to be predicted. For example, if the geometry and dimensions of a lava bed or regional strike-slip fault are known, the geometry of accompanying fractures can be inferred. Geological and mechanical analyses together can identify stress concentrations in the earth's crust, describe the nature of the stress concentrations, and yield useful descriptions of the fracture distributions. This approach is an economical way to estimate fracture heterogeneity in an aquifer or reservoir because it does not

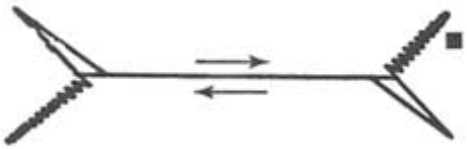

FIGURE 2.11 Map showing small faults and associated structures. From Rispoli (1981). The correspondence between the locations of the increasing and decreasing mean stress values near the fracture tips in Figure 2.10b and the dilating and constricting structures around the natural faults is remarkable.

require expensive equipment or large numbers of personnel. It can also be used in conjunction with the tools described in other parts of this report. It should be noted, however, that the task of predicting subsurface fractures is more difficult in complexly deformed areas and, obviously, when information about the regional structures is limited.

FRACTURE PROPAGATION AND INTERNAL STRUCTURES

The stress field around the fracture tip controls fracture propagation (Figure 2.8) and is characterized by a stress intensity factor (K_m), which is a function of the applied stress and the fracture geometry (Equation 2.2). Each fracture mode (I, II, and III) referred to previously has a particular stress intensity factor (K_I, K_{II}, and K_{III}), that can be calculated (Lawn and Wilshaw, 1975). According to linear elastic fracture mechanics, a fracture will propagate when the stress intensity factor exceeds a critical stress intensity factor or fracture toughness (K_{IC}, K_{IIC}, and K_{IIIC}), which is assumed to be a material property and expresses the intrinsic resistance to fracture propagation. For mode I loading the circumferential tensile stress at a small distance from the fracture tip is largest in the plane of the fracture. Therefore, joints propagate in their own plane perpendicular to the direction of the greatest tension near the joint front. As noted earlier (Figures 2.6 and 2.7), an absolute remote tensile load is not required for joint formation. Remote compressive loads can induce localized tensile stresses, as can the presence of flaws with high fluid pressure (Secor, 1965, 1968; Hubbert, 1972; Price, 1974).

The formation and propagation mechanisms of shearing-mode fractures are enigmatic. Although fracture toughnesses for mode II and mode III (K_{IIC}, K_{IIIC}) fractures exist conceptually, they have not been measured reliably in the laboratory, and it is not completely clear how they influence faults that link together by opening-mode fractures (e.g., Segall and Pollard, 1983b).

As a fault propagates, slip on it increases, and this fact has important hydrologic effects. Few faults in nature and few shear fractures in laboratories slip without significantly deforming either the material between the sliding surfaces or the adjacent wall rock. Slip commonly results in zones of brecciated rock and zones of gouge along faults. Zones of breccia can have relatively high hydraulic conductivities. Gouge zones, in contrast, tend to be highly impermeable. Breccia zones and gouge zones for large faults can reach hundreds of meters in thickness. As a result, portions of some faults are extremely conductive while others are practically impermeable. In addition, fault slip commonly juxtaposes different types of rocks. This can cause the hydraulic character of opposing sides of a fault to differ sharply.

The style of fault formation depends on the stress state during slip and on the lithologic and physical properties of the host rock. For example, faulting in porous sandstone occurs by a combination of collapsing of pores and fragmenta

tion of sand grains (Engelder, 1974; Aydin, 1978; Jamison and Stearns, 1982; Figure 2.9b). This deformation is localized into a narrow band (Figure 2.12a, b) in which grain size, porosity, and permeability can be markedly reduced. The reduction in permeability perpendicular to a narrow zone of deformation bands may be as large as three orders of magnitude (Pittman, 1981; Seeburger et al., 1991; Logan, 1992; Antonellini and Aydin, 1994).

In laboratory compression tests on low-porosity rocks such as granite, shear fractures form by a rather intricate process. First, en-echelon dilating microcracks open perpendicular to the direction of least compression; when these coalesce,

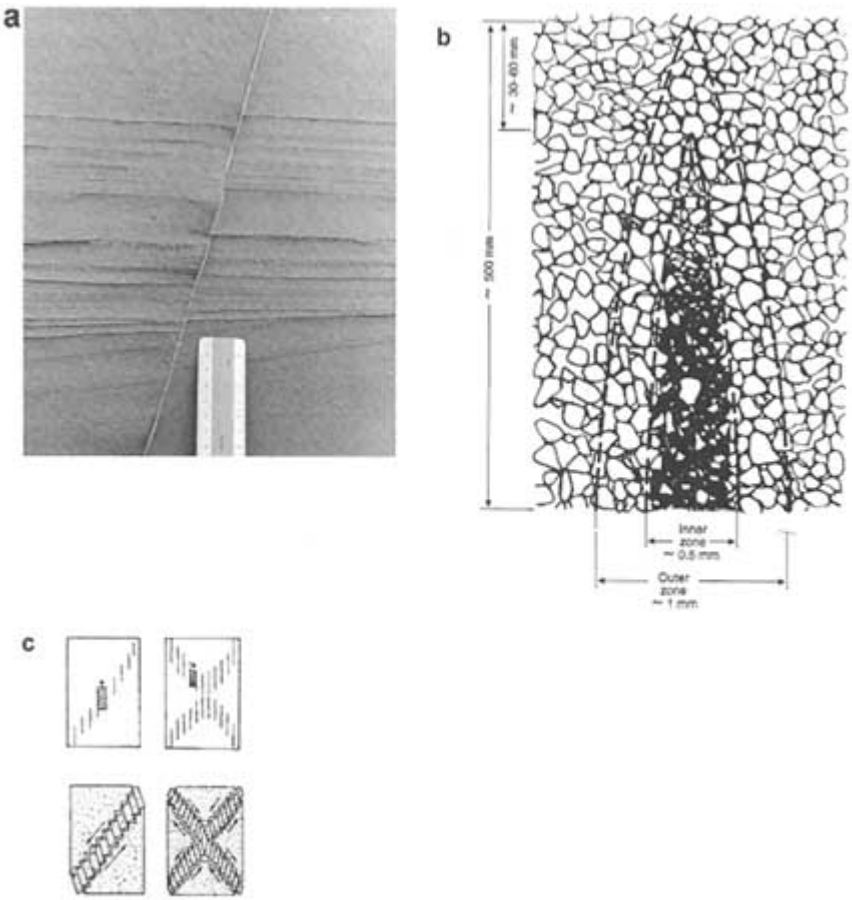

FIGURE 2.12 (a) A small fault in sandstone. From Aydin (1978). (b) Schematic drawing of the fault's tip showing the internal structures. From Aydin (1978). (c) A series of drawings showing the development of small faults in granitic rocks failed in compression tests. From Peng and Johnson (1972).

rock bridges between the cracks rotate and fail, and a shear fracture results (Peng and Johnson, 1972; Horii and Nemat-Nasser, 1985; Reyes and Einstein, 1991), as shown in Figure 2.12c. The localization of microcracks during loading is fairly well understood (for a review see Einstein and Dershowitz, 1990) thanks to improved stiff loading frames and acoustic emission techniques (e.g., Lockner et al., 1992). The en-echelon arrangement of microcracks apparently reflects the fact that each microcrack influences the location of the next microcrack (Du and Aydin, 1991; Olson and Pollard, 1991; Reches and Lockner, 1994).

The mechanics of fault propagation, the nature of friction and slip on faults, and permeabilities across faults are still poorly understood (Rice, 1992, 1993). There is a great need to understand the micromechanical processes of faulting in a host of common geological media (e.g., unconsolidated sediments, shale, sandstone, limestone, granite), the localization of deformation into zones, and possible effects of deformation on fluid flow.

FRACTURE GEOMETRIES

The shapes and dimensions of natural fractures are not well known, partly because the entire extent of a fracture is extremely difficult to observe in three dimensions and partly because a significant effort has not been devoted to such observations. Below are summaries of available information on the geometry of single joints and faults.

Geometry of Single Joints

The geometry of a joint depends on how it propagates and terminates. As a result, joint geometry is controlled by such factors as the geometry of the fractured rock mass, loading conditions, and interactions with neighboring fractures. For example, joints in layered rocks are commonly formed perpendicular to the layers. A joint is initiated at a flaw and propagates away from the flaw if sufficient energy is provided by the loading system. The joint in Figure 2.3a was initiated at a sedimentary irregularity on the bottom of a layer, whereupon the fracture propagates with a nearly semicircular front. Once the propagation front reaches the top boundary of the layer, the front propagates laterally and becomes nearly perpendicular to bedding. This manner of propagation is common in sedimentary rocks (Bahat and Engelder, 1984; Engelder, 1987). Using joint surface features, Engelder and Lacazette (1990) described the growth of joints in siltstone-sandstone beds, which they interpreted in terms of a natural hydraulic fracturing mechanism. A long joint in a single thin layer can be depicted as rectangular, with a lateral dimension much larger than the vertical dimension. The lateral dimension of an individual joint is typically a few tens of meters to a few hundreds of meters. Laubach (1992), for example, presents data from the Frontier Formation in Wyoming that shows maximum joint lengths of about 40 m.

In layered rock masses, joint segments in adjacent layers commonly join to form a composite joint (Helgeson and Aydin, 1991) that presumably still has a roughly rectangular geometry (Figure 2.13). The existence of thin shale laminae between the layers may cause offsets and discontinuities in the composite joints, as illustrated in the figure. Thick shale units usually impede jointing, thereby causing the strata-bound joints, that is, joints contained in certain stratigraphic units.

In volcanic rocks, thermally driven joints form perpendicular to cooling surfaces. Individual joints are also composites of joint segments (Figure 2.14) formed by cycles of incremental growth. Their longest dimension (vertical in the figure) is also perpendicular to the cooling surface. For rocks emplaced at or near the earth's surface, the cooling surface is usually the upper and lower surfaces of the unit, so the longest dimension is usually vertical. For more

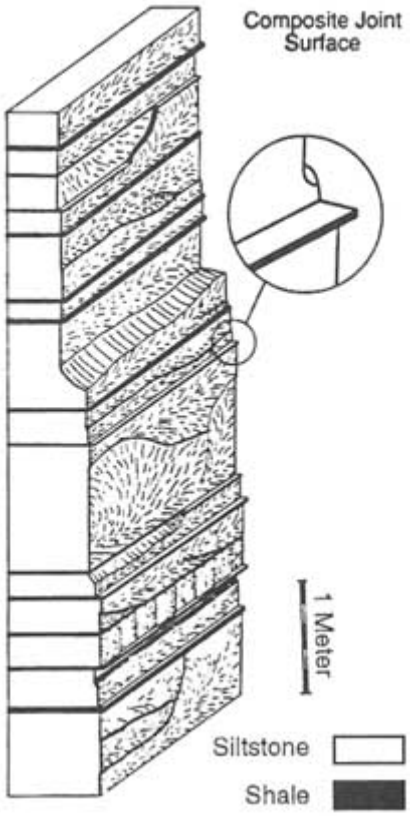

FIGURE 2.13 A composite joint surface in siltstone multilayers separated by thin shale laminae. From Helgeson and Aydin (1991).

information about the relationships among lava flow thickness, cooling rate, incremental growth, and joint dimensions, see DeGraff and Aydin (1993).

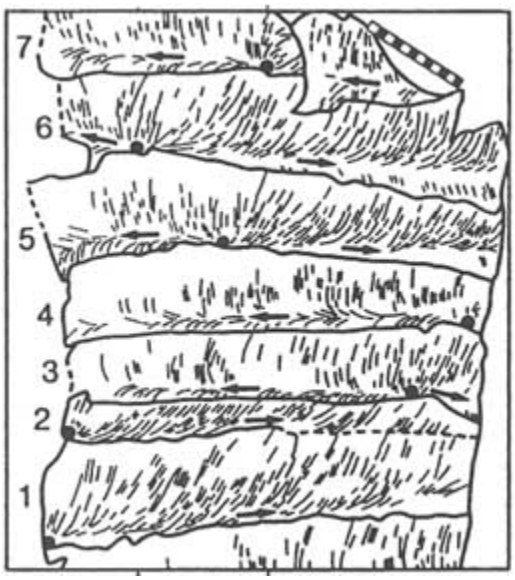

FIGURE 2.14 Addition of segments representing incremental growth of a cooling joint from a composite joint surface in a basaltic lava flow. From DeGraff and Aydin (1987).

The geometries of single joints in massive rocks or very thick sedimentary layers have not been studied in a comprehensive manner but clearly can be complex. The patterns of surface markings on many joints in massive rocks resemble the pattern of Figure 2.3a, suggesting that the joints are initially circular or elliptical. As they grow, however, portions of the joints may twist out of plane, giving them an appearance vaguely similar to a multibladed screw propeller. Further growth of the joints occurs either by the propagation of a few of these segments or by new "blades" twisting off the older ones. This twisting tends to develop most spectacularly in massive rocks, but it also occurs on a small scale in thinly layered rocks, with a fringe of fractures twisting out of plane along joint margins near bedding interfaces.

Interpreting the trace geometries of joints (i.e., the pattern of intersections between joints and the earth's surface) is somewhat problematic given that the three-dimensional geometry of joints in massive rocks is rarely known. Nonetheless, data on joint trace lengths commonly are collected to describe joint geometries because these data are accessible. Segall and Pollard (1983a) mapped a joint system (shown in Figure 2.15a) in the granitic rocks of the Sierra Nevada, California. The joint trace-length frequency distribution is of the form

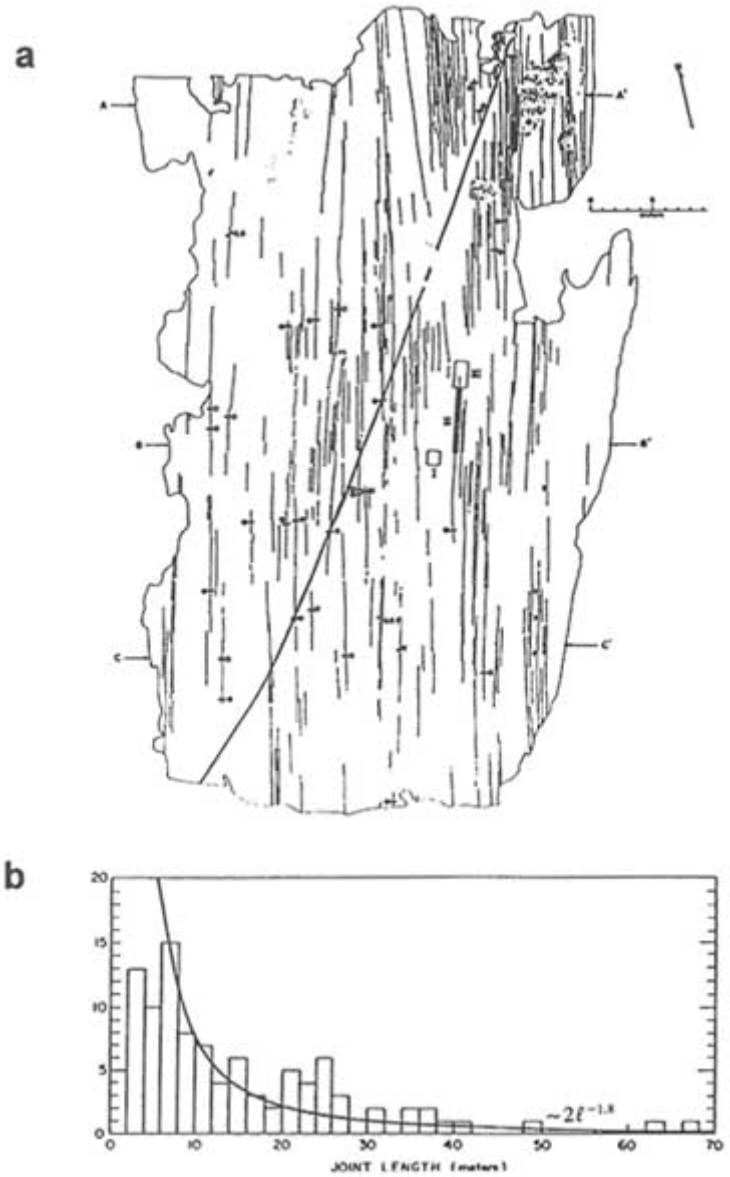

FIGURE 2.15 (a) Map of a joint set in granitic rocks of the Sierra Nevada, California. (b) Joint length-frequency distribution for the set in *a*. The curve has the form of $(2l)^{-1.8}$. From Segall and Pollard (1983a).

$f(l) \sim (2l)^{-1.8}$, with the longest joint trace length being about 70 m. A distribution function obtained from another location has the form $f(l) \sim (2l)^{-1.3}$ and apparently indicates a less developed state of fracturing.

Detailed studies of three-dimensional outcrops are necessary for deciphering the geometry of individual joints in both layered and massive rock bodies such as sandstone and granite. Experimental and theoretical models simulating three-dimensional joint growth under various environmental and loading conditions can be helpful in developing a conceptual framework for predicting joint geometry in the subsurface.

Geometry of Single Small Faults

The geometries of single small faults in certain ways resemble those of joints (Aydin, 1978; Segall and Pollard, 1980; Martel et al., 1988). The maximum in-plane dimensions of small faults are several tens of meters, and, like joints, the trace geometries of individual small faults are discontinuous. In other aspects the geometries differ. Small faults tend to be somewhat thicker than joints, which commonly are of hairline thickness. The trace geometry of a small fault is fairly straight when traversed along the direction of slip, but a wavy geometry is common in the direction perpendicular to slip (e.g., Aydin and Johnson, 1978; Power et al., 1987). New fractures of all modes can develop at the margin of a fault, and fault growth effects commonly complicate the geometry of a small fault. As a result, identification of fault ends and measurement of fault length become problematic. Thus, even though field observations on the outcrop scale of small individual faults (Aydin, 1978; Segall and Pollard, 1983a,b) suggest that they are usually short (i.e., several tens of meters), fault zones (discussed later) with large displacements can be much longer.

FRACTURE SETS

Fracture sets comprise a number of approximately parallel fractures of the same type and age. Fracture sets can be described by the areal and vertical extent, the spacing or density of individual fractures, and the orientation distribution. This information can be used to assess the physical connections between individual fractures, which influences fluid flow. Determination of fracture aperture, which, as noted previously, is the size of the opening measured normal to the fracture walls, is problematic because the original fracture opening is rarely preserved. For the purpose of present-day fluid flow, present fracture aperture distribution is important and is addressed in the next chapter.

Among the physical characteristics of fracture sets, the spacing of individual fractures (particularly for joints) has attracted the most attention. Many workers (Lachenbruch, 1962; Price, 1966; Hobbs, 1967; Ladiera and Price, 1981; Verbeek and Grout, 1984; Narr and Suppe, 1991) contend that the spacing of joints is

proportional to the thickness of the fractured layer as displayed by the field data in Figure 2.16. Also, it has been suggested that joint spacing depends on the elastic properties of rocks (Price, 1966; Hobbs, 1967). For example, the joint spacing of coal cleats is smaller than that of less stiff rock of comparable thickness.

Although joint-spacing laws of various forms have been proposed, recent experimental and numerical studies (Wu and Pollard, 1991; Rives et al., 1992) suggest that joint spacing evolves with time, strain magnitude, strain rate, and loading cycle (Figure 2.17). These studies suggest that joint spacing decreases with increasing total strain, increasing number of loading cycles and decreasing strain rate. It has also been suggested that in some cases joint spacing may evolve spatially by selective growth of some joints (Geyer and Nemat-Nasser, 1982; Dershowitz and Einstein, 1988; Pollard and Aydin, 1988; DeGraff and Aydin, 1993). The process of selective growth is influenced by the initial distribution of flaws and the propagation and interaction of joints. Even though joint spacing evolves with increasing joint development, present experimental results suggest the existence of final limiting values for well-developed joint systems (Wu and Pollard, 1991). Joint spacing is one of the most crucial parameters for fracture flow. The evolution of joint spacing distribution in terms of the mechanical factors referred to above needs to be further studied by field, experimental, and theoretical means.

Fault Sets

Faults commonly form sets that have different geometric properties than joints. The reason for this fact is that the length and spacing of faults may be related to the magnitude of slip across the faults, and faults have much greater variation in the magnitude of slip than joints have variation in the magnitude

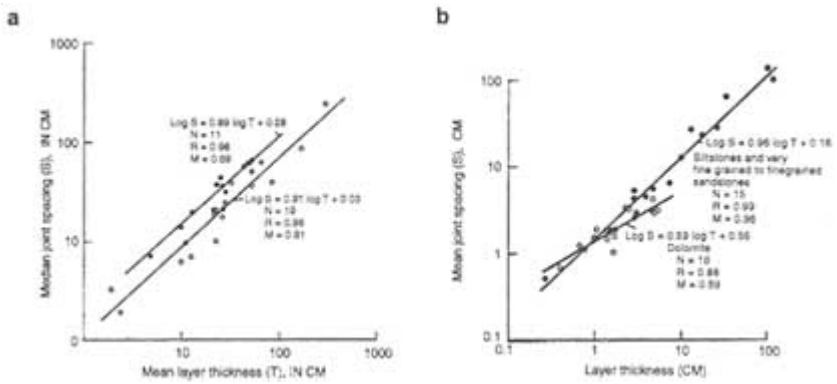

FIGURE 2.16 (a) Joint spacing-layer thickness relationship. (b) Joint spacing in different rock types. From Verbeek and Grout (1984).

of dilation. Recently, attempts have been made to characterize statistically the relationships between fault length and maximum slip (Walsh and Watterson, 1988; Marrett and Almendinger, 1991; Cowie and Scholz, 1992) and between fault length and frequency distribution (see, for example, Heffer and Bevan, 1990). Both relationships appear to be characterized by a power law across a broad range of scales. The development of faults is a complex process, and they may form by several mechanisms. So it only makes sense to compare fault lengths and spacings for faults that have formed in a similar manner.

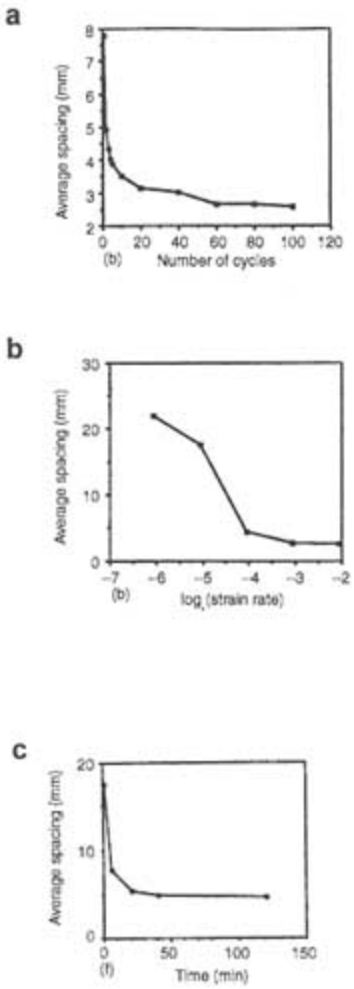

FIGURE 2.17 Variations of joint spacing as a function of (a) cyclic loading, (b) strain rate, and (c) time. From Wu and Pollard (1991).

Figure 2.18 shows the development of a fault set in granitic rock of the Sierra Nevada. Here, faults actually originated from joints (Segall and Pollard, 1983a). The initial spacing of the faults was controlled by the spacing of the joint set. Once developed, simple and compound fault zones (Figure 2.18) have their own particular slip, length, and spacing relationships.

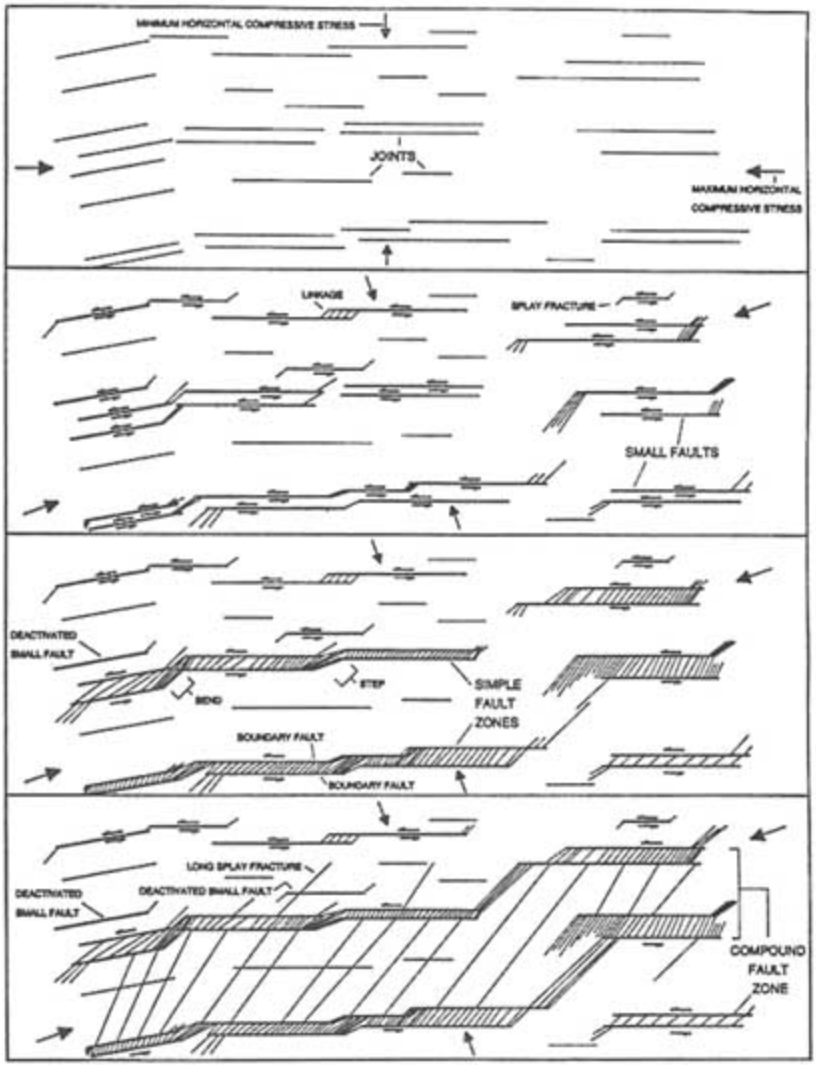

FIGURE 2.18 Schematic illustration of the development of strike-slip faults and strike-slip fault zones in granitic rocks of the Sierra Nevada, California. From Martel (1990).

INTERACTION AND LINKAGE OF JOINTS

Interaction between joints influences how they are spaced and clustered, their effective lengths, and hence their connectivities. For example, the horizontal dimensions of individual joints rarely exceed several tens of meters, as explained earlier. However, individual joints and other opening-mode fractures may be connected to form long linear arrays. Adjacent fractures may overlap slightly and link with a hook geometry over a broad range of scales (Figure 2.19). The geometry of overlap, and the existence of connecting fractures, is strongly influenced by, among other things, the state of stress (Olson and Pollard, 1991). If the differential regional stress is small (i.e., there is a nearly hydrostatic state of stress), the tendency of nearby fractures to interact and connect is strong (Figure 2.20). For a large differential stress the tendency for linkage is weak, so joint traces are straight and linear and overlap for long distances without being connected. The joints in such a system would be poorly connected, and the hydraulic communication between the joints would be low, even though individual joints are long and straight.

INTERACTION AND LINKAGE OF FAULTS

Faults commonly occur in en-echelon geometry at a broad range of scales (Segall and Pollard, 1980; Horii and Nemat-Nasser, 1985; Martel et al., 1988; Aydin and Schultz, 1990; Martel, 1990; Reyes and Einstein, 1991). Understanding the interaction and linkage between en-echelon faults is even more important for fluid flow than it is for en-echelon joints. The stepover zones along faults are broadly and pervasively fractured (Segall and Pollard, 1980). For example, the extensional stepover regions may form efficient conduits for fluids (Sibson, 1981; Aydin and Nur, 1982) in a direction perpendicular to shearing (Martel and Peterson, 1991). Large crustal-scale stepovers, however, may provide rather heterogeneous fluid flow pathways because of uneven internal fracture distribution.

There has been significant progress in understanding the mechanics of fault interactions in the past 15 years. The first papers on this topic were based on mechanical models that provided the stress fields associated with interacting faults (Rodgers, 1980; Segall and Pollard, 1980; Horii and Nemat-Nasser, 1985; Reyes and Einstein, 1991). These models have been used to interpret the observed deformation caused by fault interaction. For example, Figure 2.21 shows theoretical modeling results for the stress field around two en-echelon mode II fractures and field observations of secondary features at a real fault step. Note the increasing stress magnitudes at the overlap region and the orientations of the principal stresses. The secondary features observed in the field are located where the stresses are concentrated and are oriented consistent with the principal stresses

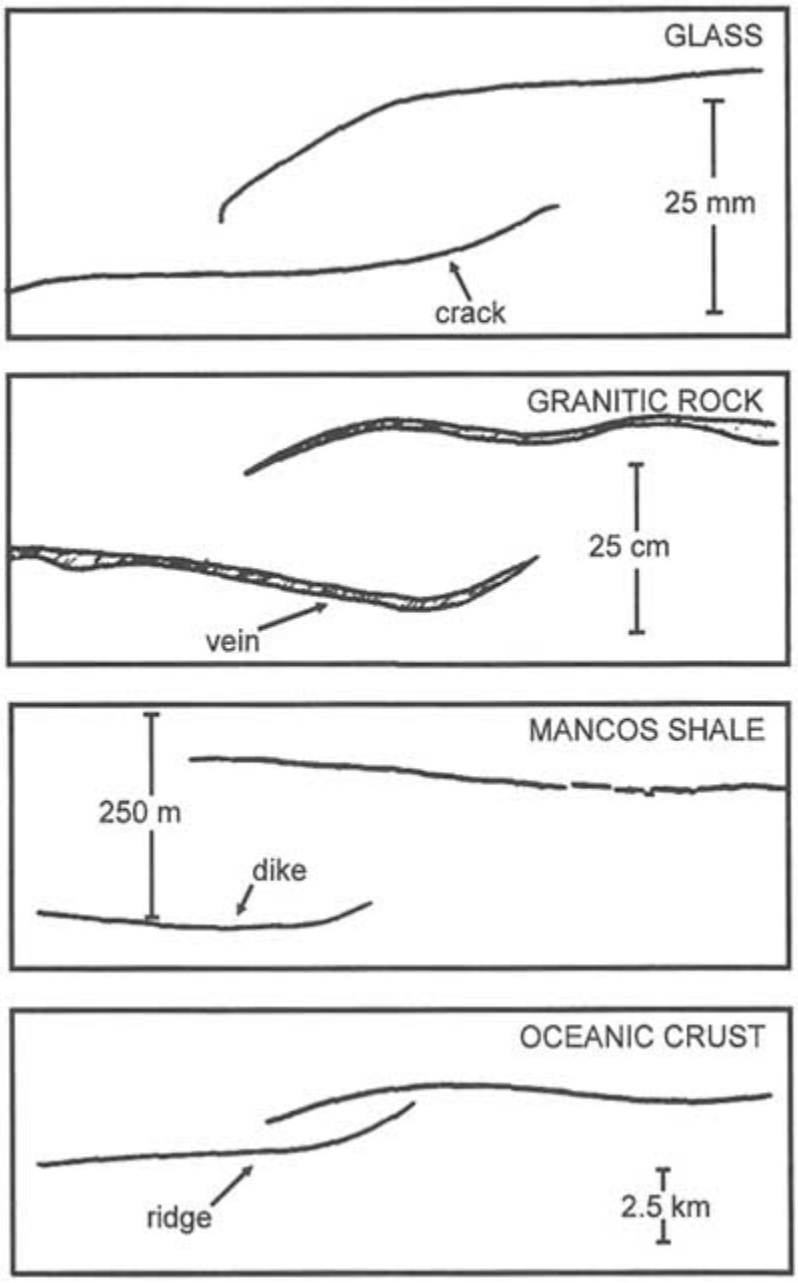

FIGURE 2.19 Overlapping geometry of en-echelon dilating fractures at various scales. From Pollard and Aydin (1984).

(e.g., the calcite-filled cavities are parallel to and the cleavages (pressure solution surfaces) are perpendicular to the tick marks of Figure 2.21b).

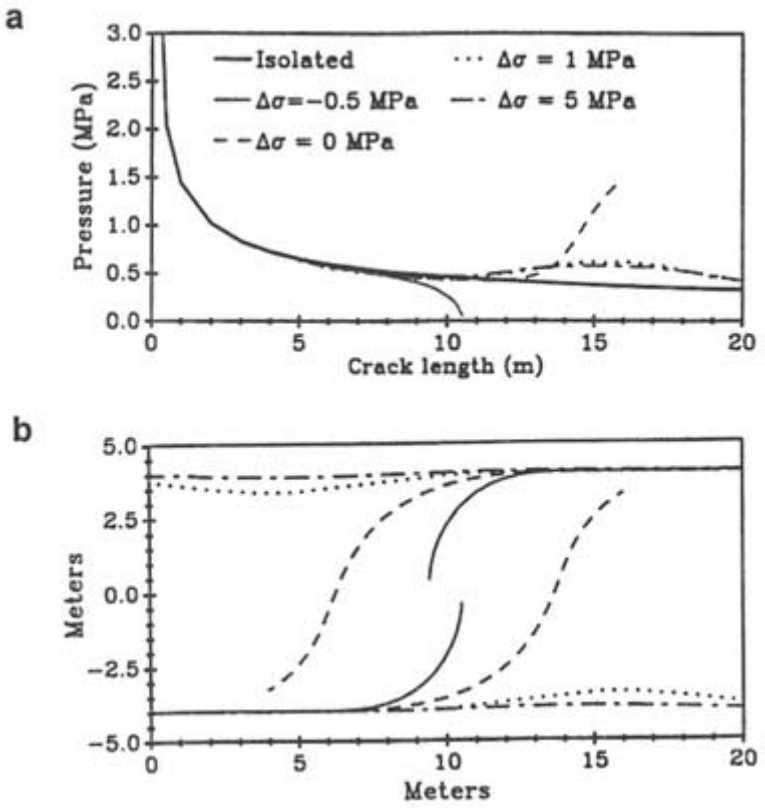

FIGURE 2.20 (a) Influence of the state of stress on the overlap and the linkage geometry of en-echelon fractures. (b) Various fracture paths for corresponding loading systems shown in *a*. From Olson and Pollard (1989).

It has been shown by field observation and field experiments that interaction zones can, in fact, contribute significantly to fluid flow (Sibson, 1981; Aydin et al., 1990; Martel and Peterson, 1991; see Chapter 8). The overlapping parts of en-echelon faults such as those illustrated in Figures 2.18 or 2.21c are regions of extension. Extensional regions tend to form extensional fractures (mode I), which are good conduits for flow because they are open. These open fractures tend to be oriented parallel to the intermediate stress direction responsible for faulting. Thus, permeability will be enhanced in that direction unless these features are completely filled with precipitates such as calcite or quartz. It is common to observe rhomboidal-shaped veins in fault steps; they are a record of old flow regimes in these extensional regions.

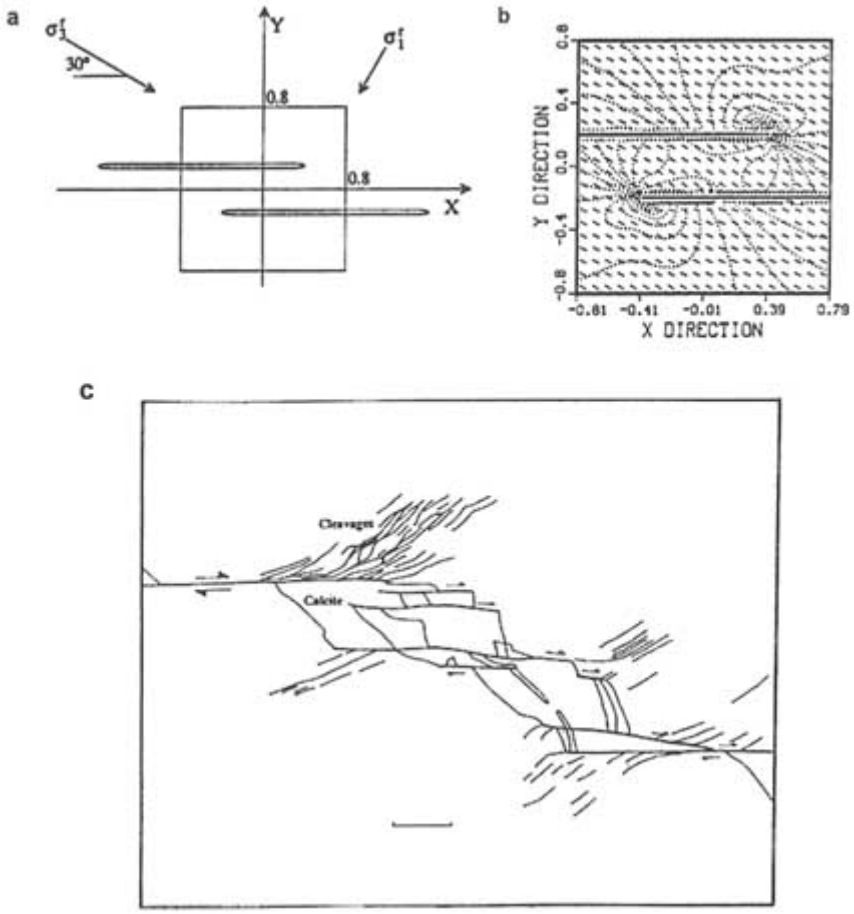

FIGURE 2.21 (a) Loading configuration. (b) Stress distribution around two en-echelon mode II fractures in an elastic plate subjected to biaxial compressive principal stresses. Contours (dotted) indicate the relative magnitude and tick marks the orientation of the principal compressive stress. (c) An array of en-echelon faults and the associated secondary structures. The calcite fillings at the extensional steps and pressure solution cleavages in the contractional quadrants are consistent with the stress field shown in *b*. Friction on the faults is assumed to be 0.6. The scale indicator at bottom center in (c) represents 0.5 mm. From Ohlmacher (1991).

A reversal in the direction of movement of the faults in Figures 2.18 or 2.21c would change the extensional regions to compressional regions. The permeability of compressional regions is not well understood, but compression may cause extensional fractures and thus increase permeability locally. Although it is known that extensional fractures tend to form in complex faults, it is not known

how they intersect and connect in three dimensions to form networks for fluid flow. A general rule is that the overlapping parts of the en-echelon faults and the area between them under extension may provide fluid pathways and that the direction of high permeability tends to be that of the intermediate principal stress unless these features are completely filled by mineral precipitates.

FRACTURE ZONES

Joints and faults commonly occur in sets localized into narrow tabular bands. In fact, many topographic lineaments mentioned in the literature with horizontal lengths of several tens of kilometers (Wise, 1976; Nur, 1982) are actually fracture zones. These zones are important for fluid flow because of their great extent, connectivity, and conductivity and will be described in detail in this section.

Joint Zones

Joint zones occur in all rock types. Figures 2.22 to 2.25 illustrate many examples from clastic rocks of the Colorado Plateau. Joint zones in the sandstones of the Colorado Plateau have been described by many investigators, each using a slightly different terminology (joint zones by Hodgson, 1961, and Engelder, 1987; zoned joints by Dyer, 1983; joint swarms by Laubach, 1991; and joint zones or fracture swarms by Cruikshank and Aydin, 1994). Some of the structures appear to be different both geometrically and perhaps genetically. For example, Hodgson's joint zones, based on his schematic diagrams (e.g., his Figure 12), contain few joints with short overlaps and appear to be related to either breakdown of parent joints (segmentation of an initially continuous joint) or progressive formation of an array of en-echelon joints. Dyer's zoned joints include a few parallel or highly overlapped joints (Figure 2.23). Laubach's joint swarms represent a cluster of many joints, some of which have strikingly different orientations (Figure 2.24). Hodgson's and Dyer's joint zones are systematic with regular spacing that is weakly related to the thickness of the fractured units; Laubach's swarms are not as systematic and appear to have highly variable widths. The joint zones described by Cruikshank and Aydin are localized and limited in extent with respect to other joints in the network. The geometry of this type of joint zone depends on structure, geology, and deformation history (slip along preexisting joints and bedding planes).

Many mechanisms may be responsible for the zonal character of joints. One of them, breakdown or segmentation of a parent joint (Pollard et al., 1982), is well known. Dyer (1983) proposed that the crack-tip stress field ahead of a propagating joint and some lithologic factors were responsible for the clustering he observed. On the basis of numerical modeling, Olson (1990) suggested that the propagation velocity of fractures may cause joint localization. Specifically, the more sensitive the fracture propagation velocity is to the degree of the stress

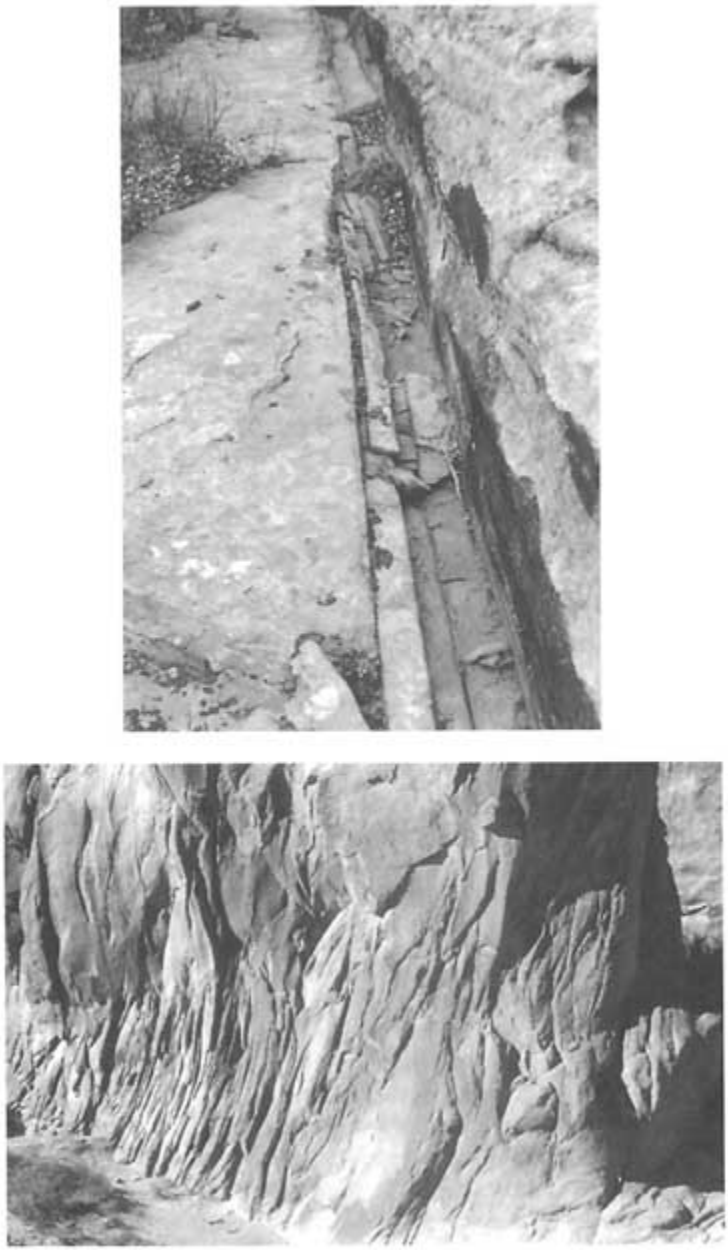

FIGURE 2.22 Two joint zones in the Entrada Sandstone, Arches National Park, Utah. Photographs by A. Aydin.

concentration at the fracture tip, the more common the fracture clustering. This notion was later exploited by Renshaw and Pollard (1994), who numerically produced systematic joint zones (Figure 2.25) controlled primarily by the sensitivity of the propagation velocity of the model fractures to the magnitude of the stress concentration.

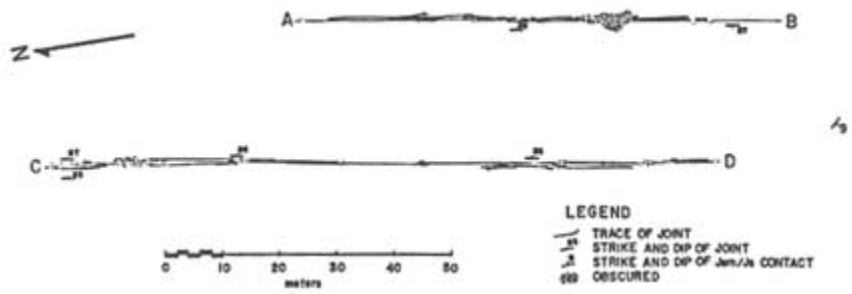

FIGURE 2.23 Zoned joints in sandstone. Note two zones each with about two parallel joint traces. From Dyer (1983).

It is difficult to test the dependence of zonal formation of joints on the fracture propagation velocity in natural conditions. However, data on the effects of fracturing rate on fracture localization are available from cooling joints. DeGraff and Aydin (1987) proposed that fan-shaped cooling fractures (Figure 2.26a, b) with much smaller spacings (compared to existing fractures) form when surface water infiltrates into growing fractures; the infiltration of water accelerates the rate of cooling, thermal stressing, and, consequently, fracturing.

Available knowledge of the geometry of, and mechanisms for, joint zones is inadequate. Because the contribution of fracture zones to the fluid flow in fractured rocks may be substantial. A better understanding of this subject is needed.

Fault Zones

Fault zones are invariably heterogeneous. Although commonly depicted as planar, most fault zones contain series of segments that are not coplanar (Scholz, 1990). Thus, the overall shape of a fault zone is somewhat irregular, and its thickness is variable. Both opening-mode and shearing-mode fractures are common in fault zones, and the orientation and distribution of these fractures are typically nonuniform. The composition of fault zones also can be heterogeneous, with blocks of sparsely fractured rock juxtaposed against lenses of gouge (mechanically and/or chemically altered fine-grained material). A variety of precipitated minerals is common in fractures and cavities along fault zones. The heterogeneous structure and composition of fault zones result in heterogeneous hydraulic properties (Caine et al., 1993; Forster et al., 1994).

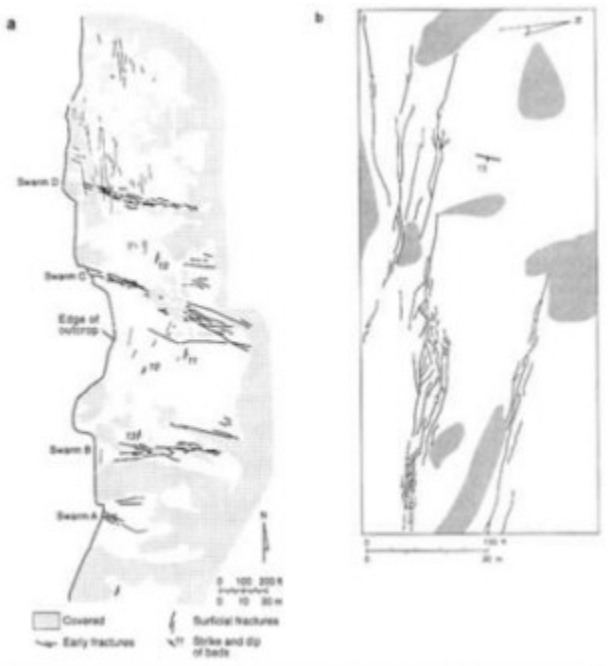

FIGURE 2.24 (a) Map showing patterns of joint swarms in sandstone. From Laubach (1991). (b) Details of swarm D in the map. From Laubach (1992).

We understand at a general level some causes of the heterogeneous structure of fault zones. Variations in the overall shape of a fault zone contribute to markedly heterogeneous stress fields along a fault zone (e.g., Segall and Pollard, 1980; Bilham and King, 1989), and this heterogeneity leads to a nonuniform fracture distribution. In addition, as stress fields change through time, fault zones can be reactivated and as a result develop increasingly intricate and varied distributions of fractures. The positions, orientations, and spacings of major slip surfaces in many fault zones are dictated largely by preexisting macroscopic flaws. Fault zones in sedimentary rocks commonly initiate and form along bedding planes (e.g., Boyer and Elliot, 1982). Fault zones in granites and metamorphic

rocks commonly form along preexisting planes of weakness such as compositional layering (Brown et al., 1989), metamorphic foliations (e.g., Choukrone and Gapais, 1983), joints (Segall and Pollard, 1983a,b; Martel et al., 1988), and dikes (Lisle, 1989; Martel and Peterson, 1991). Faults in the volcanic rocks of Yucca Mountain in Nevada appear to form along preexisting cooling joints (U.S. Geological Survey, 1984). Because macroscopic planes of weakness are inherent in most rock masses, they strongly influence how fault zones develop.

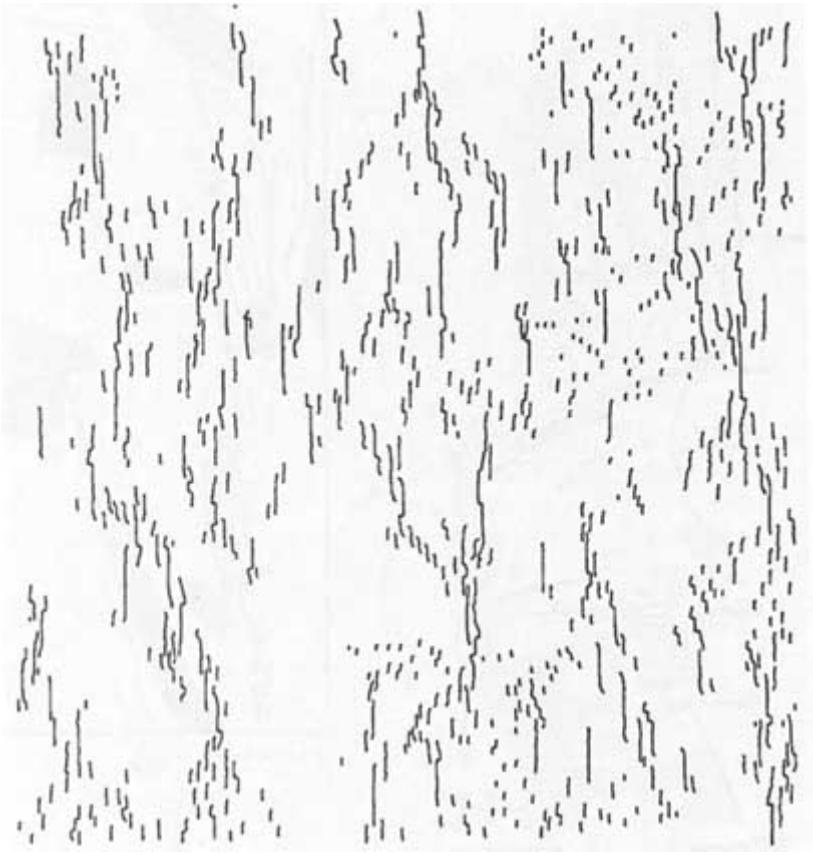

FIGURE 2.25 Numerically produced joint zone network. From Renshaw and Pollard (1994).

Fracturing along fault zones tends to evolve differently in different rock types. For example, fault zones in some sandstones develop by the sequential formation of closely spaced small faults (Figure 2.27a,b). The resulting fault zone can contain many small faults that collectively form a thick mass of crushed, low-permeability material (Aydin and Johnson, 1978; Antonellini and Aydin,

1994). A different style of fracturing has been documented (Martel et al., 1988) in some massive granitic rocks where fault zones formed as preexisting non-coplanar faults were linked by oblique fractures (Figure 2.28). A third style of fracturing has been documented in clay cakes deformed in the laboratory (Figure 2.29). The clay cake faults develop as a series of fractures form and then coalesce (Riedel, 1929; Wilcox et al., 1973); the resulting pattern resembles the fracture pattern observed along many natural faults (Skempton, 1966; Tchalenko, 1970; Wilcox et al., 1973). These findings collectively suggest that the grain-scale structure and lithology of rocks influences fault zone formation.

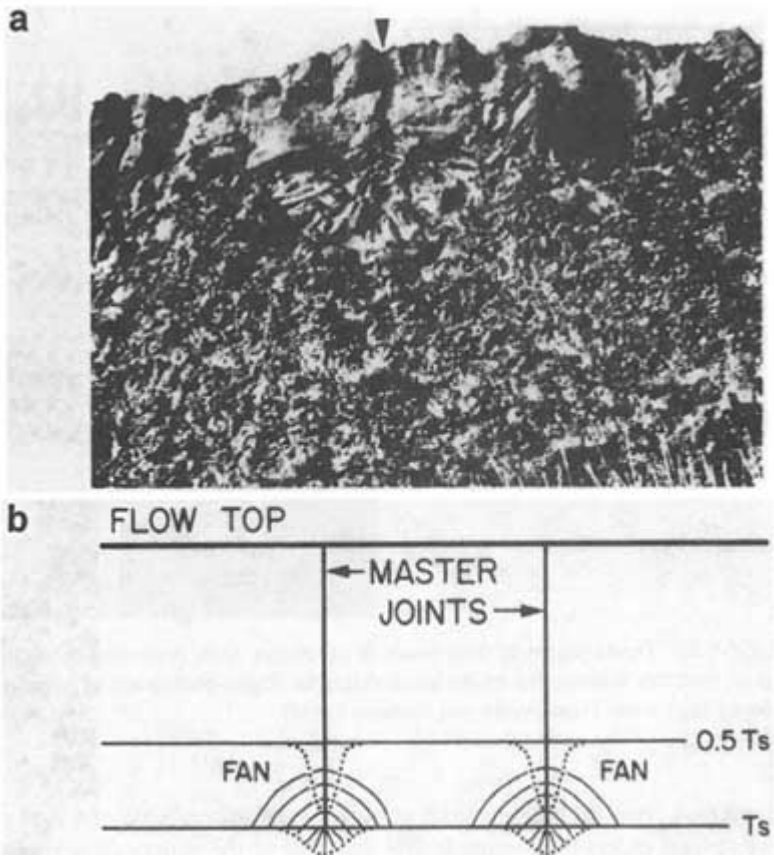

FIGURE 2.26 (a) Photograph of fan-shaped cooling joints in basaltic lava flow. (b) Schematic diagram showing joint formation by accelerated cooling, perhaps caused by additional surface water. From DeGraff and Aydin (1987).

The hydraulic properties of fault zones tend to vary with rock type, consistent with differences in the inherent macroscopic flaws and grain-scale fabrics in

different rock types. In highly porous sandstones the permeability of a fault zone can be several orders of magnitude less than that of the surrounding sandstone (Antonellini and Aydin, 1994). Nonconductive faults, also referred to as sealing faults, are widely recognized by the oil and gas industry to cause pronounced flow heterogeneities in porous clastic rocks. In contrast, in low porosity rocks the permeability of a fault zone tends to exceed the permeability of the host rock. For example, large-scale field tests (e.g., Black et al., 1990) demonstrate that the average hydraulic conductivity of fault zones in granitic rocks is three or four orders of magnitude higher than that in unfaulted granite and can approach the hydraulic conductivity of fine-grained sandstone. These conductivity contrasts can dominate the subsurface hydrology.

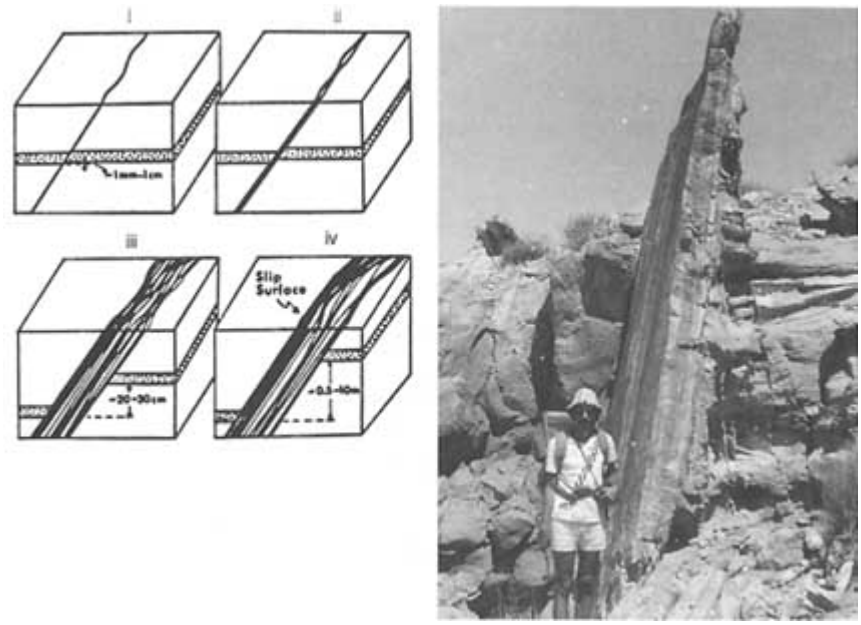

FIGURE 2.27 Development of fault zones in sandstone. Left, sequential development of a fault structure is illustrated by the block diagrams. Right, photograph of a fairly well-developed fault zone. From Aydin and Johnson (1978).

The hydraulic properties of an individual fault zone can vary significantly as a function of position along the zone. The distribution of fractures and fracture-filling materials are prime factors affecting hydraulic heterogeneity. Field measurements (e.g., Power et al., 1987) and laboratory tests (Tsang and Witherspoon, 1981) indicate that the conductivity of an individual slip surface will vary depending on the detailed shape of the surface and the magnitude of the local compressive stress acting across it.

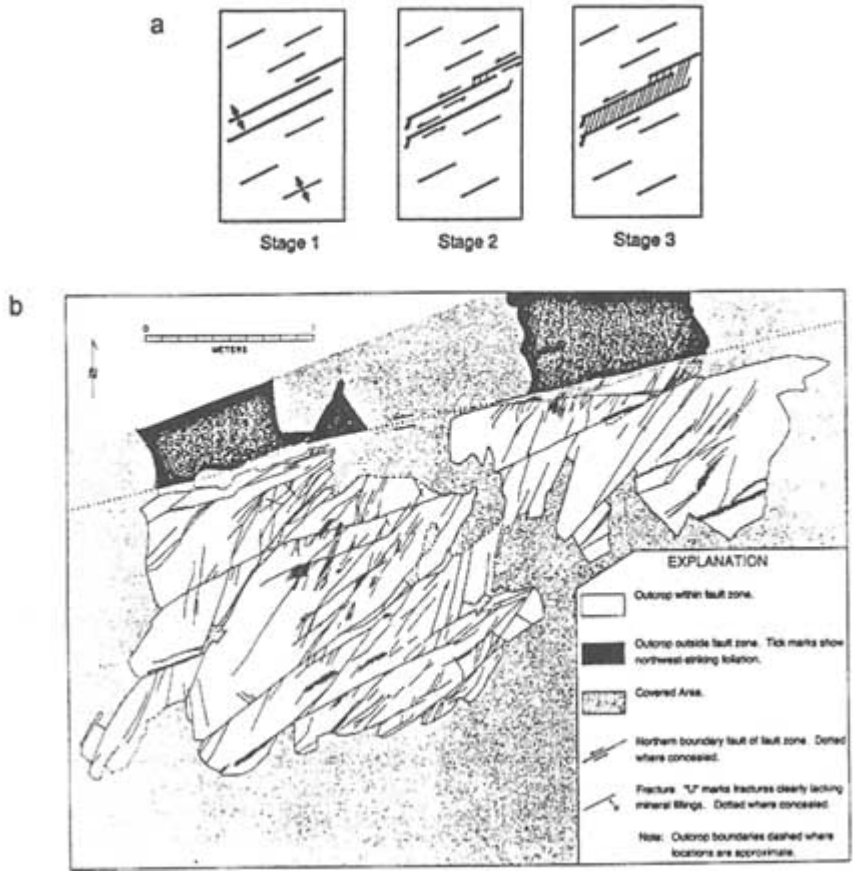

FIGURE 2.28 Development of fault zones in granitic rocks. (a) The structures and their sequential development in three stages. From Martel et al. (1988). (b) A well-developed fault zone and its internal fractures. From Martel (1990).

MULTIPLE SETS OF FRACTURES

The formation of one fracture set promotes and controls the initiation of additional sets by providing new stress concentrators and barriers for the deforming system in a changing stress regime. It is, therefore, not surprising that the occurrence of multiple sets of fractures is the rule rather than the exception. Patterns of multiple joint sets are markedly different from those of faults.

Multiple-Joint Patterns

The simplest multiple-joint patterns comprise two sets. Possible geometries for this case are shown schematically in Figure 2.30a-f. Where shorter and

discontinuous fractures about longer and more continuous fractures, the sequence of fracturing is generally easy to interpret; the shorter set formed after the longer set. In isotropic rocks, if the intersection angle is nonorthogonal, the second set formed under a different stress system, because joints form along a principal plane and, by definition, the principal planes are orthogonal for a given loading system. The two orthogonal sets may be formed simultaneously, however, because both orientations could lie in the principal planes. A situation in which one joint set crosses the other without any deflection or stepping is not possible if the older set was open at the time the younger set formed. However, such cross-cutting may occur in two cases: (1) when the first set is under a large normal compression, which results in a high resistance to slip in the plane of these fractures (Renshaw and Pollard, 1994), and (2) when the older fractures are filled with minerals during the younger propagation event and thus do not constitute void spaces. Two orthogonal joint sets are frequently observed in nature, but this pattern is but one of the many possible patterns.

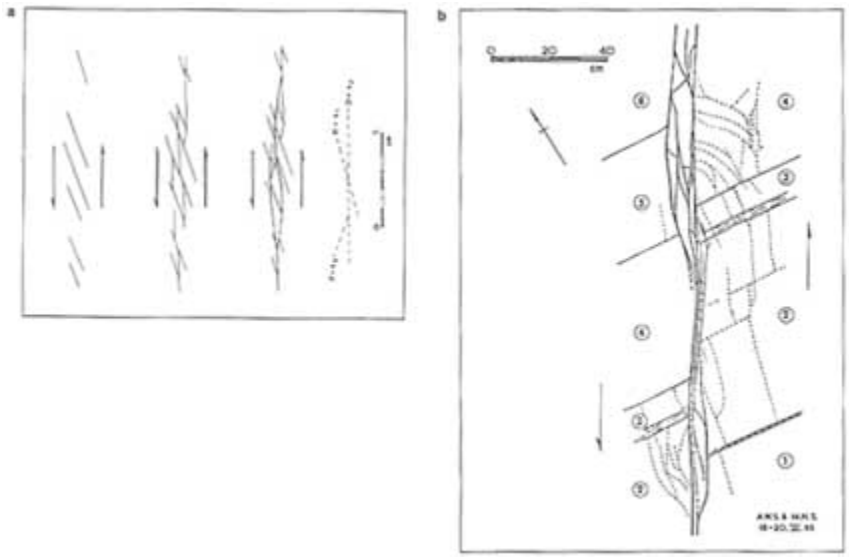

FIGURE 2.29 Development of fault zones in pelitic rocks. (a) Sequential development of structures in a clay cake. (b) A natural fault zone mapped in the field. From Skempton (1966).

Joint patterns comprising more than two sets also can exist. Perhaps the simplest of these is a polygonal pattern produced by shrinkage during cooling or drying processes (Figure 2.30i–j). These joints form sequentially in cooling lavas. They are initially four sided but evolve to yield a hexagonal pattern in the interior of a flow, where the thermal stress field is approximately homogeneous

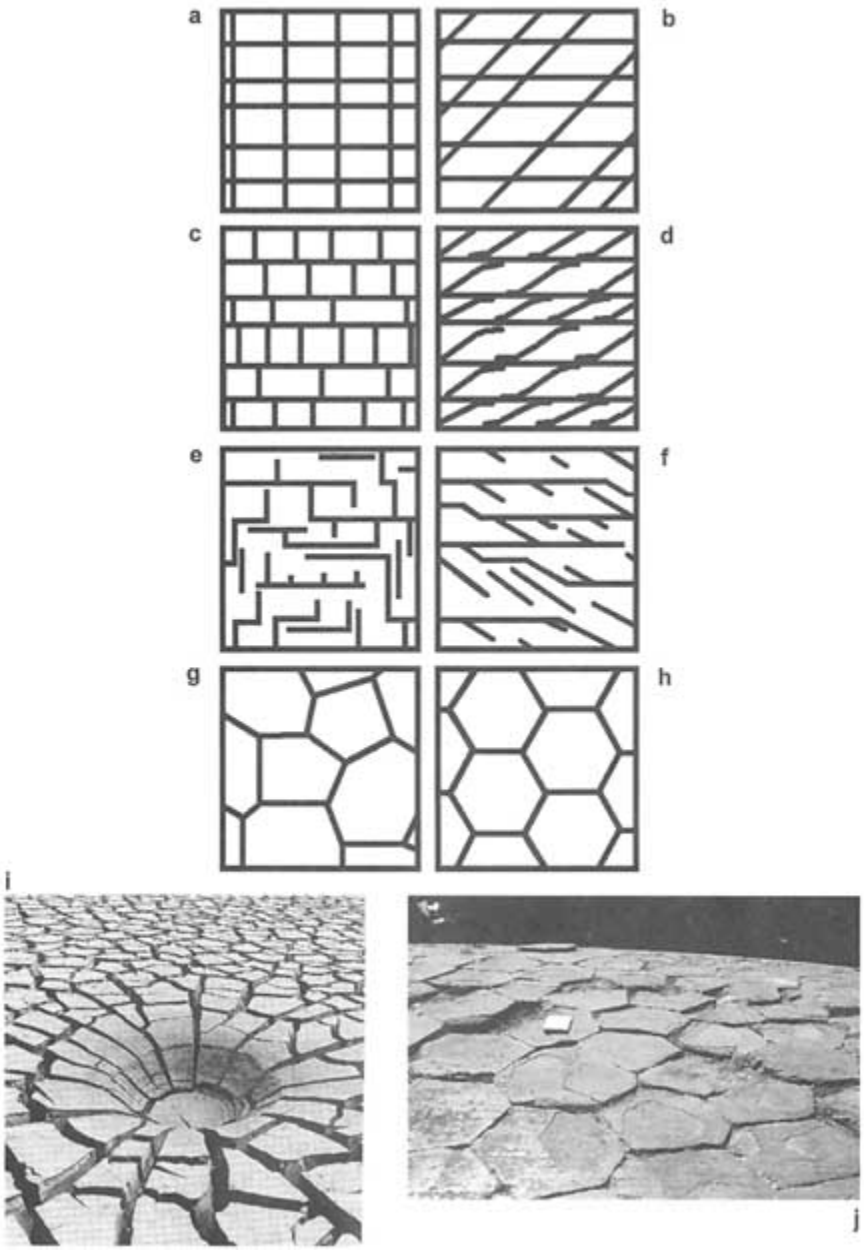

FIGURE 2.30 (a–h) Schematic illustration of major multiple-joint patterns. From Pollard and Aydin (1988). (a–f) Two joint sets with different intersection angles. (g–h) Polygonal joint patterns. (i–j) Polygonal fracture patterns in mud (from Birkeland and Larsen, 1989) and lava (from Aydin and DeGraff, 1988).

(Aydin and DeGraff, 1988). The size of hexagons and the spacing of joints are determined primarily by the rate of temperature change (DeGraff and Aydin, 1993). Because the top and bottom of a flow cool simultaneously but at different rates, joint spacing is different in the fractures formed by propagation from the top surface downward than in those formed by propagation from the bottom surface upward. These two "tiers" are commonly distinguishable. For flows with a thickness of less than several meters, one tier dominates the joint pattern (Figure 2.31a). Flows with moderate thickness (up to 40 m) have two tiers (Figure 2.31b); the upper tier or entablature has smaller and less regular spacing, with an implication of a greater hydraulic conductivity of the fracture system, whereas the lower tier or colonnade has wider and consistently regular spacing. Spacing evolves from narrower to wider as the fracture systems grow from the top and bottom surfaces (DeGraff and Aydin, 1993). Because fracture conductance is

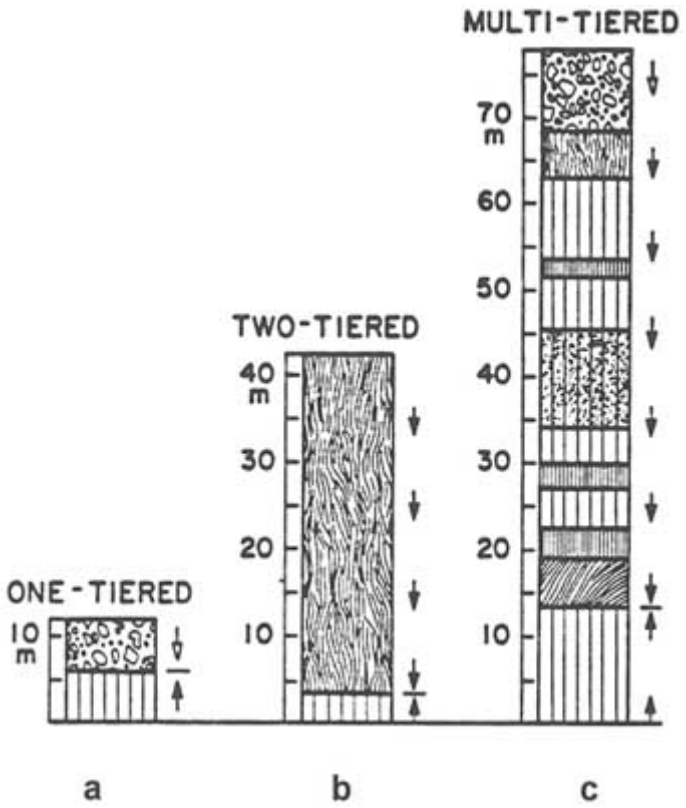

FIGURE 2.31 Fracture patterns in lava flows. From DeGraff (1987). (a) Thin flow with one-tiered columnar joints. (b) Two-tiered flow. (c) Multitiered flows. Arrows indicate vertical fracture propagation direction.

roughly proportional to the aperture cubed, a single fracture of aperture $2b$ is much more permeable than two fractures of aperture b. This, if the total fracture porosity is constant from the top to the bottom of a flow, the total hydraulic conductivity of the fracture system should increase from the top to the bottom. Other factors also affect the permeability of lava flows. The upper parts of many flows contain numerous vesicules formed by gas expansion during emplacement. These vesicules, if connected, will increase the hydraulic conductivity of the fracture system in the upper part of the flow (Wood and Fernandez, 1988) and possibly in the thin zone where the two tiers interact and meet. The intersection zone of the two-fracture system is schematically shown as a line in Figure 2.31b; however, in reality, this zone includes horizontal intersecting fractures. Some flows, especially those with greater thicknesses, are multitiered (Figure 2.31c). For multitiered flows the previous statements regarding joint spacing and the inferred relative conductivities of the uppermost and lowermost parts of the flow apply. However, the tiers in the inner parts of the flows may have variable joint spacings. Joint spacings in the inner parts of the flows are usually controlled by local environmental conditions, such as the availability of water cooling (Long and Wood, 1986; DeGraff et al., 1989). For multitiered flows the assessment of relative conductivities requires greater care.

Perhaps the most common environment for multiple-joint sets with more than two sets are terranes or plutons that have experienced multiple episodes of deformation (Spencer, 1959; Wise, 1964). It is difficult to identify a particular geometry for these occurrences, even though several have been suggested in the literature. Modeling fracture evolution in terranes with multiple deformation histories is hampered by the difficulty of determining proper boundary conditions and accounting for the possible effects of preexisting inhomogeneities.

Multiple-joint patterns may persist for several kilometers in the horizontal direction. In most cases, however, the orientations and angular relationships between joint sets change from one area to another, producing various domains with spatially distinctive patterns (Figure 2.32a) presumably related to the spatial and temporal inhomogeneities in the stress field during the development of fracture systems. In Figure 2.32b, which shows a fracture network in the Arches National Park, intersecting relationships suggest a progression of fracturing from the bottom right side to the top left side of the photograph. Based on the rule that opening fractures form perpendicular to the least principal stress, it can be inferred that the orientation of the least principal stress has changed, as shown schematically by the arrows in Figure 2.32c. The existence of several distinct joint domains on the flanks of a salt anticline in Arches National Park, Utah, indicates that such changes have occurred frequently there (Cruikshank and Aydin, 1995). It has been suggested that the diagenetic history of jointed rock also plays a role in sequential fracturing (Lorenz and Laubach, 1994).

There is evidence that joint orientation also changes vertically from one rock unit to another (Helgeson and Aydin, 1991; Figure 2.33). This makes it difficult

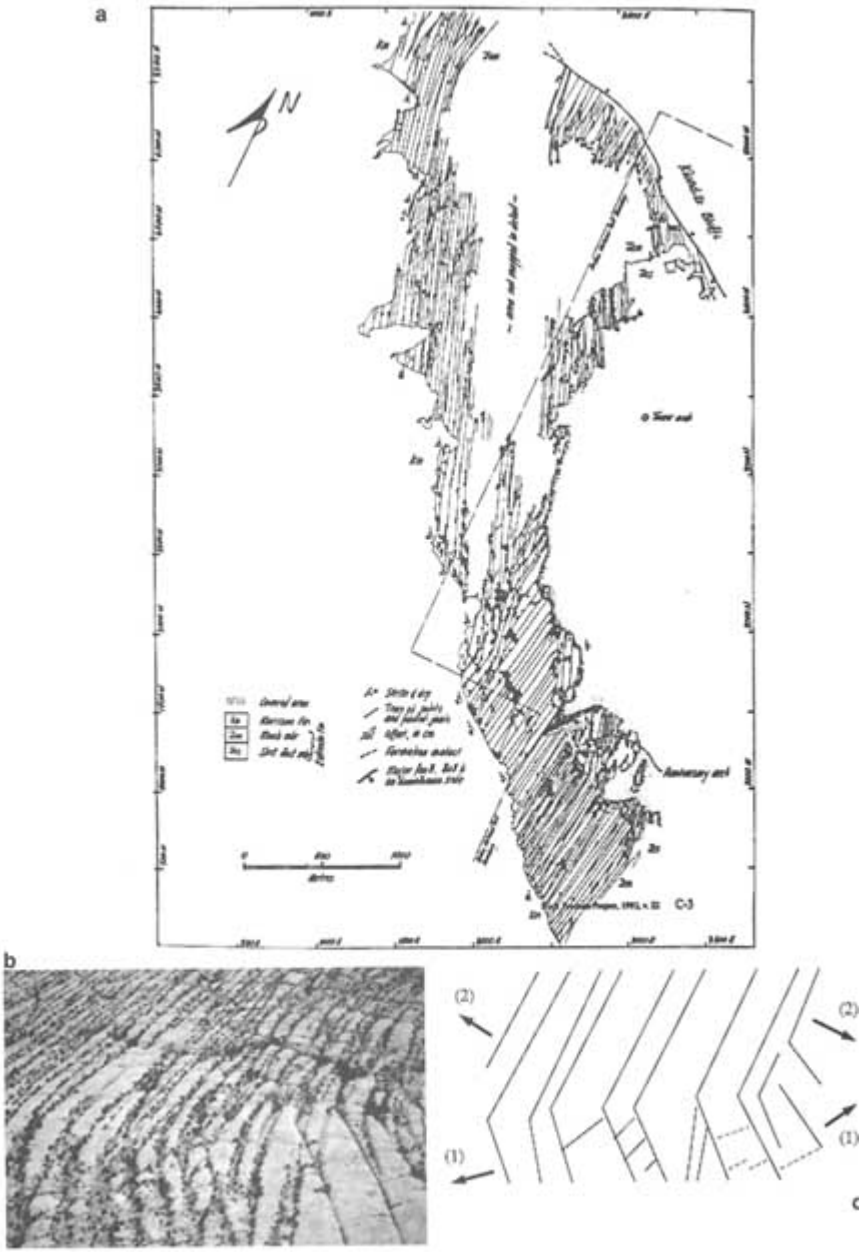

FIGURE 2.32 (a) Joint domains on the flanks of a salt anticline in the Arches National Park, Utah. From Cruikshank and Aydin (1995). (b) Photograph of two adjacent joint domains in the upper left part of the map. Photo by A. Aydin. (c) Two stress orientations (1 and 2) thought to be responsible for the systematic joint sets defining the two domains.

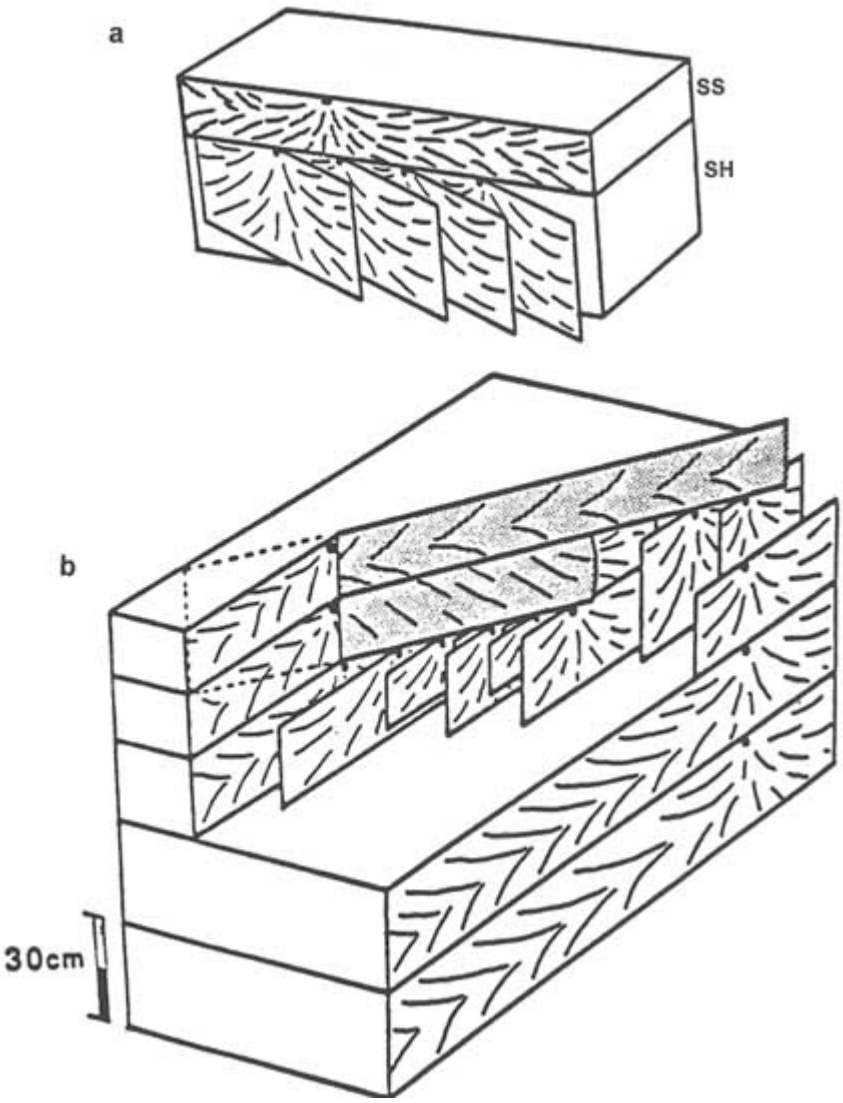

FIGURE 2.33 Block diagrams showing vertically changing joint orientation. From Helgeson and Aydin (1991). (a) Relatively simple system showing a new set of joints forming at the lower front of a previous joint. (b) A more complicated fracture evolution in which new joints initiate at the lower lateral fronts of the previous joints.

to project the orientation of a joint set at the surface to underlying units. It also reduces the vertical conductivity of joints because of the limited contact area among joints in different orientations.

One of the crucial tasks remaining for better understanding of multiple-joint patterns is the possible causes for changes in the orientation of joint sets to produce distinctive joint domains. A survey of fracture patterns in various sandstone formations of the Colorado Plateau and experimental simulation of the formation and geometric characteristics of fracture domains indicate that fracture domain boundaries provide the best fracture connectivity. Primary fracture sets with different orientations can be well connected there. Furthermore, secondary fracture sets usually are more closely spaced in the domain boundaries. Consequently, domain boundaries can be areas of enhanced hydraulic conductivity.

Multiple Fault Patterns

Faults show the most diversity of all the fracture patterns; consequently, they are poorly understood. The overview here describes a few of the most commonly observed fault patterns and the associated fracturing.

Normal Faults

In map view, normal faults appear either as parallel traces or as pairs of parallel traces with zigzag geometries (Figure 2.34a, b) corresponding to either plane strain or three-dimensional strain, respectively (Aydin and Reches, 1982; Reches, 1983). Figure 2.34c depicts fracture pattern in the Austin Chalk in Texas that appears to suggest plane-strain deformation because of the existence of two sets of normal faults. This concept of plane-strain deformation is probably applicable also to conjugate fault patterns of other major fault types.

Sand box and clay cake experiments are commonly used to simulate faulting (Riedel, 1929; Cloos, 1955; Naylor et al., 1986; McClay and Ellis, 1987). These experiments have been successful in reproducing patterns observed in nature (e.g., Figure 2.35a). They are also useful for visual demonstration of particular faulting styles and for testing the validity of certain boundary conditions and fault geometries. Numerical models also have been used to simulate normal fault geometries. Figure 2.35b illustrates a distinct element model developed by Saltzer (1992) and Saltzer and Pollard (1992) that accounts for the inhomogeneous and blocky nature of deforming rock. This model has promise for generating realistic normal fault patterns and for testing the role of boundary conditions in experimentally produced fault systems.

Listric faults (Figure 2.36) are intricate networks of normal faults that cut deep into the crust and decrease in dip with depth (Proffett and Dilles, 1984). The deep subhorizontal portion of a listric fault is commonly referred to as a detachment fault. Above the detachment fault is a series of steeply dipping faults

that define a series of wedge-shaped blocks (Xiao et al., 1991). The sizes of these blocks seem to be controlled by material properties and the forces driving the faulting. New sets of high-angle normal faults may be added to the system if the old ones rotate enough and become inactive (McKenzie and Jackson, 1986; Nur et al., 1986). Paleomagnetic techniques (Nur et al., 1986) have been used successfully to determine the amount of rotation in many regions. The magnitude of the rotation is controlled primarily by the amount of slip across the faults.

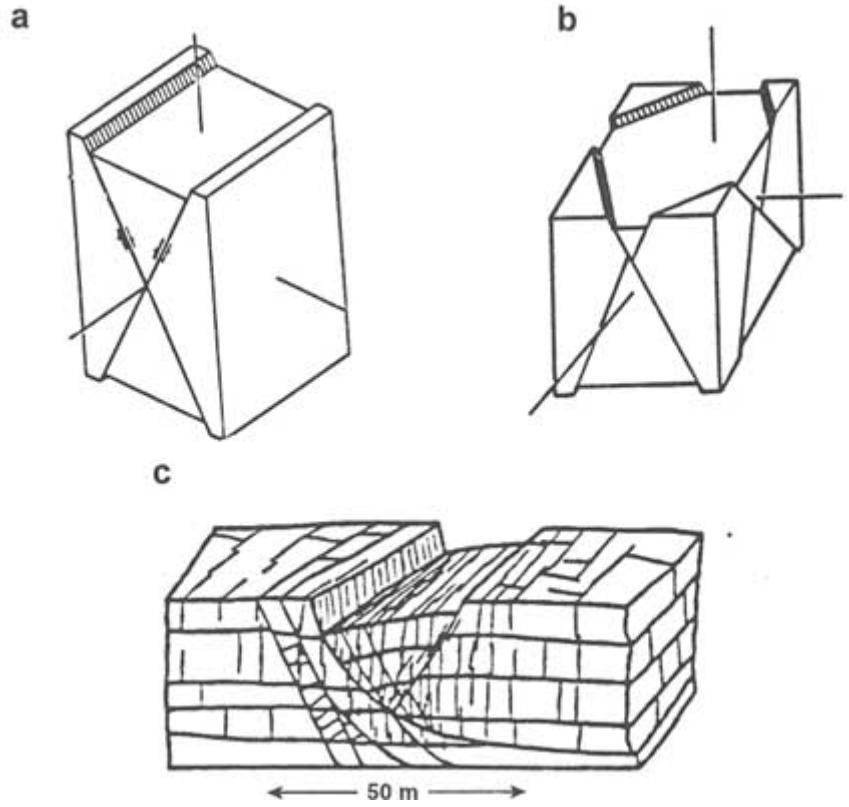

FIGURE 2.34 (a) Two sets of normal faults for plane-strain deformation. (b) Four sets of normal faults accommodating three-dimensional strain. (c) Fracture pattern that includes two sets of faults and one set of joints bisecting the fault sets in the Austin Chalk. Parts *a* and *b* from Reches (1983); (c) from Friedman and Wiltschko (1992).

The spacing of normal faults is more complex than that of joints. However, the thickness of the faulted unit is still an important factor; that is, larger spacing is expected for normal faults in thicker units (Mandl, 1988). Normal faults are commonly segmented like other fracture types and have complicated interaction features (Schwartz and Coppersmith, 1984; Wu and Bruhn, 1992; Antonellini,

1992). The nature of these geometries and the underlying mechanics of normal fault interaction are poorly known.

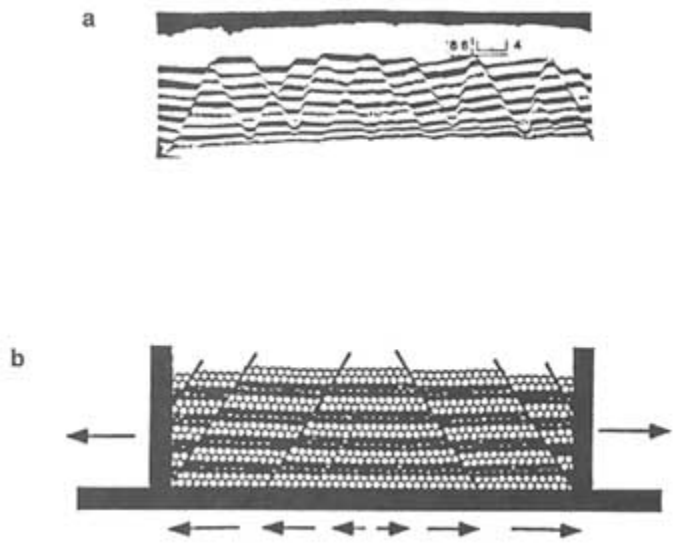

FIGURE 2.35 (a) A normal fault pattern produced experimentally in a sand box. From McClay and Ellis (1987). (b) A normal fault pattern produced by the distinct element model simulating the boundary conditions in the sand box experiment above. From Saltzer (1992).

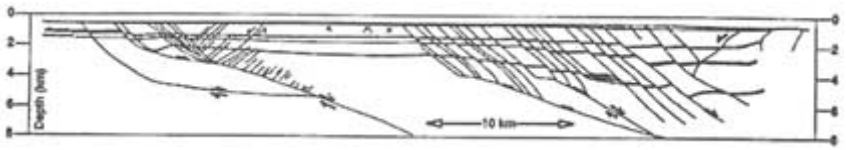

FIGURE 2.36 Normal fault patterns in cross section (seismic profile from Xiao et al., 1991).

Normal faults accommodate extension in the earth's crust. As a result, intuition suggests that there may be openings along normal fault systems that are greater than those of other fracture systems and that might be especially conductive, but these relationships have not been demonstrated. However, it has been suggested (Sibson, 1981; Moore and Vrolijk, 1992) that it is easier to have hydrofracturing in environments conducive to normal faulting.

Thrust Faults

The geometry of thrust faults also tends to be complex, especially as viewed in cross section perpendicular to a fault strike. Many thrust fault systems contain

a series of imbricate faults that merge into a subhorizontal fault at depth. The location of this deep subhorizontal detachment fault is usually controlled stratigraphically (Figure 2.37a). A thrust system commonly contains other stratigraphically controlled subhorizonal faults that are linked by more steeply inclined imbricate faults (e.g., lower-right portion of Figure 2.37a). This geometry has been detected in ancient as well as tectonically active environments (Figure 2.37b). The dip angle and perhaps the spacing of the major thrust faults are influenced by several parameters, including the friction coefficient and fluid pressure along the detachment faults and the fluid pressure in thrust sheets (Suppe, 1985).

The transport of fluids along the low-angle detachment zone, or decollement, and related imbricate faults has been demonstrated in submarine accretionary environments (see Moore and Vrolijk, 1992, for a review). It has been estimated that the velocity of channelized fluid flow along thrust faults in accretionary environments is three to four orders of magnitude faster than the flow through the matrix sediments. The hydrology of accretionary wedges has been modeled

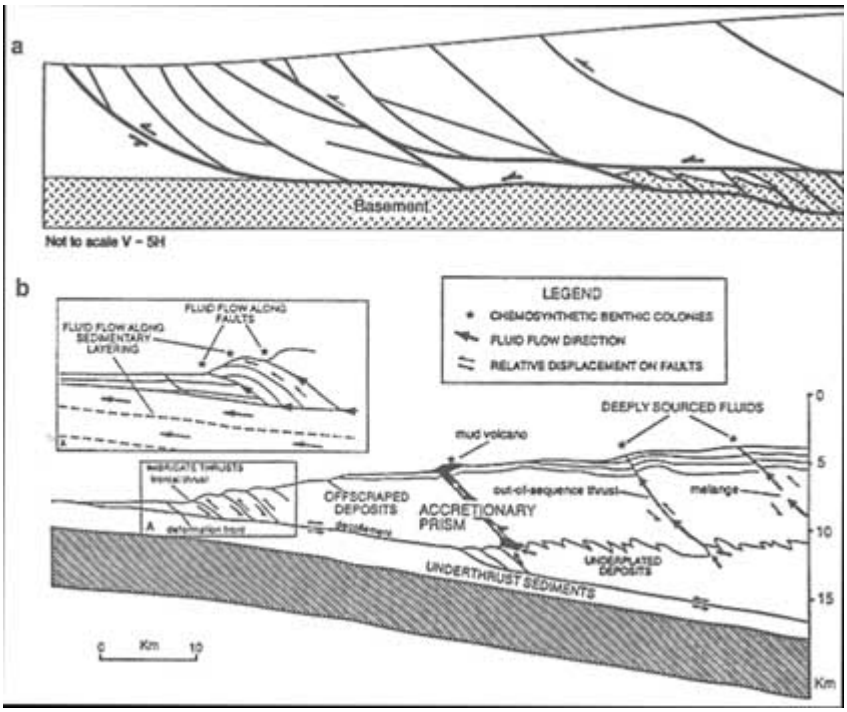

FIGURE 2.37 (a) An idealized pattern of thrust faults. From Boyer and Elliot (1982). (b) Idealized pattern of faults in an accretionary wedge and the pattern of fluid migration. From Moore and Vrolijk (1992).

numerically (Henry and Le Pichon, 1991; Henry and Wang, 1991). However, the details of fluid flow are poorly understood because fluid transport appears to be episodic and because the architecture of the fault zones and the fracture conductance distributions are not well known. Moore et al. (1988) suggested that fractures in the fault zones dilate episodically under high fluid pressure, producing an interconnected network responsible for fluid transport. Fluid transport can then cause the faults to seal, which allows the fluid pressure to build up and dilate the fault.

The geometry of the fractures in the wedges between the faults must be determined to understand the fracture distribution of a reservoir or aquifer in a thrust setting (Figures 2.36 and 2.37). At this scale, as pointed out by Price (1988), an ensemble of small-scale structures of various types, including deformed bedding planes, have complex geometric and temporal relationships. One example is a thrust sheet in the Appalachian Mountains where shearing and dilating fractures were mapped (Ohlmacher and Aydin, 1995; Figure 2.38). Small shearing fractures commonly occur subparallel to bedding interfaces, producing openings at the stepover areas known as pull-aparts (see Figure 2.21c). These openings are filled by minerals. Recurrent shear motions along the fractures reopen the fractures, and a new layer of mineralization is precipitated, which may be inferred as evidence of an episodic flow system. A network of veins or filled dilating fractures perpendicular to the shearing fractures (Figures 2.38a–d) also is common.

A similar structural assemblage is observed with intermediate-sized thrust faults that cut across bedding (Figures 2.38b, e) where offsets are several tens of meters. Normal and strike-slip faults may form at an oblique angle to low-angle thrust faults in larger-scale fault systems (Figure 2.38c, f). Different fracture networks develop for certain structural assemblages at different scales during deformation. An understanding of this hierarchy of the networks would be useful for efforts to understand larger fractures in thrust belts. Identifying other commonly occurring outcrop-scale patterns should improve the ability to visualize internal structures of aquifers, reservoirs, and waste disposal sites and to interpret the geophysical data discussed in Chapter 4 of this report.

Strike-Slip Faults

Strike-slip faults have some geometric similarities to joints. They are both usually vertical and form a series of parallel or subparallel traces with en-echelon geometry in map view. The spacing of the faults is not well understood, but crustal-scale examples suggest that it is somewhat related to the thickness of the faulted unit as it is for other fractures. Complexities in the geometries of strike-slip faults occur at bends along fault traces and at discontinuities between the fault segments. Complex faulting also occurs in the areas between parallel strike-slip faults.

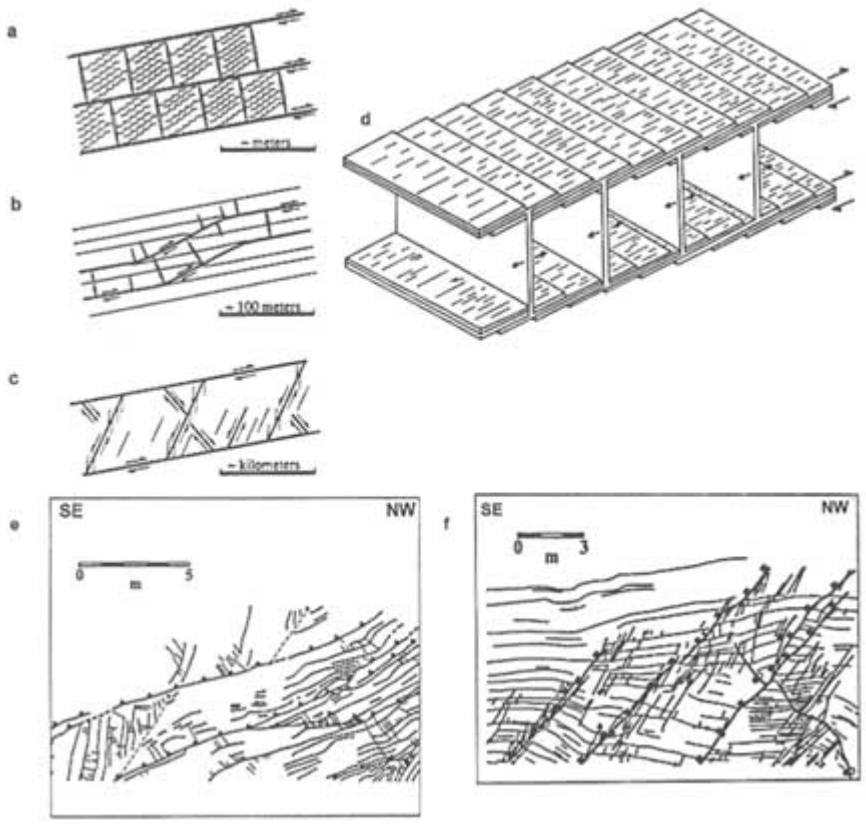

FIGURE 2.38 Fracture networks at different scales in a fold and thrust belts. From Ohlmacher and Aydin (1995). (a) Bedding interface faults and the connecting veins. (b) Intermediate-sized faults with offsets on the order of several meters cutting across bedding interfaces locally. (c) Large thrust faults with offsets larger than a few hundred meters forming a sheet deformed by a series of faults. (d) Array of en-echelon thrust faults at a low angle to the interfaces and veins perpendicular to the array; distance between parallel faults ranges from a few centimeters to several meters. (e) Map showing a thrust fault offsetting bedding and the axis of a syncline (dashed lines in the figure). (f) Map showing normal faults situated in a thrust sheet bounded by two thrust faults.

Interactions between en-echelon strike-slip faults produce a broad range of structures. These faults can be classified into two groups: those accommodating extension in extensional steps (Figure 2.39a) and those accommodating contraction in contractional steps (Figure 2.39b, c). Other examples with different modes of connecting fractures are provided in Figure 2.39c–e. The extensional steps and major overlapping faults are fluid pathways, as evidenced by the localization of veins, springs, and mud and magma volcanoes (Sibson, 1981; Aydin and Nur, 1982; Aydin et al., 1990).

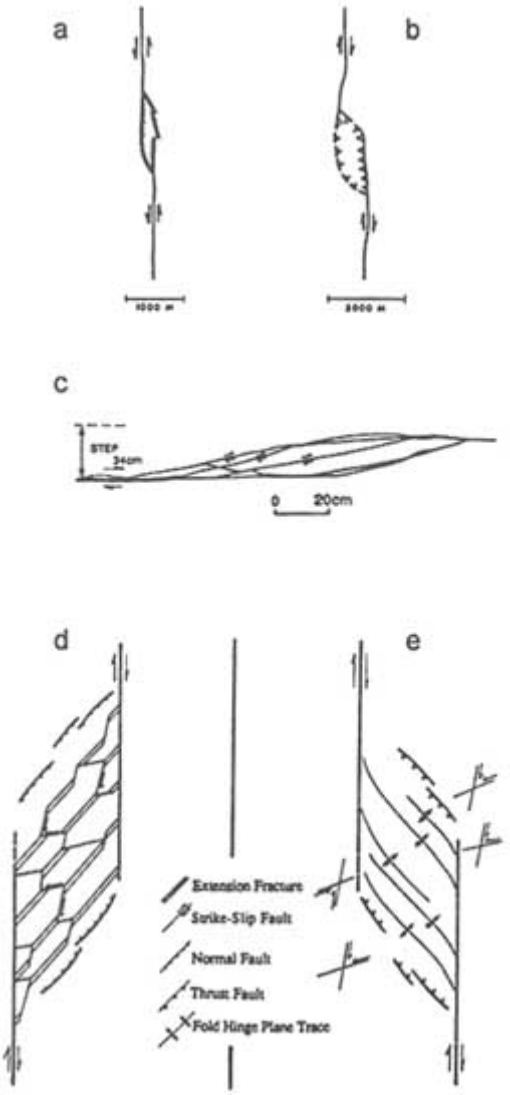

FIGURE 2.39 Examples of fault-interaction features in strike-slip faults. (a) Extensional step with connecting normal faults. From Aydin and Nur (1982). (b) Contractional step with connecting thrust faults. From Aydin and Nur (1982). (c) Contractional step with cross faults with the same kinematics as major en-echelon faults, right lateral strike-slip. From Cruikshank et al. (1991). (d) Extensional step. From Brown and Sibson (1989). (e) Contractional step. From Brown and Sibson (1989). Note the complex system of fractures proposed for the extensional step and a series of echelon folds observed in the contractional step.

Interactions between parallel strike-slip faults produce domains with characteristic fractures and faults. Figure 2.40a–c illustrates some outcrop-scale examples. Some additional examples are provided in Figure 2.41, where crustal-scale strike-slip faults occur in a variety of rock types. The map is a compilation showing fault patterns in the Greater San Francisco Bay Area. Some of the patterns attributed to fault interaction can be identified in this map. For example, the area between the Calaveras (CFZ) and the Hayward/Roger Creek (HFZ) faults is marked by an uplift, and the contractional structures are either subparallel or at an angle to the major strike-slip faults. Structures between parallel faults such as the San Andreas (SAFZ) and the San Gregorio-Hosgri (SG-HFZ) faults (Figure 2.41) are more complicated, but they can be considered a counterpart of the extensional structures between the parallel faults illustrated in Figure 2.40.

The mechanics of interaction and formation of structures associated with strike-slip stepovers have been studied by using two-dimensional models (e.g., Segall and Pollard, 1980). However, three-dimensional models will prove to be useful in addressing the change of the stress system and in predicting structures in the vertical dimension. This is particularly important because extensional steps may have significant fluid conductivity in the vertical direction. Together with field-based models, these numerical techniques are ripe for application.

SCALING UP FRACTURE PROPERTIES

As the foregoing discussion makes clear, fractures exist over a broad range of scales, from the scale of rock grains to the scale of tectonic plates. Intriguingly, fracture patterns at one scale are in many cases at least qualitatively similar to patterns at an entirely different scale (see, e.g., Figures 2.18, 2.20, 2.38, 2.39). The hierarchical similarities provide a rationale for extrapolating fracture pattern data from one scale, such as the scale of a borehole or outcrop, to another, such as that of a hydrocarbon reservoir. Fracture data generally are scaled up: details of fracture patterns are best resolved in small rock masses, yet the behavior of large rock masses is usually of greater interest.

Many investigators have examined how to quantitatively scale fracture data (e.g., LaPointe and Hudson, 1985; Turcotte, 1992; Cox and Wang, 1993; Gillespie et al., 1993; and references therein). Various fracture characteristics have been treated, such as trace length, orientation, spacing, clustering, surface roughness, and aperture. In addition to well-established geostatistical techniques based on semivariogram analysis (e.g., LaPointe and Hudson, 1985), the relatively new techniques of fractal analysis (Mandelbrot, 1982; Barton and Hsieh, 1989; Turcotte, 1992) have attracted considerable attention. In addition to quantitatively describing features that appear similar at different scales, fractal analyses are well suited to features that are in some way discontinuous; both factors make fractal analyses attractive in examining fractures. Fractal-like concepts have also been applied to the modeling of fluid flow in fractures (Barker, 1988).

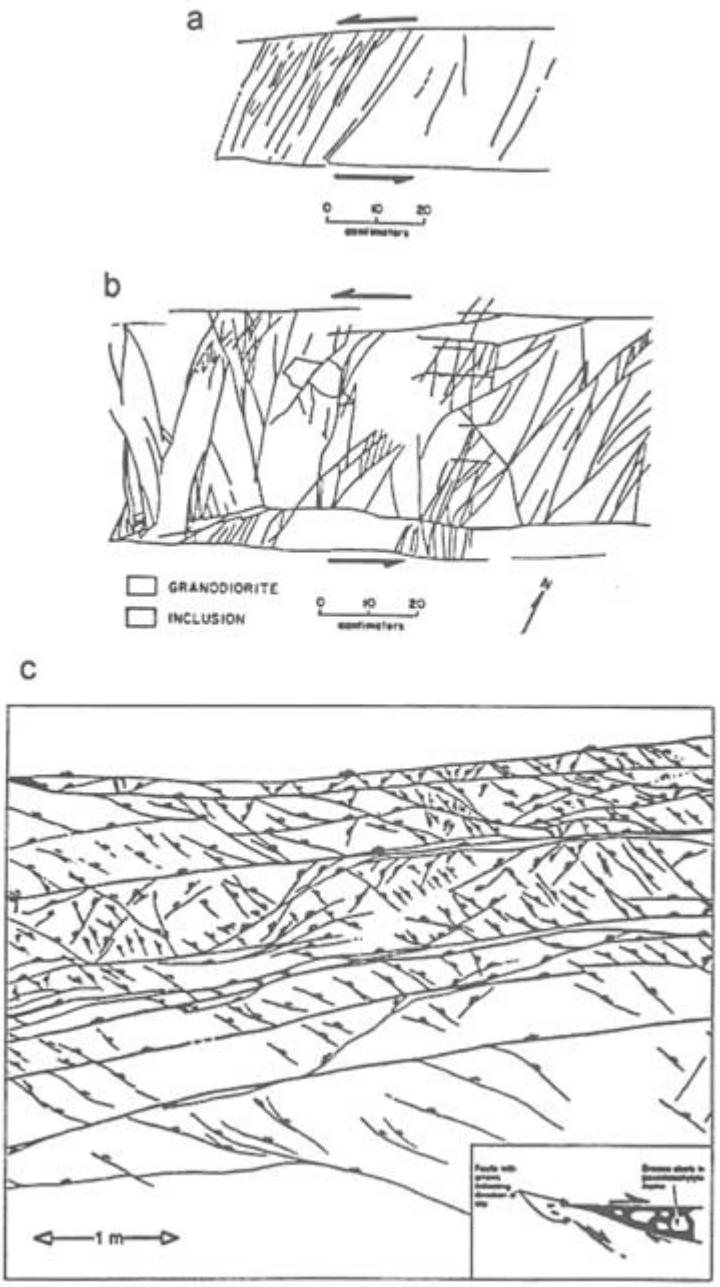

FIGURE 2.40 Structures between parallel strike-slip faults in crystalline rocks. Parts *a* and *b* from Segall and Pollard (1983b); (c) From Swanson (1992), unpublished map.

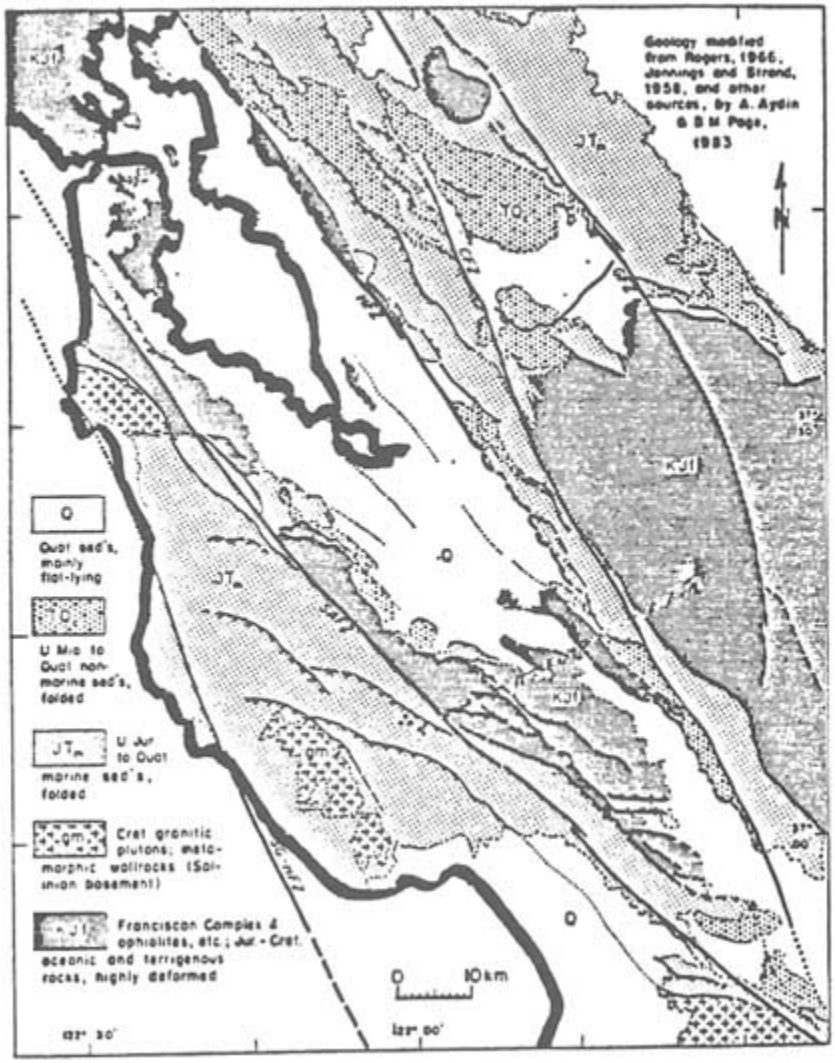

FIGURE 2.41 Geological map of the Greater San Francisco Bay Area (compiled by Aydin and Page, 1984) showing major strike-slip faults and their associated structures.

Fracture patterns typically have been described by using fractals in terms of the fractal dimension *D*, which quantifies the degree to which curves or surfaces fill space over a range of scales. Straight lines have a fractal dimension of 1, and planes have a fractal dimension of 2, but noninteger fractals are possible, too. Of the numerous applications of fractal analysis to fractures in rock (e.g., Scholz and Aviles, 1986; Power et al., 1987; Turcotte, 1992; Odling, 1992; Cox

and Wang, 1993; Gillespie et al., 1993), one of the most widely used is the box-counting method for determining the fractal dimension of fracture traces on a map (e.g., Barton and Hsieh, 1989). In this application a square mesh containing boxes of side length r is placed on a map of fracture traces, and the number of boxes N_r containing at least one fracture is tallied. This process is repeated for different mesh sizes, and log N_r is plotted against log (1/r). The spatial distribution of fracture traces is considered to have a unique fractal dimension D if the resulting plot is described well by a straight line of slope D (Figure 2.42). Not only can fracture trace lengths distributed according to a power law (e.g., Figure 2.15) be described with a constant fractal dimension (Gillespie et al., 1993), but fracture trace data collected at a variety of scales (Figure 2.42) have been fit by

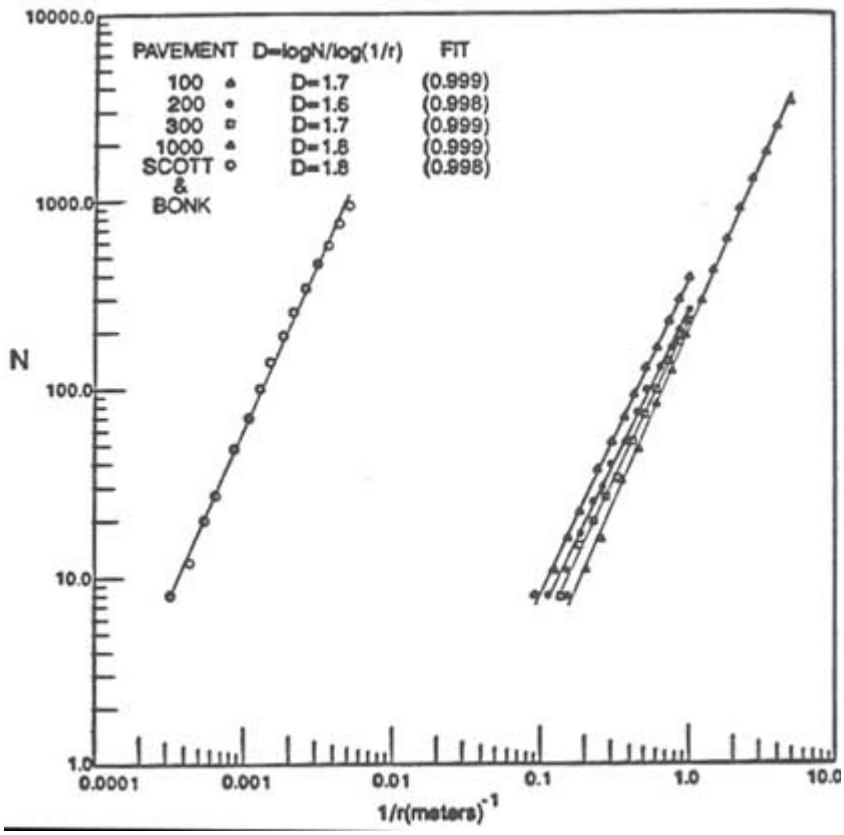

FIGURE 2.42 Fractal plots for fracture trace networks on pavements at Yucca Mountain, Nevada, mapped by Scott and Bonk (1984). The term N is the number of cells containing portions of at least one fracture trace, r is the length of a cell side in a given grid mesh, and D is the slope of the line on the plot of log N versus log (1/r). From Barton and Hsieh (1989).

a single fractal dimension (Barton and Hsieh, 1989). These findings suggest that fractal methods could be potent scaling tools.

Despite their potential power, however, the use of existing fractal methods to describe fracture patterns is still controversial for several reasons. For example, different fractal techniques generally give somewhat different fractal dimensions for a given data set (Cox and Wang, 1993). Even a single technique can yield different fractal dimensions. Box counting, for example, yields a fractal dimension that is sensitive to the orientation of the grid (Barton and Hsieh, 1989) and can change significantly with scale (Gillespie et al., 1993; Walsh and Watterson, 1993). There is also some debate as to the benefits of reducing to a single number the varied data on size distribution, orientation, linkage, spatial density, and roughness of natural fracture patterns (Gillespie et al., 1993). Perhaps one of the most problematic aspects of the technique is the difficulty in testing it rigorously. Cataloging all fractures of all scales in a large region is not feasible, and the individual fracture data sets used to calculate fractal dimensions usually span a scale range of no more than two orders of magnitude or so (e.g., Figure 2.42). Although individual data sets collected at different scales may appear to share a common fractal dimension, the collective data may not (Figure 2.43). For reasons such as these, many researchers still regard fractal analyses as experimental.

Proper scaling of the geometry and hydraulic properties of fractures remains a critical task. Current fractal methods may be useful for scaling certain fracture characteristics, but their use as rigorous quantitative tools is still controversial. Stochastic methods that blend aspects of deterministic mechanical methods and fractal scaling methods (Martel et al., 1991; see also Chapter 6) appear to be a promising avenue of research. Tests of fractal analyses on three-dimensional fracture data also will be enlightening.

IMPLICATIONS FOR FRACTURE NETWORK MODELS

All of the essential information about fractures should eventually be conceptualized in a model such as those discussed in Chapter 6 (Figures 6.11–6.14). This conceptualization should include the important variations for natural fractures. For example, since various fracture types have different flow properties, care should be taken in representing fracture types in models. Natural fractures have inhomogeneous distributions of densities and apertures, even along a single fracture. Fractures with the same fluid flow properties along their entire lengths, or large blocks of unfractured matrix between broadly spaced faults, probably do not exist (Nelson, 1987). Not all the natural fractures in a network are identical. Localized fracture zones are important and in some cases may provide almost all the yield, as illustrated in other chapters of this report. The behavior of the matrix at a fracture surface may be different from one fracture type to another and, for the same fracture type, from one rock type to another. Finally, the effects

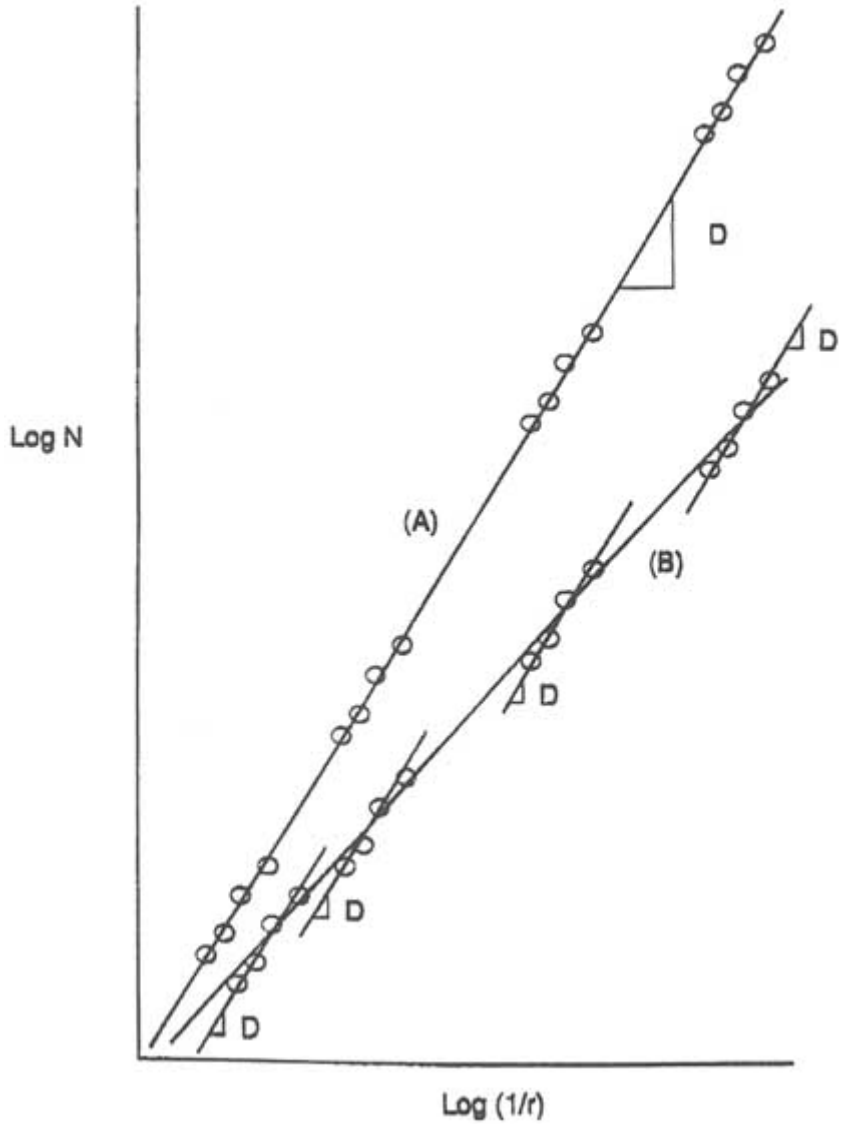

FIGURE 2.43 Hypothetical fractal dimension plots showing four sets of data collected at different scales. The slopes of the plotted curves give the fractal dimension *D*. (A) The fractal dimension is constant at all scales; all four data sets plot along a common line. (B) The fractal dimension changes as the scale changes; the four data sets plot along a gentle curve. In (B) each individual data set could be described well by a single common fractal dimension, yet the fractal dimension of the entire data collection is not constant. Courtesy of S. J. Martel.

of the present-day stress field on the opening of fracture sets should be taken into account.

It is quite clear that there is no single model that can represent all natural fracture network patterns and their flow properties. It is also clear that a better conceptual understanding of the geology, physics, and hydraulics of major fracture types is essential for a meaningful representation of fracture networks.

The spatial and temporal variations of fracture geometry in terms of the state of stress, fracture type, rock type, and scale pose many problems that need to be addressed in order to build useful models for simulating fluid flow in fractured media (see Chapter 6 for further discussion of this issue). Incorporating the most fundamental characteristics of fractures summarized in this chapter into conceptual models for fracture networks is an important first step.

Appendix 2.A

Diagenetic Enhancement Of Natural Fracture Permeability

The conventional rock mechanics model of natural fracture permeability is based on open channels between the asperities and mismatches between rough surfaces that create small voids through which fluid can flow (Figure 2.A1). However, in many rock masses, particularly hydrocarbon reservoirs, natural fractures do not possess the clean unaltered surfaces assumed in this conventional representation of fracture permeability; rather, they possess surfaces on which mineralization and dissolution have occurred. This alteration can range from growth of single crystals on fracture walls to total infilling of the fracture by mineral cements (Figure 2.A2) or, in soluble rocks such as carbonates, localized dissolution of the fracture walls.

The extent of any permeability enhancement resulting from diagenetic alteration of the fracture faces depends predominantly on the degree of alteration. Sporadic single crystals may not substantially influence the behavior of the fracture from that predicted by the surface roughness model, whereas localized clusters of mineralization can create crystalline bridges propping the fracture open (Figure 2.A1d and 2.A2b). In this way, highly conductive fluid pathways are created, with apertures of several millimeters even under high in situ stress

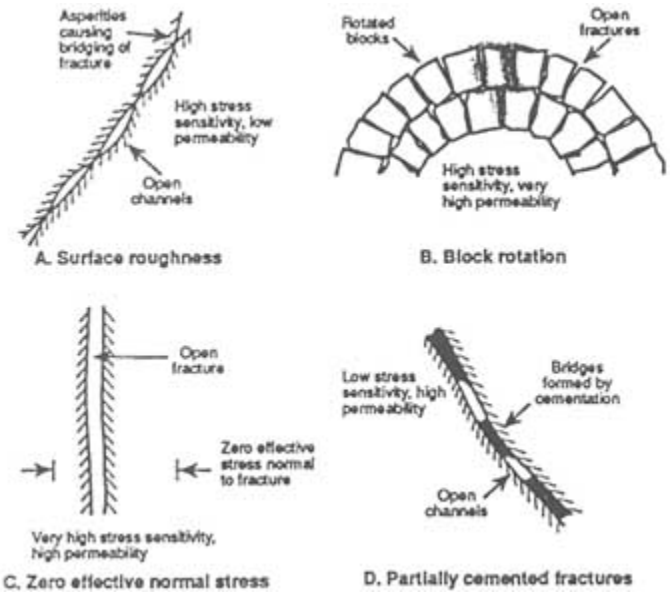

FIGURE 2.A1 Mechanisms promoting natural fracture permeability at depth. From Dyke (1996).

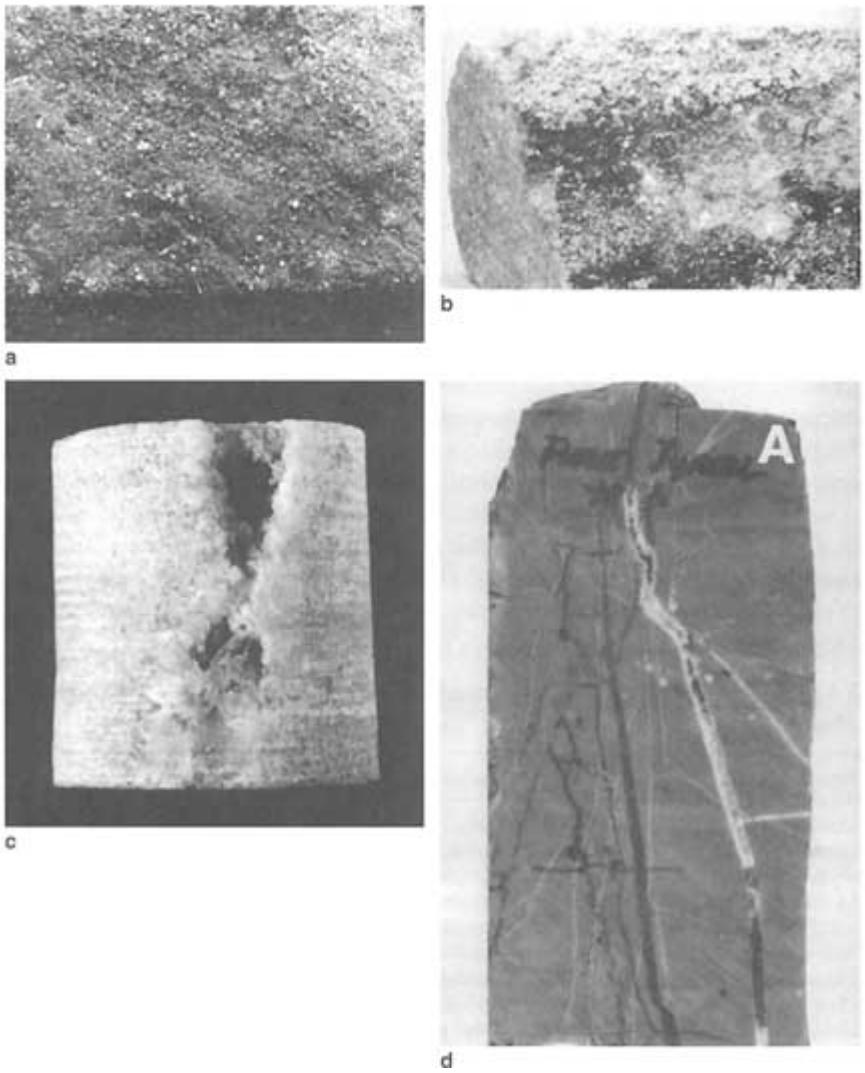

FIGURE 2.A2 Diagenetically modified natural fractures. (a) Sparsely distributed crystals of pyrite and calcite propping open a fracture in sandstone. (b) Euhedral and subhedral calcite crystals in a fracture in sandstone. The fracture face is stained by oil, which in turn is partly overlain by drilling mud. The euhedral crystals and mud invasion indicate substantial in situ apertures along discrete flow channels. (c) Calcite-lined flow channel in sandstone. Mud losses during drilling and high production indicate that this represents fracture permeability, not just unconnected porosity. Sample diameter is 1 in. (d) Partially and totally cemented fractures in dolomite. The dark staining in the open fracture is oil.

conditions. However, if mineralization proceeds to completion and the fracture is infilled, permeability can be destroyed rather than enhanced (Figure 2.A2d).

FRACTURE CHARACTERISTICS

Recognizing the existence of mineral cements and their influence on natural fracture permeability is not as easy as it might initially appear. Mineralization may be so subtle that fracture surfaces need to be examined with a microscope for it to be recognized (Kulander et al., 1990). In many cases a fracture is identified by way of the minerals decorating it, so incomplete mineralization causes some natural fractures in drill cores to go undetected. In addition, distinguishing between connected and unconnected void spaces in a heavily mineralized fracture in a drill core can be impossible because only a small portion of a fracture will be intersected by a drill core. Hence, core description can be regarded only as an indicator of fracture porosity rather than of fracture permeability.

Diagenesis enhances natural fracture permeability in a wide range of rocks (e.g., carbonate, clastic, metamorphic) and involves a wide range of mineral cements, including calcite, dolomite, ankerite, pyrite, iron hydroxide, and quartz (Table 2.A1). Well-formed (or euhedral) crystals generally grow in open fractures

TABLE 2.A1 Examples of Hydrocarbon Reservoirs Containing Partially Mineralized Fractures

Reservoir	Lithology	Fracture Description
Ekofisk, North Sea	Chalk	Partially mineralized tectonic and stylolitic fractures
Lisburne, Alaska	Limestone	Partial infill of calcite
W. Edmond, Oklahoma	Limestone	Occasional fractures partly sealed by recrystallization
La Paz, Venezuela	Limestone	Euhedral calcite covers walls of open fractures
Ain Zalah, Iraq	Limestone	Partially infilled fractures up to 0.75 in. (1.9 cm) wide
Beaver River, Canada	Dolomite	Fractures partially infilled with calcite
Ellenburger, Texas	Dolomite	Incomplete filling of interfragment pores by cement
Clear Fork, Texas	Dolomite	Partially filled fractures
Little Knife, N. Dakota	Carbonate	Small amounts of mineralization on fracture surfaces
Dnieper-Donets, Russia	Carbonate	Partially infilled with calcite, pyrite, and dolomite
Dagestan, Russia	Carbonate	Partially cemented with calcite and iron hydroxide
Oriskany, Pennsylvania	Sandstone	Open joint planes partly sealed by projecting crystals
Altamont-Bluebell, Utah	Sandstone	Quartz and calcite lining walls of open fractures
North Appleby, Texas	Sandstone	Delicate fracture lining and bridging material show that fracture was open in subsurface
Multiwell, Colorado	Sandstone	Crystal growth from the fracture wall is only partial
Pembina, Canada	Sandstone	Euhedral quartz lines opposing walls in open fractures
Big Sandy, Kentucky	Shale	Fracture planes often coated with crystalline dolomite, which may act as a proppant
Santa Maria, California	Chert/shale	Partially healed by secondary quartz
Lytton Springs, Texas	Serpentine	Intermittently locked together by cement

SOURCE: Dyke (1996).

(Figure 2.A2b), whereas subhedral and anhedral crystals develop as fractures become more completely sealed. Poorly formed crystals thus suggest lower permeability in a fracture (Figure 2.A2d). Additional examples of the effectiveness of mineral cements in "locking open" natural fractures and their range of morphological diversity are presented by Nelson (1985) and Laubach (1988).

INFLUENCE OF DIAGENESIS ON FRACTURE BEHAVIOR

Diagenetic modifications of natural fractures influence the way a fracture system will respond to changing fluid flow conditions. A small proportion of the fractures may dominate flow and be locked open at large apertures by stiff mineral cement bridges. These range in size from microscopic single crystals to polycrystalline bridges of large contact area. The magnitude of the influence of the diagenetic modification is related to the nature of these cement bridges.

INFLUENCE OF LARGE DRAWDOWNS ON FRACTURE PERMEABILITY

Natural fracture permeability is usually considered to be highly sensitive to an increase in the effective stress acting normal to the fracture. Many hydrocarbon reservoirs are subjected to massive decreases in pore pressure yet display no decrease in permeability during long-term production histories. Diagenetic modification may be one of several mechanisms that allow natural fractures to be relatively insensitive to changes in effective stress. Indeed, Morrow et al. (1990), in testing fractures partially infilled with calcite from the Multiwell Experiment, measured pressure sensitivities for fracture permeability that were in close agreement with the pressure sensitivity of the stiff matrix permeability.

Appendix 2.B

Fracture Patterns In Frontier Formation Sandstones, Southwestern Wyoming

It is known that fracture pattern controls fluid flow in fractured rocks. However, it is not usually possible to see the fracture pattern at depth. One approach to making inferences about the nature of fluid flow in rocks that cannot be seen is to be able to gain information about the fracture pattern from understanding how the fractures formed. Studies of fracture formation in areas where the fracture pattern is exposed can help in this regard. An example of such a study was carried out in the Frontier Formation sandstones of Western Wyoming.

The Upper Cretaceous Frontier Formation comprises alternating sandstone and shale that accumulated in the western part of the Cretaceous Western Interior Seaway, a foreland basin flanked to the west and southwest by the Cordilleran thrust belt. The Frontier Formation in southwestern Wyoming lies in the western part of the Green River Basin and is exposed in the limbs of an open, angular-hinged syncline above a thrust fault. The syncline, a north-trending, fault-bend fold produced during eastward transport of the thrust sheet, contains rocks that were displaced about 8 to 16 km east of their site of deposition.

Most fractures in these exposures are joints or veins oriented normal to bedding. Two prominent fracture sets are evident: north-striking fractures, which formed first, and east-striking fractures, which formed later, as evidenced by abutting and crossing relationships. Beneath veneers of vein-filling calcite, plume axes on fracture faces are parallel to bedding (paleohorizontal), consistent with fracture growth in flat-lying rocks. In many beds only north-striking fractures are present, whereas in other beds only east-striking fractures occur. Consequently, adjacent beds may contain only one or the other fracture set.

The Frontier Formation outcrops are along the leading eastern edge of the thrust belt. East-striking fractures formed after north-striking fractures, when compression related to mountain building was dominant in the foreland, but primarily before local folding and faulting. The convex salient in the foreland basin at this latitude may have accentuated the tendency to form fractures with generally eastward strikes.

Stretching during basin subsidence accounts for north-striking fractures, which parallel the depositional axis of the Cretaceous foredeep. As the basin subsided, strata were stretched east-west owing to lengthening parallel to bedding as the original nearly flat depositional surface adjusted to conform to the asymmetric basin profile. Petrogenetic evidence suggests that vein-filling minerals are contemporaneous with early Frontier Formation cements.

Attributes of the two fracture sets differ. Fractures formed during slow burial (north-striking fractures) are uniformly distributed and have a narrow range of trace lengths in beds of a given thickness and composition. Figure 2.B1 illustrates typical distributions and length patterns. Regionally, north-striking fractures have

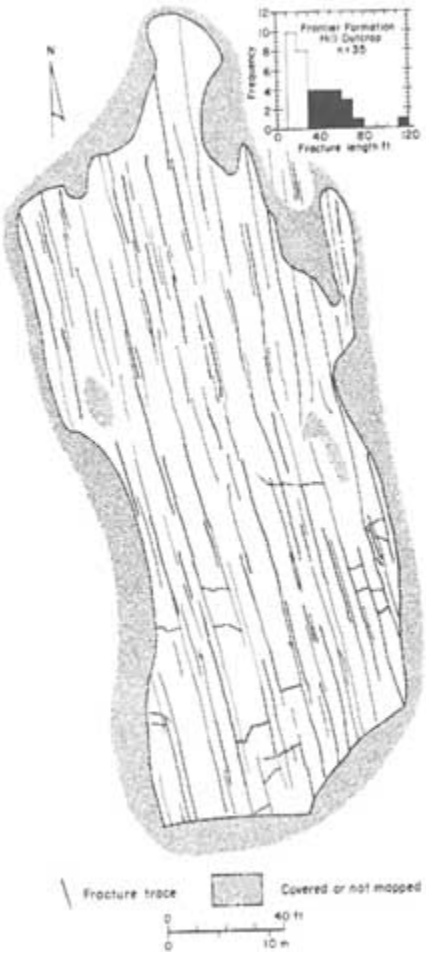

FIGURE 2.B1 Fractures formed during basin subsidence, illustrating evenly distributed, poorly interconnected fractures. Map of fracture traces on bedding plane, Little Coal Creek (Hill) outcrop, Wyoming (Sec. 31 T24N R115W). Fractures strike north-northwest, spacing is about 3 m, and variable line weight indicates relative fracture width. Disregarding fractures that do not have both ends of their traces exposed, fractures are 10 to 20 m long. Inset shows histogram of length distribution; fractures that end outside the outcrop have not been included, and that part of the distribution having numerous subsidiary fractures is shown with no pattern. From Laubach (1991).

spacings ranging from centimeters to several meters, but within an outcrop spacing generally varies by less than 30 percent of the average for that outcrop. Spacing is generally closer in thin beds and beds having extensive early cements. Contrasts in rock composition (including cement composition) and mechanically significant bed thickness can result in abrupt shifts in fracture intensity, but otherwise fractures typically are not clustered in swarms. These fractures also have a narrow range of lengths (Figure 2.B1). The distribution is even narrower if one excludes fractures less than 10 m long that are traces of hackles connected to larger fractures below the mapped surface. Here truncation effects arising from a lower cutoff in the size of mapped fracture are slight because there are few fractures mapped shorter than the measurement cutoff length of 1 m.

In contrast, the fracture set that formed during regional thrusting (east-striking fractures) is clustered into swarms containing fractures ranging widely in length (Figure 2.B2). Swarms of closely spaced fractures are typically elongated lenticular zones having widths that range from centimeters to more than 50 m. Across the margin of a swarm, fracture spacing may change abruptly from meters to centimeters. Some swarms are separated by rocks having no fractures. Other swarms are separated by areas of less closely spaced or less interconnected fractures; the swarms are not obviously periodic. Variable lengths of tectonic fractures are evident in Figure 2.B2. Exclusion of short fractures from this map introduces a significant bias; many small fractures both within and between swarms cannot be shown at this scale. Local measurements and large-scale fracture trace maps show that, locally, small fractures (centimeters to millimeters long) are abundant, and for this set the fracture length population may have a lognormal distribution.

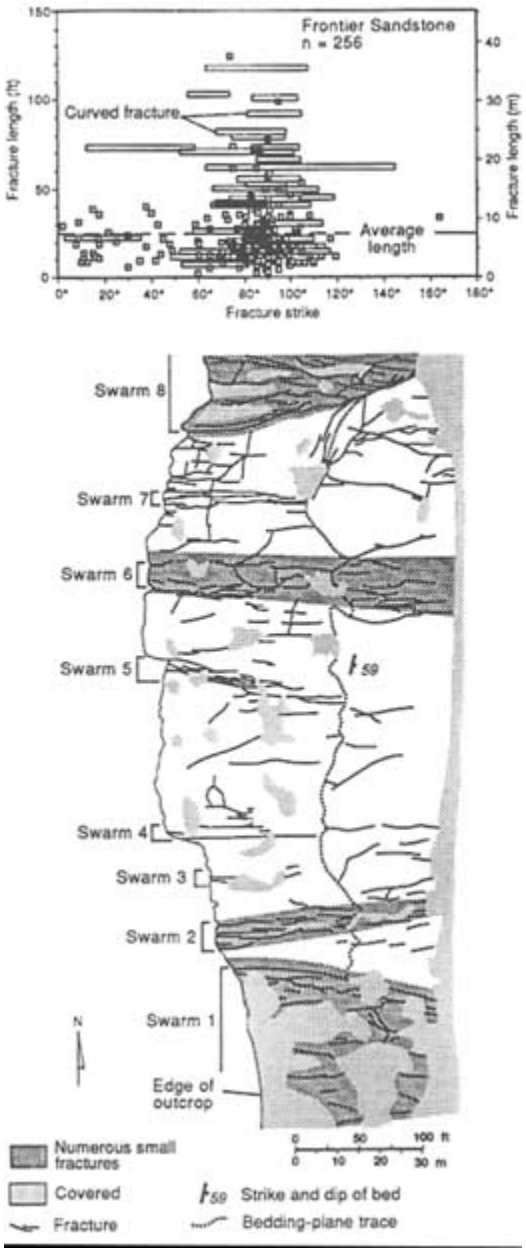

FIGURE 2.B2 East-striking fractures formed during thrusting, illustrating fracture swarms. Map of fracture traces in an outcrop in T24N R116W north of Kemmerer, Wyoming. Modified from Laubach (1992). Inset shows ranges of fracture lengths and strikes; fractures less than 1 m long are not included.

Appendix 2.C

Role Of Pore Fluids In The San Andreas Fault

Fundamental questions exist about the mechanics of deformation and slip in the San Andreas fault (SAF), such as: Why is the fault segmented at all scales into creeping and locked sections? What factors control the localization of deformation and the nucleation and recurrence of earthquakes? Why is the SAF weak both absolutely and in a relative sense compared with the adjacent plate interiors, as evidenced by heat flow measurements (Brune et al., 1969; Henyey and Wasserburg, 1971; Lachenbruch and Sass, 1973, 1980, 1992) and by apparent principal stress orientations in the adjacent plates (Mount and Suppe, 1987; Zoback et al., 1987; Oppenheimer et al., 1988; Wong, 1990)? The effective large-scale permeability of the fault zone and its adjacent country rock are key issues in the debate on the seismic behavior of the SAF.

Discovering the causes of the weakness of the SAF zone will perhaps be key to understanding the fundamental behavior of the system. Existing data (e.g., Healy and Zoback, 1988; Zoback and Healy, 1992) indicate that the frictional strength of the crust is generally consistent with the Mohr-Coulomb faulting theory, with friction coefficients in the range of 0.6 to 0.9 (from Byerlee's law). In contrast, the apparent low strength of the SAF would require a coefficient of friction of 0.1, yet the friction coefficient of even the weakest material envisioned to exist in the fault zone, montmorillonite gouge, is found to be no less than about 0.4 (Wang and Mao, 1979; Morrow et al., 1982, 1992). Furthermore, temperatures at seismogenic depths may too high to preserve this mineral. One favored alternative cause of the apparent low strength of the SAF is a very low effective stress in the fault zone caused by high fluid pore pressure.

Byerlee (1990) and Rice (1992) proposed models in which permanently high fluid pore pressure in the SAF zone can coexist with near-hydrostatic pressure in the adjacent country rock without causing hydrofracturing of the fault wall rocks. The models are identical mechanically but rely on different mechanisms to maintain the high pressure differential between the fault zone and the country rock. In Rice's model flow is allowed from the fault zone to the country rock, but the in-plane permeability of the fault zone is much higher than fault-perpendicular permeability, and the high pore pressure in the fault zone is maintained by fluid recharge from the lower crust at the root of the fault. In Byerlee's model the fault zone is sealed (i.e., there is zero effective cross-fault permeability). Fault zone fluids originally derived from the country rock are maintained at high pore pressure by compaction of fault zone materials during shearing.

Fournier (1990), Blanpied et al. (1992), Sibson (1992), Sleep and Blanpied (1992), Byerlee (1993), and Chester et al. (1993) have proposed mechanisms whereby intermittent high pore pressures are developed during the earthquake cycle by the formation of impermeable barriers through pressure-induced sealing and healing processes. Dynamic weakening mechanisms that act only during

rapid fault slip also have been proposed. These include transient high fluid pressure caused by shear heating during slip (Lachenbruch, 1980; Mase and Smith, 1987), reduction of normal stress accompanying the propagation of dilational waves along the fault (Brune, 1993), and acoustic fluidization of fault zone materials (Melosh, 1979). The latter two mechanisms do not require high fluid pressures. The critical factor in discriminating between Rice's fault-weakening model, Byerlee's (1990) model, and cyclic high pore pressure models is the origin of fault zone fluids and the hydrogeological connectivity between the fault zone and the country rock. Rice's model requires a deep crustal or upper-mantle source, whereas in the other models fluids are derived from the country rock.

REFERENCES

Antonellini, M. 1992. Geometry and distribution of deformation bands in porous sandstones, Delicate Arch area, Arches National Park, Utah. Pp. A1-A7 in the Rock Fracture Project, D. D. Pollard and A. Aydin, eds. Vol. 3. Stanford University, Stanford, Calif.

Antonellini, M., and A. Aydin. 1994. Effect of faulting on fluid flow in porous sandstones. Petrophysical Properties, American Association of Petroleum Geologists Bulletin , 78:355–377.

Antonellini, M. A., A. Aydin, and D. D. Pollard. 1994. Microstructure of deformation bands in porous sandstones at Arches National Park, Utah. Journal of Structural Geology, 16:941–959.

Aydin, A. 1978. Small faults formed as deformation bands in sandstone. Pure and Applied Geophysics, 116:913–930.

Aydin, A., and J. M. DeGraff. 1988. Evolution of polygonal fracture patterns in lava flows. Science, 239:471–476.

Aydin, A., and A. M. Johnson. 1978. Development of faults as zones of deformation bands and as slip surfaces in sandstone. Pure and Applied Geophysics, 116:931–942.

Aydin, A., and A. Nur. 1982. Evolution of pull-apart basins and their scale independence. Tectonics, 1:91–105.

Aydin, A., and B. Page. 1984. Diverse Pliocene-Quaternary tectonics in a transform environment, San Francisco Bay Region, California. Geological Society of America Bulletin, 95 (11):1303–1317.

Aydin, A., and Z. Reches. 1982. Number and orientation of fault sets in the field and in experiments. Geology, 10:107–112.

Aydin, A., and R. A. Schultz. 1990. Effect of mechanical interaction on the development of strike-slip faults with echelon patterns. Journal of Structural Geology, 12:123–129.

Aydin, A., R. A. Schultz, and D. Campagna. 1990. Fault-normal dilation in pull-apart basins: implications for the relationship between strike-slip faults and volcanic activity. Annales Tectonicae, IV:45–52.

Bahat, D. 1988. Fractographic determination of joint length distribution in chalk. Rock Mechanics and Rock Engineering, 21:79–94.

Bahat, D., and T. Engelder. 1984. Surface morphology on cross-fold joints of the Appalachian Plateau, New York and Pennsylvania. Tectonophysics, 104:299–313.

Barker, J. 1988. A generalized radial flow model for pumping tests in fractured rock. Water Resources Research, 24:1796–1804.

Barton, C. C. 1983. Systematic jointing in the Cardium Sandstone along the Bow River, Alberta, Canada. Ph.D. thesis, Yale University, 301 pp.

Barton, C. C., and P. A. Hsieh. 1989. Physical and Hydrologic-Flow Properties of Fractures. 28th International Geological Congress Field Trip Guidebook T385. P. 36. Washington, D.C.: American Geophysical Union.

Bates, R. L., and J. A. Jackson, eds. 1980. Glossary of Geology, 2d ed. Falls Church, Va.: American Geological Institute.

Bilham, R., and G. King. 1989. The morphology of strike-slip faults: examples from the San Andreas fault, California. Journal of Geophysical Research, 94:10,204–10,216.

Birkeland, P. W., and E. E. Larson. 1989. Putman's Geology, 5th ed. New York: Oxford University Press.

Black, J., O. Olsson, J. Gale, and D. Holmes. 1990. Site Characterization and Validation, Stage 4, Preliminary Assessment and Detail Predictions. Stripa Project Technical Report 91-08, Swedish Nuclear Fuel and Waste Management Company, Stockholm, p. 248.

Blanpied, M. L., D. A. Lockner, and J. D. Byerlee. 1992. An earthquake mechanism based on rapid sealing of faults. Nature, 358:574–576.

Borg, I. Y., and J. C. Maxwell. 1956. Interpretation of fabrics of experimentally deformed sands. American Journal of Science, 254:71–81.

Boyer, S. E., and D. Elliott. 1982. Thrust systems. American Association of Petroleum Geologists Bulletin, 66:1196–1230.

Brown, N. N., and R. H. Sibson. 1989. Structural geology of the Octillo Badlands antidilational fault jog, southern California. Pp. 94–109 in Fault Segmentation and Controls of Rupture Initiation and Termination. USGS Open-File Report 89-315, U.S. Geological Survey, Menlo Park, Calif.

Brown, A., N. M. Soonawala, R. A. Everitt, and D. C. Kamineni. 1989. Geology and geophysics of the Underground Research Laboratory site, Lac du Bonnet Batholith, Manitoba. Canadian Journal of Earth Sciences, 26:404–425.

Brune, J. N. 1993. Rupture mechanism and interface separation in foam rubber models of earthquakes: A possible solution to the heat flow paradox and the paradox of large overthrusts. Tectonophysics, 218(1–3):59–67.

Brune, J. N., T. L. Henyey, and R. F. Roy. 1969. Heat flow, stress, and the rate of slip along the San Andreas fault, California. Journal of Geophysical Research, 74:3821–3827.

Byerlee, J. 1990. Friction, overpressure and fault normal compression. Geophysics Research Letter, 17:2109-2112.

Byerlee, J. 1993. Model for episodic flow of high pressure water in fault zones before earthquakes. Geology, 21:303–306.

Caine, J. S., C. B. Forster, and J. P. Evans. 1993. A classification scheme for permeability structures in fault zones. Transactions of the American Geophysical Union, 74:677.

Chester, F. M., J. P. Evans, and R. L. Beigel. 1993. Internal structure and weakening mechanisms of the San Andreas fault. Journal of Geophysical Research, 98:771–786.

Choukrone, P., and D. Gapais. 1983. Strain pattern in the Aar granite (central Alps): orthogenesis developed by bulk flattening. Journal of Structural Geology, 5:411–418.

Cloos, E. 1955. Experimental analysis of fracture patterns. Geological Society of America Bulletin, 66:241–256.

Cox, B. L., and J. S. Y. Wang. 1993. Fractal surfaces: measurement and application in the earth sciences. Fractals, 1:87–115.

Cowie, P. A., and C. H. Scholz. 1992. Displacement-length relationship for faults: data analysis and discussion. Journal of Structural Geology, 14:1149–1156.

Cruikshank, K. M., and A. Aydin. 1994. Role of fracture localization in arch formation, Arches National Park, Utah. Geological Society of America Bulletin, 106:879–891.

Cruikshank, K. M., and A. Aydin. 1995. Unweaving the joints in Entrada Sandstone, southwest limb of the Salt Valley anticline, Arches National Park, Utah. Journal of Structural Geology, 17:409–421.

Cruikshank, K. M., G. Zhao, and A. M. Johnson. 1991. Duplex structures connecting fault segments in Entrada sandstone. Journal of Structural Geology, 13:1185–1196.

DeGraff, J. M. 1987. Mechanics of columnar joint formation in igneous rock. Ph.D. thesis, Purdue University, West Lafayette, Ind., p. 221.

DeGraff, J., and A. Aydin. 1987. Surface morphology of columnar joints and its significance to mechanics and direction of joint growth. Geological Society of America Bulletin, 99:605–617.

DeGraff, J. M., and A. Aydin. 1993. Effect of thermal regime on growth increments and spacing of contraction joints in basaltic lava. Journal of Geophysical Research, 98:6411–6430.

DeGraff, J. M., P. E. Long, and A. Aydin. 1989. Use of joint-growth directions and rock textures to infer thermal regimes during solidification of basaltic lava flows. Journal of Volcanology and Geothermal Research, 38:309–324.

Delaney, P. T., D. D. Pollard, J. I. Ziony, and E. H. McKee. 1986. Field relations between dikes and joints: emplacement processes and paleostress analysis. Journal of Geophysical Research, 91:4920–4938.

Dershowitz, W. S., and H. H. Einstein. 1988. Characterizing rock joint geometry with joint system models. Rock Mechanical Rock Engineering, 21(1):21–52.

Du, Y., and A. Aydin. 1991. Interaction of multiple cracks and formation of echelon crack arrays, International Journal of Numerical and Analytical Methods in Geomechanics, 15(3):205–218.

Dyer, J. R. 1983. Jointing in sandstones, Arches National Park, Utah. Ph.D. dissertation, Stanford University, Stanford, Calif., 202 pp.

Dyke, C.G. 1996. How sensitive is natural fracture permeability at depth to variation in effective stress? In Fractured and Jointed Rock Masses, Proceedings of the International ISRM Symposium on Fractured and Jointed Rock Masses. Rotterdam: A. A. Balkema.

Einstein, H. H., and W. S. Dershowitz. 1990. Tensile and shear fracturing in predominantly compressive stress fields—a review. Engineering Geology, 29:149–172.

Engelder, T. 1974. Cataclasis and the generation of fault gouge. Geological Society of America Bulletin, 85:1515–1522.

Engelder, T. 1987. Joints and shear fractures in rock. Pp. 27–69 in Fracture Mechanics of Rock, B. K. Atkinson, ed. New York: Academic Press.

Engelder, T., and P. Geiser. 1980. On the use of regional joint sets as trajectories of paleostress fields during the development of the Appalachian Plateau, New York. Journal of Geophysical Research, 85:6319–6341.

Engelder, T., and A. Lacazette. 1990. Natural hydraulic fracturing. Pp. 35-44 in Rock Joints, N. Barton and O. Stephansson, eds. Rotterdam: A. A. Balkema.

Fletcher, R. C., and D. D. Pollard. 1981. Anticrack model for pressure solution surface . Geology, 9:419–424.

Forster, C. B., J. V. Goddard, and J. P. Evans. 1994. Permeability structure of a thrust fault. Pp. 216–223 in The Mechanical Involvement of Fluids in Faulting, S. Hickman, R. L. Bruhn, and R. Sibson, eds. USGS Open File Report 94-228, U.S. Geological Survey, Menlo Park, Calif.

Fournier, R. L. 1990. A San Andreas Fault model in which maximum principal stress nearly normal to the fault is advantageous. EOS, Transactions of the American Geophysical Union, 71:1635.

Friedman, M., and D. M. Wiltschko. 1992. An approach to exploration for naturally fractured reservoirs—a generic approach with examples from the Austin Chalk. Pp. 143–153 in Geological Studies Relevant to Horizontal Drilling: Examples from Western North America, J. W. Schmoker, E. B. Coalson, and C. A. Brown, eds. Rocky Mountain Association of Geology, Denver, Colo.

Gallagher, J. J., M. Friedman, J. Handin, and G. M. Sowers. 1974. Experimental studies relating to microfracture in sandstone. Tectonophysics, 21:203–247.

Geyer, J. F., and S. Nemat-Nasser. 1982. Experimental investigation of thermally induced interacting cracks in brittle solids . International Journal of Solids and Structures, 18:344–356.

Gillespie, P. A., C. B. Howard, J. J. Walsh, and J. Watterson. 1993. Measurement and characterization of spatial distributions of fractures. Tectonophysics, 226:113–141.

Griffith, A. A. 1921. The phenomena of rupture and flow in solids. Royal Society of London Transactions, 221:163–198.

Healy, J. H., and M. D. Zoback. 1988. Hydraulic fracturing *in situ* stress measurements to 2.1 km depth at Cajon Pass, California. Geophysics Research Letter, 15:1005–1008.

Heffer, K. J., and T. G. Bevan. 1990. Scaling relationships in natural fracture: data, theory, and application. Society of Petroleum Engineers, Richardson, Tex.

Helgeson, D. E. 1990. Characteristics of joint propagation in layered sedimentary rocks. The Rock Fracture Project Workshop, 1:F1–F5. Stanford University, Stanford, Calif.

Helgeson, D. E., and A. Aydin. 1991. Characteristics of joint propagation across layer interfaces in sedimentary rocks. Journal of Structural Geology, 13:897–911.

Henry, P., and X. Le Pichon. 1991. Fluid flow along a decollement layer: a model applied to the 16 N section of the Barbados accretionary wedge. Journal of Geophysical Research, 96:6507–6528.

Henry, P., and C. Y. Wang. 1991. Modeling of fluid flow and pore pressure at the toe of Oregon and Barbados accretionary wedge. Journal of Geophysical Research, 96(20):109–120, 130.

Henyey, T. L., and G. J. Wasserburg. 1971. Water flow near major strike-slip faults in California. Journal of Geophysical Research, 76:7924–7946.

Hobbs, D. W. 1967. The formation of tension joints in sedimentary rocks: an explanation. Geological Magazine, 104:550–556.

Hodgson, R.A. 1961. Classification of structures on joint surfaces. American Journal of Science, 259:493–502.

Horii, H., and S. Nemat-Nasser. 1985. Compression-induced microcrack growth in brittle solids: axial splitting and shear failure, Journal of Geophysical Research, 90:3105–3125.

Hubbert, M. K. 1972. Natural and induced fracture orientation. American Association of Petroleum Geologists Memorandum , 18:235–238.

Inglis, C. E. 1913. Stresses in a plate due to the presence of cracks and sharp comers. Royal Institute of Naval Architects Transactions, 55:219–230.

Jamison, W. R., and D. W. Stearns. 1982. Tectonic deformation of Wingate Sandstone, Colorado National Monument. American Association of Petroleum Geologists Bulletin, 66:2584-2608.

Kulander, B. R., C. C. Barton, and S. L. Dean. 1979. The application of fractography to core and outcrop fracture investigations. METC/SP-79/3. Morgantown Energy Technology Center, Morgantown, W. Va., 174 pp.

Kulander, B. R., S. L. Dean, and B. J. Ward. 1990. Fractured core analysis: interpretation, logging, and use of natural and induced fractures in core. AAPG Methods in Exploration, No. 8, p. 88. American Association of Petroleum Geologists, Tulsa, Okla.

Lachenbruch, A. H. 1962. Mechanics of thermal contraction cracks and ice-wedge polygons in permafrost. Special Paper 70, Geological Society of America, Denver, Colo. 69 pp.

Lachenbruch, A. H. 1980. Frictional heating, fluid pressure, and resistance to fault motion. Journal of Geophysical Research, 85:6097-6112.

Lachenbruch, A. H., and J. H. Sass. 1973. Thermomechanical aspects of the San Andreas fault system. Pp. 192–205 in Proceedings of the Conference on Tectonic Problems of the San Andreas Fault System, R.L. Kovach and A. Nur, eds. Stanford University Publications in the Geological Sciences, vol. 13. Stanford University, Stanford, Calif.

Lachenbruch, A. H., and J. H. Sass. 1980. Heat flow and energetics of the San Andreas fault zone. Journal of Geophysical Research, 85:6185-6223.

Lachenbruch, A. H., and J. H. Sass. 1992. Heat flow from Cajon Pass, fault strength, and tectonic implications. Journal of Geophysical Research, 97:4995-5015.

Ladeira, F. L., and N. J. Price. 1981. Relationship between fracture spacing and bed thickness. Journal of Structural Geology, 3:179–183.

LaPointe, P. R., and J. A. Hudson. 1985. Characterization and interpretation of rock mass joint patterns. Special Paper 199, Geological Society of America, Denver, Colo., p. 37.

Laubach, S. E. 1988. Subsurface fractures and their relationship to stress history in East Texas basin sandstone. Tectonophysics, 156:37–49.

Laubach, S. E. 1991. Fracture patterns in low-permeability-sandstone gas reservoir rocks in the Rocky Mountain region. Pp. 501–510 in Proceedings, Joint Society of Petroleum Engineers Rocky Mountain Regional Meeting/Low-Permeability Reservoir Symposium. SPE Paper 21853, Society of Petroleum Engineers, Richardson, Tex.

Laubach, S. E. 1992. Fracture networks in selected Cretaceous sandstones of the Green River and San Juan basins, Wyoming, New Mexico, and Colorado. Pp. 61–73 in Geological Studies Relevant to Horizontal Drilling: Examples from Western North America, E. B. Coalson and C. A. Brown, eds. Rocky Mountain Association of Petroleum Geologists, Denver, Colo.

Lawn, B. R., and T. R. Wilshaw. 1975. Fracture of Brittle Solids. Cambridge: Cambridge University Press, 204 pp.

Lisle, R. J. 1989. Paleostress analysis from sheared dike sets. Geological Society of America Bulletin, 101:968–972.

Lockner, D. D., J. Byerlee, V. Kuksenko, A. Ponomarev, and A. Sidorin. 1992. Observations of quasistatic fault growth from acoustic emissions. Pp. 3–31 in Fault Mechanics and Transport Properties of Rocks, B. Evans and T. F. Wong, eds. New York: Academic Press.

Logan, J. M. 1992. The influence of fluid flow on the mechanical behavior of faults. Pp. 141–149 in Proceedings of the 33rd U. S. Symposium on Rock Mechanics, J. R. Tillerson and W. R. Wawersik, eds. Rotterdam: A. A. Balkema.

Long, P. E., and B. J. Wood. 1986. Structures, textures, and cooling histories of Columbia River basalt flows. Geological Society of America Bulletin, 97:1144–1155.

Lorenz, J. C., and S. E. Laubach. 1994. Description and interpretation of natural fracture patterns in sandstones of the Frontier Formation along the Hogsback, Southwestern Wyoming. Topical report to Gas Research Institute, GRI-94/0020, p. 89.

Mandelbrot, B. 1982. The Fractal Geometry of Nature. San Francisco: Freeman, 460 pp.

Mandl, G. 1988. Mechanics of Tectonic Faulting. New York: Elsevier, 408 pp.

Marrett, R., and R. W. Almendinger. 1991. Estimates of strain due to brittle faulting: Sampling of fault populations. Journal of Structural Geology, 31:735–738.

Martel, S. J. 1990. Formation of compound strike-slip fault zones, Mount Abbot quadrangle, California. Journal of Structural Geology, 12:869–882.

Martel, S. J., and J. E. Peterson, Jr. 1991. Interdisciplinary characterization of fracture systems at the US/BK site, Grimsel Laboratory, Switzerland. International Journal of Rock Mechanics and Mining Science and Geomechanical Abstracts, 28:259–323.

Martel, S. J., D. D. Pollard, and P. Segall. 1988. Development of simple strike-slip fault zones in granitic rock, Mount Abbot quadrangle, Sierra Nevada, California. Geological Society of America Bulletin, 99:1451–1465.

Martel, S. J., K. Hestir, and J. C. S. Long. 1991. Generation of fracture patterns using self-similar iterated function system concepts. 1990 Annual Report, Earth Sciences Division, Lawrence Berkeley Laboratory, Berkeley, Calif., pp. 52–56.

Mase, C. W., and L. Smith. 1987. Effects of frictional heating on the thermal, hydrologic, and mechanical response of a fault. Journal of Geophysical Research, 92:6249–6272.

McClay, K. R., and P. G. Ellis. 1987. Geometries of extensional fault systems developed in model experiments. Geology, 15:341–344.

McKenzie, D., and J. A. Jackson. 1986. A block model of distributed deformation by faulting. Journal of the Geological Society of London, 143:349–353.

Melosh, H. J. 1979. Acoustic fluidization: a new geological process? Journal of Geophysical Research, 84:7513–7520.

Moore, J. C., and P. Vrolijk. 1992. Fluids in accretionary prisms. Reviews of Geophysics, 30:113–135.

Moore, J. C., and others. 1988. Tectonics and hydrogeology of the northern Barbados Ridge: Results from Ocean Drilling Program leg 110. Geological Society of America Bulletin, 100:1578–1593.

Morrow, C. A., L. Q. Shi, and J. Byerlee. 1982. Strain hardening and strength of clay-rich fault gouges. Journal of Geophysical Research, 87:6771–6780.

Morrow, C. A., B. Radney, and J. Byerlee. 1992. Frictional strength and the effective pressure law of montmorillonite and illite clays. Pp. 69–88 in Earthquake Mechanics and the Transport Properties of Rocks, B. Evans and T.F. Wong, eds. London: Academic Press.

Morrow, N. R., K. R. Brower, S. Ma, and J. S. Buckley. 1990. Fluid flow in healed tectonic fractures. Journal of Petroleum Technology, 1310–1318.

Mount, V. S., and J. Suppe. 1987. State of stress near the San Andreas fault: Implications for wrench tectonics. Geology, 15:1143–1146.

Narr, W., and J. Suppe. 1991. Joint spacing in sedimentary rocks. Journal of Structural Geology, 13:1037–1048.

Naylor, M. A., G. Mandl, and C. H. K. Sijpesteijn. 1986. Fault geometries in basement-induced wrench faulting under different initial stress states. Journal of Structural Geology, 8:737–752.

Nelson R. A. 1985. Geologic Analysis of Naturally Fractured Reservoirs. Houston, Tex.: Gulf Publishing, 320 pp.

Nelson, R. A. 1987. Fractured reservoirs: turning knowledge into practice. Journal of Petroleum Technology, 39:407–414.

Nickelsen, R. P., and V. N. D. Hough. 1967. Jointing in the Appalachian Plateau of Pennsylvania. Geological Society of America Bulletin, 78:609–629.

Nur, A. 1982. The origin of tensile fracture lineaments. Journal of Structural Geology, 4:31–40.

Nur, A., H. Ron, and O. Scotti. 1986. Fault mechanics and kinematics of block rotation. Geology, 14:746–749.

Odling, N. E. 1992. Network properties of a two-dimensional nature fracture pattern. Pure and Applied Geophysics, 138:95–114.

Ohlmacher, G. C. 1991. Mechanics of vein, fault, and solution surface formation in Bays Mountain, southern Appalachians. Ph.D. thesis, Purdue University, West Lafayette, Ind., 210 pp.

Ohlmacher, G., and A. Aydin. 1995. Progressive deformation in the Bays Mountain Syncline, Kingsport, TN. American Journal of Science, 295:943–987.

Olson, J. 1990. Fracture mechanics analysis of joints and veins. Ph.D. dissertation, Stanford University, Stanford, Calif., 174 pp.

Olson, J., and D. D. Pollard. 1989. Inferring paleostress from natural fracture patterns: a new method. Geology, 17:345–348.

Olson, J. E., and D. D. Pollard. 1991. The initiation and growth of en-echelon veins. Journal of Structural Geology, 13:595–608.

Oppenheimer, D. H., P. A. Reasenberg, and R. W. Simpson. 1988. Fault plane solutions for the 1984 Morgan Hill, California earthquake sequence: Evidence for the state of stress on the Calaveras fault. Journal of Geophysical Research, 93:9007–9026.

Patterson, M. S. 1958. Experimental deformation and faulting in Wombeyan marble. Geological Society of America Bulletin, 69:465–476.

Peng, S., and A. M. Johnson. 1972. Crack growth and faulting in cylindrical specimens of Chelmsford granite. International Journal of Rock Mechanics and Mining Science, 9:37–86.

Pittman, E. D. 1981. Effect of fault-granulation on porosity and permeability of quartz sandstones, Simpson Group (Ordovician), Oklahoma. Bulletin of the American Association of Petroleum Geology, 65:2381–2387.

Pollard, D. D., and A. Aydin. 1984. Propagation and linkage of oceanic ridge segments. Journal of Geophysical Research, 89:10,017–10,028.

Pollard, D. D., and A. Aydin. 1988. Progress in understanding jointing over the past century. Geological Society of America Bulletin, 100:1181–1204.

Pollard, D. D., and P. Segall. 1987. Theoretical displacements and stresses near fractures in rock: with applications of faults, joints, veins, dikes, and solution surfaces. Pp. 277–349 in Fracture Mechanics of Rock, B. K. Atkinson, ed. London: Academic Press.

Pollard, D. D., P. Segall, and P. T. Delaney. 1982. Formation and interpretation of dilatant echelon cracks. Geological Society of America Bulletin, 93:1291–1303.

Power, W. L., T. E. Tullis, S. R. Brown, G. N. Boitnott, and C. H. Scholz. 1987. Roughness of natural fault surfaces. Geophysical Research Letters, 14:29–32.

Price, N. 1966. Fault and Joint Development in Brittle and Semi-brittle Rock. Oxford: Pergamon Press, 176 pp.

Price, N. 1974. The development of stress systems and fracture patterns in undeformed sediments. Proceedings of the International Society of Rock Mechanics, IA:487–496.

Price, R. A. 1988. Mechanical paradox of large scale overthrusts. Geological Society of America Bulletin, 100:1898–1908.

Proffett, J. M., and J. H. Dilles. 1984. Geologic map of the Yerington District, Nevada. in Map, Nevada Bureau of Mines and Geology, vol. 77. Reno.

Reches, A. 1983. Faulting of rocks in three-dimensional strain fields. II. Theoretical analysis. Tectonophysics, 95:133–156.

Reches, Z., and D. A. Lockner. 1994. Nucleation and growth of faults in brittle rock. Journal of Geophysical Research, 99:18,159–18,173.

Renshaw, C. E., and D. D. Pollard. 1994. Numerical simulation of fracture set formation: a fracture mechanics model consistent with experimental observations. Journal of Geophysical Research, 99:9359–9372.

Reyes, O., and H. H. Einstein. 1991. Failure mechanisms of fractured rock—a fracture coalescence model. Pp. 333–340 in Proceedings of the 7th International Congress of the International Society of Rock Mechanics, vol. 1.

Rice, J. R. 1968. Mathematical analysis in the mechanics of fracture. Pp. 192–311 in Fracture, vol. 2, H. Liebowitz, ed. New York: Academic Press.

Rice, J. R. 1992. Fault stress states, pore pressure distributions, and the weakness of the San Andreas fault. Pp. 475-503 in Earthquake Mechanics and the Transport Properties of Rocks, B. Evans and T.F. Wong, eds. London: Academic Press.

Rice, J. R. 1993. Spatio-temporal complexity of slip on a fault. Journal of Geophysical Research, 98:9885–9907.

Riedel, W. 1929. Zur Mechanik geologischer Brucherscheinungen. Zentralbl. Mineral., Abt. B, 354–368.

Rispoli, R. 1981. Stress fields about strike-slip faults inferred from stylolites and tension gashes. Tectonophysics, 75(34):T29–T36.

Rives, T., M. Razack, J. P. Petit, and K. Rawnsley. 1992. Joint spacing: analogue and numerical modeling. Journal of Structural Geology, 14:925–937.

Rodgers, D. A. 1980. Analysis of pull-apart basin development produced by en-echelon strike-slip faults. Pp. 27–41 in Sedimentation in Oblique-Slip Mobile Zones, P. F. Ballance and H. G. Reading, eds. Special Publication, International Association for Sedimentology.

Ryan, M. P., and C. G. Sammis. 1978. Cylic fracture mechanisms in cooling basalt. Geological Society of America Bulletin, 89:1295–1308.

Saltzer, S. D. 1992. Numerical modeling of crustal scale faulting using the distinct and boundary element methods. Ph.D. thesis, Stanford University, Stanford, Calif., 203 pp.

Saltzer, S. D., and D. D. Pollard. 1992. Distinct element modeling of structures formed in sedimentary overburden by extensional reactivation of basement normal faults. Tectonics, 11:165–174.

Scholz, C. H. 1990. The Mechanics of Earthquakes and Faulting. Cambridge: Cambridge University Press, 439 pp.

Scholz, C. H., and C. Aviles. 1986. The fractal geometry of faults faulting. Pp. 147–155 in Earthquake Source Mechanics, S. Das, J. Boatwright, and C. H. Scholz, eds., Monograph Series, vol. 37. Washington, D.C.: American Geophysical Union.

Schwartz, D. P., and K. J. Coppersmith. 1984. Fault behavior and characteristic earthquakes; examples from the Wasatch and San Andreas fault zones. Journal of Geophysical Research, 89:5681–5698.

Scott, R. B., and J. Bonk. 1984. Preliminary geologic map of Yucca Mountain, Nye County, Nevada, with geologic sections. USGS Open-File Report 84-494, scale 1:12,000. U.S. Geological Survey, Denver, Colo.

Secor, D. T. 1965. Role of fluid pressure in jointing. American Journal of Science, 263:633–646.

Secor, D. T. 1968. Mechanics of natural extension fracturing at depth in the earth's crust. Pp. 3–47 in Proceedings of a Conference on Research in Tectonics. Paper 68-52, Geology Survey of Canada, Ottawa.

Seeburger, D., A. Aydin, J. L. Warner, and R. E. White. 1991. Structure of fault zones in sandstone and its effect on permeability. American Association of Petroleum Geologists Bulletin, 75 (3):669.

Segall, P., and D. D. Pollard. 1980. Mechanics of discontinuous faults. Journal of Geophysical Research, 85:4337-4350.

Segall, P., and D. D. Pollard. 1983a. Joint formation in granitic rock of the Sierra Nevada. Geological Society of America Bulletin, 94:563–575.

Segall, P., and D. D. Pollard. 1983b. Nucleation and growth of strike-slip faults in granite. Journal of Geophysical Research, 88:555–568.

Segall, P., E. H. McKee, S. J. Martel, and B. D. Turrin. 1990. Late Cretaceous age of fractures in the Sierra Nevada batholith, California. Geology, 18:1248–1251.

Sibson, R. H. 1981. Fluid flow accompanying faulting: field evidence and models. Pp 593–603 in Earthquake Prediction: An International Review, Maurice Ewing Series, vol. 4, D. W. Simpson, and P. G. Richards, eds. Washington, D.C.: American Geophysical Union.

Sibson, R. H. 1992. Implications of fault-wave behavior for rupture nucleation and recurrence. Tectonophysics, 211:283–293.

Sibson, R. H. 1994. Crustal stress, faulting, and fluid flow. Pp. 69–84 in Geofluids: Origin, Migration and Evolution of Fluids in Sedimentary Basins, J. Parnell, ed. Special Publication 78, Geological Society of London.

Skempton, A. W. 1966. Some observations on tectonic shear zones. Pp. 329–335 in Proceedings of the 1st International Congress of the International Society of Rock Mechanics, Lisbon, vol 1.

Sleep, N. H., and M. L. Blanpied. 1992. Creep, compaction and the weak rheology of major faults. Nature, 359:687–692.

Spencer, E. W. 1959. Geologic evolution of the Beartooth Mountains, Montana and Wyoming, Part 2: Fracture Patterns. Geological Society of America Bulletin, 70:379–382.

Stearns, W., and M. Friedman. 1972. Reservoirs in fractured rocks. Pp. 82–106 in Stratigraphic Oil and Gas Fields; Classification, Exploration Methods, and Case Histories. American Association of Petroleum Geologists, Memorandum, No. 16 .

Suppe, J. 1985. Principals of Structural Geology. Englewood Cliffs, N.J.: Prentice-Hall, p. 537.

Tchalenko, J.S. 1970. Similarities between shear zones of different magnitudes. Geology Society of America Bulletin, 81:1625–1640.

Tsang, Y. W., and P. A. Witherspoon. 1981. Hydromechanical behavior of a deformable rock fracture subject to a normal stress. Journal of Geophysical Research, 86:9287–9298.

Turcotte, D. L. 1992. Fractals and Chaos in Geology and Geophysics. Cambridge: Cambridge University Press, 221 pp.

U.S. Geological Survey. 1984. A Summary of Geologic Studies Through January 1, 1983, of a Potential High-Level Radioactive Waste Repository Site at Yucca Mountain, Southern Nye County, Nevada. USGS Open-File Report 84-792, U.S. Geological Survey, Denver, Colo., p. 103.

Van Hise, C. R. 1896. Principles of North American Pre-Cambrian Geology: U.S. Geological Survey 16th Annual Report. U.S. Geological Survey, Reston, Va., pp. 581–874.

Verbeek, E. R., and M. A. Grout. 1984. Fracture Studies in Cretaceous and Paleocene Strata in and Around the Piceance Basin, Colorado: Preliminary Results and Their Bearing on a Fracture-Controlled Natural-Gas Reservoir at the MWX Site. USGS Open-File Report 84-156, U.S. Geological Survey, Denver, Colo.

Walsh, J. J., and J. Watterson. 1988. Analysis of relationship between displacements and dimension of faults. Journal of Structural Geology, 10:239–247.

Walsh, J. J., and J. Watterson. 1993. Fractal analysis of fracture patterns using the standard box-counting technique: valid and invalid methodologies. Journal of Structural Geology, 15:1509–1512.

Wang, C. Y., and N. H. Mao. 1979. Shearing of saturated clays in rock joints at high confining pressures. Geophysics Research Letter, 6:825–828.

Wilcox, R. E., T. P. Hardin, and D. R. Seely. 1973. Basic wrench tectonics. American Association of Petroleum Geologists Bulletin, 57:74–96.

Wise, D. U. 1964. Microjointing in basement, middle Rocky Mountains of Montana and Wyoming: Geological Society of America Bulletin, 75:287–306.

Wise, D. U. 1976. Linesmanship, guidelines for a thriving geologic artform. Pp. 635–636 in Proceedings of the 1st International Conference on New Basement Tectonics. Utah Geological Association, Salt Lake City.

Wong, I. 1990. Seismotectonics of the coast ranges in the vicinity of Lake Berryessa, Northern California. Bulletin of Seismology Society of America, 80:935–950.

Wood, W. W., and L. A. Fernandez. 1988. Volcanic rocks. Pp. 353–365 in Hydrogeology, W. Back, J. S. Rossensbein, and P. R. Seaber, eds. Boulder, Colo.: Geological Society of America.

Wu, D., and R. Bruhn. 1992. Geometry of normal fault surfaces in controlling crustal deformation and rupture segmentation. Geological Society of America Abstracts with Programs, 24 (6):69.

Wu, H., and D. D. Pollard. 1991. Fracture spacing, density, and distribution in layered rock mass: results from a new experimental technique. Pp. 1175–1184 in Rock Mechanics as a Multidisciplinary Science, Proceedings of the 32nd United States Symposium on Rock Mechanics. Rotterdam: A. A. Balkema.

Xiao, H. B., F. A. Dahlen, and J. Suppe. 1991. Mechanics of extensional wedges. Journal of Geophyical Research, 96:10,301–10,318.

Zhao, G., and A. M. Johnson. 1992. Sequence of deformations recorded in joints and faults, Arches National Park, Utah. Journal of Structural Geology, 14:225–236.

Zoback, M. D., and J. H. Healy. 1992. In situ stress measurements to 3.5 km depth in the Cajon Pass scientific research borehole: implications for the mechanics of crustal faulting. Journal of Geophysical Research, 97:5039-5057.

Zoback, M. D., M. L. Zoback, V. S. Mount, J. Suppe, J. P. Eaton, J. H. Healy, D. Oppenheimer, P. Reasenberg, L. Jones, C. B. Raleigh, I. G. Wong, O. Scotti, and C. Wentworth. 1987. New evidence on the state of stress of the San Andreas fault system. Science, 238:1105–1111.

3

Physical Properties and Fundamental Processes in Fractures

To build predictive models and understand the behavior of complex fracture systems it is necessary to understand the behavior of a single fracture under the same in situ conditions imposed on the whole system. This is true whether the fractures are represented explicitly, as in a network model, or implicitly, as in a stochastic effective medium model.

Two questions are the focus of this chapter: (1) How do flow and transport occur in a single fracture, and what factors significantly affect flow and transport properties? (2) What are the geophysical characteristics of single fractures that make it possible to detect and characterize them remotely?

This chapter emphasizes the results of theoretical and laboratory investigations. Theoretical studies, in combination with controlled laboratory tests, provide the fundamental physical properties and relationships between parameters that describe the processes of fluid flow and transport, seismic wave propagation, and electrical conduction. These fundamental relationships can then be incorporated in models of natural, more complex fracture systems. In laboratory studies, initial and boundary conditions can be controlled and experiments constructed in order to study the effects of a single or limited number of parameters. It should be noted that the physical properties of systems of fractures may be more complex than a simple linear superposition of the properties of single fractures, especially when the fractures intersect. Nonetheless, laboratory experiments can provide the basis for understanding the phenomena that govern large-scale field experiments of fracture systems.

This chapter begins with a discussion of the geometry of a single fracture and the effects of stress and genesis on that geometry. This is followed by a discussion of flow and transport and, finally, of geophysical properties.

GEOMETRIC PROPERTIES AND STRESS EFFECTS

Although fractures are often visualized conceptually as parallel plates separated by some distance (the "aperture"), there are few situations under natural conditions in which this conceptualization is accurate or meaningful. Generally, in the plane of the fracture there are regions in which the surfaces are in contact and regions, or voids, where the surfaces are not in contact. The factors that most affect the geometry of the void space are (1) the geological origin of the fracture (see Chapter 2); (2) the subsequent changes in stress brought about by natural processes and the activities of humans, such as withdrawal or injection of fluids or construction of underground openings (see Chapter 7); and (3) mineral precipitation and dissolution as fluids flow through a fracture (see Chapter 7).

The voids of a fracture form an interconnected network through which fluid flows. The concept of a fracture as a planar network of interconnected voids leads to an analogy with porous media. In fact, a better conceptualization of a fracture is that of a two-dimensional porous medium in which the fracture voids represent pores. The two-dimensionality arises because all the connections between the fracture voids are in the plane of the fracture.

There is an important difference between fracture void structure and pore structure that limits the extent of this analogy and leads to important differences in hydrological behavior between fractures and porous media. Whereas the bulk of the flow is carried in the large void spaces in both fractures and porous media, the fracture voids tend to be more cracklike in shape compared to the equant shapes of voids in porous media. Cracklike voids deform more easily under applied stress than equant voids. Consequently, the hydrological properties of fractures are subject to a much higher degree of stress sensitivity than porous media. Because fractures represent discontinuities in material properties, shear stresses can also result in deformations, leading to large changes in hydrological properties. Stress sensitivity constitutes the single greatest distinction in hydrological properties between porous media and fractures.

Another consequence of the two-dimensional nature of fractures is that flow can easily become channelized and under two-phase conditions can lead to strong phase interference. Because the pore structure is two-dimensional, flow only has the plane of the fracture to find a path around the closed void (if the matrix rock is impermeable). In porous media (or if the matrix rock is significantly permeable) the third dimension is also available.

One focus of this chapter is the effect of stress on both hydrological and geophysical properties. Fundamental to understanding these effects is a knowledge of how fracture void geometry changes under generalized stress conditions. Thus, the mechanical deformation of fractures is discussed in this section; the effects of this deformation on fluid flow and geophysical properties are discussed in subsequent sections.

The dimensions of the voids in the network certainly affect flow, but of equal if not greater importance is the connectivity of the network. At the most

fundamental level, flow and transport in a fracture are controlled by the geometric properties of the interconnected voids in the fracture. This section will first discuss these geometric properties from a purely descriptive perspective. Then the changes that occur in geometry as stresses are changed will be described.

Roughness of Fracture Surfaces

A fracture can be envisioned as two rough surfaces in contact. If the surfaces are not perfectly matched, as would be anticipated in many natural environments, there will be some regions where voids remain. Because the void space arises from a mismatch at some scale between the two surfaces of a fracture, a great deal of work has been done to quantify and model the statistics of fracture surfaces.

Surface roughness has been studied extensively because it is an important parameter in the field of tribology. Thomas (1982) gives a complete review of surface roughness measurements. Surface roughness is most commonly measured by profilometry; that is, a sharp stylus is dragged over the surface along a straight line to record the surface height in the form of a profile. For rock fractures, mechanical profilometers (Swan, 1981; Brown et al., 1986; Gentier and Ries, 1990) and optical methods (Miller et al., 1990; Voss and Shotwell, 1990) have been used to measure roughness profiles. The deviation of a surface from its mean plane as determined from these profiles is assumed to be a random process for which statistical parameters such as the variances of height, slope, and curvature are used for characterization. There are a myriad of surface roughness standards that have evolved from different applications. Thomas (1982) describes more than 20 standards that include measures such as the average deviation from the mean (also known as the root-mean-square, or rms, roughness) and peak-to-valley height.

For many rough surfaces, especially those formed in part by natural processes, such as fractures in rock (see Figures 2.3 and 2.26), the rms roughness is a function of the length of the sample (e.g., Sayles and Thomas, 1978; Brown and Scholz, 1985; Power et al., 1987). Consequently, instruments with different resolutions and scan lengths yield different values for these parameters for the same surface. The conventional methods of surface roughness characterization such as rms values are therefore plagued by inconsistencies. The underlying problem with conventional methods is that, although surfaces contain roughness components at a large number of length scales, each roughness measure depends on only a few particular length scales, which are determined by the resolution and dynamic range of the instrument. These difficulties can be overcome when the general nature of surface roughness is understood.

Two key quantities that describe a two-dimensional random process (such as the topography of rough surfaces) are the probability density function for heights and the autocorrelation function (e.g., Whitehouse and Archard, 1970) or an equivalent measure, the power spectrum (Bendat and Piersol, 1971; Bath,

1974) for texture. The probability density function describes the distribution of surface heights about the mean without regard to horizontal spatial position. The autocorrelation function or power spectrum describes the texture or spatial correlation of heights on the surface. (The power spectrum is the Fourier transform of the autocorrelation function.) This statistical description of the random processes is complete only if the process is Gaussian.

Brown and Scholz (1985) and Power et al. (1987) computed the power spectral density, $G(k)$, for various rock surfaces, natural joint surfaces in crystalline and sedimentary rocks, a bedding-plane surface, and frictional wear surfaces. Their results show that there is remarkable similarity among these surfaces. Profiles of these widely different surfaces yield power law power spectra of the form

$$G(k) = Bk^{\alpha}, \qquad (3.1)$$

where k is the wavenumber related to the wavelength λ of surface roughness according to $k = 2\pi/\lambda$. The exponent α has a fairly limited range (typically between -2 and -3). The power spectrum (and therefore the roughness) can thus be described to first approximation by two parameters: (1) the exponent α (i.e., the slope of the power spectrum on a log-log plot) and (2) the proportionality constant B (i.e., the value of $G(k)$ at $k = 1$).

This power law form of the power spectrum indicates that fracture surface topography can be represented in terms of fractal geometry where the fractal dimension of the surface, D, is related to the power spectrum exponent as $D = (7 - \alpha)/2$ (see discussions by Mandelbrot, 1982; Brown and Scholz, 1985; Brown, 1987; and Power and Tullis, 1991). This relationship is strictly true only if the phase spectrum is random and the topographic heights have a normal distribution. The fractal dimension describes the proportion of high-frequency to low-frequency roughness elements and is a measure of surface texture. For natural fracture surfaces, D falls in the range of 2 to 3, with small values representing smoother surfaces. Variations in α over different measurement scales indicate, however, that it may be unrealistic to extrapolate the power spectrum outside the range of measured wavelengths.

Void Geometry

Current understanding of the geometric properties of fracture void space has evolved from both experimental and theoretical investigations. These investigations have addressed two main issues: (1) What are the geometric characteristics at some nominal stress? (2) How do these characteristics change as stress changes? In the following discussion the term local aperture refers to the distance between the two opposing fracture surfaces measured perpendicular to the plane of the fracture.

Various techniques, each with advantages and disadvantages, have been used to characterize fracture void geometry. Representative examples of techniques described here are grouped into two categories: (1) those that use measurements of the roughness of the two surfaces composing the fracture and (2) those that involve filling the void space with a casting material. In the first category one method is to sum the surface roughness heights from both sides of the fracture to generate a "composite topography." Specifically, if the heights of the surfaces on opposing walls of the fracture are $h_1(x,y)$ and $h_2(x,y)$, measured relative to the mean level of each surface with positive values increasing outward from the surface, the composite topography is defined as $h_c(x,y) = h_1(x,y) + h_2(x,y)$. The composite topography contains only the mismatched parts of the surface roughness and represents the distribution of local apertures under essentially zero stress conditions (Figure 3.1). In a more sophisticated approach to the use of

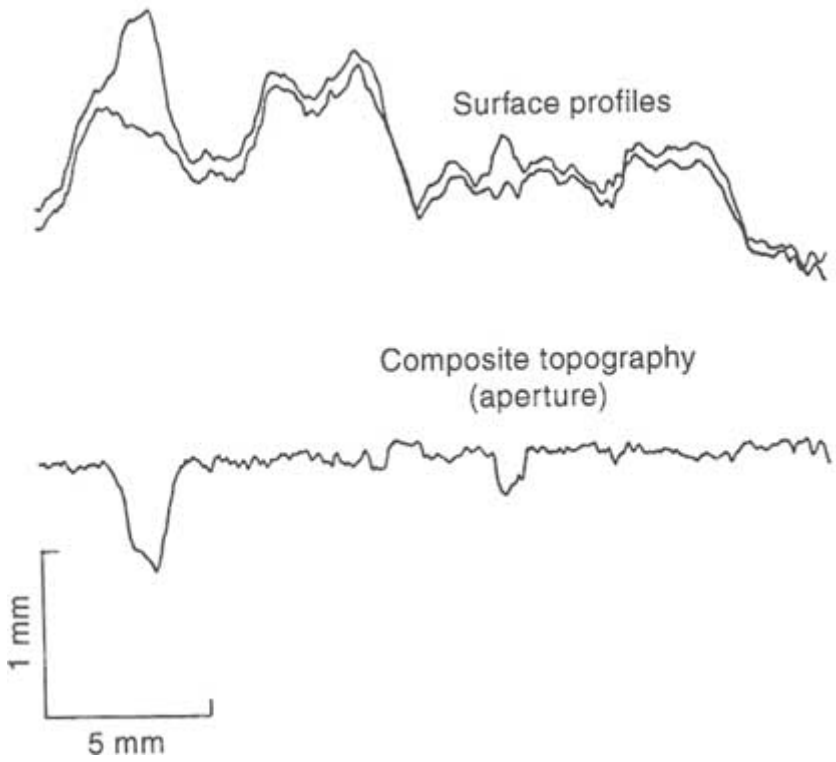

FIGURE 3.1 Example of measured matched profiles and corresponding composite topography. Notice that the high-amplitude long-wavelength components present in the profiles of the individual surfaces are not present in the composite topography. From Brown et al. (1986).

measurements of fracture surface roughness, Roberds et al. (1990) showed that the statistical properties of local apertures can be derived directly from the statistical properties of each of the opposing fracture surfaces. The advantage of methods that use surface roughness data is that such data can be easily obtained. The disadvantages are that changes from nonzero stress conditions must be inferred from models and it may be difficult to match the two halves of the fracture correctly.

In the second category are methods that involve filling the void space with different materials such as epoxy (Gale, 1987; Billaux and Gentier, 1990) or Wood's metal (Pyrak-Nolte et al., 1987a) and other casting techniques (e.g., Hakami and Barton, 1990). Epoxy castings provide good estimates of local aperture geometry, but some techniques require that the sample be sliced and consequently destroyed. Estimates of the areal distribution of void space can be obtained accurately by using Wood's metal, but it is difficult to obtain local aperture geometry. Both local aperture and void distribution can be obtained from other casting methods, but there are problems with resolution.

Although laboratory techniques have shortcomings, a number of insights concerning fracture void geometry have been provided by such measurements. Brown et al. (1986) measured matched profiles from both halves of natural joint surfaces. The power spectrum of local apertures and the composite topography were computed as well. They showed that the local aperture distribution has a power law spectrum at high spatial frequencies (short wavelengths) but flattens out at low spatial frequencies (long wavelengths), as illustrated in Figure 3.2. The crossover between the power law behavior and the flat spectrum allows a mismatch length scale to be defined as the point where the ratio of the local aperture spectrum to the spectrum of the individual surfaces reaches one-half its high-frequency value (Figure 3.2). In the simplest model this mismatch length scale is the third parameter needed to define the roughness of a fracture. This scale is essentially the largest wavelength present in the composite topography with any significant amplitude and defines the dominant roughness component of the fracture.

The results of Wood's metal injection tests on two natural granitic fractures subjected to a normal stress of 33 MPa are shown in Figure 3.3. The figure illustrates the inherent heterogeneity in the areal distribution of the void space in natural fractures. Though heterogeneous, it is also clear that the void space is spatially correlated. Nolte et al. (1989) studied the fractal properties of the void geometry of natural granitic fractures, finding that the fractal dimension, D, ranged from about 1.99 to 1.95, depending on the stress level. Further studies (Pyrak-Nolte et al., 1992) suggest that multifractal analyses of fracture void space may distinguish between successive processes that might have altered the fracture void structure.

Measurements (Gale, 1990) of an epoxy cast of a granite fracture indicate that local apertures sizes are lognormally distributed. There is an apparent relationship

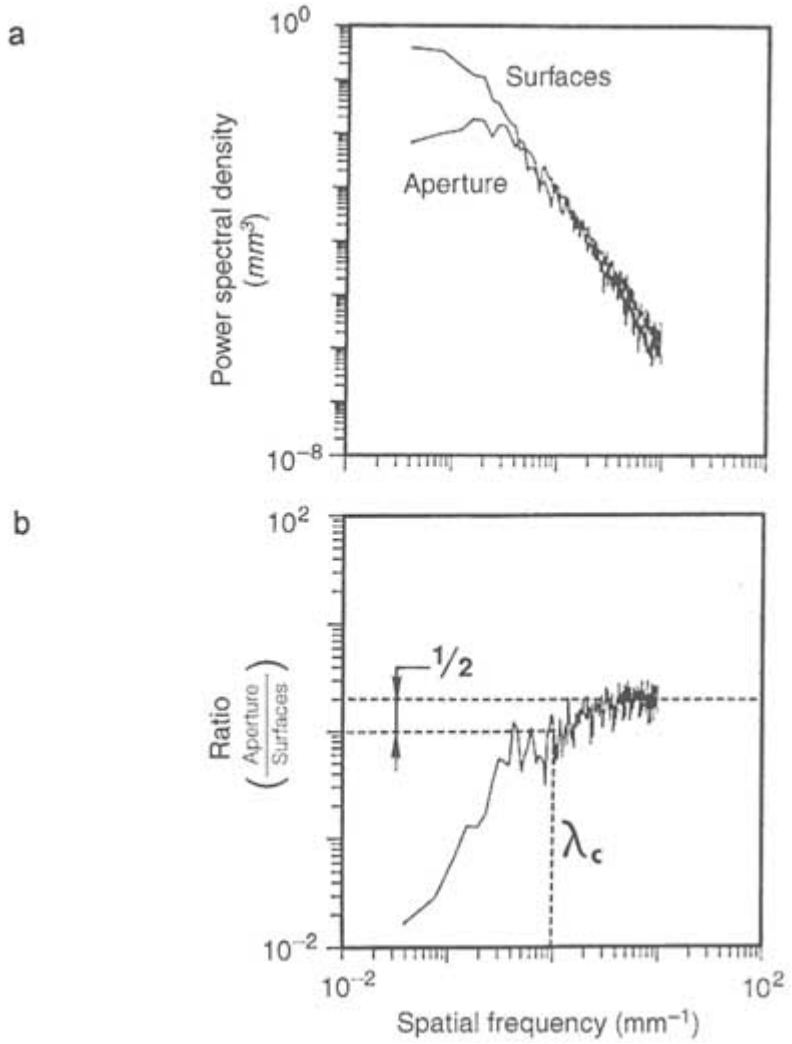

FIGURE 3.2 (a) Power spectra of the surface profiles and aperture (composite topography) shown in Figure 3.1. Notice the lack of power at low frequencies in the aperture relative to the surfaces. (b) Ratio of the aperture spectrum to the surface spectrum. A mismatch length scale λ_c can be defined by the spatial frequency at which the ratio falls to one-half its high-frequency asymptotic value. For length scales greater than λ_c the surfaces are closely matched, and for length scales less than λ_c the surfaces are mismatched. From Brown et al. (1986).

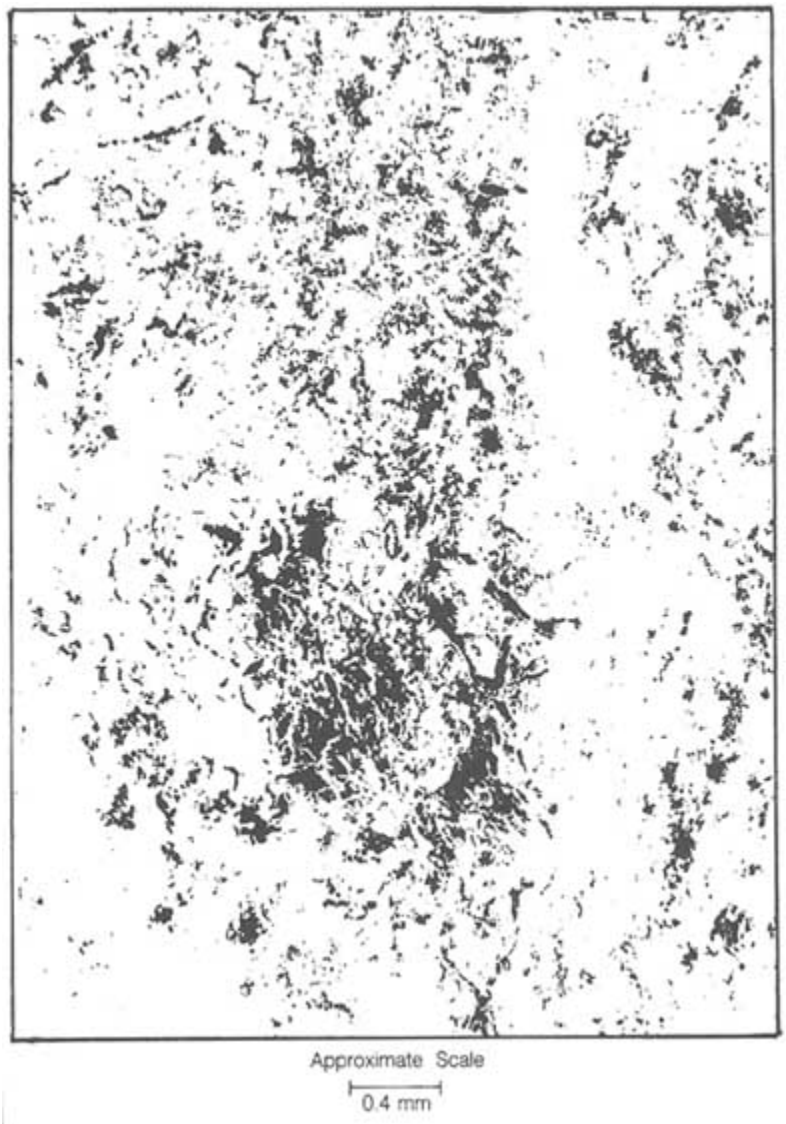

FIGURE 3.3 Composite SEM micrograph of Wood's metal casts of two natural fractures showing void space at 33 MPa effective stress. Void space, filled by Wood's metal, is shown in white; contact areas are black. From Pyrak-Nolte et al. (1992).

between local aperture size and void extent. That is, large local apertures are associated with laterally extensive voids, whereas small local apertures are associated with restricted voids.

Inferences about the statistical properties of fracture void space have been tested in a number of modeling studies. Several approaches have yielded aperture distributions that visually have properties similar to the experimental results shown in Figure 3.3. Brown (1987), Thompson and Brown (1991), and others have used the fractal properties of surface roughness measurements in combination with the mismatch length scale to generate such patterns. Moreno et al. (1988), Tsang and Tsang (1987), and others have created spatially correlated local aperture patterns, such as those shown in Figure 3.3, by using statistical techniques that assumed lognormal local aperture size distributions. Pyrak-Nolte et al. (1988) used a stratified percolation model to create spatially correlated local aperture patterns that are approximately lognormal. Although lognormal local aperture size distributions are most commonly used in models, analysis of stress/deformation data by Hopkins et al. (1990) indicate that some local aperture distributions may be bimodal.

STRESS EFFECTS ON FRACTURE VOID GEOMETRY

Deformation in a fracture can arise from either a change in fluid pressure or a perturbation of the stress field in the rock. The important stress for mechanical behavior and fluid flow in fractures is the effective stress, which is generally taken to be the normal stress on the fracture minus the fluid pressure (Terzaghi, 1936). In a three-dimensional stress field the normal stress is the component of the total stress measured perpendicular to the fracture plane. By convention in rock mechanics, compressive stresses are taken to be positive in sign, so effective stress values are usually positive. However, in some instances, such as in a hydrofracture, the fluid pressure exceeds the far-field normal stress, so effective stress values are negative.

Under transient conditions, effective stress conditions may be different in fractures and the surrounding porous media. If the matrix permeability is different than the fracture permeability, fluid pressures will be different under transient flow conditions. If matrix permeability is less than the fracture permeability, there will be a larger effective stress in the fracture than in the matrix when fluid is withdrawn. Differences in effective stresses will also arise when the pore compressibility of the rock matrix is greater than the void compressibility of the fractures. In this case, equal reductions in pore and fracture pressures will produce larger effective stress changes in the fracture than in the rock.

When the stress on a fracture changes, it will deform. Because of the importance of fractures to the mechanical behavior of rock masses, a large number of experimental investigations have addressed deformability of fractures. A good summary is presented by Einstein and Dowding (1981). The results of their work

have been incorporated into models of rock mass mechanical behavior (e.g., Roberds and Einstein, 1978). However, the following discussion is restricted to deformability from the standpoint of how it affects the process of fluid flow.

The stress on a fracture can be decomposed into two components, one in a direction perpendicular to the surface (normal) and one in a direction parallel to the surface (shear). In general, the effects of these two components are highly coupled; that is, the deformation caused by a change in one component is dependent on the magnitude of the other. Fracture surface roughness is one of the primary reasons for this coupling, as illustrated in Figure 3.4. This figure shows the distribution of voids and contacting asperities in an idealized representation of a very rough undeformed fracture. The application of shear stress to this fracture at a very low normal stress may cause one surface to ride up and over the asperities of the other, leading to large dilation. At the other extreme, at very high normal stress, the frictional forces resisting slip may exceed the strength of the rock and the asperities will be sheared off. Dilation would be minimal in this case. Deformation associated with these loading conditions is discussed later in this chapter under "Shear Stress Effects." Considerable work, as discussed below, has been carried out for the case in which only changes in effective normal stress are considered. Referring again to Figure 3.4, such studies address closure of voids where the surfaces are not in contact and deformation of asperities where the surfaces are in contact.

Normal Stress Effects

When normal stress is applied to a natural fracture in the laboratory, fracture deformation is typically nonlinear (Figure 3.5). The rate of deformation is greatest at low values of normal stress, indicating that fracture stiffness increases as normal stress increases.

A common feature of fracture deformation is a hysteresis effect during stress loading and unloading, as shown Figure 3.5. In hard clean crystalline rock fractures, hysteresis is almost entirely due to processes arising from mismatch

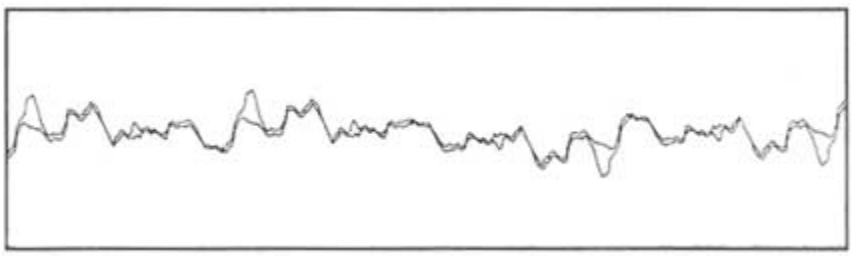

FIGURE 3.4 Cross section through a very rough fracture in the underformed state showing distribution of voids and contacting asperities.

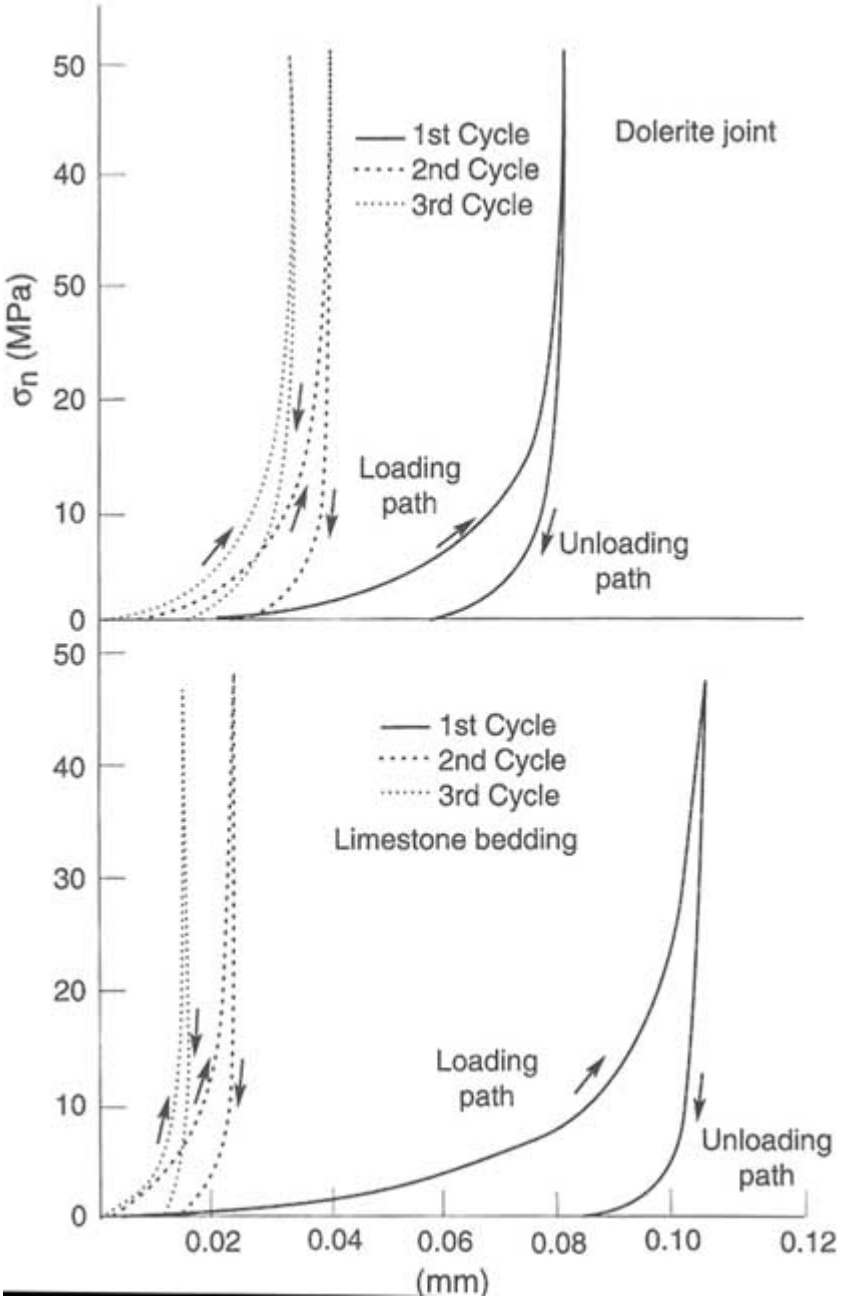

FIGURE 3.5 Measurements of the closure of natural joints under normal stress (σ_n). From Bandis et al. (1981).

(of opposing fracture surfaces) and sample disturbance. As a mismatched fracture is loaded, slight realignments of the fracture surfaces may occur or asperities may fail. In either case, the geometry of the load-bearing portions of the surface has changed, so the load deformation curve will be different. If a thick fracture infilling is present, or if the fracture is in soft, clay-bearing sediments, inelastic processes also may contribute to the hysteresis effect. After repeated cycling, Pyrak-Nolte et al. (1987a) observed that the nonlinearity of natural fracture deformation persisted without hysteresis, thus leading to the conclusion that deformation is primarily elastic. The degree to which fracture deformation is elastic is important in determining the degree to which fluid flow properties are independent of stress history. If deformation is totally elastic, the fluid flow properties of fractures will be totally dependent on the present stress state.

Elastic nonlinearity arises because as normal stress is applied the geometry of the void space changes as some voids close and additional asperities come into contact. Increased contact area results in stiffening of the fracture. This process is illustrated in Figure 3.6, which shows a Wood's metal cast of the void space in a granite fracture at different stress levels. At low stress levels, there are only a few asperities of contact surrounded by large void areas. As stress is increased, the number of contacting asperities and the contact area increase, but in a nonuniform pattern. Even at moderately high stresses, relatively large areas of void space remain, but they are connected by tortuous channels. These results

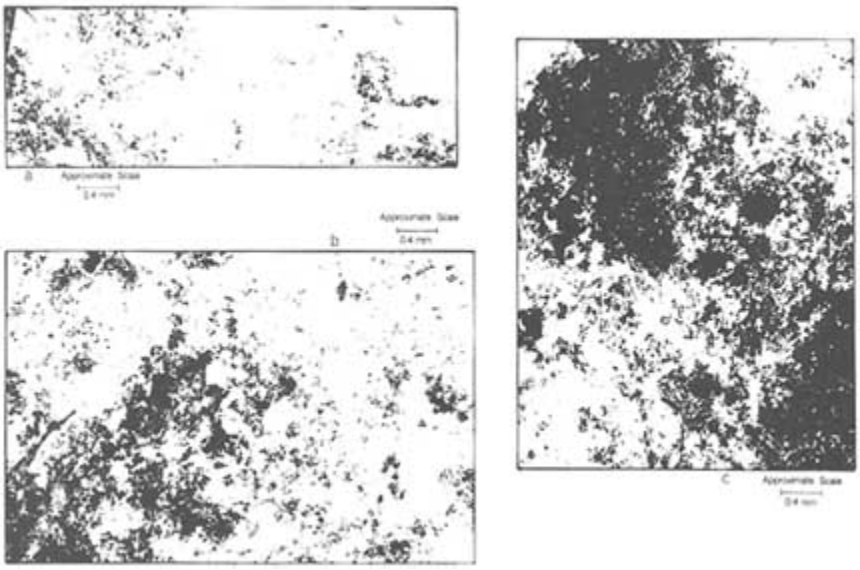

FIGURE 3.6 Composite from micrographs of a portion of a natural fracture at effective stresses of (a) 3 MPa, (b) 33 MPa, and (c) 85 MPa. Void space, filled by Wood's metal, is shown in white; contact areas are black. From Pyrak-Nolte et al. (1987a).

imply that flow must be controlled to a large extent by the location and distribution of flow restrictions or "critical necks" that connect the larger voids into continuous paths.

As explained in the following paragraphs, at least two approaches have been taken to visualize fracture deformation under normal stress. The first visualizes the fracture as being held open by asperities in contact. As stress is applied, these asperities deform and additional asperities come into contact. The second approach visualizes the fracture as a collection of voids that close as stress is applied. Other approaches have been used for developing models for mechanical deformation of fractures, but these two approaches are the most relevant to fluid flow because they allow changes in stress to be related directly to changes in the geometry of the flow path. It is frequently assumed that the geometry at the point of contact of two asperities can be represented by two touching spheres (a Hertz contact). Solutions exist for both normal and shear loading of Hertz contacts (see Mindlin, 1949; Mindlin and Deresiewicz, 1953; and Timoshenko and Goodier, 1970), from which fracture deformation under both normal and shear loading has been derived (Brown and Scholz, 1985, 1986; Yoshioka and Scholz, 1989a,b). The way in which deformations at each Hertz contact are combined to yield total fracture deformation is important; interactions between contacting asperities are often ignored, leading to underestimates of total fracture deformation.

A fracture may also be visualized as a collection of coplanar flat cracks. Under low stress, the fracture is represented by large, closely spaced cracks that close as stress is applied. As stress increases, cracks with the smallest thickness (out-of-plane dimension) to length (in-plane dimension) ratios close first, and crack spacing increases. Using fracture mechanics, analytical solutions for the deformation of noninteracting as well as interacting cracks are available (e.g., Tada et al., 1973). These solutions have led to important insights into the relationship between fracture deformation or closure measurements and changes in fracture aperture. Pyrak-Nolte et al. (1988) have shown that the volumetric deformation of a rock specimen containing a fracture subjected to stress normal to the fracture plane is equal to the deformation of the intact rock plus the changes in volume of the voids in the fracture. Stated another way, the change in void volume is exactly equal to the volumetric deformation in excess of that which would occur if the fracture were absent. This equivalence arises from conservation of volume. A consequence of volume conservation is that a given volumetric deformation corresponds to a small change in the average value of local apertures if there is a large areal percentage of voids or a large change in average aperture if there is a small areal percentage of voids. Thus, there is not a one-to-one correlation, as is often assumed, between mechanical closure and aperture closure in the fracture.

Hopkins et al. (1990) assumed an asperity model of a fracture but used the Boussinesq solution for deformation of a half-space under a distributed load (Timoshenko and Goodier, 1970) instead of the Hertz contact solution to model

asperity deformation. In this way interaction between asperities was taken into account. They showed that this approach was essentially equivalent to that of the flat-crack model.

Shear Stress Effects

Application of shear stress to a fracture can have a significant impact on void geometry because of the potential for dilation associated with relative motions of the two surfaces. Factors affecting the onset of relative motion and dilation include the magnitude of the normal stress, the roughness of the fracture, and the strength of the matrix and infilling material.

Figure 3.7 illustrates the range in shear behavior of fractures. Curve A shows the shear stress displacement of a clean rough dilatant fracture under constant normal stress. It is characterized by a rapid increase in stress up to a peak, followed by a loss in load-carrying capacity. Curve B, typical of a fracture with a thick infilling, which is usually nondilatant (Papaliangas et al., 1990), shows a more gradual increase in stress with a continuously changing slope.

The dilatancy associated with shear deformation of a fracture is illustrated in Figure 3.8. The lower curve represents the shear deformation behavior under a constant normal stress with shear stress applied in either a positive or negative direction. The upper curve shows the dilation accompanying the shear deforma

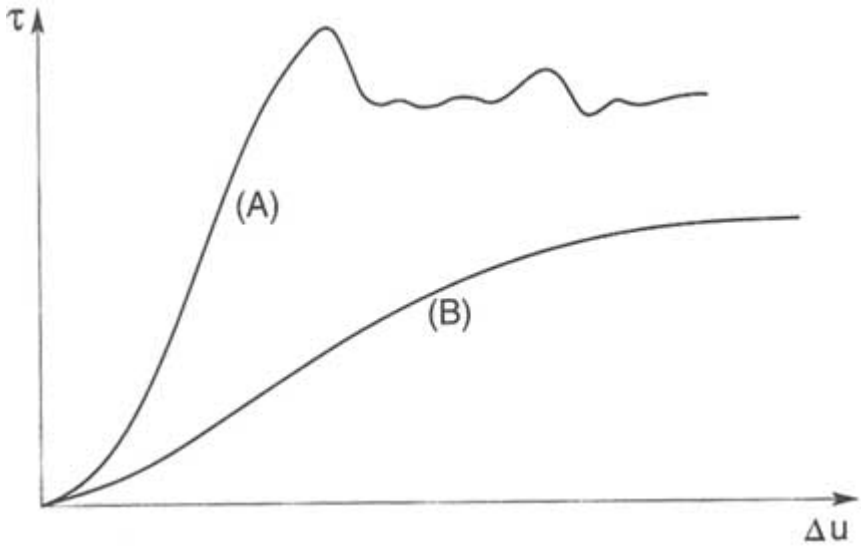

FIGURE 3.7 Curves of shear stress, τ, versus shear displacement, u, illustrating the range in shear behavior of fractures under constant normal stress. (A) dilatant behavior; (B) nondilatant behavior. From Goodman (1976).

tion. For a portion of the stress/deformation curve corresponding to elastic deformation of the fracture, there is minimal dilation. The onset of rapid dilation occurs when asperities begin to slide past one another, causing an increase in aperture. The rate of dilation increases and reaches a maximum value at the peak shear stress (Patton, 1966; Barton, 1973; Barton et al., 1985; Kutter and Otto, 1990). At this point, sufficient asperities fail to permit sliding at a nearly constant shear load. Dilation continues after the peak stress but at an ever-decreasing rate.

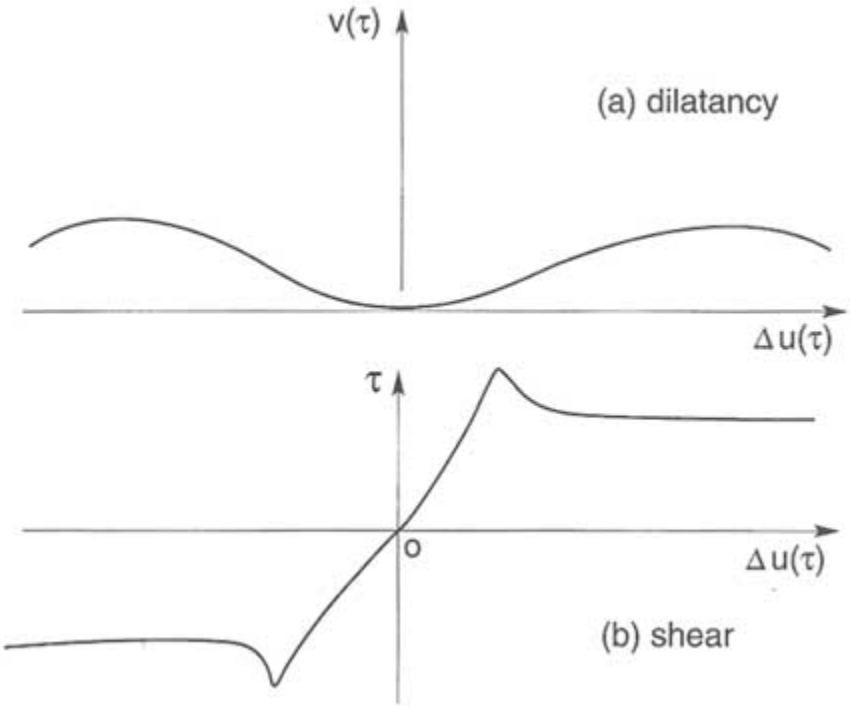

FIGURE 3.8 Illustration of dilatancy, $V(\tau)$, accompanying shear displacement, $u(\tau)$, of a rough fracture under constant normal stress. From Goodman (1976).

Although useful for conceptually describing the coupling between shear and normal stresses, the shearing of dilatant fractures under constant normal stress conditions as depicted schematically in Figures 3.7 and 3.8 usually does not occur in nature. Instead, as the fracture dilates, normal stress increases owing to the stiffness of the surrounding rock mass. Thus, normal stress changes continuously during the shearing process. In the laboratory these conditions are represented by a shear test in which the stiffness normal to the fracture is held constant (e.g., Archambault et al., 1990; Bandis, 1990). For these conditions, Ohnishi and Dharmaratra (1990) observed much lower dilation compared to shear tests under constant normal stress at identical normal stress levels. Ultimately, constitutive models must be able to describe the behavior for all types of boundary conditions.

Measurements of dilation during shear imply that the apertures of voids must be increasing. However, there is very little experimental data to quantitatively characterize these changes in void space. Gale (1990) injected resin into a fracture that was sheared under constant normal stress and found a lognormal distribution of aperture sizes, which is similar to observations of fractures under normal stress. In a numerical model, Wang et al. (1988) imposed a shear displacement on two mirror-image fractal surfaces and developed a quantitative relationship between the power spectrum of the apertures and the relative shear displacement. The mismatch length scale (cf. the earlier section, "Roughness of Fracture Surfaces") tends to increase roughly in proportion to the amount of shear displacement, implying an increase in void apertures with shear displacement.

The two approaches for modeling fracture deformation discussed earlier under "Normal Stress Effects," are not relevant, as currently formulated, to the modeling of shear deformation because neither approach accounts for frictional sliding of asperities or asperity breakage.

Effects of Fracture Origin

As discussed in Chapter 2, the hydrological properties of fracture systems are greatly influenced by their geological origin. The void structure of fractures and the hydraulic properties of the matrix depend on the origin and geological history of the rock. For example, consider two surfaces of a dilating fracture that are almost perfectly matched, with very little void space. Subsequent shearing by tectonic forces and the circulation of fluids will modify the void structure. It would be reasonable to expect that the geometry of the void space will have characteristics that reflect these processes. Void space generated by shearing motions will be affected by the magnitude of normal and shear stresses across the fracture. Shear fractures commonly have slickensides developed on fracture surfaces. In this case the surface roughness may be more highly correlated in one direction, leading to anisotropy in the void structure. Bandis et al. (1981) note that tension joints have the roughest surfaces, that beddingplane surfaces have a range of roughnesses, and that sheared joint and bedding-plane surfaces are often the smoothest.

Geological processes that lead to mineral infilling of the fracture also are important. Hydrothermal processes may alter void space by mineral precipitation or dissolution. Shearing processes can lead to formation of gouge and increasing anisotropy in permeability.

SINGLE-PHASE FLUID FLOW IN FRACTURES

Normal Stress Conditions

Most of the work on fluid flow in single fractures has been carried out under normal stress conditions. Two general techniques have been developed for

measuring the permeability of single fractures in the laboratory: radial flow and linear flow methods. In the radial flow method (Iwai, 1976; Raven and Gale, 1985), a cylindrical sample, which contains a fracture with its plane oriented perpendicular to the axis of the cylinder, is used. A small hole is drilled down the axis of the sample, intersecting the fracture plane. Fluid is injected into the hole at a constant rate, and permeability is determined from the head drop between the hole and the outside of the sample.

The linear flow method (Jones, 1975; Kranz, et al., 1979; Trimmer et al., 1980) utilizes split cylindrical samples in which the axis of the cylinder is contained in the plane of the fracture. The sample is frequently confined in a standard triaxial vessel, and a confining pressure is used to provide the normal stress across the fracture plane. Fluid is injected at one end of the sample, and permeability is determined from the pressure drop along the length of the sample. The quadrant flow method (Pyrak-Nolte et al., 1987a) approximates the flow conditions of the linear flow test. The fracture is oriented with its plane perpendicular to the sample axis, and flow is measured across the sample diameter.

The advantage of the linear flow method is that pressure drops are more uniform over the area of the fracture. Most of the head drop in the radial flow method occurs near the bored hole, so results are affected by heterogeneities in void geometry in this area.

Characteristic flow behaviors of natural fractures as a function of effective stress as observed in the laboratory are illustrated in Figure 3.9. This behavior has been observed in granite rock fractures by Gale (1982) and Raven and Gale (1985), among others, and in sedimentary rock fractures by Jones (1975) and Cook et al. (1990). Figure 3.9 shows a significant hysteresis between loading and unloading curves for the first cycle. This hysteresis is the result of slight mismatches between fracture surfaces, which produce additional pathways for fluid flow. As the load is applied, the surfaces can move slightly relative to each other, becoming better registered, or mated, and removing the effects of the mismatch. Subsequent loading results in much less hysteresis because deformations of the fractures are primarily elastic after the surfaces have become well registered.

Although the deformation of hard clean fractures is elastic, flow experiments on clay-bearing sedimentary rock (Cook et al., 1990) indicate that plastic deformation and creep can occur, causing hysteresis in flow rate measurements. Although no data are available at present, these results imply that soft infilling materials may have similar effects.

Figure 3.9 also shows that the application of normal stress results in a rapid reduction in flow rate. At high levels of normal stress, however, flow rates approach a constant, or irreducible, value. The rapid reduction in flow rate at low stress levels corresponds to closure of voids and a concomitant increase in tortuosity (see micrographs in Figure 3.6 and further discussion later, under "Relationship Between Hydraulic and Electrical Properties"). The increase in

tortuosity occurs in a heterogeneous fashion, leading to development of restrictions or "necks" between larger voids. At the highest stress levels, all flow must pass through one or more "critical necks." These restrictions are more equant in shape than the surrounding voids. Thus, the flow rate approaches a value independent of stress at high stress levels but may be orders of magnitude lower than at low stress. This has been referred to as irreducible flow (Pyrak-Nolte et al., 1987a). Mechanical closure continues at high stress levels because the large voids separated by the restrictions continue to deform.

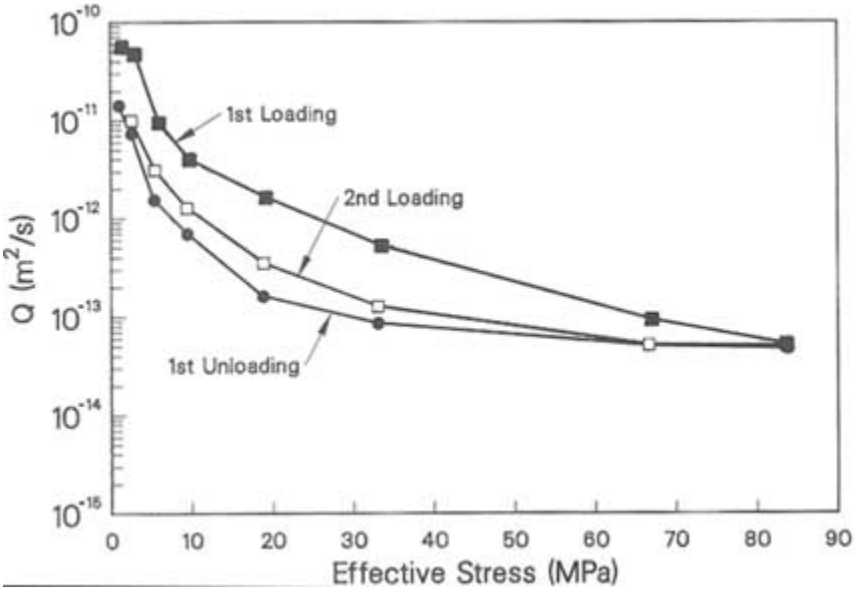

FIGURE 3.9 Flow per unit gradient as a function of effective stress for the sample shown in Figures 3.3 and 3.6. From Myer (1991).

The most common model for flow in a single fracture is the "cubic law," in which the fracture is represented by two parallel plates separated by a constant distance. The equation for one-dimensional flow between two parallel plates is

$$Q = \frac{b^3}{12\gamma}\nabla P, \qquad (3.2)$$

where Q is the volumetric flow rate per unit width (measured in the plane of the plate), b is the distance between the plates, δP is the pressure gradient, and γ is the dynamic viscosity. This equation has long been used to model macroscopic fracture flow. Recently, researchers have applied the law at a microscopic level, where the distance between fracture walls, the local aperture, is prescribed at each point in the fracture (e.g., Brown, 1987; Tsang, 1984; Thompson and Brown, 1991; see also "Relationship Between Hydraulic and Electrical Properties" later

in this chapter). The success of these models in simulating various aspects of the flow behavior observed at macroscopic scales indicates that the cubic law correctly relates local aperture and flux under laminar flow conditions and implies that, for laminar flow in fractures, viscous drag is the primary mechanism for head loss under constant flux conditions. Studies by Pyrak-Nolte et al. (1988) and Yang et al. (1989) also have shown that the geometric shapes of the local voids do not have a significant effect on flow rate. Elliptical voids and parallel-plate geometrics yield similar results. A robust analysis of the assumptions used in applying the cubic law at the local level would require complete solution of the Navier-Stokes equations in a realistic fracture void geometry.

The difficulty in applying the cubic law in the macroscopic sense (i.e., to predicting flow in a real fracture with rough walls) is in defining a representative distance between the fracture walls. Fracture openings in the field or from a core are commonly measured by using an automotive "feeler gauge." These are more nearly local aperture measurements rather than a representative distance between the fracture surfaces. In the laboratory the distance between fracture walls is often taken to be the measured mechanical closure relative to a maximum closure, under a load applied normal to the fracture surface. (Maximum closure is defined as the closure beyond which there is no deformation in excess of that in the intact rock.) This measurement is called the mechanical aperture. Another measure of the distance between the fracture walls can be obtained by measuring Q and δP and then applying Eq. 3.2 to obtain b, the hydraulic aperture. In general, the mechanical aperture and the hydraulic aperture will not be equal.

Figure 3.10 shows experimental flow rate measurements from a single fracture in claystone. The measurements were carried out over a range of conditions when the fracture was propped open with shims and with the fracture surfaces in contact and under moderate stress. The figure shows that experimental flow rate is close but not quite equal to the predicted flow rate even when the fracture is propped open. As the fracture is closed, deviation of the experimental data from the cubic law increases rapidly. Fracture permeability decreases more rapidly than predicted by the cubic law in which the variable b was assigned the value of mechanical apertures as defined above. Similar behavior has been observed in other studies (Raven and Gale, 1985; Pyrak-Nolte et al., 1987a; Gale, 1990).

For completely open fractures (fracture surfaces not in contact), analysis of data such as those presented in Figure 3.10 shows that the cubic law is valid when corrected by a friction factor, f, to account for the roughness of the fracture surfaces, that is, when Eq. 3.2 becomes (Witherspoon et al., 1980)

$$Q = \frac{1}{f}\frac{b^3}{12\gamma}\nabla P. \qquad (3.3)$$

Cook et al. (1990) showed that the friction factor could be expressed in terms of an increase in the tortuosity of the flow path in the fracture.

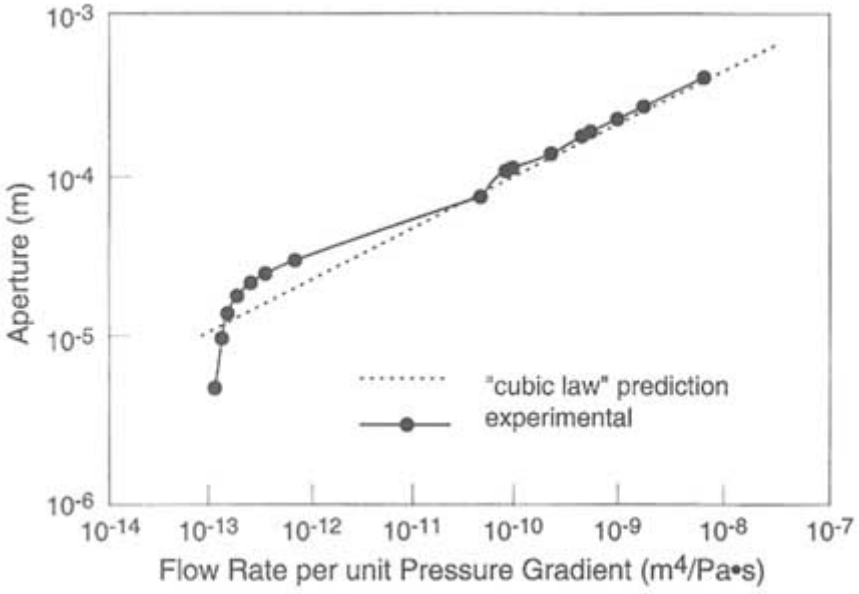

FIGURE 3.10 Flow rate through a fracture in claystone as a function of mechanical aperture (solid curve) and hydraulic aperture (broken curve) predicted by substituting the mechanical aperture into b in Eq. (3.2) and solving for $Q/\Delta P$. From Cook et al. (1990).

In some applications, such as hydrofracturing, in which negative effective stresses are common and the fracture surfaces are separated, the parallel-plate approximation (Eq. 3.2) is appropriate. For such cases, aperture is proportional to the effective stress, assuming the matrix behaves elastically. The proportionality constant can be expressed in terms of the fracture stiffness, which in turn is a function of the fracture dimensions. As a first-order approximation, a hydrofracture can be represented by a two-dimensional flat elliptical crack of length $2c$ (Figure 3.11). In this representation the axis of the injection well would be perpendicular to the page and located at the center of the crack. The relationship between the effective stress and the value of b at the crack centerline (b_{max}) is (Snedden and Elliot, 1946)

$$b_{max} = \frac{2|\sigma'|(2c)(1 - \nu^2)}{E}, \qquad (3.4)$$

where σ' is the effective stress, ν is the Poisson's ratio, and E is Young's modulus.

Lamb (1932) showed that the pressure gradient required for a particular rate of flow in an elliptical conduit of essentially zero eccentricity is 16/3 π times as great as the flow between parallel plates, all other conditions being equal. Combining Eq. 3.4 with Eq. 3.2 and multiplying by this factor gives the relationship for

flow in a flat elliptical crack: In this case the flow rate, Q, can be directly related to the effective stress.

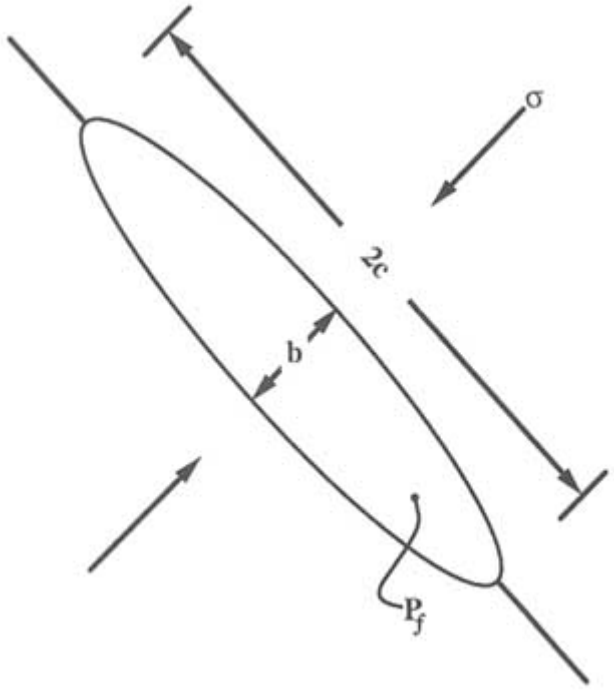

FIGURE 3.11 Deformation of a single flat two-dimensional crack with internal pore pressure P_f.

$$Q = \frac{\pi}{8\gamma}\left[\frac{2c(1 - \nu^2)|\sigma'|}{E}\right]^3 \nabla P. \qquad (3.5)$$

When the two sides of a fracture are brought into contact under normal stress, deviations from the cubic law in which b is taken as the mechanical aperture (Figure 3.10) arise because in-plane tortuosity increases and the contact area changes. The effect of increasing in-plane tortuosity has been evaluated by Walsh (1981) using an analogy with heat conduction. He derived a correction factor, $(1 - d)/(1 + d)$ as a multiplier on the right-hand side of Eq. 3.3. In this factor, d is the ratio of the contact area of asperities to the total fracture area at a given normal stress. The value of the factor decreases as the contact area increases, causing a reduction in permeability. Tsang (1984) and Brown (1987) also showed that tortuosity results in a decreased flow, with the magnitude of the effect depending on the distribution and correlation of local apertures. (See also "Relationship Between Hydraulic and Electrical Properties" later in this chapter.)

The increase in contact area with increasing normal stress causes the mean value of local aperture to decrease more rapidly than the measured mechanical aperture. This is due to the conservation of volume during elastic deformation, as discussed previously. At high stress levels, when critical necks begin to form, all flow must pass through the relatively small number of equant-shaped necks along the connected flow path. While dominating the flow, these equant-shaped necks contribute little to the total void volume change. Voids disconnected from the flow path continue to deform, leading to continued mechanical aperture changes, but flow becomes insensitive to further stress changes.

Yang et al. (1989) incorporated the conservation of volume constraint into a network model of flow in a fracture where the initial void space distribution was created by a statistical technique known as stratified percolation (Pyrak-Nolte et al., 1988). They showed that flow rate decreased more rapidly than predicted by the cubic law and suggested that a large percentage of the head drop in a fracture occurred at the critical neck along the path of the largest connected local apertures.

Cook et al. (1990) incorporated both the effects of tortuosity and conservation of void volume into a modified cubic law given by

$$Q = \left(\frac{b^3}{12\gamma}\right)\left(\frac{1-d}{1+d}\right)\frac{1}{f}\nabla P + Q_{\infty}, \qquad (3.6)$$

where b equals b_0 - (b_m + ξ), b_0 is the maximum fracture closure, b_m is the mechanical closure in response to applied normal stress, ξ *represents additional change in aperture to ensure conservation of volume, and* Q_∞ is irreducible flow.

In this equation, f accounts for the out-of-plane tortuosity and is significant only when the fracture planes are not in contact. The factor $(1 - d)/(1 + d)$, as discussed above, accounts for in-plane tortuosity. Using Eq. 3.6 and a highly idealized model to calculate void volume change, Cook et al. (1990) were able to obtain a good fit of experimental data over a range of conditions. They evaluated Q_∞ at a constant-head difference. In general, its value is a function of both the viscosity of the fluid and the applied head, and this would be included in terms of Eq. 3.6 modified by δP.

Shear Stress Conditions

As described earlier, application of shear stress can significantly alter the void space, and hence the flow, in a fracture. When dilation occurs, increases in permeability of one to two orders of magnitude have been observed (Makurat, 1985; Gale, 1990; Esaki et al., 1991). Barton et al. (1985) established empirical relationships between fracture surface roughness, mechanical properties of the wall rock, and permeability under shear stress. They showed that, under normal stresses high enough to cause asperity failure during shear, permeability may

actually decrease. Olsson (1992) ascribed the observed decreases in permeability to the formation of gouge material. He also found that the decrease was greater for rough fractures. Detailed studies of the relationship between flow and void structure under combined normal and shear stresses are not well advanced. Such studies are important for understanding flow in systems where the activities of humans result in large differences in principal stress magnitudes. Such conditions are likely to occur in civil and mining works such as underground openings, dams, and slopes where the principal stress at the free surface is zero.

Thermal and Chemical Effects

A brief discussion of the thermal and chemical effects on fluid flow in a single fracture is given here. A more complete discussion of this topic can be found in Chapter 7.

Changes in temperature may change the effective stress state in the rock mass. These stress changes may cause fractures to deform, affecting flow, as described in previous sections. It should be noted that the primary effects are actually due to thermal gradients, not temperature. Whereas a uniform temperature increase under displacement-free boundary conditions is known to affect the permeability of some intact rocks (e.g., Heard and Page, 1982), this is considered to be a second-order effect in fractures. If temperature is raised in a nearly vertical fracture intersected by a vertical borehole, the fracture will close owing to the increased hoop stress. This phenomenon has been observed in the field (Nelson et al., 1981) and has been modeled (Noorishad et al., 1984). A tunnel would be expected to experience similar effects.

Various chemical processes would be expected to have significant effects on flow in fractures, although there are few available data specific to fractures. Precipitation or dissolution would be expected to decrease or increase permeability, respectively (see Appendix 2.A). Gale and Reardon (1984) studied the precipitation of calcite along connected flow channels and observed reductions in laboratory measurements of flow in a single fracture.

The presence of clays as fracture linings could affect flow in several ways. First, as discussed previously, the mechanical deformability of the fracture may be changed (usually increased). Second, under some chemical conditions, the clays will migrate, causing significant reduction of permeability by plugging pore throats. This phenomenon has been demonstrated in porous media (Khilar and Folger, 1984) and could occur in fractures. Third, some clays are susceptible to volume change in the presence of liquids. The amount of change depends on a number of factors, including clay mineralogy, fluid chemistry, and the degree of confinement provided by the surrounding rock. Carter (1990) showed that the volumetric expansion of Na-montmorillonite clays in response to reductions in water salinity can dramatically decrease fracture permeability. These decreases, however, were observed at salinity levels much higher than anticipated based on

the traditional description of clay-particle interactions provided by the Gouy-Chapman double-layer theory (Mitchell, 1993). Results such as these illustrate the large number of questions that still remain about the effects of clay-fluid interactions on permeability.

Finally, pressure solution can affect flow, particularly at elevated temperatures. In a fracture, pressure solution may arise from stress concentrations at points of contact between asperities, and dissolved constituents will move to locations of lower stress where precipitation occurs. This process could affect flow by filling void space. Perhaps more importantly, it could also change the stiffness of the fracture. Effects of pressure solution on compaction of quartz aggregates have been studied experimentally (Sprunt and Nur, 1977), but, to the committee's knowledge, no data exist for fractures. The actual mechanism for pressure solution remains unclear, although theories have been presented by Rutter (1983), Lehner and Bataille (1984), and others.

SOLUTE TRANSPORT

Solute transport depends strongly on the distribution of velocities in the fracture. The residence time of solutes will be affected by the distribution of void sizes along connected flow paths and, of course, the path lengths. Although flow rate is dominated by the size and number of critical necks, the residence time is strongly influenced by the larger voids along the path. Consequently, the residence time could be longer than that calculated with a parallel-plate model even if the hydraulic aperture assumed in the model were obtained from flow measurements. Numerical model studies by Thompson and Brown (1991) indicate that tracer velocities may be less or greater than the average fluid velocity depending on fracture roughness and contact area. (See also "Relationship Between Hydraulic and Electrical Properties" later in this chapter.) Specifically, they found that if the fracture surfaces are rougher in one direction, the tracer velocity is less than the average fluid velocity if flow is transverse to the roughness and greater if flow is parallel to the roughness.

Variations in aperture size also may affect the dispersion of solutes in fractures. Tsang and Tsang (1987) and Tsang et al. (1988) developed a one-dimensional variable-aperture model for transport. Their numerical results showed that variations in aperture size can lead to the formation of "fast" and "slow" paths that are apparent from tracer breakthrough (or travel time) curves. These models assume that the apertures vary in a spatially correlated manner along the lengths of the channels and that their widths are constant. The effects of large volumes of fluid contained in voids of large areal extent along the flow path (e.g., Figure 3.6) are not, however, taken into account in the model.

Dispersion also is affected by the tortuosity and connectivity of multiple-flow paths. In a model in which apertures were correlated and lognormally distributed, Moreno et al. (1988) found that dispersivity (α), as reflected in the

Peclet number (α /*L*, where *L* is travel distance), was most strongly dependent on variance of the aperture distribution. Models by Smith et al. (1987) predict that the effects of connectivity and tortuosity could lead to major differences in the values of effective apertures derived from flow and tracer measurements. Such discrepancies have been observed in laboratory tests performed by Gale (1990) and Piggot and Elsworth (1990).

Piggot and Elsworth (1990) also performed tracer tests on fractures in a sheared condition. Although the fracture void volume was greater, the shape of the breakthrough curve was very similar to that obtained with the fracture in the mated condition.

Additional work is needed to more quantitatively relate geometrical properties of the void space to transport properties. It is worth reemphasizing that the limited available data show a lack of correlation between effective apertures based on hydraulic flow and transport measurements.

TWO-PHASE IMMISCIBLE FLUID FLOW

In single-phase flow, fracture geometry at the aperture scale determines flow and transport characteristics. Under two-phase immiscible fluid flow conditions, phase geometry (i.e., the geometry that is saturated with each phase) in the fracture ultimately controls the permeability to each phase, fluid pressure/saturation relationships, and solute dispersion in each phase. Phase geometry in the fracture also influences flow and transport through the surrounding porous matrix blocks by affecting hydraulic contact between the blocks. Although two-phase flow in porous media has received much attention, study of two-phase flow in fractures has only recently begun. Pressure/saturation and permeability/saturation relationships have been explored numerically and, more recently, measured in transparent rough-walled fracture analogs where phase geometry can be observed. The major difference between two-phase immiscible flow in porous media and in fractures is the two-dimensional nature of the aperture network. This increases the importance of phase interference and trapping phenomena, as discussed below.

Static and Quasi-Static Conditions

Under static conditions, viscous forces do not influence phase pressure. Therefore, assuming thermodynamic equilibrium, phase geometry in a horizontal fracture will be controlled entirely by capillary forces. The nonwetting fluid will be found in large apertures and the wetting fluid in small ones. The Laplace-Young equation (e.g., Adamson, 1990) relating the surface tension, *T*, to the pressure jump, δP, across the curved fluid-fluid interface δP dictates which phase is present at a particular location as a function of phase pressure:

$$\nabla P = T\left(\frac{1}{r_1}+\frac{1}{r_2}\right), \qquad (3.7)$$

where r_1 and r_2 are the two principal radii of curvature. For a fracture the first principal radius of curvature, r_1, is taken normal to the plane of the fracture and is equal to $b/(2\cos\alpha)$, where b is the local aperture and α is the fluid/fluid/rock contact angle. Local in-plane curvature, r_2, is assumed not to contact the rock surface and therefore is not constrained by a contact angle. In a random aperture field, assuming that curvature in the plane of the fracture is negligible and that the distribution of phases is not inhibited by lack of accessibility will lead to phase structure/pressure relationships conforming to a percolation process on a two-dimensional network, as introduced by Broadbent and Hammersley (1957). A variety of interesting results come from percolation theory, the most important being that the phase geometry is fractal and that a critical pressure exists where one phase forms an infinite connected cluster isolating the other phase (see Chapter 7 in Feder, 1988).

Numerical simulation of the percolation process on spatially correlated aperture networks has been used to evaluate phase structure as a function of pressure. Subsequent modeling of flow through each phase structure allows estimation of relative permeability as a function of pressure (Pruess and Tsang, 1990; Pyrak-Nolte et al., 1990a). These calculations indicate significant phase interference. That is, the sum of the wetting and nonwetting phase-relative permeabilities is considerably less than 1 (see Figure 3.12). Results of percolation theory on a random network also show that anisotropy in the correlation lengths (i.e., distances

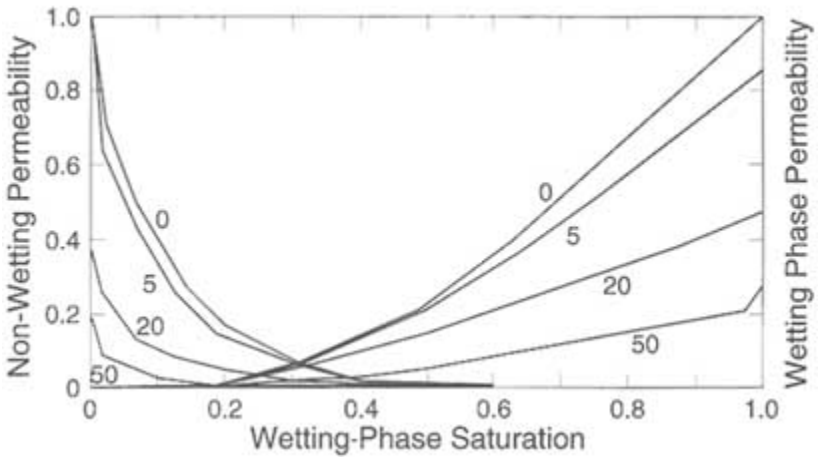

FIGURE 3.12 Effect of stress on relative permeabilities for a reduction in aperture of 5, 20, and 50 units of aperture. The saturation at which the nonwetting and wetting phase curves cross varies only a small amount with stress. From Pyrak-Nolte et al. (1990a).

over which similar values of a parameter are likely to be found) is required for the existence of two-phase mobility. This is because anisotropy can lead to the formation of parallel-connected phases. The validity of such methods for calculating two-phase fracture properties depends on the assumption that thermodynamic equilibrium predetermines phase structure for a given pressure and aperture structure. Equilibrium requires all apertures to be in a state of mutual communication. Three communication processes exist: (1) flow through the matrix that connects all apertures, (2) film flow along the fracture walls, and (3) diffusional processes. Recent experiments on a transparent cast of a natural fracture show that the interference between two phases flowing simultaneously in a fracture can be strong. At intermediate saturations, the sum of wetting and nonwetting phase-relative permeabilities was found to be much less than 1, supporting the results of numerical simulation (Persoff et al., 1991).

For a large number of situations, either communication processes do not exist or phase displacement occurs rapidly with respect to the communication processes. For these situations, accessibility of apertures to a phase (i.e., the proximity of an aperture to a phase and connection in the phase to a source or sink), places an additional control on phase geometry. If the displacement process is sufficiently slow that viscous forces can be neglected relative to capillary forces, accessibility rules may be combined with Eq. 3.7 to dictate the development of phase structure under quasi-static conditions.

Numerical models that incorporate the phase accessibility rule with Eq. 3.7, neglecting in-plane curvature, can be formulated; they conform to the process of invasion percolation introduced by Wilkinson and Willemsen (1983). Figure 3.13a shows the phase structure at breakthrough as water (the wetting fluid) supplied at the narrow boundary displaces air (the nonwetting fluid) under quasistatic conditions in a horizontal transparent rough-walled analog fracture. An example of a phase structure as simulated by the invasion percolation process on the measured aperture field for the experiment depicted in Figure 3.13a is shown in Figure 3.13b. The simulation predicts the phase structure to be much more complicated than what actually develops. Modification of the model to include in-plane curvature (r_2 in Eq. 3.7) in the calculation of aperture-phase entry pressure yields a phase structure (Figure 3.13c) comparable to those observed experimentally (Glass, 1993).

Processes by which a phase enters the fracture, including invasion from one edge of the fracture as discussed above, entry from the surrounding porous media, and entry through partitioning from the other phase, will significantly affect phase structure. As an example, Figure 3.14 shows the phase saturation structure in an air/water system in a horizontal analog fracture formed by a flat porous matrix in close contact with a roughened glass plate. Saturation/pressure relationships measured on this analog fracture/matrix system show strong hysteresis between wetting and drainage curves; nonwetting-phase entrapment reduced final wetting-phase saturation to approximately 60 percent (Glass and Norton, 1992).

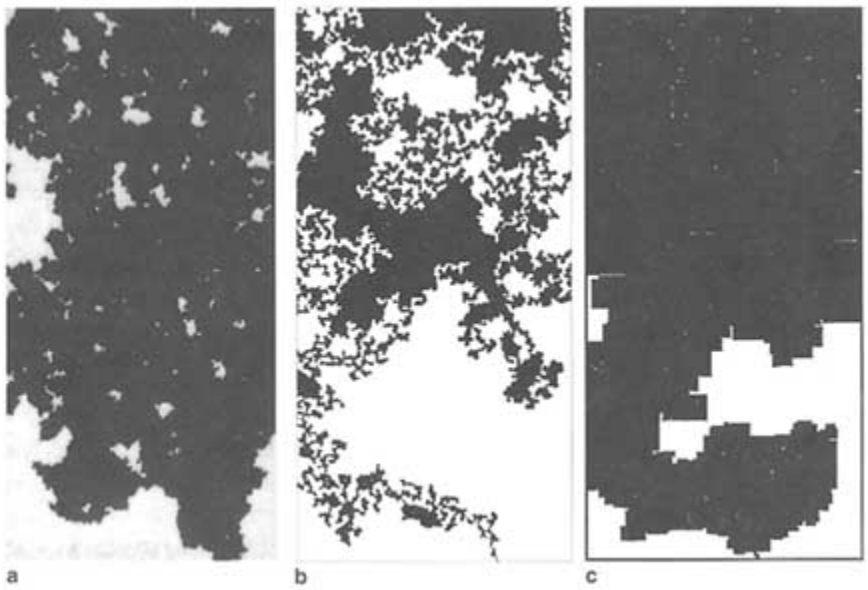

FIGURE 3.13 Phase structure at breakthrough in a rough-walled analog fracture with water (the wetting fluid, black) entry along the short side of the fracture (figure top) and air (white) exits along the other three sides of the fracture. Parts (a), (b), and (c) depict an experiment, a simulation using invasion percolation, and a simulation using a modified invasion percolation model, respectively. Simulations in parts *b* and *c* were carried out on the measured aperture field for the experiment a quarter of the size of that shown in part *a*. Gray areas in the simulation depict entrapped air phase. From Glass (1993).

For fractures that are nonhorizontal, gravity combines with capillarity under quasi-static conditions to dictate the sequence of fracture apertures that fill with the displacing phase. When the denser fluid underlies the lighter one, which is infiltrating from above, gravity tends to flatten the interface as displacement proceeds. However, if the more dense fluid is above the less dense fluid, gravity destabilizes the interface, resulting in the formation of gravity-driven fingers, even under quasi-static conditions. Experiments and simulations of gravity-driven fingering in the quasi-static limit show that the fingers widen and meander/branch as the inclination of the fracture with respect to the vertical decreases (Glass, 1993; Nicholl et al., 1993b). The opposite holds for fluids infiltrating from below. For example, air moving up into water-filled fractures will finger.

Dynamic Conditions

In situations where viscous forces are important, they combine with capillary, gravitational, and inertial forces (for large Reynolds numbers) to yield phase structure. In general, determination of the phase structure requires that the Navier-

Stokes equations for each fluid be solved with boundary conditions at the moving fluid/fluid interface incorporating a dynamic contact angle (Dussan, 1979; de Gennes, 1985). Although solution approaches based on cellular automata are under development (e.g., Stockman et al., 1990), this is still an intractable problem. Approaches that include accessibility rules and first-order viscous forces in the form of a modified invasion percolation model have been applied to porous networks and may be useful for fractures. Phase structures, however, may not be stable, and a variety of phenomena can occur, including viscous and gravity-driven fingering, flow pulsation, and blob flow (i.e., when one phase moves through another phase as a disconnected unit).

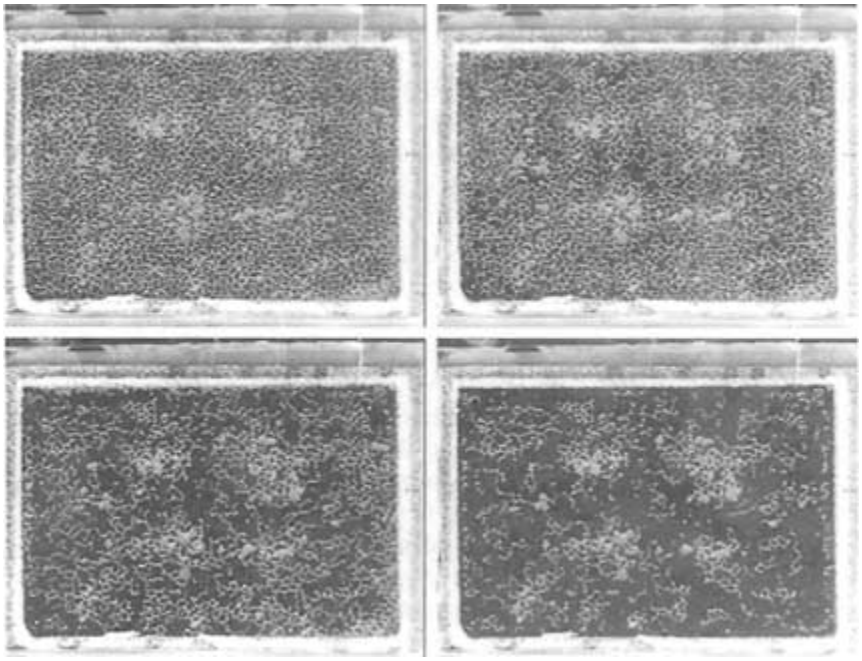

FIGURE 3.14 Growth of phase structure as a function of increasing liquid pressure (sequence is upper left, upper right, lower left, lower right) in an analog fracture/matrix system. Water (the wetting phase, black) enters the fracture from the saturated matrix. Air (the nonwetting phase, white) exits the fracture around the fracture edges. Courtesy of R. J. Glass.

Viscous and gravity-driven fingering have been studied in smooth-walled fractures (Hele-Shaw cells) as an analog for two-phase flow in porous media. Linear stability analysis of the problem shows three factors to be influential in determining interfacial stability during a steady one-dimensional vertical downward displacement of one fluid (indicated by the subscript 2 below) by another (indicated by the subscript 1 below) in a smooth-walled fracture of aperture b:

(1) the fluid viscosity difference (μ_1 - μ_2), (2) the fluid density difference (p_1 - p_2), and (3) the interfacial velocity (U) (Saffman and Taylor, 1958; Chouke et al., 1959). This result suggests instability for all wavelengths when the inequality

$$\frac{b^2 g \cos\theta}{12}(p_1 - p_2) - U(\mu_1 - \mu_2) > 0 \qquad (3.8)$$

is satisfied, where g is the gravitational acceleration and θ is the fracture inclination with respect to the gravity vector. Although several assumptions have been made to derive this equation (e.g., that the fracture is smooth walled, fluids are incompressible, disturbances are infinitesimal, and capillary forces are negligible), the relationship between buoyant and viscous forces is instructive. Flows are seen to be either stabilized or destabilized by viscosity and density differences with the interfacial velocity modifying the viscosity difference. The role of capillarity at the interface has not been included in the derivation of Eq. 3.8; however, when it is included, it limits the unstable wavelengths to be above a minimum value. Most research has concentrated on viscous-driven fingering in smooth-walled fractures in the absence of gravity (see reviews by Saffman, 1986, and Homsy, 1987). Gravity-driven fingering has been studied recently in rough-walled analog fractures for air/water systems (Nicholl et al., 1992, 1993a,b; see Appendix 3.B).

Flow pulsation and/or blob flow has been noted in several experiments in transparent analog fractures. Pulsation was observed to be a function of flow rate during relative permeability experiments (Persoff et al., 1991). Flow pulsation and blob flow also have been documented to occur as flow rate through a stable gravity-driven finger is reduced (Nicholl et al., 1993b). In both of these situations, local interactions of the wetting and nonwetting fluids yield system dynamics that have the potential to be chaotic (see Appendixes 3.B and 3.C).

SEISMIC PROPERTIES

The two properties that characterize seismic wave propagation in all media are velocity and attenuation. Velocity is a function of the elastic moduli and density of the medium. Attenuation is a measure of the energy lost from the wave as it propagates. In general, fractures cause a decrease of the modulus of elasticity of the rock and hence a reduction in seismic velocity. They also cause energy loss, leading to increased attenuation. The physical processes governing both effects are discussed in the following sections. In most applications the seismic wavelength is large compared to fracture size (areal extent) and spacing, so the effects of individual fractures are embedded in parameters describing the bulk material behavior. These effective media models are discussed in the next section. More recently, the effects of individual fractures have been modeled explicitly, as discussed later in this chapter under "Discrete Fracture Effects."

Effective Media Models

Velocity

Fractures affect the elasticity (modulus) of a rock because of the discontinuity of local elastic displacements across the fracture face. This discontinuity affects the propagation of seismic waves according to the ratio of fracture size to the seismic wavelength. Considering that any seismic pulse consists of a spectrum of wavelengths, a single fracture will act as a discrete scatterer for those wavelengths that are longer or comparable in size. The resulting radiation pattern depends on the orientation of the fracture with respect to the incident wave. Such scattering effects are common in the sonic frequency band used in acoustic logging.

More commonly (in the seismic context), fractures are small compared to seismic wavelengths; in the limit, many small scatterers are equivalent to an effective medium with decreased velocity and increased attenuation. If the fractures have a preferred orientation, the effective medium is anisotropic.

The physics of fracture-wave interaction is well understood in principle, but the complexity of natural geometries imposes the need for simplifying assumptions. A number of different approximations, utilizing different levels of phenomenology and geometric idealization, are available, as discussed below.

At the most phenomenological level, Schoenberg and Muir (1989) have presented a calculus for constructing a rock by linear combinations of grains, pores, and cracks of known compliance (normal and tangential). This formalism sidesteps all the physics connecting effective compliance to fracture geometry as well as all nonlinearities and rock-fluid mechanical interactions.

If the crack shapes are idealized as very thin oblate ellipsoids, the modulus of the rock and hence the seismic velocities are calculable in terms of aspect ratios (thickness/length) of the ellipsoids and the elastic properties of the surrounding matrix and fluids (see Budiansky and O'Connell, 1980, and references cited therein). If the crack density is small, the decrease in the modulus also is small and is well understood in terms of the properties of the matrix, the fluid, and the crack geometry. If the crack density is large, the corresponding modulus decrease is large. However, there is no consensus about how to treat the nonlinearity arising from large densities. Any theoretical treatment must be consistent with the classic work of Biot (1956) if it shares the same assumptions, such as a locally uniform value for the perturbation in pore pressure caused by the elastic wave (Thomsen, 1985).

If the thin and flat cracks are isolated from the equant pore space, the modulus decrease depends also on the crack aspect ratio and crack density (Hudson, 1980). The presence of liquid (rather than gas) in the cracks considerably stiffens them for *P*-wave propagation. However, if the cracks are hydraulically connected to the equant pore space, the liquid may squirt from crack to pore, reducing the stiffening effect (Thomsen, 1991). This mechanism and its effects on modulus were recently confirmed in experiments conducted by Rathore et al. (1991).

Attenuation

Heterogeneity causes scattering, which results in attenuation and dispersion. Fluid-filled fractures have several attenuation mechanisms that arise because of the viscosity of the fluid (Budiansky and O'Connell, 1980). At the highest (megahertz) frequencies, energy losses caused by laminar flow dominate. At ultrasonic to sonic frequencies, energy loss caused by fluid motion from cracks to pores ("squirt flow") dominates, depending on a characteristic frequency, f_s, given by

$$f_s \approx \frac{3\epsilon^3(1 - \nu^2)}{\gamma E}, \qquad (3.9)$$

where $\in$ is the crack aspect ratio (thickness/length; Budiansky and O'Connell, 1980). For brine in sandstone, with $\in$ in the range of 0.01 to 0.001, f_S is 10^3 to 10^6 Hz. However, high-viscosity fluids (e.g., hydrocarbons) can lower f_s into the seismic range (Jones, 1986). While this particular equation shows that seismic attenuation is strongly dependent on the crack aspect ratio, it implies, more generally, that attenuation is strongly dependent on fracture microgeometry.

At seismic frequencies in brine-filled rock, local flow may equalize the fluid pressure locally, and the predominant mechanism of attenuation may be global flow, as identified by Biot (1956).

Discrete Fracture Effects

It is generally accepted that one of the most important developments in seismic geophysics is improved structure resolution. There is, therefore, an emphasis on the development of high-frequency sources, particularly for cross-well or reverse (borehole to surface) vertical seismic profiling applications. Wave propagation in this case cannot be adequately represented by effective media models because the planar extent of fractures, as well as their spacing, is large or comparable to the wavelength of the propagating wave. The effects of each discrete fracture must be evaluated.

As described in the first section of this chapter, a fracture can be envisioned as a collection of voids separated by contacting asperities, all lying in a plane. Each of these voids is a scatterer, as discussed in the previous section. However, as long as the wavelength of the propagating wave is long compared to the spacing of the voids, an areal average value of the discontinuity in elastic displacements occurring at the voids can be assumed in calculations of the far-field reflected and transmitted wave fields. Such an approach is called a seismic displacement discontinuity model. Because the average displacement discontinuity is equal to the ratio of the applied stress and the mechanical stiffness of the fracture, the boundary conditions for reflection and refraction of a plane wave incident on the

fracture can be written as

$$u_{\mathrm{I}} - u_{\mathrm{II}} = \frac{\sigma}{\kappa}, \sigma_{\mathrm{I}} = \sigma_{\mathrm{II}}, \qquad (3.10)$$

where u refers to particle displacements, σ is the time-varying seismic stress, κ is the stiffness of the fracture, and the subscripts I and II refer to the media on either side of the fracture. Eq. 3.10 shows that displacements are discontinuous across a fracture by the amount σ / κ, whereas stresses are continuous. Using the boundary conditions given in Eq. 3.10, solutions for obliquely incident waves and for materials with different properties on each side of a fracture have been obtained (Schoenberg, 1980; Pyrak-Nolte et al., 1990b). The effects of multiple fractures have been modeled by Schoenberg (1983) and Pyrak-Nolte et al. (1990c). The displacement and discontinuity model predicts from a single set of assumptions that a fracture will cause a group time delay and a loss in amplitude of the transmitted wave, the magnitude of which depends on the frequency and on the ratio of fracture stiffness to the seismic impedance of the intact rock. (The term "group" refers to an energy-carrying packet of frequencies in the propagating wave. The group time is what is normally used in laboratory and field measurements to compute the seismic wave velocity.) The group time delay can be used to calculate an effective group velocity that also is time dependent (Pyrak-Nolte et al., 1987b). General characteristics of the theory are illustrated by Figure 3.15, which shows the theoretical magnitudes of the transmission and reflection coefficients and normalized group time delay for a seismic wave normally incident on a single fracture. The value $|R|$, the coefficient of reflection, increases, while the value $|T|$, the coefficient of transmission, decreases, owing to conservation of energy. The figure also shows that $|T|$ is a maximum at zero frequency, where $|R|$ is a minimum. The normalized group time delay is a maximum at zero frequency and decreases with increasing frequency. As stiffness approaches infinity, the displacement discontinuity becomes equivalent to a welded interface, and all the energy is transmitted. If the stiffness tends to zero, the displacement discontinuity reverts to the case of a free surface, and all the energy is reflected.

Fracture stiffness, κ, is defined as

$$\frac{1}{\kappa} = \frac{\delta}{\sigma}, \qquad (3.11)$$

where $\bar{\delta}$ is the areal average displacement in the plane of the fracture. The relationships between displacement in a fracture and the void geometry are discussed in detail later in this chapter under "Stress Effects on Fracture Void Geometry." Conceptually, κ can be considered the tangent to the stress displacement curve obtained in a mechanical deformation test on a fracture (cf. Figure 3.5). The tangent is taken at the value of stress representing the in situ stress (not the seismic stress) on the fractures. In actual fact it is not clear that the dynamic value of κ (for a seismic wave) is equivalent to that measured in the

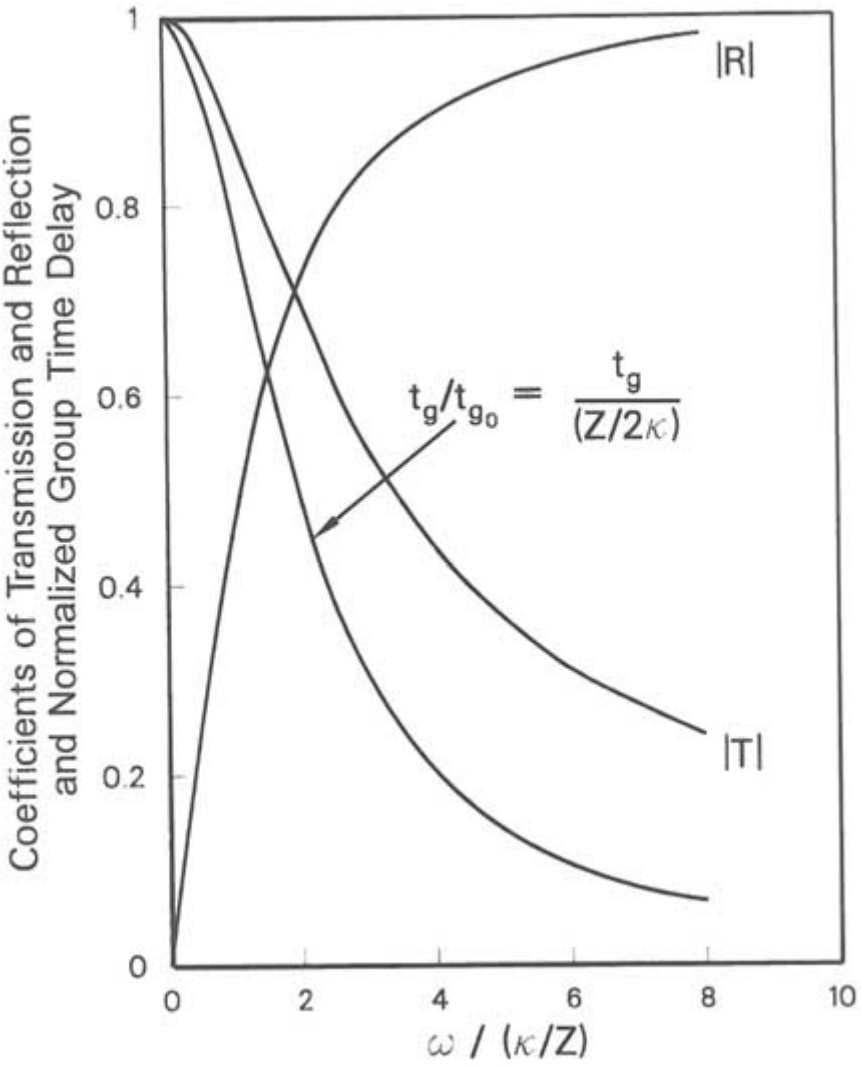

FIGURE 3.15 Magnitudes of the reflection and transmission coefficients and normalized group delay for a seismic wave normally incident on a displacement discontinuity as a function of normalized frequency; ω is circular frequency, κ is fracture stiffness, Z is seismic impedance, t_g is group time delay, $|R|$ is the coefficient of reflection, and $|T|$ is the coefficient of transmission. From Pyrak-Nolte et al. (1990b).

laboratory in a pseudostatic loading test. Work by Pyrak-Nolte et al. (1990b) suggests that the dynamic values of κ may be higher, possibly owing to frictional lockup of asperities in contact.

Although κ in general must be measured, some simple special cases have been analyzed for purposes of validation of the theoretical concept. For the very simplified geometry of a row of two-dimensional cracks of length $2c$ (e.g., Figure 3.11) with a uniform spacing of $2l$, the average displacement, $\bar{\delta}$, due to stress, σ, applied normal to the plane containing the row, is given by (Tada et al., 1973)

$$\bar{\delta} = \frac{-8\sigma l(1 - \nu^2)[ln \cos (\pi c/2l)]}{\pi E}, \qquad (3.12)$$

where E and ν are the Young's modulus and shear modulus, respectively, of the intact rock. The normal stiffness for this model can be found by combining this equation with Eq. 3.11:

$$\frac{1}{\kappa} = \frac{-8l(1 - \nu^2)[ln \cos (\pi c/2l)]}{\pi E}, \qquad (3.13)$$

Interestingly, because the expression for shear displacements under shear stress acting in the plane perpendicular to the cracks is identical to that for normal stress, the expressions for normal and shear stiffness also are equivalent, assuming frictional lockup of the contacting asperities between the cracks.

Using κ from Eq. 3.13, the wave equation can be solved to find the transmission and reflection coefficients for a row of cracks. Angel and Achenbach (1985) showed that the solution is equivalent at long wavelengths to that obtained for elastic wave scattering by a row of cracks. Myer et al. (1985) performed laboratory seismic measurements on an idealized fracture for which stiffness could be calculated by using Eq. 3.13 and found good agreement between their results and those predicted from the seismic displacement discontinuity model.

The seismic displacement discontinuity model has been compared with laboratory measurements on samples containing single natural fractures (Pyrak-Nolte, 1990a). These measurements showed that the fractures caused the frequency-dependent attenuation of both compressional and shear waves. The amount of attenuation decreased as the stiffness of the fracture increased with the addition of stress normal to the fracture. The seismic displacement discontinuity model successfully predicted the observed effects of the fractures.

If a fracture is modeled as an elastic interface, as noted above, no energy is lost in the system. To account for energy loss, which occurs when fluids or infillings such as clay are present in a fracture, a velocity discontinuity may be assumed. Solutions for Kelvin and Maxwell rheologies, which are two realizations of combined velocity and displacement discontinuity models, have been obtained (Myer et al., 1990a). Laboratory results indicate that the velocity discontinuity model provides an excellent representation of the attenuation of shear waves by

fractures containing clay and fluid of different chemistries (Suarez-Rivera et al., 1992). Field evaluation of the model is needed, however.

Appendix 3.A discusses the theory underlying this model.

Relationship to Hydraulic Properties

The geometry and volume of the void space control fluid flow and (as discussed earlier, under "Shear Stress Conditions") can be used as a basis for predicting the effects of fractures on seismic wave propagation. There should therefore be qualitative, if not quantitative, relationships between hydraulic and seismic properties of fractures.

One property important to both hydraulic and seismic behavior is the stiffness of the fracture. In an elastic system, fracture stiffness determines the change in void volume resulting from a change in applied stress. Carlson and Gangi (1985) produced a unified model that describes both the elastic and hydraulic effects of fractures. An extra degree of freedom, which describes the statistics of asperity heights, is used. In laboratory tests on natural fractures, a rank correlation between stiffness, hydraulic conductivity, and seismic amplitude is observed (Pyrak-Nolte et al., 1987a; Myer, 1991). That is, the least-stiff fracture has the highest hydraulic conductivity and lowest transmitted wave amplitude; the converse is true for the stiffest fracture. Because there is a nonunique relationship between void geometry and stiffness, the relationship between permeability and stiffness also is nonunique. However, it would be of great practical benefit to establish even empirical relationships between these parameters.

Under some conditions, the dynamic stresses imposed on a fracture by a propagating wave can produce fluid motion, the magnitude of which is a function of the fracture permeability. The energy used in producing fluid flow in turn affects wave propagation. A well-studied example is the interaction of Stonley (tube) waves with fractures intersecting a borehole. Tang et al. (1991) developed a model that relates the attenuation of the Stonley wave to the permeability of the fracture. Results of these and other studies (e.g., Paillet et al., 1987) indicate that fractures are better modeled as a thin, stress-sensitive porous medium than as parallel plates.

ELECTRICAL PROPERTIES

Bulk Properties

A number of theories have been proposed to describe bulk electrical properties based on properties of the constituents. Most commonly, a rock is considered a two-component mixture, where the mineral grains are one component and the fluid (usually a liquid) occupying the voids between the grains is the other. The volume fraction occupied by the fluid is defined as the porosity.

An empirical relationship that relates bulk resistivity to pore fluid resistivity and porosity at low frequencies was established by Archie (1942):

$$\frac{\rho_r}{\rho_w} = F = \alpha\phi^{-n}, \qquad (3.14)$$

where ρ_r is the bulk resistivity of the rock, ρ_w is the pore fluid resistivity, F is the formation factor, φ is the porosity, n is the cementation factor (approximately 1.5), and α is a dimensionless parameter (approximately unity). This equation is known as Archie's law and has found wide application in estimating porosity from resistivity measurements. Several variations of the formula exist that are considered to be more accurate for certain rock types. Archie's law is discussed in terms of the equivalent channel model by Walsh and Brace (1984).

The bulk electrical conductivity also depends on fluid saturation in the pores, assuming the matrix is nonconductive. Empirical relationships have been found that relate the percent water saturation and clay concentration to the bulk conductivity (e.g., Simandoux, 1963).

At high frequencies, equations describing electric properties become more complex, and a number of theories have been published. Some of these are reviewed by Sihvola (1989). Based on the theory of self-similar systems, Sen et al. (1981) derived a mixture formula for a two-component system known as the Bruggeman-Hanai-Sen equation. In the direct current limit, this equation reduces to Archie's law. Reasonable agreement between the mixture formula and experimental data has been reported (Shen et al., 1985; Sihvola, 1989).

In low-porosity rocks with low-conductivity pore fluids, surface conduction along grain boundaries becomes a significant factor, requiring the addition of a surface conduction term to Archie's equation (Brace et al., 1965; Magnusson et al., 1987). Hence, surface conduction will give a higher bulk conductivity than if conductivity was attributed only to the pore fluid. For clay-bearing rocks, surface conduction is usually a significant factor. Expressions for the bulk conductivity of such rocks have been given by, for example, Waxman and Smits (1968). Their expression includes a term that takes into account the dependence of the mobility of exchange cations on pore water concentration and the clay cation exchange capacity per unit volume.

The electrical conductivity of rock can vary by several orders of magnitude, depending on rock type. The extensions of Archie's law discussed above give reasonable values of conductivity for low-porosity granites with conductivities on the order of 10^{-5} siemens per meter as well as porous brine-saturated sandstone with conductivities on the order of 1 siemen per meter.

The conductivities of rocks containing conductive minerals such as graphite, pyrite, or certain ore-bearing minerals cannot be described using Archie's law or similar formulas. In such cases, conduction is dominated by the volume fraction and conductivity of the mineral grains; the contributions from porosity and pore fluids are negligible.

The porosity of a fracture is localized in a very thin planar feature. For sparse fracture spacings the fracture porosity may not be significantly larger than the matrix porosity. However, if the fractures are connected, they will provide significant paths of conduction in the rock mass. Additionally, because the void space connectivity changes with stress, fracture conductivity is stress dependent. A fractured rock mass may therefore be visualized as a matrix of one conductivity containing thin sheets of a second stress-sensitive conductivity.

The effects of the presence of such features on the bulk properties discussed above require further study. Measurements of electrical properties of fractures have rarely been undertaken. However, some insights have been gained, as discussed below, from studies using fluid flow analogies for conduction.

Relationship Between Hydraulic and Electrical Properties

The idea of comparing the hydraulic and electrical properties of rock is not new. Simultaneous measurement of fluid permeability and electrical resistivity is in fact a well-established practice for core analysis in the oil industry. The hydraulic and electrical conductivities of rock should be related because of the similarity between the differential equations describing each process. If a fracture is modeled as two parallel plates, the flow rate per unit width is given by Eq. 3.2 and the permeability, K, by analogy with Darcy's law, is $K = b^2/12$, so that

$$Q = \frac{Kb}{\gamma}\nabla P, \tag{3.15}$$

If the space between the plates is filled with an electrolyte, the electric current per unit width is proportional to the first power of the aperture according to Ohm's law

$$I = \frac{b}{\rho}\nabla V, \tag{3.16}$$

where ρ is the resistivity of the electrolyte.

From these equations it is seen that the volumetric flow rate, Q, is analogous to the electric current, I. The fluid pressure, P, is analogous to the electric potential, V, and the properties of the fluid are described by the dynamic viscosity, γ, and resistivity, ρ.

Brown (1987, 1989) assumed that the topography of the fracture surfaces varies slowly in the plane of the fracture (i.e., that the slopes are small) and that the parallel-plate results for the transport properties hold locally. Conservation of mass and charge also are assumed. Brown found that these conditions lead to Reynolds's equation for fluid flow:

$$\nabla \cdot (b^3 \nabla P) = 0 \tag{3.17}$$

and an analogous equation for the conduction of electricity:

$$\nabla \cdot (b\nabla V) = 0.$$

The local aperture b is actually a function of the spatial coordinates in the plane of the fracture (i.e., $b = b(x,y)$). These differential equations can be used to model both fluid flow and transport of electric current through a rough fracture if the aperture distribution $b(x,y)$ is known. Using a fractal algorithm, Brown (1987, 1989) generated rough surfaces, and pairs of surfaces with the same fractal dimension were placed together to form a "fracture." Calculations of the volume flow rate and electric current fields of one such fracture are shown in Figure 3.16. The electric current is more diffuse over the fracture than the fluid flow. The fluid flow is more strongly affected by the surface roughness, with the large aperture channels playing the dominant role in transport.

This observation supports the conceptual model of Tsang and Tsang (1987) for channel flow through fractures. The difference between the fluid flow and electric current fields is due to their cubic versus linear dependence on aperture. Figure 3.17 shows an overlay of the left center portions of the flow fields shown in Figure 3.16. Note that in general the fluid flow and electric current vectors do not have the same orientations. In other words, fluid particles and charged ions take different paths through the fracture.

Model results have also demonstrated that the arithmetic average aperture, when used in the parallel-plate model, overestimates both the volume flow rate and the electric current through rough-walled fractures (Brown, 1989). This is due in part to the tortuous paths both fluid particles and charged ions must take around the surface roughness elements.

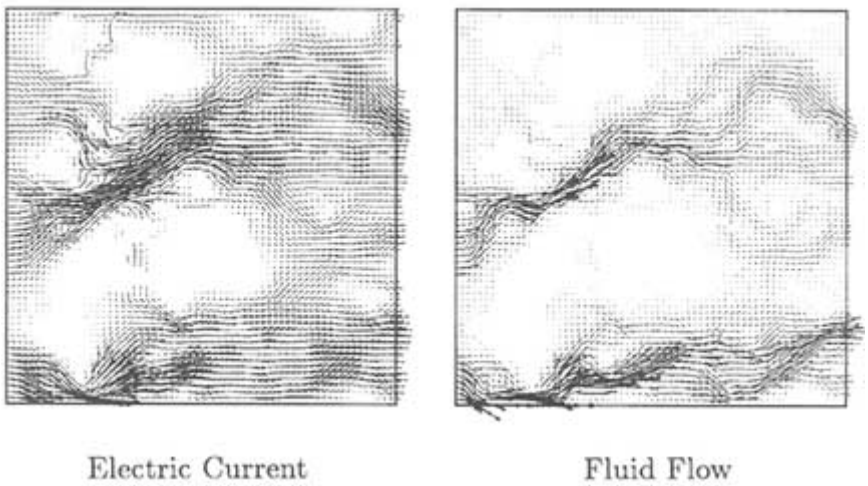

FIGURE 3.16 Electric current and volume flow rate fields of a fracture generated by using a fractal algorithm. The magnitude and direction of the local electric current and volume flow rate are represented by small arrows. From Brown (1989).

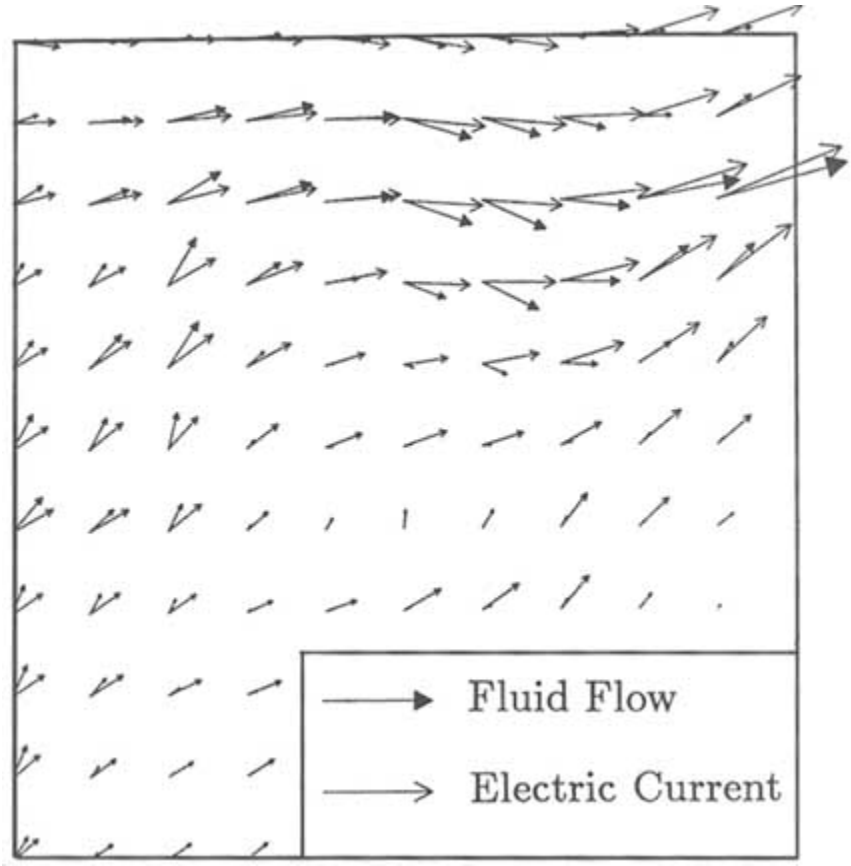

FIGURE 3.17 Overlay of the left center portions of the flow fields shown in Figure 3.16. From Brown (1989).

The relationship between hydraulic and electrical properties changes with deformation. Figure 3.18 compares hydraulic and electrical properties as a function of dimensionless aperture, b_m/h_{rms}, where b_m is the mechanical aperture and h_{rms} is the rms surface height of the fracture surfaces (Brown, 1989). Calculations were carried out for fractures generated by using surfaces with a range in fractal dimension (D). Points labeled "CV" result from apertures calculated by using conservation of volume (cf. "Normal Stress Effects" earlier in this chapter). The hydraulic (b_h) and electric (b_e) apertures are nearly the same when the surfaces are widely separated (i.e., $b_m/h_{rms} >> 1$). However, b_e becomes progressively smaller than b_h as the fracture closes. These results suggest that electrical conduc

tivity measurements underestimate the hydraulic conductivity of fractured rock and the total fracture volume by a percentage that increases as the fractures close.

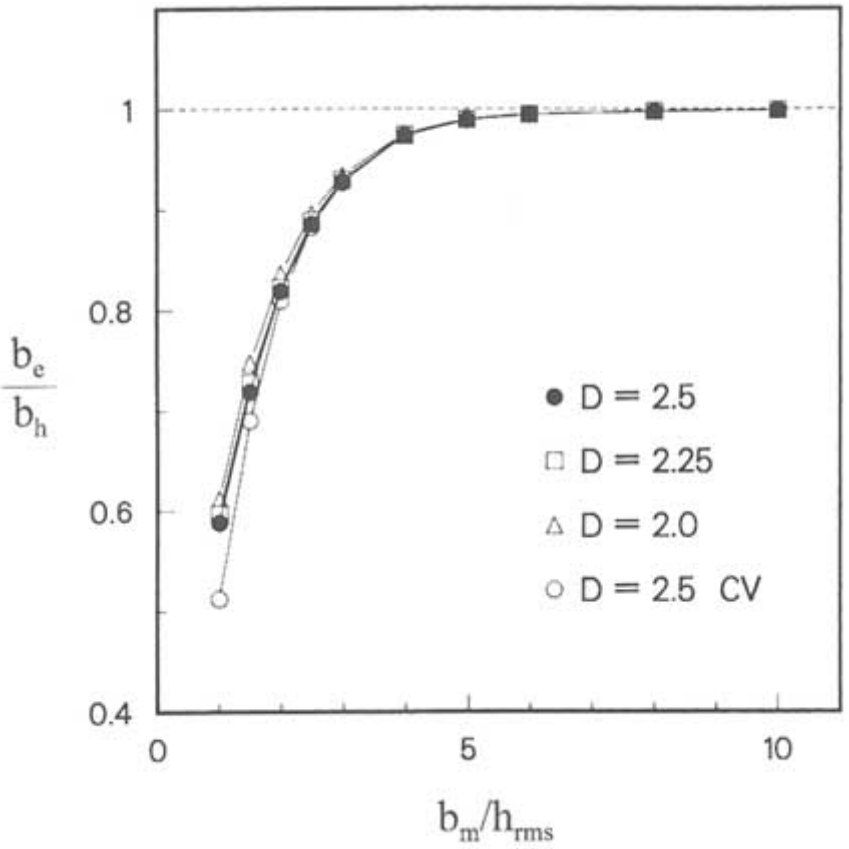

FIGURE 3.18 Ratio of the electric aperture (b_e) to the hydraulic aperture (b_h) as a function of mechanical aperture (b_m) and the rms height of the fracture surfaces (h_{rms}) for fractures with different fractal dimensions (D). "CV" denotes conservation of volume. From Brown (1989).

The results of Brown (1989) are consistent with the "equivalent channel model" presented independently by Paterson (1983) and Walsh and Brace (1984), which explains the relationship between permeability and formation factor. The essence of the equivalent channel model is the existence of a "typical" pore geometry that describes the behavior of the system. These equivalent channels are assumed to have a simple geometry, for example, cylindrical tubes for the pores in sandstones and parallel plates for microcracks in granites. The channels may not be straight. That is, the path length of the fluid may be longer than the

nominal length of the specimen. Porosity (φ) is defined as the fractional area of pore space as observed on a cross section through the specimen, and tortuosity (τ^2) is defined as the square of the ratio of the actual path length to the nominal path length.

For channels of constant cross section, such as cylindrical tubes or parallel plates, the microscopic geometry can be used to predict the macroscopic permeability (K) and formation factor (F) (Walsh and Brace, 1984):

$$K = \frac{r}{r_f}\frac{\phi}{\tau^2} \qquad (3.19)$$

and

$$F = \frac{\tau^2}{\phi}, \qquad (3.20)$$

where r is the hydraulic radius (r = radius/2 for cylindrical tubes; $r = b/2$ for parallel plates), and r_f is the shape factor ($r_f = 2$ for cylindrical tubes; $r_f = 3$ for parallel plates). In the derivation of Eqs. 3.19 and 3.20, tortuosity is assumed to be the same for the flow of fluid and electric current. By combining measurements of K and F, some useful information could conceivably be obtained about the pore geometry (i.e., a combination of τ, r, and r_f).

Conventionally in core analysis the logarithm of permeability is plotted against the logarithm of the formation factor for many specimens of a given rock type from a particular oil reservoir. If a clear relationship is observed, electrical resistivity measurements from well logging can be used to estimate the permeability. Often, there is a linear relationship between the permeability and the formation factor in logarithmic coordinates (e.g., Archie, 1942; Walsh and Brace, 1984). The slope of the line defining the relationship is s, given by

$$s = \frac{-d\log K}{d\log F}, \qquad (3.21)$$

The equivalent channel model shows that for fracture like pores s indicates how sensitive the tortuosity is to changes in fracture aperture through the following expression (Walsh and Brace, 1984):

$$\log\left(\frac{\tau^2}{\tau_o^2}\right) = \left(\frac{3-s}{1-s}\right)\log\left(\frac{b}{b_o}\right), \qquad (3.22)$$

where the subscript o indicates an arbitrary reference value. It appears that s is bounded between the values of 1 and 3. For s ÷1 the tortuosity is very sensitive to changes in aperture. It can be shown that for an ideal parallel-plate fracture, where the hydraulic aperture equals the electric aperture, s ð 3. Laboratory measurements on porous rock yield $1.5 \leq s \leq 2.8$, with a typical value close to $s = 2$ (Walsh and Brace, 1984; Bernabe, 1986, 1988).

Figure 3.19 shows the logarithm of macroscopic permeability versus the logarithm of formation factor from numerical simulations of a hypothetical rough-walled fracture generated by using rough surfaces of fractal dimension D = 2.5 (Brown, 1989). The points along this curve correspond to various values of dimensionless aperture (b_m/h_{rms}; see Figure 3.18). The curve is nonlinear; its slope varies from about -3 when the fracture walls are separated ($b_m/h_{rms} > 4.25$) to about -2 when the walls are in intimate contact ($b_m/h_{rms} << 4.25$). This implies that when the surfaces are widely separated the tortuosity is not sensitive to changes in aperture. This agrees with intuition because, when the surfaces are separated, changes in aperture should not significantly change the lengths of the

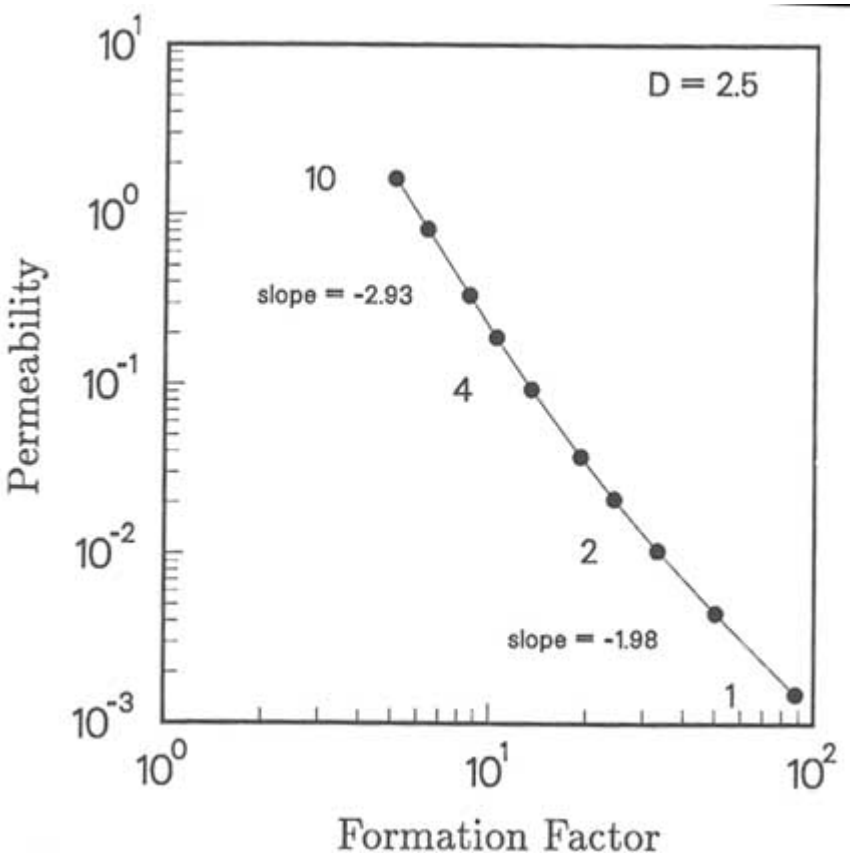

FIGURE 3.19 Permeability as a function of formation factor for a fracture composed of surfaces with fractal dimension D = 2.5. The permeability and formation factor were computed by using the hydraulic and electric apertures for the fracture. The labels 1, 2, 4, and 10 refer to the dimensionless aperture b_m/h_{rms}. Slopes are given for the two intervals 1–2 and 4–10. From Brown (1989).

streamlines. When the fracture surfaces are in contact, however, the tortuosity becomes increasingly sensitive to changes in aperture, as shown by the change of slope in Figure 3.19. Therefore, the parallel-plate model, which does not account for the extra path length, will overestimate both the volume flow rate and the electric current.

SUMMARY

With few exceptions, any fracture can be visualized as two rough surfaces in contact. In cross section the voids and solid areas representing asperities in contact are analogous to the pores and grains of porous media. Consequently, the general equations describing flow, transport, and chemical processes are equally applicable in fractures and porous media. One major difference between the two is that the void space of the fracture is interconnected in one plane, so the fracture is best described as a two-dimensional porous medium. The second major difference is that the void space of fractures tends to be more cracklike in shape than that of porous media. This difference leads to greater stress-sensitive properties of fractures. The observed flow and transport behavior of fractures can, to a great extent, be explained in terms of the geometry of the void space and the changes in this geometry brought about by changes in effective stress and fluid chemistry.

Further work is needed to characterize the statistical properties of fracture void space and how these properties vary with rock type, geological origin, and changes in stress. Although understanding the roughness of surfaces is an important element of such studies, more emphasis is needed on direct characterization of the void space; it is not at all clear what relationship, if any, there is between the roughness of the fracture surfaces and the geometric properties of the void space that remains when the fractures are in a mated condition. Both the geometric properties of the void space and the fracture surface roughness need to be described as stochastic processes.

The change in fracture void geometry owing to an applied normal stress can be effectively modeled for many rock types, assuming the rock is a linearly elastic material. This assumption is not sufficient when the applied stresses involve a combination of normal and shear stresses. Even though extensive effort has been directed toward measuring the mechanical deformation and strength of fractures under combined normal and shear stresses, there is only rudimentary understanding of the relationship between the measured mechanical response and changes in void geometry, which affect flow or transport properties.

The basic phenomenological relationships between single-phase flow, void geometry, and changes in normal stress are well understood. The cubic law adequately models flow under laminar conditions at any point in a fracture. However, under changing effective stress conditions, there is not an equivalence between the change in aperture required by the cubic law and the macroscopic

deformation of the fracture under changing stress. Additional measurements of void volume change can be made, but they are cumbersome. The most feasible alternative is direct measurements of permeability, either in the laboratory or in the field, under effective stress representative of in situ conditions. This further implies that models that incorporate a coupling of stress and flow should do so through a permeability-stress relationship, rather than through a permeability-aperture relationship.

Very little is understood about the basic phenomenological relationships between single-phase flow and fracture void geometry under combined normal and shear stresses, or between multiphase multicomponent flow and fracture void geometry under any conditions. More emphasis should be placed on measurements on natural fractures or casts of natural fractures. It is clear that these processes depend strongly on the statistical properties of the void space, including the interconnectivity and spatial distribution, but it is not yet clear what statistical measures are representative of typical fractures.

Although direct measurement of flow properties is required, there is still a need for developing quantitative relationships between microscopic measurements of fracture void geometry and macroscopic flow properties. Direct measurements of fracture aperture, such as field measurements using "feeler" gauges, should be used in engineering practice in the same manner as measurements of pore sizes in rock. Methods for using microscopic void geometry to predict macroscopic flow properties also should be investigated. For example, effective medium theory and critical path analyses (Doyen, 1988; David et al., 1990) have been applied to describing flow throughout the three-dimensional void structure of porous rock. These or other techniques, when combined with analysis of void closure under stress, could lead to a better quantitative understanding of the relationships between void structure and flow in fractures.

For many engineering applications, detailed analysis of fracture void space or direct measurements of flow and transport properties may not be feasible. There is a need to establish relationships between the geological origin of fractures and flow and transport properties. As discussed previously, the geological history of a fracture will have important effects on its surface characteristics and hence on hydrological properties. The data bases needed for such relationships, such as those established by Barton et al. (1985), should be expanded.

The presence of fractures in a rock mass causes a reduction in seismic velocity and an increase in attenuation. These two effects form the basis for characterization of fractures by seismic methods. The effects of fracture properties on seismic velocity are well understood. Changes in velocity arise primarily from changes in the effective elastic modulus of the rock. Attenuation arises from a number of processes, including scattering, fluid motion, and viscous damping. Further work is required to develop quantitative predictive relationships for these effects. The incentive for pursuing such research is that the effects of fractures

on attenuation are usually considerably greater, in terms of percent changes, than their effects on velocities.

Depending on seismic wavelengths, fractures can be represented by effective properties of the bulk medium or as discrete entities. Information gained from seismic measurements when fractures are represented by effective properties is limited to fracture density and orientation assuming fractures result in anisotropic elastic properties. Modeling of discrete fractures has the potential to provide information on location and orientation. Further testing at field scales is needed to assess the applicability of the discrete fracture theories discussed in this chapter.

Electrical conductivity is strongly related to porosity of the rock mass. The contribution of fractures to this porosity is the primary basis for use of electrical measurements for characterizing fractured rock masses. This porosity, however, is localized in the plane of the fracture. An area requiring further study is the effect of this localization on bulk effective properties that are measured in the field.

Recent studies have indicated that qualitative, and perhaps quantitative, relationships exist between the hydrological properties of single fractures and their geophysical properties. Additional theoretical, laboratory, and field-scale work is needed to confirm and improve the understanding of these relationships.

Appendix 3.A

Seismic Displacement Discontinuity Theory

The seismic displacement discontinuity theory has been applied to modeling of cross-hole measurements in a basalt rock mass (King et al., 1986). *P*-wave measurements were made in four horizontal drillholes spaced 3 m apart in the wall of a drift (Figure 3.A1) at a depth of about 46 m above the water table. The fracture characteristics of the basalt are shown schematically in Figure 3.A1. The primary fracture set, which is nearly vertical, was formed between basalt columns that range in thickness from about 0.2 to 0.4 m. A secondary cross-cutting fracture set also is present. The wavelength of the *P*-waves is about 0.1 m.

The effects of the primary vertical fracture set on *P*-wave propagation are illustrated in Figure 3.A2. This figure shows typical examples of the first arriving *P*-wave pulses for three different borehole pairs. The pulse labeled "C1-C2" propagated between boreholes C1 and C2 (Figure 3.A1) in a direction parallel to the primary fracturing. The pulse "C4-C2" propagated obliquely to the primary

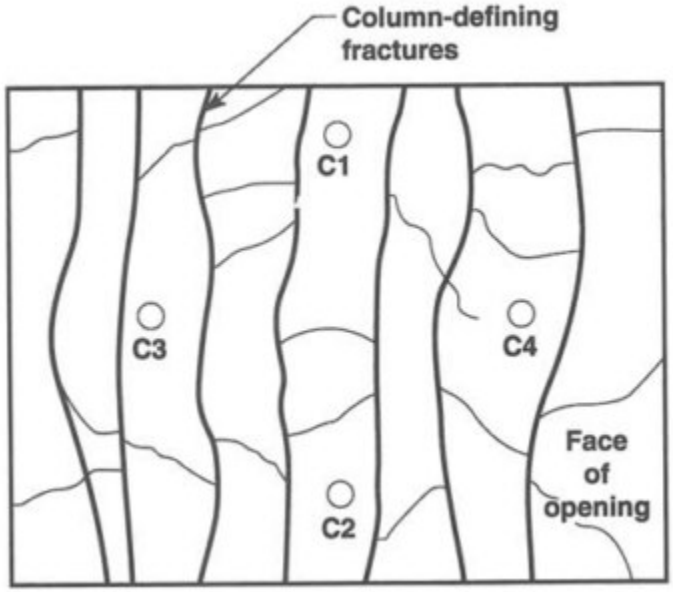

FIGURE 3.A1 Illustration of borehole configuration and fracture characteristics in crosshole field test. From Peterson et al. (1993).

fractures, whereas pulse "C3-C4" propagated orthogonally to the primary fractures. The differences in arrival times shown in the figure reflect the differences in wave velocities for the different propagation directions. It is seen that waves traveling obliquely to the primary fractures were slowed and attenuated with respect to fracture-parallel waves. The waves were almost completely attenuated in the direction perpendicular to the fractures.

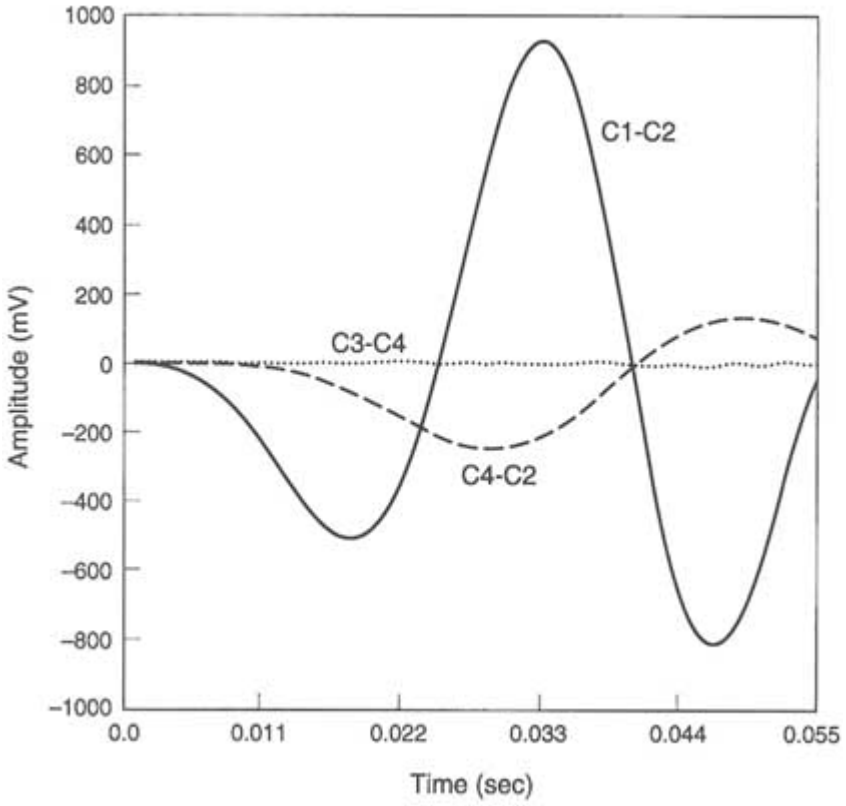

FIGURE 3.A2 Typical first arriving *P*-wave pulses from different borehole pairs. From Peterson et al. (1993).

In modeling the field results it was assumed that the observed differences in arrival times were due to the effects of the vertical fractures. In other words, except for differences due to travel path length, it is assumed that pulses traveling between all boreholes would be identical to those propagating vertically between C1 and C2 were it not for the effects of the vertical fractures. Pulses propagating between C1 and C2 were therefore used as reference pulses. The time delays and attenuations of pulses traveling in other directions were predicted by using

the seismic displacement discontinuity theory. The only parameters that needed to be estimated in the analysis were fracture frequency and fracture stiffness.

Figure 3.A3 shows results of the modeling of a typical pulse propagated between holes C4 and C2. Shown are the reference pulse, the measured pulse, and the predicted pulse assuming the wave propagated at a 45° angle of incidence across three fractures, each with a stiffness of 5×10^{11} Pa/m. It is seen that the seismic displacement discontinuity theory is able to predict the time delay, amplitude, and frequency characteristics of the measured pulse with a high degree of accuracy. For waves traveling between C3 and C4, six fractures were assumed because of the increased travel distance, but the stiffness of each fracture was held constant at 5×10^{11} Pa/m. As can be seen in Figure 3.A4, the theory predicted that the increased number of fractures should completely attenuate the pulse.

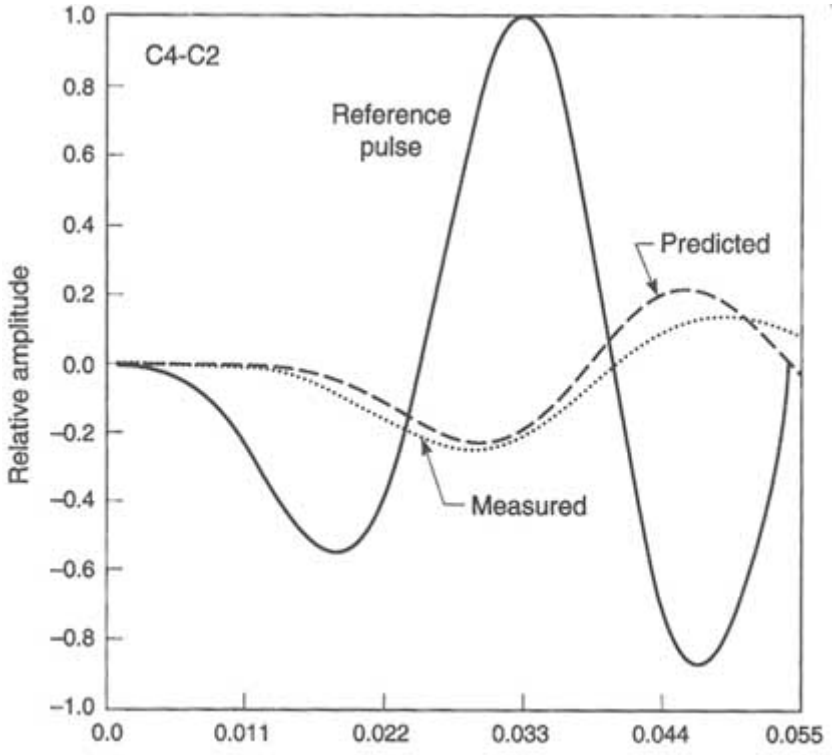

FIGURE 3.A3 Comparison of predicted and observed results for a pulse traveling between boreholes C4 and C2. From Peterson et al. (1993).

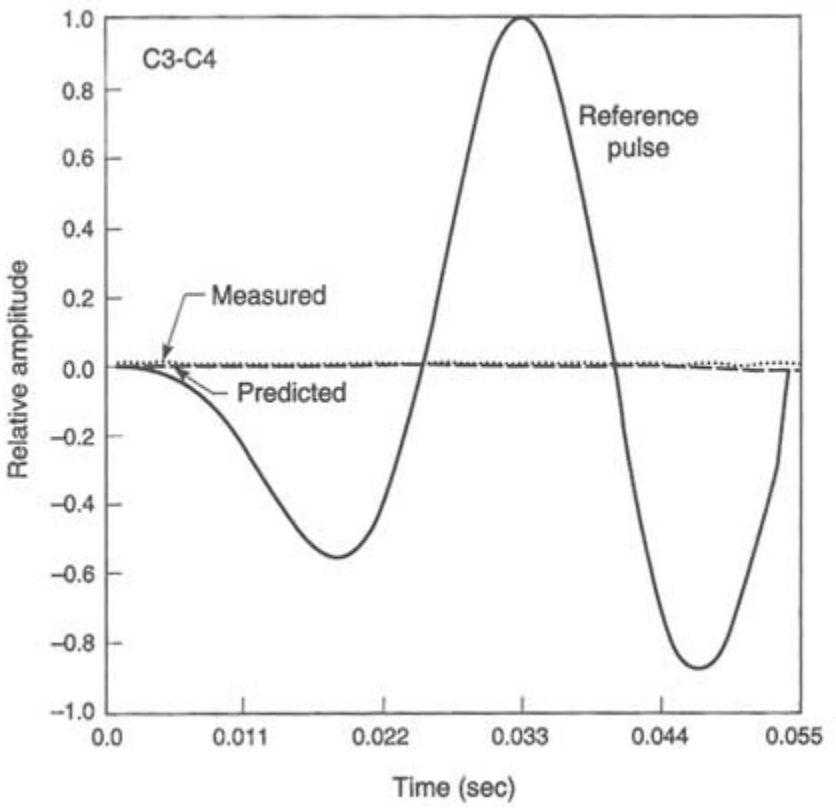

FIGURE 3.A4 Comparison of predicted and observed results for a pulse traveling between boreholes C3 and C4. From Peterson et al. (1993).

Appendix 3.B

Gravity-Driven Infiltration Flow Instability

Consider a rock unit containing extensive, initially dry, inclined fractures that outcrop at the surface. A typical fluid source for infiltration into such fractures is surface ponding resulting from a locally intense rainfall event. Preferential flow associated with local fracture heterogeneity or differential supply of fluid will introduce finite-amplitude perturbations to the infiltration front, as shown in Figure 3.B1 for a transparent analog system. The driving force in the advancing front is the sum of gravitational (δ_g) and capillary (δ_c) gradients. Assuming that

FIGURE 3.B1 Stable infiltration front initiated from application of a finite slug of fluid (black) into an initially dry fracture (white). Note that there are five significant perturbations to the front. From Nicholl et al. (1993b).

air (Ψ_a) and water (Ψ_w) entry pressure heads are independent of flow velocity, δ_c can be approximated as

$$\nabla_c \approx \frac{\psi_a - \psi_w}{L_f} \qquad \text{(B1)}$$

where L_f describes the down-gradient length of the connected fluid column (Nicholl et al., 1992). During the initial stage of infiltration, fluid is freely available to the fracture; hence, no drainage behind the front occurs ($\Psi_a = 0$) and capillary forces act to reinforce flow ($\delta_c > 0$). Preferential flow occurs to regions of small L_f, thereby damping the initial finite-amplitude perturbations and stabilizing the front.

If fluid supply to the fracture is interrupted (i.e., the fluid supply becomes exhausted), the front can only advance by draining pores along its trailing edge. The introduction of a drainage pressure ($\Psi_a < 0$) causes δ_c to reverse direction and oppose flow. As a result, flow to the front is redistributed from regions of small L_f (large δ_c) to regions of large L_f (small δ_c) that develop into fingers (Figure 3.B2). The unstable front therefore bypasses significant portions of the fracture plane, advancing farther and faster than would be expected for an equivalent uniform front. The velocity of individual fingers is a function of system hydraulic parameters, δ_c and L_f (Nicholl et al., 1992). As a finger advances, it leaves a partially wetted region behind (Figure 3.B2). The consequent loss of fluid causes the finger to slow and eventually halt in the fracture. Individual fingers therefore terminate in a fluid cluster that is "frozen" in place by capillary forces.

An unstable front will bypass significant portions of the fracture plane. Consequently, the volume of rock brought into hydraulic communication by a single infiltration event will be larger than that expected for an equivalent uniform front. Furthermore, at times short with respect to matrix imbibition and evaporative redistribution, the wetted structure created by unstable infiltration will have a significant effect on subsequent fracture infiltration. Ensuing infiltration events will preferentially follow the existing wetted structure. As the flow path is prewetted, finger velocity is increased over that observed in a dry fracture and very little fluid is lost during passage (Nicholl et al., 1993a,b). In effect, virtually the entire volume of an infiltration event is applied to the frozen fluid clusters associated with the previous event, restarting their movement and providing a mechanism for rapid recharge and solute transport.

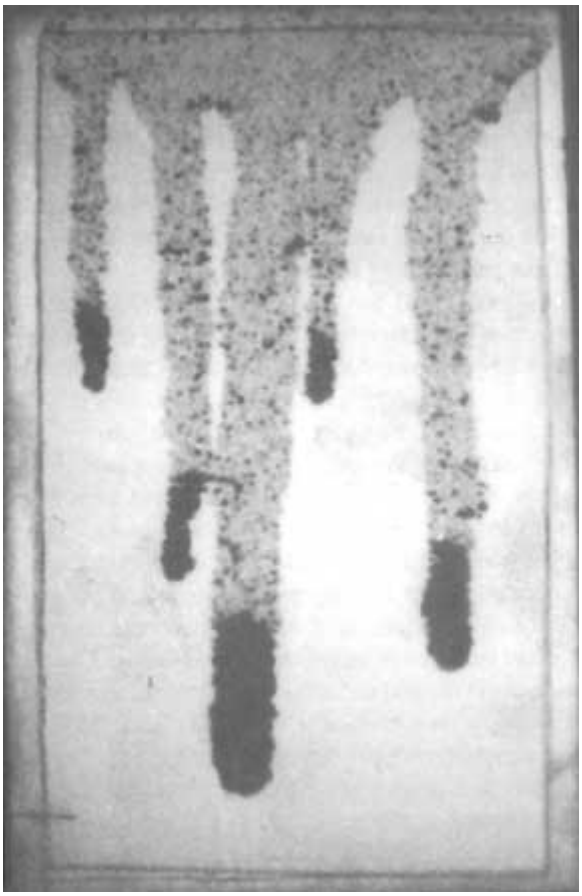

FIGURE 3.B2 Fingers originating from the stable front seen in figure 3.B1. Partially saturated regions (mottled regions) are wetted near field capacity of the analog fracture. Courtesy of R. J. Glass.

Appendix 3.C

Influence of Two-Phase Structure On Fracture Permeability And Solute Transport

Under steady-state conditions, flow in a single-phase along the plane of a fracture is confined to the connected network of apertures filled by that phase. Decreasing phase saturation reduces the fraction of the fracture plane available for flow. The resultant decrease in cross-sectional area and increased flow tortuosity reduces the relative permeability for the phase.

Nicholl and Glass (1994) used a transparent analog rough-walled fracture to explore the effects of phase structure on fluid permeability and solute dispersion. Flow through the connected phase of a two-phase structure exhibited a channelization that was not observed under single-phase conditions (Figures 3.C1, 3.C2, and 3.C3). Path tortuosity of the channelized flow was observed to increase with complexity of the phase structure and size of the entrapped regions. Disconnected regions filled by the flowing phase are entirely isolated from flow under steady-state conditions. In addition, even in the connected regions, highly tortuous flow paths tend to bypass significant portions of the connected phase structure. This creates dead zones that do not actively participate in flow but communicate with active regions through diffusion. As a result, the average cross-sectional area of the connected phase structure is larger than the effective flow area.

For phase structures formed under nonequilibrium conditions, aperture filling may not follow a simple pressure/size relationship (Glass, 1993), further complicating the phase structure/permeability relationship. The fluid phase shown in Figure 3.C1 occupies 81.2 percent of the fracture plane. However, fluid permeability was only 14.3 percent of that measured at 100 percent saturation.

As expected from the previous discussion, two-phase wetted structure significantly affects solute dispersion. Flow channelization creates differential advection in the plane of the fracture (Figures 3.C2 and 3.C3). Velocity differentials introduced by local variations in cross-sectional area also act to increase dispersion. Dead zones created by flow tortuosity act to significantly extend the tail of the residence time distribution curve.

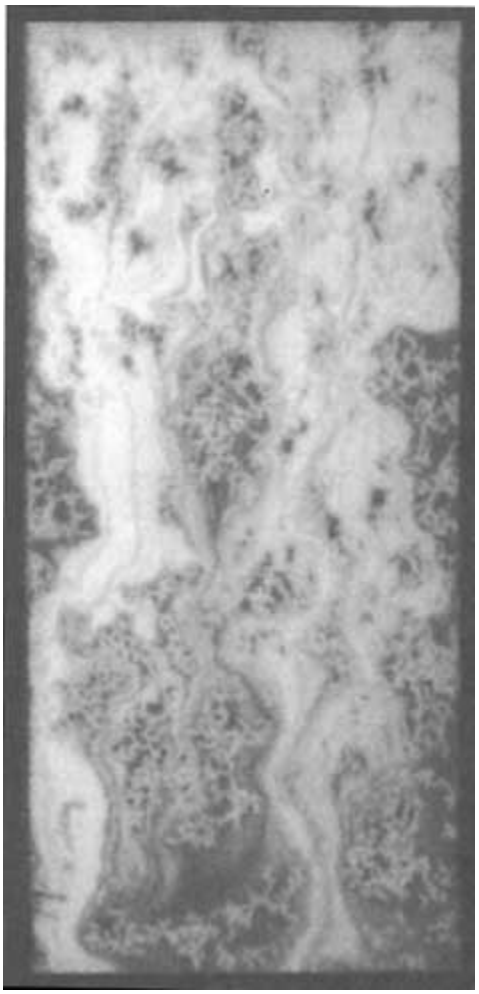

FIGURE 3.C1 Steady-state wetted structure in a transparent analog fracture. Dark areas are filled with dyed water; light regions are entrapped air. From Nicholl and Glass (1994).

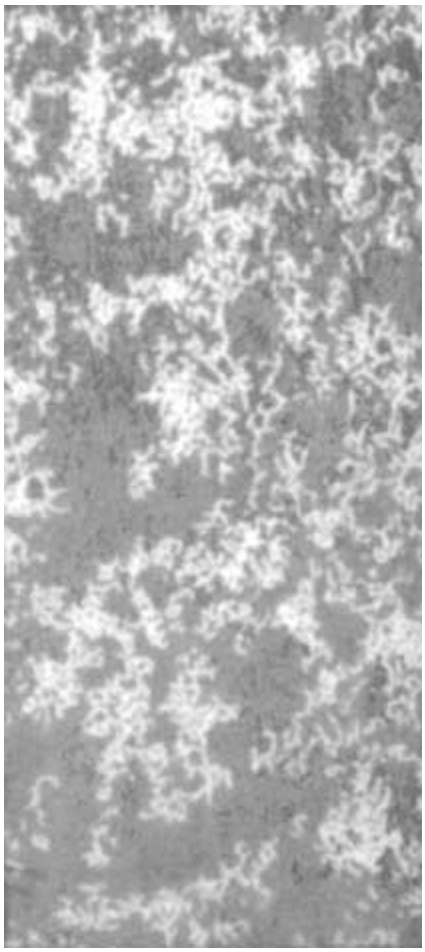

FIGURE 3.C2 Tracer pulse consisting of clear water entering the two-phase wetted structure in Figure 3.C1 from a constant flow boundary. From Nicholl and Glass (1994).

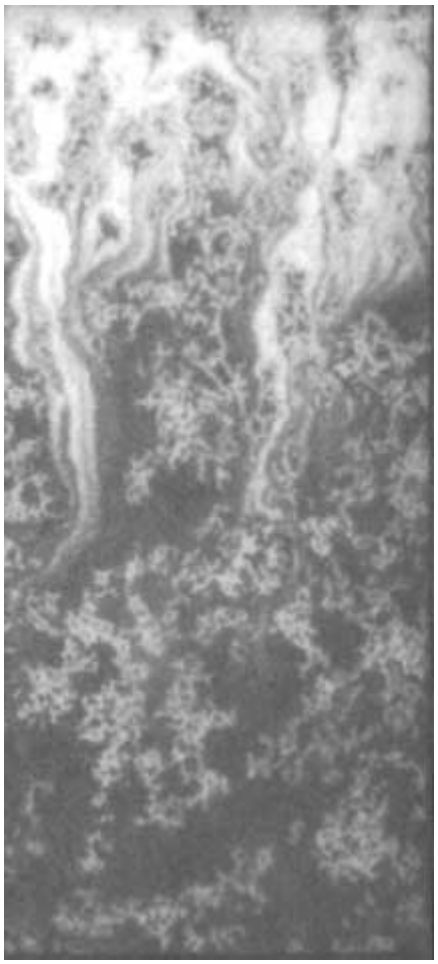

FIGURE 3.C3 Further development of the tracer pulse shown in Figure 3.C2. Note wholly isolated regions and dead zones that communicate by diffusion. From Nicholl and Glass (1994).

REFERENCES

Adamson, A. W. 1990. Physical Chemistry of Surfaces, 5th ed. New York: John Wiley & Sons, 777 pp.

Angel, Y. C., and J. D. Achenbach. 1985. Reflection and transmission of elastic waves by a periodic array of cracks. Journal of Applied Mechanics, 52:33–41.

Archambault, G., M. Fortin, D. E. Gill, M. Aubertin, and B. Ladanzi. 1990. Experimental investigations for an algorithm simulating the effect of variable normal stiffness on discontinuities shear strength. Pp. 141–148 in Rock Joints, Proceedings of the International Symposium on Rock Joints, Loen, Norway, W. Barton, and E. Stephansson, eds. Rotterdam: A. A. Balkema.

Archie, G. E. 1942. The electrical resistivity log as an aid in determining some reservoir characteristics. Transactions of the American Institute of Mechanical Engineering, 146:54–62.

Bandis, S. C. 1990. Mechanical properties of rock joints. Pp. 125–140 in Rock Joints, Proceedings of the International Symposium on Rock Joints, Loen, Norway, W. Barton and E. Stephansson, eds. Rotterdam: A. A. Balkema.

Bandis, S., A. C. Lumsden, and N. R. Barton. 1981. Experimental studies of scale effects on the shear behavior of rock joints. International Journal of Rock Mechanics and Mining Science and Geomechanics Abstracts, 18:1–21.

Barton, N. 1973. Review of a new shear-strength criterion for rock joints. Engineering Geology, 7:287–332.

Barton, N., S. Bandis, and K. Bakhtor. 1985. Strength, deformation and conductivity coupling in rock joints. International Journal of Rock Mechanics and Mining Sciences and Geomechanics Abstracts, 22(3):121–140.

Bath, M. 1974. Spectral Analysis in Geophysics. New York: Elsevier.

Bendat, J. S., and A. G. Piersol. 1971. Random Data, Analysis and Measurement Procedures. New York: John Wiley & Sons.

Bernabe, Y. 1986. Pore volume and transport properties changes during pressure cycling of several crystalline rocks. Mechanics and Materials, 5:235–249.

Bernabe, Y. 1988. Comparison of the effective pressure law for permeability and resistivity formation factor in Chelmsford granite. Pure and Applied Geophysics, 127:607–625.

Billaux, D., and S. Gentier. 1990. Numerical and laboratory studies of flow in a fracture. Pp. 369–373 in Rock Joints, Proceedings of the International Symposium on Rock Joints, Loen, Norway, W. Barton and E. Stephansson, eds. Rotterdam: A. A. Balkema.

Biot, M. A. 1956. Theory of Propagation of Elastic Waves in a Fluid-Saturated Porous Solid. I. Low-Frequency Range. Journal of the Acoustics Society of America, 28(2):168.

Brace, W. F., A. S. Orange, and T. R. Madden. 1965. Effect of pressure on the electrical resistivity of water-saturated crystalline rocks. Journal of Geophysical Research, 70:5669–5678.

Broadbent, S. R., and J. M. Hammersley. 1957. Percolation Processes. I. Crystals and Mazes. Cambridge Philosophical Society Proceedings, 53:629–641.

Brown, S. R. 1987. Fluid flow through rock joints: the effect of surface roughness. Journal of Geophysical Research, 92(82):1337–1347.

Brown, S. R. 1989. Transport of fluid and electric current through a single fracture. Journal of Geophysical Research, 94(B7):9429–9438.

Brown, S. R., and C. H. Scholz. 1985. Broad bandwidth study of the topography of natural rock surfaces. Journal of Geophysical Research, 90:575–582.

Brown, S. R., and C. H. Scholz. 1986. Closure of rock joints. Journal of Geophysical Research, 91:4939–4948.

Brown, S. R., R. L. Kranz, and B. P. Bonner. 1986. Correlation between the surfaces of natural rock joints. Geophysics Research Letter, 13:1430–1433.

Budiansky, B., and R. J. O'Connell. 1980. Bulk dissipation in heterogeneous media. Solid Earth Geophysics and Geotechnology, New York: American Society of Mechanical Engineers, 42:1.

Carlson, R. L., and A. F. Gangi. 1985. Effect of cracks on the pressure dependence of P-wave velocities in crystalline rocks. Journal of Geophysical Research, 90(B10):8675–8684.

Carter, J. J. 1990. The effects of clay coating on fluid flow through simulated rock fractures. M.S. thesis, University of California, Berkeley.

Chouke, R. L., P. van Meurs, and C. van der Poel. 1959. The instability of slow immiscible, viscous liquid-liquid displacements in porous media. Transactions of the American Institute of Mining Engineers, 216:T.P. 8073.

Cook, A. M., L. R. Myer, N. G. W. Cook, and F. M. Doyle. 1990. The effect of tortuosity on flow through a natural fracture. Pp. 371–378 in Rock Mechanics Contributions and Challenges, Proceedings of the 31st U.S. Symposium on Rock Mechanics, W. A. Hustrulid and G. A. Johnson, eds. Rotterdam: A. A. Balkema.

David, C., Y. Gueguen, and G. Pampoukis. 1990. Effective medium theory and network theory applied to the transport properties of rock. Journal of Geophysical Research, 95(B5):6993–7005.

de Gennes, P. G. 1985. Wetting: statics and dynamics. Reviews of Modern Physics, 57:827–863.

Doyen, P. M. 1988. Permeability, conductivity, and pore geometry of sandstone. Journal of Geophysical Research, 93(B7):7729–7740.

Dussan, V. 1979. On the spreading of liquids on solid surfaces: static and dynamic contact lines. Annual Review of Fluid Mechanics, 11:371–400.

Einstein, H. H., and C. H. Dowding. 1981. Shear resistance and deformability of rock discontinuities. Pp. 177–219 in Physical Properties of Rocks and Minerals, Y. S. W. Touloukian, R. Judd, and R. E. Ray, eds. New York: McGraw-Hill.

Esaki, T., H. Hojo, T. Kimura, and N. Kameda. 1991. Shear-flow coupling test on rock joints. Pp. 389–392 in Proceedings of 7th International Congress on Rock Mechanics. Rotterdam: A. A. Balkema.

Feder, J. 1988. Fractals. New York: Plenum Press, 283 pp.

Gale, J. E. 1982. The effects of fracture type (induced versus natural) on the stress-fracture closure fracture permeability relationships. Pp. 290–298 in Issues in Rock Mechanics, Proceedings of the 23rd U.S. Symposium on Rock Mechanics, R. Goodman and F. Henze, eds. New York: Society of Mining Engineers of AIME.

Gale, J. E. 1987. Comparison of coupled fracture deformation and fluid flow models with direct measurements of fracture pore structure and stress-flow properties. Pp. 1213–1222 in Rock Mechanics, Proceedings of the 28th U.S. Symposium on Rock Mechanics, I. W. Farmer, J. J. K. Daemen, C. S. Desai, C. E. Glass, and S. P. Neuman, eds. Rotterdam: A. A. Balkema.

Gale, J. 1990. Hydraulic behavior of rock joints. Pp. 351–362 in Rock Joints, Proceedings of the International Symposium on Rock Joints, Loen, Norway, W. Barton and E. Stephansson, eds. Rotterdam: A. A. Balkema.

Gale, J. E., and E. J. Reardon. 1984. Effect of groundwater geochemistry on the permeability of grouted fractures. Canadian Geotechnical Journal, 21(1):8–20.

Gentier, S., and J. Ries. 1990. Quantitative description and modeling of joint morphology. Pp. 375–382 in Rock Joints, Proceedings of the International Symposium on Rock Joints, Loen, Norway, W. Barton and E. Stephansson, eds. Rotterdam: A. A. Balkema.

Glass, R. J. 1993. Modeling gravity-driven fingering in rough-walled fractures using modified percolation theory. Pp. 2042–2052 in Proceedings of the Fourth Annual International High-Level Radioactive Waste Management Conference. La Grange Park, Ill.: American Nuclear Society.

Glass, R. J., and D. L. Norton. 1992. Wetted region structure in horizontal unsaturated fractures: water entry through the surrounding porous matrix. Pp. 717–726 in Proceedings of the Third Annual International High-Level Radioactive Waste Management Conference. La Grange Park, Ill.: American Nuclear Society.

Goodman, R. E. 1976. Methods of Geological Engineering Discontinuous Rock. St. Paul: West Publishing Co.

Hakami, E., and N. Barton. 1990. Aperture measurements and flow experiments using transparent replicas of rock joints. Pp. 383–390 in Rock Joints, Proceedings of the International Symposium on Rock Joints, Loen, Norway, W. Barton and E. Stephansson, eds. Rotterdam: A. A. Balkema.

Heard, H. C., and L. Page. 1982. Elastic moduli, thermal expansion, and inferred permeability of two granites to 350°C and 55 megapascals. Journal of Geophysical Research, 87 (B11):9340–9348.

Homsy, G. M. 1987. Viscous fingering in porous media. Annual Review of Fluid Mechanics , 19:271–311.

Hopkins, D. C., N. G. W. Cook, and L. R. Myer. 1990. Normal joint stiffness as a function of spatial geometry and surface roughness. Pp. 203–210 in Rock Joints, Proceedings of the International Symposium on Rock Joints, Loen, Norway, W. Barton and E. Stephansson, eds. Rotterdam: A. A. Balkema.

Hudson, J. A. 1980. Overall properties of a cracked solid. Mathematical Proceedings of the Cambridge Philosophical Society, 88:371.

Iwai, K. 1976. Fundamental studies of fluid flow through a single fracture. Ph.D. thesis, University of California, Berkeley.

Jones, F. O. 1975. A laboratory study of the effects of confining pressure on fracture flow and storage capacity in carbonate rocks. Journal of Petroleum Technology, Jan., pp. 21–27.

Jones, T. D. 1986. Pore fluids and frequency-dependent wave propagation in rocks. Geophysics, 51 (10):1939–1953.

Khilar, K. L., and H. S. Folger. 1984. The existence of a critical salt concentration for particle release. Journal of Colloid and Interface Science, 101(1):214–224.

King, M. S., L. R. Myer, and J. J. Rezowalli. 1986. Experimental studies of elastic-wave propagation in a columnar-pointed rock mass. Geophysical Prospecting, 34(8):1185–1199.

Kranz, R. L., A. D. Frankel, T. Engelder, and C. H. Scholz. 1979. The permeability of whole and jointed Barre granite. International Journal of Rock Mechanics and Mining Science and Geomechanics Abstracts, 16:225–234.

Kutter, H. K., and F. Otto. 1990. Influence of parallel and cross joints on shear behavior of rock discontinuities. Pp. 243–250 in Rock Joints, Proceedings of the International Symposium on Rock Joints, Loen, Norway, W. Barton and E. Stephansson, eds. Rotterdam: A. A. Balkema.

Lamb, H. 1932. Hydrodynamics, 6th ed. Cambridge: Cambridge University Press.

Lehner, F. K., and J. Bataille. 1984. Nonequilibrium thermodynamics of pressure solution. Report No. 25, Division of Engineering, Brown University, Providence, R.I., 52 pp.

Magnusson, K. A., S. Carlsten, and O. Olsson. 1987. Crosshole investigations—physical properties of core samples from boreholes F1 and F2. Stripa Project IR 87-10. Stockholm: Swedish Nuclear Fuel and Waste Management Company (SKB).

Makurat, A. 1985. The effect of shear displacement on the permeability of natural rough joints. Pp. 99–106 in Proceedings Hydrogeology of Rocks of Low Permeability, Tucson, Ariz., International Association of Hydrogeologists, Memoires XVII .

Mandelbrot, B. B. 1982. The Fractal Geometry of Nature. San Francisco: W. H. Freeman and Co.

Miller, S. M., P. C. McWilliams, and J. C. Kerkering. 1990. Ambiguities in estimating fractal dimensions of rock fracture. Pp. 471–478 in Rock Mechanics Contributions and Challenges, Proceedings of the 31th U.S. Symposium on Rock Mechanics, W. A. Hustrulid and G. A. Johnson, eds. Rotterdam: A. A. Balkema.

Mindlin, R. D. 1949. Compliance of elastic bodies in contact, Journal of Applied Mechanics, 16:259–269.

Mindlin, R. D., and H. Deresiewicz. 1953. Elastic spheres in contact under varying oblique forces. Journal of Applied Mechanics, 20:327–344.

Mitchell, S. K. 1993. Fundamentals of Foil Behavior, 2d ed. New York: John Wiley & Sons.

Moreno, L., Y. W. Tsang, C. F. Tsang, F. V. Hale, and I. Neretnieks. 1988. Flow and transport in a single fracture: a stochastic model and its relation to some field observations. Water Resources Research, 24(12):2033–2048.

Myer, L. 1991. Hydromechanical and seismic properties of fractures. Pp. 397–409 in Proceedings of the 7th International Rock Mechanics Congress, vol. 1

Myer, L. R., D. Hopkins, and N. G. W. Cook. 1985. Effects of contact area of an interface on acoustic wave transmission. Pp. 549–556 in Research and Engineering Applications in Rock Mechanics, Proceedings of the 26th U.S. Symposium on Rock Mechanics. Rotterdam: A. A. Balkema.

Myer, L. R., L. S. Pyrak-Nolte, and N. G. W. Cook. 1990a. Effect of single fractures on seismic wave propagation. Pp. 476–473 in Rock Joints, Proceedings of the International Symposium on Rock Joints, Loen, Norway, W. Barton and E. Stephansson, eds. Rotterdam: A. A. Balkema.

Myer, L. R., L. J. Pyrak-Nolte, D. Hopkins, and N. G. W. Cook. 1990b. Seismic characterization of fracture properties. Pp. 908–914 in Proceedings of First Annual International High-Level Radioactive Waste Management Conference, vol. 1. La Grange Park, Ill.: American Nuclear Society.

Nelson, P. H., R. Rachiele, and J. S. Remer. 1981. Water inflow into boreholes during the Stripa Heater Experiments. LBL-12574, Lawrence Berkeley Laboratory, Berkeley, Calif.

Nicholl, M. J., and R. J. Glass. 1994. Wetting phase permeability in a partially saturated horizontal fracture. Pp. 2007–2019 in Proceedings of the 5th International Conference on High-Level Radioactive Waste Management. La Grange Park, Ill.: American Nuclear Society.

Nicholl, M. J., R. J. Glass, and H. A. Nguyen. 1992. Gravity-driven fingering in unsaturated fractures. Pp. 321–332 in High-Level Radioactive Waste Management, Proceedings of the Third Annual International Conference, vol. 1. La Grange Park, Ill.: American Nuclear Society.

Nicholl, M. J., R. J. Glass, and H. A. Nguyen. 1993a. Wetting front instability in an initially wet unsaturated fracture. Pp. 2061–2070 in Proceedings of the Fourth Annual International High-Level Radioactive Waste Management Conference, vol. 2. La Grange Park, Ill.: American Nuclear Society.

Nicholl, M. J., R. J. Glass, and H. A. Nguyen. 1993b. Small scale behavior of single gravity-driven fingers in an initially dry fracture. Pp. 2023–2032 in Proceedings of the Fourth Annual International High-Level Radioactive Waste Management Conference, vol. 2. La Grange Park, Ill.: American Nuclear Society.

Nolte, D. D., L. J. Pyrak-Nolte, and N. G. W. Cook. 1989. The fractal geometry of flow paths in natural fractures in rock and the approach to percolation. PAGEOPH, 131(1/2):271.

Noorishad, J., C. F. Tsang, and P. A. Witherspoon. 1984. Coupled thermal-hydraulic-mechanical phenomena in saturated fractured porous rocks: numerical approach. Journal of Geophysical Research, 89(B12):10365–10375.

Ohnishi, Y., and P. G. R. Dharmaratra. 1990. Shear behavior of physical models of rock joints under constant normal stiffness conditions. Pp. 267–273 in Rock Joints, Proceedings of the International Symposium on Rock Joints, Loen, Norway, W. Barton and E. Stephansson, eds. Rotterdam: A. A. Balkema.

Olsson, W. A. 1992. The effect of slip on the flow of fluid through a fracture. Geophysics Research Letters, 19(6):541–543.

Paillet, F. L., A. E. Hess, C. H. Cheng, and E. Hardin. 1987. Characterization of fracture permeability with high-resolution vertical flow measurements during borehole pumping. Ground Water, 25(1):28–40.

Papaliangas, T., A. C. Lumsden, S. A. Hencher, and S. Manolopoulou. 1990. Shear strength of modeled filled rock joints. Pp. 275–282 in Rock Joints, Proceedings of the International Symposium on Rock Joints, Loen, Norway, W. Barton and E. Stephansson, eds. Rotterdam: A. A. Balkema .

Paterson, M. S. 1983. The equivalent channel model for permeability and resistivity in fluid-saturated rocks—a reappraisal. Mechanics and Materials, 2(4):345–352.

Patton, D. F. 1966. Multiple modes of stress failure in rock. P. 509 in Proceedings of the First International Congress on Rock Mechanics, vol. 1. Lisbon: Bertrand.

Persoff, P., K. Pruess, and L. Myer. 1991. Two-phase flow visualization and relative permeability measurement in transparent replicas of rough-walled rock fracture. Lawrence Berkeley Laboratory Report 30161, presented at the 16th Workshop on Geothermal Reservoir, Engineering, Stanford, Calif.

Peterson, J. E., Jr., D. Hopkins, and L. Myer. 1993. Application of seismic displacement discontinuity theory to Hanford data. Pp. 1006–1009 in Expanded Abstracts with Biographies, 1993 Technical Program: 63d Annual Meeting and International Exhibition, Society of Exploration Geophysicists.

Piggot, A. R., and D. Elsworth. 1990. Laboratory studies of transport within a single rock fracture. Pp. 397–404 in Rock Joints, Proceedings of the International Symposium on Rock Joints, Loen, Norway, W. Barton and E. Stephansson, eds. Rotterdam: A. A. Balkema.

Power, W. L., and T. E. Tullis. 1991. Euclidean and fractal models for the description of rock surface roughness. Journal of Geophysical Research , 96(B1):415–424.

Power, W. L., T. E. Tullis, S. R. Brown, G. N. Boitnott, and C. H. Scholz. 1987. Roughness of natural fault surfaces. Geophysics Research Letters, 14:29–32.

Pruess, K., and Y. W. Tsang. 1990. On two-phase relative permeability and capillary pressure of rough-walled rock fractures. Water Resources Research, 26(9):1915–1926.

Pyrak-Nolte, L. J., L. R. Myer, N. G. W. Cook, and R. A. Witherspoon. 1987a. Hydraulic and mechanical properties of natural fractures in low permeability rock. Pp. 225–232 in Proceedings of 6th International Congress of Rock Mechanics, vol. I. Rotterdam: A. A. Balkema.

Pyrak-Nolte, L. J., L. R. Myer, and N. G. W. Cook. 1987b. Seismic visibility of fractures. Pp. 47–56 in Rock Mechanics, Proceedings of the 28th U.S. Symposium on Rock Mechanics. Rotterdam: A. A. Balkema.

Pyrak-Nolte L. J., N. G. W. Cook, and D. D. Nolte. 1988. Fluid percolation through single fractures. Geophysics Research Letters, 15(11):1247–1250.

Pyrak-Nolte, L. J., N. G. W. Cook, and L. R. Myer. 1990a. Stratified percolation model for saturated and unsaturated flow through natural fractures. Pp. 551–558 in Proceedings of First Annual International High-Level Radioactive Waste Management Conference, vol. 1. La Grange, Ill.: American Nuclear Society.

Pyrak-Nolte, L. J., L. R. Myer, and N. G. W. Cook. 1990b. Transmission of seismic waves across single fractures. Journal of Geophysical Research, 95(B6):8617–8638.

Pyrak-Nolte, L. J., L. R. Myer, and N. G. W. Cook. 1990c. Anisotropy in seismic velocities and amplitudes from multiple parallel fractures. Journal of Geophysical Research, 95 (B7):11345–11358.

Pyrak-Nolte, L. J., L. R. Myer, and D. D. Nolte. 1992. Fractures: finite-size sealing and multifractals. PAGEOPH, 131(1/2):271.

Rathore, J. S., F. Fjaer, R. M. Holt, and L. Reulie. 1991. Acoustic anisotropy of synthetics with controlled crack geometrics. European Association of Exploratory Geophysicists Convention Abstracts, 53:538–539.

Raven, K. G., and J. E. Gale. 1985. Water flow in a natural rock fracture as a function of stress and sample size. International Journal of Rock Mechanics and Mining Science and Geomechanics Abstracts, 22(4):251–261.

Roberds, W. J., and H. H. Einstein. 1978. Comprehensive model for rock discontinuities. Journal of the Geotechnical Engineering Division, 104(GT5):553–569.

Roberds, W. J., M. Iwano, and H. H. Einstein. 1990. Probabilistic mapping of rock joint surfaces. Pp. 681–691 in Rock Joints, Proceedings of the International Symposium on Rock Joints, Loen, Norway, W. Barton and E. Stephansson, eds. Rotterdam: A. A. Balkema.

Rutter, E. H. 1983. Pressure solution in nature, theory and experiment. Journal of the Geological Society (London), 140:725–740.

Saffman, P. G. 1986. Viscous fingering in Hele-Shaw cells. Journal of Fluid Mechanics, 173:73–94.

Saffman, P. G., and G. I. Taylor. 1958. The penetration of a fluid into a porous medium or Hele-Shaw cell containing a more viscous liquid. Proceedings of the Royal Society of London, A245:312–331.

Sayles, R. S., and T. R. Thomas. 1978. Surface topography as a non-stationary random process. Nature, 271:431–434.

Schoenberg, M. 1980. Elastic wave behavior across linear slip interfaces. Journal of the Acoustical Society of America, 68(5):1516–1521.

Schoenberg, M. 1983. Reflection of elastic waves from periodically stratified media with interfacial slip. Geophysical Prospecting, 31:265–292.

Schoenberg, M., and F. Muir. 1989. A calculus for finely layered anisotropic media. Geophysics, 54 (5):581–589.

Sen, P. N., C. Scala, and M. H. Cohen. 1981. A self-similar model for sedimentary rocks with application to the dielectric constant of fused glass beads. Geophysics, 46:781–795.

Shen, L. C., W. C. Savre, J. M. Price, and K. Ahtavale. 1985. Dielectric properties of reservoir rocks at ultra-high frequencies. Geophysics, 50:692–704.

Sihvola, A. H. 1989. Self-consistency aspects of dielectric mixing theories. IEEE Transactions on Geoscience and Remote Sensing, 27:403–415.

Simandoux, P. 1963. Mesures dielectrique en milleux poreux, application a mesure des saturations en eaux, etude du comportement des massifs argileux. Rev. de l'institut Francais du Petrole, (Suppl.).

Smith, L., C. W. Mase, and F. W. Schwartz. 1987. Estimation of fracture aperture using hydraulic and tracer tests. Pp. 453–463 in Rock Mechanics, Proceedings of the 28th U.S. Symposium on Rock Mechanics, I. W. Farmer, J. J. K. Daemen, C. S. Desai, C. E. Glass, and S. P. Neuman, eds. Rotterdam: A. A. Balkema.

Sneddon, I. N., and A. A. Elliott. 1946. The opening of a griffith crack under internal pressure. Quarterly of Applied Mathematics, IV:262.

Sprunt, E. S., and A. Nur. 1977. Destruction of porosity through pressure solution. Geophysics, 42:726–741.

Stockman, H. W., C. T. Stockman, and C. R. Carrigan. 1990. Modeling viscous segregation in immiscible fluids via lattice gas automata. Nature, 348:523.

Suarez-Rivera, F. R., N. G. W. Cook, and L. R. Myer. 1992. Study of the transmission of shear waves across thin liquid films and thin clay layers. Pp. 937–946 in Rock Mechanics, Proceedings of the 33rd U.S. Rock Mechanics Symposium, J. R. Tillerson and W. R. Warvenish, eds. Rotterdam: A. A. Balkema.

Swan, G. 1981. Tribology and the characterization of rock joints. Pp. 402–407 in Proceedings of the 22nd U.S. Symposium on Rock Mechanics. Cambridge: Massachusetts Institute of Technology.

Tada, H. P., P. C. Paris, and G. K. Irwin. 1973. The Stress Analysis of Cracks Handbook. Helbertown, Pa.: Del Research Corp.

Tang, X. M., C. H. Cheng, and F. L. Paillet. 1991. Modeling borehole Stoneley wave propagation a permeable in-situ fracture. Pp. GG1–GG25 in Society of Professional Well Log Analysts Annual Logging Symposium, 32nd, Transactions. Houston, Tex.: Society of Professional Well Log Analysts.

Terzaghi, K. 1936. The shearing resistance of saturated soils. Pp. 54–56 in Proceedings of the International Conference on Foundation Engineering, Graduate School of Engineering, Harvard University. Boston: Spaulding Moss Co.

Thomas, T. R. 1982. Rough Surfaces. New York: Longman.

Thompson, M. E., and S. R. Brown. 1991. The effect of anisotropic surface roughness on flow and transport in fractures. Journal of Geophysical Research, 96(B13):21923–21932.

Thomsen, L. 1985. Biot-consistent elastic modeli of porous rocks: low-frequency limit. Geophysics, 50(12):2797–2807.

Thomsen, L. 1991. Elastic anisotropy due to aligned cracks in porous rock. European Association of Exploratory Geophysicists Convention Abstracts, 53:244–245.

Timoshenko, S. P., and J. N. Goodier. 1970. Theory of Elasticity, 3d ed. New York: McGraw-Hill.

Trimmer, D., B. Bonner, H. C. Heard, and A. Duba. 1980. Effect of pressure and stress on water transport in intact and fractured gabbro and granite. Journal of Geophysical Research, 85 (B12):7059–7071.

Tsang, Y. W. 1984. The effect of tortuosity on fluid flow through a single fracture. Water Resources Research, 20:1209–1215.

Tsang, Y. W., and C. F. Tsang. 1987. Channel model of flow through fractured media. Water Resources Research, 23(3):467–479.

Tsang, Y. W., C. F. Tsang, I. Neretnieks, and L. Moreno. 1988. Flow and tracer transport in fractured media: a variable aperture channel model and its properties. Water Resources Research, 24(12):2049–2060.

Voss, C. F., and L. R. Shotwell. 1990. An investigation of the mechanical and hydraulic behavior of tuff fractures under saturated conditions. Pp. 825–834 in High-Level Radioactive Waste Management. La Grange Park, Ill.: American Nuclear Society.

Walsh, J. B. 1981. Effect of pore pressure and confining pressure on fracture permeability. International Journal of Rock Mechanics and Mining Science and Geomechanics Abstracts, 18:429–435.

Walsh, J. B., and W. F. Brace. 1984. The effect of pressure on porosity and the transport properties of rock. Journal of Geophysical Research, 89:9425–9431.

Wang, J. S. Y., T. N. Narasimhan, and C. H. Scholz. 1988. Aperture correlation of a fractal fracture. Journal of Geophysical Research, 93(B3):2216–2224.

Waxman, M. H., and L. J. M. Smits. 1968. Electrical conductivities of oil-bearing shaley sands. Transactions of the Society of Petroleum Engineers, 243:107–115.

Whitehouse, D. J., and J. F. Archard. 1970. The properties of random surfaces of significance in their contact. Proceedings of the Royal Society of London , Series A, 316:97–121.

Wilkinson, D., and J. F. Willemsen. 1983. Invasion percolation: a new form of percolation theory. Journal of Physics A: Math. Gen., 16:3365–3376.

Witherspoon, P. A., J. S. Y. Wang, K. Iwai, and J. E. Gale. 1980. Validity of cubic law for fluid flow in a deformable rock fracture. Water Resources Research, 16:1016.

Yang, G., N. G. W. Cook, and L. R. Myer. 1989. Network modeling of flow in natural fractures. Pp. 57–64 in Proceedings of the 30th U.S. Symposium on Rock Mechanics, A. W. Khair, ed. Rotterdam: A. A. Balkema.

Yoshioka, N., and C. H. Scholz. 1989a. Elastic properties of contacting surfaces under normal and shear loads. 1. Theory. Journal of Geophysical Research, 94:17681–17690.

Yoshioka, N., and C. H. Scholz. 1989b. Elastic properties of contacting surfaces under normal and shear loads. 2. Comparison of theory with experiment. Journal of Geophysical Research, 94:17691–17700.

4

Fracture Detection Methods

This chapter addresses methods for the remote detection and characterization of fractures in the subsurface. These indirect detection methods are mainly geophysical in nature and rely on the physical principles introduced in Chapter 3. Recent advances in theory and in available technology have greatly increased our ability to detect fractures at depth and to characterize their properties. Many of these techniques were first introduced for other purposes and have been refined for use in fracture detection and characterization.

Fractures in the subsurface are zones of anomalous physical properties that can be detected remotely by various means, ranging from simple extrapolation of surface observations to sophisticated seismic and electromagnetic soundings. In general, methods that probe deeply into the subsurface have a poor ability to spatially resolve the locations of fractures and those with shorter ranges have correspondingly better resolutions. Some exceptions to this rule exist in certain circumstances and are noted below; however, the rule is sufficiently strong that the discussion here is organized according to the range and resolving power of the methods. Geophysical fracture detection methods naturally divide themselves into three distinct scales: (1) large scales associated with surface soundings, (2) intermediate scales associated with surface-to-borehole and borehole-to-borehole soundings, and (3) small scales associated with measurements made on rocks immediately adjacent to a borehole or tunnel. Table 4.1 provides a general overview organized by the type of method, which thus serves as a cross-reference for the discussion below.

Fracture detection methods rely on the fact that fractures are *thin* compared to their lengths and heights; that is, they are essentially two-dimensional anoma

TABLE 4.1 Fracture Detection Methods

Method	Length Scale of Investigation and Resolution	Remarks	Chapter Reference in this Volume
Differential methods	0.1–5,000 m	Most of the methods below best detect actual flow if performed both before and after a known stimulus.	Chapter 4
Elastic methods: seismic band (10-100 Hz)	100–5,000 m	Zero shear modulus in fracture fluid is critical.	Chapter 3 Chapter 4
P-wave reflection (2D)	[1–2 λ (velocity)][a] [1/4 λ (amplitude)]	Surface methods best detect horizontal fractures; fracture shape is critical.	Chapter 3 Chapter 4
P-wave reflection (3D)	[1–2 λ (velocity)] [1/8 λ (amplitude)]	Very subtle features recognizable in patterns.	Chapter 3 Chapter 4
S-wave reflection (2D)	[1–2 λ (velocity)] [1/4 λ (amplitude)]	Surface methods best detect vertical aligned fractures.	Chapter 3 Chapter 4
P-wave vertical seismic orofiling (VSP) (including offset, reverse)	[<1 λ (velocity)]	Minimizes overburden difficulties; fractures cause tube waves.	Chapter 3 Chapter 4
S-wave 3C vertical seismic profiling (VSP)	[< 1 λ (velocity)]	Minimizes overburden difficulties.	Chapter 4
P-wave tomography	10–100 m [1/2 λ (velocity)]	Zero shear modulus in fracture fluid is critical.	Chapter 4 Chapter 4
Cross-hole reflections	10–100 m [1/2 λ (velocity)]	Zero shear modulus in fracture fluid is critical.	Chapter 3 Chapter 4
Coupled methods	100–5,000 m [< 1 λ (velocity)]	Iteration of reflection and transmission inversion steps.	Chapter 3 Chapter 4

Elastic methods: sonic band (2-20 kHz)	0.1–10 m	Zero shear modulus in fracture fluid is critical.	Chapter 3 Chapter 4
P-wave transmission (acoustic Log, 1D)	[1–2 λ (velocity)] [1–2 λ (amplitude)]	Best detects fractures oriented transverse to rays.	Chapter 3 Chapter 4
Acoustic waveform Log, *P* and *S*	[1–2 λ (velocity)] [1–2 λ (amplitude)]	Best detects fractures oriented transverse to rays.	Chapter 3 Chapter 4
Acoustic emissions	10–100 m [1–10 m]	Emissions accompany fracture growth (e.g., during hydrofrac pumping operations).	Chapter 4
Elastic methods: ultrasonic band (200-2,000 kHz)	0.1–5 m	Fracture aperture is critical.	Chapter 3 Chapter 4
Borehole televiewer	10–30 cm [0.3–5 cm]	Detects fractures in boreholes.	Chapter 4
Electrical methods	10–300 m	Contrasting resistivity of fracture-filling fluid is critical.	Chapter 3 Chapter 4
Electric sounding	[1–10 m]	Best detects horizontal fractured zones.	Chapter 4
Electric profiling	[1–10 m]	Best detects vertical or dipping fractured zones.	Chapter 4
Electric resistivity tomography	[1–10 m]	Still under development.	Chapter 4
Formation microscanner (FMS)	[0.1–3 cm]	Best detects open fractures.	Chapter 4
Electromagnetic methods	[10–300 m]	Contrasting resistivity of fracture-filling fluid is critical.	Chapter 3 Chapter 4
Electromagnetic sounding	[3–10 m]	Best detects horizontal fractured zones.	Chapter 4
Electromagnetic profiling	[3–10 m]	Best detects vertical or dipping fractured zones.	Chapter 4
Electromagnetic tomography	[3–10 m]	Best detects conductive anomalies, like fluid-filled fractures.	Chapter 4
Radar methods	3–100 m	Contrasting resistivity of fracture-filling fluid is critical.	Chapter 3 Chapter 4
Ground-penetrating radar (reflection)	[0.1–5 m]	Conductive overburden presents difficulties, limits penetration.	Chapter 4

Method	Length Scale of Investigation and Resolution	Remarks	Chapter Reference in this Volume
Borehole radar (reflection)	[1–5 m]	Determines both location and orientation from a single borehole.	Chapter 4
Radar tomography (transmission)	[2–10 m]	May be used to image velocity, attenuation, or differences over time.	Chapter 4
Conventional well logs	0.1-10 m	Near-borehole environment.	Chapter 4
Neutron log	[0.1 m]	Detects clay and porosity in fracture washouts.	Chapter 4
Resistivity log	[0.1 m]	Detects clay in fractures and washouts.	Chapter 4
Density log	[0.1 m]	Detects clay in fractures and washouts.	Chapter 4
Gamma ray log	[0.1 m]	Detects radioactive fillers, rock-type identification.	Chapter 4
Caliber log	[0.01 m]	Detects borehole enlargement.	Chapter 4
Temperature log	[0.01 m]	Detects temperature changes owing to flow in fracture system.	Chapter 3 Chapter 4
Fluid conductivity log	[0.01 m]	Detects salinity changes owing to flow in fracture system.	Chapter 4
Fluid replacement log	1–100 m [1–10 m]	Detects salinity changes owing to flow in fracture system.	Chapter 4
Geological observation	0.1–500 km	Surface lineations, structures, etc., may indicate fractures at depth.	Chapter 2 Chapter 4
Satellite airborne imaging	1–500 km [1–100 m]	Direct observation of lineaments and inference of fractures from geological structures.	Chapter 2
Core inspection	[0.1–10 cm]	Core may not be representative.	Chapter 4
Optical imaging	[0.1–10 cm]	Borehole fluid must be clear.	Chapter 4

Tiltmeter methods	100–2,000 m	Expansion of fracture by hydrofrac pumping operations is critical.	Chapter 3 Chapter 4
Flowmeters	1–100 m	Directly detects fracture flow.	Chapter 3 Chapter 4
Heat-pulse flowmeter	[1–10 m]	Directly detects fracture flow.	Chapter 4
Electromagnetic flowmeter	[1–10 m]	Still under development.	Chapter 4
Acoustic doppler flowmeter	[1–10 m]	Still under development.	Chapter 4

[a] λ is the wavelength of seismic or sonic energy.

lies. In addition, because they are commonly organized into one or more sets, each of which has a preferred spatial orientation, fractures commonly impose some anisotropy in physical properties on the rock mass. This anisotropy may be an important characteristic for fracture detection, especially when the anisotropy is simple and not aligned with other fabric (such as bedding planes) in the rock mass. In mildly deformed bedded rocks, fractures are commonly oriented nearly vertical, with a single preferred azimuth, or two orthogonal azimuths. Several of the detection techniques rely on this characteristic. However, in tectonically active areas, there may be several sets of fractures or fracture zones with a variety of orientations.

The methods listed in Table 4.1 detect fractures indirectly. Typically, the reduced data from each detection method (e.g., seismic travel times) must be *inverted* to yield estimates of local rock properties (e.g., seismic velocities). Normally, these rock properties are not fracture properties (e.g., fracture density). Instead, the fracture properties must be indirectly *deduced* from the rock properties. This deduction requires the help of rock property theory (see Chapter 3), which may unavoidably rely on strong idealizations of fracture geometry. These fracture properties are not always the properties (e.g., fracture permeability) of direct interest in many applications. Instead, they must be *interpreted* from the deduced fracture properties. This interpretation requires higher levels of subjectivity than the first (inversion) or the second (deduction) steps.

SURFACE METHODS

Seismic Reflection

Elastic properties can be determined at greater ranges than electric or electromagnetic properties; hence, seismology is the technique most widely used to explore the deep subsurface. Seismological investigations use *P* waves, in which the rock deforms (compresses and dilates) along the direction of wave travel (as with ordinary sound in air), or *S* waves, in which the rock deforms (shears) transverse (or perpendicular) to the direction of wave travel. *S* waves may be further classified according to polarization (i.e., the orientation of the transverse deformation); this distinction is ignored in most seismological studies but turns out to be crucial for fracture detection. Some of the energy of *P* waves is converted to *S* waves at reflecting horizons, and these *S* waves also return to the surface, where they can be detected and analyzed.

In reflection seismology a controlled seismic source (or a closely spaced array of sources) imparts energy into the ground. The energy travels through the rock, reflects off features (e.g., lithologic boundaries and fractures) where the rock properties change abruptly, and returns to the surface, where it is received and recorded at many points. The receivers, which are a closely spaced array of sensors, record the vertical component of the seismic motion, one or two horizon

-tal components, or all three components. Shear waves are not transmitted by fluids, so in a conventional marine survey the receivers record only the pressure pulse (*P* wave). Each recording consists of a digital record, several seconds long, of arriving energy from all paths. After each shot, the source and receivers are moved to new locations, and the procedure is repeated.

Extensive data processing is required to extract useful information from this voluminous data set. An elementary step in this data processing gathers together the records corresponding to reflections under the common midpoints of various source-receiver pairs. The records are digitally stretched in time so that obliquely traveling waves arrive at the same adjusted time as vertically traveling waves; then the records are averaged together. This is called *stacking*.

In conventional two-dimensional (2-D) surveys the sources and receivers are distributed and moved together along a straight line on the surface, and the processed data are displayed in a format similar to a 2-D vertical section of the subsurface below that line. More common in recent times is the 3-D survey, where both sources and receivers are distributed in a 2-D pattern on the surface. As these patterns are moved in a swath across the surface, the investigated region is a 3-D volume of rock, and the processed data are presented to the interpreter in vertical, horizontal, or oblique slices through this volume.

These same principles apply even if the survey is not conducted at the earth's surface but from a tunnel or borehole.

P Waves

P-wave reflection seismology at near-vertical incidence is the primary means by which most of the world's oil and gas reservoirs have been found. However, this technique is not very sensitive to the presence of vertical fractures, as evidenced by the lack of consistent success at finding the "sweet spots" (i.e., the zones of fracture concentration) in fractured reservoirs. This is due to the insensitivity of near-vertically traveling *P* waves to the presence of vertical fractures (Hudson, 1980; Thomsen, 1995; see Chapter 3).

In modern surveys, seismic data are not necessarily restricted to near-vertical raypaths. Typically, the maximum source-receiver offset can be adjusted so that the reflections at the target depth span an angular aperture of 25° or more. Obliquely traveling *P* waves are affected by vertical fractures, both in velocity and attenuation, if their rays do not lie in the plane of the cracks (see Chapter 3). Hence, when data from a set of such oblique paths are processed into a conventional seismic reflection section, the zones of intense fracturing may appear as velocity or amplitude anomalies, most commonly as "dim spots." Kuich (1989) discusses how such techniques have been used to locate fractured oil reservoirs in the Austin Chalk fields in central Texas.

Garotta (1989) discusses the limitations of this technique, noting that dim spots may occur for a number of other reasons, not involving fractures at all. To

test whether a particular dim spot is due to fractures, it is useful to look for the characteristic azimuthal anisotropy of fractures by collecting data along another survey line that crosses the dim spot at some angle (usually 90°) to the first survey line. Fractures are indicated by an azimuthal variation in the dimness of the stacked reflection at the intersection point or in the amplitude variation with source-receiver offset. This procedure is expensive and must be repeated separately for each spot to be investigated. An additional complication is that the set of oblique raypaths from the crossing survey line averages a different volume of rock than for the first survey line. When comparing the two data sets, the possibility of confusing lateral heterogeneity with anisotropy arises. However, in offshore areas this technique may be the only one available because the *S*-wave techniques discussed below are not applicable, for *S* waves are not transmitted by fluids.

In situations where near-horizontal fracture zones are present, vertically traveling *P* waves can be used to indicate their size and orientation, although individual fractures cannot be resolved (Green and Mair, 1983). An example is shown in Figure 4.1, where reflections obtained from a subhorizontal fracture zone or fault are compared to acoustic televiewer (BHTV; see "Borehole Imaging

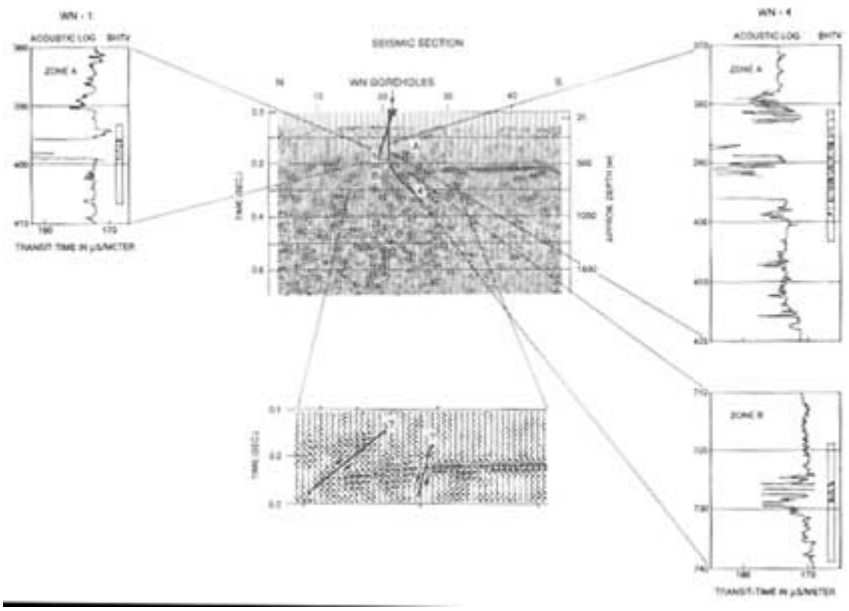

FIGURE 4.1 Comparison of a conventional *P*-wave reflection seismogram with acoustic televiewer image logs. The image logs show the distribution of fractures where two boreholes penetrate the reflector at locations close to the center of the seismic line. Modified from Green and Mair (1983).

Logs" in the section of this chapter entitled "single-Hole Methods") images of fractures intersecting boreholes near the center of the seismic section. The scale differences between the remote seismic sounding and the local borehole measurements are apparent in the figure. The *P*-wave reflections indicate a single, horizontally continuous fracture zone, whereas the borehole images indicate a great deal of variability in the local distribution of fractures in the fracture zone. This illustrates the low spatial resolving power of remote sensing methods, like seismic reflection, when used to probe to depths of several kilometers.

Three-dimensional seismic data (usually *P*-wave data) are remarkable for their ability to detect subtle features in the subsurface. For example, differences in the amplitudes of reflected waves may be too slight to be noticeable on a vertical section from a 2-D survey, yet they may form a distinctive pattern that is easily recognized on a horizontal section from a 3-D survey. Figure 4.2 shows a horizontal section through the 3-D survey of an oil field in Oman. The section clearly shows a pattern of orthogonally intersecting quasi-linear features, interpreted to be the seismic expression of sets of regional faults and fractures. These features are oriented vertically and in two orthogonal horizontal directions by the stress (or paleostress) field. The fractures form preferred pathways for the movement of fluids; the difference in seismic velocities between oil-filled and brine-filled rocks accounts for the linear features in the image. Advanced processing and color displays further enable the recognition of such subtle patterns.

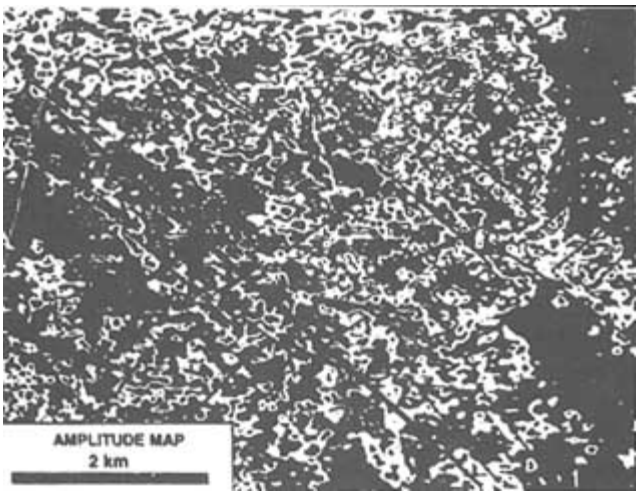

FIGURE 4.2 Horizontal section (more precisely, a map of processed reflection amplitudes, corresponding to constant reflection times) over a portion of the Yibal oil field, in Oman, showing patterns of near-orthogonal lineations interpreted as vertical faults and fractures. From Paillet (1993).

In 3D surveys on land the source and receiver patterns may include sufficient distribution of azimuths that the amplitude variation with offset of reflected *P* waves is measurable (cf. Lefeuvre and Desegaulx, 1993). This "azimuthal AVO" effect also is indicative of the presence of fractures, following the principles of Chapter 3.

S Waves

As discussed in Chapter 3, seismic shear waves are markedly influenced by aligned fractures, even though their wavelengths may be much greater than the size of the fractures. If the fractures are uniformly distributed and small compared to the wavelength, the waves propagate as though in a homogeneous anisotropic medium. By contrast, if the wavelength is small compared to the fractures, the waves will be scattered. However, long waves can penetrate much deeper into a rock mass than short waves (the range is approximately proportional to the wavelength), thus permitting deep investigation.

Anisotropies in the rock arising from aligned fractures split incident shear waves into two modes: (1) one polarized roughly in the plane of predominant fracturing and (2) one polarized roughly perpendicular to this plane. Of course, both of these shear modes are polarized roughly perpendicular to the raypath. To visualize this fact, imagine a pile of business cards standing on edge, with the spaces between the cards representing a set of vertical fractures. Imagine your hands holding the cards (from above and below), with your palms flat and horizontal, representing the wave fronts of a vertically traveling wave. Orient your fingers across the cards (representing shear motion in that direction), and shear the deck of cards sideways. It deforms easily, shearing along the zones of weakness between the cards (the fractures), indicating that the deck (representing a rock mass) is compliant for this sense of shear. With your palms still flat and horizontal, orient your fingers along the cards and try to shear the deck in that direction. It is much stiffer for this sense of shear because you must deform the cards themselves, without help from the zones of weakness between them.

Shear waves polarized obliquely to the fractures resolve themselves vectorially into these two particular directions, determined by the rock mass. These two modes travel at different speeds; the faster mode is polarized in the plane of the fractures. The difference in speed depends on the degree of fracturing. In a simple case (see Chapter 3) the delay depends on the dimensionless fracture density, η, defined for penny-shaped cracks as

$$\eta = N_v \langle l^3 \rangle / 8 \qquad (4.1a)$$

$$= \frac{3}{4\pi} \frac{\phi_f}{\epsilon}, \qquad (4.1b)$$

where N_v is the number of fractures per unit volume (called the fracture density elsewhere in this report), and $\langle l^3 \rangle$ is the average of the cube of the fracture

length. The second formulation above (Eq. 4.lb) gives the nondimensional fracture density in terms of the fracture porosity, $_f$, and crack aspect ratio, ε, the ratio of fracture thickness to fracture length. In a simple 2-D case (see Hestir and Long, 1990), the 2-D analog of parameter η (rather than, e.g., $_f$ or N_v) controls the fracture network permeability. The theory is valid for fractures that are small compared to a seismic wavelength, that is, for microfractures up through joints; however, the $< l^3 >$ factor in the equation indicates that a few large cracks will dominate the behavior of the fracture network.

Differences in arrival times of the two shear-wave modes after propagation through an interval several wavelengths thick provide stable averages of the nondimensional fracture density over that interval. Using typical oil industry acquisition practice, for example, average velocity differences of as little as 1 percent can be measured reliably. It is possible to measure such small differences even though neither velocity is known to within 10 to 20 percent of its absolute value. This is because shear modes both travel through the same rock and share the same uncertainties (e.g., the same unknown thickness of the interval), as with an interferometer (Thomsen, 1988). It follows that the average nondimensional fracture densities can be determined with similar high sensitivity and similar low spatial resolution. Recent advances in the application of these principles have come because of the capability to manipulate the source polarization and to record all signal components.

Petroleum industry experience has shown (e.g., Willis et al., 1986) that a low "background" density of fractures ($\eta = 0.01$) is ubiquitous in sedimentary rocks and that failure to account for it may result in uninterpretable shear-wave data. Such low fracture densities may not correspond to fracture permeabilities of great production significance; however, they may affect the subsurface fluid pressure regime. This happens because fractures may penetrate formations (e.g., shales) that would otherwise form pressure seals, thus establishing hydraulic continuity and a local hydrostatic pressure gradient over thousands of meters of section. See Powley (1990) for a discussion of these "subsurface fluid compartments."

It is possible to apply *S*-wave reflection analysis by using converted *P* waves (i.e., *P* → split *S* waves; Garotta, 1989) to detect vertical fractures at depth. Of course, such an application involves only one source polarization. However, a single horizontal source orientation with two horizontal receiver components can provide sufficient information for the analysis (Thomsen, 1988). Meadows and Winterstein (1994) report the detection and characterization of an artificial hydraulic fracture via analysis of the reflection of split shear waves back to the surface. Macbeth (1991) discusses the practicality of various methods to estimate shear-wave anisotropy from raw seismic data.

These seismic techniques for fracture detection can be expensive. A full acquisition scheme (three source orientations, three-component receivers) may be two to five times as expensive as a traditional one-source vertical recording

survey. If only one or two horizontal sources with two horizontal receivers are used, the cost is still roughly one and one-half to three times the traditional cost. Garotta (1989) argues that a traditional vertical or explosive source, using three-component receivers, recording *P* waves converted to split *S* waves is sufficient, making the marginal cost almost negligible. Research in the next few years will determine the utility of these less expensive alternatives.

S wave methods work best in rocks that are structurally simple (e.g., horizontal beds), with simple anisotropy owing to aligned vertical cracks. In the future it may be possible to deal with more complicated situations, using the full power of the raw (prestack) data. A recent conference, summarized by Crampin (1991), provides a good cross-section of recent advances.

Electrical and Electromagnetic Methods

Detection of water-filled fractures by electrical and electromagnetic methods is possible because water-filled fractures generally have higher electrical conductivities than intact rock. This higher conductivity is attributed to the connected geometry of the fracture, the mobility of conductive ions in the water saturating the fracture, and the conductivity of clay minerals present as fracture linings or as alteration products in the adjacent rocks (see Chapter 3). Obviously, these effects are more apparent if the surrounding rocks have low porosities. A number of different methods have been developed since the beginning of the century, when these methods were first formulated.

Electrical Methods

Electrical methods utilize what from a functional viewpoint may be considered as direct current (DC). That is, the electric fields satisfy the Laplace equation. In practice, frequencies of a few Hertz are normally used, so that noise from other frequencies can be filtered out. Two electrodes are used to inject current into the ground, and two electrodes are used to measure the voltage caused by the current. A number of different electrode configurations have been invented since the beginning of the century, but only a few are commonly used (Figure 4.3). Results are normally presented as "apparent resistivity," which is calculated from the ratio of measured voltage to injected current, multiplied by a geometric factor that depends on the configuration of the electrodes.

These configurations are normally used in two modes, sounding or profiling. In the sounding mode the separation between electrodes is changed (e.g., increased), while the center of the array remains at the same location. In profiling mode the relative positions of the electrodes are kept constant, while the entire electrode array is moved along a profile, with measurements taken at regular intervals. In principle, sounding gives information on changes in resistivity with depth, whereas profiling gives information on lateral changes in resistivity. Today,

computer technology makes it possible to use multi-electrode arrays that allow a combination of profiling and sounding to be performed simultaneously. The dipole-dipole and pole-dipole arrays (Figure 4.3) are most commonly used in combined surveys.

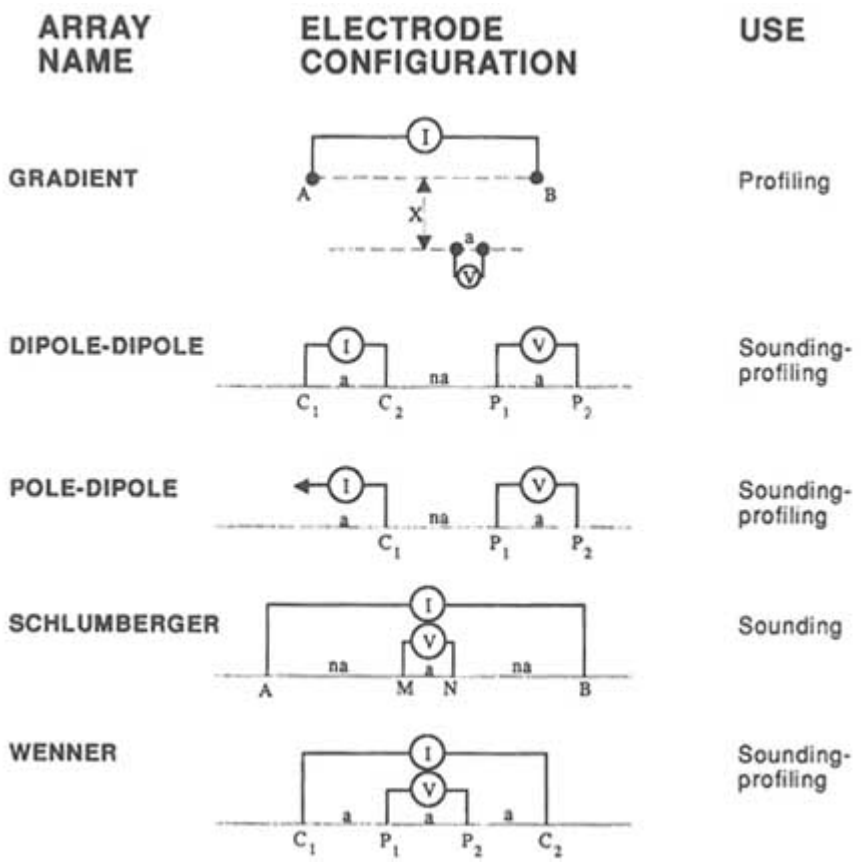

FIGURE 4.3 Common arrays used in resistivity surveys. Symbols: A, B, and C are current electrodes; M, N, and P are potential electrodes; V is voltage, I is current, a is electrode separation, n is an integer multiplier, and x is the separation distance between injection and measurement electrodes.

Electrical soundings are made to investigate the earth beneath the sounding point, most commonly in horizontally stratified environments where the method is used to find the depth, thickness, and electrical properties of different strata. In this context, "Schlumberger sounding" is a standard technique in the search for horizontal aquifers in such environments (Ward, 1990). This and similar techniques can only be used to detect fracture systems that are semihorizontal.

The presence of steeply dipping fracture systems causes distortions in the data that can be erroneously interpreted in terms of horizontal stratification. The fact that the electric fields satisfy the Laplace equation implies that resolution deteriorates rapidly with depth. Hence, deep electrical soundings can only be expected to detect larger fracture zones. The resolving power of electrical sounding can be quantified through numerical modeling (e.g., Rijo et al., 1977; Johansen, 1977; Ward, 1990).

Electrical profiling has the capability to detect steeply dipping fractures and fracture zones and, if combined with sounding, can make rough estimates of the dip of the zones. Resolution of fractures and precision in location are normally excellent if the fractures extend to the surface. However, in many cases, fractured bedrock is covered with overburden having electrical properties similar to those of the fracture zones. In practice, this limits resolution and prevents detection of fractures and minor fracture zones. In combined sounding and profiling, the effects of overburden and loss of resolution with depth inhibit accurate estimates of dip. The effects of overburden with different conductivities and thicknesses have been investigated through extensive theoretical work and numerical modeling. Based on this work, estimates can be made of attainable resolution and deductibility in different environments. Generally speaking, resolution and depth penetration are proportional to electrode separation (Dey et al., 1975; Coggon, 1973; Barker, 1989). General quantitative estimates are difficult to make, so scoping calculations are useful in defining survey layout and expected results.

Electrode arrays may be rotated around the center point in order to obtain measurements of electrical resistivity as a function of azimuth. If the overburden is horizontally isotropic and the bedrock contains vertical fractures, the measurements appear more resistive if soundings are directed transverse to the fracture planes. This is termed *directional sounding* and has been applied by Lieblich et al. (1991, 1992a,b) at several sites in New England.

Electromagnetic Methods

Electromagnetic methods utilize electric and magnetic fields in the earth that satisfy the diffusion equation, which ignores the "displacement currents" that are necessary for true wave propagation. This implies that anomalies in the data, attributed to anomalous conductors in the ground, in most cases are caused by induced currents. Electromagnetic methods commonly use frequencies from a few hundred Hertz to about 100 kHz. Lower frequencies may be used to investigate large-scale structures (e.g., magnetotelluric techniques).

Electromagnetic methods commonly use noncontacting sources or receivers, in the form of loops that measure one or more of the magnetic field components. Some instrumentation also makes use of the electric field. Noncontacting sources offer an advantage, compared to electrical methods, with respect to ease of use and efficiency in the field. Electromagnetic data can be collected from airplanes

or helicopters, allowing large areas to be surveyed quickly and at relatively low cost.

Some common electromagnetic methods are presented in Figure 4.4. Like electric methods, electromagnetic methods can be used for sounding, profiling, or a combination thereof. For some applications it is advantageous to use planewave sources, that is, sources located sufficiently far away that the primary field appears to be a plane wave in the survey area. In other applications, sources and receivers are separated by fixed finite distances.

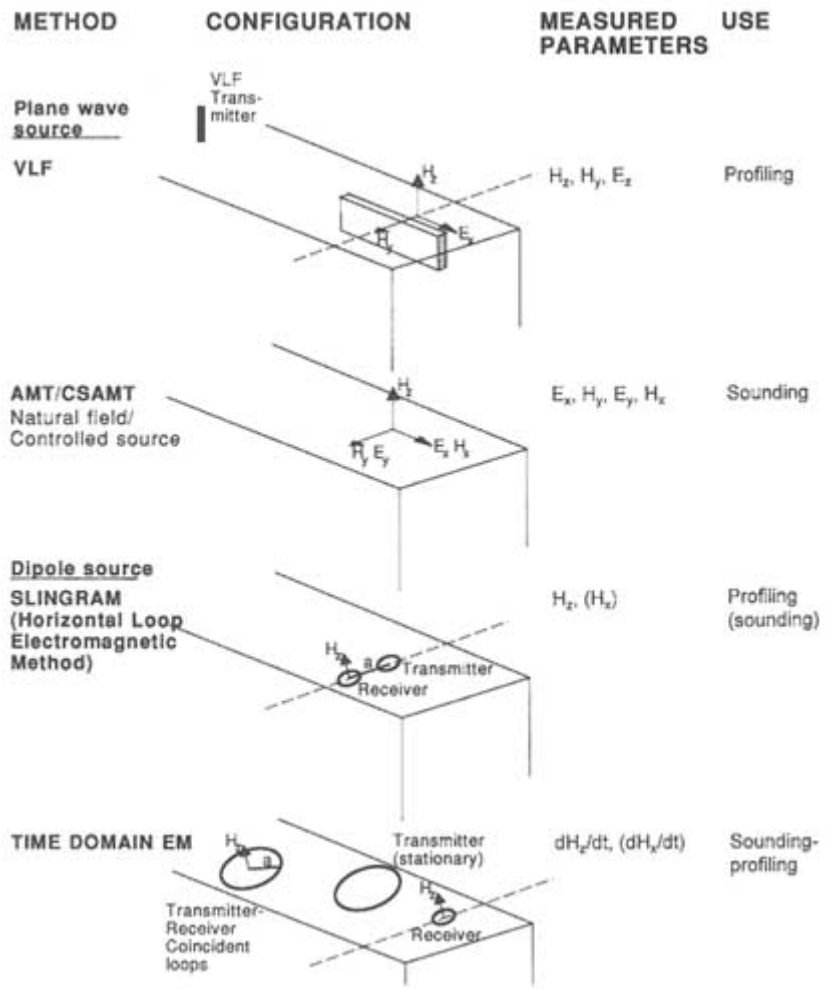

FIGURE 4.4 Common electromagnetic methods in geophysical sounding. H_x, H_y, and H_z are the components of the magnetic field; E_x, E_y, and E_z are the components of the electric field.

Modern electromagnetic equipment normally allows measurements over a wide frequency band. This can be achieved in two ways: through the use of multiple fixed frequencies (frequency domain) or by sampling the real-time response of a transmitted pulse (time domain). Mathematically, frequency and time domain methods are equivalent; the choice of domain depends mainly on practical considerations during instrument design and on noise reduction considerations.

The "skin depth" is used as a measure of the depth of penetration for electromagnetic methods. The skin depth is the distance over which a plane wave decreases in magnitude by the factor 1/*e* (where *e*, Euler's number, is approximately 2.72). The skin depth is proportional to the square root of the ratio of resistivity to frequency, so that penetration decreases with decreased ground resistivity and/or increased frequency. This implies, for example, that penetration will be poor if there is a clay-rich overburden. The actual depth of penetration for a specific method or instrument depends on the source-receiver configuration and the sensitivity and signal-to-noise ratio of the instrumentation used. It is roughly proportional to the average skin depth at a specific survey location.

When used in the sounding mode, electromagnetic methods are poor at resolving buried resistive layers but good at detecting conductive layers. This is because the electromagnetic response is from induction currents that are concentrated in the conductive layers. Thus, these methods can be used to detect semihorizontal fracture zones. Resolution deteriorates with depth owing to the diffusive nature of the electromagnetic field. Consequently, sounding methods detect fracture zones better than individual fractures at depth.

In profiling mode, overburden normally masks information about the underlying bedrock. A large fraction of the anomalies observed by using the SLINGRAM or Horizontal Loop Electromagnetic Method (HLEM), for example, are caused by localized overburden thickening, which in many cases is caused by differential weathering of the bedrock at a fracture zone. However, indirect indications of the existence of steeply dipping fracture zones may be obtained (Villegas-Garcia and West, 1983). In such cases it is not possible to estimate the dip of the fracture zone because the induced current does not flow through the zone itself. Generally speaking, dip estimates of fracture zones based on electromagnetic measurements are uncertain because currents induced at depth are much smaller than those induced closer to the surface. Thus, the measured anomalies are only weakly dependent on dip (Ketola and Puranen, 1967).

Ground-Penetrating Radar

Ground-penetrating radar (GPR) uses electromagnetic energy to obtain information about the subsurface. Use of the word "radar" implies that the electric and magnetic fields in this case satisfy the wave equation, which includes

the "displacement currents." In principle, GPR is similar to reflection seismic techniques (Figure 4.5). The radar produces a short pulse of high-frequency (10- to 1,000-MHz) electromagnetic energy, which is transmitted into the ground. Propagation of the radar signal depends on the electric properties of the rock, mainly the dielectric constant and electrical conductivity. These properties are primarily controlled by fluid content and the presence of clay minerals. Where these properties change abruptly in the subsurface, part of the energy is reflected back to the surface.

An important consequence of the applicability of the wave equation is that resolution is of the same order as the dominant wavelength. In combination with probing ranges of many wavelengths, this implies that detailed information can be obtained on structures located "far" away (i.e., in the probing range). In some sense this is equivalent to "seeing" through the rock. The radar range is roughly proportional to the first power of the resistivity of the rock. In highly resistive granites, probing ranges of about 100 m are regularly obtained for frequencies in the 20- to 100-MHz range (Holloway et al., 1992; Olsson et al., 1992). In

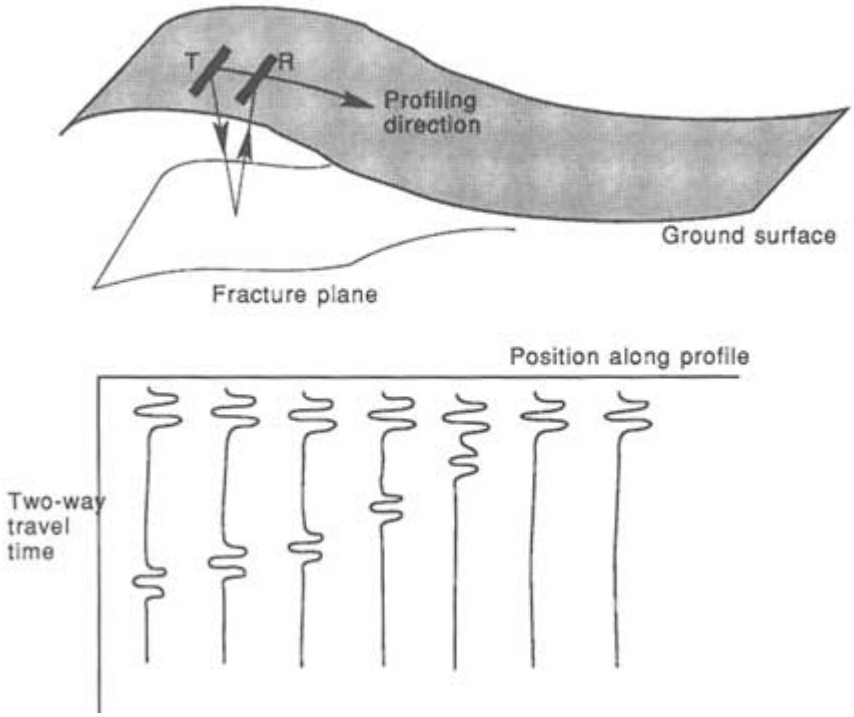

FIGURE 4.5 Schematic illustration of ground-penetrating radar used in profiling mode. T is the transmitter; R is the receiver.

other resistive rock types, probing ranges of 10 to 20 m are common. In highly conductive media such as clays, probing ranges are commonly only a few meters. Probing range decreases with increasing frequency, but resolution improves. Frequencies in the range of 500 to 1,000 MHz make it possible to obtain detailed information on structures in a few meters of the surface. For example, high-frequency radar is regularly used in the investigation of roads and other structures for fractures, rebars, voids, asphalt, and concrete thickness.

In principle, GPR is an excellent tool for finding fractures. For example, GPR surveys on granitic outcrops at the Underground Research Laboratory in Manitoba, Canada (Holloway et al., 1992) located semihorizontal fracture zones to depths of 70 to 80 m below the surface (Figure 4.6). However, as with all electric or electromagnetic methods, conductive overburden presents a problem because it prevents significant energy from penetrating into the underlying bedrock. In cases when significant overburden is present, very little information on bedrock structures will be obtained. However, GPR can be used to estimate the thickness of the overburden or to investigate its internal structure. The effectiveness of GPR in indicating fracture zones is illustrated by comparing the number

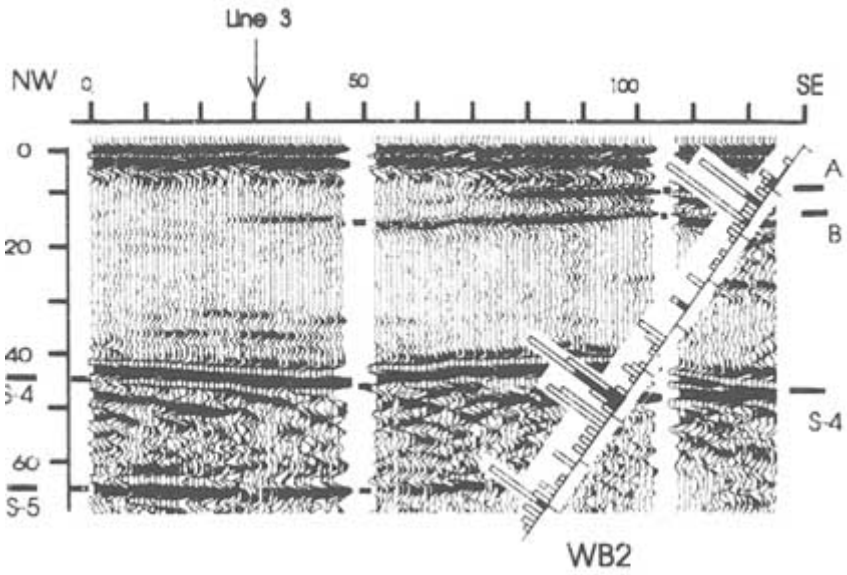

FIGURE 4.6 Semihorizontal fracture zones observed by ground-penetrating radar along a profile measured on granitic outcrops at the Underground Research Laboratory, Manitoba, Canada, showing distribution of fractures along borehole WB2. Reflectors S-4 and S-5, seen at depths of 40 to 50 m and 65 m, respectively, are verified by increased fracture frequency observed in the slanted borehole NB2. The smallest bars indicate single fractures; the other bars are scaled accordingly. From Holloway et al. (1992).

of closed fractures (indicated by open solid bars) and open fractures (solid bars) in borehole WB2 drilled through the section imaged with the GPR in Figure 4.6.

In summary, GPR is an excellent tool for mapping fractures or fracture zones with high resolution in the absence of overburden. If overburden is present, it can be used to map the structure of the overburden. If GPR is used in boreholes and tunnels, the problems caused by the overburden can be avoided. The capabilities and applications of borehole radar are discussed in a later section.

Tiltmeters

Tiltmeters installed on or below the earth's surface can detect volumetric strains in the subsurface. These strains can result from active hydraulic fracturing or from poroelastic or thermoelastic strains resulting from fluid injection at less than fracture pressure.

For fracturing operations the depth of fracturing is normally controlled by the placement of packers in the hole. The vertical extent, azimuth, and horizontal length of these features are indirectly controlled by varying the pumping pressure and can be monitored by using tiltmeters. A circular array of tiltmeters, typically with a radius 40 percent of the nominal fracture depth and sensitive to tilts of 10^{-9} radians, can delineate the azimuth and volume of fracturing. (The dimensions of the fractures also can be inferred from these data; e.g., Lacy and Smith, 1989.) Tiltmeter data are used to determine how well the operator has succeeded in engineering these fractures. For fluid injection, tiltmeter data can be used to determine the pore pressure distribution in the subsurface by relating the observed deformation to changes in effective stress. Tiltmeter data can also provide an approximate estimate of the permeability tensor.

One specific application of tiltmeter measurements to hydraulic fracture studies is the identification of fracture orientation changes around boreholes. These changes occur in response to changes in the direction of principal stress in rock around the borehole. For example, the minimum principal stress may be horizontal immediately adjacent to the borehole wall and vertical away from the local stress concentration produced by the borehole. In such situations, borehole imaging techniques will indicate vertical fractures in the wellbore. However, tiltmeters arrayed around the wellbore will indicate a symmetrical distribution of tilt away from the borehole during fracture inflation. These tiltmeter measurements indicate the presence of horizontal fractures, signaling that the vertical fractures observed in the wellbore have rotated to horizontal positions as they propagate away from the wellbore. Such results have been reported (R. H. Morin, U.S. Geological Survey, 1992, personal communication) for a 365-m-deep hydraulic fracture generated in granitic rocks on the western side of the Sierra Nevada uplift in California.

Geological Observations

Fracture orientations observed visually at the surface are commonly preserved at depth, as discussed in Chapter 2. Surface fractures may be observed in road cuts or river cuts or as lineaments on air photos or satellite imagery. Schmidt (1985) gives an example of how surface exposures can be used to constrain subsurface fracture occurrences. Even when fractures are not visible at the surface, air photos and surface geophysical or geological maps can serve as valuable guides in designing borehole networks or excavations to sample fractures and to identify possible relationships between fracture distributions and large-scale geological structures.

BOREHOLE-BOREHOLE AND BOREHOLE-SURFACE METHODS

For most surface characterization techniques, overburden introduces difficulties because of its attenuation properties and the high contrast in its properties compared to the underlying rock. In many cases the overburden acts as a filter that obscures information about the subsurface, requiring the use of complex correction procedures to obtain useful information. Boreholes and tunnels provide access to measurement points below the ground surface, allowing many of the problems introduced by the overburden to be avoided. The main advantages of performing measurements underground is that they provide subsurface confirmation of the surface measurements. They also allow surface measurements (e.g., seismic reflection data) to be tied directly to lithology and structure. Many of the measurement techniques applied at the ground surface, which were presented in the previous section, can be applied in boreholes with appropriate modifications.

Compared to surface surveys, borehole measurements sometimes require complex (and compact) sensors. Furthermore, the measurement locations are restricted to a few lines through the space represented by the boreholes and tunnels. Borehole investigations are also more costly than comparable surface surveys, owing to higher drilling and measurement costs.

The techniques discussed in this section apply to the determination of rock properties at considerable distances from the measurement locations; that is, they are remote sensing techniques. The subject of near-borehole measurements is deferred to the section "Single-Hole Methods," later in this chapter.

Remote sensing techniques are based on the propagation of waves, either seismic or electromagnetic, through the rock. As from the surface, these techniques can be applied in either transmission or reflection mode. It should be recognized that a combination of transmission and reflection data normally are collected during a survey, but in most surveys only one of the data sets is actually used. Remote sensing is done with sources and receivers placed in the same borehole, in different boreholes, or one in the borehole and the other at the

ground surface. Depending on the application, these surveys are referred to by different "trade" names, but the principles are the same.

Vertical Seismic Profiling

The vertical seismic profile (VSP) survey method provides a compromise between the large scale of surface seismic soundings and the fine scale of borehole logs. The VSP survey is performed by using a surface seismic source and receivers located in the wellbore. The method was originally designed to verify travel time versus depth inversions for surface surveys but has since been expanded to include a variety of applications (White, 1983; Balch and Lee, 1984). The smaller spatial scales and the depth control given by the borehole allow inversions of somewhat higher frequencies than those typical of conventional surface seismic surveys. The higher frequencies provide greater spatial resolution of the target area. At the same time, these conditions restrict the volume of rock that can be investigated to the vicinity of a borehole.

The simplest form of a VSP survey places the source as close to the wellhead as practicable (i.e., zero offset). If the source is placed some distance away from the wellhead, the survey is referred to as an offset VSP survey. If several offset source positions (located on a line leading away from the borehole) are used, it is called a walkaway VSP survey. If the source is in the borehole and the receivers are on the surface, it is a reverse VSP survey (an RVSP). There may be one receiver station or many for each source. If the borehole is deviated from the vertical, other configurations are possible. For example, in a walkabore survey both source and receiver are translated together, so that the raypaths are always vertical. For a 100-m-deep borehole, the volume of investigation in a typical VSP survey would range from 100 to about 1,000 m in diameter.

Other types of *P*-wave VSP surveys have been used successfully to characterize fracture zones in crystalline rock. Carswell and Moon (1989) used a walkaway VSP survey to characterize semihorizontal fault zones at the Underground Research Laboratory in Manitoba, Canada. The experiment was successful in mapping several fracture zones; however, wide-angle reflections and mode conversions limited the useful data window at large offsets.

A new technique for processing VSP-type data for the identification of fracture zones was developed within the framework of the International Stripa Project by Cosma et al. (1991). Referred to as image space processing, it is based on the assumption that fracture zones are planar reflectors in a constant-velocity host rock. This assumption has been found to be valid in many crystalline rock environments. This processing method determines the statistical significance of possible reflectors by comparing their strengths with the noise level in the data. It has proved to be very useful in detecting fracture zones in crystalline rock, as it allows enhancement of very weak reflections caused by fracture zones.

Recent developments in VSP technology related to fracturing of reservoirs include the use of three-component geophones to register *S* waves (see "*S* Waves," in the section on "Seismic Reflection," earlier in this chapter). The borehole environment is particularly amenable to split shear-wave analysis, because interference from reflection effects at the ground surface is avoided (Crampin et al., 1986). Shear-wave splitting of vertically traveling *S* waves is assumed to be caused by preferentially aligned fractures, and the magnitude and orientation of shear-wave splitting reflect the frequency and orientation of such fractures. The first field application of this technique was in a geothermal environment at The Geysers (Majer et al., 1992). Winterstein and Meadows (1991a,b) reported a correlation between the orientation of the faster shear waves and in situ stresses (1991a) and significant changes in polarization orientation and magnitude with depth (1991b). Liu et al. (1993) discuss the detailed characterization of multiple subsurface fracture sets, using VSs, RVSs, and cross-hole surveys to measure the azimuthal anisotropy of shear-wave velocity and attenuation at the Conoco Borehole Test Facility in Oklahoma.

One particular form of VSP survey, the VSP hydrophone tube-wave analysis, has been found especially useful for detection of fractures intersecting boreholes. "Tube waves" are confined to the interior and neighborhood of the borehole, and travel somewhat slower than shear waves in rock. This method uses hydrophones suspended in a fluid-filled borehole to detect tube waves generated by the interaction of *P* waves from the surface source with hydraulically conductive fractures that intersect the borehole. When source strength is corrected for geometrical spreading, the amplitude of the tube waves generated by this interaction can be related to fracture hydraulic conductance (Hardin and Toksöz, 1985; Hardin et al., 1987). The relative variation of amplitudes of the tube waves from different offset source azimuths can be used to estimate the strike and dip of the permeable fractures. VSP tube-wave surveys have been compared to other geophysical and hydraulic data at several fractured rock sites and have generally been found to agree qualitatively but not always quantitatively with these data (Paillet et al., 1987; Paillet, 1991a). Used in this manner, VSP is not exactly a remote sensing method because the information obtained represents properties of fractures where they intersect the borehole.

Transmission Tomography

Transmission measurements are normally made between boreholes, between a borehole and the ground surface, or both. Measurements are commonly made of travel times and amplitudes of first arrivals, which directly yield the average velocity and attenuation for the wave type used. The basic idea behind tomographic reconstruction is that information about the properties of the interior of a volume can be obtained through measurements performed at the boundary. For this purpose, multiple source and receiver locations are required to probe the volume of investigation with multiple crossing rays, each a source-receiver combi

nation (e.g., Figure 4.7). The travel time and amplitude data for each transmitter-receiver pair are assumed to represent the average of material properties of the rock along the raypath. In tomographic inversion the task is to reconstruct the velocity or attenuation distribution in the interior of the investigated volume from these averages.

To obtain an estimate of the unknown property at a given point, it is necessary that several rays pass close to the same point and that the rays have different directions and thus different information content. The requirement that several rays pass within each volume (of roughly spherical shape) with dimensions on the order of a wavelength places constraints on the borehole geometry. In practice, this implies that the source and receiver positions, and hence the boreholes, must be located in the same plane. Three-dimensional tomography is possible in principle, but in practice it is difficult to obtain ray coverage dense enough for reasonable resolution in three dimensions.

In borehole-to-borehole—or cross-hole—measurements, data on both travel time and amplitude of the direct wave between transmitter and receiver (i.e., the first arrival) can be extracted. Consequently, two types of tomograms can be constructed: one based on travel times that resolves the distribution of velocity, and the other that resolves the distribution of attenuation. The latter type has only recently been applied, but a number of good examples exist. It is assumed that the travel time, t_i, for the ith ray can be constructed as the line integral of inverse velocity ("slowness"), $1/v(x)$, along each ray L_i:

$$t_i = \int_{L_i} \left(\frac{1}{v(x)} \right) dx. \qquad (4.2)$$

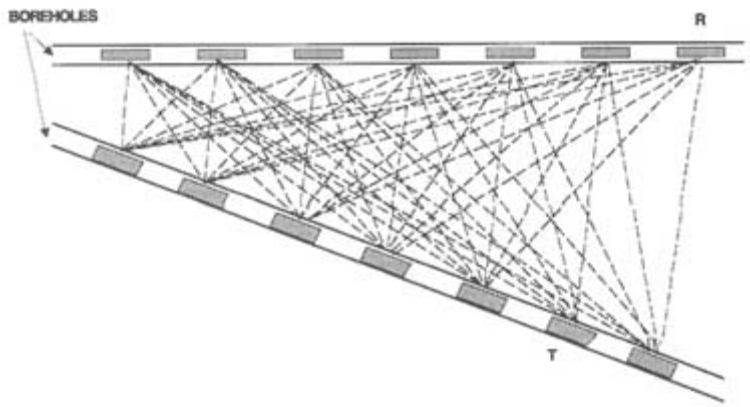

FIGURE 4.7 Schematic configuration of sources and receivers for transmission tomography between boreholes, also called borehole-to-borehole or cross-hole tomography. R is the receiver; T is the transmitter.

The amplitudes cannot be obtained from the line integral directly, but by taking the logarithm of the amplitudes the problem can be linearized:

$$\alpha_i r_i = \int_{L_i} \alpha(x)dx = ln\left[\frac{E_0 a_s(\theta_1) a_r(\theta_2)}{r_i E_i}\right], \qquad (4.3)$$

where α_i is the total attenuation along ray i, r_i is the distance between transmitter and receiver, α is the local attenuation at position x, E_0 is a normalization constant, E_i is the measured (vector) amplitude, $a_s(\theta_1)$ is a function describing the radiation pattern of the source, and $a_r(\theta_2)$ is the corresponding function for the receiver. An inversion of the logarithm of the received amplitudes should give an estimate of the distribution of attenuations in the plane of investigation. Examples of a slowness tomogram and an attenuation tomogram of the same rock mass are given in Figure 4.8.

The slowness and attenuation tomograms exhibit small differences in the location of anomalies. A possible explanation for the observed differences, to some extent supported by data from the International Stripa Project, is that the increased slowness corresponds to open fractures (increased porosity), while the

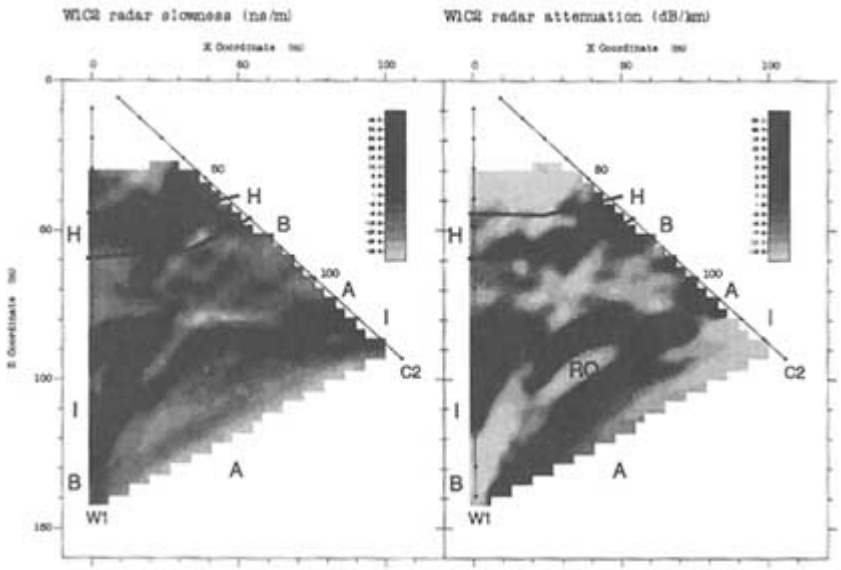

FIGURE 4.8 Tomographic reconstruction of a borehole section in the Stripa mine using 60-MHz radar, showing radar slowness (left) and radar attenuation (right). Arrows and letters give the positions of fracture zones inferred from these and other data. From Olsson et al. (1992).

increased attenuation is caused by alteration of the rock (the presence of clay minerals). This hypothesis is based on the fact that increased slowness is mainly due to increased water content, while increased attenuation is mainly due to increased electrical conductivity.

If velocity contrasts are smaller than 10 to 15 percent, ray bending according to Snell's law can be neglected, and the raypaths, L_i, can be assumed to be straight lines. This makes the system of equations linear. The straight-ray assumption can also be justified, even if velocity contrasts are larger, when there are low-velocity anomalies embedded in a high-velocity medium, as demonstrated by Dyer and Worthington (1988). This situation frequently occurs when mapping fracture systems (low-velocity anomalies) in crystalline rock. The straight-ray assumption is normally not useful if there is a general velocity gradient over the investigated area. This is commonly the case in sedimentary basins where velocity generally increases with depth.

Tomographic inversion can be performed either with transform methods or series expansion methods. Integral transform methods (e.g., the inverse plane-wave transform) are commonly used in medical tomography, where the angular ray coverage of the investigated region is quite complete. In geophysical tomography there is generally incomplete angular ray coverage (i.e., sources and/or receivers cannot be located on all sides of the region of investigation), and ray bending is significant in many cases. This makes series expansion methods more useful. In these methods the target region is assumed to consist of a discrete set of pixels, and the measured property is formed as the sum of the pixel values along the raypath. This approximates the physical problem as a matrix equation, which must be solved numerically.

If raypaths are straight, there is a linear relationship between travel time and slowness or inverse velocity (Eq. 4.2), or between amplitude and attenuation (Eq. 4.3). However, if ray bending is significant, the system is nonlinear because the length of the raypath becomes a function of the slowness. To obtain a solution of the nonlinear system, a series of linearized problems are solved iteratively. The system of travel time equations is generally large, sparse, ill posed, and overdetermined; it may also be underdetermined. "Overdetermined" means that there are more data available than unknowns; the data are mutually inconsistent (in the strict sense), so that a solution is found that "best" fits the data. "Underdetermined" means that the data are not sufficient to determine all of the unknowns, for example, those pertaining to pixels with insufficient illumination by the rays.

The system of equations is solved by using some minimization criterion for the difference between the model solution and the measured data. Several iterative inversion algorithms have been devised and are referred to by acronyms such as ART, SIRT, and CG (for a description, see Ivansson, 1986). These methods generally yield similar results; there are standard methods for determining the validity of the solutions in light of the problems mentioned above. It is also

possible to solve the equation system by direct inversion, but this is normally not done because of the very large number of unknowns and the long computing times required.

Resolution of a tomogram depends in a complex manner on a number of factors. At best, resolution is no better than about one-quarter the dominant wavelength. It also depends on the ray pattern (density and angular coverage), geological structure, noise levels, and placement accuracy of source-receiver positions. In practically all geological applications, sources and receivers cannot be located on all sides of the investigated area. This leads to artifacts or errors in the reconstructed image, particularly in parts of the plane where the ray density is low or the rays are nearly parallel. These problems have been discussed in a number of papers (e.g., Nolet, 1987; Dyer and Worthington, 1988a, b; Bregman et al., 1989; Krajewski et al., 1989). Limited ray coverage generally leads to smearing of anomalies. The effect of ray coverage can be quantified by computing the ability of the data to resolve each pixel (Nolet, 1987). Errors due to noise, zero-time offset, and inadequately known source and receiver locations are more difficult to quantify.

Tomographic inversion normally assumes that the medium is isotropic. However, this method requires a large angular distribution of raypaths in order to include rays with different information content. This inevitably exposes the technique to artifacts if the medium is in fact anisotropic. It is easy to see that small travel time differences owing to large velocity differences in small anomalous areas may be comparable in magnitude to those caused by even weak velocity anisotropy throughout the entire region crossed by the rays. One way to handle this problem is to use all the raypaths to define an average anisotropy. Then all the travel times are adjusted to remove the differences caused by this average anisotropy (Majer et al., 1990; Olsson et al., 1991). The residual differences in travel times are then assumed to be due to heterogeneities alone. One difficulty with anisotropy correction is that the variation in travel times caused by fracture zones that are aligned with the fabric of the rock may be removed by the correction. The difference between heterogeneity and anisotropy is blurred in this case.

Tomographic surveys can be repeated to indicate some change of state in the rock, occurring between the initial and subsequent surveys. This is called difference or alterant tomography. For example, this technique makes it possible to study groundwater flow paths through rock. Saline tracer injected into the rock increases the attenuation of radar waves. Tomographic inversion of the difference in attenuation data before and after injection of tracer provides an image of the location and amount of tracer in the tomographic plane. Multiple repetition measurements provide data on the spreading of tracer as a function of time (Olsson et al., 1991). A fuller discussion is given later in this chapter under "Fluid Flow Monitoring Using Geophysical Methods."

Seismic Tomography

Seismic cross-hole tomography can be applied at a variety of scales, ranging from detailed engineering studies on the meter scale to reservoir studies on the kilometer scale. The frequencies used vary with the scale of investigation from a few tens of hertz for kilometer-scale investigations to tens of kilohertz for meter-scale investigations.

To obtain large cross-hole probing ranges, powerful seismic sources are required. Explosives can provide the necessary power, but their use must be restricted to avoid damage to the borehole. Commonly applied sources include air guns, electric sparkers, down-hole hammers, and piezoelectric sources. To avoid borehole damage, these sources provide limited energy output and can be used only for shorter ranges. Further development of new seismic borehole sources is needed. A promising technique is to use nonimpulsive sources where the signal is extended in time (e.g., swept-frequency sources, whose total energy may be substantial), but the instantaneous power rate is small.

Either hydrophones, which sense the scalar pressure pulse in the borehole fluid caused by the wave, or geophones, which are clamped to the borehole wall and sense the vector motion of the wave, are used as receivers. These instruments sense the velocity of the medium caused by the wave. In detailed engineering applications, three-component accelerometers are sometimes used because of their high-frequency response.

Comprehensive studies of fracture characterization with seismic tomographic techniques have been performed in nuclear waste disposal programs. In situ tests have generally been successful in mapping the location and properties of fracture zones (Sattel and Gelbke, 1987; Bregman et al., 1989; Cosma, 1990; Majer et al., 1990; Tura et al., 1991). An example from a detailed characterization of a fracture zone at the Grimsel test site in the granitic Alps of Switzerland, using sources and receivers on all four sides of the investigated area, is shown in Figure 4.9.

Radar Tomography

Borehole radar normally implies the application of a pulsed source. Radar wave propagation is only feasible in resistive formations, for example, crystalline rocks, limestones, and salt formations. Tomographic surveys have been performed using frequencies in the range of 20 to 500 MHz, corresponding to wavelengths of approximately 5 to 0.2 m in rock. Useful cross-hole ranges for the lower frequencies can be more than 100 m. Fracture zones normally appear in the tomographic images as regions of low velocity and increased attenuation compared to the surrounding rock. Radar has also been used successfully to map saline tracer transport through fractured rock by repeated tomographic measure

ments (e.g., Olsson et al., 1991). Increases in radar attenuation caused by a saline tracer can be used to estimate flow porosity (Olsson et al., 1991).

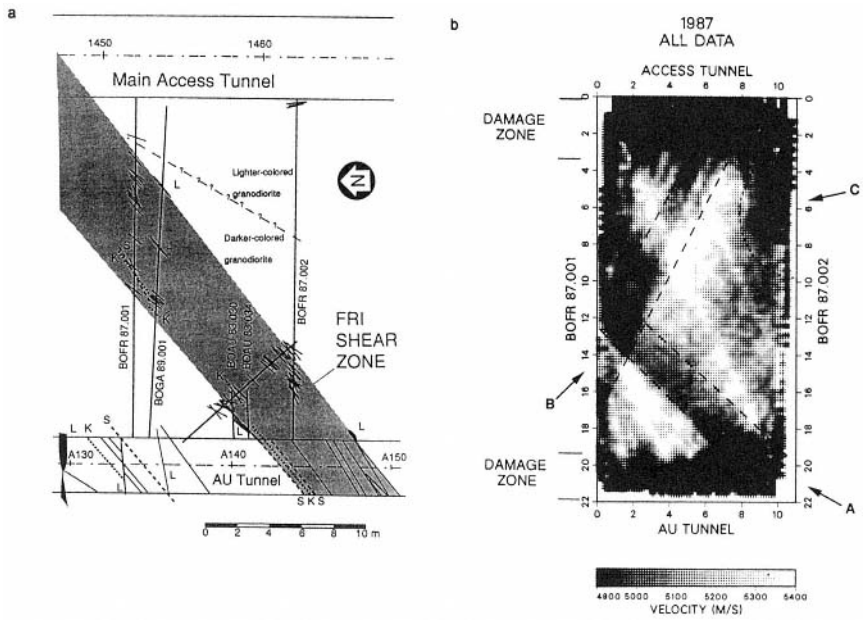

FIGURE 4.9 (a) Geological plan view of the FRI fracture zone at the Grimsel test site that is intersected by two parallel tunnels. (b) Seismic tomogram obtained with complete (four-sided) coverage by inverting the 1987 data. From Majer et al. (1990).

An example of a radar attenuation and seismic velocity tomogram from the same borehole section is shown in Figure 4.10. The low-velocity and high-attenuation anomalies correspond to fracture zones, with widths ranging from 1 to 8 m, intersecting a granite intrusion. The agreement between seismic and radar results is remarkable considering that they represent different physical properties of the rock mass.

Electromagnetic Tomography

There are also a number of continuous-wave electromagnetic systems that can be used for cross-hole surveys. Some work in the high-frequency range (above 10 MHz), where wave propagation is the dominant phenomenon in resistive rock types. These systems are normally used for attenuation tomography and yield resolutions comparable to the pulsed-radar systems described above.

There are also a few systems that use frequencies of a few hundred kilohertz. In this frequency range, diffusion processes dominate, which results in an inherent loss of resolution. An investigation method of this type is the radio imaging

method, which is applied in underground openings to characterize resistive beds (e.g., coal seams) surrounded by more conductive strata. The resistive bed acts as a wave guide because the waves are less attenuated in the resistive rock; ranges of several hundred meters can be obtained (Stolarczyk, 1990). Faults can be detected indirectly as changes in affected coal seams. Because fractures are usually less resistive than their surroundings, this method is infrequently used for fracture detection.

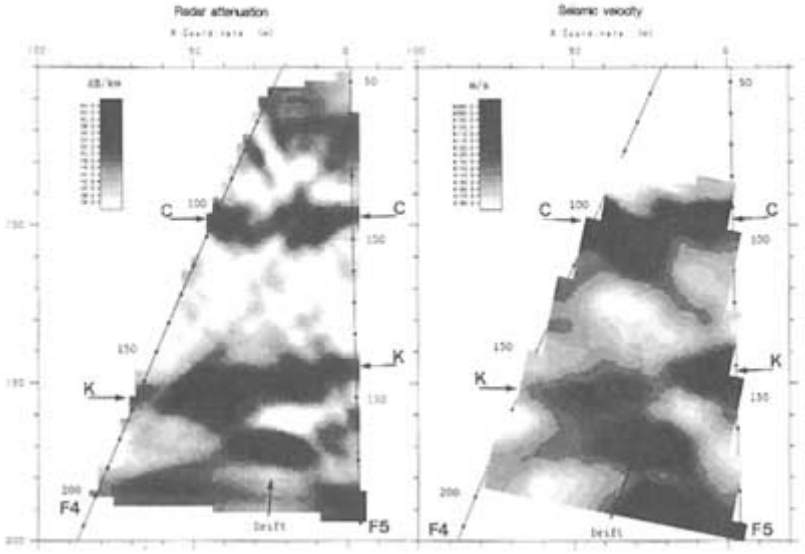

FIGURE 4.10 Tomographic reconstruction of borehole Section F4-F5 at the Stripa mine. Left, radar attenuation data; right, seismic velocity data. From Olsson et al. (1992).

Horizontal magnetic dipoles (vertical loops) located in drifts or boreholes are used as sources and receivers. This results in a vertical electric field component between the conductive layers, with the magnetic field component horizontally polarized in the seam. Data from multiple sources and receivers can be inverted by tomographic techniques to yield maps of electric properties in the resistive bed. Interpretation of the reconstructed images normally requires the knowledge and skill of a geologist.

Three-dimensional inversion schemes for electromagnetic data require modeling the forward problem repeatedly. Successful inversion requires a great deal of high-quality data from many sources (Alumbaugh and Morrison, 1993; Lee, 1993).

Electric Resistivity Tomography

Inversion techniques for cross-hole direct-current electric data also have been developed and are commonly referred to as electrical resistivity tomography. In

this case the inversion assumes that the media satisfy the Laplace equation. Laplace methods inherently have a lower resolving power. Inversion techniques based on iterative finite-element algorithms (Yorkey et al., 1987; Daily and Owen, 1991) and alpha centers (Shima and Saito, 1989; Shima, 1990) have been developed and tested on synthetic and field data. Results appear promising, but further research is required to resolve issues concerning resolution and uniqueness of solutions in geological environments.

Borehole Reflection Methods

Reflectivity is not an intrinsic property of rock; instead, it is a function of the differences in rock properties and the distance over which such differences occur. Hence, derivation of rock properties based on reflection data is difficult. Instead, reflections primarily give information on the geometric characteristics of geological features.

Cross-Hole Seismic Reflection

The image space processing technique discussed earlier has been applied to reflection data from borehole-to-surface, borehole-to-borehole, and borehole-to-tunnel surveys (e.g., Blumling et al., 1990; Cosma, 1991). Seismic reflection techniques can also be applied in tunnels (during excavation) to predict the occurrence of fracture zones or other geological features that may disrupt excavation work ahead of the tunnel face (Sattel et al., 1992).

Borehole Radar

The borehole radar technique was developed during the 1980s and is now available for commercial use. One of the most significant contributions to the technique was made by the international Stripa Project, where new equipment, processing, and interpretation techniques were developed. The new system can be used for single-hole reflection measurements and for cross-hole reflection and tomography surveys.

A recent development is a directional antenna that senses the direction of the received radiation. This makes it possible to uniquely determine the orientation of a fracture zone from measurements in a single borehole (Sandberg et al., 1991). Figure 4.11 shows the main components of the short-pulse directional borehole radar system developed in the Stripa Project. It includes a computer unit that is used for control of measurements, data storage, presentation, and analysis. The transmitter and the directional receiver are connected to the control unit through optical fibers; power is supplied through downhole batteries. The system uses dominant frequencies in the range of 20 to 60 MHz, corresponding to wavelengths in most rock types of 6 to 2 m. The transmitter in the directional

radar system is equipped with an electrical dipole antenna aligned with the borehole axis. The receiver is sensitive to the direction of the incoming radiation, and this makes it possible to find the location of a reflector relative to the borehole (see Appendix 4.A).

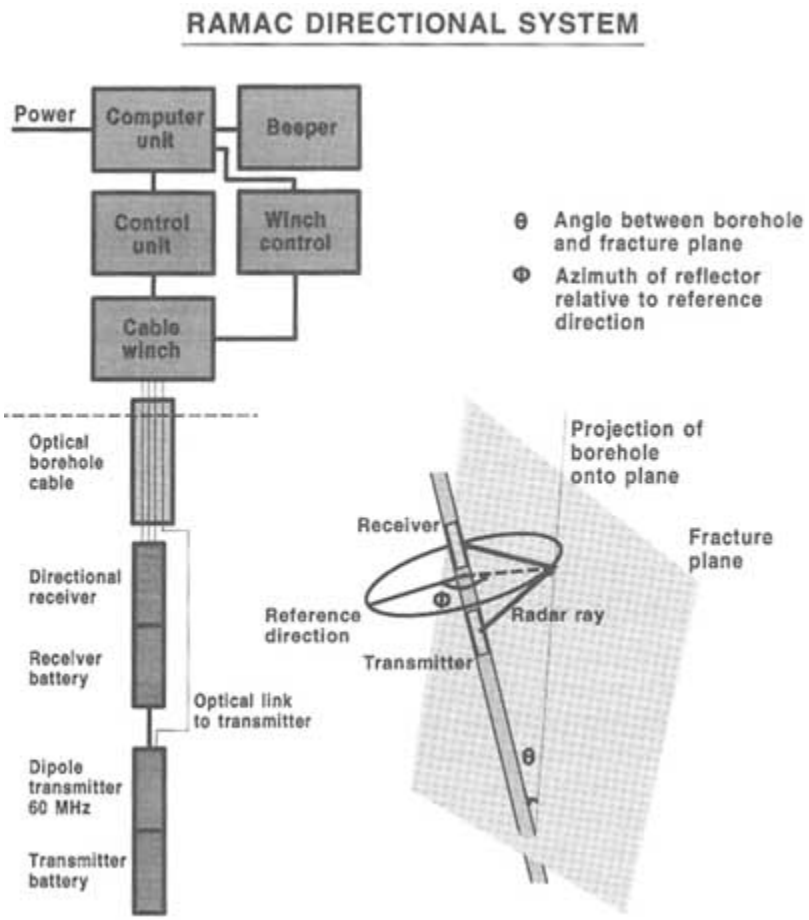

FIGURE 4.11 Main components of the short-pulse directional borehole radar system. From Olsson (1992).

Evaluation of borehole radar data enables understanding the observed features with respect to physical properties, orientation, and size. Reflections are caused by differences in electric properties and can be understood from general arguments concerning wave propagation. In this respect the general characteristics of radar-and seismic-wave propagation are similar and have been described in numerous textbooks (e.g., Stratton, 1941; Telford et al., 1976; Claerbout, 1985).

Features with large contrasts in electric properties will cause strong reflections, independent of their thickness. For example, a thin metallic foil is sufficient for total reflection of radar waves. In the typical case in which the contrast in properties is low, a certain minimum thickness is required to give a reflection that stands above background. This is referred to as the detectable limit and is sometimes taken to be about one-thirtieth the dominant wavelength. For borehole radar applications, this corresponds to about 10 cm (thicker than a single fracture). Hence, borehole radar will detect fracture zones, clusters of fractures, and tectonized zones rather than single fractures. The capability to detect features with a thickness of about 10 cm has been verified in the Stripa Project mine, where a reflector was identified by using radar and was later excavated and found to be a 10-cm-wide tectonized zone.

Borehole radar detection ranges vary considerably, depending on the conductivity of the host medium. In highly resistive granites or rock salt, probing ranges of about 100 m or greater are common; ranges in conductive clays or brine-saturated porous sandstones can be so short that the method is virtually useless in such environments.

Coupled Inversion of Transmission and Reflection Data

In most cross-hole measurements where pulsed sources are used, the entire waveform form is recorded. In most cases only the time or amplitude of the first arrival is used for tomographic inversion, as described in the previous section. However, the entire waveform contains information about the structure of the rock and can be included in the data inversion. An inversion algorithm of this type is termed *diffraction tomography*. Principles for the 2-D case have been outlined by Wu and Toksöz (1987), who provide several synthetic examples showing that reconstructed images of rock properties with satisfactory resolution could be obtained from cross-hole configurations. Pratt and Worthington (1988) tested the 2-D algorithm in an ultrasonic tank experiment and obtained reasonable agreement with the experimentally defined velocity distribution. They recognized that the use of point sources to characterize 2-D objects (i.e., a 2.5-D geometry) requires extensions to the original scheme outlined by Wu and Toksöz. Tura et al. (1991) used a pseudospectral finite-difference technique to investigate the applicability of the Born approximation to actual data. Although the results were not as good as desired, they showed that diffraction tomography may become practical if the first-arrival wavelet can be removed from the data. Further experience is needed before the practical applicability of diffraction tomography can be resolved.

The velocity field obtained from tomographic inversion of transmission data can also be used as input to image construction (depth migration) with reflection data. Velocities derived from transmission data are used to obtain a more exact velocity field, which is then used as a priori information in the interpretation

of reflection data. Reflection and transmission data can be used iteratively to successively improve the seismic image of the subsurface regions (Lines, 1991). These procedures are commonly referred to as seismic reflection tomography and are applied to surface measurements. An integrated scheme for wave equation and tomographic inversion of borehole data also has been suggested by Pratt and Goulty (1991).

Acoustic Emissions

Acoustic emissions (AEs) normally accompany the growth of fractures. These microseismic events, containing measurable frequencies of 10 to 1,000 Hz, can be detected at ranges of several hundred feet in competent rock (Lacy and Smith, 1989) and frequently indicate the presence of a fractured zone rather than a single isolated fracture (Wills et al., 1992). It is known from laboratory and small-scale field experiments that seismic signals are generated during and after the hydrofracture process (Lockner and Byerlee, 1977; Solberg et al., 1977).

Acoustic emissions have been used to infer the effects of fluid injections and hydrofractures on scales ranging from laboratory to field (Pearson, 1981; Batchelor, 1982; Majer and McEvilly, 1982; Majer et al., 1983; Majer and Doe, 1986). Acoustic emissions are used to identify the location of fluids injected into "tight" rock. For years earthquake seismologists have been concerned with characterizing the seismic signals generated from slip along a discontinuity in the earth; AEs are no different except for their size. AEs are used to specify the dynamic source properties (fracture orientation, dimensions, slip orientation, time history of slip, and stress distribution) from the seismic waveforms.

The dominant mechanism in these signals is shear, rather than tensile slip. Because of the relatively high frequency of the AE, it may offer a real-time method for monitoring with greater resolution than tilt or magnetic measurements. In the past, most efforts have used single or multicomponent sensors, either on the ground surface (if there is no weathered overburden) or in a nearby borehole, to detect *P* and/or *S* waves (Power et al., 1976; Smith et al., 1978; Nyland and Dusseault, 1983). In an important large-scale field experiment, Baria and Green (1986) observed that when a viscous fluid is used for injection, the AEs are more likely to be tensile events, whereas lower-viscosity injection fluids yield shear events.

In deeper injections, slip is more likely to develop on preexisting fractures if there is a large differential stress. In such a case, the change in pore pressure would more likely cause shear failure on preexisting planes. (It must be kept in mind, however, that such AE activity is possible without significant fluid flow.) On the other hand, if new fractures are created, tensile failure would be expected. In the case of grouting, the pressures are held well below the breakdown point, so no tensile failures should occur. The question of the relationship of AE activity to fluid flow is then crucial. Does AE activity mean fluid flow in the same area

as the AE events, or is it mainly a pressure buildup without significant fluid flow? These and other questions regarding the significance and characteristics of the seismic signals can be addressed by analyzing acoustic emissions.

To avoid the high attenuation of the near-surface layer, receivers are normally placed in boreholes. The orientation of the clamped three-component receiver is determined from the signals received on each component from controlled sources, usually fired at a number of azimuths on the surface. Then the direction of acoustic emissions caused by the hydraulic fracturing is determined by resolution of the *P*-wave arrival on the three components, and the distance is estimated from the difference between the *P*- and *S*-wave arrival times. Alternatively, if several wells are available for monitoring, the location of the slip event can be determined from *P* waves recorded in single-component receivers, or hydrophones, by standard triangulation methods.

AE studies have proven especially useful in complex geothermal reservoirs, where downhole transducers cannot be readily inserted into the hostile environment and where transmission losses from remote seismic sources can be severe. Acoustic emissions induced by pressure and temperature changes in the reservoir rock can be related to the thermomechanical deformation of the reservoir. Acoustic emissions can be used to interpret the nature of reservoir deformation, to characterize the nature of fracture formation and propagation, and to interpret the location and geometry of fractures in the reservoir. A detailed description of the application of acoustic emission methods to reservoir studies is given in the discussion of fracture studies at The Geysers Geothermal Area in Chapter 8.

SINGLE-HOLE METHODS

Boreholes and tunnels provide the only direct means of access for measurements of fracture properties at depth. Most geophysical logging methods were designed to meet the need for measurements performed in situ, adjacent to a borehole, and in sample volumes small enough to significantly improve spatial resolution over that obtained from surface or surface-to-borehole methods. The primary drawbacks of geophysical logging in fracture applications include the effects of the borehole and drilling damage on the fracture in the measurement volume, and the restriction of sampling to the immediate vicinity of the borehole. This spatial restriction introduces significant bias in the characterization of fracture populations because boreholes are not very effective in sampling fractures, especially those aligned parallel to the borehole axis. The need to sample enough of the formation adjacent to the borehole to offset the effects of drilling damage and the effects of the fluid column on the geophysical measurements also impacts the ability to resolve fractures. Despite these important limitations, measurements made in the immediate vicinity of boreholes are very useful in characterizing fractures and fluid flow through fractures in a number of important applications.

Core Inspection

One of the most obvious and direct methods for characterizing fractures in situ is core examination. Samples containing fractures are commonly obtained by conventional rotary coring. This method is suitable for hard crystalline rocks where samples generally remain intact. It is usually found that in crystalline rocks the amount of core recovered is inversely proportional to the density of the fractures and the intensity of weathering associated with fracturing. Fracture samples in softer sedimentary formations are sometimes recovered in a relatively natural state by analogous methods, by using "shale" bits rather than diamond coring bits, or by driving the sampling barrel directly into the formation.

The orientation of recovered samples may be determined by comparing the core with oriented borehole image logs (Paillet, 1991a) or by orienting the core barrel during drilling. Core orientation is frequently determined by drilling slightly off vertical (usually by 15 or 20 degrees at a known azimuth) and fitting the core barrel with a gravitationally oriented scribe that scores the core on the downward side as it is extruded into the barrel. However, this technique is impractical for long boreholes.

Fractures are usually described as they are recovered from the core barrel. A qualitative or semiqualitative measure of fracture density is given by the "rock quality designation" factor, which is defined as the ratio of recovered core more than 4 in. (about 10 cm) long and of good quality to the total drilled length and is expressed as a percentage. Another measure of fracture density is the number of fractures intersecting the core per unit length. However, core is commonly lost or the core barrel is filled with rubble in many intensely fractured intervals, strongly biasing such fracture frequency determinations.

Fractures are also described by their openness or apparent ability to conduct fluids. In a simple example, fractures might be described as closed, open, and opened by drilling. A fourth classification, rubble, is sometimes added to include sections of core that are so badly broken that it is not practical to refit the many broken and ground pieces together. In many cases it is these very rubblized zones that dominate fluid flow.

In more sophisticated studies the degree and type of weathering associated with fracture faces is recorded. This information might include the chemical composition and nature of staining films on mineral grains, the width of alteration halos, and the amount of various infilling minerals. Fracture apertures may be estimated by measuring the diameter of isolated crystals deposited on the fracture faces. It is assumed that these crystals grew in place in the fracture, so that their size is a lower limit of the size of the opening in which they developed.

Although core inspection would appear to be a simple and direct method for characterizing fractures, it has several important drawbacks. The method can be slow and prohibitively expensive. Core samples provide a very small volumetric sample of the fracture, especially when core diameters are only a few centime

ters. Small samples are not necessarily representative of fractures in the surrounding rock mass. Even small core samples are likely to have been damaged during drilling, and core recovery may be poor in the intensely fractured and weathered parts of the rocks that provide most of the hydraulic conductivity. Hence, core studies may not be reliable for determining characteristics of dominant fractures or fracture zones.

Even with these drawbacks, cores provide useful direct evidence of the hydraulic and geological properties of fractures and host rocks. The use of core is most effective when it is related to geophysical well logs from the borehole. Core analysis can be used to relate geophysical measurements of the rock to geochemical and hydraulic properties of more intrinsic interest. The geophysical measurements can then be used to determine fracture properties in intervals where core is missing. The combined analysis of core and geophysical logs provides information on fractures that is not available when the techniques are applied separately.

Conventional Well Logs

Conventional measurements or logs made in boreholes, quasi-continuously over extended intervals, are a tried and proven way for determining the properties of the rocks adjacent to the wellbore. As a general class of measurements, well logs have both specific advantages and significant drawbacks. The unique advantages of well logs are (1) they provide a consistent one-dimensional profile of rock properties expressed in terms of a consistent length scale, (2) they provide measurements of rock properties in situ, and (3) they provide multiple independent measurements of rock properties that can be used to solve for multiple independent variables. The disadvantages of well logs are (1) they measure properties that may not be of direct interest and that are not uniquely related to the properties that are of direct interest; (2) they represent measurements on rocks that are disturbed by drilling; (3) they may average rock properties with those of the borehole fluid; and (4) they have a directional bias because they sample along the direction of the wellbore rather than in three dimensions.

The advantages of logging can be illustrated with a few common examples:

- A limited number of laboratory test data on discrete samples can be correlated with geophysical log measurements at specific depths; the rest of the logs then show how the lab data might be extrapolated between sample points.
- Core samples are subject to damage during recovery and desiccation after recovery, so a comparison between core results and logs can be used to infer the extent and nature of possible damage during drilling and recovery.
- In many surface geophysical soundings, a single geophysical property (e.g., electrical resistivity) is mapped over a depth section. When such a property depends on more than one variable (e.g., electrical resistivity depends on water

salinity, pore size, and clay mineral fraction), multiple geophysical logs can be used to identify methods for uncoupling these dependencies.

These examples illustrate the advantages of well logging as a general investigation technique giving fine-scale (sample volumes ranging from 10 cm to 10 m in diameter) descriptions of the properties of rocks and sediments encountered by boreholes.

Geophysical logging has been applied to fracture identification and characterization for many years (Keys, 1979). The identification of fractures by most conventional logs is complicated by the borehole itself and the fluids it contains (Figure 4.12). Most geophysical logs are designed to resolve beds thicker than about 10 cm; they have great difficulty in clearly defining the properties of thinner

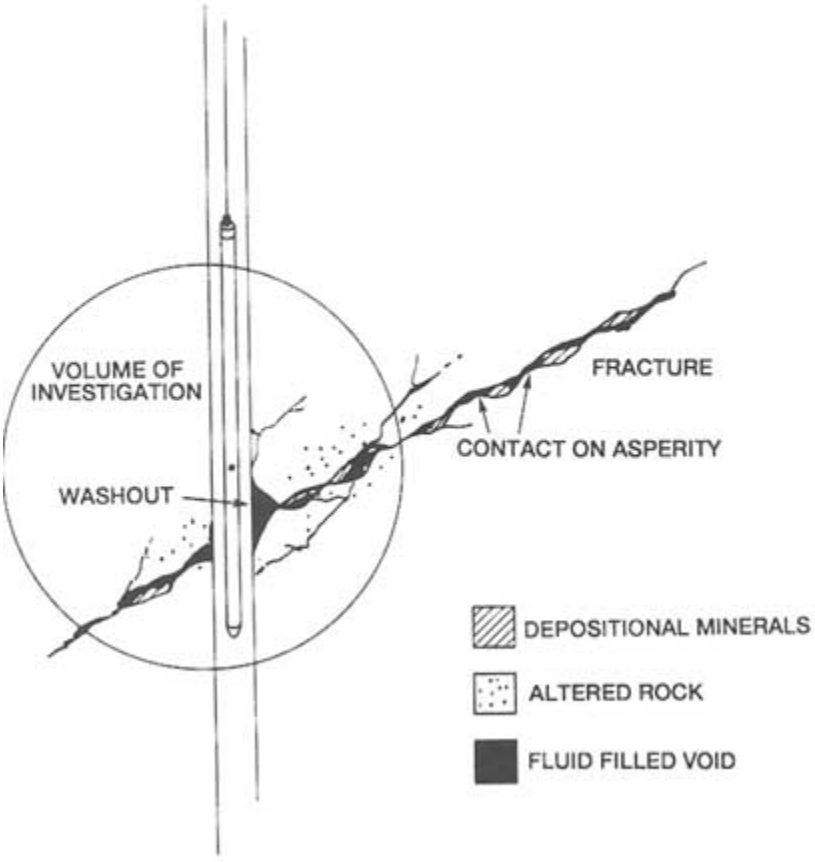

FIGURE 4.12 Schematic example of natural fractures intersecting a borehole and the geophysical volume of investigation.

beds, whose properties are averaged with those of surrounding beds. In this context, individual fractures such as those illustrated in Figure 4.12 might be considered "thin beds," with thicknesses usually less than a few centimeters for most individual fractures. If fracture zones are present or if concentrations of subparallel fractures are associated with faults and geological contacts, the thickness may be great enough that the average property of the zone will be indicated by the geophysical measurement. Even then, the properties of fractures will be averaged with those of the intervening rock and borehole fluids.

There are practical approaches to fracture analysis using conventional geophysical logs that are almost always based on physical effects indirectly related to fractures. The model of a typical fracture illustrated in Figure 4.12 was generated by breaking the rock fabric along grain boundaries, imposing some slippage along the face, and then allowing recontact of the two rock faces at asperities. Subsequent movement of fluids through the voids between asperities allows for alteration of rock around the fracture and deposition of minerals in some of the openings. The geophysical response to fractures indicated in most conventional well logs is associated with these alteration halos and with the mechanical enlargement of the borehole at the point where the fracture intersects the borehole wall. These are indirect effects, and their magnitudes may be related in a qualitative way to the "size" of the fracture. However, precise relationships between numbers, spacings, and apertures of fractures are almost impossible to define on the basis of these measurements. Appendix 4.B discusses the typical response of several conventional logs to fractures.

One of the recognized drawbacks in geophysical logging of fractured rocks is the effect of sample volumes on resolution. Because most conventional geophysical logging measurements average the properties of rocks over equant volumes about 0.3 m in diameter, these measurements are relatively insensitive to the presence of individual fractures. One class of logging tools, known collectively as micrologging devices, has been designed to improve vertical resolution for the detection of thin beds and fractures. These logging tools are modified versions of conventional neutron, gamma density, and electrical resistivity devices, with closely spaced sources and receivers or closely spaced electrodes embedded in pads that are pressed against the borehole wall. The short source-to-detector or electrode spacings are associated with sampling volumes only a few centimeters in diameter. These logging probes are used extensively in the coal industry, for example, where accurate measurements of the tops and bottoms of coal-bearing strata are of great economic importance. Microelectrical resistivity probes are also used extensively in the petroleum industry to estimate the properties of "mudcake" (a layer of drilling mud at the borehole wall) and the invaded zone immediately behind the mudcake. The sensitivity of microneutron and microdensity logs to borehole wall roughness caused by mechanical damage during drilling (known as rugosity in the logging industry) severely limits their use in some applications. Microresistivity logs have been useful in identifying fractures and

fracture zones in boreholes, but these devices have been largely superseded by more sophisticated microresistivity tools, especially the formation microscanner, which is capable of producing images of the borehole wall. The formation microscanner is described in the next section, along with other borehole wall imaging devices.

Other types of logs can sometimes be used to provide information about water movement related to fractures. For example, temperature logs measure temperature in the well as a function of depth. When borehole temperatures are at equilibrium with the local wall rocks, the temperature log accurately reflects the local formation temperature. When water is circulating along the wellbore, departures from the geothermal gradient indicate where water is entering or existing from the borehole. Fluid conductivity logs provide similar information because changes in fluid conductivity may indicate where entry or exit of water induces sharp contrasts in dissolved solids contents.

Natural circulation of water in boreholes is almost always too slow to be measured with conventional impeller flowmeters, which require vertical velocities of at least a few feet per second in order to turn the most sensitive impeller blades (Hess, 1986). However, measurable flows can be induced by pumping, if the pumping does not dewater the wellbore. Conventional flowmeter measurements during pumping can sometimes be an effective means of identifying conductive fractures that intersect the borehole (Keys and Sullivan, 1979). Temperature and fluid conductivity logs obtained during production or injection may likewise be effective methods for identifying the depths at which producing fractures intersect boreholes (Keys, 1979; Keys and Brown, 1985).

One specialized application for geophysical well logs is geothermal reservoir characterization. Most geothermal reservoirs produce hot water from fractures, but the elevated temperatures and high mineral contents of geothermal waters result in an intense interaction between fractures and water during drilling and well regulation. High temperatures, the presence of water and steam, and corrosive fluids affect the performance of logging equipment. Hostile borehole conditions also degrade the wall rock, making it more difficult to characterize fractures using geophysical logging methods. The general approach used in log analysis for geothermal applications is similar to that outlined previously for more general fracture studies. However, the difficult borehole environment greatly complicates data interpretation.

Logging equipment must be designed to withstand the elevated temperatures and pressures typically encountered in geothermal wells. Conventional logging cables cannot be used at temperatures above 150°C, and the most advanced geothermal logging cables are limited to temperatures below about 300°C. Electronic components and circuits are built to fit into specially designed dewar flasks. The presence of both steam and water limits the performance of some equipment. The high pressures encountered in geothermal reservoirs require that logs be obtained by running the logging cable through pressure control devices or "lubri

cators," which greatly complicates the operational aspects of logging. Examples of the application of fracture characterization methods to well logging in geothermal studies are given by Keys and Sullivan (1979) and Paillet and Morin (1988).

Borehole Imaging Logs

One of the most direct and effective methods for detecting fractures in boreholes is borehole wall imaging. Many devices based on optical, acoustic, or electrical techniques have been designed to provide photographs or other images of the borehole wall, so the intersection of fractures with the borehole can be "seen" and described (Paillet et al., 1990). Optical devices include photoelectric transformers, conventional cameras operated remotely from a wireline and television cameras operated remotely using coaxial cable. These cameras are used extensively in shallow water wells and other near-surface applications for a variety of borehole and casing inspection tasks.

Fracture detection applications are sometimes limited because cameras require clear borehole fluids, and they commonly image the borehole at oblique angles using local illumination sources that produce shadows, which interfere with fracture detection and interpretation (Paillet et al., 1990). Furthermore, the data are not in digital form initially, and so are not amenable to sophisticated processing. However, under the right conditions, these logs can produce striking images of fractures.

The digital borehole scanner (DBS) is a new logging tool that provides optical, true-color images of a borehole wall (Figure 4.13). The digitally recorded data yields very high resolution images, enabling detailed measurement of fractures, identification of fracture mineralization, and observation of other microscale properties not generally available with other instruments (Cohen, 1996). The primary components of the DBS system are the white light source, rotating mirror, magnetic compass or gyroscope, and photoelectric transformer. The mirror rotates at 3,000 rpm, simultaneously illuminating the borehole wall and directing the reflected light through a lens and into a photoelectric transformer. The transformer measures the intensity of the red, blue, and green light wavelengths and converts them to digital form. The data stream passes through an azimuth and a depth gauge and the data is stored on digital tape. A scrolling, unrolled image of the borehole wall is stored and simultaneously recorded on videotape.

Since the tool records high-resolution color images, mineral-filled fractures, open fractures, zones of discoloration due to rock alteration by fluids, and even gouged and altered zones can be detected. Fracture features are easier to detect in lighter color rocks such as granites and gneisses than in darker colored rocks such as shale. The maximum vertical resolution of the DBS instrument is 0.001 mm, and the horizontal resolution depends on the diameter of the borehole. For a 17 cm well, the resolution can be 0.5 mm. In general, the DBS can provide borehole images with resolutions comparable to photographs of core.

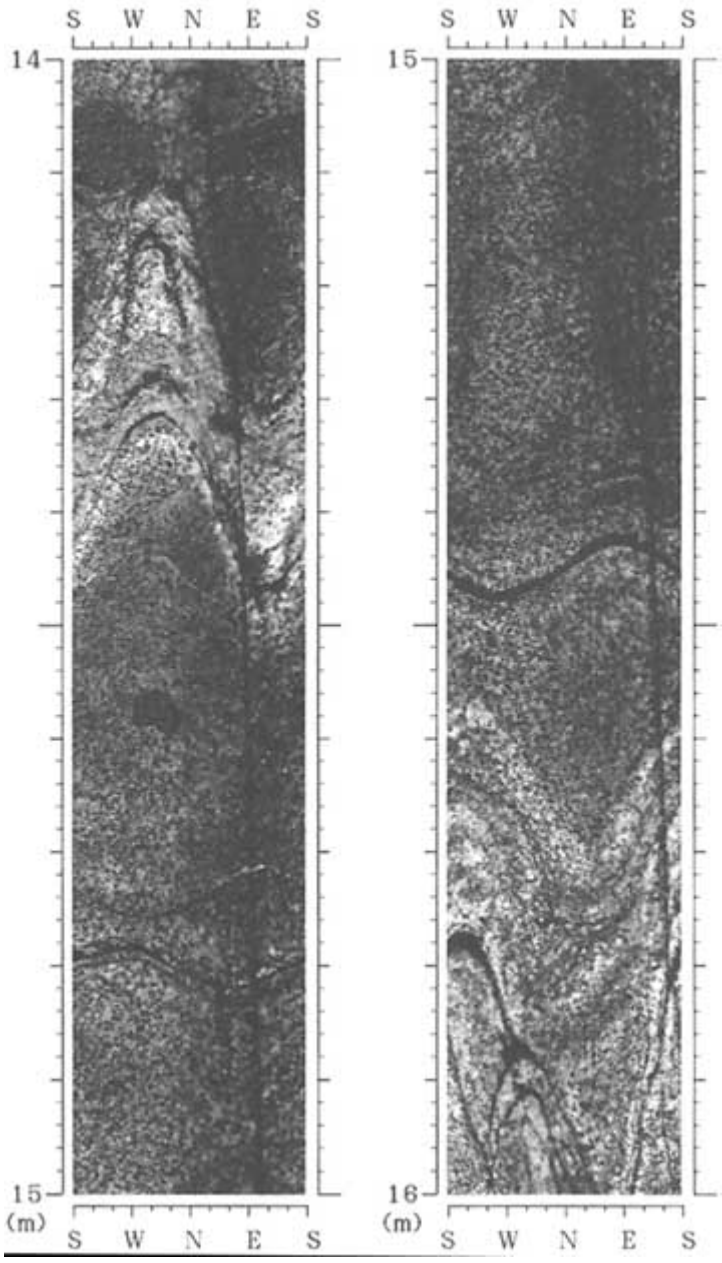

FIGURE 4.13 A color visual band digital scanner borehole log of fractured granite using the CORE borehole scanner (shown here in black and white). The dark vertical line is an artifact of the cable. Fractures are clearly evident. Reproduced with permission of CORE Corporation, Tokyo, Japan.

Television cameras require coaxial cable rather than conventional wireline. For these reasons, acoustic and electrical imaging methods are the most frequently used techniques to investigate the distribution of fractures and properties of fractured rocks in boreholes more than 50 m in depth.

The first acoustic imaging method consistently used in fracture characterization was the borehole televiewer (BHTV; Zemanek et al., 1970). The modern BHTV uses an ultrasonic beam with centerband frequency of 500 KHz to 1.5 MHz and a beam diameter of 0.5 to 1.0 cm. The BHTV operates by scanning the borehole wall at a rate of about three revolutions per second while the probe is steadily drawn along the borehole. The transducer is fired at a rapid rate and serves as both the source of the acoustic pulse and the receiver for the reflected signal. In the earliest version of this instrument the borehole image was recorded in the form of a photographic display of the intensity of reflection (Figure 4.14a). The BHTV image is oriented with respect to the local magnetic field by a downhole magnetometer. The image is split along the apparent north azimuth and "unwrapped" for display.

The intersection of the fracture with the borehole wall scatters acoustic energy, producing dark sinusoidal features on the image. The image allows the geophysicist to interpret the strike and dip of fractures, although deviation surveys are required to determine the local orientation of the borehole, so that measured orientations can be corrected for borehole orientation and for deviation between local magnetic field and true north (Kierstein, 1983; Lau, 1983). The apparent thickness of the linear feature identified on the BHTV log may be taken as a qualitative indicator of fracture "size" or aperture. However, this thickness depends on both the actual fracture aperture and the beam width and represents the fracture where it has been affected by drilling. For these reasons the interpretation of fractures using BHTV logs is at best semiquantitative.

Figure 4.14c shows a BHTV log from a granite batholith where a smooth core-hole wall provides optimum conditions for imaging. This BHTV log is compared with a synthetic televiewer image constructed by using fracture descriptions given from inspection of oriented core of the same interval. The comparison shows that on the BHTV log most of the open fractures are clearly "larger" than closed fractures. However, some of the closed fractures appear to be as large as the open ones, especially the uppermost set of parallel closed fractures. The crumbling of the layers of rock between these sealed fractures (a process known as spalling) has probably resulted in local enlargement of the fractures at the borehole wall. These fractures appear to be open fractures, comparable in size on the BHTV log to those identified by core inspection as truly open and conductive.

A second example (Figure 4.14b) illustrates that BHTV data can sometimes provide a more representative depiction of fractures than core. In the figure, core photographs are compared to BHTV logs for a borehole in granite (Paillet et al., 1985). The BHTV log indicates a single, large, near-vertical fracture, with faint indications of near-horizontal fractures close to the bottom of the larger fracture.

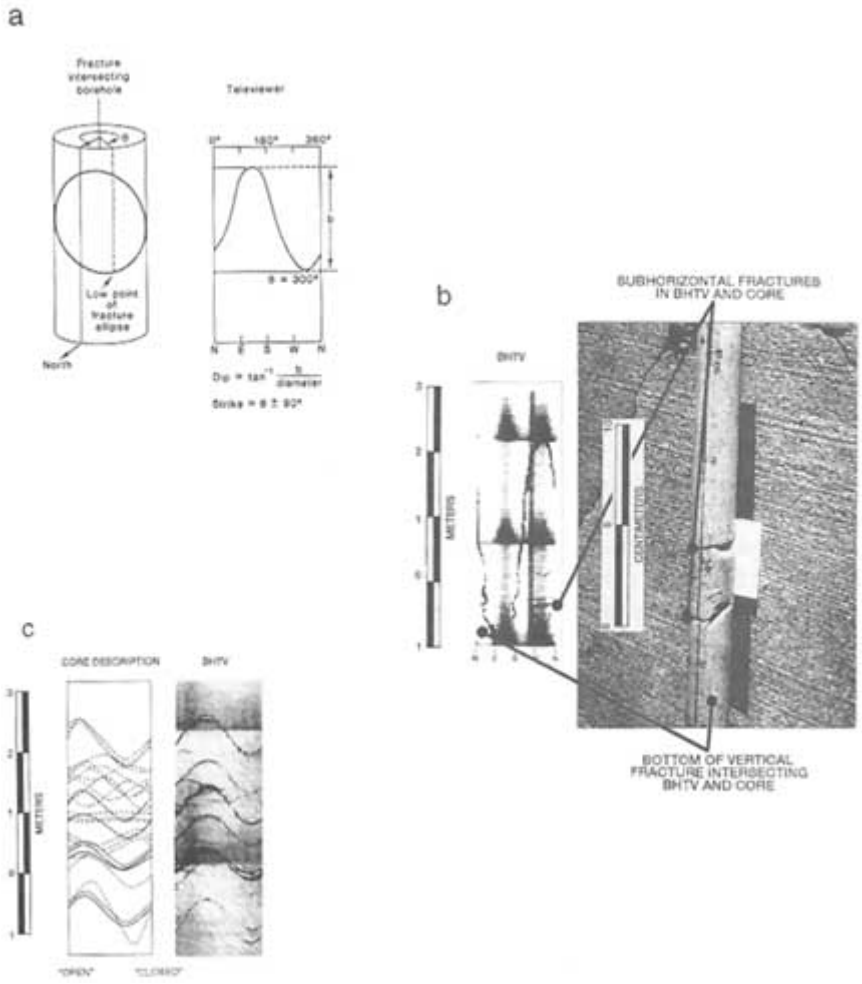

FIGURE 4.14 Acoustic borehole televiewer (BHTV) logs: (a) Schematic illustration of fracture representation by a BHTV image of the borehole wall. (b) Compression of BHTV log from a granite pluton in Manitoba, Canada, with the corresponding interval of core, indicating that apparently open horizontal fractures in core were closed in situ. (c) Example of BHTV log on right compared with core fracture description for oriented core in the same granite pluton, where closed fractures (sealed by minerals in core) are shown by dotted lines and open fractures are shown by solid lines. From Paillet et al. (1985).

The core has separated on two of the horizontal fractures, and the near-vertical fracture is barely visible as a tight fracture in the intact core. The subhorizontal fractures were nearly closed under confining pressure in situ as indicated by the BHTV log, but opened during core recovery. Although fractures shown in BHTV

logs are commonly affected by drilling damage, at least they are shown under in situ stress conditions as modified by the presence of the borehole. This is especially important in intensely fractured intervals where core is not recovered or comes out of the core barrel as rubble.

BHTV has been a reliable and tested means of borehole imaging in fracture studies for nearly two decades. In recent years the conventional approach in BHTV logging of photographing and displaying an image of the intensity of ultrasonic reflections with an oscilloscope has been modified in a number of useful ways (Paillet et al., 1990; Maki et al., 1991). An important variant is the recording of reflection time, rather than amplitude, thus giving the distance to the reflector (often referred to as an "acoustic caliper"). Further, the BHTV signal is now routinely recorded on conventional video recorder systems in the field and digitized in the laboratory. A few BHTV prototype probes now digitize reflection intensity and two-way travel time directly for each source pulse and store them on magnetic disks. Various image enhancement techniques have been used in conjunction with PC graphics packages to produce a wide variety of useful displays (Barton et al., 1991; Barton and Zoback, 1994). As an example, Figure 4.15 shows a three-dimensional side view of a borehole surface; the software allows for rotation of images and indexing along the borehole axis. The

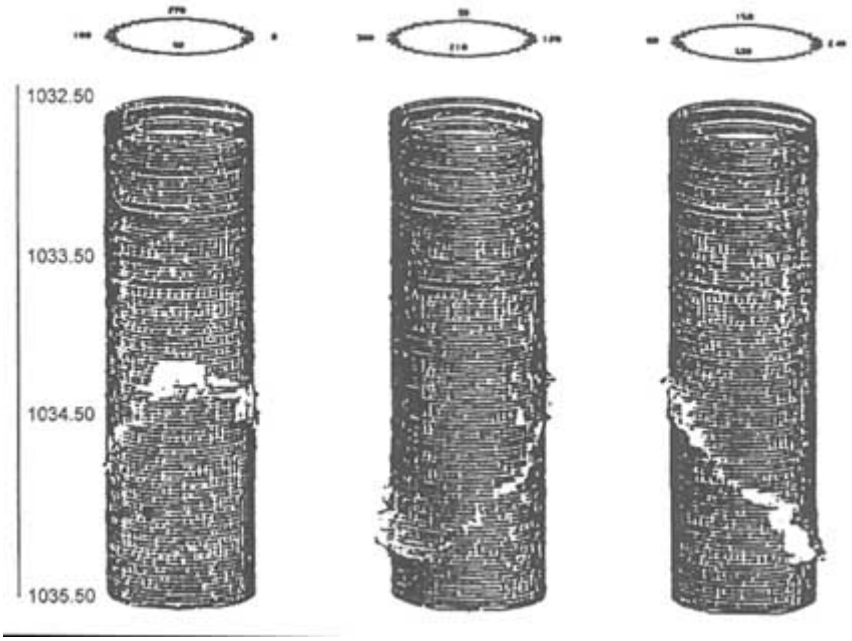

FIGURE 4.15 Example of three-dimensional side view of borehole-fracture intersection generated by digital processing of BHTV data. From Barton (1988).

advantage of such a display is the ability to represent the fracture/borehole intersection in three dimensions, without the severe vertical-scale compression of conventional BHTV displays. Reduced-scale versions of BHTV logs can be directly depth correlated with other geophysical logs; this reduction in scale is a useful advance made possible by the digitization of the BHTV signal.

There have been recent important improvements in televiewer logging transducers. The most significant of these improvements is the ability to focus the acoustic source beam and to optimize the degree of focus for specific borehole conditions (Paillet et al., 1990; Maki et al., 1991). The focused acoustic beam is achieved by fabricating the source transducer with a concave surface. The degree of concavity determines the amount of beam focus and the radial interval over which focus is achieved. In the most advanced BHTV-like systems, the transducer is formed by a series of concentric piezoelectric transducers that can be fired in a sequence to produce optimum focusing for a given local borehole diameter and fluid impedance.

Although acoustic imaging systems have been the most frequently used method for identifying fractures in situ, electrical imaging systems have become available in recent years. The first commercially available version of this system was known as the formation microscanner or FMS (Dennis et al., 1987; Ekstrom et al., 1987; Bourke, 1989; Paillet et al., 1990). The FMS system is an outgrowth of the conventional dipmeter, where the four electrical pads of the dipmeter have been enlarged to include many more individual electrodes. The electrical response of the four pads is processed to produce four vertical "strips" showing the detailed pattern of electrical resistivity of the formation. FMS data provide a visual indication of fine sedimentary structure as well as fractures. A typical FMS image of fractures is illustrated in Figure 4.16. The images in this figure show that FMS systems can provide an effective display of fractures in comparison to the BHTV. The latest applications of FMS use independent measurements of fluid conductivity to relate the measured electrical anomaly associated with the fracture to fracture aperture (Hornby et al., 1992).

Probably one of the most important limitations of this system in fracture studies is the incomplete azimuthal coverage of the wellbore provided by the FMS image. This can make it difficult to determine fracture strike and dip in some situations. This limitation is offset by the much greater operational simplicity of FMS logs. Both television and televiewer logs are run at very slow speeds, and both are affected by borehole fluids. The opacity of borehole fluid is frequently a problem with remote optical image (television) logging, and viscous drilling mud can severely degrade televiewer log performance (Paillet and Goldberg, 1991). In contrast, the FMS log can be run at typical logging speeds and under typical logging conditions, and the FMS logging sonde is not affected by the many operational delays typically associated with the much more electromechanically sensitive optical and acoustic imaging devices.

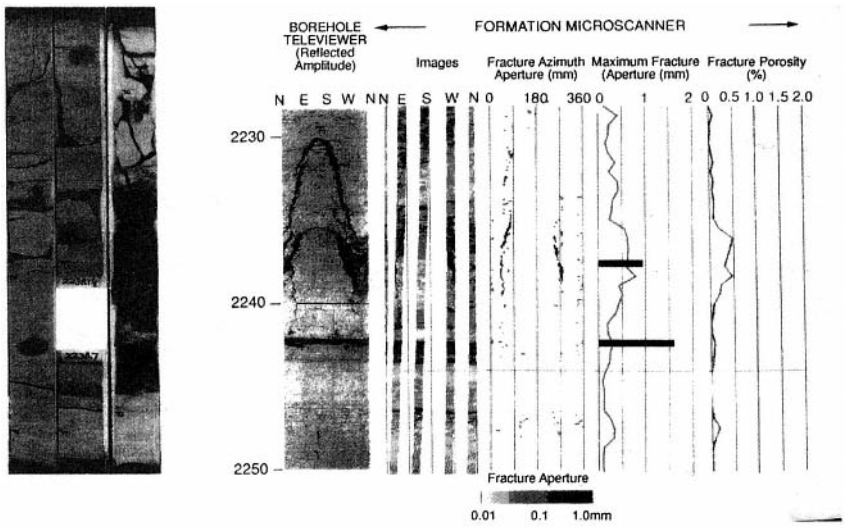

FIGURE 4.16 Comparison of fractures in a sandstone formation as indicated on (left) core samples, (center) BHTV log, and (right) FMS log. From Hornby et al. (1992).

Until recently, acoustic and electric borehole imaging devices have been extensively used in fracture studies despite the much greater potential spatial resolution of optical imaging devices. As noted previously, there are practical problems with optical imaging, such as opacity of drilling fluids, shadows cast from light sources, and lack of digital data or processing. Most of these problems appear to have been solved with at least one of the latest optical borehole imaging systems (Kamewada and Hu, 1990). This downhole digital optical imaging system provides digital image data with reliable color at a spatial resolution significantly better than that available from acoustic or electrical imaging systems such as the FMS and BHTV. This system functions in boreholes filled with clear fluid or air, and the digitized image data can be processed by state-of-the-art image enhancement software, such as that described by Paillet et al. (1990). An example of the image obtained with this new device is illustrated in Figure 4.17. This system appears to have all of the advantages described for televiewer and FMS logging systems coupled with a significantly improved spatial resolution. In addition, the system provides true color images suitable for description of lithology and identification of alteration halos and mineral staining adjacent to fractures.

Acoustic Waveform Logging Methods

Acoustic waveform logs (AWFLs) are obtained by recording the complete pressure signal at an array of receivers located some distance along the borehole

axis from a conventional transducer. Early attempts to develop this method applied established seismic data processing techniques in a scaled-down version of conventional acoustic refraction and reflection methods (Christensen, 1964). In well-consolidated rocks, such techniques can identify both *P* waves and *S* waves in

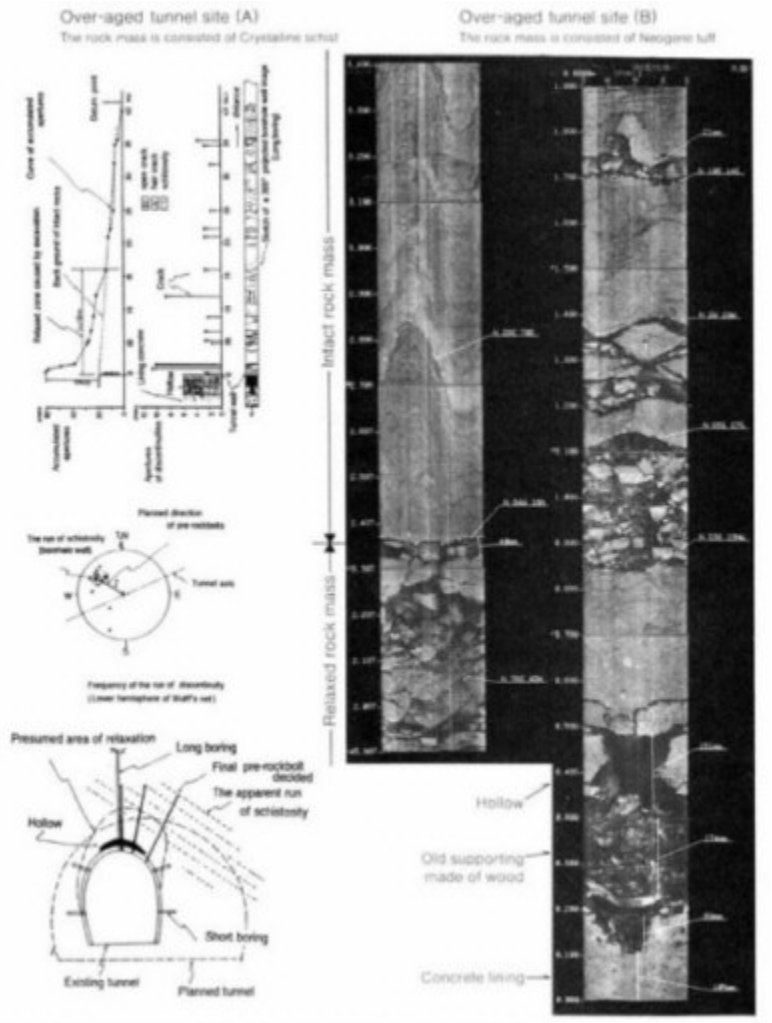

FIGURE 4.17 Example of digitally processed, downhole television data obtained in fractured bedrock. From Kamewada and Hu (1990).

the wavetrain. However, little success was achieved in evaluating the properties of fractures previously identified on BHTV (or other imaging) logs until the approach was modified (Paillet, 1980, 1985a,b; Figure 4.18).

In analyzing AWFL data it must be remembered that the fractures may be large compared to the wavelength. The waves may therefore scatter from the fractures, rather than propagate through them as through an effective medium.

Examples of AWFL data for typical fractures are given in Figure 4.19. For nearly horizontal fractures, all of the wave modes comprising the composite waveform are attenuated, because all waves must travel across the fracture between source and receiver. The example shown in Figure 4.19a illustrates the variation of shear-wave amplitudes, plotted as the mean square amplitude of acoustic energy in a window centered on the shear arrival. The same display shows the amplitude of the Stoneley or tube wave, a guided wave mode confined

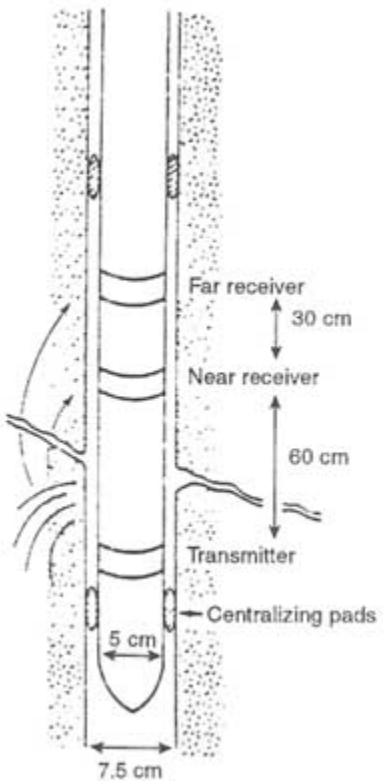

FIGURE 4.18 Schematic illustration of acoustic waveform logging as a scaled-down refraction study of fractures and adjacent rock. The technique records the changes in the refracted acoustic waveforms caused by propagation across permeable fractures. From Paillet (1980).

mostly to the fluid column, which is known to be sensitive to borehole wall permeability (Rosenbaum, 1974; Paillet, 1983, 1991c; Burns, 1990). The second example (Figure 4.19b) illustrates AWFL data for a near-vertical fracture, where there is some azimuth of the borehole wall where acoustic waves can propagate through unfractured rock, no matter where the logging tool is positioned. Such a condition occurs whenever the distance over which the fracture intersects the borehole exceeds the source-to-receiver distance of the logging tool. In Figure 4.19b

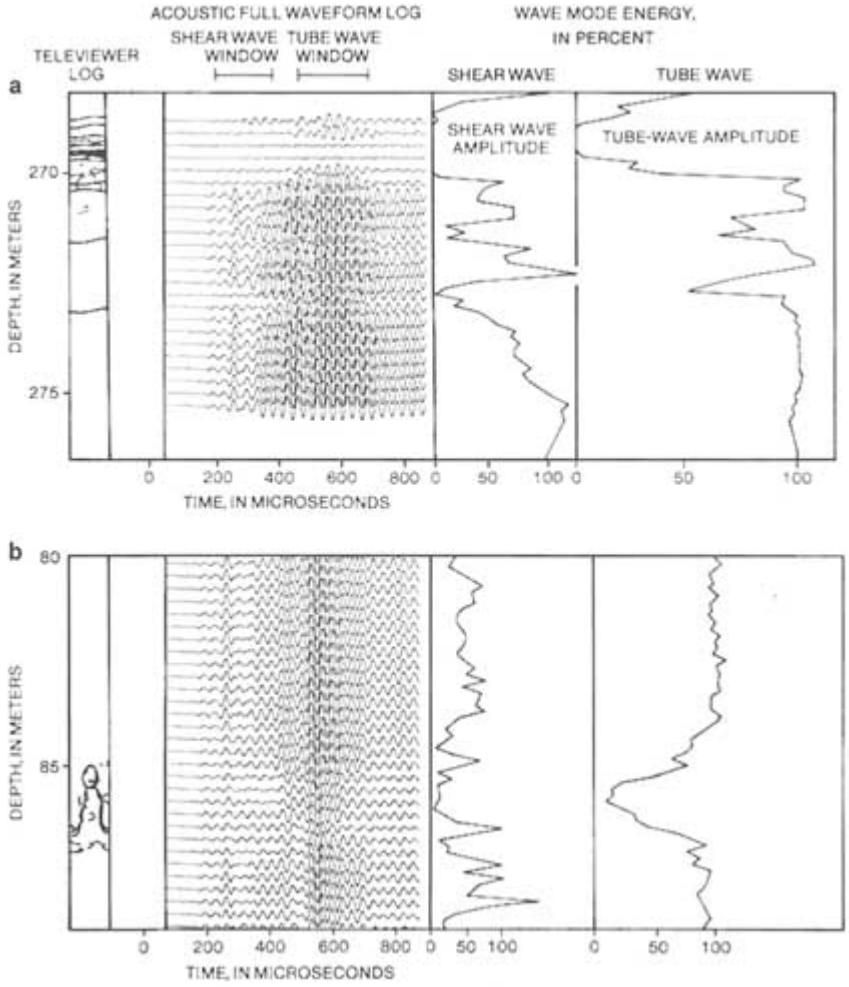

FIGURE 4.19 Examples of AWFL data for (a) nearly horizontal fracture zone and (b) nearly vertical fracture. Both data sets are from small-diameter coreholes in granite. From Paillet (1993).

the shear-wave amplitude does not show a simple anomaly that correlates with the fracture very well, but the tube-wave amplitude remains surprisingly consistent in correlation with the fracture. Experiment and theory indicate that tube-wave amplitude can be related to the fluid conductivity of fractures. For example, Paillet (1983, 1991b) shows that the interval-integrated tube-wave amplitude deficit (the shaded area indicated in Figure 4.19b) correlates with independent measurements of fracture-fluid conductance.

Attempts to construct a rigorous theory relating fracture properties to tube-wave amplitude and velocity have not been as successful. Early plane-fracture models indicate that tube waves are reflected but not attenuated by fractures having effective hydraulic apertures, such as those illustrated in Figure 4.19b. In contrast, the data show that there is significant attenuation without measurable reflections. Multifrequency experiments further confirm that reflections are absent at typical acoustic logging frequencies (10 to 30 kHz) and only become important at frequencies below 5 kHz (Paillet, 1984). At these lower frequencies, the intensity of tube-wave reflections is a better indicator of fracture permeability than attenuation (Hornby et al., 1989, 1992). Furthermore, the lower frequencies are associated with longer acoustic wavelengths, which produce a larger effective volume of investigation, thus making the method suitable for larger, more transmissive fractures. In this sense the two methods complement each other: the high-frequency amplitude methods can be used for fine-scale fractures, and the lower-frequency reflection method is appropriate for larger fracture zones.

The discrepancy between theory and experiment has only recently been resolved (Paillet et al., 1989a) by considering more complex fracture models that account for the heterogeneity and contacts along asperities of real fractures. An example of a model for a set of AWFL data in the crossover frequency range (where both amplitude and reflection methods apply) is illustrated in Figure 4.20.

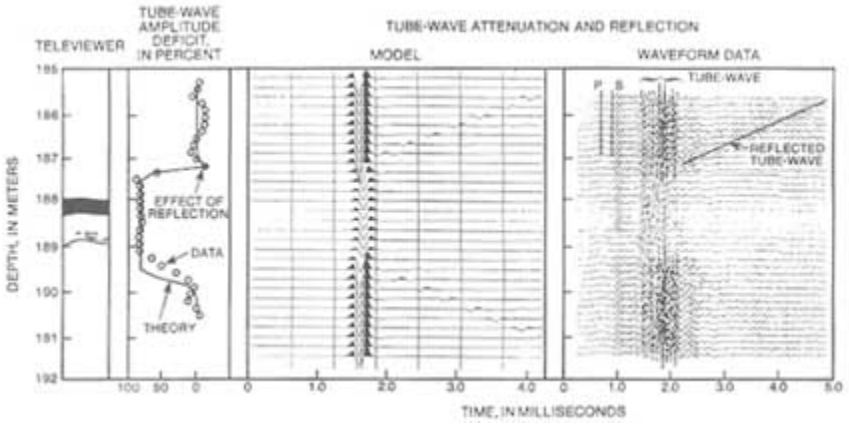

FIGURE 4.20 Comparison of AWFL data obtained by using a 5-kHz source in granite with synthetic seismograms computed for tube-wave propagation. From Paillet (1993).

There is a good agreement between the dynamic wave propagation models and AWFL data (Tang and Cheng, 1989). It is also important to note that comparison of these results to permeability measured at near steady state using conventional straddle packer and injection tests must include a complex hydraulic impedance factor related to the dynamic version of Darcy's law that applies to flow at acoustic frequencies (1 to 30 kHz).

A new generation of shear-wave logging tools is under development. These tools utilize two orthogonal (in the horizontal plane) dipole sources and receivers, so that the multisource/multireceiver analysis of split shear waves at the surface (see "*S* Waves," earlier in this chapter) and in the VSP context (see "Vertical Seismic Profiling," earlier in this chapter) may be utilized to detect fractures in the borehole. In the past two years, such "crossed-dipole" tools have been marketed worldwide by several service providers.

High-Resolution Flowmeter Methods

The availability of borehole imaging methods for fracture identification and other geophysical logs for fracture characterization provides effective methods for describing fractures that intersect exploratory boreholes. However, this near-borehole data does not provide useful information about connections between fractures and the larger-scale groundwater flow systems. Established techniques to locate flow systems are based on geochemical analyses of groundwater samples, tracer studies, and radar and seismic tomography. However, recently developed logging techniques that utilize high-resolution flowmeters provide the capability to investigate how the population of fractures intersected by a borehole is related to flow paths in the surrounding rock. A number of different flowmeters are being developed, including heat pulse (Hess, 1986; Hess and Paillet, 1990), electromagnetic (Molz and Young, 1993), acoustic-doppler (Almén and Zellman, 1991), and laser-doppler systems (Momii et al., 1993). These systems are just now becoming available for routine use in geotechnical studies.

The application of high-resolution flowmeters to fracture characterization can be illustrated by the performance of the heat pulse flowmeter, which works by measuring the time required for heat, which is produced by a short current pulse on a wire screen placed across the flow, to be convected 2 cm up or down the borehole (Figure 4.21). The latest version of this system increases sensitivity by means of an inflatable packer, which is designed to block the annulus around the measurement section of the tool, thereby forcing all of the flow to pass through the measurement section. Tool response is calibrated in the laboratory by relating the inverse of pulse travel time in inverse seconds to borehole discharge in liters per minute. Calibration studies demonstrate that the heat pulse flowmeter can resolve flows as small as 0.01 liters per minute.

Two case studies of high-resolution flow logging (see Appendix 4.C) discuss potential applications of these newly developed flow measurement techniques.

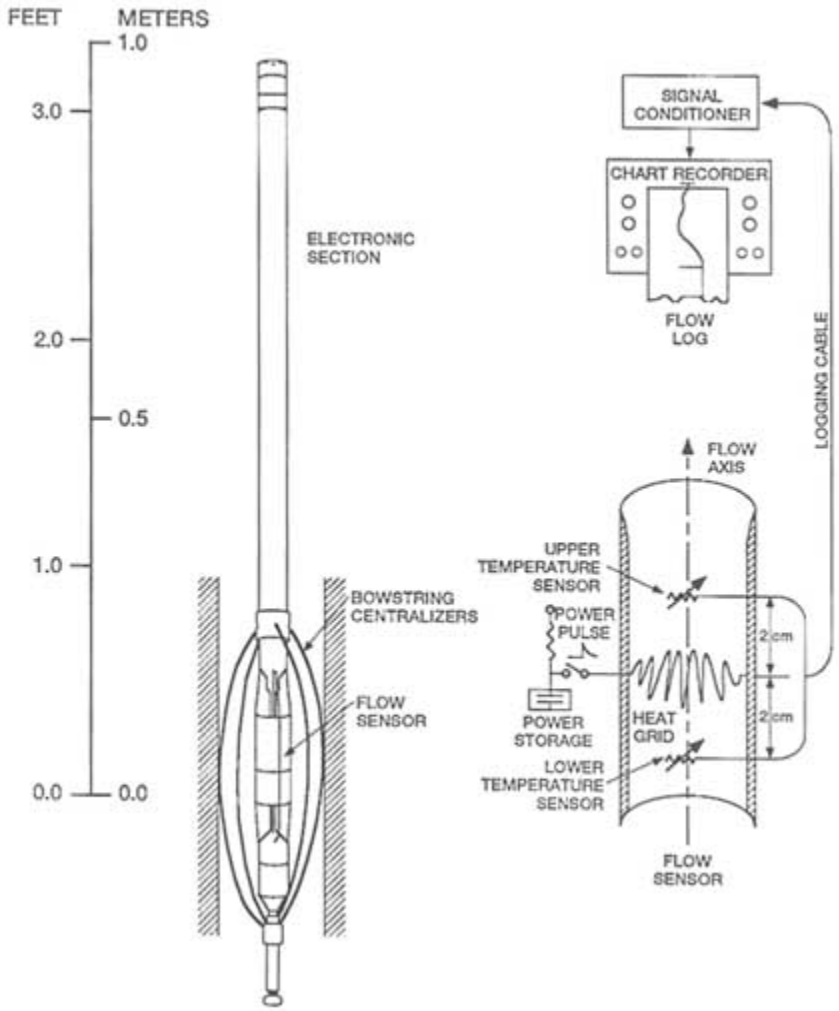

FIGURE 4.21 Schematic illustration of the operating principles and probe configuration for the heat pulse flowmeter. From Hess and Paillet (1990).

These methods seem especially useful in bridging the gap between small-scale measurements of conventional well logging and intermediate-scale measurement techniques such as straddle packer tests and borehole-to-borehole sounding.

Fluid replacement logging is a recently developed technique for the identification of permeable fractures that intersect the borehole (Tsang et al., 1990). The method provides estimates of electrical conductivity and the pH of fluids entering the borehole, as well as the depths and relative permeabilities of fractures

or fracture zones. The technique involves replacement of the fluid column in the borehole with deionized water and measurement of electrical conductivity of the fluid column over time as formation waters enter the borehole. The analysis assumes a diffusion process to infer both inflow rates and the electrical resistivity of the inflowing water.

Fluid replacement logs are compared to other geophysical logs for a borehole in fractured granitic rocks in Figure 4.22. The flowmeter and fluid replacement data show where water is entering the borehole during production. The fluid replacement log data provide a slightly better resolution than the high-resolution flowmeter analysis. Although fluid replacement logging is somewhat more time consuming and cumbersome than flowmeter logging, both techniques are effective in identifying the fracture zones associated with inflow to this borehole.

FLUID FLOW MONITORING USING GEOPHYSICAL METHODS

The best way to detect and characterize the actual flow of fluid in fractures is through differential measurements—that is, measurements before, during, and after the application of a known perturbation of the fluid system. For example, Wills et al. (1992) detected acoustic emissions and tiltmeter strains during a hydrofrac treatment, which indicated that the main fracture was surrounded by a large process zone (an area of inelastic deformation, suggesting the existence of seismic activity). They also performed simple cross-well tomography, detecting the fracture zone as a "shear-wave shadow zone" through which shear waves

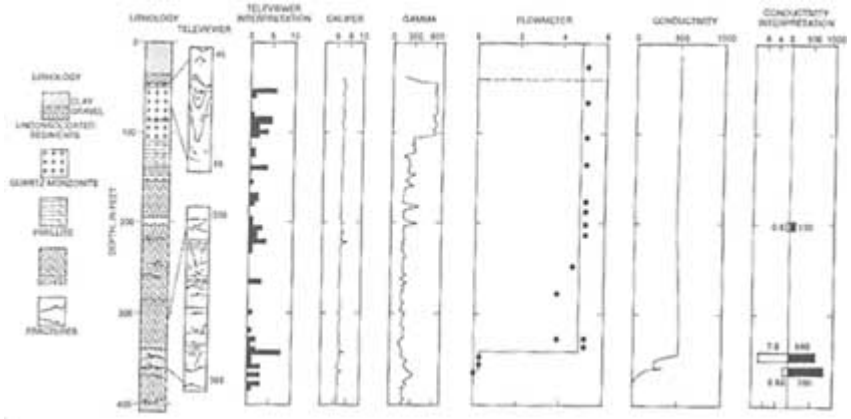

FIGURE 4.22 Example of fluid replacement logging in a borehole in fractured granite rocks in southeastern New Hampshire. Most of the geophysical logs are explained in previous sections of this chapter. The BHT data have been analyzed by assigning a size score to each fracture on a scale of one to five and then summing the total scores in depth intervals. From Vernon et al. (1993).

did not propagate. They detected fracture closing as inflections in the pressure decline curve (following classical arguments) and correlated these with changes in the seismic measurements.

The dependence of bulk electric properties on pore fluids allows monitoring of fluid flow by electrical or electromagnetic methods. Normally, it is difficult to distinguish between permeable and impermeable fractures through electrical methods because their electrical properties are similar, especially when the impermeable fractures are filled with gouge, clay minerals, or other alteration products.

Remote sensing methods normally provide very little information concerning large-scale hydraulic connections in fractured systems. However, changes in the conductivities of pore fluids may be measured by using electric or electromagnetic methods. In general, measurements are collected at several times, and changes are assumed to be due to differences in physical properties of the pore fluid or to changes in fracture geometry. Changes in pore fluid conductivity can be caused deliberately by injection of brine solutions during tracer experiments or inadvertently by leachates from landfills (contaminants may be more conductive than natural groundwater) or from mining operations. Hence, these methods can be used to measure the distribution of flow in fractured systems and to monitor confinement systems.

Electrical methods are usually applied by installing an electrode array in the area to be investigated (e.g., downstream from a landfill). The electrical resistances between pairs of electrodes are monitored during an appropriate time period. The geometrical distribution of resistivity changes will indicate if, when, and where changes in groundwater conductivity have occurred. In most cases, arrays are set up to monitor the lateral spread of contaminants (e.g., Van et al., 1991), but information on the vertical distribution also can be obtained by using sounding techniques (described in "Seismic Reflection," earlier in this chapter).

Electromagnetic methods (e.g., Tangential Electric Mode, Slingram; see Figure 4.4) also have been used for monitoring purposes. Profiles across the survey are normally remeasured at regular intervals, and the observed changes are interpreted in terms of contaminant locations (Hanson et al., 1991). Induction logging is also a useful technique for monitoring conductive plumes if boreholes are available (McNeil, 1990).

The limited resolution of electrical and electromagnetic methods also applies when they are used for monitoring purposes. A possible source of error when these methods are used for shallow monitoring of groundwater flow is a change in saturation owing to variations in precipitation or to freezing. These changes can cause annual variations in resistivity that must be removed from the data.

Tomographic techniques have higher resolutions than electric or electromagnetic methods. The basic principle is to produce a reference tomogram before injection of a conductive tracer into the fracture system. Tomographic measurements are then repeated at regular intervals to get "snapshots" of the distribution

of the tracer. Increases in radar attenuation can be attributed to the presence of saline tracer and allow the tracer mass to be estimated (Olsson et al., 1991).

There are a number of examples where repeated borehole radar tomography has been used to map the transport of a brine tracer in fractured granite. Figure 4.23 shows the difference tomogram obtained after continuous injection of saline tracer into a fracture zone. The tracer can be seen to follow the fracture zone from the injection point to the adjacent boreholes, which act as drains. The

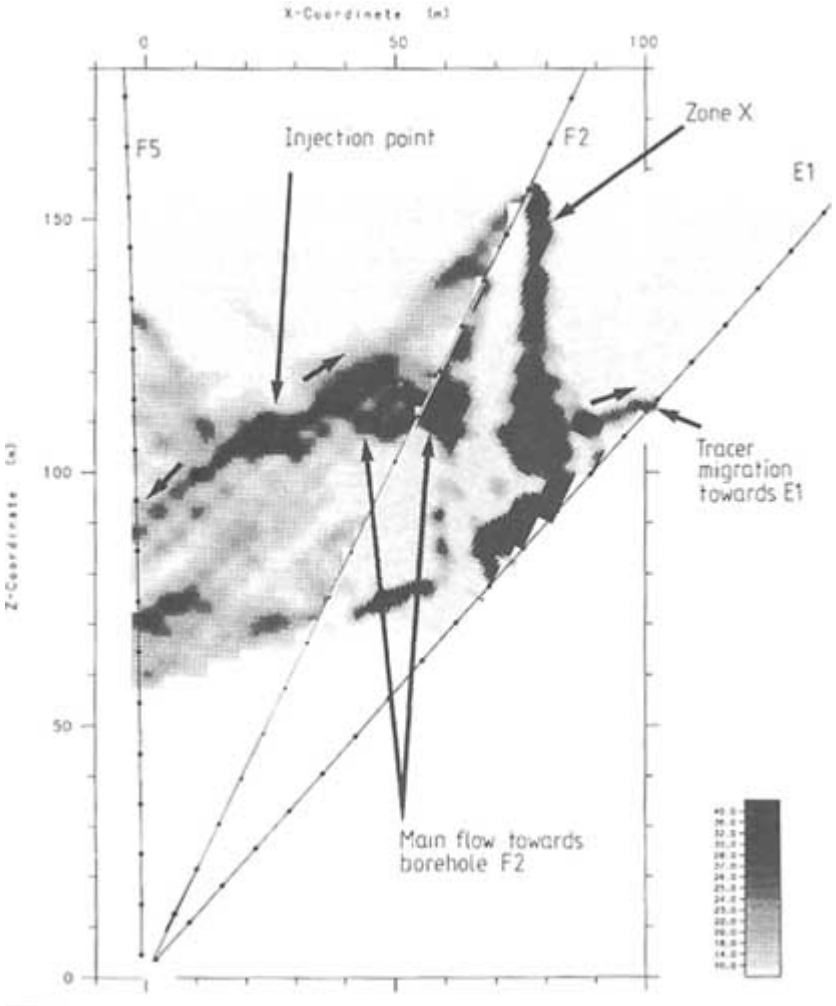

FIGURE 4.23 Increase in radar attenuation (dark regions) owing to injection of saline tracer (0.5 percent NaCl) into a fracture zone. From Andersson et al. (1989).

irregular distribution of tracer in the fracture zone is clearly demonstrated. Several intersecting tomograms were obtained at the same site. They were internally consistent and in agreement with the observed tracer inflows to the draining boreholes.

These tomography methods are especially significant for studies of flow in fractures. Almost all geophysical tomograms disclose distributions of physical properties that are only indirectly related to flow. For example, radar tomograms of fractured crystalline rocks show the distribution of alteration clays and other electrically conductive minerals. These patterns of anomalous radar transmission are likely to be indirectly related to the three-dimensional distribution of fractures, but they do not provide direct evidence of fluid flow. However, repeated borehole tomograms obtained before and during brine injection do provide unambiguous direct evidence of the three-dimensional distribution of flow. This distinction makes the brine injection studies (e.g., Olsson et al., 1992) more significant for flow system identification than other seismic, electric, and radar tomography studies given in the literature.

Radar difference tomography also has been used to map the spreading of grout in dams (Andersson et al., 1991) and to monitor the progress of the flame front in oil shale retorting (Daily, 1984). This technique has also been used to monitor the progression of flood fronts in thermal-enhanced oil recovery (Justice et al., 1989). Difference tomography has been used to map the location of new fractures induced by blasting (Cumerlato et al., 1991). In principle, any operation that alters the compressibility of the fracture-filling fluid (e.g., by changing the saturation state) should be detectable by difference tomography.

DISCUSSION

The preceding sections have discussed a broad array of fracture detection methods. These methods are summarized in Table 4.1. The following methods are particularly useful at various detection distances:

- for detection at great distances, seismic methods based on split shear waves;
- for detection at moderate distances, the directional borehole methods;
- for detection in the borehole, the televiewer, FMS, and scanner methods; and
- for characterization of the actual flow associated with fracture systems, the high-resolution flowmeter methods and radar difference tomography.

The objectives of most studies are to both detect and characterize fractures. The properties of interest include the physical characteristics of the fractures (e.g., orientation, size, shape, fluid and mineral content), and hydraulic properties (e.g., permeability and its variability with pressure).

With any of the geophysical detection methods, raw data (e.g., voltages from a measuring instrument) are acquired and processed into a form suitable for inversion to estimate physical properties of the rock mass (e.g., seismic velocity). This inversion may be computationally intensive and may rely on oversimplified theories. Nevertheless, there is broad consensus on the validity of these methods, and their resolution and uniqueness are well understood.

In contrast, the inference of fracture parameters (e.g., fracture size) from these physical properties is open to considerably greater debate. (The term *inference* is used rather than inversion to emphasize a lesser degree of reliability.) In most cases the theory that guides this inference involves strong assumptions about the properties of the fracture (e.g., that it has the shape of a prolate ellipsoid) that are not readily defensible. Further, these fracture parameters tend to be lumped parameters (e.g., the nondimensional fracture density as given by Eq. 4.1) rather than a single fracture characteristic. This inference, even if correct, still retains significant uncertainty with respect to fluid flow. For this reason, multiple studies using different methods that produce different lumped parameters are clearly useful for constraining fracture properties.

Finally, few detection methods allow direct interpretation of these inferred fracture characteristics in terms of fracture flow. (An interpretation is less scientifically based and less reliable than either an inference or an inversion.) Perhaps the best exceptions to this generalization are methods that track differences over time (e.g., see preceding section on radar tomography). Changes in tomographic images over time in response to induced changes in flow provide convincing evidence that these images can be used to characterize flow through fracture systems.

Given the breadth of methodologies evident in Table 4.1, it might seem unnecessary to look for new methods of acquisition, processing, and inversion. However, major new methods have recently been developed (e.g., split shear waves that do not rely on oversimplified theories. Additionally, advancements in technology continue to allow for significant refinements to older methods (e.g., the borehole imaging devices).

By contrast, progress is clearly needed in the inference process in order to obtain better estimates of fracture properties. In particular, the deduction process should rely less heavily on unsupportable assumptions. This may require the use of more data (e.g., the entire signal, not just the first breaks, for seismic data) or better experiments (e.g., broader-band sources, downhole sources) in the deduction process.

Finally, there is the need to better learn how to interpret the hydraulic properties of direct interest from the inferred fracture parameters. The best hope for improvement lies in the application of multiple methods in the inference step, repeated over time as the fracture system responds to a known stimulus. The numerical modeling methods discussed in Chapter 6 have an important role to play in this effort.

Appendix 4.A

Directional Borehole Radar System

IN a reflection measurement with a directional borehole radar system (Sandberg et al., 1991), the transmitter and receiver are kept at a fixed separation while lowered together into the borehole. Measurements are normally made at 0.5-m depth intervals to avoid spatial aliasing. A measurement along a single borehole produces three independent radar images (one dipole image and two orthogonal directional component images) that must be combined in order to find the orientation of the reflectors.

In practice, inversion of directional radar data is made by using an interactive program. The program calculates the radar reflection maps for the dipole and the directional signal for every 10 degrees of azimuth. Reflectors are marked in the radar maps, and models corresponding to plane or point reflectors are adjusted to fit each observed reflector (Figure 4.A1, left). The depth of intersection and the angle between the borehole and the reflector are displayed automatically. Then the azimuth is changed until the minimum directional signal is found for a particular reflector (Figure 4.A1, right). There are two minima, and the correct azimuth is determined by comparing the phase of the directional signal at maxi

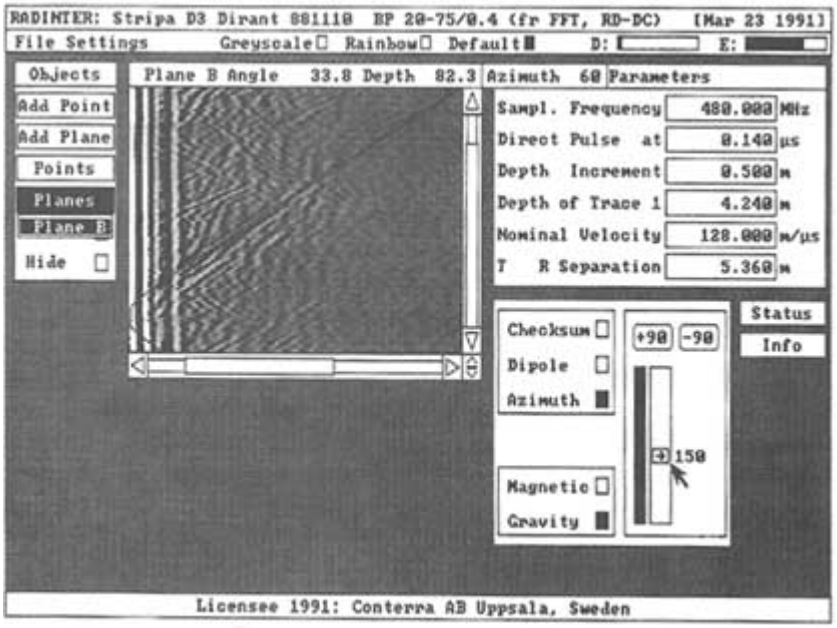

FIGURE 4.A1 Screen display of a commercially available software product for interactive interpretation of directional radar data. Reproduced with permission of MALÅ GeoSciences, Malå, Sweden.

mum signal strength with the phase of the dipole signal. The dip and strike of the fracture plane can be calculated if the orientation of the borehole is known. The azimuth can normally be determined with an accuracy of ±5° for data with good signal-to-noise ratio. For weak reflectors in a noisy environment, it may not be possible to find the azimuth with that accuracy.

During a reflection measurement in a borehole, the reflection point traces a line on the fracture plane (see Figure 4.18). It is along this line that the existence and orientation of the fracture plane are actually known. The reflectors detected can then be plotted (e.g., with a 3-D computer-aided design system) at the locations in space where the reflections actually occurred. In this way, 3-D visualization of actual fracture locations makes it possible to construct models of the fracture pattern recognizing the information actually available. Figure 4.A2 illustrates reflectors observed from different boreholes at the SCV (Site Characterization and Validation) site at the Stripa project's mine (see Chapter 8) and the assignment of reflectors to different fracture zones.

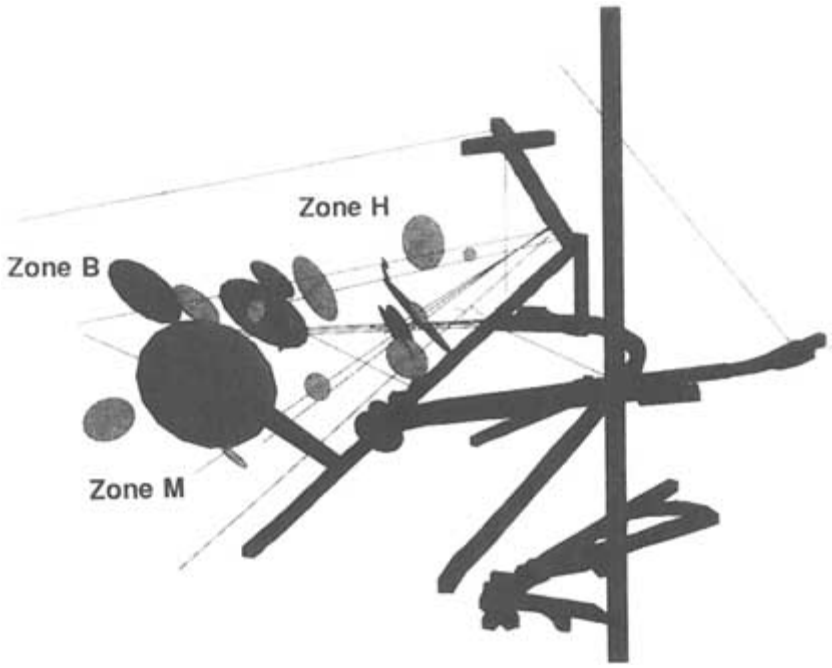

FIGURE 4.A2 Distribution in space of radar reflections derived from single-borehole directional radar data at the Site Characterization and Verification (SCV) site at the Stripa Project's mine. Different shades indicate reflectors interpreted as belonging to different fracture zones. From Olsson (1992).

Appendix 4.B

Summary Of Conventional Log Applications In Fracture Studies

Geophysical well logs can be used to determine the physical properties of rocks encountered by boreholes, whether or not cores and other sample data have been recovered during drilling. Figure 4.B1 gives a summary of the applications of conventional well logs to fractures as described by Keys (1979) and Paillet (1993). The figure gives a schematic illustration of the fractures as they might look in core samples and shows how the presence of each fracture might be represented in each of the logs. In many cases the rock volume sampled by the measurement is so large relative to the fracture that the open fluid-filled passages in the fracture are a negligible volumetric fraction of the sample volume. Therefore, the geophysical measurement is much more sensitive to the indirect effects of the fracture, such as fracture mouth enlargement at the wellbore or alteration surrounding the fracture, than to the permeability or hydraulic aperture of the fracture. Electric and neutron logs appear to be especially sensitive to clay mineral alteration and infilling (Nelson et al., 1983; Katsube and Hume, 1987). These logs and the density log are also sensitive to borehole wall enlargement or

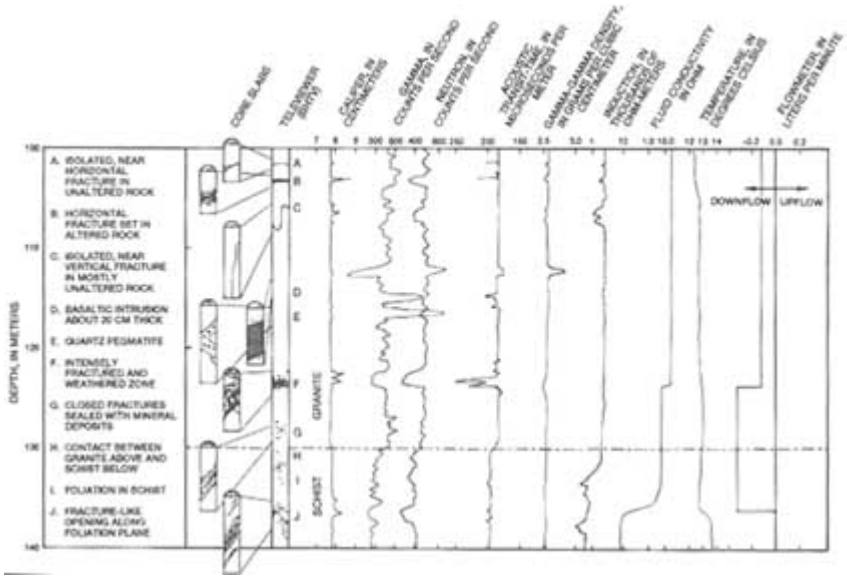

FIGURE 4.B1 Comparison of fracture permeability interpreted from borehole televiewer image logs with results of high-resolution flowmeter measurements of flow under ambient hydraulic head conditions and permeability measured by packer isolation-hydraulic injection tests for two boreholes in fractured dolomite at a site near Rockford, Illinois. From Paillet (1991d).

borehole wall roughness, known as "rugosity" in the well logging literature (Keys, 1979; Paillet, 1991a). All of the fracture responses listed in Figure 4.B1 represent idealized measurements where isolated fractures and their local alteration halos are embedded in homogeneous unfractured crystalline rock. In many situations the host rocks are foliated, cross-cut by sedimentary beds or intrusions, or intensely fractured and altered, so the "idealized" log responses associated with individual fractures cannot be recognized.

The natural gamma ray log is not sensitive to borehole enlargement and is only moderately sensitive to alteration minerals. In some situations, gamma ray logs are used to indicate fractures because radioactive minerals such as uranium and radium may be deposited in fractures in acidic plutonic rocks such as granite. But this response is generally inconsistent, and such fracture-related concentrations of radioisotopes cannot be reliably distinguished from similar deposits lodged in veins and pegmatites (Aguilera, 1979; Paillet, 1991a).

Conventional acoustic logs frequently indicate a response to fractures related to effects other than alteration and borehole enlargement. The first arrival may be only minimally delayed, but its small amplitude prevents detection. Instead, subsequent pulses are detected. This produces an abrupt decrease in acoustic velocity. These fracture-associated spikes are known as "cycle skips" and may serve as fracture indicators. Most modern acoustic logging systems are designed such that routine signal processing rejects these anomalies, and, hence, the log almost always ignores fractures.

Conventional caliper logs measure the average diameters of boreholes (using several spring-loaded arms) and are useful for detecting fractures. As shown in Figure 4.B1, fractures are usually associated with large spikelike anomalies on caliper logs. These spikes represent the effects of mechanical enlargement of fracture mouths during drilling. Experience demonstrates that caliper logs indicate the depths where almost all significant fractures and fracture zones intersect boreholes. However, the spike is a secondary effect related to alteration and drilling damage, and there are situations where caliper logs show absolutely no indication of the presence of fractures. Generally, such fractures are not hydraulically significant.

The schematic application of conventional logs to fracture characterization is illustrated by a typical suite of logs from fractured crystalline basement rocks in New Hampshire (Figure 4.B2). In this figure the caliper log shows anomalies associated with some of the major fractures (label "A" in the figure), and the natural gamma log indicates a major change in lithology below about 46 m (label "B" in the figure). The neutron log illustrates responses associated with major fracture zones (label "C" in the figure); there is also a gamma ray anomaly that may be associated with radioisotope concentrations in one of the fractures (label "D" in the figure). Electrical resistivity anomalies associated with both borehole enlargement and alteration are indicated by the response of the single-point resistance log (label "E" in the figure). The resistivity log indicates a major shift

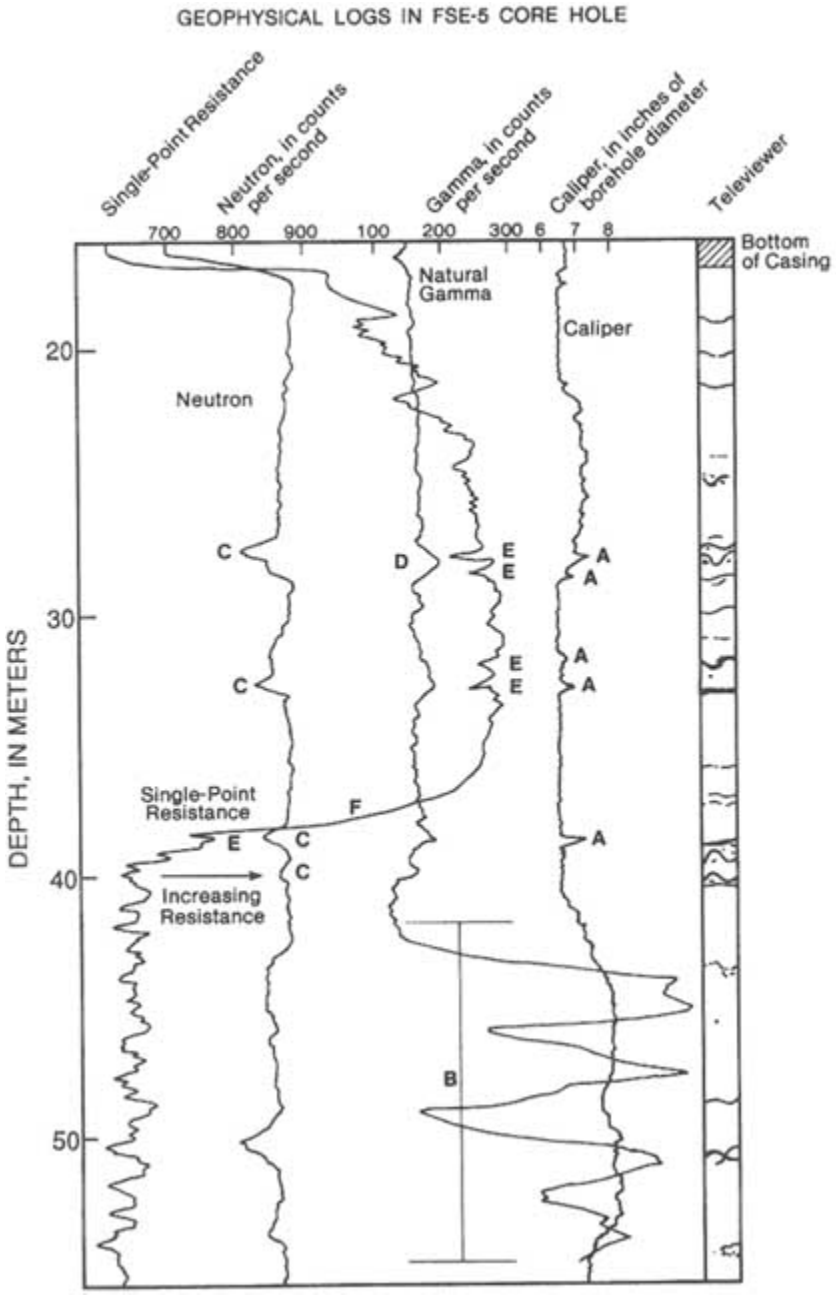

FIGURE 4.B2 Example of conventional caliper, resistance, neutron, and gamma logs for a borehole in granitic crystalline rocks in New Hampshire.

at about 41 m, where fresh water circulating from above exists through one of the fractures, leaving more saline groundwater in the deeper part of the borehole. All of these fracture indicators may be compared to the televiewer log (see "Borehole Imaging Logs" in this chapter) for this well, which gives an image of the fractures intersecting the borehole wall. The televiewer image indicates the orientation and relative size of fractures. Note the extent to which the geophysical logs respond to the most prominent fractures on the televiewer image and fail to indicate many of the smaller and possibly closed fractures.

Appendix 4.C

Flowmeter Case Studies

An example of the use of the heat pulse flowmeter to identify fracture connections to larger-scale flow systems is illustrated in Figure 4.C1, which shows the caliper log for a borehole in fractured schist north of New York City. The BHTV image indicates a high density of fracturing in this rock mass; there are fractures intersecting every meter of this borehole over the entire depth of more than 100 m. This borehole was drilled to investigate a contamination site, and water level monitoring indicated transient drawdowns apparently related to pumping of water wells in the area. This situation raised important practical

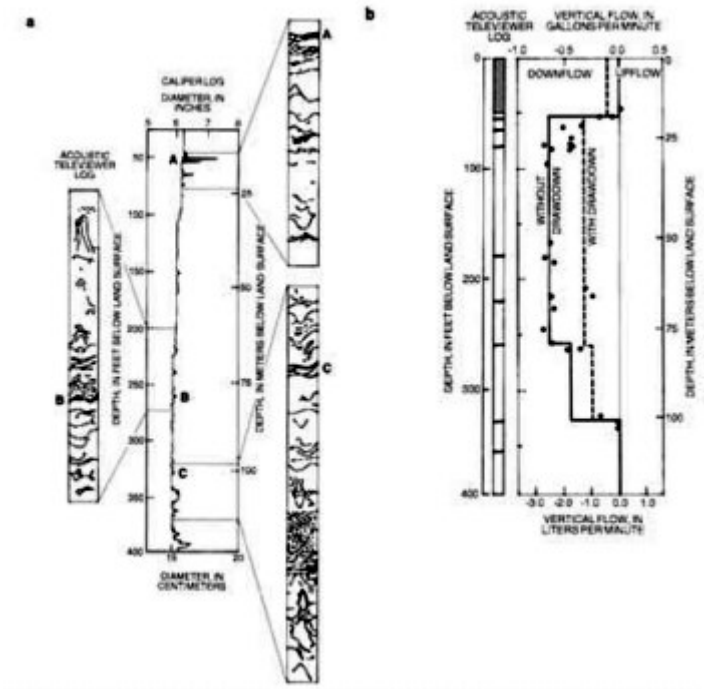

FIGURE 4.C1 Example of high-resolution flowmeter measurements used to define fractures connected to larger-scale flow systems for a borehole in fractured schist in New York. (a) Distribution of fractures indicated by caliper and BHTV logs; (b) distribution of vertical flow under ambient conditions. From Hess and Paillet (1990).

problems about where to install packers to isolate flow systems and to ensure effective sampling of the potential contaminant plume.

Vertical velocity profiles generated with the heat pulse flowmeter showed that, although there were many open fractures intersecting the borehole, fluid actually entered and exited it during the pumping transients at only three depths. Furthermore, each of these entry and exit points could be associated with specific sets of fractures identified on the BHTV image. The individual flow measurements made with the flowmeter are shown in Figure 4.C1b; they show considerable scatter. This scatter is the result of a continuously changing flow regime as drawdowns in adjacent water wells fluctuate. The entry and exit points are resolved by scanning the borehole for the general characteristics of the flow and then making repeat measurements above and below suspected entry or exit fractures.

The most important result of this study was the identification of the three fracture zones that are connected to larger-scale flow systems. The high-resolution flowmeter data allowed these three points to be identified and subsequently isolated with only two packers. The characteristics of these three flow systems could then be monitored over time, and each zone could be sample while the packers prevented cross-contamination of zones.

A second example of high-resolution flow logging for fracture characterization is illustrated by the logging of a potential water well before and after hydraulic stimulation. In the crystalline basement uplift in suburban areas around Boulder, Colorado, domestic water supplies are furnished by wells drilled in fractured granitic rocks. Although these rocks were intensely fractured by at least two separate tectonic events, production statistics indicate that approximately 20 percent of the wells drilled produce less than the 2 liters per minute generally needed for household use (Paillet et al., 1989b). Most of these "dry" wells can be salvaged by a stimulation process whereby fractures are opened by pressurization below a packer and propped by injection of sand into the open fractures. An example of the changes induced by the stimulation of a well is illustrated in Figure 4.C2 (Paillet et al., 1989b). Caliper and BHTV logs before and after stimulation indicate that the borehole is intersected by a number of fractures and that the stimulation process produced no measurable change in these fractures in the immediate vicinity of the borehole. However, flowmeter measurements during injection indicate that stimulation has changed the pattern of fracture connectivity because two relatively minor fractures were capable of accepting about 10 times as much water under the same recharge conditions after stimulation. The large decrease in outflow at the uppermost fracture is attributed to a small rise in water level in the well after stimulation, saturating a previously unsaturated fracture that had accepted much of the recharge during the prestimulation experiment.

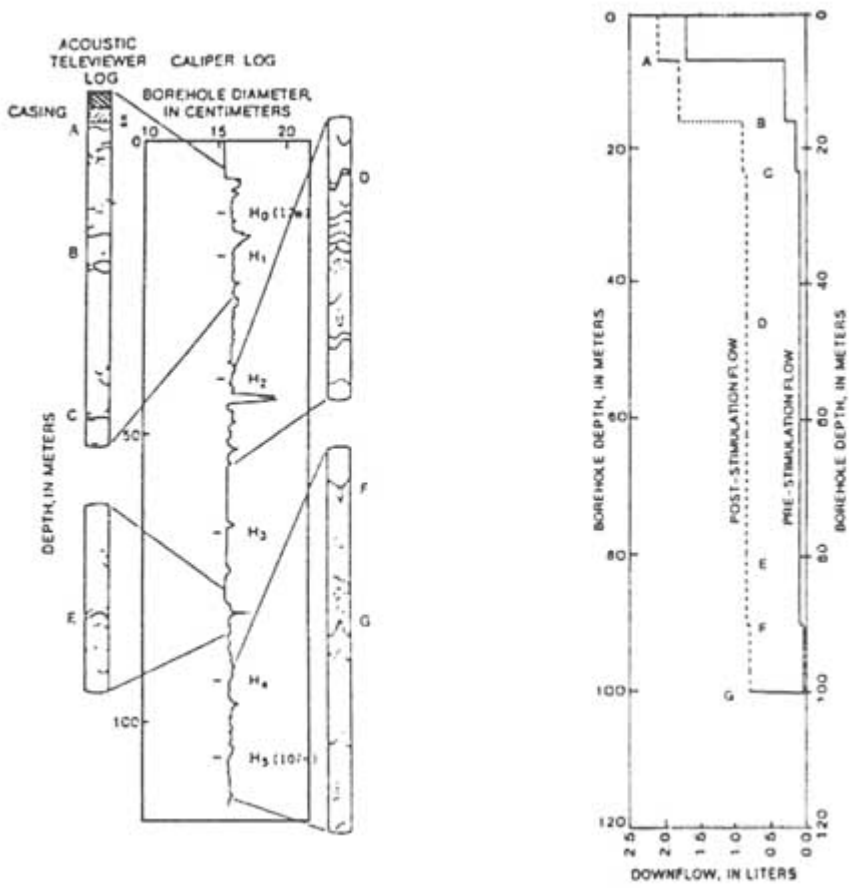

FIGURE 4.C2 Example of high-resolution flowmeter measurements used to characterize changes in fracture properties induced by hydraulic stimulation at a site in Colorado. Left, distribution of fractures indicated by caliper and BHTV logs; right, distribution of vertical flow under about 7 m of hydraulic head during injection before and after stimulation. From Paillet et al. (1989b).

Appendix 4.D

Example Of Shear-Wave Anisotropy In Fractured Reservoirs

Shear waves have properties that make them very attractive for characterizing fractured rock. When shear waves propagate through an anisotropic material, their polarization (the direction of the transverse deformation) is controlled by the material's anisotropy rather than by the source. The study of fractured reservoirs has shown that in such cases fracturing is the dominant cause of seismic anisotropy.

Figure 4.D1 is a schematic representation of shear-wave propagation in a homogeneous medium with aligned fractures. The incident wave is shown to be

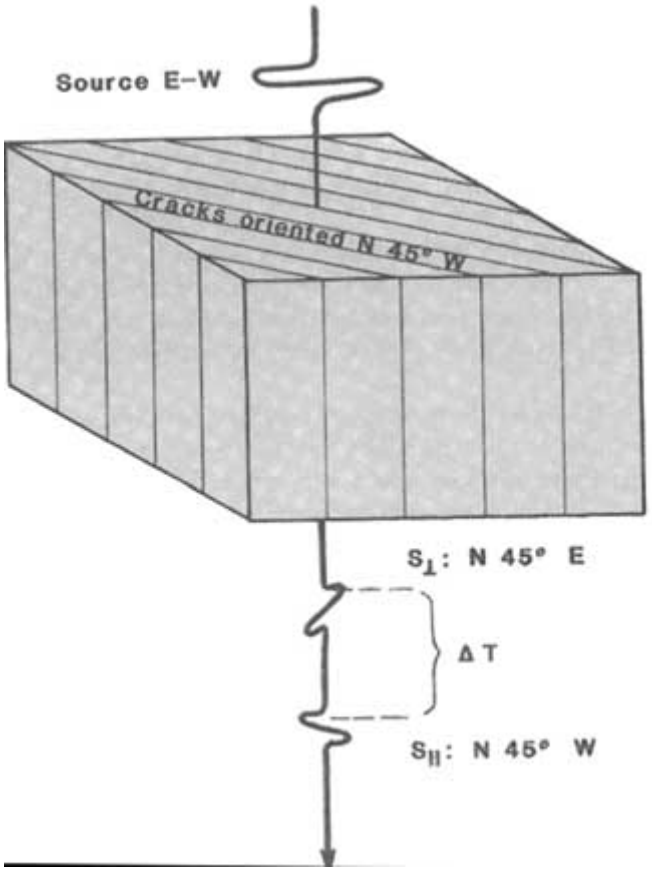

FIGURE 4.D1 Schematic illustration of shear-wave propagation in a homogeneous medium with aligned fractures. From Martin and Davis (1987).

polarized east-west. While traveling through the fractured interval, the incident wave splits into two shear waves—a fast wave polarized parallel to the fractures (N45W) and a slow wave polarized perpendicular to the fractures (N45E). After leaving the fractured interval, both shear waves propagate with the same velocity but have different polarizations and travel times, which were established by the fractured interval. The orientation of the fractures can be determined from the polarization of the first-arriving shear wave.

Digital processing of shear-wave recording allows them to be resolved into the components parallel and perpendicular to the natural coordinate system (a coordinate system assumed to be defined by fracture orientation). The presence of fracturing is seen in travel time differences between parallel and perpendicular orientations, and the orientation of fracturing is determined from the rotation angles.

The use of shear-wave anisotropy information is demonstrated by a case history from a seismic reflection survey of the Silo field in southeastern Wyoming (Martin and Davis, 1987). This field is a naturally fractured reservoir that produces oil from chalks within the late Cretaceous Niobrara formation at depths of about 2,440 m. Because the production in this field is controlled by the orientation and density of fractures, a multicomponent seismic line was obtained to record both *P* waves and shear waves.

Figure 4.D2 shows a *P*-wave reflection profile with a *P*-wave VSP (vertical seismic profile) from a nearby well. The VSP gives depth control to the seismic travel times. The *P*-wave profile clearly shows the Niobrara formation (labeled "Kn") at 1.7 s, about 2,744 m (9,000 feet) in depth, but there is no fracture information.

Figure 4.D3 shows the parallel (left) and perpendicular (right) shear-wave reflection sections. Various reflections, labeled A through F, clearly show fracture induced time delays between sections, with reflection C, the top of the Niobrara, having a 120-ms time difference. The parallel polarized section (left side) has less travel time because these shear waves are faster. A shear-wave VSP acquired in a nearby well, and polarized perpendicular to fracturing, is shown in the perpendicular reflection section (right side). The observed delay times between orthogonally polarized shear waves correlate with both mapped fracture orientations and fracture intensities inferred from production data throughout the Niobrara formation.

This example demonstrates the utility of split shear waves for mapping from the surface the locations, orientations, and intensities of fractures at great depth.

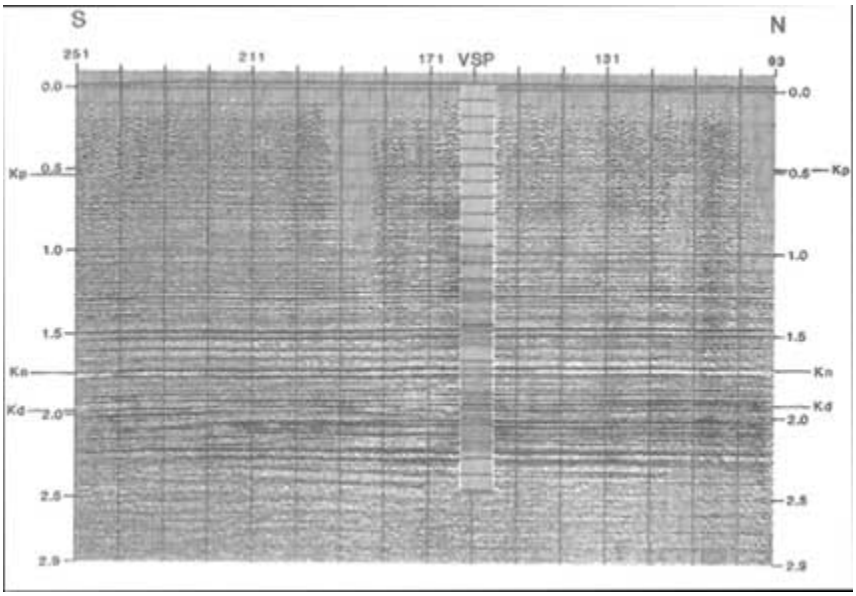

FIGURE 4.D2 *P*-wave reflection profile and *P*-wave vertical seismic profile from a well in the Silo field in southeastern Wyoming. The *y* axis represents two-way travel time. From Martin and Davis (1987).

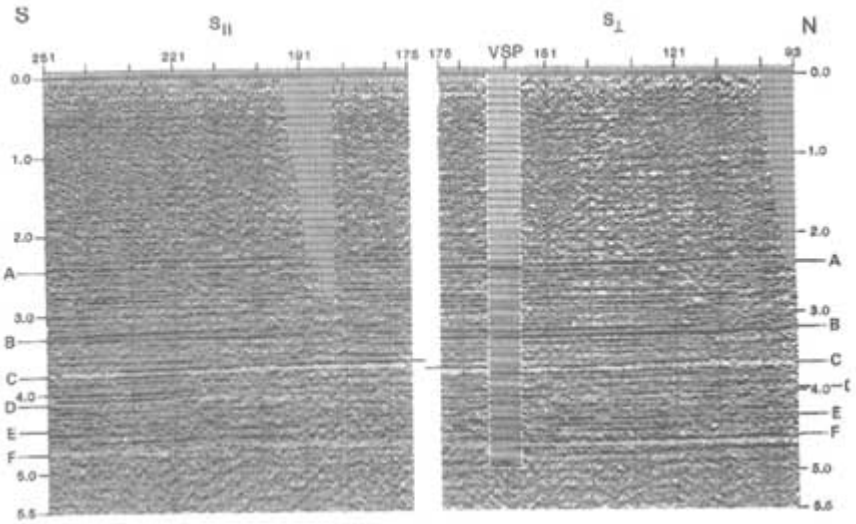

FIGURE 4.D3 Parallel (left) and perpendicular (right) shear-wave vertical seismic profiles from the Silo field in southeastern Wyoming. From Martin and Davis (1987).

REFERENCES

Aguilera, R. 1979. Naturally Fractured Reservoirs. Tulsa, Okla.: Petroleum Publishing.

Alford, R. M. 1986. Shear data in the presence of azimuthal anisotropy. Pp. 476–479 in Society of Exploration Geologists Convention Expanded Abstracts. Tulsa, Okla.: Society of Exploration Geologists.

Almén, K. E., and O. Zellman. 1991. Äspö Hard Rock Laboratory—field investigation methodology and instruments used in the preinvestigation phase, 1986–1990. SKB TR 91-21. Stockholm: Swedish Nuclear Fuel and Waste Management Co.

Alumbaugh, D. L., and H. F. Morrison. 1993. Electromagnetic conductivity imaging with an iterative Born inversion. IEEE Transactions on Geoscience and Remote Sensing , 31 (4):758–763.

Andersson, P., E. Gustafsson, and O. Olsson. 1989. Investigation of flow distribution in a fracture zone at the Stripa mine, using the radar method results and interpretation. SKB TR 89-33. Stockholm: Swedish Nuclear Fuel and Waste Management Co.

Andersson, P. M., B. G. Linder, and N. R. Nilsson. 1991. A radar system for mapping internal erosion in embankment dams. Water Power & Dam Construction, July:11–16.

Balch, A. H., and M. W. Lee, eds. 1984. Vertical Seismic Profiling: Techniques, Applications, and Case Histories. Boston, Mass.: International Human Resources Development Corp.

Baria, R., and A. S. P. Green. 1986. Seismicity induced during a viscous stimulation at the Camborne School of Mines Hot Dry Rock Geothermal Energy Project in Cornwall, England. Pp. 120–121 in European Association of Exploration Geophysics Expanded Abstracts. Zeist, Netherlands: European Association of Exploration Geophysics.

Barker, R. D. 1989. Depth of investigation of collinear symmetrical four-electrode arrays. Geophysics, 54:1031–1037.

Barton, C. A. 1988. Development of in situ stress measurement techniques for deep drillholes. Ph.D. dissertation, Stanford University, Stanford, Calif.

Barton, C. A., and M. D. Zoback. 1994. Stress perturbations associated with active faults penetrated by boreholes: possible evidence for near-complete stress drop and a new technique for stress magnitude measurement. Journal of Geophysical Research, 99 (B5):9373–9390.

Barton, C. A., L. G. Tessler, and M. D. Zoback. 1991. Interactive image analysis of borehole televiewer data. Pp. 265–284 in Automated Pattern Analysis in Petroleum Exploration, I. A. P. S. Sengupta, ed. New York: Springer-Verlag.

Batchelor, A. S. 1982. The stimulation of a hot dry rock reservoir in the Cornubian Granite, England. In Proceedings of the 8th Workshop on Geothermal Reservoir Engineering.

Blumling, P., C. Cosma, M. Korn, C. Gelbke, and B. Cassel. 1990. Geophysical methods for the detection of discontinuities ahead of the tunnel face. NAGRA TR 90-07. Wettingen, Switzerland: Swiss National Cooperative for Radioactive Waste Disposal (NAGRA).

Bourke, L. T. 1989. Recognizing artifact images of the formation microscanner. Pp. WW1-WW25 in the 30th Annual Logging Symposium Transactions. Houston, Tex.: Society of Professional Well Log Analysts.

Bregman, N. D., R. C. Bailey, and C. H. Chapman. 1989. Crosshole seismic tomography. Geophysics, 54:200–215.

Burns, D. R. 1990. Acoustic waveform logs and the in-situ measurement of permeability—a review. Pp. 65–78 in Geophysical Applications for Geotechnical Investigations, F. L. Paillet and W.R. Saunders, eds. ASTM STP 1101. Philadelphia, Pa.: American Society for Testing and Materials.

Carswell, A., and W. M. Moon. 1989. Application of multioffset vertical seismic profiling in fracture mapping. Geophysics, 54:737–746.

Christensen, D. M. 1964. A theoretical analysis of wave propagation in fluid-filled drill holes for the interpretation of three-dimensional velocity logs. Pp. K1–K130 in 5th Annual Logging Symposium Transactions. Houston, Tex.: Society of Professional Well Log Analysts.

Claerbout, J. F. 1985. Imaging the Earth's Interior. Oxford: Blackwell.

Coggon, J. H. 1973. A comparison of IP electrode arrays. Geophysics. 38:737–761.

Cohen, A. 1996. Hydrogeologic Characterization of Fractured Rock Formations: A Guide for Ground-water Remediators. Report in preparation, Lawrence Berkeley Laboratory, Berkeley, Calif.

Cosma, C. 1990. Fracture characterization by seismic and sonic methods, techniques applied during Phase III of the Stripa Project. Pp. 85–95 in Proceedings of the 3rd NEA/SKB symposium on in-situ experiments associated with the disposal of radioactive waste. Paris: Organization for Economic Cooperation and Development, Nuclear Energy Agency .

Cosma, C. 1991. Seismic imaging techniques applied to rock engineering. Pp. 37–49 in Proceedings of the 1st Society of Exploration Geophysicists of Japan International Symposium on Geotomography. Tokyo: Society of Exploration Geophysicists of Japan.

Cosma, C., P. Heikkinen, and S. Pekonen. 1991. Improvement of high resolution seismics: Part I, Development of processing methods for VSP surveys; Part II, Piezoelectric signal transmitter for seismic measurements. Stripa Project TR 91-13. Stockholm: Swedish Nuclear Fuel and Waste Management Co.

Crampin, S. 1991. A decade of shear-wave splitting in the earth's crust. Geophysical Journal International, 107(3):387–408.

Crampin, S., I. Bush, C. Naville, and D. Taylor. 1986. Estimating the internal structure of reservoirs with shear-wave VSP's. Geophysics: The Leading Edge of Exploration, 5(11):85.

Cumerlato, C. L., V. J. Stachura, and D. R. Tweeton. 1991. Assessing presplit blast damage with crosshole seismic tomography. Pp. 514–517 in Society of Exploration Geophysicists Expanded Abstracts. Tulsa, Okla.: Society of Exploration Geophysicists.

Daily, W. 1984. Underground oil-shale retort monitoring using geotomography. Geophysics, 49:1701–1707.

Daily, W., and E. Owen. 1991. Cross-borehole resistivity tomography. Geophysics, 56:1228–1235.

Dennis, B., E. Standen, D. T. Georgi, and G. O. Callow. 1987. Fracture identification and productivity predictions in a carbonate reef complex. SPE 16808, Society of Petroleum Engineers, Richardson, Tex., pp. 579–588.

Dey, A., W. H. Meyer, H. F. Morrison, and W. M. Dolan. 1975. Electric field response of two-dimensional inhomogeneities to unipolar and bipolar configurations. Geophysics, 40:615–632.

Dyer, B. C., and M. H. Worthington. 1988a. Seismic reflection tomography—a case study. First Break, 6:354–365.

Dyer, B., and M. H. Worthington. 1988. Some sources of distortion in tomographic velocity images. Geophysical Prospecting, 36:209–222.

Ekstrom, M. P., C. A. Dahan, M. Y. Chen, P. M. Lloyd, and D. J. Rossi. 1987. Formation imaging with microelectrical scanning arrays. The Log Analyst, 28(3):294–306.

Garotta, R. 1989. Detection of azimuthal anisotropy. Pp. 861–863 in European Association of Exploration Geophysicists, 51st Annual Meeting Extended Abstracts, Zeist, Holland.

Green, A. G., and J. A. Mair. 1983. Subhorizontal fractures in a granitic pluton: their detection and implications for radioactive waste disposal. Geophysics, 48(11):1428–1449.

Hanson, J. C., D. R. Tweeton, M. J. Friedel, and L. J. Dahl. 1991. A field test of electromagnetic methods for the detection of conductive plumes. Pp. 569–572 in Society of Exploration Geophysicists (SEG) Expanded Abstracts. Tulsa, Okla.: Society of Exploration Geophysicists.

Hardin, E. L., and M. N. Toksöz. 1985. Detection and characterization of fractures from generation of tube waves. Pp. II1–II21 in 26th Annual Logging Symposium Transactions. Houston, Tex.: Society of Professional Well Log Analysts.

Hardin, E. L., C. H. Cheng, F. L. Paillet, and J. D. Mendelson. 1987. Fracture characterization by means of attenuation and generation of tube waves in fractured crystalline rock at Mirror Lake, New Hampshire. Journal of Geophysical Research, 92(B8):7989–8006.

Hess, A. E. 1986. Identifying hydraulically conductive fractures with a slow-velocity borehole flowmeter. Canadian Geotechnical Journal, 23(1):69-78.

Hess, A. E., and F. L. Paillet. 1990. Applications of the thermal-pulse flowmeter in the hydraulic characterization of fractured rocks. Pp. 99–112 in Geophysical Applications for Geotechnical Investigations, F. L. Paillet and W. R. Saunders, eds. ASTM STP 1101. Philadelphia, Pa.: American Society for Testing and Materials.

Hestir, K., and J. Long. 1990. Analytical expressions for the permeability of random two-dimensional poisson fracture networks based on regular lattice percolation and equivalent media theories. Journal Geophysical Research, 95(B13):21565–21582.

Holloway, A. L., K. M. Stevens, and G. S. Lodha. 1992. The results of surface and borehole radar profiling from permit area B of the Whiteshell research area, Manitoba, Canada. Special Paper 16, 329-337. Espoo: Geological Survey of Finland.

Hornby, B. E., D. L. Johnson, K. W. Winkler, and R. A. Plumb. 1989. Fracture evaluation using reflected Stoneley-wave arrivals. Geophysics, 54(10):1274–1288.

Hornby, B. E., S. M. Luthi, and R. A. Plumb. 1992. Comparison of fracture apertures computed from electrical borehole scans and reflected Stoneley waves: an integrated interpretation. The Log Analyst, 32(1)50–66.

Hudson, J. A. 1980. Overall properties of a cracked solid. Mathematical Proceedings of the Cambridge Philosophical Society, 88:371.

Ivansson, S. 1986. Seismic borehole tomography—theory and computational methods. Proceedings of the Institute of Electrical and Electronic Engineers, 74:328–338.

Johnsen, H. K. 1977. A man/computer interpretation system for resistivity soundings over a horizontally stratified earth. Geophysical Prospecting, 25:667–691.

Justice, J. H., A. A. Vassiliou, S. Singh, J. D. Logel, P. A. Hansen, B. R. Hall, P. R. Hutt, and J. J. Solanki. 1989. Acoustic tomography for monitoring enhanced oil recovery. The Leading Edge, 8(2):12–19.

Kamewada, S., and S. G. Hu. 1990. Application of a borehole image processing system to the survey of a tunnel. Pp. 51–58 in Rock Joints, Proceedings of the International Symposium on Rock Joints, Loen, Norway, W. Barton, and E. Stephannson, eds. Rotterdam: A. A. Balkema.

Katsube, T. J., and J. A. Hume. 1987. Permeability determination in crystalline rocks by standard geophysical logs. Geophysics, 52(3):342–352.

Ketola, M., and M. Puranen. 1967. Type curves for the interpretation of Slingram (horizontal loop) anomalies over tabular bodies. Report of Investigations #1. Espoo: Geological Survey of Finland.

Keys, W. S. 1979. Borehole geophysics in igneous and metamorphic rocks. Pp. 1–26 in the 20th Annual Logging Symposium Transactions. Houston, Tex.: Society of Professional Well Log Analysts.

Keys, W. S., and R. F. Brown. 1985. Effects of artificial recharge on the Ogallala aquifer, Texas. USGS Water Supply Paper 2251, U.S. Geological Survey, Reston, Va.

Keys, W. S., and J. K. Sullivan. 1979. Role of borehole geophysics in defining the physical characteristics of the Raft River geothermal reservoir, Idaho. Geophysics, 44(6):1116–1141.

Kierstein, R. A. 1983. True location and orientation of fractures logged with the acoustic televiewer (including programs to correct fracture orientation). USGS Water Resources Investigations Report 83-4275, U.S. Geological Survey, Reston, Va.

Krajewski, C., L. Dresen, C. Gelbke, and H. Ruter. 1989. Iterative tomographic methods to locate seismic low-velocity anomalies: a model study. Geophysical Prospecting, 37:717–752.

Kuich, N. 1989. Seismic fracture identification and horizontal drilling: keys to optimizing productivity in a fractured reservoir, Giddings Field, Texas. Transactions of the Association of Geological Societies, 34:153-158.

Lacy, L. L., and X. Smith. 1989. Fracture azimuth and geometry determinations. Pp. 357–375 in SPE Monograph 12: Recent Advances in Hydraulic Fracturing. Richardson, Tex.: Society of Petroleum Engineers.

Lau, J. S. O. 1983. The determination of true orientation of fractures in rock cores. Canadian Geotechnical Journal, 20(2):209–221.

Lee, K. H. 1993. Three-dimensional interpretation of electromagnetic (EM) field data using a nonlinear inversion scheme. Paper presented at the Computational Technology Initiative for the Oil and Gas Industry, Santa Fe, N.Mex., June 20–24.

Lefeuvre, F., and P. Desegaulx. 1993. Azimuthal anisotropy analyzing with *P*-waves: the AVOAVAZ approach. European Association of Exploration Geophysicists Abstracts, 55:C031.

Lieblich, D. A., J. W. Lane, and F. P. Haeni. 1991. Results of integrated surface geophysics studies for shallow subsurface fracture detection at three New Hampshire sites. Proceedings of Society of Exploration Geophysicists (SEG) Convention Expanded Abstracts. Tulsa, Okla.: Society of Exploration Geophysicists.

Lieblich, D. A., F. P. Haeni, and R. E. Cromwell. 1992a. Interactive use of surface geophysics methods to indicate subsurface fractures at Tibbitts Road, Barrington, New Hampshire. USGS Water Resources Investigation Report 92-4012, U.S. Geological Survey, Reston, Va.

Lieblich, D. A., F. P. Haeni, and J. W. Lane. 1992b. Interactive use of surface geophysics methods to indicate subsurface fractures in Milford, New Hampshire. USGS Water Resources Investigation Report 92-4056, U.S. Geological Survey, Reston, Va.

Lines, L. 1991. Applications of tomography to borehole and reflection seismology. The Leading Edge, 10:11–17.

Liu, E., S. Crampin, J. H. Queen, and W. D. Rizer. 1993. Velocity and attenuation anisotropy caused by microcracks and macrofractures in azimuthal reverse VSPs. Canadian Journal of Exploration Geophysics, 29(1):177–188.

Lockner, D., and J. Byerlee. 1977. Hydrofracture in Weber sandstone at high confining pressure and differential stress. Journal of Geophysical Research, 82:2018–2026.

Macbeth, C. 1991. Inversion for subsurface anisotropy using estimates of shear-wave splitting. Geophysical Journal International, 107(3):585–595.

Majer, E. L., and T. W. Doe. 1986. Studying hydrofractures by high frequency seismic monitoring. International Journal of Rock Mechanics and Mineral Science, 23(3):185–199.

Majer, E. L., and T. V. McEvilly. 1982. The Stripa acoustic emission experiment. Pp. 569–582 in Proceedings of a Workshop on Hydraulic Fracturing for Stress Measurements, USGS Open File Report 82-1075, U.S. Geological Survey, Reston, Va.

Majer, E. L., T. V. McEvilly, and T. W. Doe. 1983. Laboratory studies of acoustic emissions (AE) in salt during hydrofracturing. EOS, Transactions of the American Geophysical Union, 64 (45).

Majer, E. L., L. R. Myer, J. E. Peterson, K. Karasaki, J. C. S. Long, S. J. Martel, P. Blumling, and S. Vomvoris. 1990. Joint seismic, hydrogeological and geomechanical investigations of a fracture zone in the Grimsel Rock Laboratory, Switzerland. NAGRA TR 90-49. Wettingen, Switzerland: Swiss National Cooperative for Radioactive Waste Disposal (NAGRA).

Majer, E. L., R. H. Chapman, W. D. Stanley, and B. D. Rodriguez. 1992. Monograph on The Geysers Geothermal Field, Special Report 17, Geothermal Resources Council, Davis, Calif.

Maki, V., S. Gianzero, R. Strickland, H. N. Kepple, and M. V. Gianzero. 1991. Dynamically focused transducer applied to the cast imaging tool. Pp. HH1–HH24 in 32d Annual Logging Symposium Transactions. Houston, Tex.: Society of Professional Well Log Analysts.

Martin, M. A., and T. L. Davis. 1987. Shear-wave birefringence: a new tool for evaluating fractured reservoirs. Geophysics: The Leading Edge of Exploration, 6(10):22.

McNeil, J. D. 1990. Use of electromagnetic methods for groundwater studies. Pp. 191–218 in Geotechnical and Environmental Geophysics, vol. 1, S.H. Ward, ed. Tulsa, Okla.: Society of Exploration Geophysicists.

Meadows, M. A., and P. F. Winterstein. 1994. Seismic detection of a hydraulic fracture from shear-wave VSP data at Lost Hills Field, California. Geophysics, 59:11–26.

Molz, F. J., and S. C. Young. 1993. Development and application of borehole flowmeters for environmental assessment. The Log Analyst, 34(1):13–23.

Momii, K., K. Jinno, and F. Herein. 1993. Laboratory studies on a new LDV system for horizontal groundwater velocity measurement in a borehole. Water Resources Research, 29:283–291.

Nelson, P. H., K. A. Magnusson, and R. Rachiele. 1983. Applications of borehole geophysics at an experimental waste storage site. Geophysical Prospecting, 30:910–934.

Nolet, G. 1987. Seismic Tomography. Dordrecht, Holland: D. Reidel.

Nyland, E., and M. Dusseault. 1983. Fire flood microseismic monitoring results and potential for process control. Journal of Canadian Petroleum Technology, March–April:61–68.

Olsson, O., ed. 1992. Site characterization and validation. Final report, Stripa Project, TR 92-22. Stockholm: Swedish Nuclear Fuel and Waste Management Co.

Olsson, O., P. Anderson, and E. Gustafsson. 1991. Site characterization and validation—monitoring of saline tracer transport by borehole radar measurements. Final report, Stripa Project TR 91-18. Stockholm: Swedish Nuclear Fuel and Waste Management Co.

Olsson, O., L. Falk, O. Forslund, L. Lundmark, and E. Sandberg. 1992. Borehole radar applied to the characterization of hydraulically conductive fracture zones in crystalline rock. Geophysical Prospecting, 40:109–142.

Paillet, F. L. 1980. Acoustic propagation in the vicinity of fractures which intersect a fluid-filled borehole. Pp. DD1–DD30 in 21st Annual Logging Symposium Transactions. Houston, Tex.: Society of Professional Well Log Analysts.

Paillet, F. L. 1983. Acoustic characterization of fracture permeability at Chalk River, Ontario. Canadian Geotechnical Journal, 20(3):468–476.

Paillet, F. L. 1984. Field tests of an acoustic sparker source for waveform logging . Pp. GG1–GG25 in 25th Annual Logging Symposium Transactions. Houston, Tex.: Society of Professional Well Log Analysts.

Paillet, F. L. 1985a. Problems in fractured-reservoir evaluations and possible routes to their solution. The Log Analyst, 26(6):26–41.

Paillet, F. L. 1985b. Borehole acoustic applications in rock mechanics. Pp. 207–219 in Proceedings of the 26th U.S. Symposium on Rock Mechanics. Rotterdam: A. A. Balkema.

Paillet, F. L. 1991a. Use of geophysical well logs in evaluating crystalline rocks for siting of radioactive waste repositories. The Log Analyst, 33(2):85–107.

Paillet, F. L. 1991b. High-resolution flow logging in observation boreholes during hydraulic testing of fractured-rock aquifers. Pp. L1–L23 in 32d Annual Logging Symposium Transactions. Houston, Tex.: Society of Professional Well Log Analysts.

Paillet, F. L. 1991c. Qualitative and quantitative of fracture permeability using acoustic full-waveform logs. The Log Analyst, 32(3):256–270.

Paillet, F. L. 1991d. Comparing geophysical logs to core and cross borehole flow logging in the Mirror Lake drainage basin. U.S. Geological Survey Toxic Substances Hydrology Program, Proceedings of the Technical Meeting, Monterey, California. March 11–15. G. E. Mallard and D. A. Aronason, eds. USGS Water Resources Investigation Report 91-4034, U.S. Geological Survey, Reston, Va.

Paillet, F. L. 1993. Application of borehole geophysics in the characterization of flow in fractured rocks . USGS Water Resources Investigation Report 93-4214, U.S. Geological Survey, Reston, Va.

Paillet, F. L., and C. H. Cheng. 1991. Acoustic Waves in Boreholes—The Theory and Application of Acoustic Full-Waveform Logs. Boca Raton, Fla.: CRC Press.

Paillet, F. L., and D. Goldberg, 1991. Acoustic televiewer log images of natural fractures and bedding planes in the Toa Baja borehole, Puerto Rico. Geophysical Research Letters, 18 (3):501–504.

Paillet, F. L., and R. H. Morin. 1988. Analysis of geophysical well logs obtained in the state 2-14 borehole, Salton Sea geothermal area, California. Journal of Geophysical Research, 93 (B11):12,981–12,994.

Paillet, F. L., W. S. Keys, and A. E. Hess. 1985. Effects of lithology on televiewer-log quality and fracture interpretation. Pp. JJJ1–JJJ30 in the 26th Annual Logging Symposium Transactions. Houston, Tex.: Society of Professional Well Log Analysts.

Paillet, F. L., P. Hsieh, and C. H. Cheng. 1987. Verification of acoustic waveform and seismic VSP measurement of fracture permeability. Pp. PP1–PP21 in the 28th Annual Logging Symposium Transactions. Houston, Tex.: Society of Professional Well Log Analysts.

Paillet, F.L., C.H. Cheng, and X.M. Tang. 1989a. Theoretical models relating acoustic tube-wave attenuation to fracture permeability—reconciling model results with field data. Pp. FF1–FF24 in the 30th Annual Logging Symposium Transactions. Houston, Tex.: Society of Professional Well Log Analysts.

Paillet, F. L., J. Waltz, and R. E. Boyle. 1989b. Geophysical log investigation of formation changes produced by hydraulic fracture stimulation in a crystalline-bedrock aquifer. Pp. EE571–EE594 in Proceedings of the Third Symposium on Borehole Geophysics for Minerals and Geotechnical Logging. Houston, Tex.: Society of Professional Well Log Analysts.

Paillet, F. L., C. Barton, S. Luthi, F. Rambow, and J. Zemanek. 1990. Borehole Imaging. SPWLA Reprint Series. Houston, Tex.: Society of Professional Well Log Analysts.

Paillet, F. L., R. T. Kay, D. Yeskis, and W. Pedler. 1993. Integrating well logs into a multiple-scale investigation of a fractured sedimentary aquifeu. The Log Analyst, 34(1):13–23.

Pearson, C. 1981. The relationship between microseismicity and high pore pressures during hydraulic stimulation experiments in low permeability granitic rocks. Journal of Geophysical Research, 86(B9):7855–7865.

Pickett, G. R. 1960. The use of acoustic logs in the evaluation of sandstone reservoirs. Geophysics, 25(1):250–274.

Power, D. V., C. L. Shuster, R. Hay, and J. Twombly. 1976. Detection of hydraulic fracture orientation and dimensions in cased wells. Journal of Petroleum Technology, pp. 1116–1124.

Powley, D. 1990. Pressures and hydrogeology in petroleum basins. Earth Science Reviews, 29:215–226.

Pratt, R. G., and C. H. Chapman. 1992. Travel-time tomography in anisotropic media: application. Geophysical Journal International, 109(1):20–37.

Pratt, R. G., and N. R. Goulty. 1991. Combining wave-equation imaging with travel-time tomography to form high-resolution images from crosshole data. Geophysics, 56:208–224.

Pratt, R. G., and M. H. Worthington. 1988. The application of diffraction tomography to cross-hole seismic data. Geophysics, 53:1284–1294.

Rijo, L., W. H. Pelton, E. C. Feitosa, and S. H. Ward. 1977. Interpretation of apparent resistivity data from Apodi Valley, Rio Grande Do Norte, Brazil. Geophysics, 42:811–822.

Rosenbaum, J. H. 1974. Synthetic microseismograms: logging in porous formation . Geophysics, 39:14–32.

Sandberg, E. V., O. L. Olsson, and L. R. Falk. 1991. Combined interpretation of fracture zones in crystalline rock using single-hole, cross-hole tomography and directional borehole-radar data. The Log Analyst, 32(2):108–119.

Sattel, G., and C. Gelbke. 1987. Non-destructive rock testing with seismic crosshole tomography. Pp. 845–848 in Society of Exploration Geophysicists (SEG) Convention Expanded Abstracts. Tulsa, Okla.: Society of Exploration Geophysicists.

Sattel, G., P. Frey, and R. Amberg. 1992. Prediction ahead of the tunnel face by seismic methods—pilot project in Centovalli Tunnel, Locarno, Switzerland. First Break, 10(1):19–25.

Schmidt, R. D. 1985. Fracture zone dewatering to control ground water inflow in underground coal mines. RI 8981, pp. 4–16. Washington, D.C.: U.S. Department of the Interior, Bureau of Mines.

Shima, H. 1990. Two-dimensional automatic resistivity inversion technique using alpha centers. Geophysics, 55:682–694.

Shima, H., and H. Saito. 1989. Automatic three-dimensional resistivity inversion of crosshole data. Paper presented at European Association of Exploration Geophysicists meeting, June, West Berlin, Germany .

Smith, M. B., G. B. Holman, C. R. Fast, and R. J. Covlin. 1978. The azimuth of deep penetrating fractures in the Wattenburg field. Journal of Petroleum Technology, 30:185–193.

Solberg, P., D. Lockner, and J. Byerlee. 1977. Shear and tension hydraulic fractures in low permeability rocks. PAGEOPH, 115:191–198.

Stolarczyk, L. G. 1990. Radio imaging in seam wave guides. Pp. 187–209 in Geotechnical and Environmental Geophysics, vol. 3, Ward, S. H., ed. Tulsa, Okla.: Society of Exploration Geophysicists.

Stratton, J. A. 1941. Electromagnetic Theory. New York: McGraw-Hill.

Tang, X. M. and C. H. Cheng. 1989. A dynamic model for fluid flow in open borehold fractures. Journal of Geophysical Research, 94(B6):7567–7576.

Telford, W. M., L. P. Geldart, R. E. Sherif, and D. A. Keys. 1976. Applied Geophysics. Cambridge: Cambridge University Press.

Thomsen, L. 1988. Reflection seismology over page 146 anisotropic media. Geophysics, 53(3):304–313.

Thomsen, L. 1995. Elastic anisotropy due to aligned cracks in porous rock. Geophysical Prospecting, 43:805–829.

Tsang, C. F., P. Hufschmied, and F. V. Hale. 1990. Determination of fracture inflow parameters with a borehole fluid conductivity logging method. Water Resources Research, 26(4):561–578.

Tura, M. A. C., L. R. Johnson, E. L. Majer, and J. E. Peterson. 1991. Application of diffraction tomogrophy to fracture detection. Geophysics, 57(2):245-257.

Van, G. P., S. K. Park, and P. Hamilton. 1991. Monitoring of leaks from storage ponds using resistivity methods. Geophysics, 56:1267–1270.

Vernon, J. H., F. L. Paillet, W. H. Pedler, and W. J. Griswold. 1993. Applications of borehole geophysics in defining the wellhead protection area for a fractured crystalline bedrock aquifer. The Log Analyst, 34(1):41–57.

Villegas-Garcia, C. J., and G. F. West. 1983. Recognition of electromagnetic overburden anomalies with horizontal loop electromagnetic survey data. Geophysics, 48:42–51.

Ward, S. H. 1990. Resistivity and induced polarization methods. Pp. 147–189 in Geotechnical and Environmental Geophysics, vol. 1, S. H. Ward, ed. Tulsa, Okla.: Society of Exploration Geophysicists.

White, J. E. 1983. Underground Sound: Application of Seismic Waves. New York: Elsevier.

Willis, H. A., G. L. Rethford, and E. Bielouski. 1986. Azimuthal anisotropy: occurrence and effect on shear-wave data quality. Pp. 470–481 in Society of Exploration Geophysicists (SEG) Convention Expanded Abstracts. Tulsa, Okla.: Society of Exploration Geophysicists.

Wills, P. B., D. C. DeMartini, H. J. Vinegar, and J. Shlyapobersky. 1992. Active and passive imaging of hydraulic fractures. Geophysics: The Leading Edge of Exploration, 11(7):15–23.

Winterstein, D. F., and M. A. Meadows. 1991a. Shear-wave polarizations and subsurface stress directions at Lost Hills field. Geophysics, 56:1331–1348.

Winterstein, D. F., and M. A. Meadows. 1991b. Changes in shear-wave polarization azimuth with depth in Cymric and Railroad Gap oil fields. Geophysics, 56:1349–1364.

Wu, R. S., and M. N. Toksöz. 1987. Diffraction tomography and multisource holography applied to seismic imaging. Geophysics, 52:11–25.

Yorkey, T. J., J. G. Webster, and W. J. Tompkins. 1987. Comparing reconstruction algorithms for electrical impedance tomography. IEEE Transactions in Biomedical Engineering, 34:843–852.

Zemanek, J., E. E. Glenn, L. J. Norton, and R. L. Caldwell. 1970. Formation evaluation by inspection with the borehole televiewer. Geophysics, 35:254–269.

5

Hydraulic and Tracer Testing of Fractured Rocks

Hydraulic and tracer tests are field methods for investigating fluid flow and chemical transport in the subsurface. They generally involve artificially inducing perturbations into the subsurface and measuring the resulting responses. In a hydraulic test the perturbation is created by injecting or withdrawing fluid from a borehole. The response is the change in fluid pressure in the same or nearby observation boreholes. In a tracer test a concentration perturbation is created by introducing a solute (tracer) into the subsurface. The movement of this solute is monitored by sampling for solute concentration at locations downstream from the tracer introduction point.

This chapter provides an overview of field techniques and methods of analysis and their advantages and limitations, but the intent is not to provide a manual for hydraulic and tracer testing. The discussion is limited to hydraulic and tracer tests under single-phase, isothermal flow conditions in which the solute concentration is sufficiently dilute that density effects can be neglected. Not covered are hydraulic and pneumatic tests for evaluation of the vadose zone. Hydraulic and transport properties are assumed to remain constant during the tests. In other words, it is assumed that coupling between fluid pressure and rock stress is negligible and that chemical reactions (such as precipitation) that alter fracture openings do not occur. These conditions are generally satisfied when testing at depths of less than a few hundred meters and when the induced pressure perturbation is relatively small (e.g., less than 10 bars). In contrast, the testing of deep petroleum or geothermal wells commonly involves large changes in fluid pressure to the extent that fractures are opened or closed. This coupling is addressed in Chapter 7, but it is beyond the scope of this report to discuss hydraulic tests in these settings.

The popular notion that hydraulic and tracer tests are methods to "measure" hydraulic and tracer properties is somewhat misleading. In reality, the analysis of a hydraulic or tracer test is a modeling exercise consisting of two steps. The first step is to choose a model to represent flow and transport in the rock mass. In the petroleum industry this step is commonly known as the diagnostic phase. The choice of model is based on knowledge of the rock mass and the behavior of the test response. After a model is chosen, the second step is to determine values of model parameters such that model-computed responses match the field responses. This step is known as parameter estimation. If the model-generated response cannot be made to match the field response, the model must be revised. In other words, model selection and parameter estimation are an iterative process. In some cases there may be insufficient information to identify a unique model or a unique set of parameters for a given model. When faced with such nonuniqueness, several possible models and/or parameter sets may need to be considered until additional information is collected to better define the flow system. The hydraulic and transport properties determined from a hydraulic or tracer test are not unique. They must be considered within the context of the model chosen for analysis.

HYDRAULIC TESTS

In groundwater investigations, hydraulic tests are used to obtain estimates of hydraulic conductivity and specific storage of the aquifer medium. The term "transmissivity" refers to the product of hydraulic conductivity and aquifer thickness. "Storativity" is the product of specific storage and aquifer thickness. In the petroleum industry the properties obtained are permeability and total compressibility.

The distinction between hydraulic conductivity and transmissivity, or specific storage and storativity, is clear-cut when testing a porous medium, but confusion may arise in fractured rocks, as illustrated by the following example. Consider a rock mass containing a single extensive horizontal fracture bounded by impermeable rock. A borehole is drilled through this fracture, and a packer test is conducted in a test interval of length L containing this fracture (Figure 5.1a). If a porous-medium approach is used to analyze the test data and flow is assumed to be confined to a porous slab of thickness L (Figure 5.1b), a transmissivity T and hydraulic conductivity, K (= T/L), of the test interval can be calculated. For this particular example, however, the computed hydraulic conductivity is not representative of the rock mass because its value depends on the length of the test interval. If the length of the test interval is doubled (Figure 5.1c), the calculated hydraulic conductivity is halved. The transmissivity, however, is independent of the length of the test interval as long as no additional permeable fractures are encountered as the test interval is lengthened. To the extent that a single fracture can be viewed as an aquifer, it is useful to assign the transmissivity of the interval

to the fracture. Thus, fracture transmissivity is a term that is receiving increasing usage. The point of this example is not to discourage the use of hydraulic conductivity in test analysis but to emphasize the importance of reporting the test results with sufficient detail on the method of analysis so that readers are not misled.

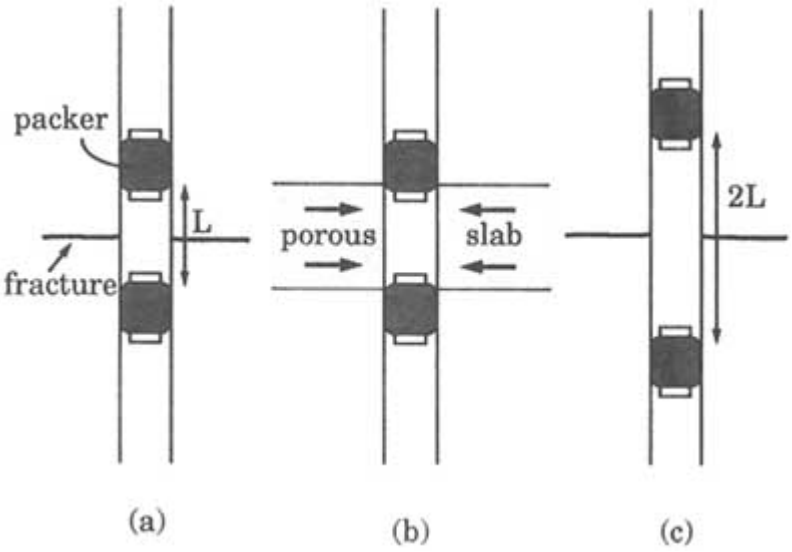

FIGURE 5.1 Packer test for determining transmissivity. (a) Packer interval of length L straddling a single fracture. (b) Packer interval of length L straddling a slab of fractured rock considered a porous medium. (c) Packer interval of length $2L$ straddling a single fracture.

Hydraulic Testing in a Single Borehole

In many subsurface investigations, particularly during the initial exploratory phase, hydraulic measurements (e.g., hydraulic head and flow rate) are restricted to individual boreholes. These tests are known as single-borehole hydraulic tests. Although single-borehole tests do not yield as much information as tests involving multiple boreholes, they offer the advantage of economy and speed. Single-borehole tests are commonly used for deep geological investigations because of the prohibitive expense of drilling multiple boreholes. Single-borehole tests are also used in some geotechnical investigations where time constraints preclude extensive testing with multiple boreholes.

Open-Borehole Versus Packer Tests

Single-borehole hydraulic tests can be performed in two configurations: in an open borehole or with packers. In an open-borehole test the entire uncased portion of a borehole is tested. Open-borehole tests are easy to set up and do not require expensive test equipment. They provide information on the hydraulic properties of the tested rock mass as a whole. They also provide valuable information for the design of packer tests, for example, on the expected range of pumping or injection rates. It is advantageous to conduct open-borehole tests prior to packer tests.

There are several disadvantages to open-hole tests. First, water inflow zones in the borehole cannot be located unless a flowmeter survey (Chapter 4) is conducted during pumping. Second, if the borehole penetrates several fractures or rock formations, the test response will be controlled by the most permeable zone, and little information will be obtained on the less permeable portion of the borehole. Third, when performed in low-permeability rocks, the test response may be dominated by wellbore storage effects (explained below), which complicate the interpretation of test data.

Packer tests utilize two or more packers to isolate a portion of the borehole for testing. Depending on the application, the test interval can vary from tens of centimeters to tens of meters in length. Packers can be used to isolate an individual fracture, a group of fractures, or an entire rock formation. In some test programs, a fixed test interval length is chosen, and the borehole is tested in consecutive sections throughout its length to obtain a hydraulic conductivity profile. Other test programs concentrate on testing only the more permeable portions of the borehole. In such cases the test intervals may vary in length, depending on borehole conditions as inferred from geophysical logs.

Test Procedures

The basic procedure of a single-hole hydraulic test is to inject or withdraw fluid from a test interval while measuring the hydraulic head in the same test interval. Prior to testing, borehole conditions are allowed to reequilibrate following installation of test equipment. Test equipment can be set up in many different ways, examples of which can be found in Zeigler (1976), Bennett and Anderson (1982), and Bureau of Reclamation (1985). In a packer test the hydraulic heads above and below the test interval are monitored to check for fluid leakage around the packers. Leakage can result from poor packer seals or the presence of "short-circuiting" fractures between the test interval and the rest of the borehole. When testing at depth, temperature in the test interval should be monitored because a change in temperature resulting from thermal disequilibrium (e.g., if the rock was cooled by drilling fluid prior to the test) can cause anomalous responses (see, e.g., Pickens et al., 1987).

During injection or withdrawal, the head change should be sufficiently large that the flow rate is measurable but not so large as to alter the hydraulic properties of the rock mass. A high injection head can open existing fractures and increase their transmissivities. In an extreme case, hydraulic fracturing can result. Conversely, a large reduction in head during fluid withdrawal can cause dissolved gas to come out of the solution. Gas bubbles lodged in fractures can reduce their transmissivities.

Five common procedures for single-hole hydraulic tests are discussed below: (1) constant-flow tests, (2) constant-head tests, (3) slug tests, (4) pressure pulse tests, and (5) drillstem tests. Figure 5.2 shows schematic plots of head and flow

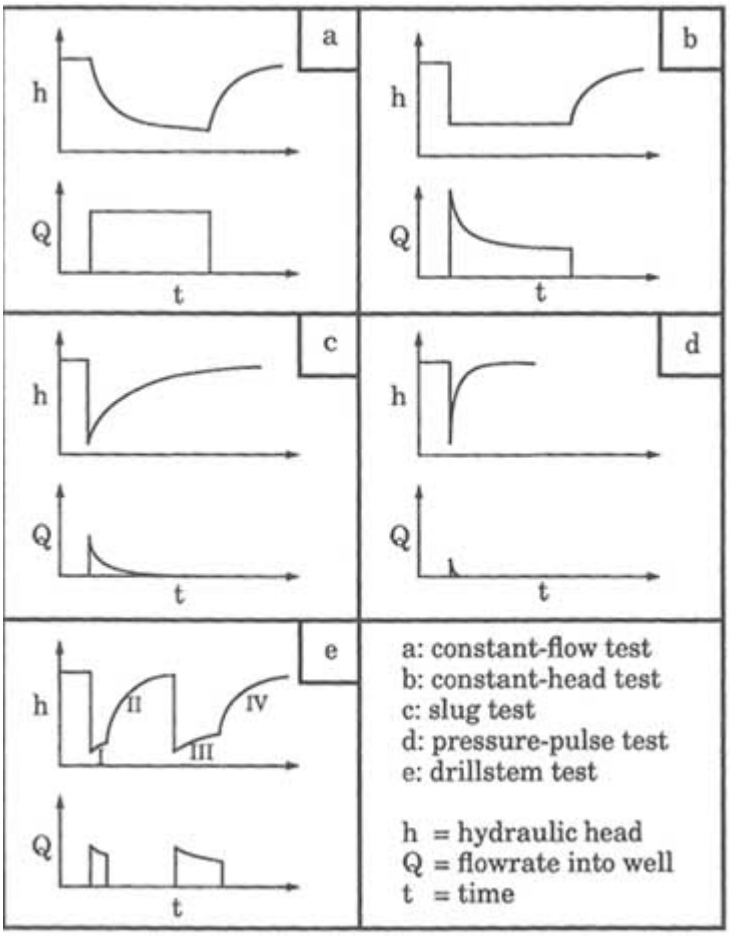

FIGURE 5.2 Schematic plots of hydraulic head and flow rate versus time for single-hole hydraulic tests.

rate versus time for these tests. Typically, the decision on which test to perform is based on the expected transmissivity of the test interval, the volume of rock to be sampled, and the availability of time and equipment. Test duration can range from 10 minutes in a geotechnical investigation to many days in a petroleum or water production test. Other factors being equal, a test of longer duration, involving a larger volume of injected or withdrawn fluid, will sample a larger volume of rock in the vicinity of the borehole. Quantifying the volume of rock sampled by these tests is a topic of current research.

The constant-flow pumping test (Figure 5.3), in which fluid is withdrawn at a constant rate from the test interval, is the most common test method in the

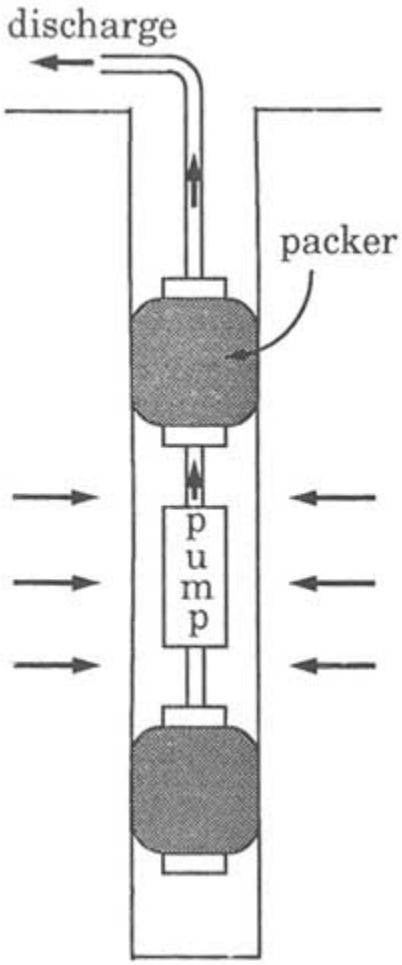

FIGURE 5.3 Equipment setup for a constant-flow pumping test in a single borehole.

groundwater and petroleum industries. Despite its popularity, this test is not without drawbacks. When performed with packers, the test is equipment intensive because a submersible pump must be used (Figure 5.3). Because most pumps operate over a limited discharge range, it is necessary to know the approximate transmissivity of the test interval in order to select the appropriate pump. Consecutive interval testing along a borehole becomes impractical, as the transmissivity variation from one test interval to another necessitates frequent changing of pumps. When testing an interval of low transmissivity, constant flow can be difficult to maintain and the pump can stall. For these reasons, constant-flow pumping tests are commonly reserved for testing more permeable intervals. An exception to this generalization occurs when testing in an environment where the hydraulic head is higher than the discharge point (e.g., in an underground facility, a naturally flowing well). In this case a constant outflow can be controlled by a flow regulator and a pump is not needed.

During a constant-head test (Figure 5.4), fluid is injected into or withdrawn from a test interval while keeping the head of the test interval at a constant value. Constant-head injection is common practice in geotechnical investigations. Constant-head withdrawal is practical when testing in an underground chamber. If the hydraulic head in the test interval is higher than the chamber floor, the test interval can be opened to free drainage. A key advantage of constant-head testing is that it generally presents no special technical difficulties when applied to test intervals of low transmissivity, as long as the flow rate is measurable. The effects of wellbore storage also are minimal, which simplifies data analysis.

A slug test (Figure 5.5) is performed by rapidly raising or lowering the fluid level in the pipe string or tubing connected to a test interval and monitoring its recovery to an equilibrium level. Typically, the test equipment includes a downhole valve in the test interval (Figure 5.5). After the packers are inflated, the test interval is isolated from the pipe string by closing the downhole valve. The fluid level in the pipe string is then raised or lowered by addition or removal of fluid. At the start of the test, the downhole valve is opened so that the hydraulic head in the pipe string is imposed on the test interval. If the fluid level in the pipe string were to be raised, fluid would drain from the pipe into the rock. If the fluid level was lowered, fluid would drain from the rock into the pipe. The downhole valve is kept open until the fluid level recovers to its equilibrium position. Slug tests are suitable for test intervals of moderate to low transmissivity. The test duration depends on the transmissivity of the test interval and the inside diameter of the pipe string. Lower transmissivities and larger pipe diameters lead to longer test times. Because pipe diameter can be varied, the duration of a slug test is controllable to a limited extent.

A pressure pulse test (Bredehoeft and Papadopulos, 1980) is similar in concept to a slug test, with the exception that the downhole valve is closed after the hydraulic head in the test interval is abruptly increased or decreased. The downhole valve is opened just long enough for the head in the pipe string to be

transmitted into the test interval. Alternatively, the initial head disturbance can be created by using a hydraulic piston to inject a known volume of fluid into the test interval. The duration of a pressure pulse test depends on the transmissivity and the "system compressibility" of the test interval. System compressibility is

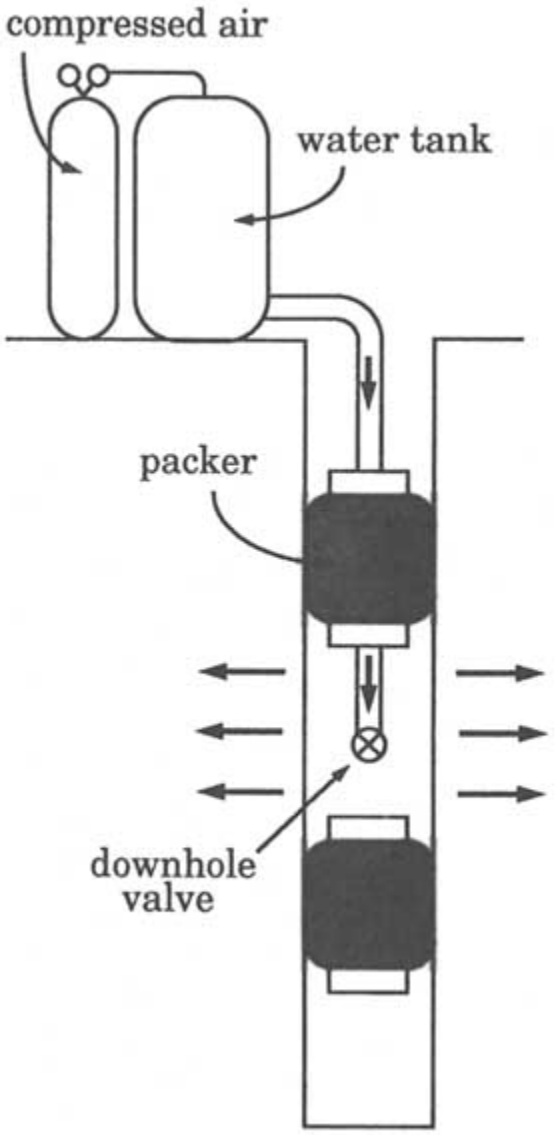

FIGURE 5.4 Equipment setup for a constant-head injection test in a single borehole.

a function of the fluid compressibility and the compliance of the test equipment (e.g., Neuzil, 1982). Because head recovery is controlled by compressibility effects rather than filling or draining fluid from the pipe string, the duration of a pressure pulse test is much shorter than that of a slug test, all other factors being equal. For this reason, the pressure pulse test is commonly applied to test intervals of very low transmissivity. However, the volume of rock tested by a pressure pulse test is significantly smaller than that tested by a slug test.

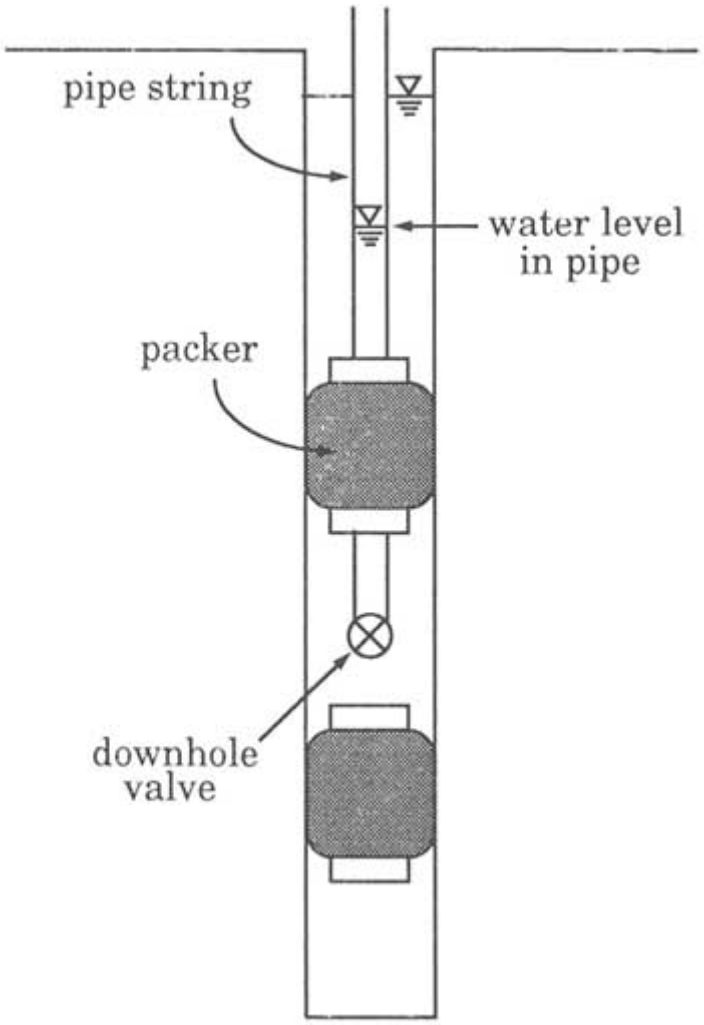

FIGURE 5.5 Equipment setup for a slug test in a single borehole.

The drillstem test was originally developed in the petroleum industry for testing wells before casing is installed. The equipment for a drillstem test is similar to that for a slug test. After the packers are inflated, the downhole valve (known as the tester valve in the petroleum industry) is shut and fluid is removed from the pipe string. The actual test comprises four stages (identified as I, II, III, and IV in Figure 5.2e). The first stage is the initial flow period, when the tester valve is opened for five to 10 minutes, allowing formation fluid to enter the pipe string. During the second stage, which lasts about an hour and is known as the initial shut-in period, the tester valve is shut so that fluid pressure in the test interval can recover toward the undisturbed formation pressure. In the third stage the tester valve is opened for the final flow period of approximately an hour. This is followed by the fourth state, final shut-in period of one to two hours, when the tester valve is again closed and the pressure in the test interval is allowed to recover. The flow period of a drillstem test is equivalent to a slug test, and the test data can be analyzed in the same fashion.

Discussions of drillstem testing can be found in petroleum texts such as that by Earlougher (1977). Karasaki (1990) has proposed a variant of the drillstem test that consists of only one flow period, with the shut-in occurring at the time when the initial head drop has recovered by 50 percent. According to Karasaki, such a procedure improves the estimation of formation properties when a skin of low permeability (e.g., a mudcake) surrounds the wellbore.

Models of Single-Borehole Hydraulic Tests

Many common models of single-borehole hydraulic tests assume that the tested rock can be approximated as an isotropic homogeneous porous medium. Simple additions such as a highly transmissive fracture intersected by the borehole can be included in the analysis. The assumption of isotropy is made for a practical reason: reliable methods to characterize anisotropy generally require multiple boreholes. Homogeneity is assumed because the test response in a single borehole is insensitive to changes in hydraulic properties far from the test interval. Unless flow boundaries are close to the test interval, they are difficult to detect with confidence. For these reasons, models for single-borehole hydraulic tests are primarily concerned with fluid flow in the immediate vicinity of the test interval.

Flow in the vicinity of the test interval can be envisioned in terms of three basic geometries: spherical flow, radial flow, and linear flow. Combinations of these geometries are possible. The discussion of these geometries below assumes that flow is caused by pumping from the test interval, causing a drawdown in hydraulic head. To the extent that the head change is sufficiently small that the hydraulic conductivity is not changed, the discussion is equally applicable to an injection test, in which case the flow direction is merely reversed.

Spherical flow geometry describes fluid flow toward a spherical cavity in a homogeneous porous medium of infinite extent in all directions (Figure 5.6a). Equipotential surfaces are concentric spheres around the spherical cavity. When applied to hydraulic testing, the cavity can represent a short test interval, the length of which is not significantly greater than the borehole diameter (Figure 5.6b). Spherical flow is commonly characterized as "three-dimensional" because the hydraulic head varies in the three spatial dimensions.

Radial flow geometry describes flow toward a well that pumps from a homogeneous layer of infinite lateral extent (Figure 5.7a). This flow geometry serves as the model for a well test in a confined aquifer, which is bounded above and below by impervious materials. In the aquifer, equipotential surfaces are cylinders centered about the well axis. Thus, radial flow is also known as cylindrical flow. When applied to fractured-rock testing, the layer of porous medium represents a horizontal fracture zone or a single fracture bounded by impermeable rock (Figure 5.7b). Radial flow is commonly characterized as "two-dimensional" because the hydraulic head varies in the plane perpendicular to the well axis but remains constant along the direction parallel to the axis.

Linear flow geometry describes flow that is unidirectional, that is, flow that does not vary in space (Figure 5.8a). An example of linear flow is flow to a well that intersects a highly transmissive vertical fracture that extends a long distance

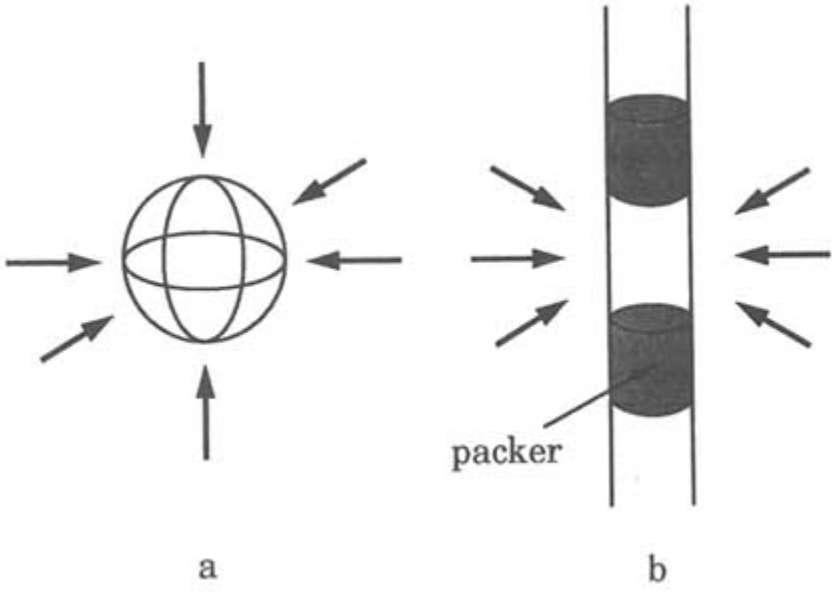

FIGURE 5.6 (a) Spherical flow to a cavity in a homogeneous porous medium. (b) Flow to a short test interval in a borehole that approximates spherical geometry.

from the well. The fracture acts effectively as an extension of the wellbore (Figure 5.8b), increasing its efficiency in extracting fluid from surrounding rock. Flow does not converge toward the well axis but is oriented in the direction perpendicular to the fracture plane. Equipotential surfaces are planar and parallel to the fracture plane. For this reason, linear flow is commonly characterized as "one-dimensional" flow.

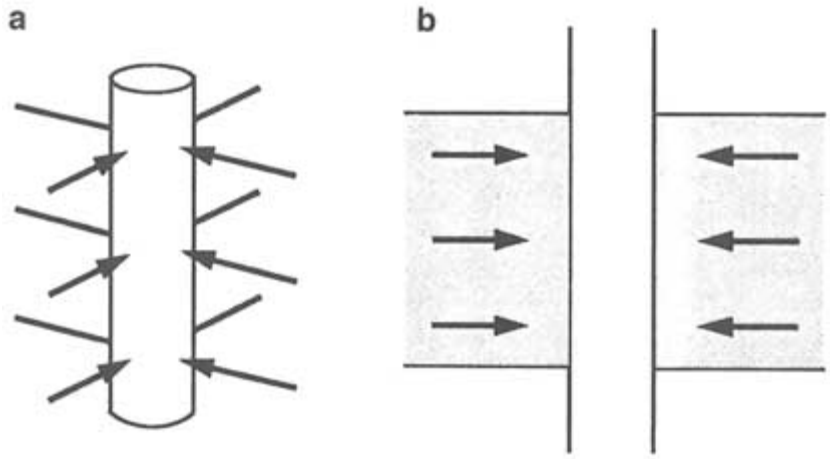

FIGURE 5.7 (a) Radial flow to a cylinder in a homogeneous porous medium. (b) Flow in a layer of porous medium confined above and below by impervious material.

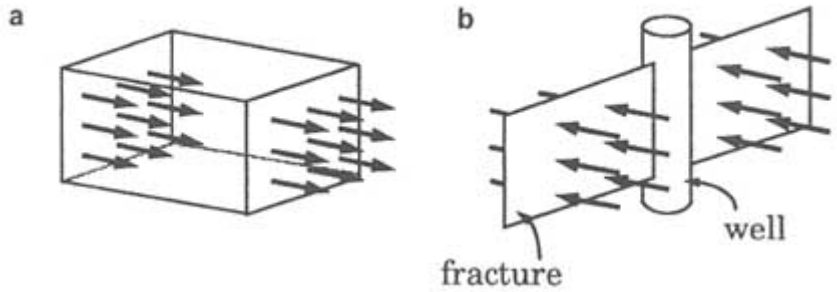

FIGURE 5.8 (a) Linear flow in a homogeneous porous medium. (b) Flow to a well that intersects a highly transmissive vertical fracture. The fracture acts as an extension of the wellbore.

Combinations of the three basic geometries described above are possible, Figure 5.9 illustrates flow toward a test interval whose length is significantly

longer than the wellbore diameter in an infinite porous medium. In the vicinity of the test interval, flow is nearly radial, whereas far from the borehole, it is nearly spherical. Such a flow pattern is termed *radial spherical*. Another example of combined flow geometries is illustrated by flow to a well intercepting a highly transmissive fracture (Figure 5.10). Flow is nearly linear where the fracture intersects the wellbore. At a large distance away from the wellbore, flow is nearly radial. This flow pattern is termed *linear radial*.

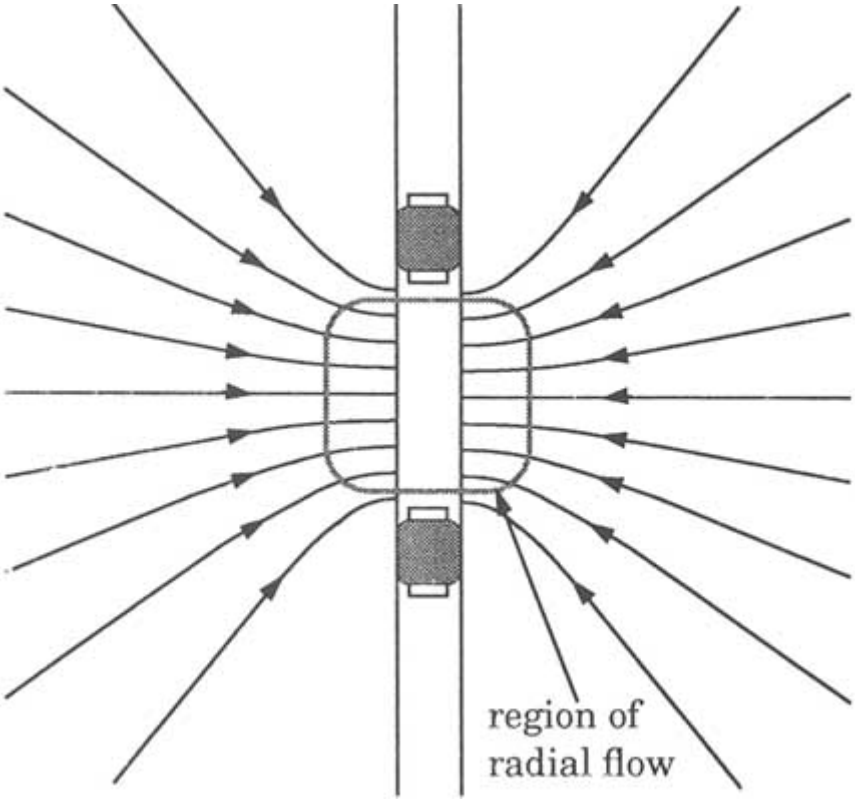

FIGURE 5.9 Radial-spherical flow. Flow is nearly radial close to the test interval and nearly spherical far from the test interval.

Barker (1988) introduced the concept of a fractional flow dimension to hydraulic test analysis. This concept provides a novel approach to interpreting hydraulic tests. The fractional flow dimension describes the power relationship between the distance from the test interval and the area available for flow. For spherical flow the area (A) available to flow is $4\pi r^2$ (i.e., the area of a sphere of radius r), where r is the distance from the test interval. For radial flow, A =

$2\pi rb$ (i.e., the area of a cylinder of radius r and height b). For linear flow the area is a constant value independent of r. The relationship between A and r can be generalized as $A = \alpha_d r^{d-1}$, where d is the Euclidean integer dimension (d = 1, 2, or 3), and α_d is a proportionality constant that is a function of d. In introducing the concept of fractional flow dimension, Barker allowed d to take nonintegral values. For example, a dimension between 2 and 3 represents a hybrid flow geometry between radial and spherical.

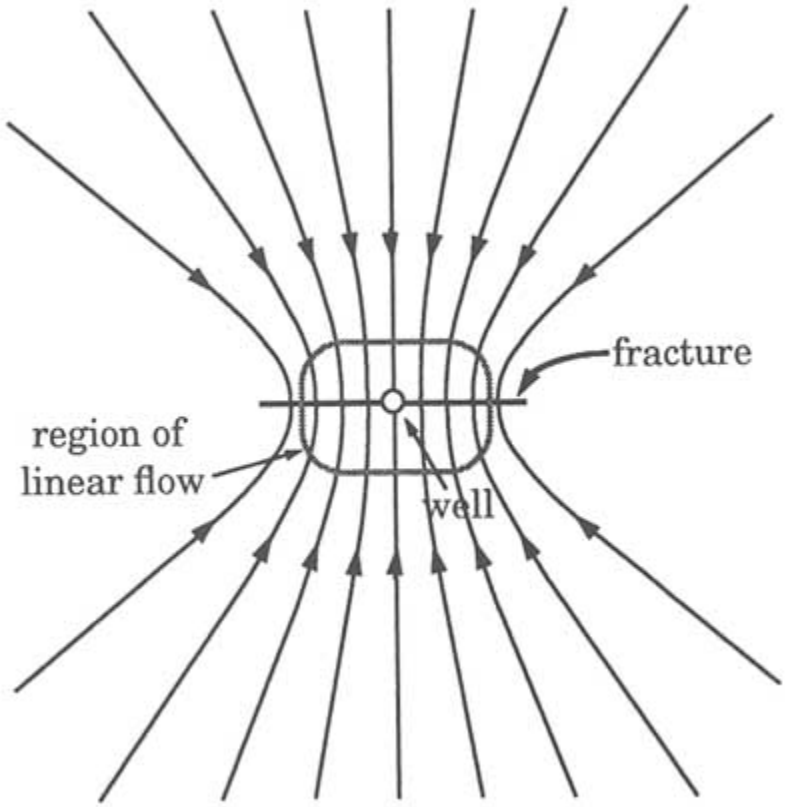

FIGURE 5.10 Areal view of linear-radial flow to a well intersecting a highly transmissive vertical fracture. Flow is nearly linear where the wellbore intersects the fracture and is nearly radial far from the well and fracture.

The physical meaning of a fractional flow dimension is unclear, but Barker speculates that it describes a fracture network that exhibits fractal geometry. That is, the fractional flow dimension may be related to the fractal dimension of the fracture network. Polek (1990) showed that the flow network of such fractal objects is a subset of the geometric network. In the cases he studied, the flow

dimension, as determined by using Barker's (1988) approach, is less than or equal to the fractal dimension.

Mathematical analysis of models having the flow geometries described above is the subject of numerous papers in the groundwater and petroleum literature (e.g., Streltsova, 1988; Dawson and Istok, 1991). In many cases the models are sufficiently simple that analytical solutions can be found to the initial boundary value problem. The analytical solution is a mathematical formula that expresses drawdown and discharge as functions of time and model parameters. The availability of analytical solutions is highly advantageous for model selection and for gaining insight into how well model parameters can be estimated from field data.

Knowing the characteristic forms of the analytical solutions can be highly beneficial for selecting a flow model to analyze the hydraulic tests. For a constant-flow test a plot of the log of drawdown versus the log of time illustrates the contrasting behaviors for different flow geometries. Figure 5.11 shows the responses for the three Euclidean flow dimensions (n = 1, 2, and 3 for linear, radial, and spherical geometries, respectively). If the flow is spherical (i.e.,

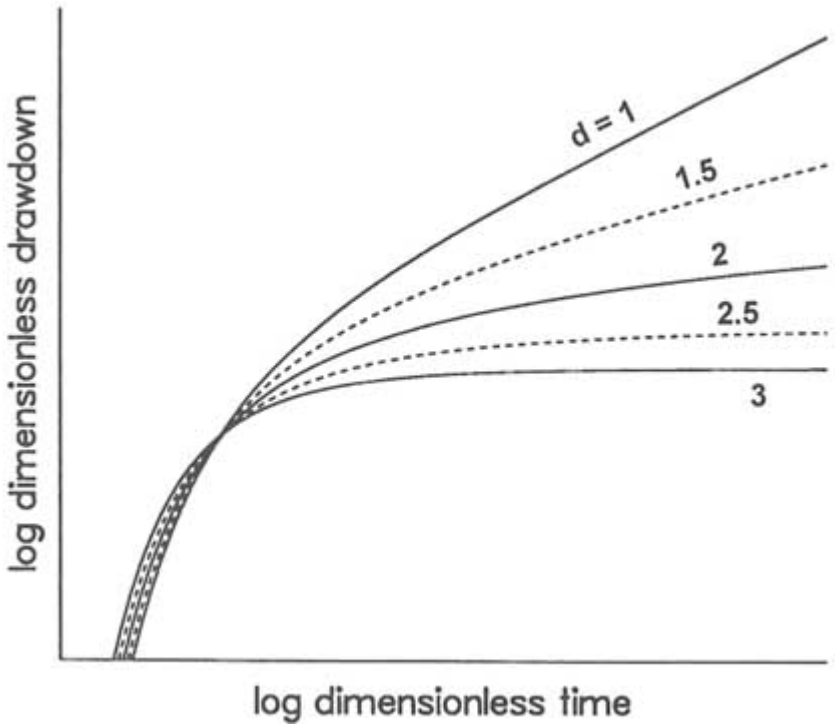

FIGURE 5.11 Plot of log dimensionless drawdown versus log dimensionless time for a constant-flow test. Numbers are flow dimensions. After Barker (1988), Figure 2.

d = 3), the drawdown initially increases with time but later approaches a constant value. If the flow is linear (i.e., d = 1), the drawdown plots as a straight line with slope 0.5 at late time. If the flow is radial (i.e., d = 2), the shape of the drawdown curve is intermediate between that of linear flow and spherical flow. For a constant-head test a similar comparison can be made by plotting the log of the inverse well discharge rate versus the log of time (Figure 5.12). Table 5.1 summarizes the characteristic behaviors of analytical solutions for different flow geometries.

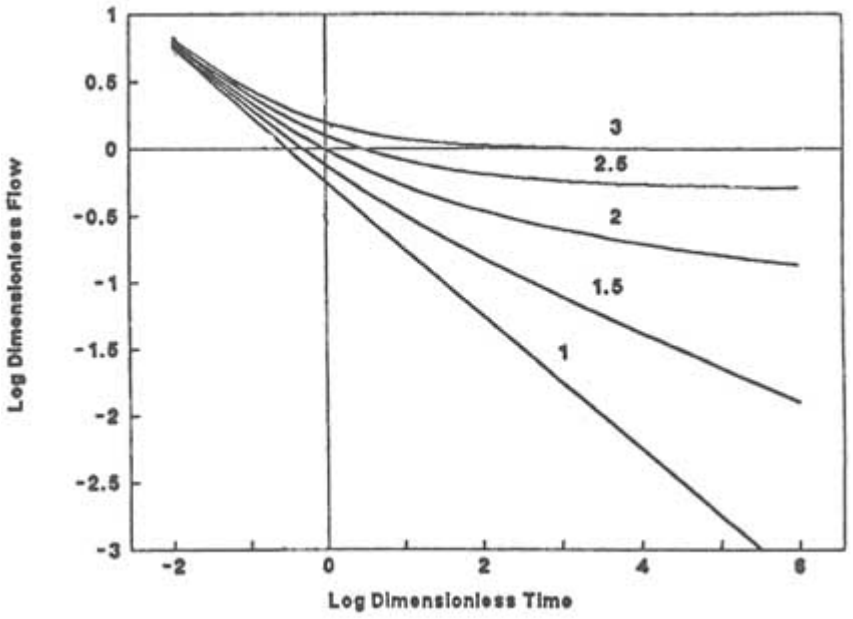

FIGURE 5.12 Plot of log dimensionless well discharge rate versus log dimensionless time for a constant-head test. Numbers are flow dimensions.

TABLE 5.1 Characteristic Behavior of Constant-Flow and Constant-Head Tests with Different Flow Geometries

Flow Geometry	Constant-Flow Test	Constant-Head Test
Spherical	Constant s at late time	Constant Q at late time
Radial	s proportional to log t at late time	$1/Q$ proportional to log t at late time
Linear	s proportional to $t^{1/2}$ at late time	$1/Q$ proportional to $t^{1/2}$ during entire test

Note: s denotes drawdown, t denotes time, and Q denotes discharge rate.

Introduction of fractional flow dimensions has provided a new approach to hydraulic test analysis, but indiscriminant application of the method can lead to meaningless results. Because fractional-dimension-type curves can match a large range of hydraulic responses, there is a strong temptation to apply this analysis exclusively. In some cases a different interpretation may be more meaningful. For example, consider radial flow to a well in a two-dimensional flow system (such as a fracture plane) that is heterogeneous with respect to both transmissivity, *T*, and storativity, *S.* Suppose the well pumps from a local region of lower *T* and *S* (compared to their average values). In the vicinity of the pumping well, both *T* and *S* will appear to increase with radial distance from the well. If the hydraulic test is of a short duration, the well response will be controlled by the hydraulic properties of the near-well region. The response will be similar to that of a flow domain with a fractional flow dimension larger than 2. Conversely, if the well pumps from a local region of higher *T* and *S*, the response will be similar to that of a flow domain with a fractional flow dimension less than 2. The application of a fractional flow dimension model to analyze the test response in this example yields a flow dimension that is an artifact of the heterogeneity in the flow domain. To interpret this dimension as characterizing some scaling feature of the entire flow field is erroneous.

A final model discussed here is the double-porosity model, which was developed to describe flow in a fractured porous medium. Such a medium is assumed to comprise a network of fractures bounding intact porous blocks. The fractures have high permeability and low storage, whereas the blocks have low permeability and high storage. The fractures provide the pathways for flow to the well, and the blocks provide the main source of water. Figure 5.13 illustrates the drawdown behavior during a constant-flow test in a well with radial flow geometry. Initially, most of the pumped water comes from the fractures, and the head in the fractures drops rapidly (period A). As pumping continues, the blocks begin to supply water to the fractures, causing the head in the fractures to stabilize and the head in the blocks to drop (period B). As the heads in the fractures and blocks equalize, both systems produce water to the well, although the blocks are the dominant source (period C). The combined fracture-block response is operative for the rest of the test.

Estimation of Model Parameters

Parameter estimation is essentially a fitting procedure. After a model is selected, the model parameters (hydraulic properties) are adjusted until the model computed drawdown and flow rate match the field data. A steady-state analysis attempts to match only that portion of the field data collected after steady state is achieved. A transient analysis attempts to match the drawdown and flow rate for the entire duration of the test. Steady-state analysis is simple because parameter estimation reduces to the direct application of a simple formula to determine the

hydraulic conductivity or transmissivity. However, the analyst must accept a number of assumptions (e.g., flow geometry), the validity of which may be uncertain. Transient analysis, although more complicated, offers the advantage that the flow geometry may be inferred from the field data.

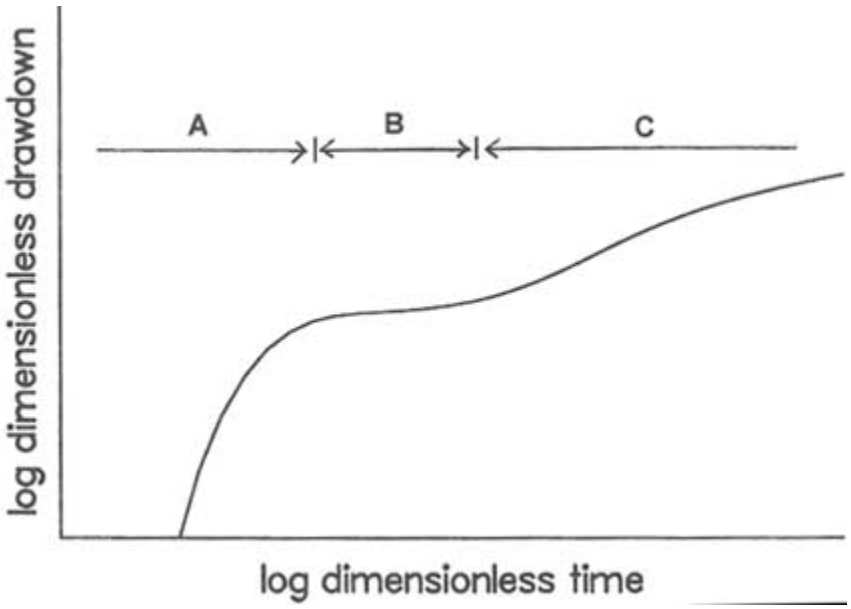

FIGURE 5.13 Plot of log dimensionless drawdown versus log dimensionless time for a constant-flow test with radial flow geometry for the double-porosity model. After Moench (1984), Figure 3.

It is somewhat ironic that steady-state analysis is generally applied to constant-head or constant-flow tests of relatively short duration (tens of minutes). Typically, the test is performed until both the flow rate and the hydraulic head in the test interval reach "stable" values, which is often taken to mean that the instrument readings do not change over several minutes. The stabilized head change and flow rate constitute the data from the test. If radial flow is assumed, the Theim formula (e.g., Bear, 1979) is used to compute the transmissivity of the test interval. For radial-spherical flow, formulas by Hvorslev or Moye yield the hydraulic conductivity of the rock in the vicinity of the test interval (Zeigler, 1976). Linear flow is generally not assumed in steady-state analysis.

Steady-state analysis is subject to errors from two sources. First, for tests of short duration, conditions may be far from steady state. Second, for certain flow patterns, a true steady state does not exist. Theoretical and field analyses show that the transmissivity or hydraulic conductivity determined from a steady-state analysis is often higher than the same quantity determined from a transient

analysis. Therefore, results of steady-state analyses should be considered as order-of-magnitude estimates.

Transient analysis can be done graphically or with computer software. The graphical method involves plotting the analytical solution and the data on separate sheets of graph paper and matching one to the other. The plot of the analytical solution is known as a *type curve* in the groundwater field, and the curve-matching procedure is known as *type curve analysis*. Recently, the use of automated computer analysis programs has gained popularity. The programs are based on regression techniques and are commonly set up so that the analyst can quickly try a number of different models. This interactive approach is desirable because the data may be matched equally well by type curves generated from different flow models. In such situations one may have to accept a range of hydraulic properties values until additional information becomes available to better guide selection of the flow model.

In principle, transient analysis yields the transmissivity and storativity if radial flow is assumed or hydraulic conductivity and specific storage if spherical flow is assumed. In practice, it is difficult to determine the storativity or specific storage with confidence from single-hole tests. During a constant-flow or constant-head test, storage effects are dominant only during the relatively short period (generally seconds to minutes) at the start of the test. The data during this period are commonly influenced by other factors, such as the inability to achieve constant flow or head instantly at the start of the test, that are neglected in the model.

In analyzing slug-test data, there is even greater uncertainty in determining storativity or specific storage because the analytical solutions for radial and spherical flow geometries are represented by a family of type curves. Figure 5.14 illustrates type curves for radial flow. Each curve corresponds to a different value of a dimensionless parameter that is a function of storativity and well geometry. For small values of storativity, the type curves are similar in shape, so it is difficult to obtain a unique match to the test data. A slight change of match from one type of curve to another can change the resultant storativity by an order of magnitude. The same problem occurs in the analysis of pressure pulse and drillstem tests.

To overcome the difficulty in selecting type curves, the method of matching to a derivative-type curve was introduced (Bourdet et al., 1989). The derivative-type curve is a plot of the derivative of the head with respect to the log of time against time (Figure 5.15). The shapes of derivative-type curves are somewhat more distinctive from one another and therefore provide an improved basis for curve matching. Test data must be of sufficient quality (i.e., accurate and free of noise) that their derivatives can be calculated for matching to the derivative curves.

Wellbore Storage and Skin Effects

Wellbore storage and skin effects are two factors that must be taken into account when analyzing single-borehole tests. Wellbore storage effect is due to

the fact that, when the water level is lowered in an open borehole during the early part of a constant-rate pumping test, the actual rate of water removal from the formation is less than the pump discharge. If the rate at which water is removed from the wellbore is insignificant in comparison with the rate at which water is pumped from the formation, the wellbore storage effect is negligible. This is generally the case when testing highly transmissive aquifers. When testing low-permeability rocks, however, the pumping rate is generally low, and a significant portion of the pumped water may be derived from the wellbore. When wellbore storage dominates the test response, a plot of log drawdown versus log time is a straight line of unit slope. Neglecting this effect will result in erroneous interpretation of the hydraulic test. In packer tests the change in hydraulic head is not associated with a change in water level. Wellbore storage can generally

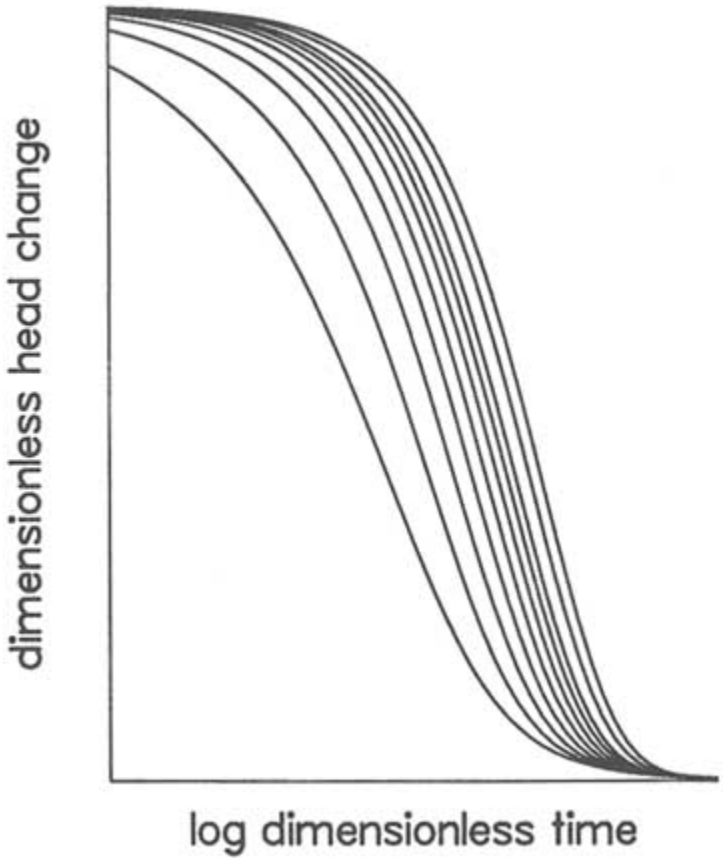

FIGURE 5.14 Plot of dimensionless head change versus log dimensionless time for a slug test with radial flow geometry. After Cooper et al. (1967), Figure 3.

be neglected except when testing borehole intervals of very low transmissivity, in which case equipment compliance could create a wellbore storage effect.

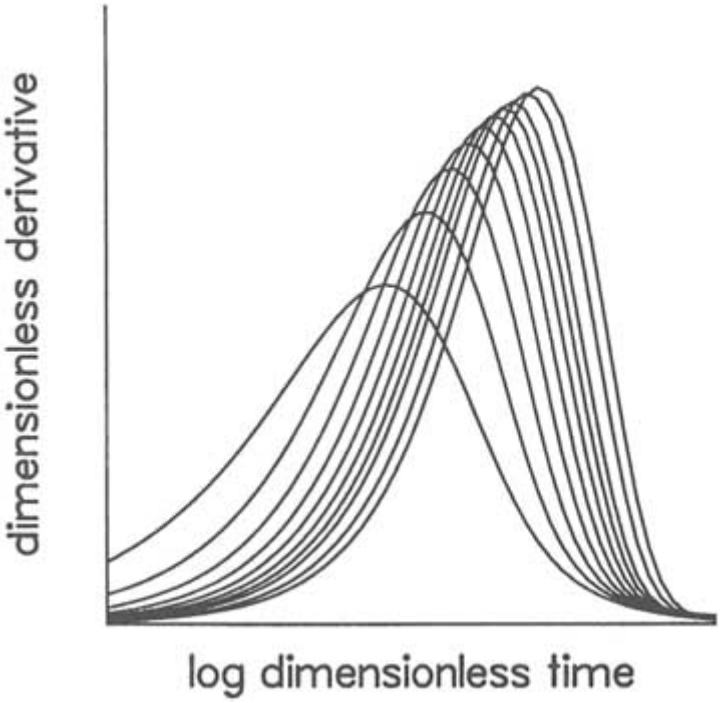

FIGURE 5.15 Plot of dimensionless derivative of head with respect to log of time versus log of dimensionless time for a slug test with radial flow geometry. Each curve corresponds to a different value of dimensionless parameter that is a function of storativity and well geometry. After Karasaki et al. (1988), Figure 4.

The term *skin effect* was originally introduced in the petroleum literature to describe the change in permeability of the borehole wall as a result of drilling. The region of altered permeability is known as the skin, and the effect of the skin is described by a quantity known as the skin factor. If the permeability is reduced owing to invasion of drilling mud, the skin factor is positive and drawdown in the well during pumping is greater than drawdown in the absence of skin. If the permeability is increased because of well development, the skin factor is negative and drawdown is less than in the absence of skin. In fractured rocks where water or air is used as the drilling fluid, alteration of the borehole wall should be minimal. However, the highly heterogeneous nature of fractured rocks can give the impression of a skin effect. For example, if a borehole intersects a locally tight portion of a fracture, the region around the borehole may appear to

be surrounded by a positive skin. In general, independent information is needed to determine whether this effect is due to wellbore damage, formation damage, or testing of a low-permeability region.

The effects of wellbore storage and skin can be included in a model by specifying the appropriate boundary condition at the test interval. In many cases the two effects can be combined into a single dimensionless term that is a function of the storativity, skin factor, and the known geometry of the wellbore (Ramey et al., 1975; Sageev, 1986). As in the case of a slug test, a family of type curves exists for analyzing a constant-flow test with wellbore storage and skin effects (Figure 5.16), and the test data must be matched by using type curve analysis. Derivative-type curves also can be used to aid matching. For radial flow the test analysis yields the transmissivity and a quantity that is a function of storativity and skin factor. In general, the storativity and skin cannot be separately computed without additional information.

Hydraulic Testing with Multiple Boreholes

Multiple-borehole hydraulic tests are also known as interference tests or cross-hole tests. Like single-borehole tests, multiple-borehole tests can be per

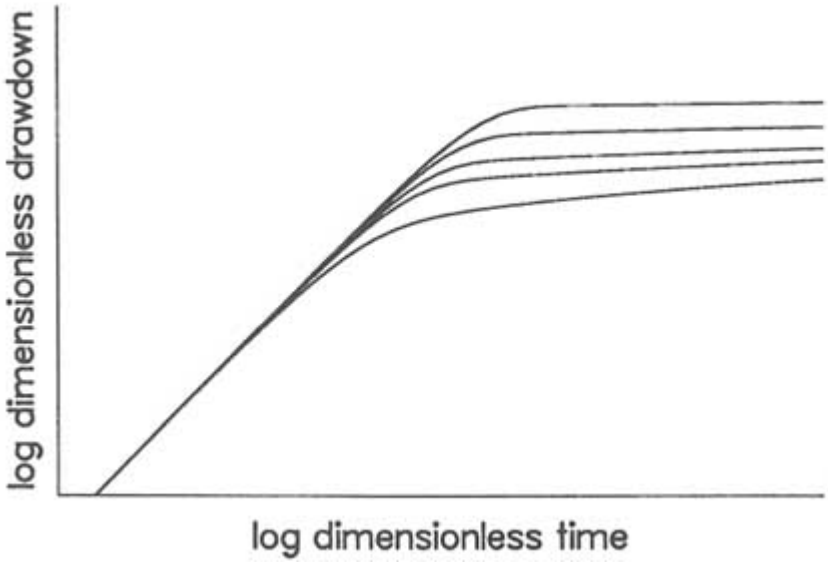

FIGURE 5.16 Plot of log dimensionless drawdown versus log dimensionless time for a constant-flow test with radial flow. Different type curves correspond to different values of a dimensionless parameter that is a function of storativity, wellbore storage, and skin factor. After Bourdet et al. (1989), Figure 1.

formed on open boreholes or on packer-isolated intervals. In the open-borehole configuration, fluid is pumped from one well and drawdown is observed in the pumped well and nearby observation wells. This is the traditional aquifer test in a groundwater investigation, or the interference test in the petroleum industry. When packers are used, fluid is pumped from a "pumped interval" in one borehole, and drawdown is monitored in "observation intervals" in nearby boreholes. In testing rocks of low permeability, injection may be easier than pumping. For more permeable rocks, however, injection may be impractical because it requires a large source of water on the site.

Multiple-borehole tests offer a number of advantages over single-borehole tests. Multiple-borehole tests sample a larger volume of the rock mass. Consequently, the calculated value of the specific storage or storativity is subject to much less uncertainty. If the rock mass is treated as a porous medium, the anisotropy of the rock mass can be investigated. If flow is controlled by several highly transmissive fractures and the test objective is to characterize the interconnection between these fractures, multiple-borehole testing is indispensable.

Pumping at a constant rate is the common method to conduct multiple-borehole tests, but varying the pumping rate in a systematic fashion can be advantageous when hydraulic tests are affected by nearby activities such as well drilling, testing, or underground operations. If these disturbances obscure the response of the hydraulic test, data analysis will be very difficult. To remedy this situation, Black and Kipp (1981) proposed the "sinusoidal pressure test," which calls for varying the pumping rate or the hydraulic head in a sinusoidal manner. This strategy is similar to that of the "pulse test" in the petroleum industry (Johnson et al., 1966), where the pumping scheme consists of alternating periods of pumping and no pumping. The sinusoidal test causes the head response in the observation intervals to also vary in a sinusoidal manner. In the presence of interference by other activities, the sinusoidal response can be extracted from the hydraulic head data. However, the distance over which the test response can be observed in a sinusoidal test is generally less than that of a constant flow test. In actual application (e.g., Noy et al., 1988) the frequency of the sinusoid ranges from one to several cycles per day.

Test Procedures

The setup of a multiple-borehole test is highly dependent on the test objective and subsurface conditions. Because generalizations are difficult to make, the discussion below uses five examples to illustrate the different ways of setting up multiple-borehole tests for different conditions.

Example 1. A large, horizontal, areally extensive fracture is bounded by rock of sufficiently low hydraulic conductivity to be considered impermeable. A multiple-borehole test setup is illustrated in Figure 5.17. All the packer intervals contain the fracture, which is the sole feature that is investigated.

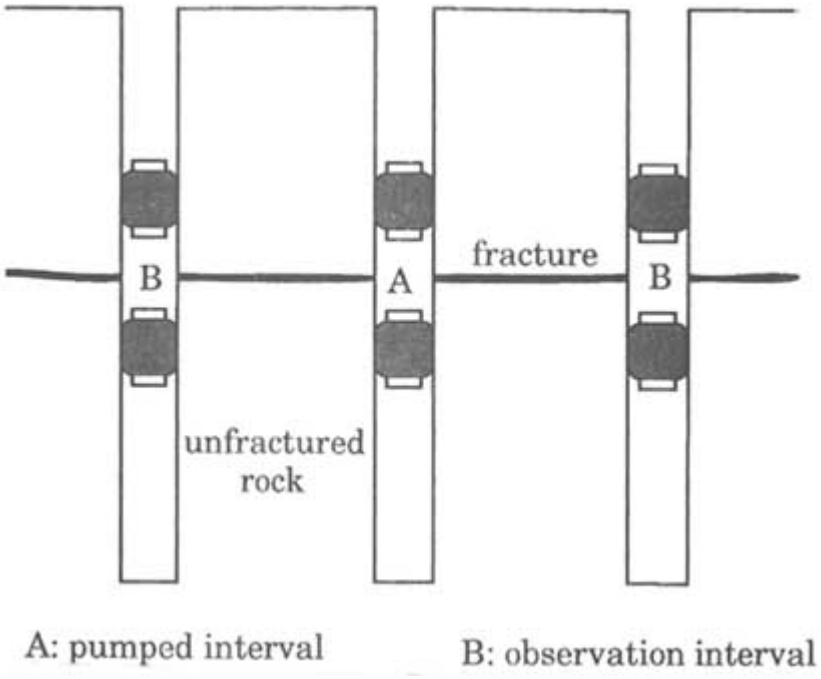

FIGURE 5.17 Example setup of a multiple-borehole hydraulic test in a rock containing a single extensive fracture.

Example 2. The rock mass bounding the large horizontal fracture in Example 1 is either permeable or contains a network of smaller fractures. In this case, pumping from the large fracture induces flow through the surrounding rock mass. The test setup shown in Figure 5.18 includes observation intervals to monitor drawdown and estimate hydraulic properties in the large fracture and the surrounding rock mass.

Example 3. A sedimentary rock, such as limestone or dolomite, contains highly transmissive horizontal fractures along bedding planes. These fractures are hydraulically connected by smaller vertical fractures, as shown in Figure 5.19. (A similar style of fracturing can occur in crystalline rock, although the large horizontal fractures may not be associated with bedding planes.) A multiple-borehole test in such a setting may call for pumping from one bedding-plane fracture and monitoring drawdown in the pumped fracture as well as in the overlying and underlying fractures.

Example 4. A densely fractured rock mass can be considered a porous medium. The systematic orientation of the fractures imparts anisotropy to the hydraulic conductivity. The test objective is to determine the hydraulic conductivity tensor of the rock mass, as opposed to the transmissivity of any individual

fracture. As shown in Figure 5.20, the test setup involves pumping from a packed-off interval in one borehole and monitoring drawdown in observation intervals arranged in a three-dimensional pattern around the pumping interval.

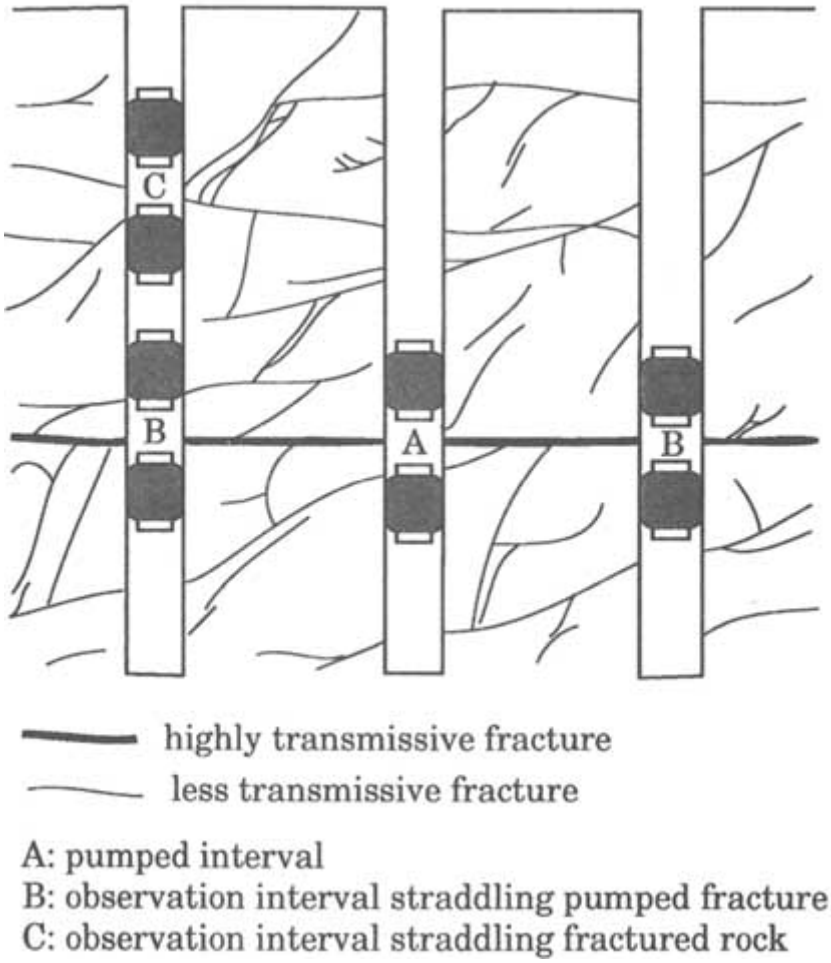

FIGURE 5.18 Example setup of a multiple-borehole hydraulic test in a rock containing an extensive and highly transmissive fracture with a network of less transmissive fractures.

Example 5. In this structurally complex setting, there are horizontal, inclined, and vertical fracture zones cutting through the rock mass, which is itself fractured (Figure 5.21). The greater complexity of this site, compared to the previous examples, requires a more extensive program of field characterization. A well-coordinated multidisciplinary approach is critical to its success. At an early stage, the investigation may be aimed at establishing the presence of the fracture zones.

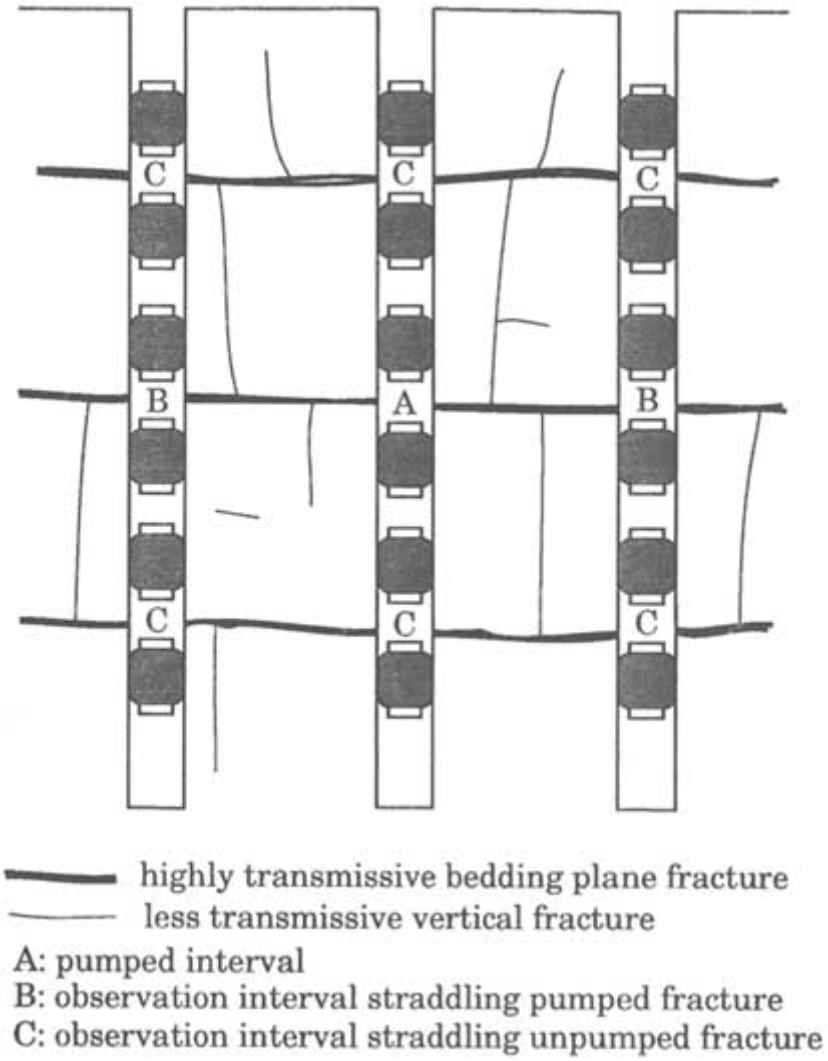

FIGURE 5.19 Example setup of a multiple-borehole hydraulic test in a rock containing highly transmissive horizontal bedding-plane fractures that are interconnected via less transmissive vertical fractures.

Identification of these zones requires extensive drilling, geological mapping, and geophysical investigations. Hydraulic tests may be limited to a single borehole or a few nearby boreholes. As a conceptual picture of the underground begins to emerge, full-scale, multiple-borehole tests, such as the one illustrated in Figure 5.21, can be conducted to investigate how the fracture zones are interconnected.

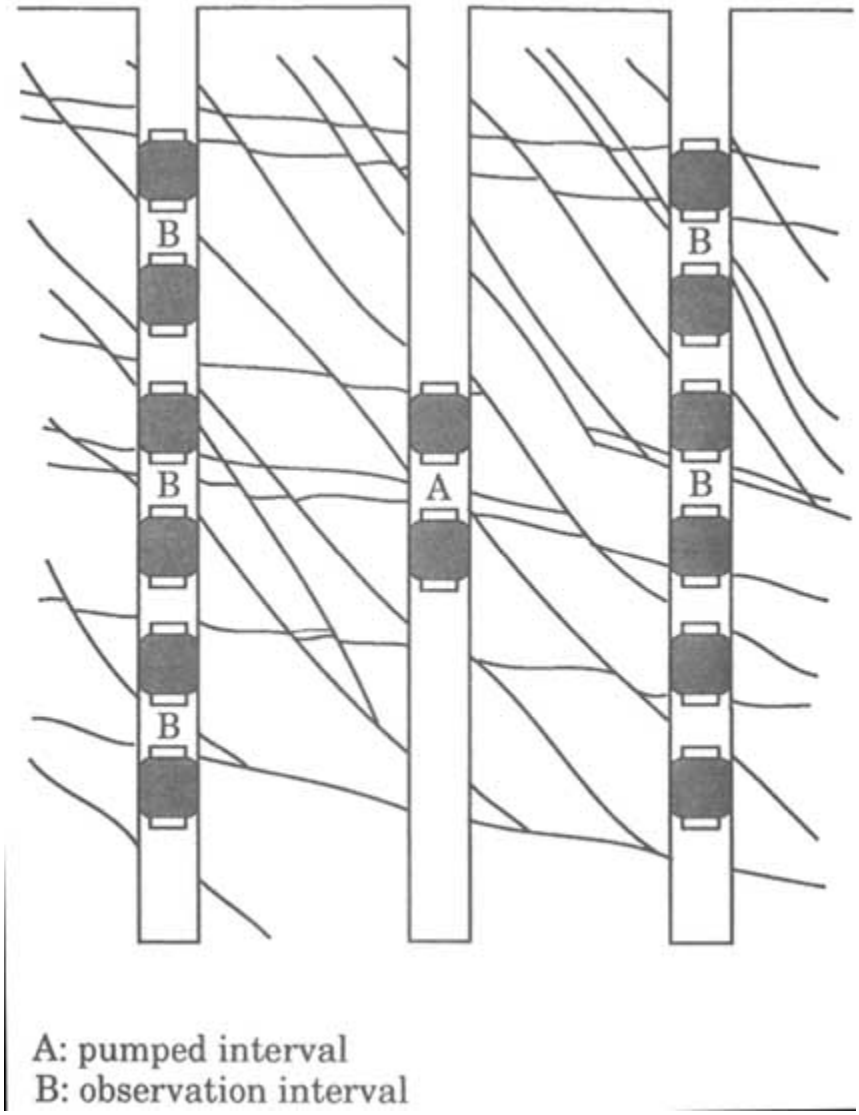

FIGURE 5.20 Example setup of multiple-borehole hydraulic test to determine the hydraulic conductivity tensor of a rock containing a dense and well-connected network of fractures.

Models of Multiple-Borehole Hydraulic Tests

Some models of multiple-borehole hydraulic tests can be adopted from models developed for porous media flow. For example, the single fracture in Example 1 above can be modeled as a thin confined aquifer, and the fracture in

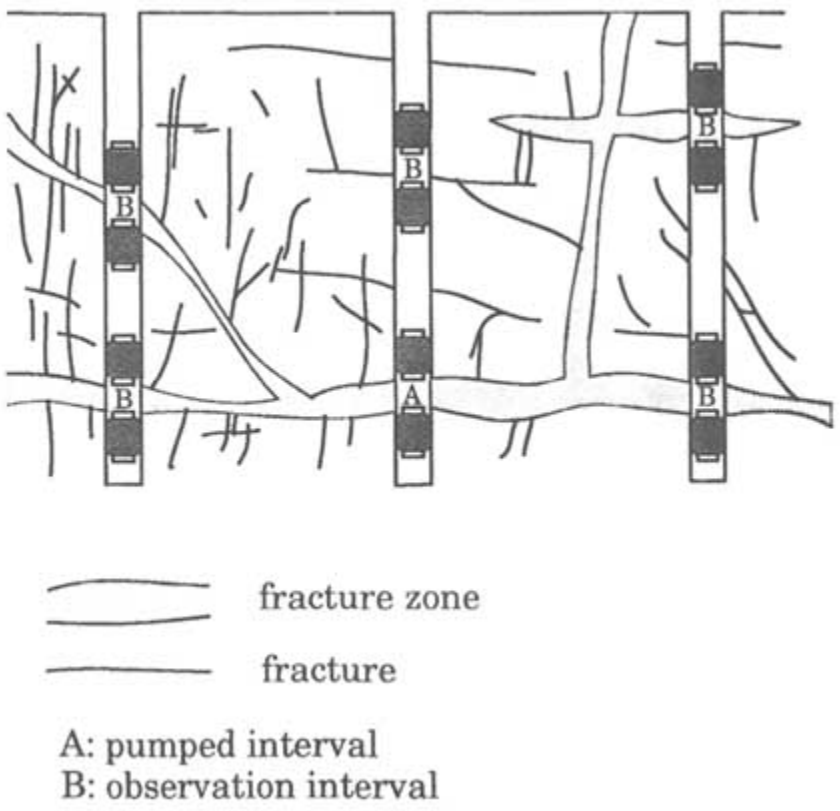

FIGURE 5.21 Example setup of a multiple-borehole hydraulic test in a rock mass with multiple sets of fractures and fracture zones.

Example 2 can be modeled as a leaky aquifer. (*Leakage* is a term used in groundwater hydrology to refer to the flow between an aquifer and an overlying or underlying layer of lower-permeability rock.) The multiple-fracture system in Example 3 can be treated as a multiple-aquifer system, with the bedding-plane fractures taking the role of the aquifers, and the rock layers (containing vertical fractures) taking the role of the aquitards. Models of this type have been developed by Hantush (1967) and Neuman and Witherspoon (1972). If the rock is treated as an anisotropic porous medium, as in Example 4, the method used to interpret the anisotropic permeability tensor from the well test data (see Appendix 5.B) developed by Hsieh et al. (1985) may be applicable.

To obtain analytical solutions to these models, homogeneity is generally assumed. (As noted earlier, the availability of an analytical solution is highly advantageous for analysis of test data.) Nonetheless, field experience indicates that fractured rocks are generally highly heterogeneous. In many cases, models

based on the homogeneity assumption are not capable of fully simulating the test response in fractured rocks. When testing in such an environment, the field hydrologist is commonly faced with test responses that are uncommon in porous media settings. For example, a nearby observation well may show no response, whereas a faraway well may show a large drawdown, even though these two observation wells lie along the same direction from the pumping well.

Accounting for heterogeneity of the rock mass requires a numerical model that is capable of simulating fluid flow through regions of variable hydraulic properties. To model a field setting such as that in Example 5, one approach is to use a numerical model (such as a finite-element model) that treats the fracture zones as highly transmissive elements and the fractured rock mass as porous blocks. Another approach may be the equivalent discontinuum model discussed in Chapter 6. At this level of analysis, there is little distinction between the methods discussed in this chapter and the modeling techniques discussed in Chapter 6.

Estimation of Model Parameters

If a model having an analytical solution is chosen to analyze the hydraulic test, the model parameters can be estimated either by type curve or automated computer matching. However, as noted earlier, the assumption of homogeneity required by the analytical solution is frequently inconsistent with the heterogeneous nature of fractured rocks. When faced with such heterogeneities, the analyst may be tempted to separately analyze the response in each observation interval as if the rock mass is homogeneous and isotropic. This approach yields a range of hydraulic property values, which are commonly interpreted as a qualitative measure of the heterogeneity of the rock. Such a simple approach is appealing, but it can be seriously wrong. Each separate analysis must be based on the assumption that the drawdown at the observation interval is due to the total rate of fluid removal at the pumping interval. However, in a heterogeneous formation, the low-permeability regions yield less fluid and consequently suffer lower drawdowns than higher-permeability regions. A separate analysis of observation intervals situated in low-permeability regions will yield erroneously high permeability values because the total fluid production is erroneously ascribed to a low drawdown. However, when the analysis assumes a heterogeneous rock mass, small drawdown correctly indicates relatively low permeability in the vicinity of the observation.

If a numerical model is used to analyze the hydraulic test, the analyst must decide on the parameterization of the model, that is, how to assign hydraulic properties to each cell or element of the model grid. On one extreme, each cell can have a different set of hydraulic properties. Such a "fine" zonation scheme is ideal for representing a highly heterogeneous rock mass, but the resulting model contains a large number of model parameters. On the other extreme, the

model grid can be divided into a smaller number of zones, with each zone having its own set of hydraulic properties. For example, a large region of rock mass may be lumped into a homogeneous zone, and major features such as highly transmissive fracture zones are treated as separate zones. Such a "coarse" zonation scheme does not represent all the details of the heterogeneity, but it results in a smaller number of parameters.

Parameter estimation for a numerical model amounts to choosing the model parameters such that the model-computed heads match the observed heads. This matching can be done by trial and error or by numerical inverse methods (e.g., Yeh, 1986). Computer programs that implement inverse methods are not yet widely available, but the modern approach to hydraulic test analysis in heterogeneous formations is clearly moving in this direction. Numerical inversion is faster than a trial-and-error approach and may provide a quantitative indication of the uncertainty of the estimated model parameters. The use of computer inversion programs allows the analyst to quickly try different parameterization schemes in order to select the most appropriate one.

For inverse methods there is a tradeoff between uniqueness and closeness of match (see, e.g., Carrera and Neuman, 1986). In general, the fewer the parameters in the model, the more likely they can be uniquely identified. On the other hand, fewer parameters limit the ability of the model to match certain field responses. Adding more parameters to the model may allow it to simulate a broader range of test responses, but the inverse algorithm may not be able to converge to a unique set of model parameters. The use of numerical inversion methods requires thoughtful judgments by the analyst. This topic is addressed further in Chapter 6.

TRACER TESTS

Tracer tests are generally applied (1) to explore connectivity in the subsurface and (2) to determine transport properties (e.g., kinematic porosity and dispersivity) and chemical reaction parameters, such as the distribution coefficient for mass transfer between liquid and solid phases (adsorption). In the first application (exploring subsurface connection), the approach is similar to that used for karst studies, where tracers are commonly used to investigate the possible connection between, say, a solution opening and a spring. The following discussion focuses on the second application, the determination of transport properties and chemical reaction parameters.

Solute Transport Processes

The discussion of tracer tests below is prefaced with a short review of key processes that control solute transport. Some of these processes are well known in porous media theory, for example, advection, dispersion, and adsorption.

Other processes, such as channelized transport and matrix diffusion, are concepts developed in the study of transport in fractured rocks.

Advection and Dispersion

The concepts of advection and dispersion in fractured rocks are identical to those in porous media. Advection refers to the movement of the tracer caused by the movement of the host fluid. When observed in detail, this movement is extremely complicated, as fluid velocity can vary on all scales: across the aperture of the fracture, in the fracture plane, from one fracture to another, and from one part of the fracture network to another part. To describe every detail of this movement would be impractical. In the classical approach to transport modeling, only the "average" velocity field is described. In concept, the average is taken over an appropriate volume, so small-scale variations are smoothed out. These averages represent the large-scale features of the velocity field. For example, the average velocity field may be uniform flow, radially converging flow to a pumping well, or recirculating flow from an injection well to a pumping well. The transport of tracer along this average flow field is referred to as advection.

Because the average velocity field does not capture all the details of the velocity distribution, advective transport does not fully describe tracer movement. The small-scale variations that are not described by the average velocity field will cause the tracer to spread and mix. When molecular diffusion is added to this spreading and mixing process, the result is what is commonly known as dispersion.

The classical approach assumes that dispersion can be treated as a Fickian (diffusive) process, but modern analyses suggest that this assumption is not always valid (Dagan, 1986; Gelhar, 1986). In a heterogeneous formation the solute must travel a certain distance before Fickian dispersion is established. Because tracer tests are commonly conducted over a relatively short distance, the validity of assuming Fickian dispersion remains an open question that awaits further research.

The magnitude of the dispersivity term depends on how much detail is known about the heterogeneity of the rock. If little is known about heterogeneity and the rock is modeled as hydraulically uniform, the dispersivity derived from a tracer test will appear to be large. If more is known and the rock is modeled as nonuniform, the dispersivity derived from a tracer test will be smaller.

Fracture Channels and Channelized Transport

Two processes have been recognized to be of special importance in fractured rocks. They are transport in fracture channels and channelized transport. A fracture channel is a long narrow region of enlarged aperture formed at the intersection of two fractures or by processes such as shearing (see Chapter 3). Transport

along enlarged fracture intersections could be significantly greater than transport along grooves on fracture planes. Channelized transport arises from the nonuniform velocity of fluid and solute transport in a variable-aperture fracture. Flow and transport are concentrated in narrow regions following pathways of least resistance.

The term *channeling* can refer either to transport in fracture channels or to channelized transport. Similarly, a *channel* can mean either a fracture channel or the narrow pathways of least resistance. However, Tsang and Tsang (1989) pointed out that transport in fracture channels is not the same as channelized transport. Fracture channels are fixed in orientation and position, whereas pathways of least resistance vary according to the flow direction. In addition, channelized transport does not require the presence of fracture channels. The computer simulation of Tsang and Tsang demonstrates how flow and transport tend to concentrate along narrow pathways in variable-aperture fractures (Figure 5.22). If the flow direction changes, the pathways of least resistance also change.

Diffusion into Stagnant Water and Rock Matrix

When flow is channelized in a fracture, significant portions of the fracture may be occupied by relatively stagnant or slow-moving water. Tracer moving through the channels can diffuse into this stagnant water. Tracer can also diffuse from the mobile water flowing in the connected fractures into the stagnant water residing in unconnected or dead-end fractures. Tracer can also diffuse from fractures into the rock matrix if the matrix has significant porosity. The net effect of these diffusive processes is a retardation of the apparent movement of the tracer compared to that of the water. As a general rule, the longer the duration of the tracer test, the more significant the effects of diffusion into stagnant water and rock matrix.

Adsorption

In the context of tracer testing, adsorption refers to the tendency of the solute to attach to solid phases in the host rocks. In a fractured rock, certain tracers can adsorb onto fracture surfaces, especially if the surfaces are coated with alteration products such as clay. The effect of reversible adsorption is similar to that of diffusion into stagnant water: the apparent movement of the tracer is retarded. If the tracer diffuses into the matrix and is adsorbed onto surfaces in the rock matrix, retardation can be greatly increased compared to that for adsorption on fracture surfaces. This is because the specific surface (i.e., adsorptive surface per bulk volume of rock) of the rock matrix grains is significantly greater than the specific surface of the fractures. Consequently, a larger quantity of tracer can be adsorbed on the rock matrix than on fractures.

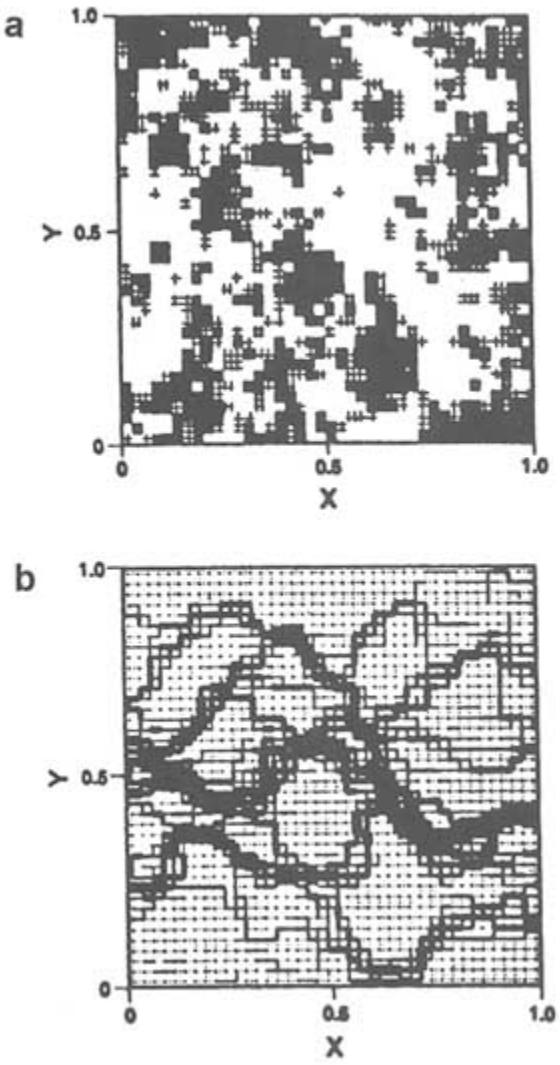

FIGURE 5.22 Computer simulation of channelized transport in a fracture with variable aperture. (a) Aperture distribution in the fracture plan. Lighter shading corresponds to larger aperture. (b) Flow rate distribution in the fracture plan, assuming constant-pressure boundaries on left and right and no-flow boundaries on top and bottom. Line thickness is proportional to the square root of the flow rate. From Tsang et al. (1991), Figure 5.

Field Methodology

A tracer test is conducted by introducing one or more chemicals (tracers) into the groundwater and measuring their concentrations over some time period at various sampling points downstream from the tracer introduction point. It is desirable to determine the distribution of the tracer in space and time, but this goal is usually not achievable. The number of sampling points (usually boreholes) is necessarily limited, so test data consist of concentration-versus-time curves (breakthrough curves) obtained at each sampling point.

The selection of tracers is a critical component in the design of tests. Using tracers with appropriate properties can help identify dominant transport mechanisms. Ideally, one of the tracers should move at the same velocity as the water. This tracer should be chemically inert during the course of the tracer test. That is, it should not decay, adsorb onto the rock, or react with other tracers. However, if diffusion into stagnant water or rock matrix occurs, even a chemically inert tracer will show an apparent retardation. In this regard, using several inert tracers with different coefficients of molecular diffusion can help quantify this effect. Adsorptive tracers can be used to investigate the sorptive properties of the fracture surfaces and rock matrix.

Natural Gradient Tracer Test

In a natural gradient tracer test, a tracer is injected into the groundwater system and is allowed to be transported by natural movement of the groundwater. The spatial distribution of tracer concentration is monitored by sampling from a grid of wells located down gradient from the injection point(s) (Figure 5.23). In general, water samples must be collected from different depths in each monitoring well to define the concentration distribution in three dimensions.

A natural gradient tracer test is perhaps the ideal method for the study of solute movement under natural or prevailing conditions because the prevailing groundwater condition is not disturbed, except for the brief period when the tracer is injected. From a theoretical point of view, the ability to define the spatial distribution of tracer concentration is highly desirable because such data allow direct calculations of tracer mass, velocity, and dispersion. For these reasons, several large-scale natural gradient tracer tests have been conducted in granular (e.g., sand) aquifers in recent years (e.g., Mackay et al., 1986; LeBlanc et al., 1991).

The natural gradient tracer test is generally expensive and difficult to apply in fractured rocks. In contrast to a granular aquifer at shallow depth, where multilevel samplers can be easily installed, fractured rock sites require numerous wells for sampling. Furthermore, tracer distributions in fractured rocks tend to be highly irregular. If, as some researchers argue (e.g., Tsang and Tsang, 1989; Abelin et al., 1991a,b), the tracer travels along channels that occupy small portions

of the fracture planes, the tracer distributions in fractured rocks may resemble a braided network of one-dimensional pathways. In such a setting, sampling from a grid of wells may miss a significant portion, or even all, of the tracer mass.

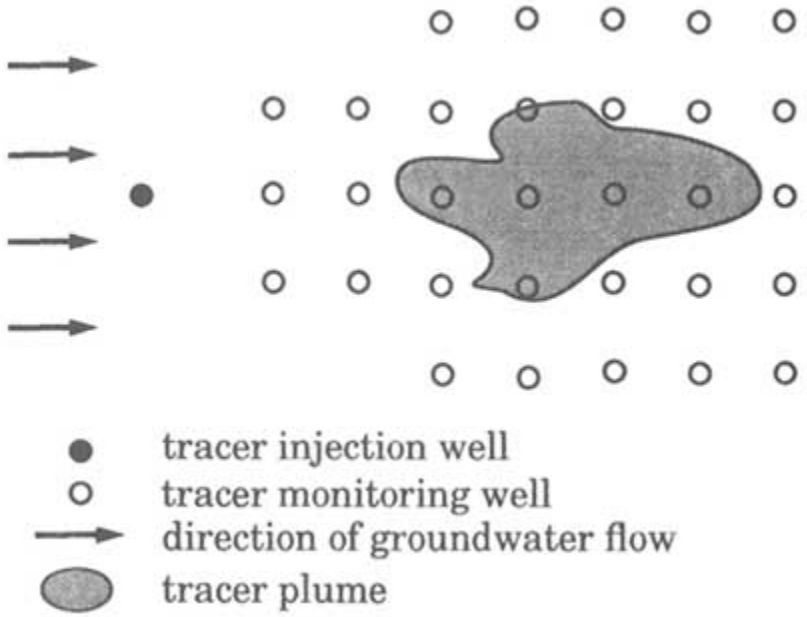

FIGURE 5.23 Setup of a natural gradient tracer test.

Another problem with conducting a natural gradient tracer test in fractured rocks is the difficulty of collecting water samples that are representative of in situ conditions. This problem is especially severe for rocks of low permeability and porosity. In such setting, the extraction of water samples from tight fractures is a difficult task. Furthermore, the amount of water in the wellbore causes a significant dilution of in situ water. It is possible to back-calculate the concentration of in situ water from well-mixed wellbore water, but the result is inexact.

To obtain a representative sample of in situ water, it is necessary to purge the wellbore water by pumping for a period of time before collecting the sample. In a low-porosity formation, such pumping may significantly distort the flow field. Using packers to hydraulically isolate the fracture to be sampled will reduce the amount of purging required; however, standard packer equipment does not completely eliminate the problem of wellbore dilution. The development of specialized packer equipment (Novakowski and Lapcevic, 1994) to reduce well-bore volume would strongly enhance the ability to collect representative in situ water samples from fractures.

Divergent Flow Tracer Test

In a divergent flow tracer test, water is injected into a recharge well at a constant rate. After a steady flow field is established, the tracer is added into the recharge water either as a pulse or a step increase. The tracer concentration is then monitored at one or more wells in the vicinity of the recharge well (Figure 5.24). The advantage of this test is that the tracer is quickly forced into the flow system, so the test condition can be accurately represented by a simple mathematical model. In addition, if multiple sampling wells are used, a larger volume of rock can be investigated compared to the convergent flow tracer test discussed below. The disadvantages of the divergent flow tracer test are that a large water supply may be required for injection, the recharge water may clog the fractures, and the tracer is left in the rock at the end of the test. In addition, sampling from the monitoring well is subject to the same difficulties as discussed above: (1) the tracer may bypass the monitoring wells by flowing along channels

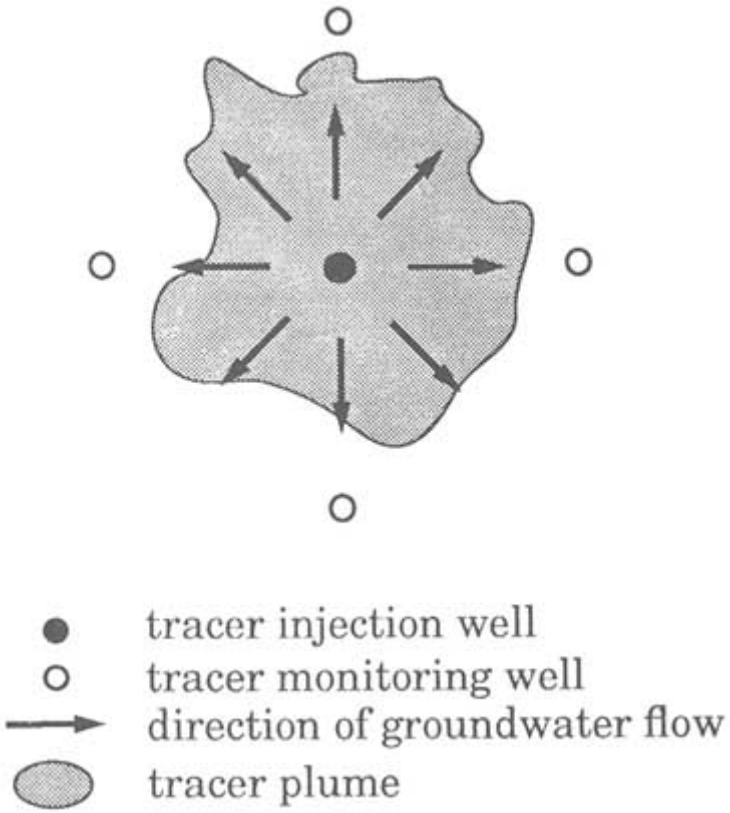

FIGURE 5.24 Setup of a divergent flow tracer test.

that are not intersected by or hydraulically connected to them; (2) the monitoring wells may intersect tight portions of fractures from which it is difficult to extract water samples; (3) when sampling from the monitoring wells, the in situ water may be strongly diluted by the wellbore water; and (4) in most cases there are not enough monitoring wells to allow calculation of the tracer mass in the subsurface.

Convergent Flow Tracer Test

In the convergent flow tracer test, water is pumped from a well until a steady flow field is established. A tracer is then injected, ideally as a pulse, into the flow system through a "tracer injection" well (Figure 5.25). The arrival of the tracer at the pumping well is monitored by sampling the pumped water. This test avoids the sampling difficulties discussed above. Also, the amount of tracer recovered can be readily computed, and, under optimal circumstances, a large portion of the injected tracer is removed at the end of the test. However, injecting the tracer as a pulse into the flow system can be difficult to achieve. A common practice is to inject the tracer and then a certain volume of clean water. However, field experience suggests that such a practice does not flush all the tracer from

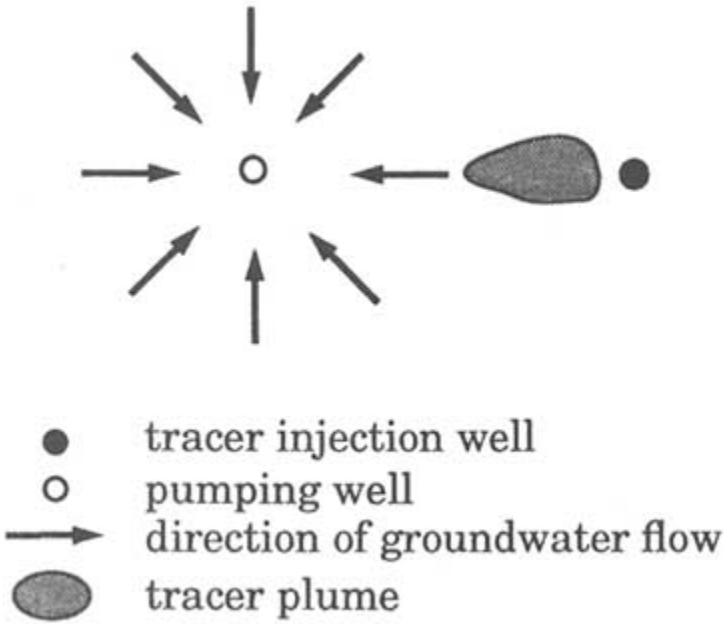

FIGURE 5.25 Setup of a convergent flow tracer test.

the borehole into the flow system. If some tracer remains in the borehole and slowly enters the flow system, the concentration-versus-time curve at the pumped well will have a long tail, which complicates the test analysis.

Because the convergent tracer test samples the relatively narrow flow region between the tracer injection well and the pumping well, it is desirable to introduce tracer at several injection wells to increase the volume of investigation. Simultaneous injection into several wells requires the use of different tracers that do not chemically interfere with each other. If the same chemical is to be used at different injection wells, the tracer from one injection well must be near fully recovered before the chemical is injected into another well. Such a sequential injection scheme will generally require onsite analysis of tracer concentration in the pumped water in order to determine tracer recovery. Appendixes 5.D and 5.E describe such tests.

Two-Well Tracer Test

The two-well tracer test involves pumping from one well while recharging another well (Figure 5.26). Ideally, the pumping and recharge rates should be identical. In practice, however, the recharge rate is commonly less than the pumping rate owing to clogging of fractures. After a steady-state flow field (known as a doublet) is established, a tracer is added to the recharge water as a pulse or a step increase. Tracer arrival at the pumped well is monitored by sampling the pumped water. The two-well tracer test is attractive because the pumped water can be used as the recharge water, thus eliminating the logistical problem of obtaining an independent water supply for a divergent flow tracer test or disposing of the pumped water during a convergent flow tracer test. The main disadvantage of the two-well tracer test is in the analysis of data. In a doublet flow field, the travel time from the recharge well to the pumping well varies with the streamline along which the tracer travels. Thus, the shape of the breakthrough curve is primarily controlled by the different travel times of the tracer along different streamtubes and not by the dispersion in each streamtube. Consequently, the effect of dispersion is not as evident as in the convergent or divergent tracer tests. To improve the sensitivity to dispersion, Welty and Gelhar (1989) recommend that a pulse injection of tracer be used in this test, rather than a step rise in concentration.

Borehole Dilution Test

In a granular aquifer the borehole dilution test is a method for estimating the groundwater flow flux in the vicinity of a well screen. When applied to a fractured rock formation, the test yields the volumetric rate of groundwater flow through a packed-off interval of a wellbore. To conduct the test, a tracer is introduced into the packed-off interval of the wellbore and continually mixed.

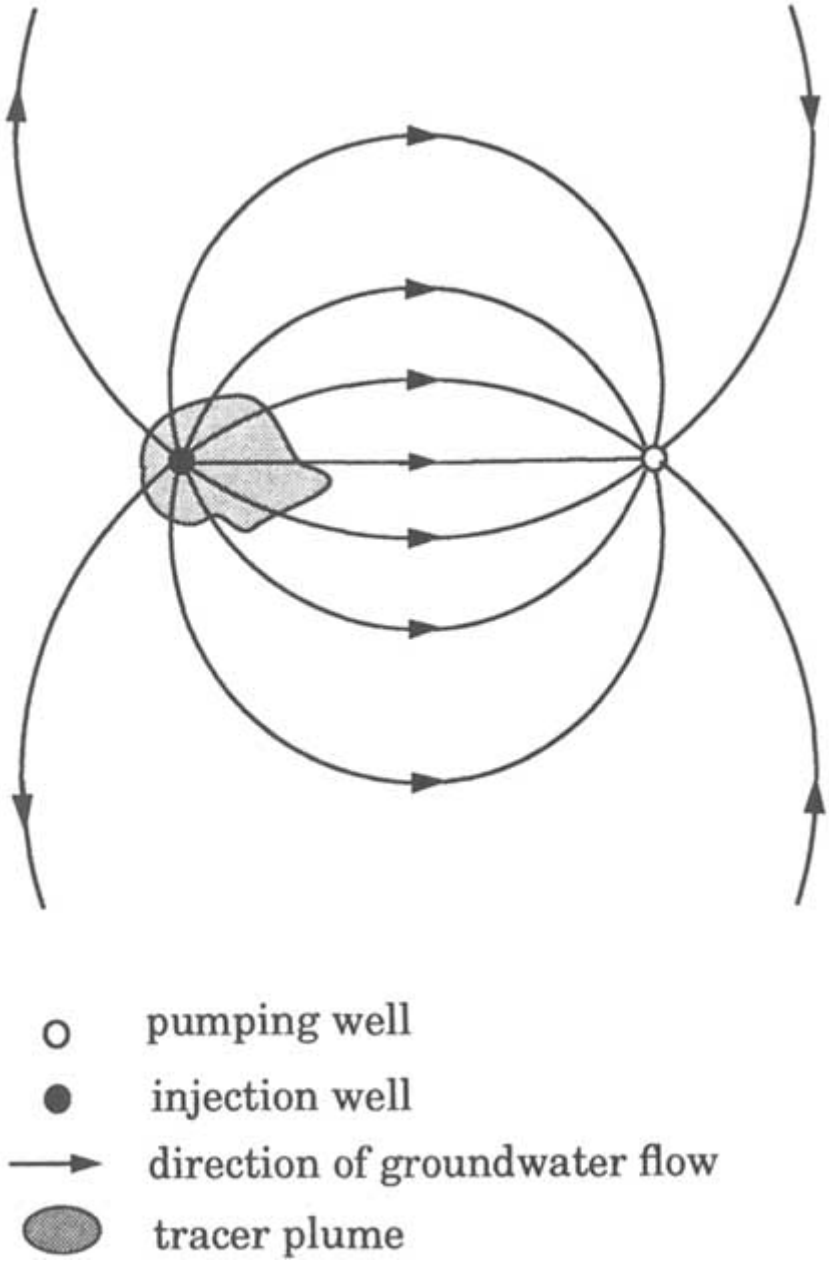

FIGURE 5.26 Setup of a two-well tracer test.

The flow of groundwater into and out of the wellbore is allowed to flush out the tracer. By monitoring the tracer concentration in the wellbore with time, the volumetric rate of groundwater flow through the well can be determined.

Analysis of Tracer Tests

The analysis of a tracer test is similar to that for a hydraulic test. It requires the selection of a model (diagnosis) and the adjustment of model parameters until the model-computed breakthrough curves match the observed breakthrough curves (parameter estimation). For a model with an analytical solution, parameter estimation can be done by type curve matching in the same manner as for the hydraulic test. Although relatively uncommon in the past, the use of inverse methods to determine transport properties is likely to become more widespread.

Despite the similarity in their general approaches, tracer test analysis can be substantially more difficult than hydraulic test analysis. The greater difficulty arises from the fact that flow and transport processes respond differently to heterogeneities in fractured rocks. Dispersion and diffusion during fluid flow tend to smooth out the effects of heterogeneities. Solute transport during a tracer test is usually dominated by advection, which does not smooth out the effects of heterogeneities. Thus, in a heterogeneous formation, solute distribution tends to be significantly more irregular than the pressure distribution. This implies that the flow field or velocity distribution must be characterized in greater detail for transport modeling than for fluid flow modeling.

The unequal effects of rock heterogeneity on flow and transport are demonstrated by the computer simulation of Smith et al. (1987). Figure 5.27 a illustrates the aperture distribution in a rough-wall fracture, which forms one of the more dominant fractures in a three-dimensional fracture network. Figure 5.27b shows the head distribution that results when a well pumps from the center of the fracture plane. Although the lines of equal potential are not perfect circles (which would be the case if the aperture were uniform), their shapes are more or less circular. For this highly idealized case, one might conclude that even though the fracture is not uniform, representing it as having uniform properties would capture the main features of the hydraulic response. However, the same cannot be said for transport. Figure 5.27c shows the water (and tracer) travel time from any point in the fracture to the pump. Note that the travel times from different points at equal distances from the well can differ substantially. For example, the travel time from point A to the well is less than two time units, whereas the travel time from point B is almost four time units. For a fracture having a highly variable distribution of aperture, the variation in transport times may be even larger.

Despite the complexities of flow and transport in fractured rocks, simple models, which are derived from single- or dual-porosity media assumptions and are based on advection and Fickian dispersion, continue to be the popular choice for analyzing tracer tests. A good summary of these models is given by Welty

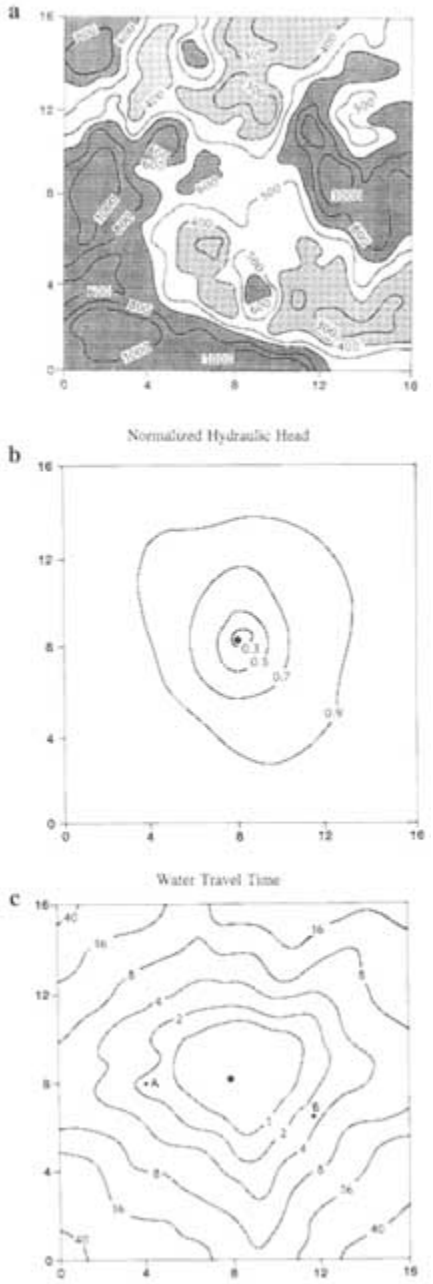

FIGURE 5.27 Computer simulation of flow and transport to a well pumping from a single fracture. (a) Distribution of fracture aperture. (b) Distribution of normalized hydraulic head. (c) Distribution of travel time to the pumping well. From Smith et al. (1987), Figure 4.

and Gelhar (1989). Recent advances that account for factors such as mixing in the wellbore are summarized by Moench (1989). Diffusion into the rock matrix can be incorporated by inclusion of an additional term into the transport equation, as shown by Maloszewski and Zuber (1985). A similar approach was used by Raven et al. (1988) to account for diffusion into stagnant water. The adequacy of using simple analytical models to analyze tracer tests in fractured rocks is open to question. Given the highly heterogeneous nature of fractured rocks, flow paths are likely to be highly complex, and therefore not well described by simple flow geometries such as those shown in Figures 5.25 and 5.26. Analyses based on simple models would likely lead to nonunique interpretations. A realistic analysis might require a numerical model to simulate flow and transport in a heterogeneous domain. The use of such models, however, would likely require extensive geological, geophysical, and hydraulic data as supportive information.

Some researchers have proposed to model the effects of channeling with a set of parallel one-dimensional transport models. The reasoning behind this approach is that, if the channels do not intersect each other, the transport in each channel can be analyzed separately as transport in a one-dimensional flow field. In addition, if the transport process in a channel can be modeled by classical advection and dispersion processes, analytical solutions are readily available. Thus, analysis of a breakthrough curve amounts to separating it into a number of component curves, each of which represents transport through a separate channel. By fitting an analytical solution to each component curve, the average velocity, dispersivity, and a dilution factor for each channel can be calculated. The dilution factor accounts for the portion of the injected tracer that enters the channel.

The separation of breakthrough curves into component curves has gained popularity because the procedure provides a simple way to analyze tracer test data that are not amenable to analysis using standard advection-dispersion models. For example, breakthrough curves for some tracer tests in fractured rocks show multiple peaks. By invoking the channel model, the individual peaks can be attributed to transport through individual channels (Figure 5.28a). A similar approach can be applied to breakthrough curves having very long tails. In this case the long tail is attributed to tracer transport along channels with successively lower velocities (Figure 5.28b).

A weakness of the channel model is that a certain degree of arbitrariness can be required in its application and interpretation. This is especially evident when analyzing breakthrough curves with long tails, which can be broken down into nonunique combinations of component curves. These component curves do not necessarily represent transport through actual channels in the fractures. Furthermore, even if the hypothesized channels are realistic representations of flow paths in the rock, these channels are particular to the flow geometry of the tracer test. In a different flow geometry, different channels will develop. It is as yet unclear how the characterization of channels in one flow geometry can be used

to characterize transport in a different flow geometry. Theoretical development in this area would significantly advance the interpretation of tracer tests in fractured rocks.

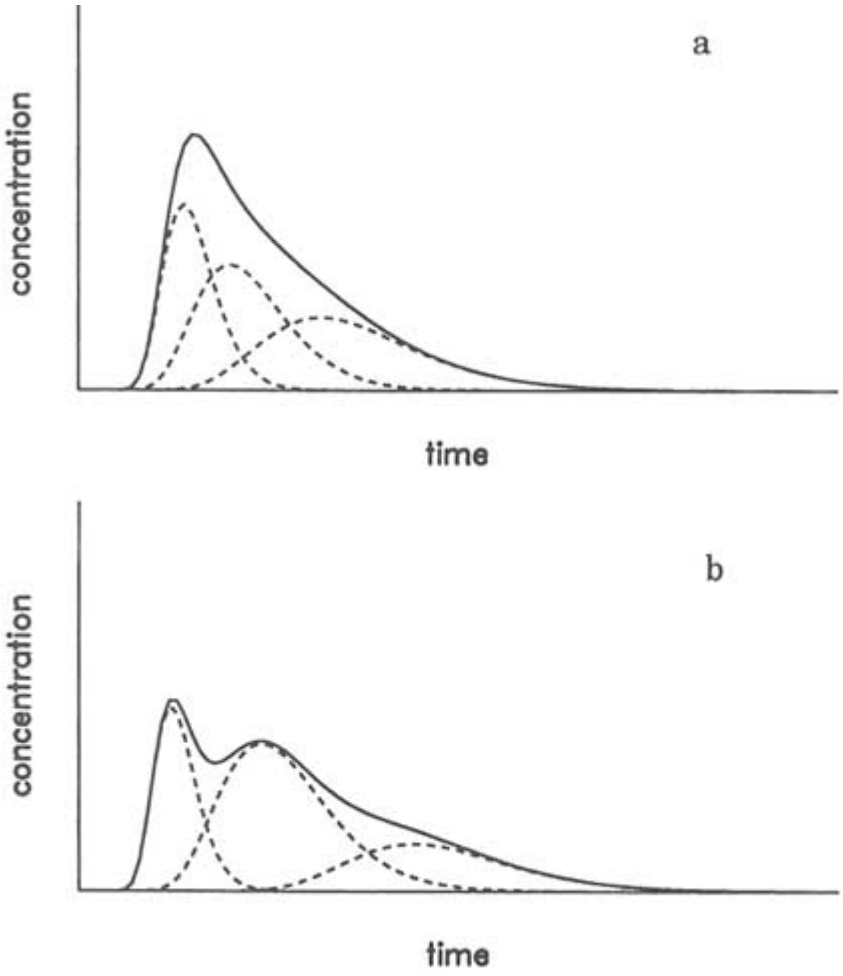

FIGURE 5.28 Separation of a breakthrough curve (solid line) into component curves (dashed lines). (a) Single peak case. (b) Multiple-peak case.

Research Needs

The highly heterogeneous nature of fractured rocks remains a major source of difficulty in modeling solute transport. A major research need is to develop

approaches to deal with this heterogeneity. Simple models based on uniform properties can frequently be calibrated to match the breakthrough curve from a single sampling point, but they are likely to fail in a calibration attempt that involves multiple breakthrough curves from several sampling points. In this regard the development of efficient numerical models of solute transport, coupled with parameter estimation algorithms, will greatly facilitate the analysis of tracer tests.

On a theoretical level, the development of alternative approaches that are not based on the classical advection/Fickian dispersion model may lead to new solutions. An example of such an approach, based on stochastic fracture networks, is discussed in Chapter 6. Another development that may lead to useful results is the solute flux approach advocated by Dagan et al. (1992). In this approach the variable of interest is the mass of solute discharged through a control surface. The control surface may be a wellbore, the discharge area of a groundwater flow system, or a compliance surface at some distance from a waste disposal site. Because the quantity of interest is found by integrating the mass flux across the entire surface, the result may be subject to less uncertainty compared to point concentrations.

On a practical level, the development of improved tools for in situ sampling would enhance the execution of tracer tests. In particular, packer equipment that minimizes the wellbore volume will substantially improve the ability to sample in situ fluid while reducing the need to pump a large volume of fluid to purge the well. Such equipment has been developed and used at the Grimsel test site in Switzerland (see Appendix 5.G). However, the most significant advancements in field methods will likely come from remote detection of the tracer distribution in the rock mass. The use of electromagnetic tomography to map the location of a salt solution is currently limited to two-dimensional cross sections. Three-dimensional images can, in principle, be obtained from a large number of two-dimensional cross sections. There are, however, practical and cost limitations. If the three-dimensional distribution of solute can be visualized, there is a much better chance of describing its movement.

Appendix 5.A

Example Of A Conductive Network Exhibiting Fractal Geometry

The key concepts of a fractal object are scaling and dimension. Scaling implies that the small-scale features of the object appear in some sense like the larger-scale features (self-similarity or self-affineness). The dimension of a fractal object can take on nonintegral values. To understand these concepts, consider the two networks of conductive elements in Figure 5.A1. The left network is a regular Euclidean network. The right network approximates a fractal network, known as a modified Sierpinski gasket. (The smaller conductive elements are not shown.) The scaling feature of this fractal network is evident. Now assume that a well pumps from the center of each network. At a distance r from the well, the "area" available to flow can be determined by drawing a circle of radius r centered at the well and counting the number of conductive elements intersected by the circle. For the regular Euclidean network, the number of conductive elements intersected by the circle is linearly proportional to the radius r. In terms of the area-distance relationship, $A = \alpha d r^{d-1}$; the exponent d - 1 is unity. The flow dimension of this network is 2, which is consistent with the standard notion of Euclidean geometry. For the fractal network, however, the number of conductive elements intersected by the circle of radius r is proportional to $r^{0.59}$. The flow dimension in this network is 1.59. Compared to the Euclidean network, the lower dimension of the fractal network is due to the fact that as the circle increases in radius it encounters successively larger regions without conductive elements. In this sense the fractal network can be viewed as a partially connected network of conductive elements.

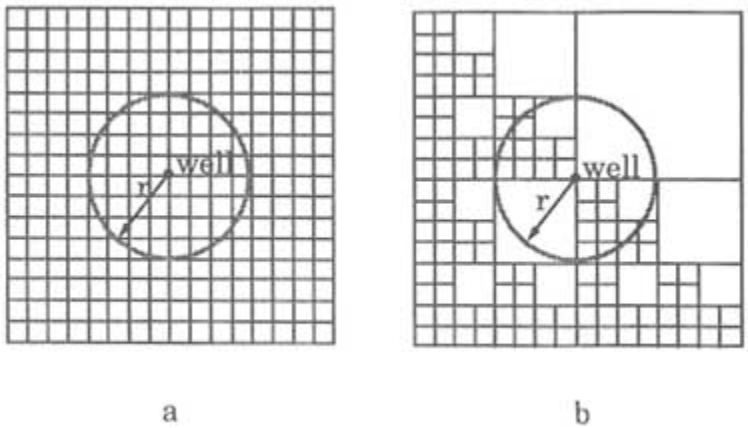

FIGURE 5.A1 Two networks of conductive elements. (a) A Euclidean network of dimension two. (b) A fractal network (modified Sierpinski gasket) of dimension 1.59.

Appendix 5.B

Using A Multiple-Borehole Test To Determine The Hydraulic Conductivity Tensor Of A Rock Mass

If a fractured rock mass is viewed as a homogeneous anisotropic porous medium, the hydraulic conductivity is a second-order symmetric positive-definite tensor with six independent components. Determining these components will require testing with a relatively short pumping interval, so that, in the absence of boundaries, spherical flow will be established in the vicinity of the pumped interval. In theory, data from a minimum of six observation intervals, arranged in a three-dimensional pattern around the pumped interval, are needed. In field applications, where the assumption of homogeneity is not strictly satisfied, additional observation intervals are required so that the hydraulic conductivity components can be determined statistically. The test data are analyzed to compute the directional hydraulic diffusivity (directional hydraulic conductivity divided by specific storage). If the rock mass can be represented as a homogeneous porous medium, a three-dimensional plot of the square root of the directional hydraulic diffusivity versus direction should form an ellipsoid. If the directional hydraulic diffusivities fluctuate so severely that they do not form an ellipse in any meaningful sense, this is a direct indication that the tested rock does not behave as a homogeneous porous medium. This criterion is similar in concept to that proposed by Long et al. (1982). However, because of the difference in flow geometry, the two criteria may not be identical.

A hydraulic test conducted in the Oracle granite north of Tucson, Arizona, illustrates this application (Hsieh et al., 1985). The test was conducted in three boreholes —H-2, H-3, and H-6—drilled in a triangular pattern. The distance between boreholes ranged from 7 to 11 m. Figures 5.B1 a–c show the square roots of directional hydraulic diffusivities (dots) and the cross sections of the fitted ellipses along vertical planes between well pairs. Figure 5.B1 d is an oblique view of the cross sections oriented in three dimensions. Figure 5.B1 e is an oblique view of the fitted ellipsoid. Although the directional hydraulic diffusivities show a scatter owing to nonuniformities in the local rock properties, their square roots can be fitted to an ellipsoid. This result suggests that the tested rock behaves hydraulically in a manner not too different from that of a homogeneous anisotropic porous medium.

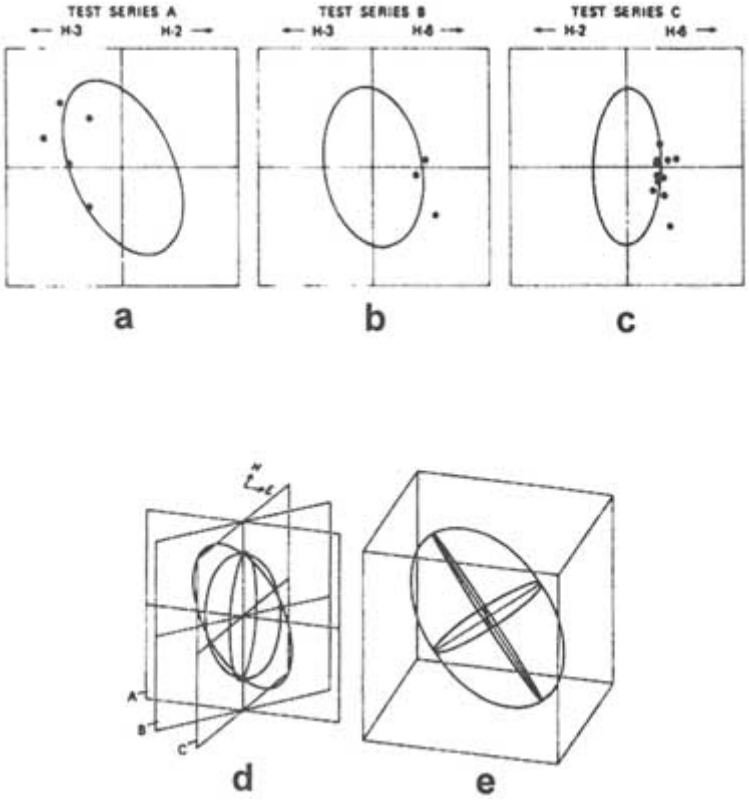

FIGURE 5.B1 Hydraulic conductivity ellipsoid determined by multiple-borehole testing in the Oracle granite north of Tucson, Arizona. (a)–(c) Polar plots of square roots of directional hydraulic diffusivities (dots) and cross sections of the fitted ellipse along vertical planes between well pairs. (d) Oblique view of cross sections (a) through (c). (e) Oblique view of filled ellipsoid. From Hsieh et al. (1985), Figure 12.

Appendix 5.C

Using A Numberical Model And Inverse Method To Analyze A Multiple-Borehole Hydraulic Test

Detailed subsurface characterization of a 200 m × 150 m × 50 m block of monzonitic gneiss at the Chalk River Nuclear Laboratories in Ontario, Canada, revealed the presence of four fracture zones (Raven, 1986). As shown in Figure 5.C1, fracture zone 1 is nearly horizontal and extends throughout the site; fracture zones 2 and 3 are, respectively, horizontal and inclined and cover only part of the site; and fracture zone 4 is vertical. The rock mass itself also is fractured and permeable. A multiple-borehole hydraulic test was conducted by pumping from well FS-10 and monitoring hydraulic heads in packer-isolated intervals in the other wells.

Carrera and Heredia (1988) modeled this site by using a finite-element model in which the fracture zones were explicitly modeled as two-dimensional planar features and the rock mass was represented as a continuum. To maintain a small number of model parameters, homogeneity was assumed in each fracture zone and in the rock mass, although hydraulic properties could differ from one zone to another. The initial model consisted of nine parameters, which were estimated by using a numerical inversion program. Subsequent revisions of the initial model included dividing fracture zone 1 into two homogeneous subzones and increasing the hydraulic connection between fracture zones by allowing higher hydraulic conductivities to occur at local regions in the rock mass between fracture zones. The final model, consisting of 13 parameters, yielded computed drawdowns that closely matched the observed drawdowns. Carrera and Heredia (1988) concluded that, even though single-borehole tests showed that the fracture zones are highly heterogeneous, the assumption of homogeneous fractures is adequate for modeling

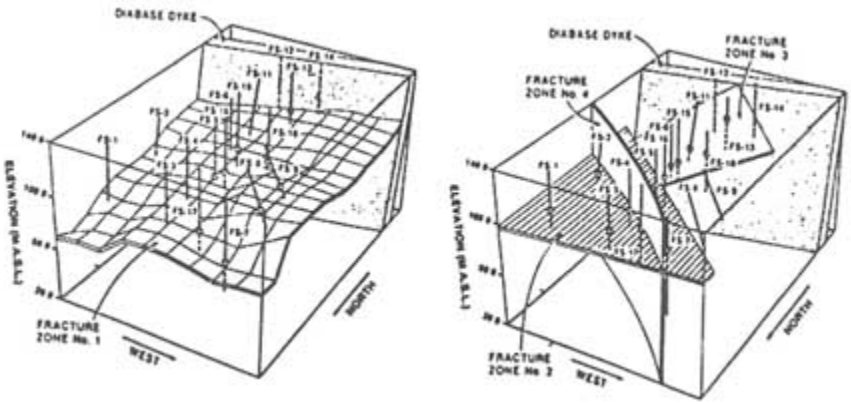

FIGURE 5.C1 Fracture zones in a block of monzonitic gneiss at the Chalk River Nuclear Laboratories in Ontario, Canada. From Raven (1986).

multiple-borehole hydraulic tests. This implies that the head distribution in the flow system is primarily controlled by the contrasting hydraulic conductivities of the fracture zones versus that of the rock mass. The internal variation of hydraulic conductivity in a fracture zone or in the rock mass has little effect on the observed flow pattern.

Appendix 5.D

A Radially Convergent Flow Tracer Test In A Fractured Chalk Formation

A radially convergent flow tracer test performed by Garnier et al. (1985) illustrates the importance of matrix diffusion and adsorption. The test was performed in a fractured chalk formation approximately 9 m thick, from which a well pumps at a rate of 20.8 m^3 per hour. Four tracers (deuterium, uranine, iodine, and carbon-13) were injected simultaneously into the same borehole as a concentrated pulse at a distance of 10.22 m from the pumping well. The observed breakthrough curve at the pumping well is shown in Figure 5.D1. The concentration of each tracer was normalized by their respective injective masses to allow for comparison.

If the four tracers all behave in the same way during transport, their normalized breakthrough curves will be identical. Figure 5.D1 shows that this is not the case. Of the four tracers, uranine has the largest molecular weight and therefore the lowest coefficient of molecular diffusion. A relatively small diffusion into the chalk matrix can account for the high peak of the uranine breakthrough curve. In contrast, the lower peaks for deuterium and iodine can result from their higher coefficients of molecular diffusion and therefore greater diffusion into the chalk

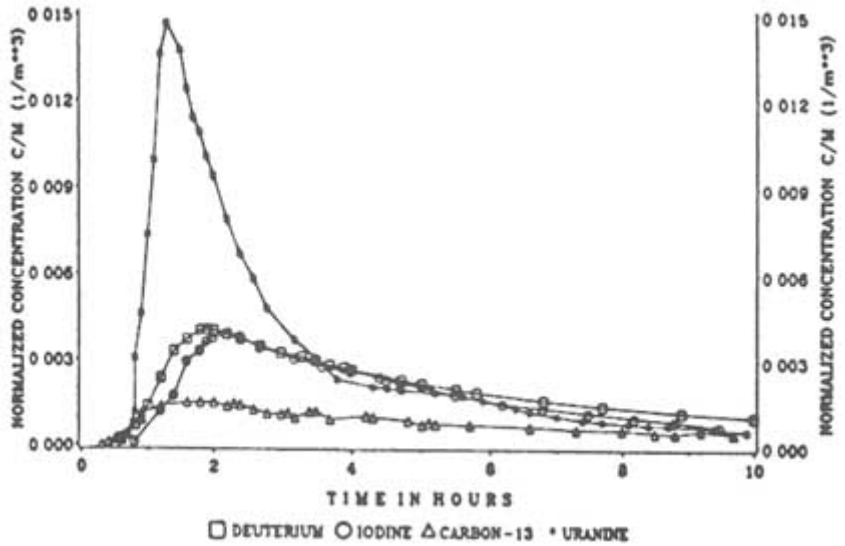

FIGURE 5.D1 Breakthrough curves of four tracers during a radially converging flow tracer test performed by Garnier et al. (1985). From Maloszewski and Zuber (1992), Figure 5.

matrix. Finally, the very low peak of carbon-13 suggests that it was lost by adsorption in the matrix.

To analyze this tracer test, Maloszewski and Zuber (1990) developed a one-dimensional transport model that accounts for advection, Fickian dispersion, matrix diffusion, and matrix adsorption that involves both an instantaneous equilibrium reaction and a nonequilibrium kinetic reaction of the first order. Calibration of the model yielded a fracture porosity of about 0.3 percent, a matrix porosity of about 40 percent, and a dispersivity of about 200 cm.

Appendix 5.E

A Large-Scale Flow And Tracer Experiment In Granite

Between 1984 and 1987, a large-scale flow and tracer experiment was performed by I. Neretnieks and co-workers in the Stripa Project mine in Sweden. Because the mine is situated beneath the water table and is kept at atmospheric pressure, it acts as a sink to which groundwater discharges. The experiment took place in an underground site that consisted of a 75-m-long main drift and a crossing arm 25 m in length. To measure the rate and distribution of this inflow, the entire ceiling and the upper part of the walls were covered with nearly 380 plastic sheets, which were used to collect water seeping from the rock (Figure 5.E1). For a period of over one and a half years, nine different tracers were injected continuously into nine intervals in three boreholes drilled vertically upward from the ceiling of the main drift. Tracer concentration was sampled from the plastic sheets for more than two years.

The results of this experiment, reported by Abelin et al. (1991a, 1991b), illustrate the complexities encountered in the analysis of solute transport in fractured rocks. The heterogeneity of the flow system can be observed in the highly uneven distribution of the water inflow rates, the highest occurring near one end of the crossing arm. The tracers, however, emerged in the central part of the main drift. Of the nine injected tracers, three were not detected during the course of the experiment. Of the tracers that reached the drift, recovery varied from 2.8 percent to 65.8 percent. The less-than-complete recovery may be due to the movement of tracers into pathways that do not lead to the drift and the

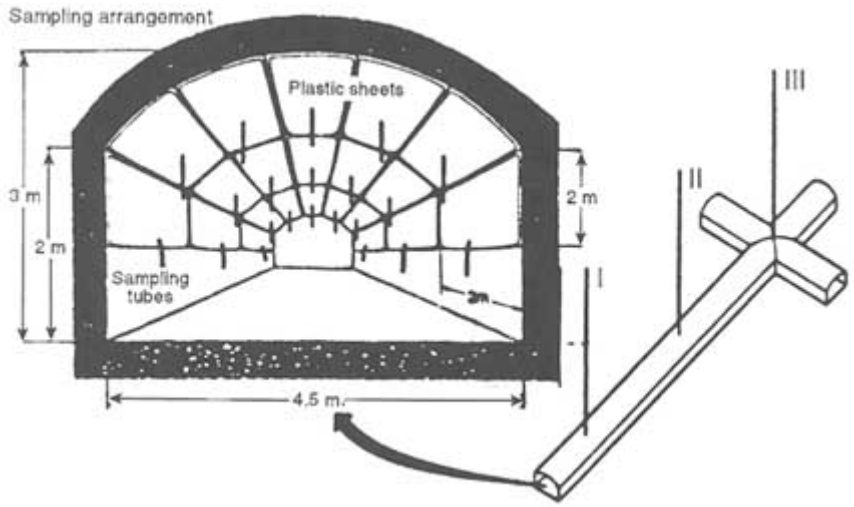

FIGURE 5.E1 Underground site in Stripa Project mine where a large-scale flow and tracer experiment was performed. From Abelin et al. (1991a), Figure 2.

diffusion of tracers into regions of stagnant water. The first possibility was verified by the detection of a tracer in a nearby drift of the Stripa mine complex. The complex's flow system suggests that knowledge of the groundwater hydraulics and flow paths is critical for the design and analysis of tracer tests in fractured rocks.

Appendix 5.F

Diagnostic Well Test Analysis At The Fracture Research Investigation

The Fracture Research Investigation (FRI) in the Grimsel Rock Laboratory, which is located in the Alps in southern Switzerland, provides an excellent example of diagnostic well test analysis. A hydrologically active and accessible fracture zone was selected for investigation, and five studies were jointly undertaken (Majer et al., 1990). A detailed geological investigation provided background information. Extensive cross-hole tomographic studies imaged the fracture zone, which was observed crossing two parallel drifts. Hydrological tests were designed based on the results of the geological and geophysical investigations.

Hydraulic tests were planned in two boreholes drilled from the two drifts using the 1987 tomography results (Figure 5.F1). Each test consisted of pumping water in a given interval at a constant pressure and monitoring in all the other intervals. Test 1 was undertaken to provide a hydrological characterization of the main fracture zone that was identified in the tomographic images (feature A in Figure 5.F1). Packers were placed such that they confined the main fracture zone as tightly as possible in order to minimize wellbore storage and isolate the hydrological system (Figure 5.F2). This isolated interval (interval I1.2) was used as the inflow interval, and pressure was monitored in all the other intervals. Based on these results (Wyss, 1988), feature A is clearly the most significant hydrological feature at the FRI site.

Figure 5.F3 shows the pressure transient interference data at various observation points during Test 1. Note that the interval I3.1 responded most markedly during pumping. The response data at I3.1 are compared to the theoretical response in Figure 5.F4. As can be seen from the figure, the pressure observed at I3.1 is significantly lower than predicted by the analytical solution, although the shapes of the curves are almost identical. The analytical solution assumes that the fracture is infinite, isotropic, and homogeneous. Therefore, conditions must exist where one or more of the above assumptions are not appropriate. A number of violating conditions may exist, including:

- *Skin*: there is a low-permeability zone around the injection well, that is, a skin that causes the effective pressure at I1.2 to be lower.
- *Anisotropy*: the fracture is anisotropic, and the maximum permeability direction is oriented vertically.
- *Leakage*: there is leakage from the fracture to the adjacent rock, so the pressure is more dispersed.
- *Boundary effect*: the boundary effect of the laboratory tunnel keeps the pressure low in I3.1.

Skin effect is usually suspected when an anomalous result is obtained. However, the flow rate curve (not shown) does not match any of the skin curves, and

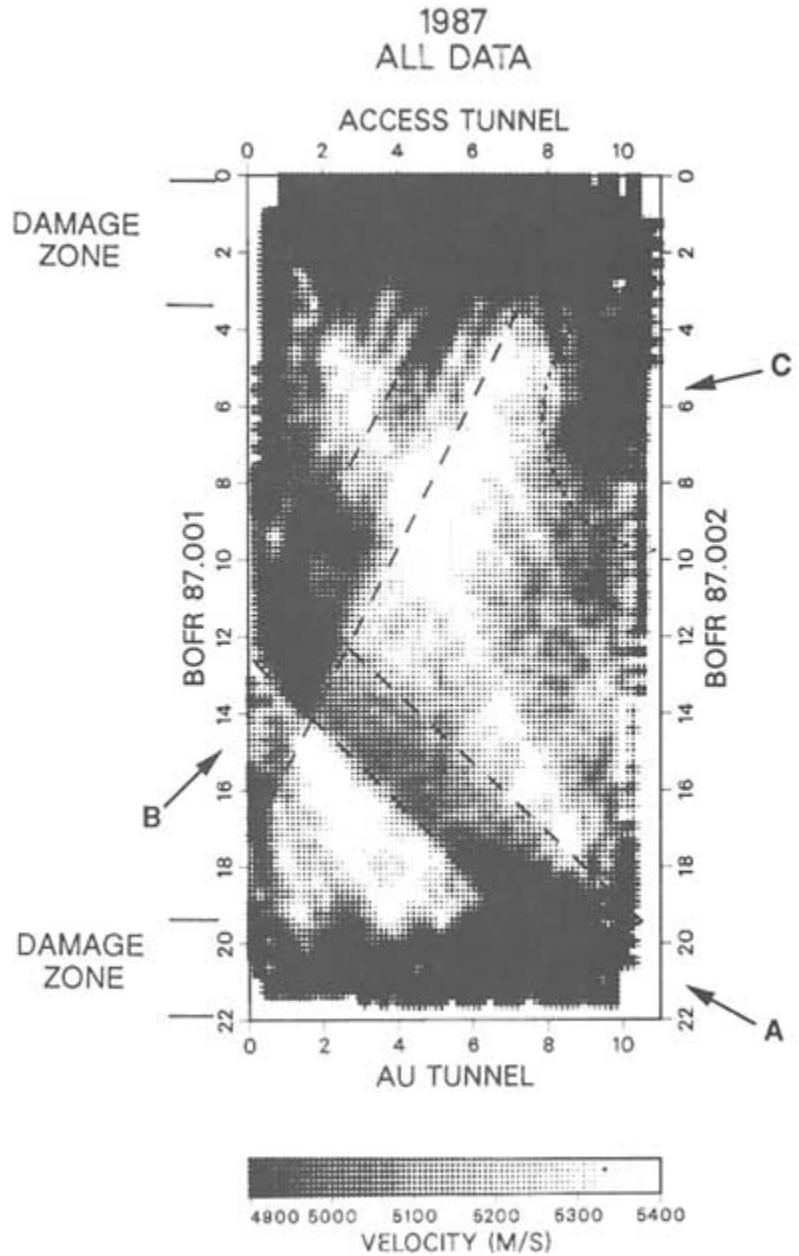

FIGURE 5.F1 Tomographic image of the FRI site obtained from the algebraic reconstruction technique (ART) invasion seismic data collected during 1987 survey. From Majer et al. (1990).

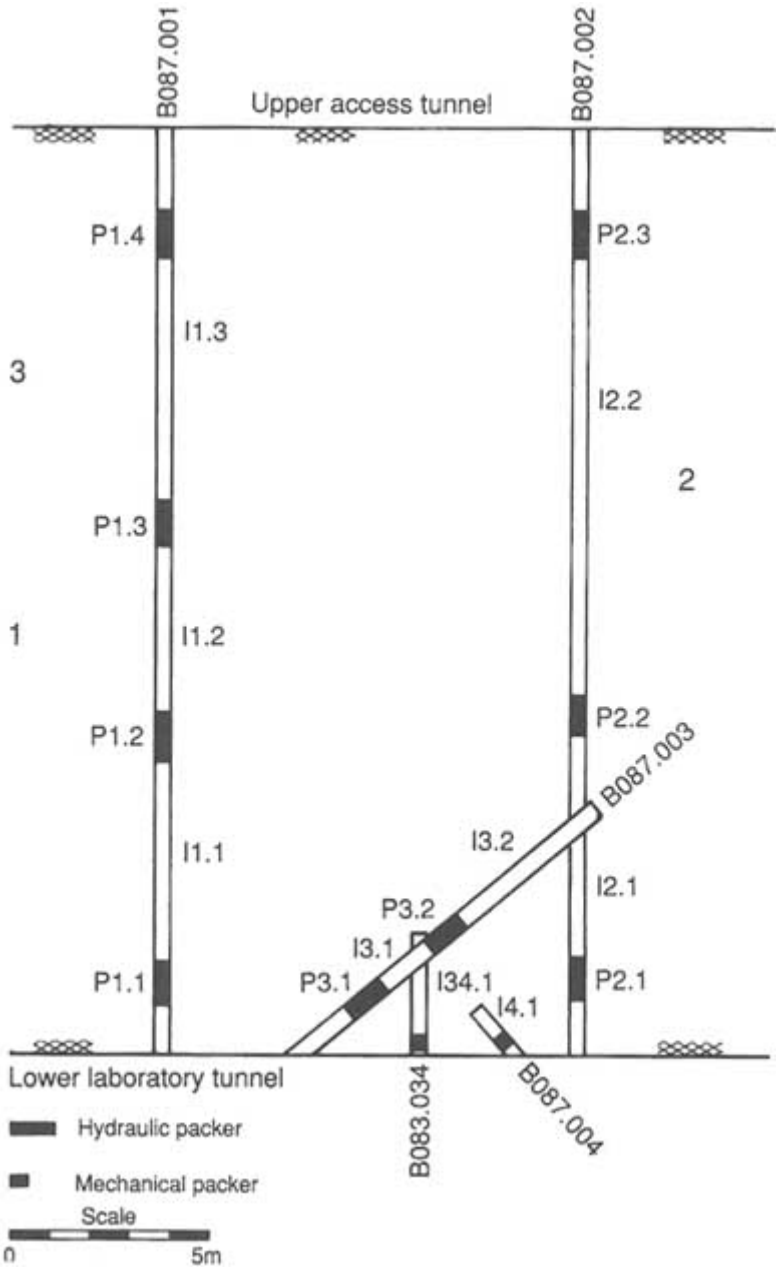

FIGURE 5.F2 Packer locations used in hydraulic tests at the FRI site. From Majer et al. (1990).

the match for I3.1 is not very good. Therefore, it seems that the conventional skin effect cannot explain the observed behavior. Alternatively, if a constant pressure drop independent of the flow rate is assumed at the borehole wall, the flow rate curve would not exhibit the skin effect. Although the no-skin curve is closer to the observed curve, it still does not explain the observed inflection in the flow rate curve.

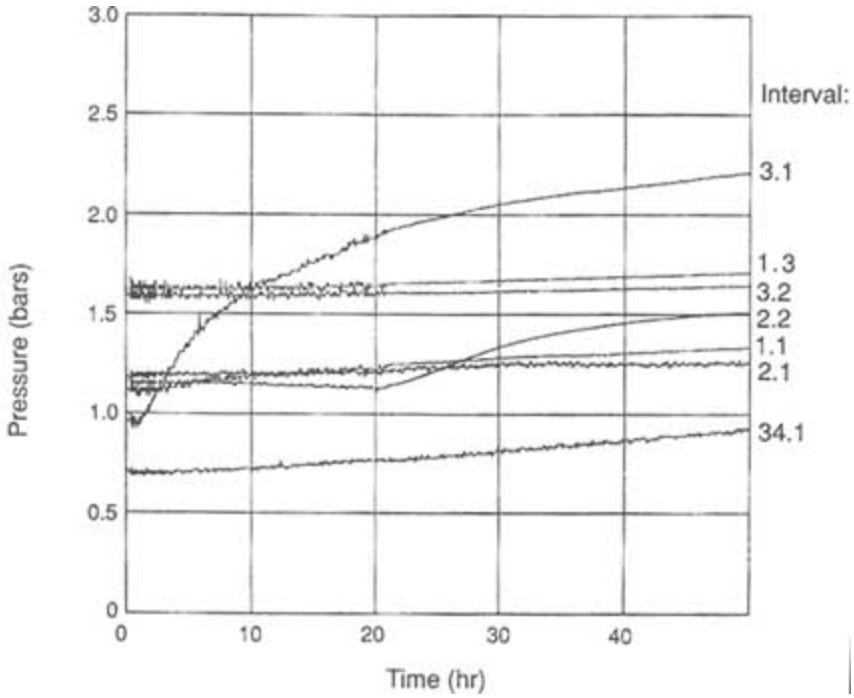

FIGURE 5.F3 Interference buildup data for test 1 at various observation points. From Majer et al. (1990).

Geological observations indicate that the fracture zone may be highly anisotropic with the highest permeability in the vertical direction. Thus, injected water may flow preferentially in the vertical direction. As a result, the observed pressure head in the horizontal direction in interval I3.1 may be lower than for the isotropic case. Analytical solutions for flow to a well in an anisotropic medium can be obtained through a transformation of coordinates (Kucuk and Brigham, 1979). However, an unreasonably large anisotropy ratio (2×10^9) is necessary to explain the pressure drop. Therefore, it is unlikely that anisotropy is the sole cause for the low-pressure measurement.

As can be seen from Figure 5.F3, small interference responses were observed at various intervals that are not in the plane of the fracture zone. This implies

that there is leakage from the fracture zone into adjacent rocks, which may explain why the interference response in I3.1 was low. The solution for pressure in a constant-pressure test in a leaky aquifer is not readily available in the literature. However, if the thickness of the rock into which leakage occurs is assumed to be of finite size and the leakage is at quasi-steady state, the solution presented by Da Prat et al. (1981) for a double-porosity medium can be used. The match between the flow rate data and the Da Prat solution (not shown) is very good, but the match between the pressure data and the solution in I3.1 (not shown) is poor. The theoretical pressure is too high compared to the data because in the model the rock is assumed to be of finite size.

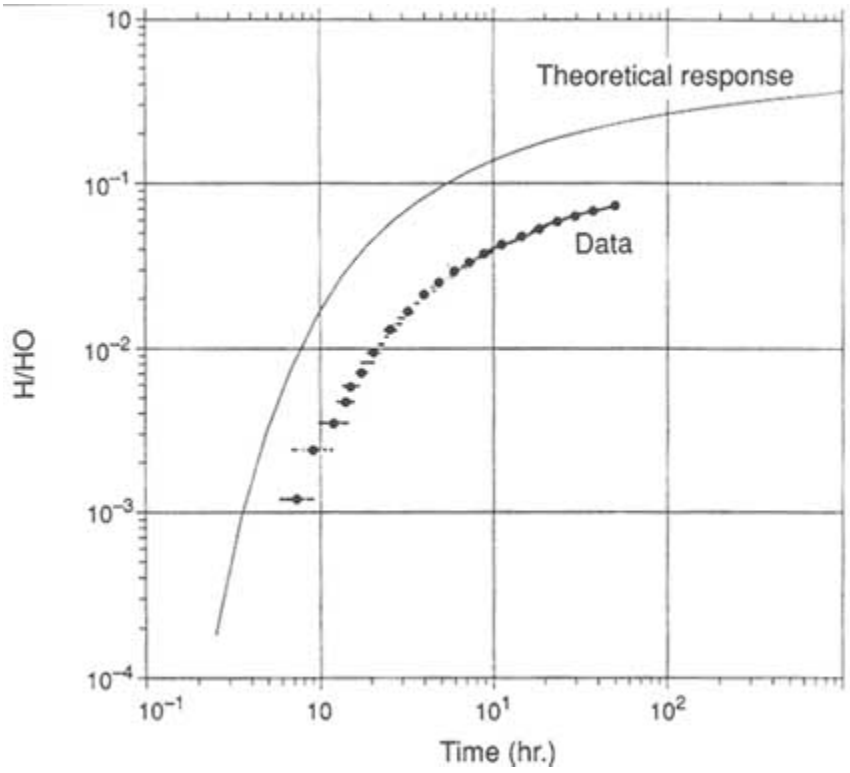

FIGURE 5.F4 Comparison between interference buildup data for test 1 and the theoretical response curve. From Majer et al. (1990).

Leakage into an infinite-sized rock was considered through a Laplace space solution for the normalized pressure in the fracture zone at a nondimensional distance, *rD*, under a constant-pressure test with leakage into an infinite-sized rock. Values of drawdown and flow for the Laplace space solution are plotted in Figures 5.F5 and 5.F6 for various combinations of fracture and matrix proper

ties. Also plotted are the observed data. The match with the interference data in I3.1 is much better than in Figure 5.F4. However, the match between the data and the theoretical curves at long times is not good. In particular, the observed flow rate data are much flatter than the theoretical curves at long times (Figure 5.F6).

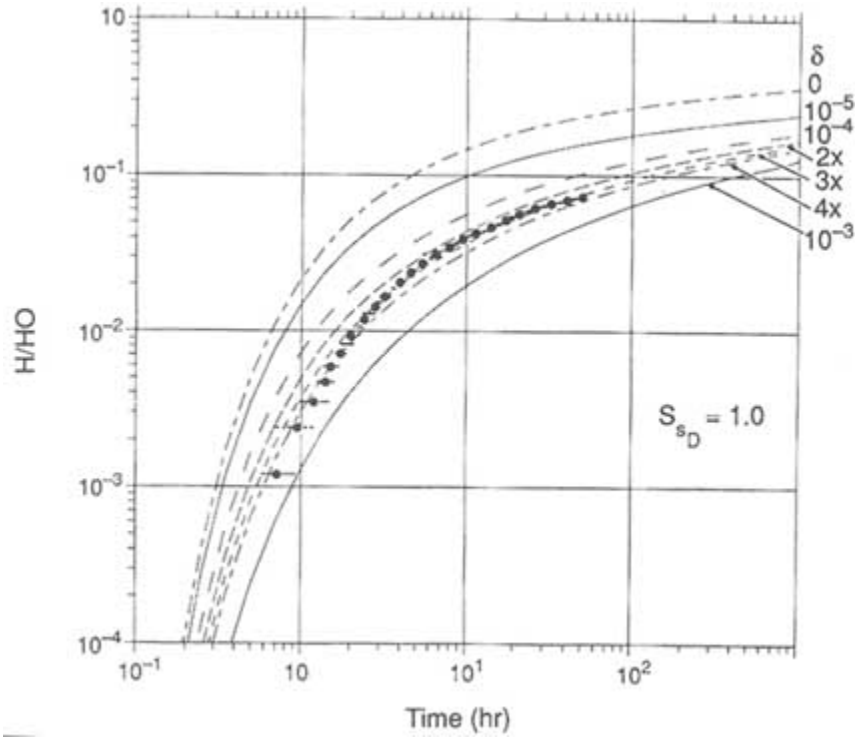

FIGURE 5.F5 Comparison of drawdown and flow for leakage into an infinite-sized rock with data from I3.1. From Majer et al. (1990).

Nonetheless, the concept of leakage appears to explain the trend of the data: low interference pressure and flattening of the flow rate curve at long times. The weak hydraulic connection between I1.2 and I2.2 may be through this low-permeability rock matrix. It is worth noting that the 1988 seismic tomography results (Figure 5.F1) indicate the existence of a feature (feature B) that extends diagonally from the access tunnel toward borehole 87.001. This may be a conduit for the leaking water. This localized leakage is not taken into account by the analytical solution; it could explain the low pressure in I3.1 and the flattening of the flow rate curve.

Hydraulic tests have confirmed the hydrological significance of this fracture zone, which was previously identified by seismic tomography. It appears that the majority of flow occurs in the relatively thin fracture zone that connects I1.2

and I3.1 (feature A). A weak but definite hydrological connection between I1.2 and I2.2 also was observed. Feature B in Figure 5.F1, which extends diagonally from the access tunnel to borehole 87.001, may partially explain this hydrological connection.

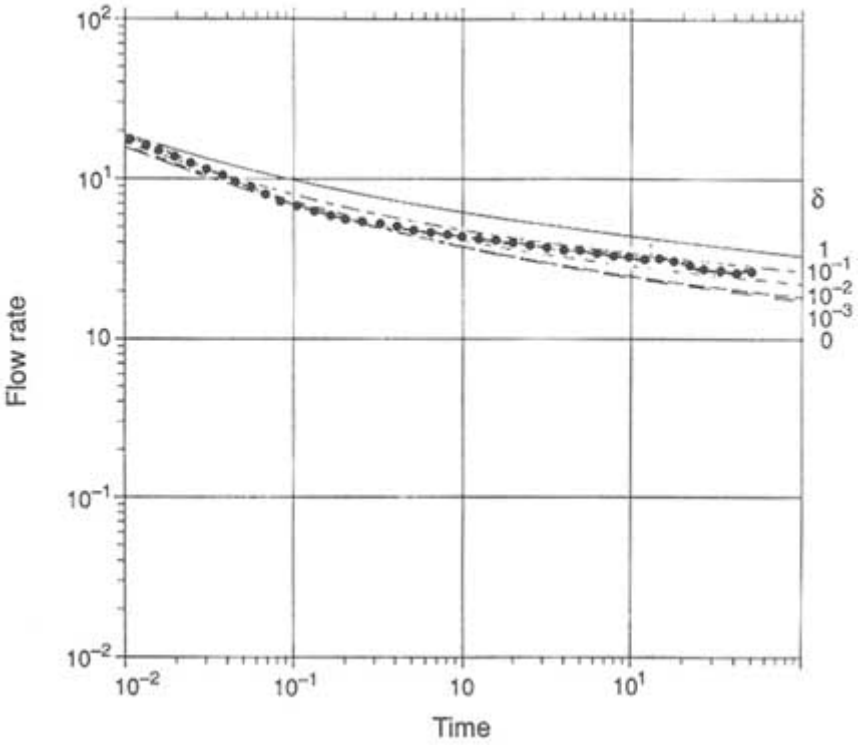

FIGURE 5.F6 Comparison of drawdown and flow for leakage into an infinite-sized rock with data from I2.1. From Wyss (1988).

Appendix 5.G

The Fracture Zone Project At Finnsjön

The fracture zone project sponsored by SKB (Swedish Nuclear Fuel and Waste Management Co.) was run between the years 1984 and 1990 at the Finnsjön site, which is located in central Sweden about 140 km north of Stockholm. Its main goal was to characterize a major fracture zone in crystalline bedrock, especially the flow and transport properties of a fracture zone, the localization of potential pathways for groundwater flow, and transport of solutes essential for the safety assessment of a nuclear waste repository.

At the Finnsjön site, there are a number of gently dipping fracture zones (0° to 30° to the horizontal), which are common in such crystalline rock formations (Andersson, 1993). Geological identification and characterization of these fracture zones were accomplished through a broad range of geological, geophysical, geomechanical, geochemical, and hydrological investigations.

Through these investigations, a gently dipping fracture zone, zone 2, was defined in nine boreholes in an area of about 1,500 × 500 m in the northern part of the Finnsjön Rock Block at depths of 100 to 300 m. This zone was singled out for detailed flow studies aimed at understanding flow and transport in the zone and interactions with surrounding bedrock. Flow measurements on this zone included piezometric measurements, single-hole hydraulic tests at different scales, interference tests, groundwater flow measurements, and tracer tests, radially converging and dipole.

A number of hydrological modeling efforts were then undertaken. These efforts were carried out in conjunction with field experiments, so there was a close interaction between modeling and field measurements. In this interaction the modeling and field measurements mutually support each other; measurements can be used to test and improve the predictive ability of models, and models can be used to design and interpret field measurements. The overall sequence of this interaction was as follows:

- model predictions of interference tests
- interference tests
- updated flow models based on interference tests
- predictions of radially converging tracer tests
- radially converging tracer tests
- comparison of model predictions with radially converging tracer tests
- prediction of dipole tracer test, and
- comparison of model predictions with dipole tracer test.

The main conclusion regarding flow in zone 2 showed that the zone, which is about 100 m thick, is composed of two to five highly transmissive sections (T = 1 - 4 × 10^{-4} m^2/s). These highly transmissive sections have widths of

about 0.5 m. Interference tests showed that the uppermost section was interconnected over distances of several hundred meters, and tracer experiments showed travel times differing by a factor of 10 between two observation boreholes at approximately the same distance from an injection borehole. Modeling efforts showed that zone 2 has a complicated structure where transport occurs in a few well-defined pathways and that this heterogeneity must be an important component in transport models.

REFERENCES

Abelin, H., L. Birgersson, J. Gidlund, and I. Neretnieks. 1991a. A large-scale flow and tracer experiment in granite 1. Experimental design and flow distribution. Water Resources Research, 27(12):3017–3117.

Abelin, H., L. Birgersson, L. Moreno, H. Widen, T. Agren, and I. Neretnieks. 1991b. A large-scale flow and tracer experiment in granite 2. Results and interpretation. Water Resources Research, 27(12):3019–3135.

Andersson, J. E., L. Ekman, R. Nordquist, and A. Winberg. 1991. Hydraulic testing and modeling of a low-angle fracture zone at Finnsjon, Sweden. Journal of Hydrology, 126:45–77.

Andersson, P. 1993. SKB Report 93-20, Swedish Nuclear Fuel and Waste Management Co., Stockholm.

Barker, J. A. 1988. A generalized radial flow model for hydraulic tests in fractured rock. Water Resources Research, 24(10):1796–1804.

Bear, J. 1979. Hydraulics of Groundwater. New York: McGraw-Hill.

Bennett, R. D., and R. F. Anderson. 1982. New pressure test for determining coefficient of permeability of rock masses. Technical Report GL-82-3, U.S. Army Engineer Waterways Experiment Station, Vicksburg, Miss., p. 61.

Black, J. H., and K. L. Kipp. 1981. Determination of hydrogeological parameters using sinusoidal pressure test: a theoretical appraisal. Water Resources Research, 17(3):686–692.

Bourdet, D., T. M. Whittle, A. A. Douglas, and Y. M. Pirard. 1983. A new set of type curves simplifies well test analysis. World Oil, 196:95–106.

Bourdet, D., J. A. Ayoub, and Y. M. Pirard. 1989. Use of pressure derivative in well test interpretation. SPE Formation Evaluation, 4(2):293–302.

Bredehoeft, J. D., and S. S. Papadopulos. 1980. A method for determining the hydraulic properties of tight formations. Water Resources Research, 16(1):233–238.

Bureau of Reclamation. 1985. Ground Water Manual. Denver: U.S. Department of the Interior, Bureau of Reclamation, p. 480.

Carrera, J., and S. P. Neuman. 1986. Estimation of aquifer parameters under transient and steady-state conditions: 2. Uniqueness, stability, and solution algorithm. Water Resources Research, 22(2):211–227.

Carrera, J., and J. Heredia. 1988. Inverse modeling of Chalk River block. NAGRA Technical Report 88-14, National Cooperative for the Disposal of Radioactive Waste (NAGRA), Baden, Switzerland, 117 pp.

Cooper, H. H., J. D. Bredehoeft, and I. S. Papadopulos. 1967. Response of a finite-diameter well to an instantaneous charge of water. Water Resources Research, 3(1):263–269.

Dagan, G. 1986. Statistical theory of groundwater flow and transport: Pore to laboratory, laboratory to formation, and formation to regional scale. Water Resources Research, 22(9):120S–134S.

Dagan, G., V. Cvetkovic, and A. Shapiro. 1992. A solute flux approach to transport in heterogeneous formations 1. The general framework. Water Resources Research, 28 (5):1369–1376.

Da Prat, G., H. Cinco-Ley, and H. J. Ramey, Jr. 1981. Decline curve analysis using type curves for two-porosity systems. Society of Petroleum Engineers Journal, Society of Petroleum Engineers of AIME, pp. 354–362.

Dawson, K. J., and J. D. Istok. 1991. Aquifer Testing: Design and Analysis of Pumping and Slug Tests. Chelsea, Mich.: Lewis Publishers, p. 344.

Earlougher, R. C., Jr. 1977. Advances in Well Test Analysis. Dallas: Society of Petroleum Engineers of AIME, p. 264.

Gelhar, L. W. 1986. Stochastic subsurface hydrology from theory to applications. Water Resources Research, 22(9):135S–145S.

Garnier, J. M., N. Crampon, C. Preaux, G. Porel, and M. Vreulx. 1985. Tracage par 13-C, 2-H, I-et uranin dans la nappe de la craie senonienne en ecoulement radial convergent (Bethune, France). Journal of Hydrology, 78:379–392.

Hantush, M. S. 1967. Flow to wells in aquifers separated by a semipervious layer. Journal of Geophysical Research 72(6):1709–1720.

Hsieh, P. A., S. P. Neuman, G. K. Stíles, and E. S. Simpson. 1985. Field determination of the three-dimensional hydraulic conductivity tensor of anisotropic media 2. Methodology and application to fractured rocks. Water Resources Research, 21(11):1667–1676.

Johnson, C. R., R. A. Greenkorn, and E. G. Woods. 1966. Pulse testing: A new method for describing reservoir flow properties between wells. Journal of Petroleum Technology, Dec.:1599–1604.

Karasaki, K. 1990. A systematized drillstem test. Water Resources Research, 26(12):2913-2919.

Karasaki, K., J. C. S. Long, and P. A. Witherspoon. 1988. Analytical models of slug tests. Water Resources Research, 24(1):115–126.

Kucuk, F., and W. E. Brigham. 1979. Transient flow in elliptical systems. Society of Petroleum Engineers Journal, pp. 401–410.

LeBlanc, D. R., S. P. Garabedian, K. M. Hess, L. W. Gelhar, R. D. Quadri, K. G. Stollenwerk, and W. W. Wood. 1991. Large-scale natural gradient tracer test in sand and gravel, Cape Cod, Massachusetts 1. Experimental design and observed tracer movement. Water Resources Research, 27(5):895–910.

Long, J. C. S., J. S. Remer, C. R. Wilson, and P. A. Witherspoon. 1982. Porous media equivalents for networks of discontinuous fractures. Water Resources Research, 18(3):645–658.

Mackay, D. M., D. L. Freyberg, P. V. Roberts, and J. A. Cherry. 1986. A natural gradient experiment on solute transport in a sand aquifer 1. Approach and overview of tracer movement. Water Resources Research, 22(13):2017–2029.

Majer, E. L., L. R. Myer, J. E. Peterson, Jr., K. Karasaki, J. C. S. Long, S. J. Martel, P. Blumling, and S. Vomvoris. 1990. Joint seismic, hydrogeological, and geomechanical investigations of a fracture zone in the Grimsel Rock Laboratory. Report LBL-27913, NDC-14, Lawrence Berkeley Laboratory, Berkeley, Calif., 173 pp.

Maloszewski, P., and A. Zuber. 1985. On the theory of tracer experiments in fissured rocks with a porous matrix. Journal of Hydrology, 79:333–358.

Maloszewski, P., and A. Zuber. 1990. Mathematical modeling of tracer behavior in short-term experiments in fissured rocks. Water Resources Research, 26(7):1517–1528.

Maloszewski, P., and A. Zuber. 1992. On the calibration of mathematical models for the interpretation of tracer experiments in groundwater. Advances in Water Resources, 15:47–62.

Moench, A. F. 1984. Double-porosity models for a fissured groundwater reservoir with fracture skin. Water Resources Research, 20(7):831–846.

Moench, A. F. 1989. Convergent radial dispersion: A Laplace transform solution for aquifer tracer testing. Water Resources Research, 25(3):439–447.

Neuman, S. P., and P. A. Witherspoon. 1972. Field determination of the hydraulic properties of leaky multiple aquifer systems. Water Resources Research, 8(5):1284–1298.

Neuzil, C. E. 1982. On conducting the modified "slug" test in tight formations. Water Resources Research, 18(2):439–441.

Novakowski, K. S., and P. A. Lapcevic. 1994. Field measurements of radial solute transport in fractured rock. Water Resources Research, 30(1):37–44.

Noy, D., J. Barker, J. Black, and D. Holmes. 1988. Crosshole investigations—Implementation and fractional dimension interpretation of sinusoidal tests. Stripa Project Technical Report 88-01, Swedish Nuclear Fuel and Waste Management Co., Stockholm, 62 pp.

Pickens, J.F., G.E. Grisak, J.D. Avis, D. W. Belanger, and M. Thury. 1987. Analysis and interpretation of borehole hydraulic tests in deep boreholes: principles, model development, and applications, Water Resources Research, 23(7):1341–1375.

Polek, J., K. Karasaki, J. Barker, and J. Long. 1989. Flow to wells in fractured rock with fractal structure. In Fractal Aspects of Materials, J. H. Kaufman, J. E. Martin, and P. W. Schmidt, eds. Materials Research Society.

Ramey, H. J., Jr., R. G. Agarwal, and I. Martin. 1975. Analysis of 'slug test' or DST flow period data. Journal of Canadian Petroleum Technology, July-Sept.:37–47.

Raven, K. G. 1986. Hydraulic characterization of a small groundwater flow system in fractured monzonitic gneiss. National Hydrology Research Institute Paper No. 30, Inland Waters Directorate Series No. 149, Environment Canada, Ottawa, Canada.

Raven, K. G., K. S. Novakowski, and P. A. Lapcevic. 1988. Interpretation of field tracer tests of a single fracture using a transient solute storage model. Water Resources Research, 24 (12):2019–2032.

Sageev, A. 1986. Slug test analysis. Water Resources Research, 22(8):1323–1333.

Smith, L., C. W. Mase, and F. W. Schwartz. 1987. Estimation of fracture aperture using hydraulic and tracer tests. Pp. 453–463 in Rock Mechanics, Proceedings of the 28th U.S. Symposium, Tucson, Arizona, June 21–July 1. Farmer, I. W., J. J. K. Daemen, C. S. Desai, C. E. Glass, and S. P. Neuman, eds. Rotterdam: A. A. Balkema.

Streltsova, T. D. 1988. Well Testing in Heterogeneous Formations. New York: John Wiley & Sons, 413 pp.

Tsang, C. F., Y. W. Tsang, and F. V. Hale. 1991. Tracer transport in fractures: Analysis of field data based on a variable-aperture channel model. Water Resources Research, 27(12):3095–3106.

Tsang, Y. W., and C. F. Tsang. 1989. Flow channeling in a single fracture as a two-dimensional, strongly heterogeneous permeable medium. Water Resources Research, 25(9):2076–2080.

Welty, D., and L. W. Gelhar. 1989. Evaluation of longitudinal dispersivity from tracer test data. Report 320, Ralph M. Parsons Laboratory for Water Resources and Hydrodynamics, Massachusetts Institute of Technology, Cambridge.

Wyss, E., 1988. Kurzbericht zu den ersten hydrogelogischen Untersuchungen im Rahmen des Versuches FRI. SOLEXPERTS Field report to the Swiss National Cooperative for the Storage of Nuclear Waste (internal document).

Yeh, W. W. G. 1986. Review of parameter identification procedures in groundwater hydrology: The inverse problem. Water Resources Research, 22(2):95–108.

Zeigler, T. W. 1976. Determination of rock mass permeability. Technical Report S-76-2, U.S. Army Engineer Waterways Experiment Station, Vicksburg, Miss., 114 pp.

6

Field-Scale Flow and Transport Models

Previous chapters have addressed fracture geometry, physical and geomechanical properties of single fractures, fracture detection, and the interpretation of hydraulic and tracer tests. All of these elements must be integrated when developing a mathematical model to represent fluid flow and solute transport in fractured media. The focus of this chapter is mathematical models and the model-building process. The process of building a hydrogeological model crosses discipline boundaries, demanding the combined expertise of geologists, geophysicists, and hydrologists.

The hydraulic properties of rock masses are likely to be highly heterogeneous even within a single lithological unit if the rock is fractured. The main difficulty in modeling fluid flow in fractured rock is to describe this heterogeneity. Flow paths are controlled by the geometry of fractures and their open void spaces. Fracture conductance is dependent, in part, on the distribution of fracture fillings and the state of stress. Flow paths may be erratic and highly localized. Local measurements of geometric and hydraulic properties cannot easily be interpolated between measurement points. In contrast, granular porous media, although also heterogeneous, commonly exhibit smoothly varying flow fields that are amenable to treatment as equivalent continua. Model studies of fluid flow and solute transport in fractured media that do not address heterogeneity may be doomed to failure from the outset.

The formulation of a hydrogeological simulation model is an iterative process. It begins with the development of a conceptual model describing the main features of the system and proceeds through sequential steps of data collection and model synthesis to update and refine the approximations embodied in the

conceptual model. The conceptual model is a hypothesis describing the main features of the geology, hydrological setting, and site-specific relationships between geological structure and patterns of fluid flow. Mathematical modeling can be thought of as a process of hypothesis testing, leading to refinement of the conceptual model and its expression in the quantitative framework of a hydrogeological simulation model.

The relationship between the conceptual model, laboratory and field measurements, and the hydrogeological simulation model is illustrated in the flow chart in Figure 6.1. Simulation models are usually used as tools for enhancing understanding of flow systems as an aid in reaching management or design decisions. Three basic questions must be addressed before a model can be used as a site-specific design tool. First, does the conceptual model provide an adequate

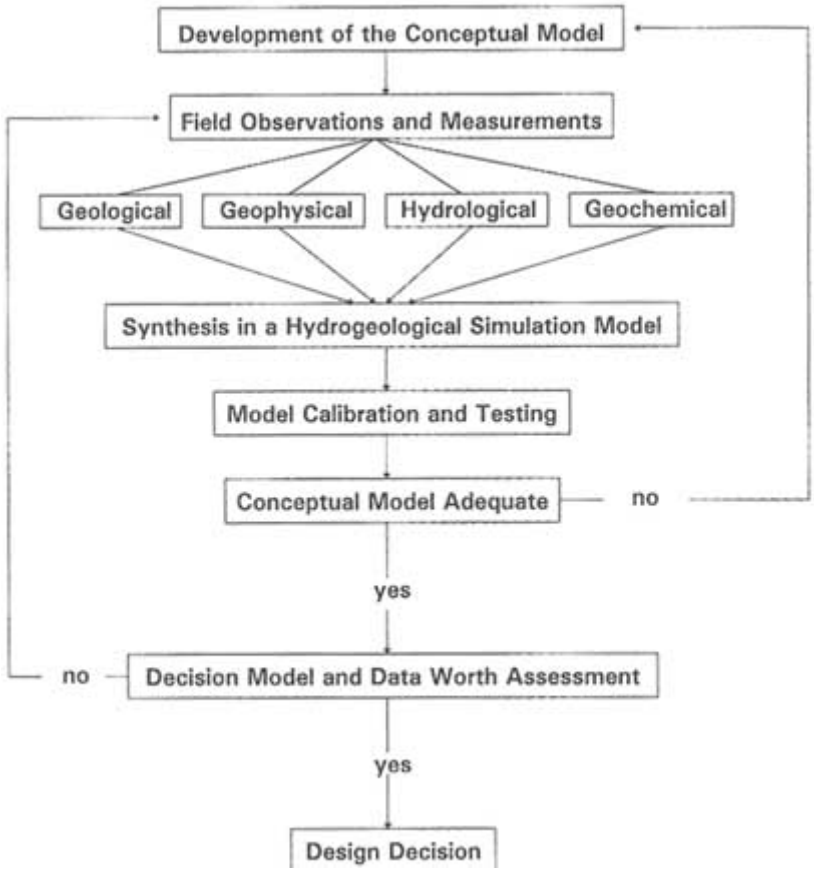

FIGURE 6.1 Flow chart identifying steps involved in the development of a hydrogeological simulation model for the purpose of reaching a management or design decision.

characterization of the hydrological system? If not, it should be revised and reevaluated. Second, how well does the model perform in comparison with competing models? Model results are nonunique. Consequently, field measurements may be successfully matched using fundamentally different conceptual and mathematical models. A model that successfully reproduces field measurements is not necessarily correct or validated. An important test of any model is to see how well it predicts behavior under changed hydrological conditions. Once the conceptual model is accepted, a third question must be asked: is the data base adequate to estimate the model parameters with sufficient reliability that the associated prediction uncertainties are acceptable in light of the intended application of the model in the decision process? If not, additional data collection is justified. In most instances this latter question is best addressed in an economic framework (Freeze et al., 1990).

The flow chart in Figure 6.1 is not unique to fractured geological media. It outlines the modeling process for any hydrogeological system. It is commonly the case, however, that these three questions are considerably more difficult to resolve when dealing with fractured media in comparison to problems involving fluid flow through granular porous media.

The purpose of this chapter is twofold: (1) to summarize recent views on the development of conceptual models of fluid flow and transport in fractured porous media and (2) to discuss and assess the state of the art in mathematical modeling and to identify research needs to advance modeling capabilities. The chapter focuses on general issues of model design. Mathematical formulations, numerical techniques, and specific computer codes are not included in the discussion. The chapter reviews the ways different types of simulation models incorporate the heterogeneity of a rock mass.

Much of the experience involving the simulation of fluid flow and solute transport in fracture systems has developed through the application of dual-porosity models in reservoir analyses. An extensive literature exists on the use of these models (e.g., Warren and Root, 1963; Kazemi, 1969; Duguid and Lee, 1977; Gilman and Kazemi, 1983; Huyakorn et al., 1983a,b; to name but a few). Although dual-porosity models are included in this discussion, greater emphasis is placed on more recent models that accommodate more complex fracture geometries than normally assumed in dual-porosity models. In addition, the discussion in this chapter is limited to fracture systems and model applications where it is not necessary to consider the effects of fracture deformation on fluid flow. This topic is addressed in more detail in Chapter 7.

DEVELOPMENT OF CONCEPTUAL AND MATHEMATICAL MODELS

Overview

Figure 6.1 highlights the central role of the conceptual model in the modeling process. When formulating a conceptual model to describe conductive fractures

and their permeabilities, three factors come into play: (1) the geology of the fractured rock, (2) the scale of interest, and (3) the purpose for which the model is being developed. These three factors determine the kinds of features that should be included in the conceptual model to capture the most important elements of the hydrogeology.

Geology of the Fractured Rock

A geological investigation seeks to identify and describe fracture pathways. These pathways are determined by material properties, geometry, stress, and geological history of the rock. There are two end members that describe the distribution of fracture pathways: (1) a system dominated by a few relatively major features in a relatively impermeable matrix, as commonly observed in massive crystalline rocks, and (2) a system dominated by a network of ubiquitous, highly interconnected fractures in a relatively permeable matrix, as might be found in an extensively jointed, layered rock with strata-bound fractures. Fracture systems exist at many levels between these two extremes in many different rock types. A geological investigation attempts to identify which features of a fracture system, if any, have the potential to dominate the hydrology.

Scale of Interest

A fracture system may be highly connected on a large scale, but it may be dominated by a few, relatively large features when viewed on a smaller scale. Classical thinking holds that the larger the scale of interest, the more appropriate it is to represent fractured rock in terms of large regions of uniform properties. The major problem then becomes one of estimating the large-scale properties from small-scale measurements. More recently, some workers have suggested that there are fracture features at all scales of interest. For these cases the traditional strategy of representing the rock as having large regions of uniform properties is less likely to be adequate. A series of new approaches are being developed to address fracture representation at large scales.

Purpose for Which the Model Is Being Developed

The level of detail required in the conceptual model depends on the purpose for which the model is being developed—for example, whether it will be used to predict fluid flow or solute transport. Experience suggests that, for average volumetric flow behavior, predictions can be made with a relatively coarse conceptual model provided data are available to calibrate the simulation model. Thus, a continuum approximation may be used to predict well yields with sufficient accuracy, even if a fracture network is poorly connected. For solute transport a considerably more refined conceptual model is needed to develop reliable predic

tions of travel times or solute concentrations because of the sensitivity of these variables to the heterogeneity of fractured systems (Chapter 5). A more specific description of fracture flow paths may also be necessary to identify recharge areas for a well field located in a fractured medium.

The importance of identifying fracture pathways in contaminant transport problems can be visually demonstrated by observations from a laboratory model. Figure 6.2 illustrates the development of a solute plume in a fractured porous medium constructed from blocks of porous polyethylene. In this experiment a tracer was injected into a permeable matrix block for a period of 75 minutes, and its distribution was mapped. The pattern of spreading is complex and strongly dependent on the local structure and hydraulic properties of the network.

To this point, the conceptual model has been expressed in terms of a hypothesis describing the heterogeneity of the rock mass. In a more general sense, a conceptual model encompasses all of the assumptions that go into writing the mathematical equations that describe the flow system. Decisions are required about whether the problem at hand involves saturated or unsaturated flow, isothermal or nonisothermal conditions, single-phase or multiphase flow, and reactive or nonreactive solutes. Issues related to the development of conceptual models for these more complex processes are explored in the final section of this chapter.

The development of an appropriate conceptual model is the key process in understanding fluid flow in a fractured rock. Given a robust conceptual model, different mathematical formulations of the hydrogeological simulation model will likely give similar results. However, an inappropriate conceptual model can easily lead to predictions that are orders of magnitude in error.

Development of a Conceptual Model

The steps in building a conceptual model of the flow system include (1) identification of the most important features of a fracture system, (2) identification of the locations of the most important fractures in the rock mass, and (3) determination of whether and to what extent the identified structures conduct water. The important fractures are significantly conductive and connected to a network of other conductive fractures. All fractures are not of equal importance. Identification of preferred fluid pathways is crucial in the development of a conceptual model. So too is an understanding of the orientation of the fractures (or fracture sets) that contribute to flow, because these orientations provide insight into the anisotropic hydraulic properties of the rock mass.

Inferences about the relative importance of fractures can be made in a variety of ways. As described in Chapter 2, geological observation of fracture style is a powerful tool. Fractures have been studied in many locations and in many rock types, and several patterns have been identified (e.g., La Pointe and Hudson, 1985). For example, fractures may be evenly distributed in the rock mass or may occur in concentrated swarms or zones. There may be polygonal joints or

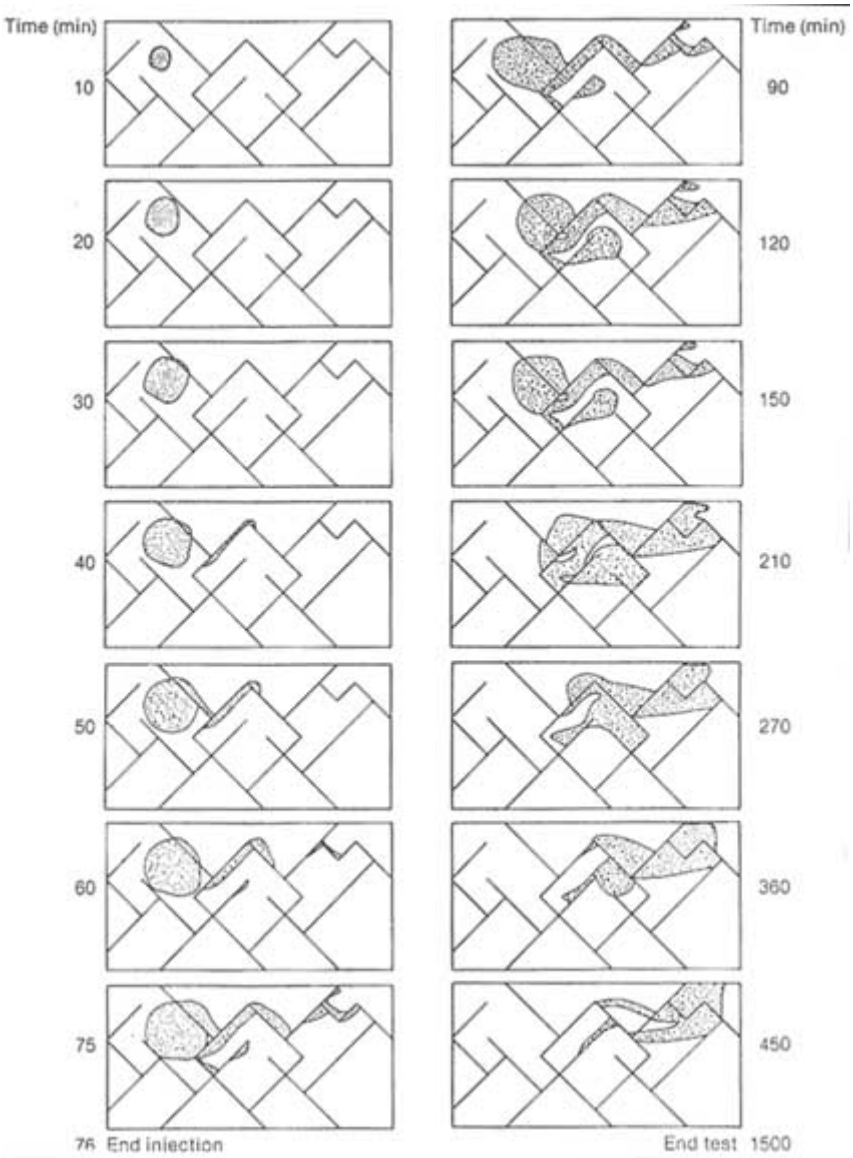

FIGURE 6.2 Laboratory experiment of tracer injection in a fractured porous medium. The model domain is 80 cm in length. Tracer was injected for 75 minutes and allowed to migrate under the influence of a uniform hydraulic gradient. The lines in the boxes represent the fracture networks. From Hull and Clemo (1987).

en-echelon features. Understandings gained through investigations of fracture style provide insights for predicting the character of fractures in unexposed parts of the rock mass.

Understanding the genesis of fractures can provide insights into the hydrological properties of the rock mass. For example, subvertical shear zones near Grimsel Pass in the Swiss Alps were studied in outcrop by Martel and Peterson (1991) and shown to have distinctly different fracture patterns depending on the orientation of the zone with respect to the fabric of the rock. Shear zones at an angle to the fabric (so-called K zones) tend to have parallel groups of fractures, whereas those parallel to the fabric (so-called S zones) have more braided, anastomosing fractures (Figure 6.3). The hydrological characteristics of these zones are likely to be quite different. K zones may have high vertical permeabilities in the vicinity of the fractures because they formed by extension; in contrast, S zones may be more uniformly, if anisotropically, permeable.

The Stripa mine in Sweden provides an example of another way to make inferences about fracture hydrology. A 50-m-long drift was excavated in the granitic rock mass, and every fracture with a trace longer than 20 cm was mapped (Figure 6.4). The rock appears to be ubiquitously fractured, with a concentration of fractures in the central 10 or 15 m of the drift (the H zone). Careful measurement has shown that essentially all the inflow comes from this zone; 80 percent of this inflow is from a single fracture (Olsson, 1992). Outside of this zone, the myriad other fractures are unimportant in contributing to the fluid influx. The zone itself does not behave as a homogeneous porous slab. It can be surmised that the flow systems in these zones are likely to be only partly connected. Fracture zones also dominate the hydrology at the Underground Research Laboratory in

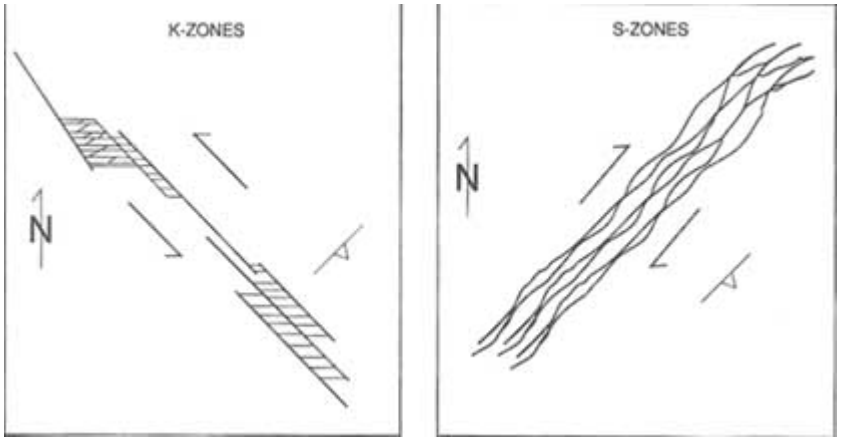

FIGURE 6.3 Schematic diagrams comparing the arrangement of fractures in K zones and S zones from the Grimsel Pass in the Swiss Alps. From Martel and Peterson (1990).

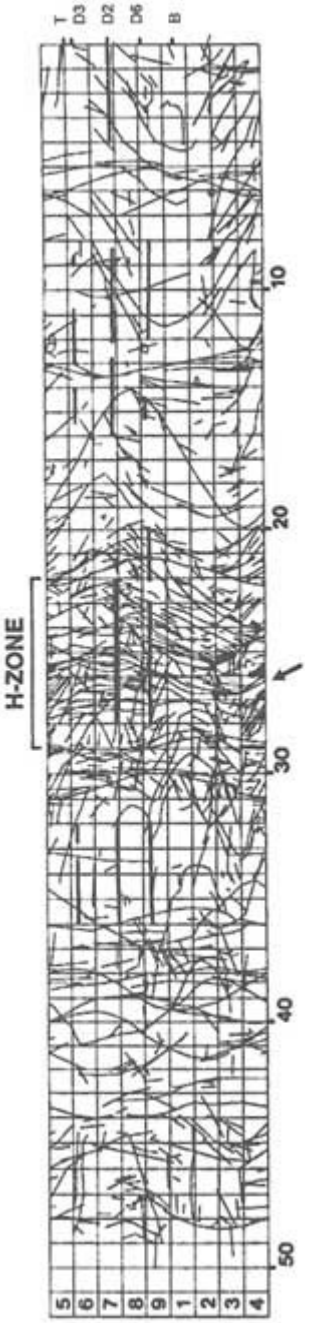

FIGURE 6.4 Fracture map from the Stripa validation drift, Sweden, showing the H fracture zone. Arrow shows the fracture that carries 80 percent of the flow into the drift. From Olsson (1992).

Canada (Davison et al., 1993) and at the Grimsel Rock Laboratory in Switzerland (Long et al., 1990).

The state of stress can be a controlling factor in determining which fractures or parts of fracture systems are important. An example is provided by a study in a fractured oil reservoir in the Ekofisk field in the North Sea (Teufel et al., 1991). Fractures with two distinct orientations were logged from boreholes; one of the sets was far more abundant than the other. Subsequent hydraulic testing showed that the direction of maximum permeability was aligned with the less abundant fracture set and that this direction was parallel to the maximum compressive stress. Apparently, fractures parallel to the maximum compressive stress tend to be open, whereas those perpendicular to this direction tend to be closed.

Once the flow-controlling fractures are identified, the next step is to define and locate them in the rock mass. Ideally, geophysical and geological data can be combined to determine the three-dimensional geometry of the major structures that might conduct water. Geological and geophysical investigations are clearly complementary. Geological investigations are well suited to identifying, locating, and characterizing exposed fractures and to determine how the fractures were formed; they are limited in their ability to determine how far to project known fractures into the rock and to detect unexposed fractures. Geophysical investigations can locate unexposed fractures, as discussed in Chapter 4, but are limited in their ability to uniquely determine the geometry of the detected fractures. Geological and geophysical methods do not generally yield quantitative information about the hydraulic and transport properties of fractures. They do provide information about the structure of the rock mass that can be used to organize hydrological investigations and interpretations.

There are two types of geological information available for integration with geophysical data: (1) geological maps of outcrops and (2) underground exposures and borehole data. The interpretation of borehole data has certain limitations. Individual borehole records typically do not allow the shapes and dimensions of fractures to be determined, nor do they provide information about fracture connectivity. In addition, the orientation of fracture zones, which can be determined from borehole measurements, can differ significantly from the orientation of individual fractures in the zone (e.g., the K zone in Figure 6.3). Methods of collecting and analyzing statistical data on fracture systems based on borehole observations are discussed in greater detail later in this chapter.

Finally, it must be determined if and how the identified fractures conduct water. There is probably no better way to see if a fracture conducts water than to pump water through it while monitoring the hydraulic response in the rock. A conceptual model of the fracture geometry provides a framework for designing this hydrological investigation. Instead of simply measuring injectivities at random, the tests can be focused on determining the hydrological properties of specific features. If the conceptual model includes a major feature, the well testing program can be designed to investigate the permeability of this feature. If there

are a number of features, the well tests can be designed to see if they are hydraulically connected. This diagnostic testing is described in Chapter 5. Geophysical tools described in Chapter 4, such as borehole flowmeters or borehole televiewers, also provide indications of the location of hydraulically conductive fractures. Under favorable circumstances, examination of the chemical composition of waters from different locations can provide an indication of water sources and whether or not the sources are mixing.

The result of this process is a model of those features of the fracture system that control the hydrology and some understanding of the nature of flow in the system. The process is by its very nature iterative. As data are collected and analyzed, the conceptual model is updated, and this may influence subsequent decisions on the types of data to be collected and on measurement techniques or locations. Revision of the conceptual model or selection of a competing model is driven by comparison of model predictions with new observations. An example of this process that emphasizes the role of geophysics is the conceptual modeling of the Site Characterization and Validation Experiment at the Stripa mine, which is discussed in Chapter 8.

Mathematical Models

Mathematical models fall into one of three broad classes: (1) equivalent continuum models, (2) discrete network simulation models, and (3) hybrid techniques. The models differ in their representation of the heterogeneity of the fractured medium. They may be cast in either a deterministic or stochastic framework. The scale at which heterogeneity is resolved in a continuum model can be quite variable, from the scale of individual packer tests in single boreholes to effective permeabilities averaged over large volumes of the rock mass. Discrete network models explicitly include populations of individual fracture features or equivalent fracture features in the model structure. They can represent the heterogeneity on a smaller scale than is normally considered in a continuum model. Some of the more recent innovations in mathematical simulation are best classified as hybrid techniques, which combine elements of both discrete network simulation and continuum approximations.

Table 6.1 presents a summary of the main classes of simulation models for fractured geological media. Included in this table are key parameters that distinguish the models. Also listed are references that illustrate recent applications of each modeling approach. The few references were chosen simply to point the direction toward the relevant literature; it is not meant to imply they are necessarily viewed as the "best" papers on a given topic. Subsequent sections of this chapter explore these model types in greater detail. Additional coverage of some of these modeling concepts can be found in a recent text by Bear et al. (1993) and in another National Research Council (1990) report on groundwater models.

TABLE 6.1 Classification of Single-Phase Flow and Transport Models Based on the Representation of Heterogeneity in the Model Structure

Representation of Heterogeneity	Key Parameters that Distinguish Models	Recent Examples
Equivalent Continuum Models		
Single porosity	Effective permeability tensor Effective porosity	Carrera et al. (1990) Davison (1985) Hsieh et al. (1985)
Multiple continuum (double porosity, dual permeability, and multiple interacting continuum)	Network permeability and porosity Matrix permeability and porosity Matrix block geometry Nonequilibrium matrix/fracture interaction	Reeves et al. (1991) Pruess and Narasimhan (1988)
Stochastic continuum	Geostatistical parameters for log permeability: mean, variance, spatial correlation scale	Neuman and Depner (1988)
Discrete Network Models		
Network models with simple structures	Network geometry statistics Fracture conductance distribution	Herbert et al. (1991)
Network models with significant matrix porosity	Network geometry statistics Fracture conductance distribution Matrix porosity and permeability	Sudicky and McLaren (1992)
Network models incorporating spatial relationships between fractures	Parameters controlling clustering of fractures, fracture growth, or fractal properties of networks	Dershowitz et al. (1991a) Long and Billaux (1987)
Equivalent discontinuum	Equivalent conductors on a lattice	Long et al. (1992b)
Hybrid Models		
Continuum approximations based on discrete network analysis	Network geometry statistics Fracture transmissivity distribution	Cacas et al. (1990) Oda et al. (1987)
Statistical continuum transport	Network geometry statistics Fracture transmissivity distribution	Smith et al. (1990)
Fractal Models		
Equivalent discontinuum	Fractal generator parameters	Long et al. (1992) Chang and Yortsos (1990)

In the process of calibrating a hydrogeological simulation model, assumptions and approximations on which the conceptual model is founded can be tested and refined. Competing models can be compared. The reality of hydrogeological simulation is that there may be a number of possible models with different combinations of geometry and media parameters that reproduce the observed response at a given point in the rock mass. Most flow and transport data from fractured rock sites are open to more or less equally successful interpretations by means of fundamentally different conceptual and mathematical models.

There is always a question about the uniqueness of the model. In selecting among different models that provide equally good matches to field measurements, two viewpoints exist. One favors a more parsimonious model, giving preference to models that are conceptually the simplest, that contain a smaller number of model parameters, and/or that contain the fewest number of quantities that are not readily measurable in the field on the same scale as they appear in the model. A second point of view favors models that are more "open ended" and look for a spectrum of structures, or distributions of permeability, that could explain the test data. Both approaches are being pursued in the research community. To evaluate these model results, there is a need for a more coordinated effort of cross-checking model predictions with field behavior, in a variety of fractured rock settings, on a variety of length scales.

Predictions of fluid flow and solute transport are normally subject to a considerable degree of uncertainty for several reasons. A fractured medium typically has a permeability structure that is highly variable and uncertain. Fluid flow and solute transport are sensitive to this heterogeneity. Changes in fluid pressure, through the effective stress, can modify the hydraulic properties of the fracture network. It is for these reasons that use of both the iterative approach and interdisciplinary investigations is critical to building confidence in model predictions. So, too, is the effort to quantify the magnitude of the uncertainty inherent in a model prediction.

In many instances, severe constraints on site characterization are encountered owing to limited project budgets, concerns about maintaining the integrity of a low-permeability rock mass, or concerns about cross-contamination of different horizons in the rock mass. There may be few boreholes in an area of several square kilometers. Funds may not be available for additional drilling or for detailed geophysical measurements. Consequently, it may not be possible to identify the positions or even the presence of connected pathways through a rock mass. Although geological models of the fracture system can be a great aid in these cases, the extent to which the hydrological model can be refined is limited. The unavoidable consequence of such constraints is the higher degree of uncertainty that is introduced into the hydrogeologic simulation model. Ideally, one would like to represent the fractured rock mass and the flow through it by models that accurately simulate the performance of each rock mass component. For the reasons just discussed, this is not possible, and all models are simplifications.

These simplifications may be introduced in the form of continuum models, in which the discontinuum character of the rock mass is neglected, or in the form of discontinuum models, which try to represent the discontinuities geometrically and mechanically. It is also possible to combine these modeling approaches. It is relevant to note that the difficulties in representing a fractured rock mass occur in many problems other than fracture flow, such as stability and deformability of the rock mass. Many of the models discussed in this chapter originate in these domains.

The simulation models listed in Table 6.1 are discussed in the following pages. The focus is on single-phase flow and transport in the saturated zone. The conceptual models that represent the heterogeneity of the rock mass are discussed with respect to the process of parameter estimation. Although their conceptual frameworks differ, all models are based on balance equations that express mass conservation in some representative volume of the rock mass. Examples of these models are described, and a few case studies are presented. The next section discusses the use of equivalent continuum models. Then alternative approaches that have been developed to address the complexities of flow peculiar to fracture systems are covered. More text is devoted to the discussion of discrete network and hybrid approaches because the hydrological community is generally less familiar with these concepts than with continuum models. One should not infer from the level of detail provided here that the committee always favors one approach over others. Models for more complex phenomena are discussed later in this chapter, including chemical processes, unsaturated flow, multiphase flow, and heat transfer. Fluid flow in deformable fractures is discussed in Chapter 7.

EQUIVALENT CONTINUUM SIMULATION MODELS

The Continuum Approximation

In a conventional equivalent continuum model, the heterogeneity of the fractured rock is modeled by using a limited number of regions, each with uniform properties. Individual fractures are not explicitly treated in the model, except when they exist on a scale large enough to be considered a separate hydrological unit (e.g., an areally extensive fracture zone). At the scale of interest, hydraulic properties of the rock mass are represented by coefficients, such as permeability and effective porosity, that express the volume-averaged behavior of many fractures. For example, Figure 6.5 shows a numerically generated fracture network. Flow through the network is calculated in many directions and is used to derive the equivalent permeability ellipse discussed below.

If the coefficients in the fluid flow and solute transport equations are viewed as being known with certainty, or if the most likely values of the variables are used, the model is deterministic. Conventional forms of the groundwater flow equation, which were developed originally for granular porous media, can then

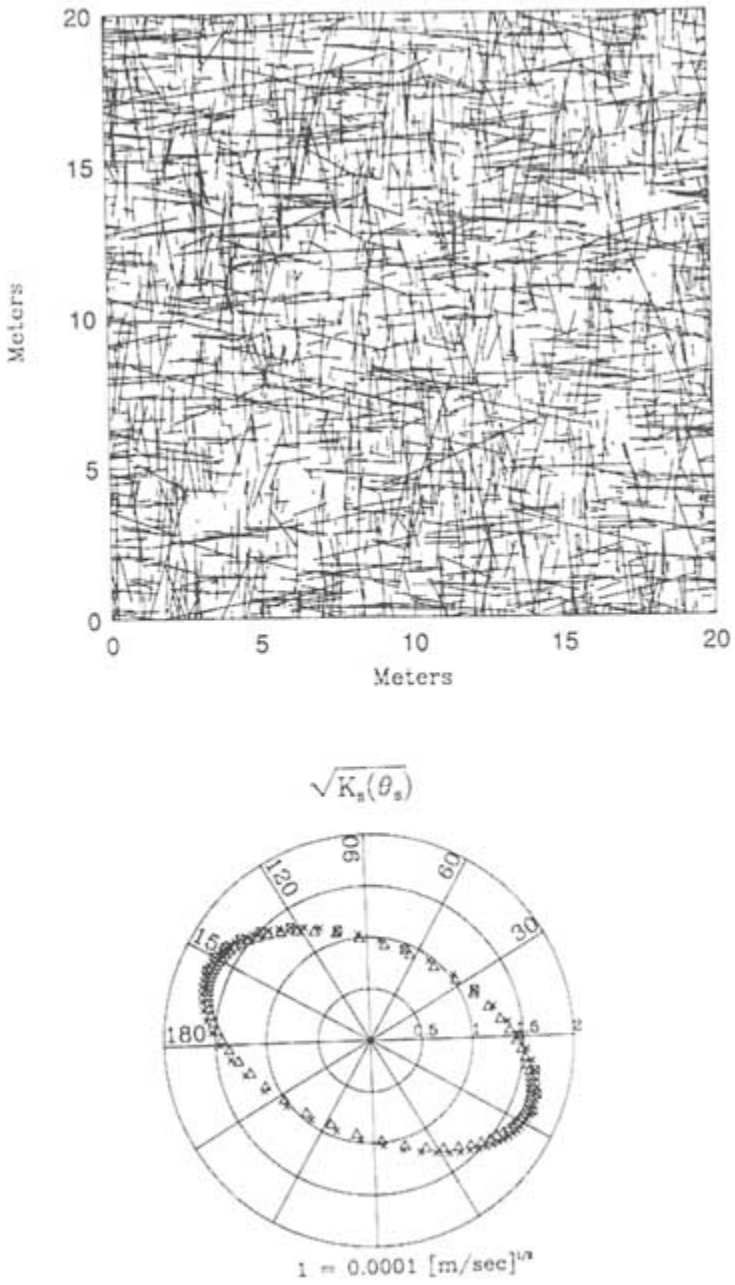

FIGURE 6.5 Deriving equivalent continuum properties. Representation of the average fluid flux through a fracture network in terms of an anisotropic permeability ellipse.

be adopted. The use of continuum approximations in a deterministic framework has been the common practice.

If the coefficients are viewed as a spatially variable random field, characterized by a probability distribution, the model is stochastic. The magnitude of uncertainty in the input parameters depends on the natural variability of the medium, knowledge of which may be limited by the number and types of measurements available to map the heterogeneity.

Averaging volumes associated with a deterministic continuum approximation must be large enough to encompass a statistically representative sample of the open, connected fractures and their variable influences on flow and transport behavior. Effectively, this means that fluid flux and solute transport are not influenced to any significant degree by any individual fracture or its interconnections with other fractures that form the conducting network. The representation of a flow region using uniform flow properties is best applied to cases where the scale of the problem is large, the fractures are highly interconnected, and the interest is primarily on volumetric flow, such as in groundwater withdrawal for water supply. Rocks that have been subject to multiple and extensive deformations, and/or those with significant matrix permeabilities, are likely to be good candidates for equivalent continuum modeling. If, however, fracture density is low or many fractures are sealed by mineral precipitates, fracture connectivity may be low and continuum assumptions less likely to be adequate.

In the saturated zone, fractures usually provide the primary pathways for fluid flow and mass transfer. Matrix blocks between the conducting fractures can significantly increase the storage properties of the rock mass. Equivalent continuum models for fractured media are of two general types, single and dual porosity. In a single-porosity model all porosity is assumed to reside in the fractures; porosity in the matrix blocks between the conducting fractures is neglected. In a dual-porosity (fracture plus matrix) model the matrix blocks are assigned a value of porosity greater than zero. Single-porosity models represent hydrology in terms of a single continuum; dual-porosity models are based on two overlapping continuua.

For fluid flow problems involving steady-state conditions (i.e., no changes in fluid storage), single-porosity models are usually adopted. The fluid flux through the rock matrix is assumed to be negligible in comparison to that in the fracture network. For problems involving transient flow (i.e., a change in fluid storage), both single- and dual-porosity models have been used. As discussed later, the choice between a single- and a dual-porosity formulation relates to the manner in which the water released from storage in the fractures and matrix blocks is characterized. For problems involving solute transport in geological media with high matrix porosities or problems with long time scales, diffusion of mass between the fractures and the rock matrix (so-called matrix diffusion) can be an important process. Matrix diffusion is normally simulated by using a dual-porosity model.

This section reviews the approaches based on conventional applications of hydraulic test data to formulate estimates of the field-scale properties of the fractured medium. These applications include both deterministic and the more recent stochastic models. Continuum approaches that make use of discrete network models as a means of estimating field-scale continuum properties of the fractured medium are discussed later in this chapter, under "Hybrid Methods: Using Discrete Network Models in Building Continuum Approximations."

Single-Porosity Models Developed in a Deterministic Framework

Fluid Flow

Single-porosity models consider flow and transport only in the open, connected fractures of the rock mass. When using a numerical model, such as a finite-difference or finite-element model, a grid is superimposed on the flow domain and values of permeability are assigned to each grid block. Estimation of permeability involves a synthesis of laboratory and in situ measurements, model calibration, and model evaluation. The rock mass is normally represented by a limited number of hydrological units, each with homogeneous properties. These units may be isotropic or anisotropic. Because fractures typically occur in sets having preferred orientations, large-scale permeabilities may be anisotropic. An excellent example of a continuum approach is provided by Carrera et al. (1990), who modeled groundwater flow in a fractured gneiss at the Chalk River site in Ontario, Canada. They carried out an inverse simulation to identify a preferred model structure and to estimate the model parameters.

Hydraulic tests provide the most direct means of examining the validity of a porous medium approximation and for estimating values of the permeability tensor (Hsieh and Neuman, 1985; Hsieh et al., 1985). Single-borehole and crosshole hydraulic tests can provide this information (see Chapter 5), typically for volumes of rock having a characteristic length scale of tens of meters. If multiple nests of boreholes are tested, the question becomes one of how to use the values measured at this scale to estimate parameters representative of other scales of heterogeneity that are invariably present. Approaches to this issue represent one of the key research topics concerning the hydrology of fractured rocks. Geological and geomechanical models have an important role to play in providing a physical basis for extrapolating data beyond the measurement scale.

At the scale of hundreds of meters (subbasin scale), hydrogeological simulation models calibrated to estimates of recharge rates, water table positions, and/or potentiometric head data may provide the most reliable approach to estimate large-scale values for the conductance of the rock mass. Geochemical data, including isotopes and age dating of groundwater, also can be valuable for calibrating and testing hydrogeological simulation models. This general approach is probably most useful when predicting gross features of the flow system. As

emphasized in Figure 6.1, hydrogeological simulation is an iterative process. Model calibration can reveal the presence of fractures that may have been poorly sampled in the field, as happens, for example, with near-vertical fracture sets in an investigation program relying on vertical boreholes with no surface exposure. In this case, comparison of model predictions and field measurements may suggest horizontal anisotropy or a higher vertical permeability than was initially anticipated. An example of this case is discussed in Appendix 6.A.

For problems involving transient flow (e.g., a hydraulic disturbance caused by a pumping or injection well), a method to account for the fluid released from storage must be chosen. If fracture densities are high and matrix blocks are small, the fractured medium is sometimes treated as one effective continuum; that is, no distinction is made between fluid residing in the fractures or the matrix. The hydraulic diffusivity of the medium is a composite value reflecting the influence of both fractures and matrix blocks. The conventional equation describing transient groundwater flow in a porous medium is used in the simulation model (e.g., Freeze and Cherry, 1979).

Solute Transport

In a single-porosity transport model, the assumption is made that solute migrates only through the open, connected fractures in the rock mass. As indicated earlier, reliable prediction of solute transport in a fractured rock mass is considerably more difficult than the corresponding flow problem. Common practice, which is fraught with uncertainty, is to adopt the continuum approximations embodied in the conventional form of the advection dispersion equation. However, the scale at which a continuum approximation is valid may be at best difficult to determine, and at worst nonexistent. To define transport, the analyst must define the pathways through the flow system. This is equivalent, in a granular porous medium, to defining the subsurface configuration of streamtubes that connect the areas of groundwater recharge to the areas of discharge from the flow domain. It is because these pathways are so difficult to define in a fractured medium that there is considerable uncertainty in a transport simulation.

If an approximation based on porous medium equivalence is adopted, values are needed for the effective porosity and dispersive properties of the open fracture network. Estimation of effective porosity is key to predicting the average rate at which the solutes will move and to determining the mobility of solutes that react with the rock matrix. Mass will disperse as it encounters various pathways through the connected fractures. Invariably, an isotropic model for dispersion is chosen, whereby spreading is governed by three dispersivity coefficients that are independent of the angle of the hydraulic gradient. In fractured media, however, spreading is probably a highly anisotropic process; the character of spreading changes for different orientations of the hydraulic gradient. There are few experimental data of sufficient reliability to identify either a representative range of values for the

dispersive properties of fractured media or the character of the early time evolution of the dispersion process.

In principle, parameter estimates for effective porosity and dispersivity can be obtained from tracer tests. Although it is feasible to design and implement tracer tests to characterize the transport properties of fracture zones (see Chapter 5), transport properties of large fractured rock volumes are more difficult to characterize. Techniques for determining effective porosity are poorly developed. There are no general analytical expressions relating network geometry and the conductance of fractures to the three-dimensional dispersion tensor, analogous to expressions that have emerged in recent years for heterogeneous porous media. Furthermore, for fractured rock systems it is unclear how observations of tracer migration at small scales can be extrapolated to larger scales. Neuman (1990, 1994) has proposed a theoretical model that characterizes the scale dependence of dispersivity on average for all rock types (porous and fractured media). The approach provides an ensemble or, most likely, value at any given scale. If confirmed by further observations, this model will be useful in relating transport properties to the heterogeneity in permeability and to the information available to describe that heterogeneity.

Dual-Porosity Models

Fluid Flow

Dual-porosity models consider fluid flow and transport in both the connected fractures and the matrix blocks. For a rock mass with large porous matrix blocks between the conducting fractures, dual-porosity models have been used to account for the release of fluid from storage in the matrix blocks into the fracture network. The geometry of the fracture network is idealized to the extent that it can be represented by a small number of geometric parameters (e.g., the average dimension of a matrix block). Several examples are shown in Figure 6.6. The rock is characterized as two overlapping continuua, and both are treated as porous media. The key hydraulic properties are the effective permeability and porosity for the fracture network, the matrix porosity and permeability, and the storage coefficients for the fractures and matrix blocks. The equation expressing fluid flow through the fracture network contains source terms to account for flow from the matrix to adjacent fractures. A second set of equations describes fluid flow in the matrix blocks. Drainage into the fracture network depends on the geometry of the fracture-matrix interface and the hydraulic diffusivity of the matrix. Normally, a uniform geometry and block length are adopted for large regions of the flow domain. Some guidance in choosing a representative value for block length can be obtained from geological logs of fracture spacing.

An example that illustrates the application of a dual-porosity model using well logs to guide the selection of block size can be found in Moench (1984).

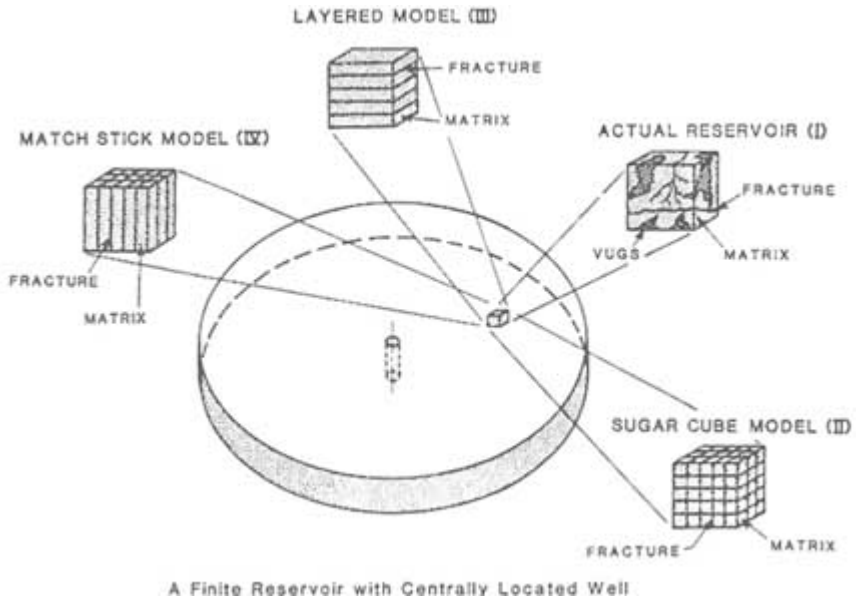

FIGURE 6.6 Idealization of a fractured reservoir adopted in a dual-porosity model. I, actual reservoir; II, sugar cube model; III, layered model; IV, match stick model. From Kazemi and Gilman (1993).

The case study deals with a well test at the Yucca Mountain site in Nevada. A borehole flow survey showed that there were five major zones of fluid entry over a vertical interval of 400 m (Figure 6.7). These zones were modeled as five horizontal zones of enhanced permeability, separated by slablike blocks of approximately 80 m thickness.

The match between the pumping test data and the type curves for the transient block-to-fracture flow model also is shown in Figure 6.7. The analysis gave values of hydraulic conductivity for the fracture system that were consistent with estimates obtained from single-borehole packer tests. Although values of hydraulic conductivity obtained for the blocks between the fracture zones were, to some degree, uncertain, estimated values from the dual-porosity model were in the range obtained by packer injection tests in intervals containing no major producing fractures. The values of hydraulic conductivity for the blocks were greater by two to five orders of magnitude than values measured on core samples, reflecting the presence of a connected fracture network in the blocks between the major fractures.

The primary advantage of dual-porosity flow models is that they provide a mechanism to account for the delay in the hydraulic response of the rock mass caused by fluid that is resident in less permeable matrix blocks. Dual-porosity

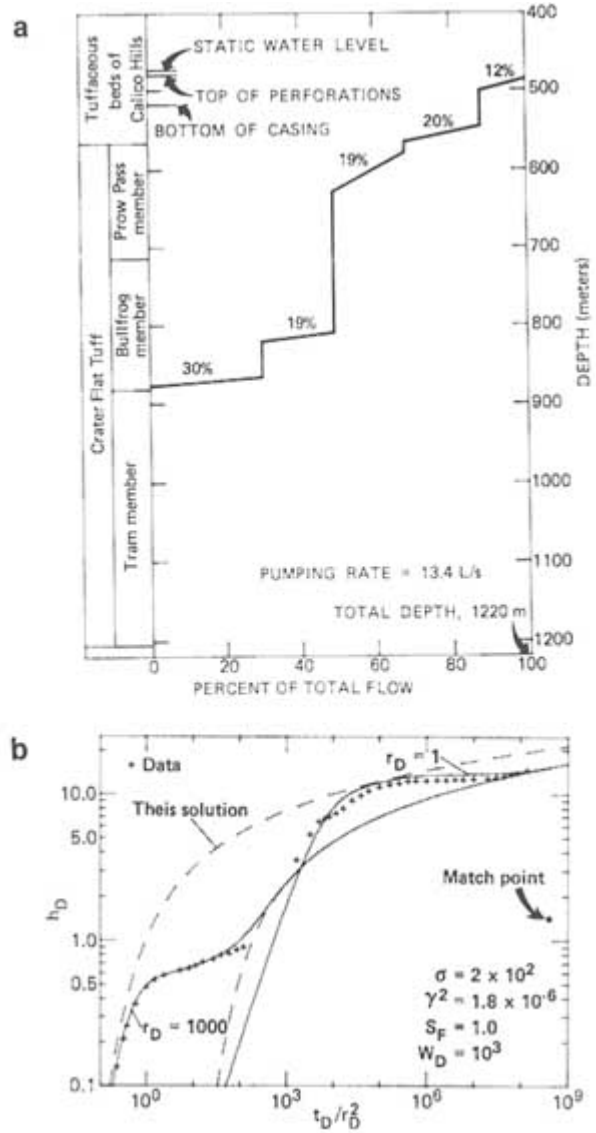

FIGURE 6.7 Interpretation of a pumping test in fractured rock at Yucca Mountain, Nevada, using a dual-porosity model. (a) Borehole flow survey showing percentage of total flow versus depth. (b) Match of the type curves for the dual-porosity model to the field data. The parameter r_D is a dimensionless distance; other parameters given in the figure describe the hydraulic properties of the fractures and blocks. The parameters h_D and t_D are a dimensionless drawdown and dimensionless time, respectively. From Moench (1984).

models have been widely used in reservoir simulation (e.g., petroleum and geothermal reservoirs). The conceptual basis of dual porosity is appealing because of its simplicity. However, experience suggests that there are limits to the prediction capabilities of dual-porosity models. Two problems can be noted with these models: (1) they over regularize the geometry of the fracture network, and (2) good parameter estimates are difficult to obtain. Quantitative criteria to guide the choice between single- and dual-porosity formulations in site-specific applications are not easily defined. The choice of the appropriate conceptual model should be tested during its development (i.e., Figure 6.1).

Solute Transport

In cases where there is the potential for substantial diffusive transfer of mass into the rock matrix blocks, it is essential to incorporate this process into the mathematical structure of the simulation model. Concentration distributions can be greatly affected in comparison to a case in which mass is restricted to the open fracture network. This situation can arise, for example, in problems of regional-scale transport or in problems involving flow through geological units with high matrix porosities, as occurs in some sedimentary rocks and fractured clays. Transport can be facilitated by colloids because their large size limits the extent of matrix diffusion (e.g., McKay et al., 1993; Ibaraki, 1994). Two approaches are possible. One, discussed in a later section, models the fractures and matrix blocks as discrete features with specific geometric coordinates. The second, which uses a dual-porosity formulation, adopts a two-continuum representation of the fractures and matrix blocks, with matrix diffusion treated in a manner analogous to the fluid exchange between the fractures and the matrix.

A good example of the strengths and limitations of a dual-porosity transport simulation was published by Reeves et al. (1991). They investigated the potential for off-site migration of radionuclides through the Culebra dolomite at the Waste Isolation Pilot Project (WIPP) site in New Mexico. The Culebra dolomite is known to be fractured. The rock matrix also is porous, with an average porosity of 15 percent. Figure 6.8 shows their prediction of solute concentrations at the WIPP boundary, calculated for three different cases: (1) a single-porosity model, with flow only through the fractures; (2) a single-porosity model using an effective porosity equal to the sum of the matrix and fracture porosity; and (3) a dual-porosity model. The importance of mass diffusion into the matrix blocks is immediately apparent, as is the effect of dual-porosity structure.

Few quantitative data are available to characterize either the geometry or continuity of fractures in the Culebra dolomite. Observations from cores indicate that fracturing is not uniform even at the local scale. Reeves et al. (1991) adopted a uniform value of 2 m for the length of a matrix block. They also assumed that the fracture network could be represented as a single set of parallel fractures. Based on a travel time performance measure, they concluded that, in terms of

the need for additional characterization, data on the matrix block length and matrix porosity ranked first and second, respectively, for a set of seven model parameters that described solute transport in the Culebra dolomite.

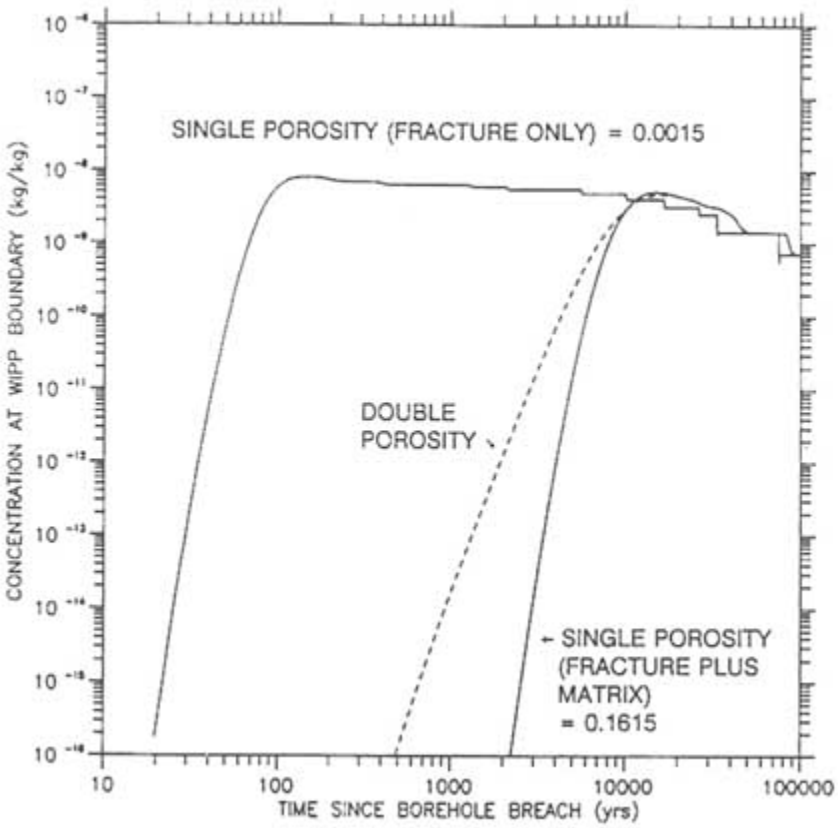

FIGURE 6.8 Example of a dual-porosity transport model. Predictions of solute concentrations for singleand dual-porosity representations of fractured rock at the WIPP site in New Mexico. From Reeves et al. (1991).

Stochastic Continuum Models

The stochastic representation of fluid flow and solute transport in heterogeneous porous media has led in recent years to a powerful new set of tools for hydrogeological analysis. These tools have also been applied to fractured geological media (e.g., Neuman, 1987). The basis of stochastic models is the representation of hydraulic properties in terms of probability models that describe the medium as a random field. In adopting a stochastic approach, the modeler

acknowledges that a complete and accurate simulation of fluid flow, or the movement of a contaminant plume in a fractured rock mass, is not a realistic goal. Instead, it is argued that predictions of plume geometry that are expressed in terms of the spatial moments of the plume (i.e., the mean position and spread of the mass about the mean position), or statements cast in probabilistic terms to describe mass breakthrough at a downstream boundary, provide a better framework for implementing and interpreting predictive simulations. The stochastic framework can also provide estimates of prediction errors in concentration and travel time. Stochastic continuum concepts have been proposed for single-porosity models, and there is no difficulty, in principle, in extending the approach to a dual-porosity formulation.

It is normally assumed that the fractured medium is heterogeneous, but the statistical parameters that describe the heterogeneity are uniform in the region of interest (statistical homogeneity). If this assumption is appropriate, the probability model characterizing the fractured medium is reduced to a form expressed in terms of a mean, variance, and three-dimensional correlation structure for each variable of interest (e.g., hydraulic conductivity and porosity). The correlation structure is a measure of the degree of spatial continuity of the hydraulic conductivity values. The many tools developed for geostatistical analysis of heterogeneous media come into play here (e.g., Isaaks and Srivastava, 1989). Estimates of hydraulic conductivity from single-hole packer tests provide the point values for statistical characterization of the heterogeneity. Figure 6.9a illustrates log hydraulic conductivity profiles obtained from straddle packer tests in several boreholes at the Oracle site in Arizona (Jones et al., 1985). The semivariogram characterizing the spatial continuity in log hydraulic conductivity is plotted in Figure 6.9b. The fractured granite is represented by a continuous but spatially varying set of hydraulic properties. Figure 6.9c is one possible representation of the hydraulic conductivity variations along a cross section connecting four boreholes. This representation preserves the values measured at the borehole locations, yielding a so-called conditional stochastic model.

Once the hydraulic conductivities have been estimated, stochastic flow theory provides equations to estimate the effective conductivity ellipse for an anisotropic porous medium (e.g., Gelhar and Axness, 1983; Dagan, 1987). These equations can also be used to estimate a set of field-scale dispersion coefficients. This approach has been illustrated for a fractured rock system by Neuman et al. (1985) and Neuman and Depner (1988). The stochastic equations also permit estimates to be made of the magnitude of the uncertainties in flow and transport predictions. As an alternative to estimating parameter values in a governing stochastic equation, multiple realizations of the hydraulic properties of the rock mass can be generated from the probability model (e.g., Figure 6.9) and used in a Monte Carlo simulation to estimate probability distributions of output variables, such as volumetric flows or groundwater travel times.

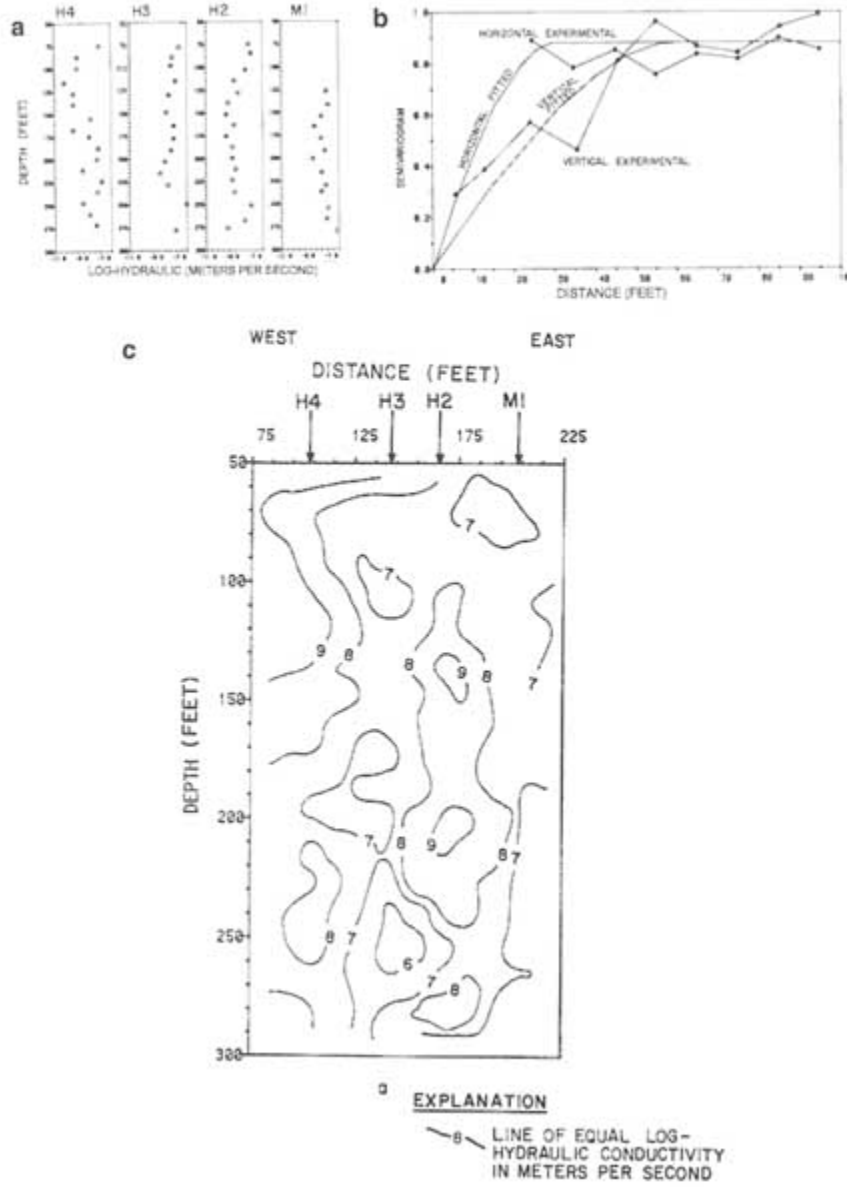

FIGURE 6.9 Geostatistical characterization of hydraulic conductivity at the Oracle site in Arizona. (a) Log hydraulic conductivity profiles from straddle packer tests in four boreholes. (b) Anisotropic semivariogram of log hydraulic conductivity. (c) Geostatistical representation of hydraulic conductivity variations from four boreholes (M1, H2, H3, H4). The plot shows a single realization generated from the conditional stochastic model. From Jones et al. (1985).

The important practical advantage of this stochastic approach is that it works directly with field measurements of hydraulic conductivity, rather than a suite of parameters characterizing network geometry. Its validity depends on the suitability of approximations embodied in the representation of the fractured rock mass as a heterogenous porous medium with a statistically homogeneous structure and in the suitability of mathematical simplifications that underlie stochastic transport theory.

Assessment of Continuum Modeling

The strength of the continuum approach lies in its simplicity; it reduces the geometric complexity of flow patterns in a fractured rock mass to a mathematical form that is straightforward to implement. For most applications that are encountered in practice, some type of continuum approach remains the preferred alternative. The two greatest limitations of deterministic continuum models of the kind most widely used today are (1) the scale at which the continuum approximation is justified can be difficult to quantify and in fact may not be justified at the scale of interest or, for that matter, at any scale and (2) the process of spatial averaging restricts model predictions to scales greater than or equal to that of the representative elemental volume (REV). The concept of the REV may be irrelevant to most field measurements, especially in fractured rock (Beveye and Sposito, 1984, 1985; Neuman, 1987, 1990). Most small-scale field measurements do not correspond to REVs. If these measurements represent a statistically homogeneous field, then under special circumstances, such as uniform mean flow in an unbounded media, an REV can be defined on a scale that exceeds many times the spatial correlation scale of the measured data (and many more times the scale of the actual local measurement) (Long et al., 1982; Neuman and Orr, 1993). Seldom can the corresponding REV scale permeability be determined directly by field tests and almost never so in low-permeability fractured rocks. In most circumstances, and especially in multiscale media of the kind fracture rocks are thought to be, an REV can never be defined. If the concept of an equivalent continuum is not applicable in reality then there may be a broad class of hydrogeological problems that are not amenable to analysis with conventional continuum models. This concern is particularly relevant in the case of solute transport.

It is common in a fracture system to find well test responses that are not normally viewed as indicative of continuum behavior. For example, for a pumping well with two observation wells, the farther observation well may respond more quickly than the nearer one. This type of response is due to the nature of fracture interconnections. While such behavior can be reproduced in a continuum model by adopting a heterogeneous hydraulic conductivity distribution (i.e., a local-scale representation of the spatial variability in hydraulic conductivity), the appropriate model structure will end up looking much like a discrete fracture model.

Stochastic continuum models, which represent the fractured rock mass as a continuous random field, represent one approach to dealing with issues of scale. The scale at which the heterogeneity is represented in the model can be tailored to the scale at which measurements of permeability are made in the field. Probabilistic predictions of fluid flow and solute transport can then be made at a larger scale.

A number of important issues have yet to be resolved in applying continuum approximations. There is the basic issue of applicability and robustness of assumptions that underlie a continuum representation. There is the issue of how to identify the scale at which the continuum approximation is valid, if there is one. There is a need to develop an understanding of what field observations, including but not limited to hydraulic interference testing, may be helpful in indicating the scale of continuum behavior. A description of the dominant fluid pathways in a fractured rock is critical in a transport simulation. Methods for implementing this information in the framework of a continuum model require further investigation, especially in the case of sparsely fractured rock masses.

DISCRETE NETWORK SIMULATION MODELS

Why Consider Discrete Network Models?

Fractured masses are composed of blocks separated by discontinuities, and therefore discontinuum models may be an attractive approach to representing these systems. Discontinuities occur at a variety of scales; they have different geometries and flow properties, and these properties may vary with location and direction. Discontinuum models must account for these complexities. In particular, the fact that discontinuities are not persistent (i.e., they are bounded by intact rock) is most significant because the characteristics of intact rock and of the discontinuity differ substantially. (This is not only so for fluid flow in a rock mass but also for rock mass stability and deformability.) The knowledge of individual fracture characteristics in situ is limited, and the persistence of fractures is not known. This so-called persistence problem can only be solved through the use of stochastic models and probabilistic approaches incorporated into these models.

Discrete network models are predicated on the assumption that fluid flow behavior can be predicted from knowledge of the fracture geometry and data on the transmissivity of individual fractures. The guiding principle is that spatial statistics associated with a fracture network, including fracture transmissivity, can be measured, and these statistics can be used to generate realizations of fracture networks with the same spatial properties. The fractures in these realizations become the conductive elements in a fracture network flow or transport model (e.g., Hudson and La Pointe, 1980; Long et al., 1982; Dershowitz, 1984; Endo et al., 1984; Robinson, 1984; Smith and Schwartz, 1984). Application of

network models to field sites requires the measurement of fracture geometry to construct models that reproduce the observed statistics of the geometry of the fracture network. This method involves choosing a stochastic rule for locating fractures and determining their orientation, extent, and conductivity. Various issues involved in collecting and analyzing statistical data on fracture networks are reviewed later in this section, followed by the outline of a number of models that have been proposed to represent the statistical characteristics of fracture networks.

Discrete network models are closely linked with concepts of stochastic simulation. Network geometry is characterized by statistical descriptions of fracture orientation, location, areal extent, and transmissivity for each of the fracture sets in the rock mass. From this statistical model it is possible to generate multiple realizations of a fracture network and to solve for fluid flow through each network. Each realization is one possible representation of the fracture network in the rock mass from which the geometric properties were mapped. For example, Figure 6.10 shows three different fracture networks, each of which is one realization from stochastic models with differing fracture densities (expressed as a scan line density, i.e., the average number of fractures per meter encountered along horizontal and vertical sample lines).

For each realization a large-order system of equations is solved to determine the distribution of hydraulic head at all points in the fracture network. This is accomplished by modeling flow in each fracture and ensuring conservation of fluid mass at fracture intersections. By averaging the flow behavior for a large number of realizations of the same stochastic model in a Monte Carlo simulation, inferences can be made about the expected behavior of the system and the variability about the mean. The behavior of interest may be fluid flux across the fracture network or, in the case of a contaminant transport problem, the travel time of solutes from a recharge boundary to the outflow boundary. This property is illustrated in Figure 6.10, where the mean and standard deviations in breakthrough time at the downstream boundary are given for the three different fracture densities. In this case the standard deviation can be interpreted as a measure of the uncertainty in predicting the time at which solutes first arrive at the downstream boundary. Similar statistics on the arrival time of mass at the downstream boundary could have been developed by using the stochastic continuum approach if, instead of characterizing the network geometry, the rock mass had been represented as a continuous random field of local-scale permeability values. This figure clearly demonstrates the strong dependence of travel time statistics on the geometric properties of the fracture network.

By conditioning the model on the location of known fractures or measured values of fluid flux, it is possible to quantify the extent to which uncertainty is reduced with the availability of specific types of field data. Anderson and Thunvik (1986) generated multiple realizations of a fracture network; each network preserved the locations of fractures that would have been mapped in a set of hypotheti

cal boreholes. As expected, they found that adding more boreholes (and thus adding information on the location of fractures as mapped on the borehole walls) decreased the uncertainty in a transport prediction. However, other factors such as fracture length, fracture line density, and the spatial correlation of aperture along a fracture exerted a strong influence on the value of the geometrical data

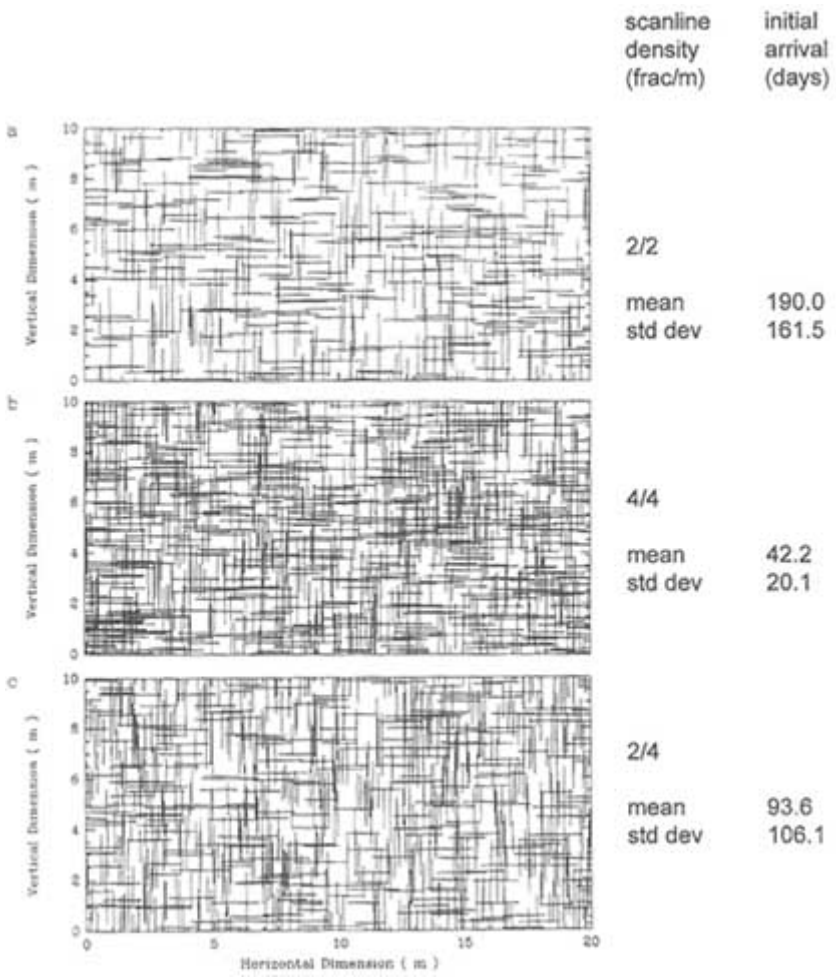

FIGURE 6.10 Examples of single realizations for three fracture systems with differing fracture densities (measured as scanline densities; see text). Numbers on the right are the mean and standard deviations of travel times for solutes that enter the left side of the systems through a single fracture and travel downstream to the right side of the systems. Modified from Smith and Schwartz (1993).

obtained from borehole logging. Knowledge of the bulk permeability of the fracture network led to a greater reduction in uncertainty than the collection of additional geometrical data on fracture location. This response occurred because knowing fracture location along a borehole does not provide information about fracture extent. The information is not sufficient to determine interconnectivity and therefore permeability (Long and Witherspoon, 1985). Conditioning on the bulk permeability provided a stronger constraint on estimates of the rate of advective mass transfer than did geometric data on fracture location without additional information on fracture connectivity, which cannot be obtained from borehole fracture intersections.

To apply discrete network models in a field setting, it is essential to have the capability for three-dimensional simulation. In these models, fractures are represented as disk-shaped or polygonal features, rather than line segments. The degree to which higher-transmissivity regions on one fracture plane connect with those on other fractures will determine the connectivity of the network, fluid pathways, and transport patterns. By modeling flow in each fracture and ensuring conservation of fluid mass at fracture intersections, a large-order system of equations is solved to determine the distribution of hydraulic head at all points in the fracture network. A number of three-dimensional flow models are described in the literature (e.g., Long et al., 1985; Shapiro and Anderson, 1985; Elsworth, 1986; Dverstrop and Anderson, 1989). Examples of the application of different three-dimensional network flow models are the studies by Dershowitz et al. (1991a), Long et al. (1992b), and Herbert et al. (1991) of the Stripa Site Characterization and Validation Experiment. Also, some work has been reported on three-dimensional network models for solute transport (Smith et al., 1985; Cacas et al., 1990; Dershowitz et al., 1991a, b; Herbert and Lanyon, 1992; Nordqvist et al., 1992; Segan and Karasaki, 1993a).

Three-dimensional network models are of three general types: (1) semi-analytical models (e.g., Long et al., 1985); (2) equivalent one-dimensional pipes arranged in three-dimensional space (e.g., Segan and Karasaki, 1993); and (3) discretized fracture planes, where a two-dimensional numerical grid is constructed in each fracture plane (e.g., Smith et al., 1985; Dershowitz et al., 1991a; Herbert and Lanyon, 1992). A network of planar fractures may require 10^5 to 10^6 nodes to adequately resolve the flow field, even for a relatively sparse fracture network. When it is necessary to generate multiple realizations of the network for analysis, computational requirements are very demanding.

One-dimensional pipe models have been adopted in an attempt to reduce the computational requirements associated with a fully three-dimensional representation. The fracture network is first generated in a three-dimensional framework and then is collapsed to a system of one-dimensional pipes to solve for fluid flow. Flow in each fracture plane is reduced to a single representative pipe centered in the middle of the fracture plane (Cacas et al., 1990) or to an arbitrary number of pipes (Segan and Karasaki, 1993). A one-to-one correspondence

between pipe properties and the actual three-dimensional geometry governing flow is theoretically possible. However, the actual geometry governing flow is rarely, if ever, known. The model parameters are probably best viewed as calibration variables rather than physically based properties of the medium.

Geological Issues in the Statistical Representation of Fracture Networks

Some geological settings may be more amenable to statistical analysis of fracture patterns than others. The statistical method will work best if (1) the fracture pattern is uniform in a statistical sense (statistical homogeneity); (2) it is possible to obtain a sample that is statistically representative; (3) the spatial distribution of fractures is not too complex, that is, it can be described by a simple rather than a compound stochastic process; and (4) the fractures used to determine fracture statistics actually do conduct fluid. Favorable conditions for discrete network modeling might best be met, for example, in some jointed rocks. These factors are similar to the conditions suited to the application of continuum models. Consequently, discrete models may also provide a method for obtaining the parameters used in continuum models, as discussed later.

Strata-bound joints that have relatively regular patterns in a given strata have been observed in bedded volcanics and sedimentary rocks such as bedded limestones (Pollard and Aydin, 1988). Joint patterns amenable to statistical analysis also have been observed in massive rocks (Segall and Pollard, 1989). Joints commonly occur in subparallel sets with variable spacing. Figure 2.30 shows some common joint system patterns. These patterns provide the basis for many of the conceptual models described below. The existence of common joint geometries with recognizable patterns has been one of the primary motivations for the statistical approach.

The nature of joint intersections is an important attribute of joint systems. Some examples are shown in Figure 2.30. If joints intersect other joints, a hydraulic connection can be formed between them. If one set terminates near another without actually intersecting, there may be no hydraulic communication.

Joint systems can exhibit complexities that affect statistical modeling of network geometry. Joint frequency may be spatially variable. Spacing can be a function of depth, lithology, or bed thickness. Joint clusters or zones also occur and may be difficult to include in a statistical model. Joints are commonly formed episodically and have segments corresponding to each episode, each with varying properties. Extensive folding and faulting of jointed rock may be responsible for the development of large dominant flow structures that are not well represented in a statistical sense. Multiple deformations can lead to preferential fracturing along preexisting planes of weakness, resulting in a style of fracturing that is very heterogeneous and complex.

It is important to recognize that, owing to a variety of geological processes, large parts of the observable fracture system may be uninvolved in fluid circula

tion. This issue points to a basic concern for the discrete fracture approach because it uses the observable fracture geometry to predict flow and transport behavior. A significant proportion of fractures may be nonconductive, because they are either closed or sealed by mineral precipitates. A model based on fracture occurrence without accounting for fractures that are nonconductive will vastly overestimate interconnectivity. This lack of interconnection is the main reason that discrete network models are chosen over equivalent continuum models, but it is also the reason that homogeneous network models may fail to capture the distribution of hydraulic conductors and consequently fail to reproduce the hydraulic behavior of the fracture network.

Evidence of hydrologically inactive fractures has been found at numerous sites. For example, at the Fanay-Augeres mine in France, thousands of fractures were mapped in tunnel walls and in boreholes from the tunnel. Models created with fracture size, orientation, and location statistics for this tunnel resulted in highly interconnected fracture networks (Long and Billaux, 1987; Billaux et al., 1989; Cacas et al., 1990). However, none of these models were able to reproduce the fundamental observation that there is no hydraulic communication between some of the boreholes. Another example is the Stripa mine, discussed earlier, where 80 percent of the water flowing into a drift was carried by one fracture, even though many of the observed fractures have the same orientation and should have roughly the same state of stress acting on them. These measurements suggested a high degree of interconnection in the observed fracture network (Herbert et al., 1991). However, out of thousands of fractures intersecting the drift, only a few conducted water.

Stochastic Models of Fracture Networks

The representation of discontinue and solution of the persistence problem only became possible with the introduction of stochastic models for representing network geometry. As will be seen below, the first stochastic fracture models had only a few stochastic characteristics; the remainder were spatially invariable. Most important, fractures (discontinuities) were unbounded, thus not providing a solution to the persistence problem. The introduction of bounded fractures came with the introduction of two models: the Baecher disk model and the Veneziano polygonal model. Most subsequent fracture network models for rock mass flow, rock mass stability, and rock mass deformation were based on these models. Although these models represented a major advance, the assumed independence of their geometric characteristics made representation of typical fracture properties such as clustering impossible. Spatial dependence in stochastic models was introduced through a variety of statistical and quasi-mechanistic concepts (Long and Billaux, 1987; Lee et al., 1990; Martel et al., 1991) and through fractal representation (Barton and Larsen, 1985). The increasing complexity of the

models brings them closer to reality but makes the inference procedures by which the field data can be transferred into the model increasingly difficult.

Two classes of stochastic models can be used to describe fracture systems. One is based on the assumption that the occurrence of one fracture has no influence on the positioning of any subsequent fracture that is generated to form the network. Fracture centers are located by using a uniform probability distribution. These models are discussed here and are reviewed in more complete detail by Dershowitz and Einstein (1988). The second class of models allows for a spatial dependence between the positioning of neighboring fractures, and it leads to networks with recognizable, scale-dependent characteristics. This latter class of models is discussed later in this chapter. Both model classes have rules for specifying fracture characteristics, including (1) the location of fractures in space; (2) the shape of fractures; (3) the extent of fractures, including truncations against other fractures; (4) the orientation of fractures; (5) the conductive properties of fractures; and (6) in some cases the conductive properties of fracture intersections.

Orthogonal Models and Their Extensions

The simplest fracture model is the orthogonal model that is based on three sets of unbounded orthogonal fractures (Figure 6.11). In two dimensions this corresponds to the network shown in Figure 2.30a. This model was characterized

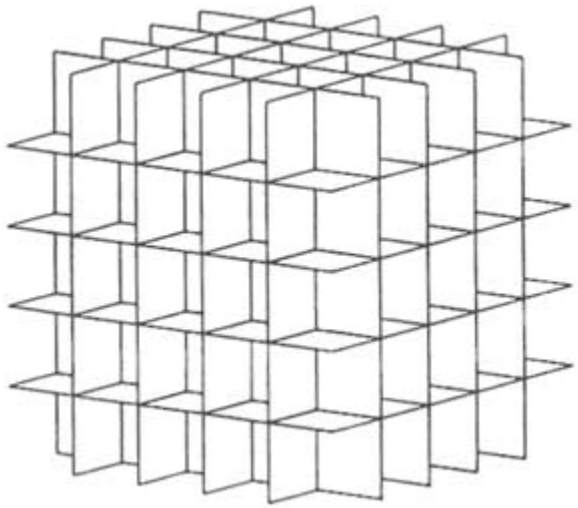

FIGURE 6.11 Three-dimensional orthogonal fracture model. From Dershowitz and Einstein (1988).

by Irmay (1955) and Childs (1957), among others. A series of models can be created as modifications of this basic structure by allowing the orientation, extent, location, and conductivity of the fractures to vary (Snow, 1965). For example, the networks in Figure 2.30 c–f can be considered two-dimensional modifications of the orthogonal model.

Poisson Plane Models

Probably the most important stochastic process used to define fracture system geometry is the Poisson process. This random process is controlled by only one parameter, a density parameter, that specifies the average density of objects in space—that is, the average number of objects (points, lines, or planes) per unit line length, unit area, or unit volume. Priest and Hudson (1976) were the first to recognize the similarity between the geometry of rock fracture systems and the attributes of Poisson processes. In particular, the distances along a line sample between objects of a Poisson process are distributed according to a negative exponential distribution. This distribution is commonly observed for fracture spacing along a scanline. The simple Poisson plane fracture model of Priest and Hudson was based on the assumption of unbounded fractures. In their model, fractures were located randomly by having each fracture pass through a point in space that is determined by a Poisson process. The orientation of the plane was then determined independently, according to an appropriate probability distribution.

More complex models are defined with bounded fractures. These models are of two types: (1) those that define fracture shape and size distribution a priori and (2) those that define a process that, in turn, defines fracture shapes and sizes. For the first type of model, fractures are usually assumed to be rectangles or ellipses. They can have any size distribution and are placed in space centered on Poisson points and oriented randomly according to any distribution specified (see Figure 6.12). Such models have been developed by Baecher et al. (1977), Barton (1978), and Robinson (1984). The Baecher model has been used in rock mechanics applications by Einstein et al. (1980, 1983) and Warburton (1980a,b) and for fracture flow modeling by Long et al. (1982, 1985) and Dershowitz (1984). The Robinson model has been used by Herbert et al. (1991) at the Stripa mine. Geier et al. (1989) proposed an extension to the Baecher model to account for the probability of fractures in one set terminating at the intersection with another set. It is also possible to use the Poisson process to create a polygonal grid of fracture elements (a pattern similar to Figure 2.30g; see Khaleel, 1989).

The second type of model defines a stochastic process to determine fracture shape and size. The usual process is to start with the unbounded Poisson planes and superimpose on them a series of Poisson lines. The lines can be created independently, as in Figure 6.13 (Veneziano, 1978), or by the lines of intersection between the unbounded Poisson planes, as in Figure 6.14 (Dershowitz, 1984).

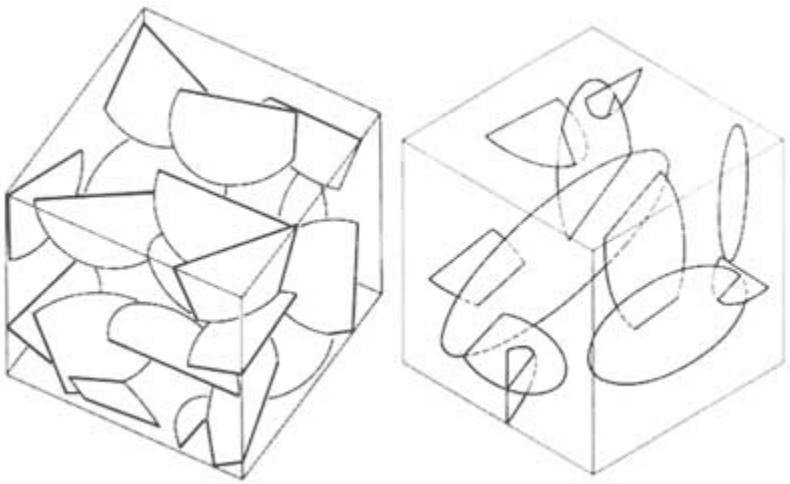

FIGURE 6.12 Baecher disk model of a fracture system. From Dershowitz and Einstein (1988).

The lines divide the planes into polygonal areas, each of which is then assigned some probability of being an open fracture. It is very easy to construct networks with coplanar fractures with these models. Veneziano (1978) demonstrated that this type of model leads to an exponential distribution of fracture trace lengths, which contrasts with the lognormal distribution found in the Baecher model. The Veneziano model has been applied to slope stability problems by Einstein et al. (1983) and to the hydrology of fractured rock masses by Rouleau (1984). Both of these applications utilized the Veneziano model in a two-dimensional trace plane only. The geometry of the Veneziano model is quite complex in three dimensions.

Estimation of Model Parameters for Statistical Models of Fracture Networks

To build a fracture network model, field data must be collected to estimate the parameters of the stochastic model used to represent the network geometry. The following data are normally required:

- Fracture location as observed in boreholes or along scanlines in either surface outcrop or subsurface excavations.
- Fracture orientation from borehole logs, core, surface outcrop, or subsurface excavations. The orientation of fractures that intersect planes may have to be estimated from apparent orientation, that is, the orientation of the trace of the fracture plane.

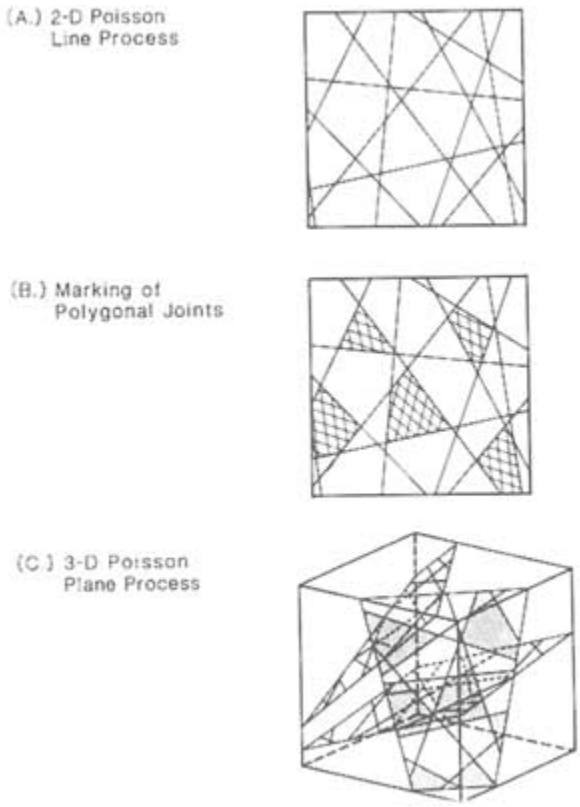

FIGURE 6.13 Veneziano polygonal model of a fracture system. From Dershowitz and Einstein (1988).

- Fracture trace length in outcrop or underground excavations.
- The percentage of fractures that terminate against other fractures as a function of orientation, as obtained from outcrop or underground excavation.
- Estimates of the transmissivity of individual fractures from hydraulic tests.

There are two approaches to using this data to parameterize the models described above. In the first approach the parameters of the model are calculated directly from the fracture statistics. This method works best for the simplest models, primarily those based on simple Poisson processes. A good example of this approach was the work of Herbert et al. (1991) at Stripa. As more of the spatial relationships between fractures are accounted for, it is harder to calculate the parameters directly. In these cases an inverse approach becomes more attractive. In the inverse approach a set of parameters is proposed for a given conceptual

model and used to generate the geometry of a fracture network. Then a series of simulated networks is sampled in a manner congruent to that used in the field: simulated boreholes or surfaces are used to collect fracture spacing, orientation, and trace length. The simulated data are compared to the real data, and adjustments are made to the model parameters to improve the fit to the observed data. In effect, this is model calibration. Dershowitz et al. (1991a) provide a good example of this approach.

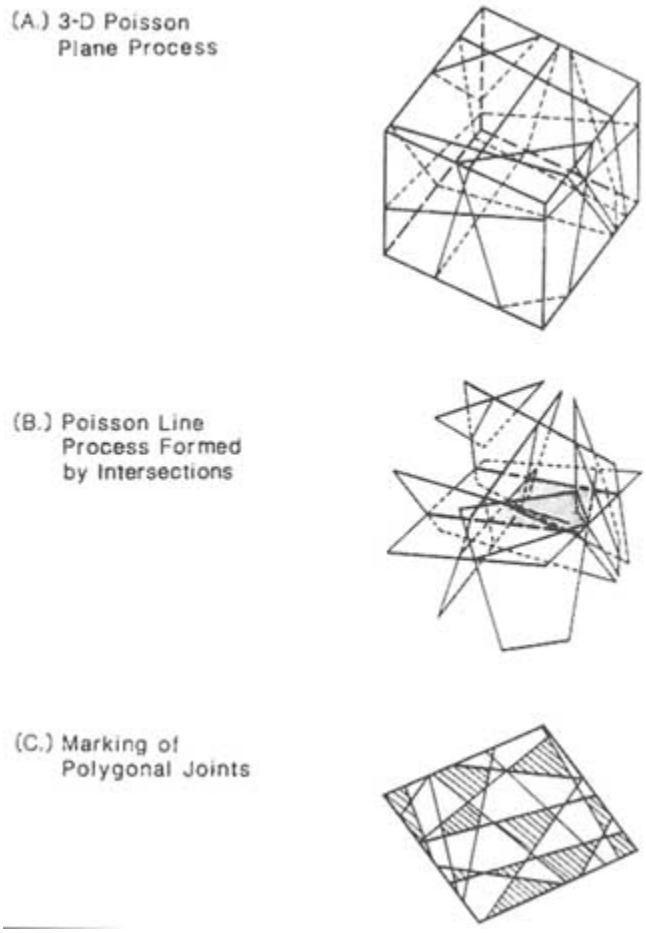

FIGURE 6.14 Dershowitz polygonal model of a fracture system. From Dershowitz and Einstein (1988).

All fracture data collection procedures are affected by uncertainties introduced by the sampling procedure (errors, biases, statistical fluctuations), which,

combined with the spatial uncertainty discussed throughout this chapter, model uncertainties, boundary condition uncertainties, and omissions, affect the representation of geology and engineering performance predictions (for a complete discussion of uncertainties in engineering geology, see Einstein et al., 1980). Of particular interest in the context of this section are the uncertainties caused by errors and biases. In the following discussion on data collection for stochastic model representation, typical biases that must be considered will be mentioned. These are only examples and they are far from complete. For a more comprehensive treatment of sampling biases and errors, including possible corrections, see Einstein et al. (1979) and Baecher (1972).

Fracture Density

To build a Poisson model, the fracture density per unit volume must be known. The advantage of the Poisson distribution is that analytical relationships exist between densities that can be measured and those that are needed to generate a network. For example, given the density of fracture intersections along a line (i.e., fracture frequency) and the fracture size and orientation distributions, it is possible to calculate the expected number of fractures per unit volume (volumetric fracture density). A simple example is for fractures with mean area, A, and a distribution of orientations, $f(\theta)$, where θ is the angle between the fracture poles and the sample line (e.g., a borehole). The fracture pole is the unit vector perpendicular to the fracture plane. The relationship between volumetric density (number of fractures per unit volume, N_v) and linear density (fracture frequency, N_L) is

$$N_L = N_v A \langle \cos \theta \rangle,$$

where $\langle \cos \theta \rangle$ is the mean orientation of the fracture set (Terzaghi, 1965). This equation shows that the probability of encountering a fracture in a borehole, N_L, is proportional to the fracture size and the number of fractures per unit volume, N_v. This probability is higher for fractures perpendicular, $\cos \theta = 1$, to the borehole than for fractures parallel to it, $\cos \theta = 0$. Consequently, if the sample lines are parallel to the fractures, it may be difficult to get a good estimate of fracture density.

Fracture Orientation

Obtaining the orientation distribution is conceptually simple but practically difficult. Errors in the construction of orientation data sets are common because the analysis is three-dimensional and there are many potential sources of error. After correction, the orientation in space of each fracture encountered in the sample is measured. The pole of each fracture is normally plotted on a stereographic projection, either a Wolff net or a Schmidt net. Then clusters can be identified and used to group fractures into sets. For each set the orientations can

be fitted to a distributional form such as a spherical normal (or Fischer) distribution (Mardia, 1972), or the sample distribution can be used itself. There is some sentiment that identification of fracture sets by an "eyeball" fit may be as effective as the more sophisticated analytical methods.

It is necessary to account for possible sampling biases. In the case of the orientation distribution, this bias arises from the difficulty in determining the orientation distribution for fracture sets parallel to the sampling line or plane. The Terzaghi (1965) approach to correcting for orientation bias is to divide the density of fractures in a similarly oriented group by $<\cos \varphi>$, where φ is the angle between the sampling line or plane and the poles of the fractures for that group, thereby increasing the frequency of fractures parallel to the sample line. This approach has the underlying assumption that the sampling of fractures nearly parallel to the borehole is representative. It is not possible to know whether the absence of fractures parallel to the borehole is real or is due to sampling bias. An alternative proposed by Martel (1992) and Martel and Peterson (1993) involves comparison of the sampled orientations with orientation distributions obtained by sampling a series of synthetic distributions in the same manner that field data were taken. In this way one can determine if the sampling scheme is sensitive to the possible choices of orientation distribution.

Fracture orientations obtained from outcrop or underground excavations can be measured directly if the fracture surfaces are exposed. Otherwise, only apparent orientations can be measured, that is, the orientation of the fracture trace. Orientation data can also be obtained from boreholes by using the logs described in Chapter 4 or from core, although there can be difficulties in getting reliable data. Cores tend to twist on extraction, causing orientation errors. Pieces may be missing or broken, making it difficult to orient sections of the core. Borehole imaging logs (Chapter 4) can be used where there is missing core. More fundamentally, the orientation of the fracture where the core was taken may not be representative of the average orientation of the fracture. On the practical side, there is probably no other effort in the analysis of fracture statistics that deserves a good-quality assurance program as much as the data collection and reduction process for fracture orientation.

Fracture Size

From available exposures, the distribution of fracture size is obtained from the orientation data and fracture trace data. Rarely, if ever, can the actual areal extent of a fracture be observed directly. The trace length sample must first be corrected for bias, as discussed below. Then the corrected trace length distribution can be used to predict the distribution for fracture area. The relationship between the trace length distribution and the size distribution depends on fracture shape. Normally, it is necessary to make an assumption about the shape of the fracture (e.g., disk-shaped) and then estimate the size distribution from the sample data.

When mapping in adits, it is important to distinguish between fractures caused by blasting and those that reflect in situ conditions. It is also important to characterize the types of fracture intersections. Fractures may either cross or one may terminate against the other. Termination can be quantified simply by noting the percentage of fractures of a given set that terminate against other fractures.

There are four biases affecting the estimation of fracture size: length bias, orientation bias, truncation bias, and censoring. Small fractures will be underrepresented, as there is a lower probability of intersecting smaller fractures than larger fractures (length bias). Fractures parallel to the sampling plane will also be underrepresented (orientation bias). Fractures shorter than a predetermined length are usually not mapped (truncation bias). A censoring bias is introduced because the sample area is finite, and the fracture traces may not be completely visible (Baecher et al., 1977). Censoring bias is most important for longer fractures, which are generally the more conductive fractures. With respect to censoring bias, fracture traces can be divided into three groups: (1) traces with both endpoints visible, (2) traces with one endpoint visible, and (3) traces with no endpoints visible. The trace length distribution of the first group can be determined. These fractures have a maximum length determined by the dimensions of the sample area. For the second group a distribution of minimum lengths can be found. For the third group all that is known is that the fracture traces are larger than the sample dimensions. Some analytical solutions to the censoring problem have been obtained by assuming a distributional form for the trace lengths (Long and Billaux, 1987; Einstein et al., 1979, vol. IV). Similarly, if a distributional form is assumed for the fracture areas, one can use the corrected trace length distribution to estimate the parameters of the area distribution (Long and Billaux, 1987). Dershowitz et al. (1991a) have developed an automated procedure for generating fractures of a given size distribution and sampling the system the same way the field data were sampled. The prospective area distributions can be easily modified until a good (but necessarily unique) match to the field data is found. If only borehole measurements are available, problems associated with obtaining estimates of fracture size can be severe.

Transmissivity of Individual Fractures

In applying a discrete network model, the characterization of transmissivity values is likely to be a dominant source of uncertainty in a flow or transport simulation. It was once thought that the hydraulic conductivity of each fracture could be obtained from a physical measurement of aperture and application of the cubic law (Iwai, 1976). As explained in Chapter 3, complications of roughness, filling, and contact area indicate that fracture transmissivity should be measured directly. Such in situ measurements have been attempted through packer tests from boreholes. An interval, as small as practical, is isolated in a borehole, and a well test is carried out. The transmissivity calculated from the test is then

attributed to the fractures intersecting the borehole interval. A number of assumptions must be made in order to obtain the distribution of fracture transmissivities from these borehole tests. Usually it is not possible to isolate single fractures. Consequently, one must decide how to distribute the observed transmissivity among the fractures that intersect the borehole interval. Further, in calculating the transmissivity, it is normal to assume that the fractures are infinite in extent and perpendicular to the borehole. Fracture intersections, branching, and terminations are not accounted for. Any correlation between fracture transmissivity and length is very difficult to determine, but such correlation significantly increases network permeability (Shimo and Long, 1987).

Local estimates of transmissivity from a number of well tests provide an initial estimate of the statistical distribution of transmissivity for individual fractures. However, these estimates are significantly affected by lack of information about the number, relative conductance, orientation, and extent of fractures intersecting the test zone and the intersection of the tested fractures with other fractures. Thus, it is usually not possible to obtain good estimates of fracture transmissivity distributions, and it is inevitable that some kind of model calibration will be required to refine the estimates of fracture transmissivity.

Calibration of a discrete network model can involve estimates for hundreds or thousands of variables (e.g., an effective transmissivity value for each fracture in the network). An even greater number of variables is introduced if the inversion seeks estimates of transmissivity for fracture segments between intersections, relaxing the assumption that each fracture has a single transmissivity. Inevitably, there will be no unique set of transmissivity values that explain the observational data. An alternative calibration strategy is to simply refine estimates of the mean and variance of the transmissivity distribution, by matching the observed variability in transmissivity to that predicted by the model.

Applications of Discrete Network Models in Media with Significant Matrix Porosity

Discrete network models are necessarily more complex in cases where (1) the permeability of the rock mass in which the fracture network is embedded is a significant fraction of the network permeability or (2) the porosity of the rock matrix is high or the time scale of interest is long enough that diffusive mass transfer becomes a factor in determining large-scale solute transport patterns. Several methods have been developed to model flow and solute transport in geological units containing a network of fractures embedded in a porous matrix. The fracture network is modeled explicitly, unlike a conventional dual-porosity model. McKay et al. (1993) have applied an analytical model describing advective/diffusive transport in evenly spaced, parallel fractures to model tracer tests at an experimental site in a fractured clay till. The principal difficulties in solving these problems numerically are the different time scales involved for transport

along the fractures and in the matrix and the need for a fine grid resolution to represent sharp concentration gradients at the fracture-matrix interface. Using a Laplace transform technique in conjunction with a finite-element model, Sudicky and McLaren (1992) have overcome these problems. Figure 6.15 provides an example showing a calculation of the concentration distribution in both the fracture network and the matrix blocks in a medium where matrix porosity is 30 percent. The concentration distribution bears little resemblance to that which would be observed in an unfractured aquitard. Similarly, matrix diffusion is effective in slowing down the rate of advance of contaminants through the aquitard, in comparison to a case where mass transport is limited to the fracture network. Dershowitz and Miller (1995) describe an implementation of a discrete fracture model in which matrix diffusion is simulated using a probabilistic particle tracking technique. Okusu et al. (1989) created a mesh generator that can discretize the matrix for any two-dimensional fracture network. Given the mesh, a variety of flow and transport models can be invoked.

Another possibility for solving this problem is to treat the fracture flow explicitly and the matrix flow semianalytically. The flow into or out of the matrix can be determined through the use of a proximity function that describes the cross-sectional area of the matrix block as a function of distance from the fracture (Pruess and Karasaki, 1982; Figure 6.16). The fracture network (Figure 6.16a) is divided into connected elements and dead-ends plus isolated fractures (Figure 6.16b). The matrix area is divided into regions that are equidistant from connected fractures (Figure 6.16c). It is then possible to construct a "proximity function" that gives the cross-sectional area of matrix as a function of proximity to a fracture containing fluid flow. This function can be used in a double-porosity model to describe fracture-matrix interactions in a statistical sense.

Assessment of Discrete Network Models

There are two views concerning the utility of discrete network models. One view is that they are primarily a tool for concept evaluation or model-based process studies (e.g., Long and Witherspoon, 1985; Smith and Schwartz, 1984). Studies of this type have proven useful in examining requirements for characterization of a fracture network as an equivalent porous medium, studying the scale dependence of the dispersion process, examining how network geometry influences spreading patterns, and evaluating issues related to the reliability of data on fracture position and orientation.

The second view is that discrete network models are practical tools for site-specific simulations (e.g., Dershowitz et al., 1991a; Herbert and Lanyon, 1992). The advantage of a discrete fracture simulation is that volume-averaging approximations are avoided at the scale of the fracture network. In cases where an equivalent continuum cannot be defined, discontinuum network simulation is a viable alternative.

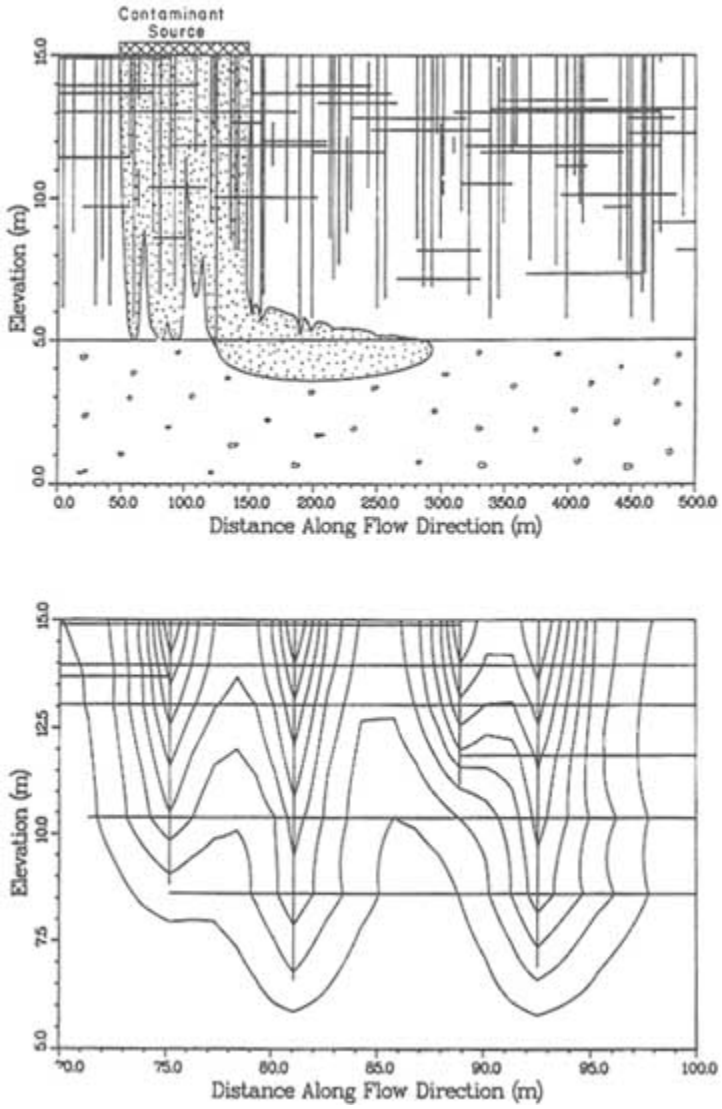

FIGURE 6.15 Prediction of solute distribution using a discrete network model in a medium where matrix diffusion is important. A fractured low-permeability aquitard overlies a permeable aquifer (lower unit). The fracture network is shown as straight lines; the contours of contaminant concentration appear as curved lines. The upper plot shows the plume at t = 200 years. Only the outer contour with a normalized concentration of 0.01 is shown. The lower plot is a detailed view of a part of the plume. The outer contour is a normalized concentration of 0.1; the contour interval is 0.1. From Sudicky and McLaren (1992).

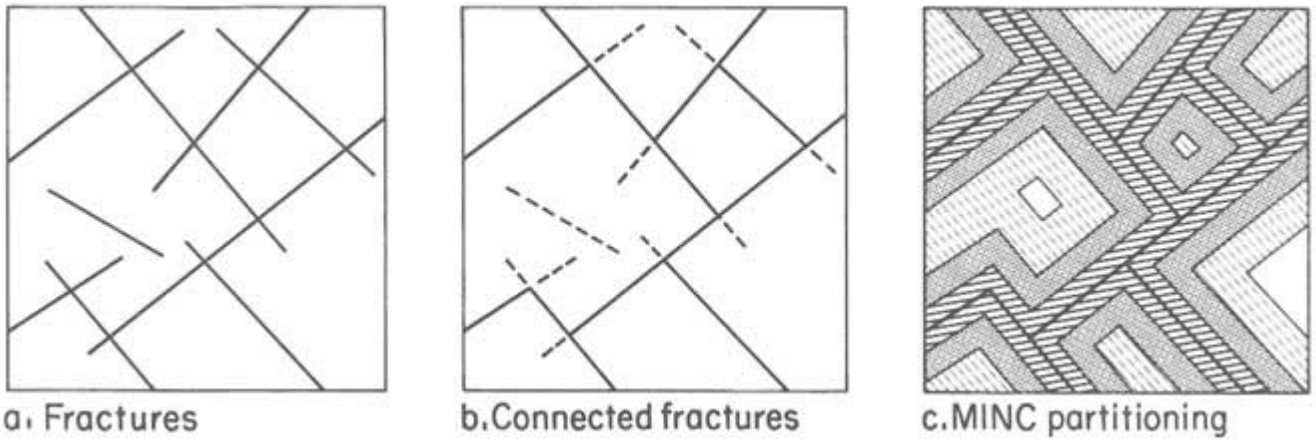

FIGURE 6.16 Illustration of the construction of a proximity function for an arbitrary two-dimensional fracture distribution. (a) Fracture network. (b) Connected fractures in the network are indicated by solid lines; extensions of the fractures that are not conductive are shown by dotted lines. (c) Division of the matrix area into regions (indicated by different patterns) that are equidistant from the connected fractures. These regions are used to calculate the proximity function. From Pruess and Karasaki (1982).

To be useful as a simulation tool, discrete network models must incorporate information concerning the dominating fracture features and their positions in three-dimensional space. These capabilities exist. The disadvantages of discrete network simulation are threefold: (1) the method requires statistical information that can be difficult to obtain, (2) it is difficult to separate the conductive fracture geometry from the nonconductive fracture geometry, and (3) the models can be complex and computationally intensive for realistic fracture densities.

These models have been useful in problems of near-field simulation over length scales of 50 to 100 m. Application to larger-scale problems will require modifications such as treating fracture zones as a single fracture in the model and screening of fractures to eliminate the less transmissive ones.

Although theoretical studies using fracture network models have provided valuable insights on how to determine equivalent continuum properties of fractured rock, it is extremely difficult to actually determine continuum properties in the field. The magnitude of permeability estimates is critically dependent on the values assigned to fracture transmissivity. Mechanical measurements of fracture aperture are of little value in this regard, as they do not capture the influence of the internal geometry of the fracture plane on the hydraulic resistance to flow. The observed fracture pattern may not be strongly related to the equivalent permeability if, for example, a significant percentage of the fractures are sealed by mineral precipitates or are closed owing to the stress regime. Billaux et al. (1989) and Cacas et al. (1990) describe how such approaches were applied in an adit at Fanay-Augeres in France and led to hydrological models that are highly overconnected compared to the real system. Calibration data of some kind (e.g., an observed fluid flux) are needed to apply these methods. Whether it be for continuum models or discrete network models, too few prediction studies have been checked against subsequent behavior.

Perhaps the most often heard comment about discontinuum models is that they are not practical. Consequently, researchers have tried to show that this style of model better captures the hydraulic system behavior of a fracture system in order to justify the apparent extra expense. The problem with discontinuum models, as for any model of fracture flow, is that it is extremely difficult to construct a field test that can prove that a model is valid. (This has led some researchers to develop pragmatic definitions of the word *validate*, shaped by what they expect to be able to accomplish rather than what would ideally constitute validation.) Most field tests designed to test and compare models have concluded that a variety of models, including discontinuum models, can reproduce the observed behavior of the system (see, e.g., Olsson, 1992). However, to focus on these projects as validation exercises is to miss the major accomplishment of such work, which is to increase understanding of the hydrology of the media involved. The particular style of modeling is much less important than whether the model includes the features that are dominating the behavior of the system. In fact, during the lifetime of the Stripa Site Characterization and Validation

Project, four teams were developing models of flow and transport for the site. (See Olsson, 1992, for an entree to this literature.) Although these models started from very different approaches, they became more similar with time as more was learned about the site and what features at the site were hydrologically important. The hydrologically dominant fracture zones had to be explicitly entered into all the models, continuum or discontinuum, in order to match the observed behavior. Whether or not the discontinuum codes were more or less efficient than the continuum codes was simply a matter of how they were applied, that is, whether they included and discretized every observable fracture or whether major zones of fractures became one large fracture in the model. These exercises have shown that discontinuum models can be used effectively and may be very efficient at reproducing the lack of connectivity in a fracture network.

HYBRID METHODS: USING DISCRETE NETWORK MODELS IN BUILDING CONTINUUM APPROXIMATIONS

Fluid Flow

Because it is difficult or impossible to measure large-scale permeability directly, it would be extremely useful to be able to estimate such values by taking some kind of average of the local-scale measurements. In the case of fracture systems, discontinuum models can provide a framework for attempting such an analysis. If it is possible to build a discontinuum model based on field data, it may be possible to obtain an estimate of large-scale continuum properties. However, all the difficulties in parameterizing discontinuum models that are described in the previous section apply as well to this endeavor. The use of discontinuum models to study how fracture systems will behave on a large scale has taken two approaches. One approach is to perform numerical flow experiments using fracture network models. The second approach reaches estimates of continuum behavior by looking at the networks as a percolation problem.

Estimation of Continuum Properties from Fracture Network Analysis

Several equations have been developed to estimate the permeability tensor by combining hydraulic data on fracture transmissivity with data on fracture frequency and orientation obtained from geological surveys. One of the first of these equations was developed by Snow (1965). Snow measured the frequency and orientation of fractures encountered in a borehole or along a scanline and combined these data with estimates of hydraulic aperture from packer tests. He assumed that all the fractures were infinite in length and could be modeled as parallel plates. An equivalent permeability tensor was calculated from the orientation and hydraulic aperture of each fracture by simply adding the components from each fracture. Oda (1985) and Oda et al. (1987) developed an analytical

formulation of the permeability tensor that applies to fractures of finite length The basic assumption underlying this formulation is that fracture density is high enough that nearly all the fractures contribute to the effective permeability. Thus, this formula applies to essentially the same cases as Snow's. From an engineering perspective, these equations are the best available to relate fracture geometry to a larger-scale hydraulic conductance. They are limited by the difficulty of obtaining representative estimates of hydraulic apertures and of distinguishing between the apparent and conductive fracture geometry. Most importantly, these methods do not account for the effect of fracture connectivity. This approach was applied to predict the hydraulic properties of fractured granite around a ventilation drift at the Stripa mine. Given estimates of an average hydraulic aperture from in situ tests, estimates of effective permeability were within one order of magnitude of measured values.

Long et al. (1982), Robinson (1984), Dershowitz (1984), and Hudson and LaPointe (1980), among others, have extended the approach of estimating continuum properties from a fracture network analysis by developing models of fluid flow in fracture networks. The fracture networks are specified by giving the location, orientation, extent, and hydraulic aperture of each fracture. The fractures are assembled into a network, and fluid flow through the network is calculated with standard numerical techniques.

The calculated behavior of these networks can be compared to that of a continuum in a variety of ways. Long et al. (1982) suggested calculating a series of directional permeabilities, $K(\theta)$ measurements. It is possible to plot $1/K(\theta)$ as a function of the gradient direction, θ, on a polar plot. This plot will be a perfect ellipse if the medium is behaving as an equivalent continuum. For a less than perfect ellipse, a regression analysis can be used to fit these data to the permeability tensor (Figure 6.17). The regression error is then a measure of how well the medium can be represented as an equivalent continuum. The idea is similar to that proposed by Hsieh et al. (1985) for analysis of interference data, as described in Chapter 5. Any of the network models described in the previous section could be used in this manner to estimate a permeability tensor.

Cacas et al. (1990) provide an interesting demonstration of an approach for estimating the large-scale permeability of fractured rock using statistical data on network geometry in combination with a model calibration using small-scale hydraulic and tracer tests. The analysis was based on data from an adit in a highly fractured granite at Fanay-Augeres, France. The injection test data consisted of 180 flow measurements, using a packer spacing of 2.5 m, obtained in 10 boreholes. Total inflow to the adit also was recorded. Data were also available from 10 tracer injection experiments, four of which yielded breakthrough curves adequate for use in model assessment. They proceeded as follows: (1) A stochastic, three-dimensional, discrete network model was constructed and used to generate a number of realizations of the fracture network. To solve for the distribution of flow in each realization, the network was reduced to a set of one-dimensional

"pipes" connecting each fracture intersection to the center of the fractures. (2) The conductance of the pipes was interpreted as a stochastic parameter and was characterized by the mean and variance of its distribution. The mean and variance of the pipe conductance were taken to be the calibration parameters. Values were estimated so that the mean and variance of the flow rates observed in the set of synthetic realizations matched the observed mean and spread in the histogram of injection flow rates. (3) The calibrated flow model was then used to generate 17 "intermediate-scale" realizations, and a hydraulic conductivity ellipse was

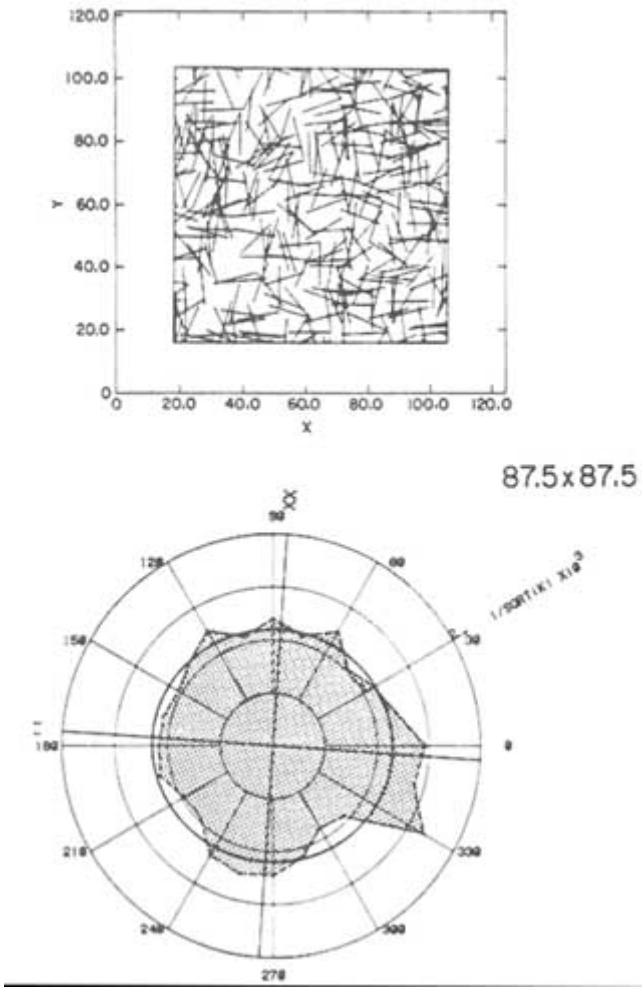

FIGURE 6.17 Example of a polar plot of the inverse of the directional hydraulic conductivity for the fracture network shown in the upper plot. From Long (1983a).

estimated for each. (4) These intermediate-scale values were averaged, using equations developed for heterogeneous porous media, to estimate a large-scale hydraulic conductivity for the rock mass surrounding the adit.

The flow model was tested by using a set of hydraulic head measurements from around the adit, together with measured inflow rates to the adit, to estimate a single hydraulic conductivity value, applicable at a scale of 100 m. The value obtained fell within the range of the global hydraulic conductivity estimated using the stochastic discrete network model. Tracer tests were then used to test the estimate of the variance of the pipe conductance. Using the calibrated flow model, 20 realizations of each tracer injection experiment were generated. A single transport parameter, related to fracture volume, was adjusted so that the peak arrival times in each set of realizations were consistent with the variation in the time of peak arrival observed in the tracer tests. To provide another test of the flow model, a comparison was made with the calibrated transport model to see if the model reproduced the observed variability in breakthrough durations. (The breakthrough duration is a function of the variance in the pipe conductance.) The distribution of the breakthrough duration times was consistent with the values observed in the tracer tests, without any additional calibration of the variance of the pipe conductances.

The study by Cacas et al. (1990) showed how field data obtained at one scale can be analyzed in a stochastic framework to provide larger-scale estimates of the hydraulic conductivity of an equivalent porous medium. In adopting a stochastic framework, they attempted to reproduce the structure of the fracture network only in a statistical sense and not in terms of identifying specific locations around the adit where the connectivity may be higher or lower than average. It is important to note, however, that this model (and the more complex model of Billaux et al., 1989, described later) failed to accurately represent the lack of hydraulic interconnection at Fanay-Augeres because it was based on apparent fracture geometry rather than conductive fracture geometry. The Fanay-Augeres experience illustrates dramatically that it is not enough to look at fracture statistics, or fracture pattern for that matter, to be able to understand the hydrology of a fracture system. It is critical that data be collected that show how the system is hydraulically interconnected. This statement implies that one must create a hydraulic signal at various points in the system and monitor whether that signal is received at other points in the system. In other words, it is critical to do interference testing and tracer testing to see if the system is interconnected. Mapping the fractures and single-well hydraulic tests simply cannot provide this critical information.

Estimation of Continuum Properties Based on Percolation Theory

As described in Appendix 6.B, percolation theory is the study of random networks of conductors. In some cases it is possible to map a discrete network

model into a simple lattice percolation model. This map, together with results from percolation theory, can be used to derive analytical expressions for the permeability of the network model (Hestir and Long, 1990).

A simple lattice percolation model is constructed by creating a lattice of conductors and randomly turning some of them off, as shown in Figures 6.18a and b. The parameter that describes this stochastic model is p, the probability that a given conductor is left on. Analytical expressions for approximating permeability in such lattices have been given in the physics literature for some time (for example, Kirkpatrick et al., 1983). These expressions give permeability in terms of p when p is near the critical probability, p_c. The critical probability p_c corresponds to the value of p below which there are only finite clusters of connected conductors (no percolation) and above which there are infinite clusters of connected conductors (percolation).

One way to develop expressions for permeability as a function of the stochastic network parameters is to relate a discrete network model to a simple percolation model. Several authors have developed relationships between permeability and the average number of intersections per fracture, ς, where ς is a measure of the connectivity (see Appendix 6.C on connectivity). This method has been implemented for two-dimensional discrete networks of random line segments (e.g., Figure 6.18c) by Robinson (1984), Hestir and Long (1990), and Berkowitz and Balberg (1993). In the work of Robinson and Hestir and Long, for example, a way was found to determine the effective values of p and z as a function of ς. Hestir and Long show that a good fit to numerical simulations of fracture network permeability can be found by using the following expression for p derived by finding the average length of a line in the lattice model as a function of p and the average length of a line in the random line model as a function of ς and then equating the two averages to get an expression of p in terms of ς:

$$p = \frac{\varsigma}{\varsigma + 2}, \qquad (6.1)$$

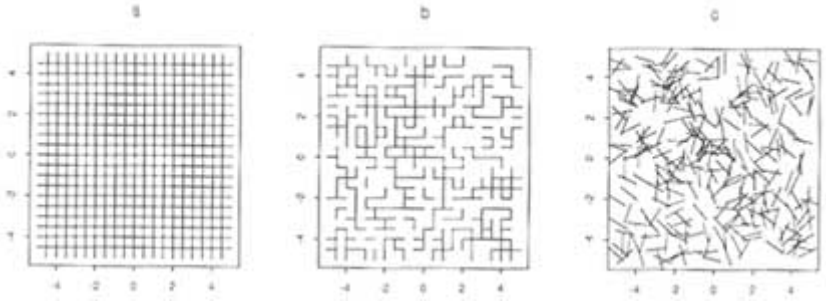

FIGURE 6.18 Percolation networks. (a) Square lattice with all conductors present. (b) Same lattice with a fraction $1 - p$ of the original conductors removed. (c) Random percolation network of uniform-length line segments.

Then, using percolation theory (see Appendix 6.B), an expression for permeability near the critical limit can be developed:

$$\frac{K}{K_S} = k\left[\frac{\varsigma}{\varsigma + 2} - \frac{\varsigma_{crit}}{\varsigma_{crit} + 2}\right]^t \qquad (6.2)$$

where K_s is a normalization constant corresponding to the case where ς is infinite, k is a constant, ς_{crit} is the value of connectivity where percolation begins, and t is a universal exponent with a value of about 1.2. This method depends on being able to calculate the average line length in the random model. This is possible for simple Poisson models but may become extremely difficult for more complex stochastic systems. This limitation prevents direct application of the method in many cases, but the general concept of connectivity and percolation behavior is expected to hold in any random network. Thus, these theories do provide an intellectual platform for understanding the development of permeability.

Solute Transport

As indicated earlier, one of the key difficulties in the formulation of a field-scale model to represent solute transport in fractured rock is estimation of the parameters that characterize the dispersive properties of the rock mass. Model studies have been used to examine equivalent porosity in much the same way that models have been used to examine equivalent permeability. Endo et al. (1984) created a mechanical transport model by tracing streamtubes through a two-dimensional network model assuming no mixing in the fracture intersections. Just as in Figure 6.17, flow and transport were examined in a variety of directions through the models. For each direction the ratio of fluid flux to mean velocity was calculated (i.e., equivalent hydraulic porosity). Endo found that even systems that behaved like equivalent porous media for flux had values of hydraulic equivalent porosity that varied with the direction of flow, as shown in Figure 6.19. In a similar manner, both tortuosity and dispersivity were found to vary significantly with flow direction. In most practical situations, with limited project budgets and short time horizons, tracer tests are not a viable option for formulating parameter estimates. One approach, based on stochastic theories of transport in heterogeneous porous media, was outlined earlier. The present section outlines a second approach, based on the development of transport characteristics at the continuum scale by simulating transport at a smaller scale using a discrete network model.

Schwartz and Smith (1988) proposed a statistical continuum model to simulate anisotropic dispersion in a network of finite-length, randomly located fractures of variable aperture. Particle tracking is at the core of the method. Solute transport is modeled by first collecting statistics on particle motion in a subdomain model using a discrete network simulation and then using these statistics in a continuum

model to simulate transport at a larger scale. Particle tracking also is used in the continuum model, so there is never a need to assign numerical values to a dispersion tensor. This, in fact, is the primary advantage of the technique. In essence, the particles are "educated" in the discrete model. Then, in the continuum model, they are able to mimic the effects of the interaction between network geometry and conductance, the orientation of the hydraulic gradient, and the resulting spreading patterns.

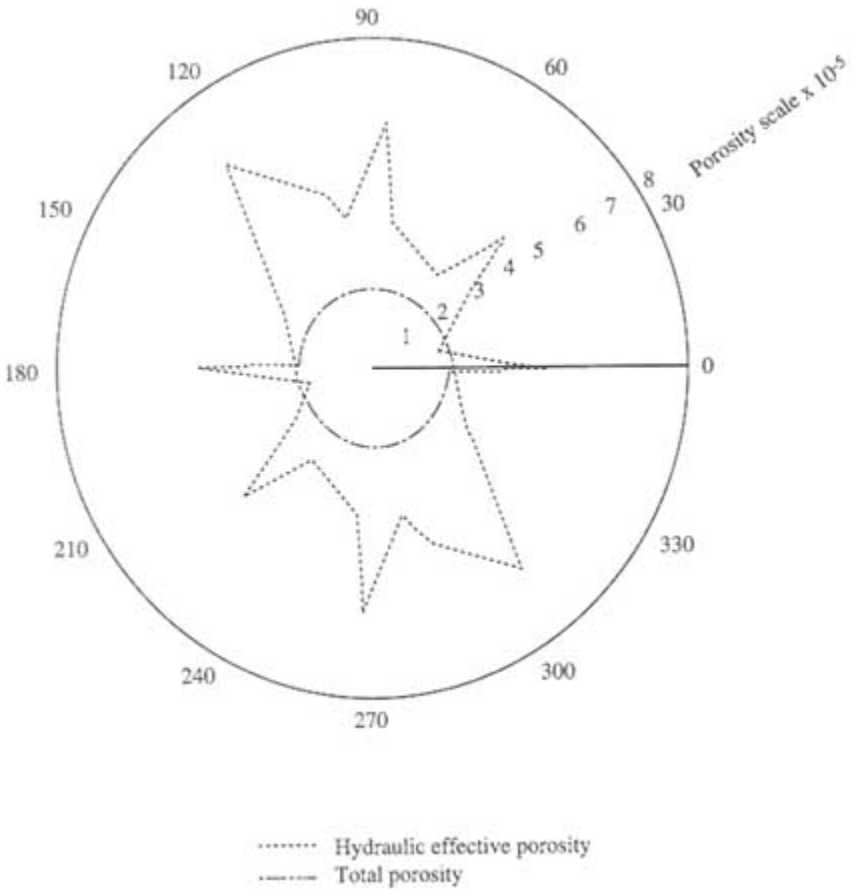

FIGURE 6.19 Polar plots of total porosity and hydraulic effective porosity for discontinuous system with mean fracture length of 50 m and linearly correlated apertures. From Endo (1984).

The discrete network model is a small piece of the much larger domain for which field-scale simulation is required, but it is intended to be representative. The basic inputs to the model are the geometric properties of each fracture set

and the distribution of transmissivity values measured at the scale of individual fractures. The continuum model provides an estimate of the expected (or average) distribution of mass and not the mass distribution that would occur in any single realization of a fracture network (Figure 6.20).

Subdomain statistics adopted by Schwartz and Smith (1988) included the mean and standard deviations in fluid velocity for each possible direction of motion, probabilities on the direction of motion away from fracture intersections, and the probability distribution of distances between fracture intersections for a given fracture set. Because the dispersion process is anisotropic, statistics must be collected for a number of different orientations of the hydraulic gradient, Smith et al. (1990) modified the approach to account for the correlation structure of the fluid velocities and used a gamma distribution, rather than a lognormal distribution, to represent the probability distribution of fluid velocities. Parney and Smith (1995) analyze the correlation between fluid velocities and the distribution of path lengths.

This approach is based on continuum approximations, and, as such, the statistical properties of the fracture network at the subdomain scale must be equivalent to those that apply at the scale of the continuum model. This requires that the fracture pattern be spatially uniform and that the fracturing be characterized by one length scale. The advantage of this technique, at least at a theoretical level, is that it deals correctly with the anisotropic dispersion process by relating spreading patterns directly to the geometric and conductive properties of the fracture network. Its limitations, which are common to all discrete network models, are the requirements that data be available to characterize both the fracture length distribution and the statistical properties of transmissivity at the scale of individual fractures and the fact that it is possible to isolate the characteristics of the conductive fracture network.

DISCRETE NETWORK MODELS WITH SCALE-DEPENDENT PROPERTIES

Basic Issues

There are two basic concerns with the stochastic models of fracture networks described earlier in this chapter. First, there are typically no mechanistic underpinnings to the proposed stochastic structure of the fracture network; their primary objective is to reproduce the statistics of fracture maps, not the spatial relationships between fractures. Second, although statistical models are based on the observable fracture geometry, in some cases a significant number or possibly even the vast majority of the observable fractures may not be open to flow. It makes little sense to base an understanding of fracture hydrology on statistical descriptions of the geometry of thousands of fractures that play a minor or no role in conducting

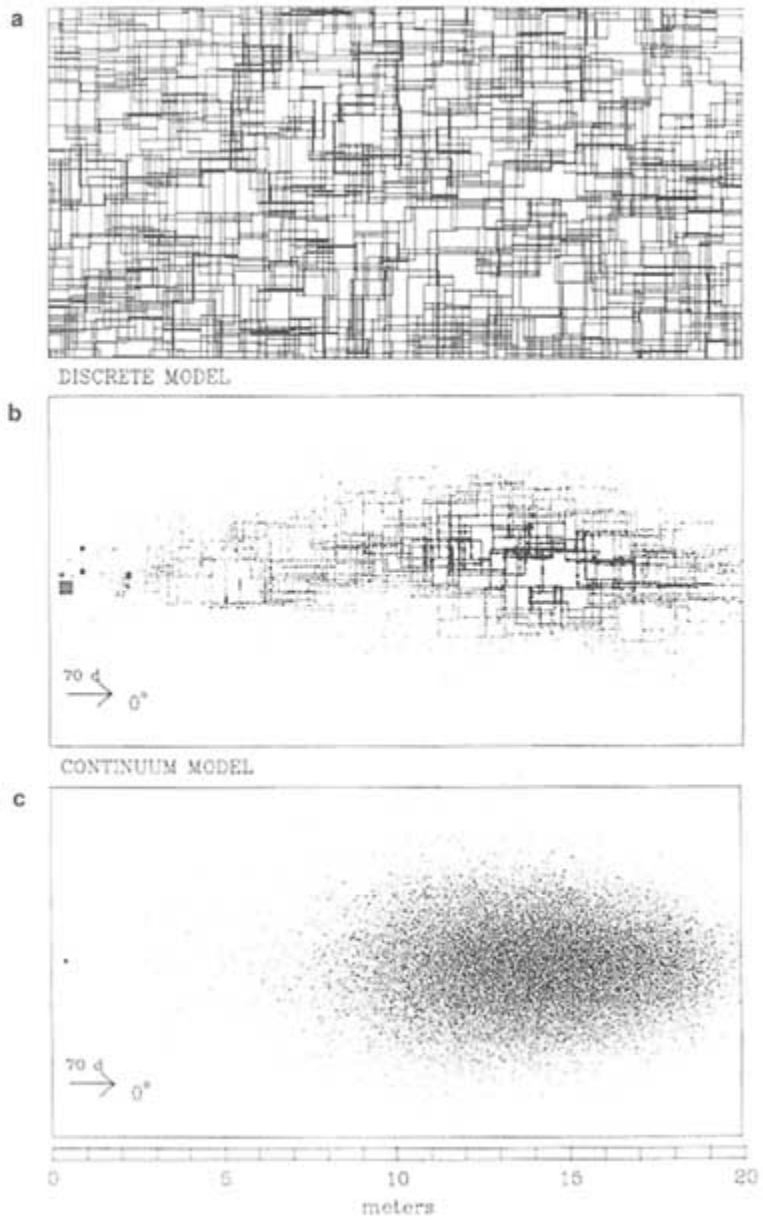

FIGURE 6.20 Statistical continuum transport model. (a) Predictions of the mass distribution within the fracture network. (b) Results using a discrete network simulation. (c) Results using a statistical continuum model. From Smith et al. (1990).

fluid. In these cases, fracture statistics may provide a poor basis for the prediction of flow behavior.

To address these concerns, discrete network models can be extended (1) to take into consideration the origin of the fractures and any statistical distribution functions arising naturally from the mechanics of fracture formation, (2) to incorporate a hierarchical structure of fractures, and (3) to be conditioned on hydrological observations. The term hierarchical refers to a superposition of fractures of many different sizes, with some genetic relationship among the different scales. The term nested structure is analogous to a hierarchical structure. Each scale influences to a varying degree the hydraulic and mechanical behavior of the rock mass. Some means also is needed to identify the more important fractures and to build the geometric model of the network with the emphasis on those fractures. The concept of conditioning discrete network models on hydrological observations usually involves an extension to cross-hole hydraulic tests from the single-borehole tests used in estimating fracture transmissivity.

Rules describing the scale dependence of the hydraulic and transport properties of geological media are being actively explored by the research community. While the discussion of scale-dependent properties is presented here in the context of discrete network models, this topic has a base that extends to all porous media. There is strong evidence from field observations of flow and transport that permeability and dispersivity vary with the scale of measurement. Several models have been suggested to represent this dependence. For example, Neuman (1990, 1994) proposed scaling relationships that treat both porous and fractured rocks as multiscale random functions defined over a continuum. We do not review this broader research issue, but the reader should be aware that these concepts underlie the application of any of the network models presented here.

Geological Evidence of Scale-Dependent Properties

There are several reasons fracture networks might be expected to have scale-dependent or hierarchical properties. Fractures are normally generated in a series of geological episodes. Each succeeding episode of fracturing is influenced by the presence of fractures formed during earlier events because of their impact on the local stress distribution and on rock strength. Dynamic systems of this type are known to produce fractal structures (Barnsley, 1988), In particular, fracture growth has been shown to depend on fracture length (e.g., Griffith, 1920; Pollard and Aydin, 1988). This relationship can lead to systems with a small number of very large features and larger numbers of smaller features, that is, features of every length scale. The implication is that the larger the domain, the larger the features one will observe. The challenge in modeling fluid flow is to include scaling in the description of fracture system geometry.

Tchalenko (1970) showed that fracture systems associated with shear zones are qualitatively similar across a wide range of scales, from tectonic faults of

kilometer-scale dimensions to fractured clay laboratory samples of centimeter scale. The similarities in structure of the fractures were interpreted by Tchalenko as indicating similarities in the deformation mechanism over this wide range of scales. In a similar manner, Martel et al. (1988) showed how the development of fault zones in the Sierra Nevada leads to the formation of several generations of fractures, each related to its parent in a similar way (see Figure 2.18).

Faults are composed of one or many interconnected fractures. At some scales, a fault may appear to be a one-dimensional trace of a single fracture, whereas at another scale the same fault may appear to consist of a two-dimensional set of interconnected subparallel fractures. A number of studies have focused on the irregularity of fault traces at a variety of scales (e.g., Scholz and Aviles, 1986; Aviles et al., 1987; Okubo and Aki, 1987; Power et al., 1987; Hirata, 1989; Power and Tullis, 1991). The basic conclusion of these studies is that single fault traces have topographies that can be described by fractal geometry. When a fault consists of multiple fractures, the fracture system has a fractal character as well.

The fractal concept incorporates scaling and hierarchical structure at a fundamental level. Measurements of the fractal geometry of fracture systems have become more common in recent years (e.g., Barton and Larsen, 1985). Analyses to date have been carried out on linear transects or planar sections of fracture systems. Most studies find power law (fractal) scaling over a wide range of length scales. LaPointe (1988) found that the fractal dimension varied with the orientation of the sample line. A comprehensive review of this work is given by Barton (1995).

In studies of scale-dependent properties, two approaches have been taken. The most common approach is to consider a statistical distribution function—say, the number of fractures in a population as a function of fracture size or the number of fractures observed along a linear transect or a drill core. This approach ignores the spatial position of the fractures and therefore the spatial correlation structure. One study analyzed data on the spatial distribution of fracture density in the form of a "surface topography" and found a power law relationship reminiscent of fractal geometry (LaPointe, 1988). In light of the anticipated importance of spatial correlation in fracture density on fluid flow and transport, the approach of LaPointe is perhaps of greater relevance in hydrological studies.

The evidence suggests that the concept of hierarchical systems is applicable to many fractured rocks. The question remains, in adopting a discrete network model, of how to generate network models that provide a realistic portrayal of these spatial structures.

Geometric Models Incorporating Spatial Relationships Between Neighboring Fractures

The network models described in earlier in this chapter apply to systems in which the fractures are distributed in the rock mass in a more or less uniform pattern. Here we account for fracture patterns that exhibit a spatial dependence

between neighboring fractures. Maps of fracture traces suggest that fracture occurrence is not independent and that fractures tend to occur in clusters. Causative mechanisms for this clustering were discussed in Chapter 2. Two approaches have been pursued: one in which a simple stochastic rule is applied to establish fracture clusters and a second in which an attempt is made to mimic the processes of fracture formation and growth.

Geometric Models Incorporating Clustering of Fractures

Long and Billaux (1987) and Billaux et al. (1989) attempted to include fracture clustering by introducing both a "mother-daughter" process for fracture spacing and an empirical variogram for fracture orientation. A network is built by first creating parent points according to a Poisson process with rate λ_p where λ_p varies in space. Once the parent points are placed, a random number of daughters are randomly placed about the parents. Fractures are assumed to occur with their centers at the daughter points. Figure 6.21 presents an example of a fracture network generated by using the parent-daughter process. The clustering of fractures and the scale dependence in the system are apparent. Estimation of the parameters of this model, using data from fracture trace mapping, is illustrated in Billaux et al. (1989).

The parameters of the parent-daughter process were derived by comparing the variogram derived from the field data with a series of theoretical variograms derived from different sets of parent-daughter parameters. An optimization procedure was used to find the theoretical variogram that matched the observed one. Hydraulic data were used to estimate fracture transmissivities. However, this model fails to reproduce the lack of fracture interconnectivity for the same reason as described above by Cacas et al. (1990).

Geier et al. (1989) summarized several models that are similar in intent to the parent-daughter models are:

- The Levy-Lee model, where fracture centers are generated sequentially using a power law expression for the spacing, with the size of a fracture being proportional to its distance from the preceding fracture.
- The "nearest-neighbor" model, in which primary, secondary, and tertiary fractures are generated in sequence. Fractures in the primary group dominate the generation of fractures in succeeding groups. Spatial density of the secondary fractures is proportional to the reciprocal of the distance to the nearest fracture.
- The "war zone" model, in which the spatial density of secondary fractures is greater in the regions between pairs of neighboring primary fractures that are subparallel.

Drift 2

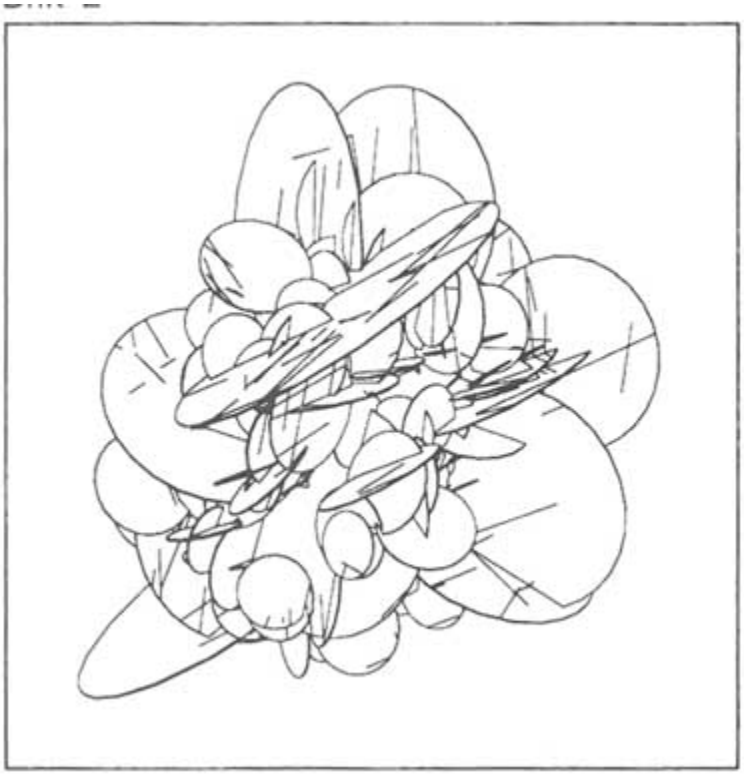

FIGURE 6.21 Example of a fracture network generated by using the parent-daughter process. From Billaux et al. (1989).

Geometric Models Based on Fracture Mechanics

Conrad and Jacquin (1975) were the first to present a two-stage fracture model designed to discriminate between fracture sets in which the fracture traces are extensive and those sets in which the fractures have an irregular pattern and truncate against the extensive fractures. These authors modeled the extensive or primary fractures as unbounded Poisson lines. In the polygons formed by the Poisson lines, finite-length fractures were generated as another series of Poisson points. These fractures were terminated where they intersected primary fractures.

Lee et al. (1990) used the Conrad-Jaquin concept of fracture hierarchy to represent different fracture patterns as they occur in nature. In this so-called hierarchical fracture trace model, fracture trace sets are modeled in a hierarchical (sequential) manner that corresponds to geological processes. Specifically, for

the case shown in Figure 6.22, the first fracture set was produced by a doubly stochastic (Cox) point process combined with an appropriate trace length and orientation distribution model; spatial correlation of trace length and orientation were considered. Fractures were thus reproduced with the appropriate lengths and clustered as in reality. The second set was created by first checking fracture independence in the first set. In case of independence, the second set was created like the first one. In the case of dependence, an appropriate correlation was considered. Also, the observed termination distribution of fractures of one set against those of the other was considered. This model has been validated against real patterns (Figure 6.22).

Geometric models of fracture networks can also be built in a way that mimics the natural genesis of fractures. If this is done alteratively, with each stage of fracturing depending on the results of the previous stage, hierarchical fracture systems can be obtained. There are a number of examples of fracture genesis models based on the physics of fracture growth—for example, Takayasu (1985), Termonia and Meakin (1986), Cox and Paterson (1989), and the references provided therein. As discussed in Chapter 2, Olson (1991) developed a model for joint formation based on continuum mechanics and linear elastic fracture mechanics that included interactions between fractures. It was shown that the crack propagation velocity determined the character of the resulting fracture system. Faster crack growth favors longer fractures formed in clusters, whereas slower crack growth results in fractures of more equal length that are equally spaced. For these models, observation of fracture patterns can help determine the parameters that govern crack growth.

A heuristic model based on the physics of fracture formation has been developed by Martel et al. (1991; see also Long et al., 1992a). Small starter cracks are placed according to a Poisson process. The cracks then grow in a recursive manner according to stochastic rules (Figure 6.23). The rules for growth are based on principles of fracture mechanics and assume that the probability of fracture growth depends on the rate of energy release as a fracture propagates. For an opening-mode fracture, the energy release rate is proportional to the square of the mode I stress intensity factor (Lawn and Wilshaw, 1975). As described in Chapter 2, the stress intensity factor for a uniformly loaded fracture scales with the square root of the length of the fracture. Accordingly, the probability of fracture growth would depend on the first power of fracture length. Principles of fracture mechanics together with experimental findings indicate that under a given load a fracture will propagate spontaneously once it reaches a critical length; below that length it will propagate more slowly, at subcritical rates.

At each iteration a fracture is assigned a probability of growing that is proportional to its length, if its length is less than some critical value, L_c. Above this critical length, all fractures have a probability of growing equal to unity. The amount of growth at each iteration is chosen randomly from a uniform distribution between zero and a maximum growth increment, $B = \Delta L/L$, where

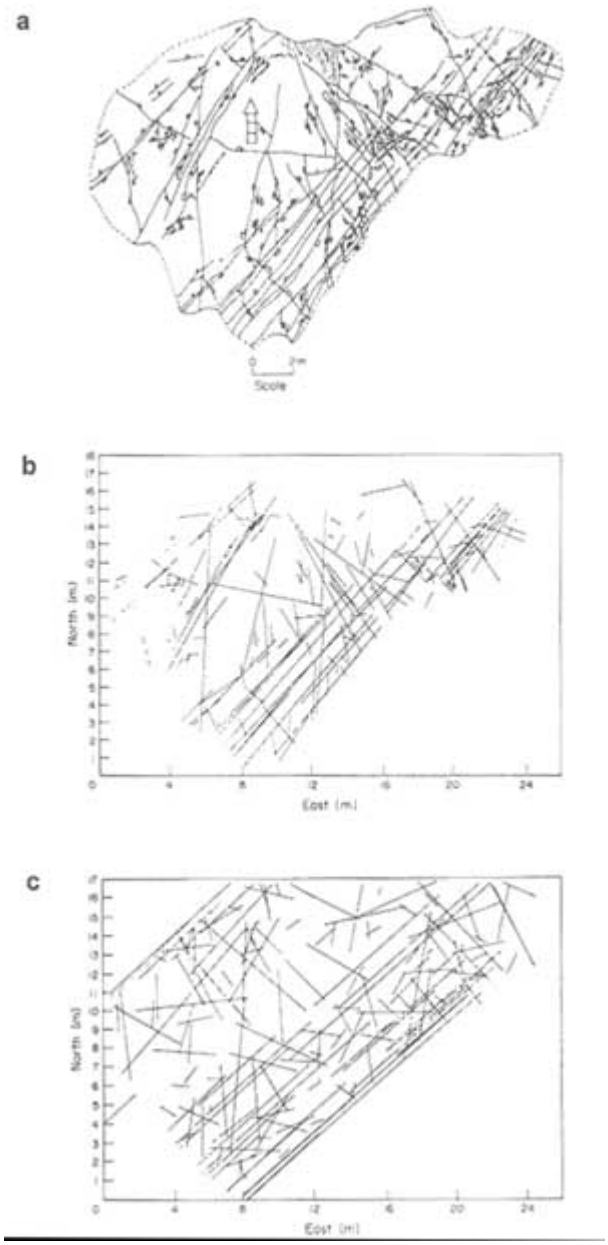

FIGURE 6.22 (a) Original trace map of PA100. From Barton and Larson, (1985). (b) Schematic representation of PA100 trace map. (c) Modeling of PA100 hierarchical fracture trace model. From Lee et al. (1990).

L is the fracture length. Thus, the choice of B is equivalent to choosing the fracture propagation rate. If fracture growth occurs, either a daughter crack can grow or the parent itself can grow. The probability of daughter versus parent growth, P_d, is a parameter of the model. The entire fracture pattern is thus determined by five parameters: L_c, B, P_d, the number of starting cracks, and the number of iterations.

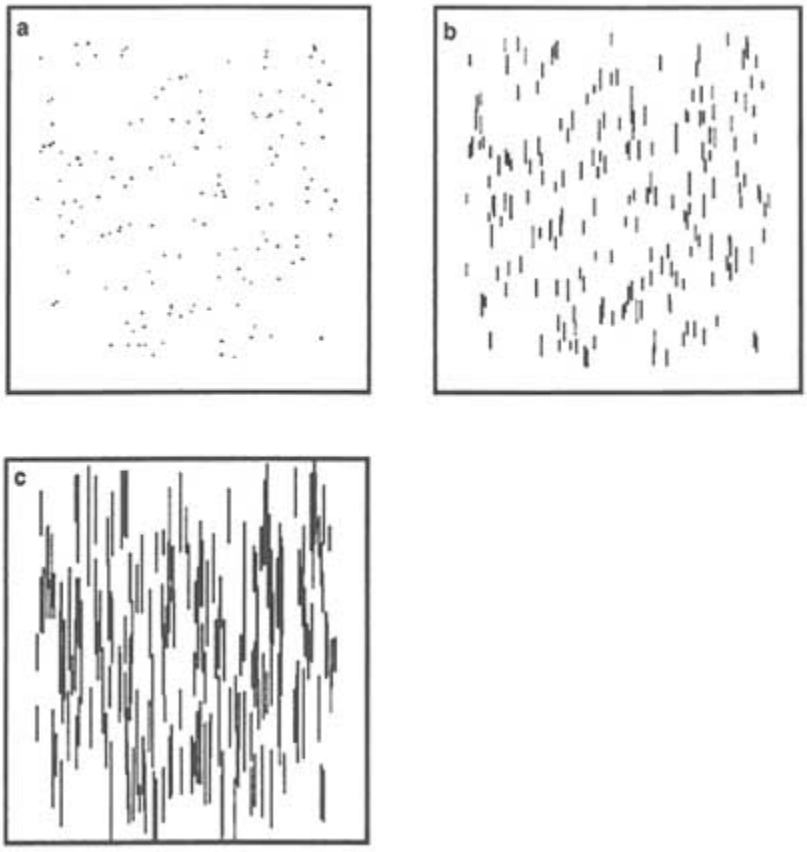

FIGURE 6.23 Development of a fracture pattern from 200 randomly located starter cracks. From Martel et al. (1991).

Flow and Transport Models

The networks created by incorporating spatial relationships between neighboring fractures typically have a wide range of trace lengths. In principle, there is no conceptual difficulty in applying discrete network models to fractures with

multiple length scales. The method, however, can be inefficient because of the high proportion of smaller-scale fractures that are typically generated. To reduce computational requirements when solving the flow and transport equations, a common approach is to simply remove fractures from the network. For example, all fractures with a transmissivity less than the mean might be eliminated on the grounds that they do not contribute significantly to the flux through the network. Hestir and Long (1990) showed that a proportion of the shortest fractures can be eliminated without changing the fracture network permeability.

Smith et al. (1990) describe a simulation approach that recognizes a hierarchy among fractures, preserving dominant fractures as discrete features (primary fractures) and modeling flow and transport in the more numerous, smaller-scale fractures by using a lumped parameter representation (to form so-called network blocks). This concept is illustrated in Figure 6.24. The network blocks are not modeled on the basis of a porous medium approximation. Rather, each network block has unique properties, in the same sense as the primary fractures. Their properties reflect the influence of the smaller-scale fractures that are grouped into the network blocks. This approach is suited to systems where fractures exhibit multiple length scales because it does not ignore the connectivity provided by the smaller-scale fractures while permitting simulation of larger-scale flow systems (Clemo, 1994).

Discrete Network Flow Models Conditioned on Hydraulic Behavior

As discussed earlier, geometric information from fracture statistics does not form a sufficient basis to construct a discrete network model. Hydraulic data must be available to define transmissivities at the scale of individual fractures. Such data are normally obtained from packer tests in single boreholes. One approach to ensure that the constructed network behaves like the real system is to condition the fracture network models using hydraulic data.

Equivalent Discontinuum Models

In an equivalent discontinuum model, flow in fractures is modeled as flow in a set of equivalent conductors, which may be regularized to lie on some form of a lattice (Odling and Webman, 1991; Long, 1993). The lattice is chosen during the formulation of the conceptual model. For example, if fracture zones are found to be the most important flow paths, as at the Stripa mine, the lattices can be confined to the planes (or slabs) representing the fracture zones. In this case the model does not explicitly include every fracture at the site but only a set of equivalent conductors in the fracture zones. In other cases it may be appropriate to construct the lattice throughout the three-dimensional space of the site. If fracture orientation is known, lattice elements can be oriented parallel to the mean orientations of the fracture sets. If the geological investigation suggests

that the fracture zones have higher vertical hydraulic conductivities, as in the K-zone at Grimsel in Switzerland, the lattice can be chosen to have vertical elements. The lattice includes any information derived a priori from the characterization process (see "Development of Conceptual and Mathematical Models," earlier in this chapter) and, in a sense, represents the conceptual model of the site.

Figure 6.25 shows a lattice developed for the Stripa Site Characterization and Validation Project (see Chapter 8). Each plane represents a major fracture zone that, in turn, contains a lattice. The equivalent discontinuum model is similar to an equivalent continuum model, except that some lattice elements are removed.

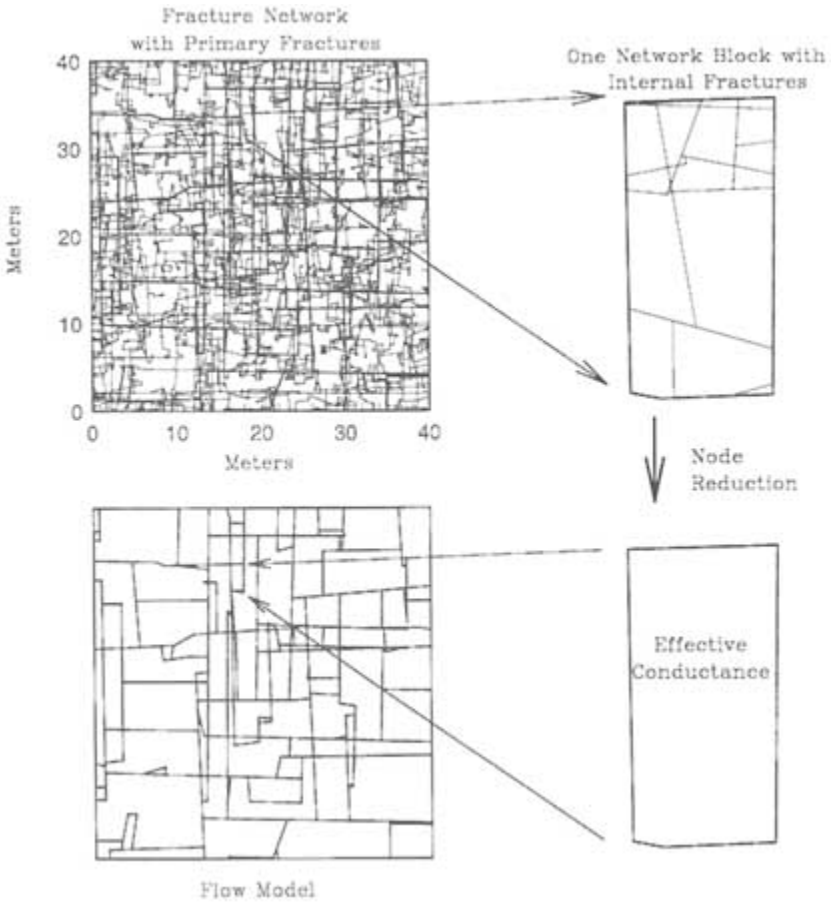

FIGURE 6.24 Division of a fracture network into primary fractures and network blocks. Primary fractures are retained as individual discrete fractures. Most fractures are grouped into network blocks, as shown for the single block that has been isolated in this schematic representation. Modified from Clemo (1994).

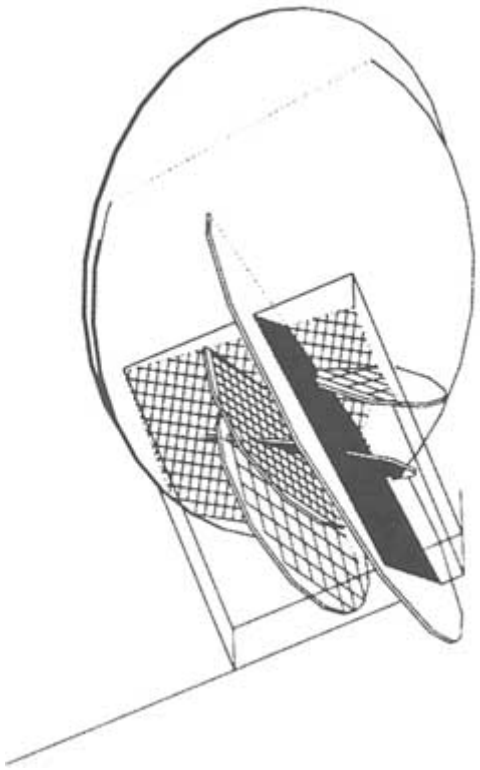

FIGURE 6.25 Three-dimensional template for an equivalent discontinuum model, from the Stripa Site Characterization Validation Project. The features shown are the seven fracture zones identified in Black et al. (1991). Each zone is represented as a disk and contains a lattice. From Long et al. (1992b).

The equivalent discontinuum model is essentially a partially filled lattice that exhibits the same hydraulic behavior as that observed in situ. Where the fracture flow system is connected, the model is connected through lattice elements. Where the flow system is unconnected, the lattice elements are unconnected. Partially filled lattices of this sort have fractal properties near the percolation threshold (Orbach, 1986). The advantages of an equivalent discontinuum model are that it represents the important larger-scale features explicitly and uses equivalent conductors to represent the average behavior of less important features. It is possible to use these models to reproduce the discontinuous hydraulic behavior of a fracture system without modeling every fracture.

An inversion technique called *simulated annealing* can be used to construct equivalent discontinuum models (Long, 1993). Simulated annealing is an optimization algorithm that finds lattice configurations that are functionally equivalent

to the observed system (i.e., a model that simulates the field behavior). To search for configurations that behave like the observed system, the simulated annealing algorithm makes a random change in the lattice. For example, a lattice element that was on may be turned off (i.e., it becomes nonconducting). For each trial configuration a well test that was conducted in the field is simulated. The "energy" of the configuration is a function of the squared difference between the observed and simulated responses. The problem of finding the "best" model then becomes one of finding configurations that have low values of the energy function. The algorithm accepts the change to the configuration if the energy is decreased over the previous configuration. If the energy is increased, the algorithm may accept the change with a probability inversely proportional to the energy increase. Thus, the solution "wiggles" out of local minima and can find the globally minimum solution.

An example of equivalent discontinuum modeling at the Stripa mine is provided by Long et al. (1992b). A fracture zone at the mine called the H-zone was intersected by a series of wells (W1, W2, C1–C5, D1–D6). Hydraulic interference testing was carried out. A two-dimensional lattice template was constructed for the H-zone. The template was designed (1) to represent as much detail as possible in the vicinity of the D-holes, (2) to have a large enough mesh to prevent the hydraulic disturbance from reaching the boundary too quickly, and (3) to keep the number of elements and bandwidth as small as possible for efficient annealing.

The total inflow to the six parallel D-boreholes (D1–D6) from the H-zone was modeled using simulated annealing. Simulated annealing produces a model that matches an interference test called the C1–C2 large-scale cross-hole test, which was conducted by pumping from the H-zone in well C1 and monitoring the other boreholes. The "best-fitting" model is shown in Figure 6.26. The annealed network is analogous to a finite-difference model of a continuum with variable connectivities, more so than being representative of actual fractures. The grid does, however, provide an explicit representation of the connectivity (or lack of connectivity) in the fracture zone. Figure 6.27 shows the match between the observed well responses and the model responses. The mesh was adjusted to calculate the effects of opening the D holes and collecting the inflow. The measured steady-state flow (0.75 liters per minute) and the predicted value (0.77 liters per minute) agree quite well.

Emerging Concepts

For fracture networks near the percolation threshold, the equivalent discontinuum models described above result in a fractal structure through the development of a percolation lattice. Several attempts have been made to model fracture systems using numerical approximations of fractals directly. Pollek (1990) built a series of random Sierpinski's gasket models with various fractal dimensions

and compared the behavior of well tests on these models to the behavior predicted by Barker (1988). Chang and Yortsos (1990) derived solutions for well test behavior on fractals, in this case fractals embedded in a porous matrix, thus explicitly addressing systems with both fracture and matrix porosity. Acuna and Yortsos (1991) constructed approximate numerical models of this fractal system to compare the well test behavior with that derived by Chang and Yortsos.

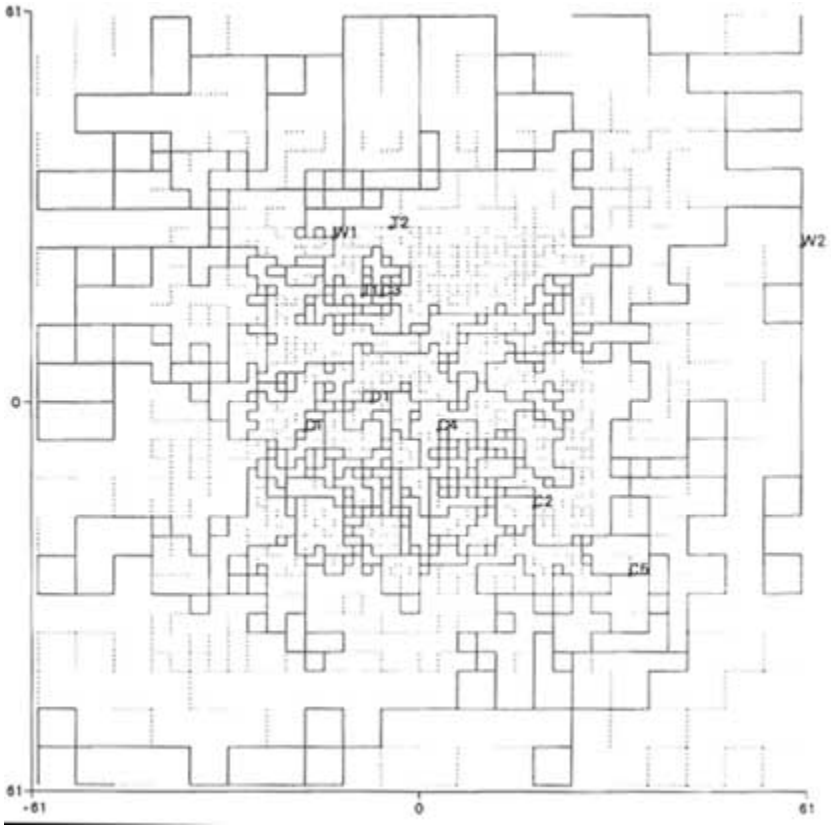

FIGURE 6.26 Two-dimensional equivalent discontinuum model of the H zone at Stripa, annealed to C1–C2 cross-hole hydraulic test. From Long et al. (1992b).

Another emerging concept involves the use of an iterated function system (IFS), which is a standard way to model self-similar geometrical structures (Barnsley, 1988). An IFS comprises an initial set of points and a set of iterative functions. At each iteration, each function in the system operates on the set of points and, according to the parameters in the function, translates, reflects, rotates, contracts, or distorts them. Over many iterations the points coalesce toward an "attractor." The IFS is designed such that the attractor is a fractal object.

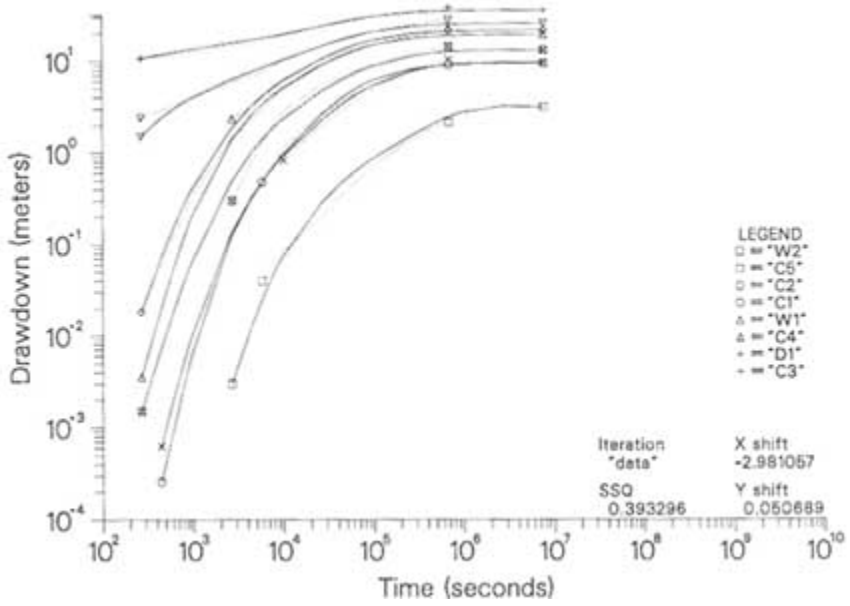

FIGURE 6.27 Comparison of the C1–C2 well test response data to the prediction of these test results provided by the equivalent discontinuum model. From Long et al. (1996).

An IFS can be used as the basis of hydrological inversion (Doughty et al., 1994; Long et al., 1996). In this case the points of the attractor are mapped into hydrological parameters (i.e., conductivity and storativity) and used to simulate a well test. For example, an attractor can be superimposed on a lattice by incrementing the conductance and storativity of the lattice elements that are close to each point on the attractor, as shown in Figure 6.28. The conductance of a lattice element can be incremented as many times as there are nearby points on the attractor. In this way the small number of parameters of an IFS defines the conductance and storativity distribution of thousands of elements.

One of the potential advantages of this approach is that it may be possible to choose subclasses of IFSs that produce features observed in a geological investigation. For example, it may be possible to find IFSs that always produce cooling fractures or a specific type of brittle shear zone. In these cases the search for appropriate models could be confined to the subclass of IFS that represents that geology. Once the form of the IFS that best explains all the data has been identified, the model will have fractal-like properties that may help to extrapolate behavior to scales that cannot be tested in reasonable time frames.

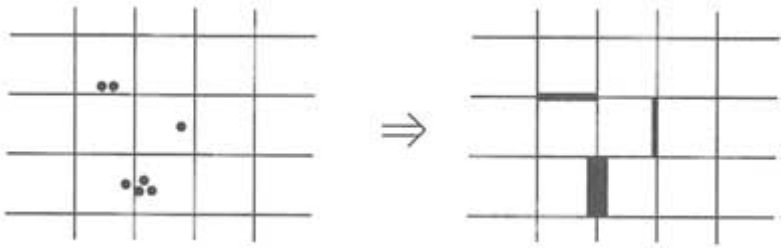

FIGURE 6.28 Step mapping between points on the attractor and increments in hydrological properties of the lattice. This example is for incrementing conductance. Points can also be used to decrement conductance. From Doughty et al. (1994).

Inverse methods applied to fractal models can be used in a manner similar to that for an equivalent discontinuum model. An inversion algorithm searches for IFS parameters that define a heterogenous system that behaves like the observed well tests. Starting with a model of the flow system based on an arbitrary IFS, the parameters of the IFS are optimized until the model produces a good match to the well test data. The advantage of the IFS inversion is that the whole system is defined by the small number of parameters that define the IFS. Consequently, there are fewer degrees of freedom in the inversion. Figure 6.29 shows preliminary models of the H zone at the Stripa mine constructed through IFS inversion using the same data as the model in Figure 6.26.

Recently, interest has been growing in neural network models. In this approach a whole series of specified conditions and outcomes are used to "teach" the neural network, which may be thought of as a "black box" of how the system works. Then, when new conditions arise, the neural network uses its "understanding" to predict system behavior. This approach can be used without even trying to define a model for the system. The approach can be purely heuristic, which may be particularly useful when hydrological data are available, but there is little information about the configuration of the fracture system. On the other hand, the approach may also involve physical understanding. This line of research is worthy of more attention.

Assessment of Scale-Dependent Discrete Fracture Models

The work on fracture growth schemes shows promise of being able to reproduce fracture patterns. The development of physically based stochastic models of fractures is an important area of research. The advantages to be gained from such models are numerous. First, the model has quantifiable parameters whose values can be estimated from observations of the fracture system. Because the model is physically based, knowledge of these parameters can aid the geologist in further understanding the fracture formation process. Second, the model param

eter estimation scheme can be used to guide the collections of field data appropriate to understand the fracture system. Finally, uncertainties about the model parameters can be used to estimate uncertainties about fracture system geometry.

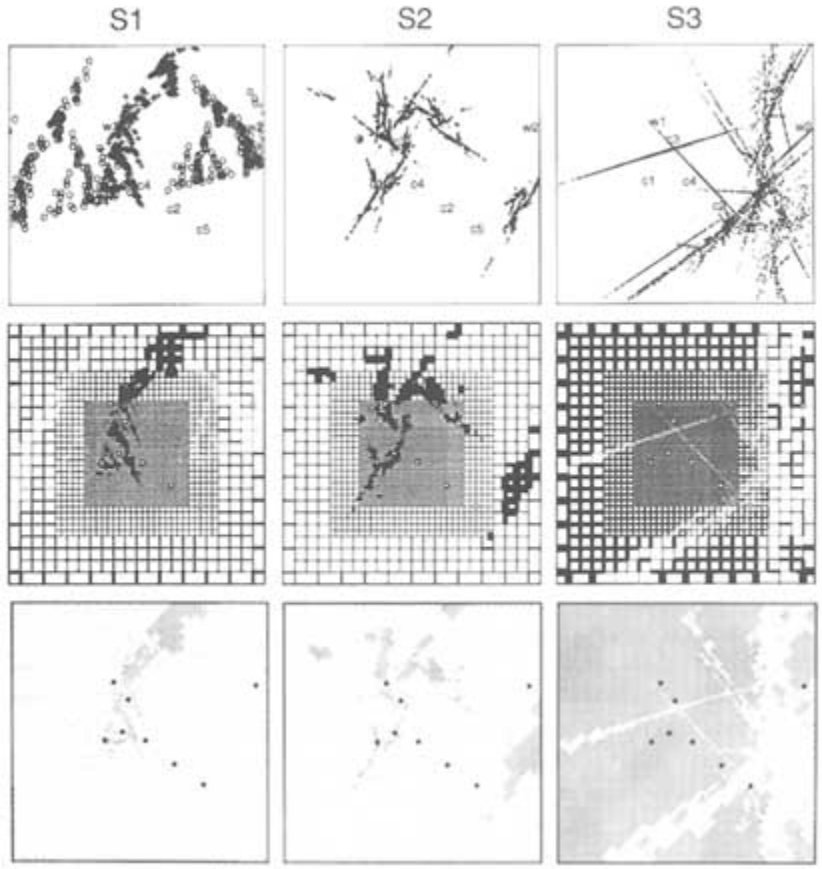

FIGURE 6.29 IFS inversion of an interference test in a fracture zone (H zone) at Stripa. Top row shows three different attractors from three different IFS schemes: left figure is for the case that the IFS increments permeability; middle figure is for incrementing and decrementing; and right figure shows the attractor for decrementing permeability. Middle row shows the resulting numerical grid. Higher conductances are shown by thicker lines. Bottom row is the average distribution of conductance that results from the attractor. Lighter colors represent lower conductances. From Doughty et al. (1994).

The idea of using cross-hole hydraulic tests to calibrate discrete network models also appears promising. Reliable hydraulic test data can be used with inversion methods to find permissible configurations for the conducting lattice. In practice, however, it can be quite difficult to obtain a good data set for analysis.

Some of the difficulties arise from the usual problems with model calibration, for example, poorly known boundary conditions and incomplete or insufficient data. Other difficulties arise because the inversion procedure must be tailored to the specific type of test data available (e.g., steady-state or transient tests).

In general, the inversion of hydraulic test data yields nonunique solutions. The problem is compounded by the generally limited availability of data. Characterization efforts must recognize from the beginning this nonuniqueness problem. If several different hydraulic well tests are available to calibrate the model, they can be combined. In principle, any combination of steady-state test data, constant flow, or constant-head transient data can be cointerpreted by the inversion. The advantage of using multiple-well tests is that each additional test provides more information about the system. Preliminary work with simulated annealing indicates that predictions based on two-well tests are significantly better than those based on one-well tests. The main drawback for combining a large number of transient tests is the potential computing requirements.

Efficient computer algorithms are being developed that may help to make simulated annealing a practical tool. Another important effort is to improve the efficiency of solution searches. For example, a priori information, such as geophysical data, can be incorporated to force the search to look for permeability anomalies where there are geophysical anomalies. Coinversion of both geophysical data and hydrological data might also be useful. Geophysical data should be used as a priori information because a significant amount of expert judgment is needed to interpret such data. This judgment would be overlooked in a coinversion.

MODELS OF MORE COMPLEX HYDROGEOLOGICAL SYSTEMS

Much of this chapter has been devoted to problems involving saturated isothermal flow in nondeforming rock masses, or the transport of nonreactive solutes. These conditions encompass a wide range of problems encountered in practice, but there are many situations where these assumptions are not valid. Examples include the disposal of radioactive waste in the unsaturated zone above the water table, migration of multiphase organic contaminants, and heat extraction from hot dry rock systems. The following review of modeling techniques for these kinds of problems is not exhaustive. Indeed, as these problems commonly involve systems of great complexity, there are significant gaps in our capabilities to model these systems at field scales. Nonlinear relationships between the media properties that characterize the conductance of a fractured rock mass and the degree of phase saturation are very difficult to quantify at field scales. Coupling between the thermal, hydrogeological, mechanical, and geochemical systems also is characteristic of these more complicated systems (see de Marsily, 1987). The objective of this section is to highlight certain issues and concerns that arise when formulating conceptual models and simulation for these more complex systems.

Modeling Flow and Transport in the Unsaturated Zone

Comprehensive research programs to investigate fluid flow and solute transport in unsaturated fractured rock have only recently been organized. The impetus to better understand the processes involved, and to develop a simulation capability, comes primarily from two sources: (1) the U.S. Department of Energy's program to evaluate the vadose zone at Yucca Mountain, Nevada, as a potential site for a high-level radioactive waste repository and (2) siting efforts for landfills and other surface-based disposal facilities in regions with deep unsaturated zones. There have been a number of refinements in conceptual models of flow in these regions. However, comprehensive understanding of the mechanisms of fluid flow in unsaturated fractured rock, matrix-fracture interactions, and spatial-temporal recharge fluxes through the vadose zone has yet to be developed. A collection of papers edited by Evans and Nicholson (1987) provides a good review of the state of the science to the mid-1980s.

In its most complete form, movement of water in unsaturated fractured rock is a problem of multiphase fluid flow (water and air phases), with the pressures in one phase influencing the mobility of the other phase. The complexity of the problem is reduced if it is assumed that the air phase is immobile and exists at constant pressure throughout the domain of interest. This approximation is routinely made in modeling water movement in unsaturated porous media.

Under conditions of partial saturation, capillary forces influence the subsurface distribution of water. Fluid saturation and hydraulic conductivity are functions of moisture content and, thus, fluid pressure. The conceptual model of fluid flow that is favored by some workers is illustrated in Figure 6.30. Fractures with larger apertures tend to desaturate before pores in the matrix blocks, so connected pathways for fluid flow will preferentially be located in the matrix blocks, with flow occurring across the fractures only at contact points (Wang and Narasimhan, 1985). As a consequence, drained fractures may act as a barrier to the infiltration of a wetting front, a reversal of the situation that occurs in the saturated zone. As water saturation increases, a limited number of connected pathways will be established along the fracture planes, especially in the smaller-aperture fractures. Once saturated, the highest fluid flux will be through the connected fracture network.

It is becoming apparent through theoretical and laboratory studies (Chapter 3) that there may be significant phase interference in fractures under conditions of unsaturated flow. In a planar fracture, when the matrix rock is relatively impermeable, the fracture behaves essentially as a two-dimensional porous medium. Under two-phase conditions, the presence of the second phase in the plane of the fracture can create barriers to the flow of the first phase, and vice versa. Since these fluids cannot use the third dimension (i.e., the matrix) to find flow paths around the other phase, the flow may be even more channelized than under conditions of saturated flow. The active flow region in the fracture may

be so small that little of the phase will be drawn into the rock matrix by capillary forces. If the fracture surfaces are sealed with minerals and the rock matrix is near saturation, downward flow to the water table may be largely confined to the fractures. A conceptual model of this system would differ significantly from the conventional view of unsaturated flow in fractured rock, which predicts that the matrix controls the flow and that fractures act as barriers to it. Indeed, this conceptual model would predict a more rapid downward transmission of fluid than the conventional model, where flow is confined to the rock matrix.

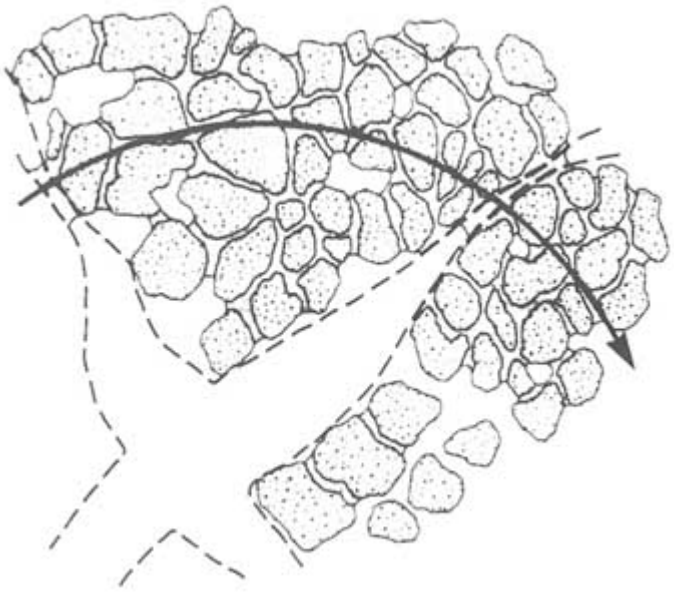

FIGURE 6.30 Conceptual model of flow in an unsaturated fractured rock. From Wang and Narasimhan (1985).

These two models describing infiltration through the vadose zone may be operative at different times as surface hydrological conditions change. The conventional model assumes that the connected fractures are drained and that water moving downward does so through matrix blocks where moisture contents and permeabilities are higher. The alternative model is based on downward infiltration through fractures, which might occur during precipitation events that promote saturation of the fractures at the ground surface. The wetting front in the connected fracture network need not coincide with that in the rock matrix. The depth of penetration of the wetting front is a complex function of fracture and matrix geometries, moisture contents, and permeability of the fracture wall.

Evidence for these two modes can be found at the Apache Leap research site in Arizona, where data suggest that recharge through unsaturated tuff occurs

along two pathways, one through fractures and the other predominantly through the rock matrix. Intermittent pulses of stream seepage penetrate to a tunnel 150 m below the ground surface in a matter of days to weeks. On an adjacent escarpment at a similar depth, geochemical evidence indicates that much older water occurs in a perched zone. It has not yet been possible to determine the percentage of the recharge to the perched zone that follows fracture and matrix-dominated pathways. At the Apache Leap site Rasmussen and Evans (1993) have demonstrated the possibility of high water intake rates on exposed fractured rock surfaces.

Two-phase flow in a fracture may never be truly steady state. Even under steady-state boundary conditions, pressure in the wetting phase will build up, eventually causing the wetting phase to displace the nonwetting phase occupying the larger, more permeable void spaces in the fracture plane. Subsequently, the pressure dissipates and the wetting phase is swept out again. Such oscillatory flow has been observed in the laboratory (Persoff et al., 1991) and possibly in the field (Olsson, 1992). A key area for research is to determine if the amplitude and period of this oscillatory flow behavior increase with the scale of the flow system as might be expected.

Rasmussen (1991) describes a technique for modeling steady-state fluid flow and advective transport in a partially saturated fracture network embedded in impermeable rock. The technique utilizes a discrete air-water interface in each fracture to separate the saturated region from the drained region. A similar approach uses accessibility and allowability criteria to determine which fractures in a network will contain water and which will contain air (personal communication, Kenzi Karasaki, Ernest Orlando Lawrence Berkeley National Laboratory). Therrien (1992) has developed an efficient three-dimensional, discrete fracture model that solves for variably saturated groundwater flow and solute transport. The matrix blocks between the discrete fractures are porous and permeable. Complex interactions caused by contrasts between the saturation, relative permeability, and pressure-head relationships for the fractures and the matrix control the redistribution of water in the system. Depending on the nature of these relationships, groundwater flow and solute transport can be controlled either by the porous matrix or the fractures. Fracture connectivity in three dimensions shown to produce very irregular hydraulic-head patterns in fractured aquitards, which can lead to the development of irregularly shaped contaminant distributions in the subsurface.

It is not known how well conventional unsaturated flow models based on porous medium approximations represent flow processes in the vadose zone. Few studies have examined how best to average the properties of the matrix and the fractures under conditions of partial saturation (Figure 6.31). The work of Peters and Klavetter (1988) is an important step forward in addressing these issues. If the majority of fractures are drained, the moisture content versus pressure head and permeability versus moisture content relationships are determined by the properties of the matrix blocks. Under these conditions it seems probable that

continuum approximations are valid. At near saturation, connected pathways through smaller-aperture fractures may develop, potentially leading to substantial increases in rock mass permeability. Properties of the fracture network will determine fluid fluxes, and the same concerns discussed earlier about continuum approximations under saturated conditions are applicable.

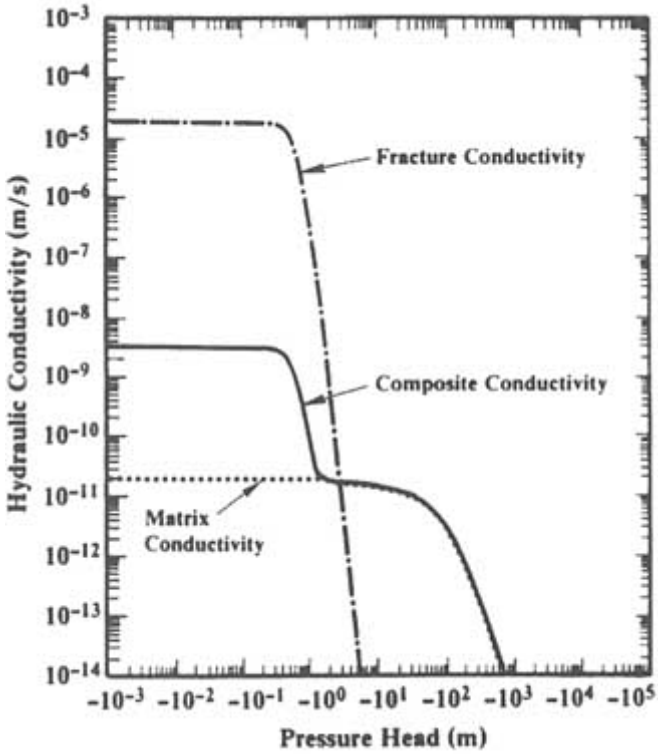

FIGURE 6.31 Hydraulic conductivity of unsaturated fractured volcanic tuff from Yucca Mountain, Nevada, plotted as a function of fluid potential. Pressure values are negative, indicating that water is held in tension. From Peters and Klavetter (1988).

To model fluid flow in unsaturated fractured rocks using currently available models, relationships must be developed for moisture content, fluid pressure, and relative permeability. Additional data are needed to develop relationships for fluid exchange between the fractures and the matrix blocks. Even in a single rock type with a uniform fracture geometry, measurements of characteristic curves representative of field-scale behavior are difficult to obtain. This issue is explored by Kwicklis and Healy (1993), using a numerical model of steady flow through a variably saturated fracture network.

Only limited work has been completed to examine how best to average the properties of the matrix and the fractures under conditions of partial saturation. In a domain containing different lithologies or spatially variable fracture geometries, data requirements seem immense. There is again the issue of how measurements made at one scale can be extended to characterize flow behavior at other scales. At scales of tens to hundreds of meters, parameter estimates may best be constrained through model calibrations using geochemical or isotopic indicators.

Modeling Multiphase Flow in Fractured Rocks

Models that simulate multiphase flow in fractured rock systems arise in petroleum reservoir engineering, in the analysis and development of some geothermal systems, and in contaminant hydrogeology. Experience with multiphase flow models has been considerably more extensive in the petroleum engineering field than in the field of groundwater hydrology. Although the models in both fields have a common basis in the physics of immiscible fluids, they address different sets of problems. For example, interest in fractured petroleum reservoirs commonly centers on prediction of oil displacement from matrix blocks under various recovery plans. Predicted pressure changes in each fluid phase are key variables in characterizing reservoir performance. In geothermal systems the phases of interest are steam and water, and an important area of concern is the generation and migration of steam with a decline in the reservoir pressure. In environmental applications an important issue concerns the redistribution of an organic solvent in a water-saturated medium that initially contains none of this phase. In this case the interest is in the spatial extent and distribution of solvent in the subsurface.

Simulation of multiphase flow (e.g., oil/water/gas) in a naturally fractured petroleum reservoir is normally carried out by using continuum approximations embodied in a dual-porosity model. A mature literature exists on this topic, and Kazemi and Gilman (1993) provide a recent overview of the models used in the petroleum industry. Balance equations are written for each fluid phase, for flow in both the fracture network and the matrix blocks. Because this is a continuum approximation based on porous medium equivalence, rates of fluid flux and capillary pressure are expressed in terms of relative permeability and phase saturation, respectively, for each of the fracture network and matrix domains.

For cases where significant fluid flow occurs between matrix blocks, the dual-porosity model has been extended to produce what are known as dual-permeability models. The fracture network and matrix blocks are viewed as two superimposed continuua, with both the fractures and the matrix forming continuous flow paths across the reservoir. Balance equations are written for multiphase flow in both the fracture network and the rock matrix. This model differs from the dual-porosity model by the addition of interblock matrix flow terms. If these additional terms are set to zero, the dual-porosity formulation is recovered. The concerns raised earlier ("Dual-Porosity Models") about the

predictive capabilities of dual-porosity models are also appropriate when discussing multiphase flow.

The escape of synthetic organic liquids (nonaqueous-phase liquids, or NAPLs) to the subsurface environment poses a significant threat to groundwater quality. Although NAPLs are typically of low solubilities, their dissolution can lead to aqueous-phase concentrations far above drinking water standards. Migration of NAPLs as a separate phase effectively creates a much larger source volume from which mass can be transferred to the aqueous phase by dissolution. The capability to make site-specific predictions of the movement of NAPLs through fractured porous media does not exist with current modeling tools.

Most NAPLs behave as nonwetting fluids, preferentially occupying the larger void spaces. The low viscosity of some NAPLs enhances their mobility. If the fluid density of a NAPL is less than that of water (e.g., gasoline), it will move downward through the vadose zone to the water table, at which point it will migrate laterally. Some fraction of the NAPL will be left behind in fractures in the rock as a residual saturation. Dense NAPLs (e.g., trichloroethylene or polychlorinated biphenyls [PCBs]) can penetrate the water table, moving downward and laterally in a pattern strongly influenced by geological structure. At sites underlain by fractured rock with low matrix porosity, the potential exists for substantial vertical and lateral migration of an NAPL as a separate phase.

Chapter 3 addresses multiphase flow at the scale of a single, rough-walled fracture. For the field problem it is necessary to extend the observations made in single fractures to models that characterize flow in an interconnected network of fractures. A conceptual model of NAPL movement in a fractured medium is shown in Figure 6.32. An NAPL will enter a water-saturated fracture only if the capillary pressure at the entrance to the fracture is greater than the entry pressure. Entry pressures are smaller for larger-aperture fractures or along segments of a fracture where the aperture is greater. The geometric properties of a fracture network are critical factors in determining large-scale migration patterns. At the local scale, NAPLs may be distributed in a very irregular manner. Perhaps the issue of greatest theoretical concern is the determination of appropriate scaling relationships for describing capillary pressure saturation and relative permeability curves at the scale of a fracture network from measurements on single fractures or blocks containing a small number of fractures.

Multiphase flow models describing NAPL migration in fractured rock could be used in practice to provide much-needed insights into physical (and chemical) processes for NAPL migration at the network scale. With respect to site-specific applications, models may have two uses. One is to estimate migration paths and the subsurface volume of residual NAPL for the design of site investigation programs. A second use is for evaluating remediation programs to remove NAPL from a fractured porous medium. However, even as the numerical capability for simulation emerges, it is unclear whether data requirements and the high sensitivity

of NAPL movement to geological structure will permit the formulation of reliable site-specific models.

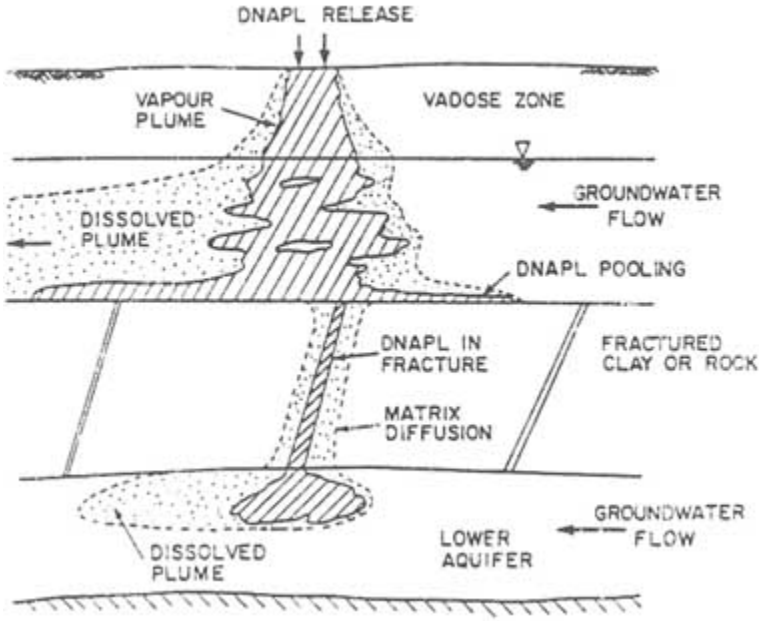

FIGURE 6.32 Conceptual model describing movement of a dense nonaqueous-phase liquid (DNAPL) downward across a fractured geological unit. The liquid has a density greater than that of the groundwater. From Kueper and McWhorter (1991).

Chemical Processes

The hydrological processes that transport dissolved solutes through an open fracture network are linked to chemical processes in the geochemical environment that act to modify solute concentrations. Perturbations of the thermal or stress regime may also initiate and maintain chemical reactions. Flow and transport of reactive solutes are a complex nonlinear system that is difficult to analyze quantitatively.

Chemical processes of interest include precipitation-dissolution reactions, redox reactions, surface sorption, complexation, and transformations of organic compounds. These reactions can occur in the fluid phase; at the interface with a fracture wall; or, as a result of diffusional mass transfer, in matrix pore spaces adjacent to the fracture. Fluid pathways in fractured media may be quite complex. Mixing of fluid with different chemistries in such media cannot necessarily be understood using conventional porous media concepts.

To account for chemical reactions during transport, a geochemical model must be coupled to the mass balance expressions that are the foundation of the fluid flow and solute transport equations. The choice of geochemical model is very much problem dependent. For example, hydrothermal ore deposits typically reflect mineralization from a relic flow system in a fractured rock. Mineralization commonly occurs as the result of a perturbation in the flow system, for instance, a rapid reduction in fluid pressures owing to fracture dilation. To model this system, fluid flow and transport models must be linked to models of the thermal and stress regimes. Time scales of interest may extend over many thousands of years, with repeated episodes of fracture opening and sealing. In principle, equilibrium speciation models of the type used in porous media simulations can serve to track the evolution of the chemical system. If the rate of advective mass transfer through the fracture network is fast relative to the rates of chemical reactions, kinetic models may be needed. The complexities of such systems are great. A quantitative framework is now emerging as a result of careful geological observation to describe in general terms the dynamic evolution of fracture-dominated hydrothermal systems.

In some ways the transport of reactive solutes away from a hazardous waste site or surface impoundment is simpler to characterize than transport in hydrothermal systems. The time scales of concern are much shorter. The thermal and stress regimes can usually be decoupled from the chemical state of the system. Temperatures and pressures are lower. Simpler geochemical models may serve to approximate the important chemical processes. In other ways the problem is more difficult, because site-specific predictions of the potential for, or extent of, off-site migration must be obtained.

Surface sorption of a trace metal or dissolved organic compound is one of the more straightforward geochemical processes to incorporate into a transport model. For problems involving transport in granular porous media, chemistry is commonly simplified. Linear exchange models are used to represent the reversible transfer of mass between the aqueous phase and the solid surface. Recent experimental evidence does, however, point to limitations in the use of a simple, reversible sorption coefficient (Vandergraaf, 1995).

When modeling geochemical processes in fractured rock, there are a number of concerns related to the geometry of flow. A key concern is determination of the contact area between the solute and the rock matrix (Moreno and Noretnieks, 1993). The contact area depends on the degree to which fluid is channelized along pathways through the fracture network, the extent of surface sorption on the fracture walls, and the access of the solute to the rock matrix. At present, it is not known how to introduce these factors into simulation models, in part because it is not known what should be measured in the field. As frequently noted in this chapter, it is difficult to characterize flow paths at the field scale in fractured rock masses. Wels and Smith (1994) suggest that retardation of solutes at the plume scale is a nonuniform, anisotropic process as a consequence

of the inverse relation between retardation and fracture aperature at the scale of individual fractures. There are also unresolved issues about the size of an averaging volume associated with a continuum approximation when comparing the cases of reactive and nonreactive solutes. Reactive transport is more difficult to simulate if the fractures that control flow (e.g., larger, well connected fractures) do not also control the geochemistry of the system. These issues require additional study, both experimental and theoretical, to provide quantitatively sound methods and models for the prediction of reactive solute transport in fractured geological media.

Modeling Heat Transfer in Fractured Rocks

In low-permeability unfractured rock, conduction is the dominant mechanism of heat transfer. Advection of heat by moving groundwater may dominate heat transfer in highly permeable or fractured rocks. An understanding of advective heat transfer is an important problem in fractured systems, with application in the analysis of geothermal systems, disposal of high-level nuclear waste, and characterization of hydrothermal circulation in the oceanic crust.

To model heat transfer in a fractured porous medium, an energy balance equation is introduced to account for conductive and either convective or advective heat transfer in the fracture network and matrix blocks. The presence of a heat source creates spatial gradients in fluid density that provide an additional driving force for fluid flow and solute transport. Fractures serve as efficient conduits for heat transfer by fluid motion, and matrix blocks can be large reservoirs of thermal energy storage. Heat exchange between the matrix and fracture network depends on rates of fluid flow in each domain and the geometry of the fracture network. The main problem in modeling a geothermal reservoir to assess its production potential is to obtain representative values for the hydrological and thermal properties of the fractured rock mass.

The flow model in a geothermal reservoir simulation may be based on single-phase or multiphase flow, depending on whether temperature and pressure conditions allow the formation of a steam phase. The fluid flow and heat transfer equations are coupled and must be solved either simultaneously or iteratively. Pruess and Wang (1987) and Bodvarsson and Witherspoon (1989) provide recent reviews of geothermal models. Most geothermal reservoir simulation models fall into one of two classes: either the rock mass is treated as a single continuum that reflects the composite properties of fractures and matrix or a double-porosity formulation is chosen. The double-porosity models are simply an extension of the models described earlier for single-phase isothermal flow. Double-porosity models assume a regular fracture geometry. Discrete features such as major through-going faults, which are key elements of many geothermal settings, may be modeled as separate hydrogeological units. Both single- and double-porosity models are based on porous medium equivalence.

Advective heat transfer in geological settings at scales where continuum approximations may not hold is an important and largely unexplored topic. This problem could be approached on a theoretical level by coupling the discrete network flow models described earlier with a heat transfer model for the fracture network and the surrounding rock mass.

SUMMARY

Issues of scale underlie and confound the development of hydrogeological simulation models. Scale issues are particularly troublesome for developing hydrogeological models of fractured media. The main difficulty is the identification and representation of the heterogeneous properties of the connected fracture network. Individual measurements of hydraulic properties in single boreholes or detailed characterization of a rock mass volume are made on a small scale relative to the scale of the simulation model. The most basic issue facing the modeling community is how to use measurements obtained at one scale to estimate model parameters that represent another scale of heterogeneity of a fractured rock mass.

The conceptual model plays a fundamental role in dealing with the issue of scale in flow and transport models. As noted previously, the conceptual model can be viewed as a hypothesis describing the main features of the geology, the hydrological setting, and site-specific relationships between geological structure and patterns of fluid flow. It provides the basis for identifying the most important features of the fracture system that need to be incorporated into the hydrogeological or transport simulation model. The simulation model is simply the mathematical expression of the conceptual model in a form that permits a quantitative assessment of system behavior or system response to perturbations. Given a robust conceptual model of the fracture system, different mathematical formulations of the simulation model will likely give similar results. However, an inappropriate conceptual model can easily lead to predictions that are in error by orders of magnitude.

The modeling process is by its very nature an iterative procedure. The steps in building a conceptual model of a flow system in fractured rock include the identification of important features of the fracture system, their location in the rock mass, and determination of the extent to which they conduct fluid. Geological models of the fracture system are an essential part of conceptual model building. As additional data are collected and analyzed, the conceptual model is revised and the hydrogeological simulation model is updated. In the process of calibrating and testing a hydrogeological simulation model, assumptions and approximations on which the conceptual model is founded can be evaluated and refined, if necessary.

Three basic questions must be addressed before a simulation model can be used as a site-specific design tool. First, does the conceptual model provide an adequate characterization of the hydrological system? Second, how well does the

simulation model compare with competing models based on different modeling concepts or different model structures? Third, is the data base adequate to estimate the simulation model parameters with sufficient reliability that the associated prediction uncertainties are acceptable in light of the intended application of the simulation model in the decision process? If not, additional data collection is justified. It is commonly the case that these questions are considerably more difficult to resolve when dealing with fractured media owing to the greater heterogeneity of the flow system.

The level of detail required in the conceptual model varies with the purpose for which the model is being developed, for example, whether it is being used to predict fluid flow or solute transport. Experience suggests that for volumetric flow predictions can be made with a relatively generalized conceptual model, provided data are available to calibrate the simulation model and average rather than local-scale behavior is required. For problems involving solute transport through fractured rock, a considerably more refined conceptual model is needed, in terms of a description of the fracture flow paths, to develop reliable predictions of travel times or solute concentrations because of the sensitivity of these variables to the heterogeneity of fractured systems.

Simulation models can be classified on the basis of how fracture system heterogeneity is incorporated into the model structure. Deterministic continuum models typically represent the heterogeneity of the fractured rock by using a limited number of regions, each with uniform properties. Individual fractures are not explicitly treated in the model, except when they exist on a scale large enough to be considered a separate hydrological unit. Stochastic continuum models represent the heterogeneity of the fractured rock as a continuous random field, with the scale of heterogeneity tailored to the scale of measurements of permeability made in the field. Discrete network models explicitly include large numbers of individual fractures that conduct fluid in the model structure. They reflect an attempt to represent heterogeneity on a scale smaller than normally considered in a continuum model.

Recent model innovations combine elements of both discrete network and continuum approximations. Within each class of model, the analysis may be structured in either a deterministic or stochastic framework, depending on whether the coefficients that characterize heterogeneity are viewed as being known with certainty (or are used as the most likely values) or are described by probability distributions.

There is a diversity of opinion on which numerical modeling approaches are most useful in practice when considered across a broad range of geological settings, scales of interest, and project budgets. In the committee's view, two points are of fundamental importance. First, it is important that a model capture the pattern of heterogeneity in the rock mass; it is less important which type of numerical model is used for representing fracture permeability. Second, no single modeling approach is superior in all instances. A limited number of model

comparisons have been attempted. In these cases most of the flow and transport data derived from the experiments can be more or less equally interpreted by means of a number of fundamentally different mathematical models. However, the experiments on which models have been compared were not designed to discern between different models.

There is also a diversity of opinion on the principles that should guide selection among competing models. Model selection involves an assessment of data availability (both geological and hydrological data), the style and scale of fracturing and the degree of heterogeneity, data reliability, and the intended application of the model. Progress in this area will come only with the availability of more experimental sites and additional experience in testing model predictions encompassing a variety of fracture styles.

The strength of the continuum approach is that it reduces the geometric complexity of the flow patterns in a fractured rock mass into a mathematical form that is straightforward to implement. Averaging volumes associated with the deterministic continuum approximation must be large enough to encompass a statistically representative sample of the open, connected fractures and their variable influences on flow and transport behavior. Effectively, this means that averaging volumes must be sufficiently large that fluid flux and solute transport are not influenced to any significant degree by any individual fracture or its interconnections with other fractures in the conducting network. For most applications that are encountered in practice, some type of continuum approach remains the preferred alternative. Its two greatest limitations are that (1) the scale at which the continuum approximation is justified can be difficult to quantify and (2) the process of spatial averaging restricts the possibility of making model predictions at scales smaller than that of the representative elemental volume. If averaging volumes are large, there may be a broad class of hydrogeological problems, especially those related to contaminant transport, that are not amenable to analysis with deterministic continuum models.

The stochastic continuum approach is built on a geostatistical representation of the spatial variability in the conductance properties of the rock mass. Its important practical advantage is that it works directly with field measurements of permeability, rather than a suite of parameters characterizing network geometry. The scale at which heterogeneity is described can be tied to the scale of field measurements. Stochastic theories provide equations for estimating larger-scale hydraulic and transport properties from the smaller-scale field measurements (Neuman and Depner, 1988). The validity of the stochastic continuum approach rests on the suitability of approximations embodied in the representation of a fractured rock mass as a heterogeneous porous medium and in the suitability of mathematical simplifications that underlie stochastic transport theory. Additional studies are needed to evaluate the capability of geostatistical models to capture the structure of a conducting fracture network (or the so-called hydraulic backbone

of the rock mass) from a suite of smaller-scale permeability measurements derived from packer tests.

Discrete network models are predicated on the assumption that fluid flow behavior can be predicted from knowledge of the fracture geometry and data on the transmissivity of individual fractures. The guiding principle is that one can measure spatial statistics associated with a fracture network, including fracture transmissivity, and use these statistics to generate realizations of fracture networks with the same spatial properties. The fractures in these realizations become the conductive elements in a fracture network flow or transport model. Discrete network models are closely linked with concepts of stochastic simulation, and they lead naturally to the adoption of Monte Carlo simulation techniques to quantify the magnitude of uncertainties in model predictions. In some circumstances, discrete network models may provide one alternate means of estimating large-scale hydraulic and transport properties of the rock mass for use in equivalent continuum models.

Two classes of models have been proposed to represent the geometric properties of fracture networks. One class is based on the assumption that the occurrence of one fracture has no influence on the positioning of any subsequent fracture that is generated to form the network. The second class of models allows a spatial dependence between the positioning of neighboring fractures and leads to networks with recognizable, scale-dependent characteristics. Both models comprise rules for specifying the location of fractures in space; the shape of fractures; the extent of fractures, including truncations against other fractures; the orientation of fractures; and the conductive properties of fractures.

In cases where an equivalent continuum cannot be defined, a discrete network simulation may be a viable alternative. This approach appears most useful in problems of near-field simulation over length scales of 50 to 100 m. Simulations at larger scales require grouping fractures into single features or elimination of less transmissive fractures. The disadvantages of discrete network simulation are threefold: (1) the method requires statistical information that may be difficult to obtain (e.g., fracture size), (2) the models are complex and computationally intensive for realistic fracture densities, and (3) there is no guarantee that a model reproducing the apparent geometric properties of a fracture network will capture its essential flow or transport features.

Geometric information from fracture statistics is not sufficient to construct a discrete network model. To be useful as a simulation tool, discrete network models must incorporate the information contained in the conceptual model concerning the properties and positions of the hydrologically dominant fractures. Hydraulic data also must be available to define transmissivities at the scale of individual fractures. The magnitude of fluid flow estimates is critically dependent on the values assigned to fracture transmissivity. Mechanical measurements of fracture aperture are of little value in this regard as they do not capture the influence of the internal geometry of the fracture plane on the hydraulic resistance

to flow. The observed fracture pattern may not be strongly related to the hydraulic backbone of the conducting fractures if, for example, a significant percentage of the fractures are sealed by mineral precipitates or closed owing to the stress regime. A model based on fracture occurrence that does not account for nonconductive fractures can vastly overestimate the connectivity of the network and will fail to capture the hydraulic behavior of the rock mass.

The latest developments in the area of discrete network simulation address two of the limitations of is method: (1) there are typically no mechanistic underpinnings to the proposed stochastic structure of the fracture network, and (2) a significant number of the observable fractures may not be open to flow. Discrete network models have been extended (1) to take into consideration the origin of the fractures and any statistical distribution functions arising naturally from the physics of fracture formation, (2) to incorporate a hierarchical structure in representing the fracture system, and (3) to be conditioned on hydrological observations. There are a number of reasons to expect that fracture networks will have scale-dependent or hierarchical properties. Some method is needed to identify the more important fractures in the fracture system and to build the geometric model of the network with the greatest emphasis on those fractures. The concept of conditioning discrete network models on hydrological observations involves an extension to cross-hole hydraulic tests from the single-borehole tests used in estimating fracture transmissivity. In this approach an inverse technique is used to construct a representation of the fracture network that is functionally equivalent to the observed system in the constraints imposed by the conceptual model.

Appendix 6.A

Model Prediction Using A Continuum Approach: The URL Drawdown Experiment

Since 1980, Atomic Energy of Canada Limited has been developing an Underground Research Laboratory (URL) in southeastern Manitoba (Davison, 1985; see Figure 8.14 for location map). This facility plays a key role in Atomic Energy's research and development program to evaluate the feasibility of geological disposal of radioactive waste in plutonic rocks in the Canadian Shield (see Chapter 8). The laboratory, excavated in crystalline rock of the Lac du Bonnet batholith, consists of a main vertical shaft approximately 450 m deep, with horizontal tunnels at different depths. Many different experiments have been carried out, or are planned, to assess current and emerging site characterization methods, to document rock mass response to tunneling and thermal loading, and to assess the current ability to model groundwater flow and solute transport in a crystalline rock site.

An experiment conducted during the construction phase of the URL, known as the URL Drawdown Experiment, was designed to evaluate the ability to model groundwater flow in fractured rock. The experiment consisted of (1) characterization of the hydrogeology of the site, (2) development of a groundwater flow model, (3) use of the model to predict hydrological perturbations owing to shaft construction, and (4) comparison of predicted perturbations to actual perturbations observed during shaft excavation.

Prior to shaft excavation, the site was investigated by surface geological mapping and geophysical surveys. Nine boreholes were cored, and 30 air percussion boreholes were drilled. Hydraulic testing consisted of single-borehole straddle packer tests and multiple-borehole hydraulic interference tests. In situ stresses also were measured, and groundwater was sampled for chemical analysis. Similar studies were performed over the larger Whiteshell Research Area to characterize the regional hydrological setting.

The site investigation revealed three major low-angle fracture zones and a number of subvertical fracture zones (see Figure 6.A1 and Chapter 8). Except for these fracture zones, the rock mass was found to be relatively unfractured. Because the fracture zones were significantly more permeable than the surrounding rock, they were believed to control groundwater flow and groundwater chemistry at the site. Detailed analysis of water samples indicated that each of the major zones in Figure 6.A1 was acting as a nearly independent flow path, with weak communication across the intervening rock mass. This generalized model was supported by the results of pumping tests conducted prior to shaft construction. Further investigation at other sites in the Whiteshell Research Area showed that the distribution of fracture zones and character of flow paths in subhorizontal fracture zones were representative of hydraulic conditions over a large part of the batholith.

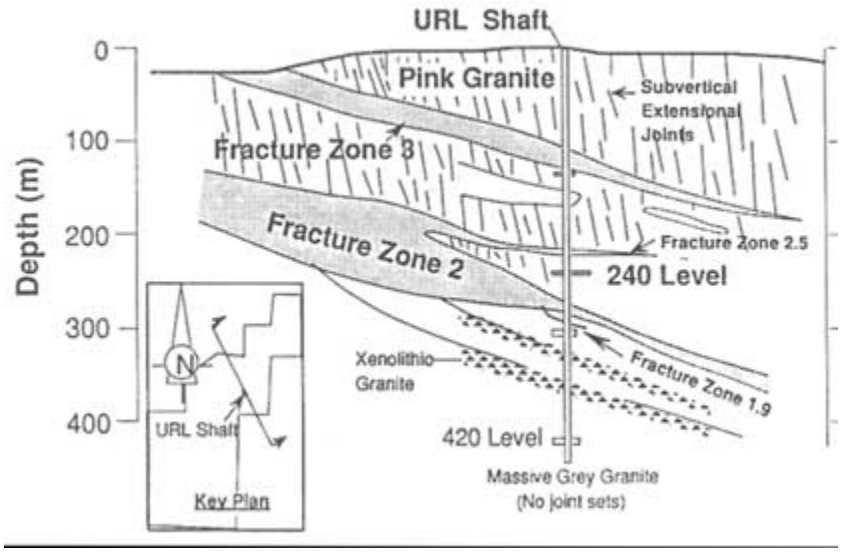

FIGURE 6.A1 Conceptual model of the rock mass at the Underground Research Laboratory (URL) in Manitoba, Canada. From Davison et al. (1993).

Based on knowledge gained from the site investigation, a model of groundwater flow was constructed. The model treated the fracture zones as discrete features and the rock mass away from the fracture zones as a porous medium. Two models were constructed at different scales. A regional-scale model was developed to define boundary conditions for a local-scale model. The regional-scale model was calibrated by adjusting recharge until the water table coincided with the land surface. The local-scale model was calibrated by adjusting parameters in fracture zones until calculated drawdowns agreed with measured drawdowns from hydraulic tests. After calibration, the local-scale model was used to predict drawdown at 171 packer-isolated intervals in the borehole monitoring network and the rate of seepage into the shaft during construction.

The URL model was relatively effective in predicting drawdown during shaft construction. Much of the success resulted from the effectiveness of site characterization prior to model development. The single most important aspect of this characterization was identification of the major geological features (the subhorizontal fracture zones) controlling flow at the site. For most of the 171 measurement locations, the magnitude and temporal variation of the drawdown were predicted to within an order of magnitude. Discrepancies between model predictions and field measurements were inversely proportional to the radial distance from the shaft; smaller discrepancies occurred at greater distances from the shaft. However, the onset of significantly measured drawdown consistently occurred 20 to 30 days earlier than predicted. This was attributed to differences

between assumed and actual shaft deepening rates, as well as the existence of extensive permeable vertical fractures providing good hydraulic communication between fracture zone 3 and the rock some 70 to 80 m above and below the zone. This situation was not detected during any of the site characterization activities carried out prior to excavation. The predicted inflow rate was approximately four times the measured rate (Figure 6.A2). This difference can be attributed in part to a combination of local effects related to the fine-scale distribution of fractures adjacent to the shaft.

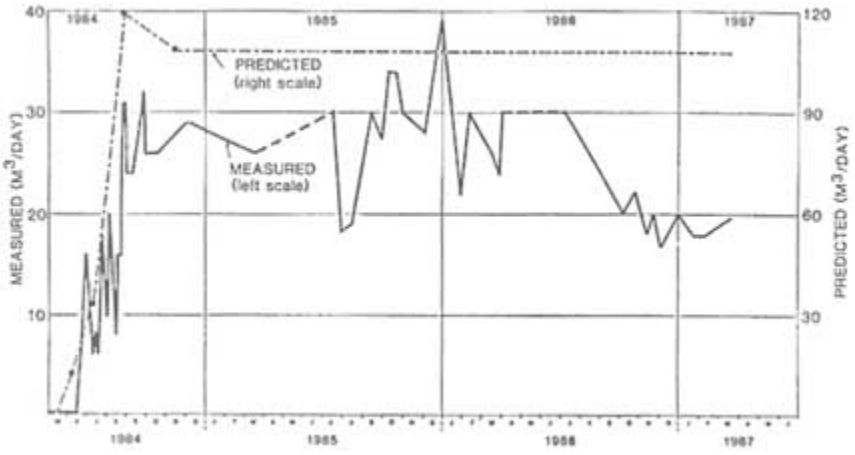

FIGURE 6.A2 Comparison of observed and predicted drawdown using a continuum model for the URL drawdown experiment. The measured inflow is plotted on the left-hand scale, and the predicted inflow on the right-hand scale. From Davision et al. (1987).

Appendix 6.B

Percolation Theory

Percolation theory is the study of random networks of conductors. The simplest example of a percolation network, a simple lattice percolation, can be constructed by creating a lattice of conductors and randomly turning some of them off. Examples of square lattices are shown in the top row of Figure 6.B1. Here, each of the conductors in the square lattice is left on with probability p ($0 \leq p \leq 1$) and turned off with probability $1 - p$. The on-off decisions are statistically independent. The fundamental parameter that describes the statistical model for percolation in this case is p. One example of a percolation network applicable to fracture models is continuum percolation, where sets of conductors are placed randomly in space and overlapping conductors are connected. An example of a continuum percolation network is illustrated in the bottom row of Figure 6.B1.

Usually percolation networks are studied using numerical simulations of finite-sized domains (Zallen, 1983). Some analytical results for infinite-sized percolation networks also are known (Kesten, 1987). These results suggest that percolation models have two basic properties. The first is the existence of a critical density of conductors. Below the critical density there are only finite-sized clusters of connected conductors (no percolation), and above the critical density there is an infinite cluster (or clusters) of connected fractures (percolation). For large, finite-sized percolation models, this means that there is a high probability that no clusters span the largest length scale when the density is below the critical value. Conversely, there is a high probability that a cluster will span the

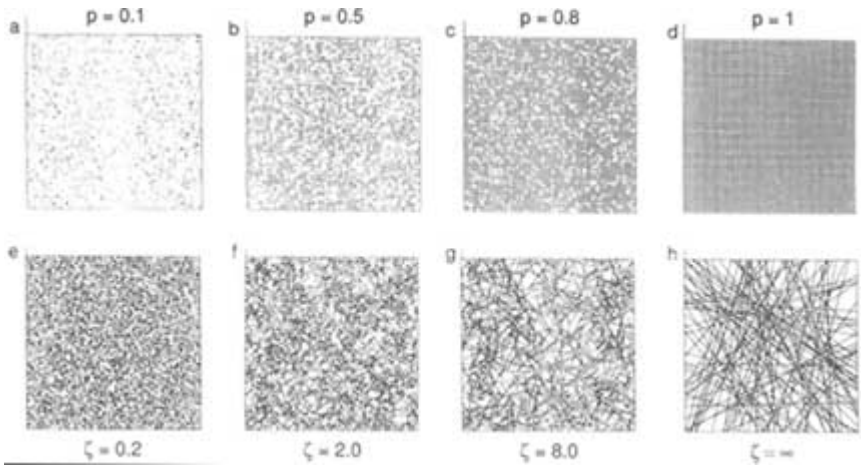

FIGURE 6.B1 Examples of fracture networks with different degrees of connectivity. Parts (a)–(d) are regular lattices that correspond to the random Poisson networks; z`(e)–(h) shown below them.

largest length scale when the density is above the critical value. For simple lattice percolation the critical density corresponds to a value for p called p_c. In the continuum percolation case the controlling parameters are the spatial density, size, and orientation of the random sets. In some cases one can find a way to map the parameters of the continuum percolation model into an effective p and then apply the results predicted by simple lattice percolation (Hestir and Long, 1990).

The second basic property of percolation networks is that universal scaling laws appear when the fracture density is near the critical value. To explain this, suppose p is near p_c and M represents a particular physical property of the percolation network, such as average permeability. Then M will be related to p in the following way:

$$M \alpha (p - p_c)^{\tau}$$

where the exponent τ is referred to as a universal scaling exponent. The term universal is used because numerical studies suggest that the exponent depends only on the dimension of the percolation model (e.g., two or three dimensions) and not the details of the model, such as the kind of lattice used or the types of random sets in the continuum percolation case.

It is reasonable to suggest that most random network models will have two basic properties: critical density and scaling laws with universal exponents. Hence, these properties are also expected to apply in the case of a network of fractures. However, there is no general way to apply these concepts in a field situation, so percolation theory can only be used as a general framework for thinking about fracture and fluid flow problems. For some example applications of percolation theory to flow in a single fracture, see Chapter 3.

Appendix 6.C

Connectivity

A flow system with many fractures can have a high or low permeability depending on the connectivity of the fracture network (Figure 6.B1). Although the term connectivity has no generally accepted definition, it is normally used to describe the subjective appearance of a fracture network. Highly connected networks are more permeable. In some cases, where there is a specific mathematical model for the fractures, connectivity can be rigorously defined.

One of the best-known cases where connectivity has been studied is the percolation model. As noted in Appendix 6.B on percolation theory, percolation networks are constructed by creating a lattice of conductors and randomly turning some of them off. Several quantities can be defined that describe connectivity in percolation networks; each is based on assigning an arbitrary point on the lattice to be the origin. Connectivity measures include (1) the expected number of conductors connected to the origin, and (2) the probability that there is a path from the origin to a point x in the lattice. This latter probability is called the connectivity function. The higher the expected number of conductors, or the greater the probability of a path between the origin and point x, the greater the connectivity, ζ.

A model that is similar to percolation networks is the continuum percolation model. One method for quantifying connectivity in these models involves choosing an arbitrary fracture and labeling it level one (Billaux et al., 1989). The fractures intersecting the level one fracture are then counted and labeled as level two fractures. Next, the number of fractures intersecting level two fractures that were not previously labeled are counted and labeled as level three fractures, and so on. The connectivity measure is given by a count of the number of fractures at each level; more connected systems have an increasing number of fractures at each level, whereas less connected systems have fewer fractures or no fractures at each level.

A third measure of connectivity is the average number of intersections per fracture (Figure 6.B1). This measure was used by Robinson (1984) and Long and Hestir (1990) for Poisson line systems. In this simplified system an analytical expression can be derived for the average number of intersections per fracture. This number is then taken to be the connectivity measure. In this case the permeability of the network is a definable function of connectivity.

Except for the Poisson line model, the other measures of connectivity described above have no known analytical description but can only be determined by numerical methods. To the extent that fracture systems can be reduced to statistical models characterizing the hydraulically active fracture system, the geometric analysis of connectivity will be indicative of permeability.

REFERENCES

Acuna, J. A., and Y. C. Yortsos. 1991. Numerical construction and flow simulation in networks of fractures using fractal geometry. Paper SPE-22703 presented at the 66th Annual Technical Conference, Society of Petroleum Engineers, Dallas, Oct. 6-9.

Anderson, J., and R. Thunvik. 1986. Predicting mass transport in discrete fracture networks with the aid of geometrical field data, Water Resources Research, 22(13):1941–1950.

Aviles, C. A., C. H. Scholz, and J. Boatwright. 1987. Fractal analysis applied to characteristic segments of the San Andreas fault. Journal of Geophysical Research, 92:331–344.

Bachu, S., ed. 1990. Parameter identification and estimation for aquifer and reservoir characterization. In Proceedings, 5th Canadian/American Conference on Hydrogeology, Calgary, Alberta, Canada, September 18-20. Dublin, Ohio: National Water Well Association.

Baecher, G. B. 1972. Site exploration: A probabilistic approach. Ph.D. thesis, Department of Civil Engineering, Massachusetts Institute of Technology, Cambridge.

Baecher, G. B., N. A. Lanney, and H. H. Einstein. 1977. Statistical description of rock properties and sampling. Pp. 5C1–5C8 in Proceedings, 18th United States Symposium on Rock Mechanics, Colorado School of Mines. Golden, Colo.: Johnson Publishing Co.

Barker, J. 1988. A generalized radial flow model for pumping tests in fractured rock. Water Resources Research, 24(10):1796–1804.

Barnsely, M. 1988. Fractals Everywhere. San Diego, Calif.: Academic Press, 396 pp.

Barton, C. C. 1995. Fractal analysis of the scaling and spatial clustering of fractures. In Fractals and Their Use in Earth Sciences, C. C. Barton and P. R. LaPointe, eds. New York: Plenum Publishing Co.

Barton, C. C., and P. A. Hsieh. 1989. Physical and Hydrologic-Flow Properties of Fractures. Field Trip Guidebook T385. Washington, D.C.: American Geophysical Union.

Barton, C. C., and E. Larsen. 1985. Fractal geometry of two-dimensional fracture networks at Yucca Mountain, Southwestern Nevada. Proceedings, International Symposium on Fundamentals of Rock Joints. Bjorkliden, Sweden: Centek Publishers.

Barton, C. M. 1978. Analysis of joint traces. Pp. 38–41 in Proceedings of the 19th U.S. Symposium on Rock Mechanics. Reno, Nev.: Conferences and Institutes.

Bear, J., C. F. Tsang, and G. de Marsily. 1993. Flow and Contaminant Transport in Fractured Rock . New York: Academic Press.

Berkowitz, B., and I. Balberg. 1993. Percolation theory and its applications to groundwater hydrology. Water Resources Research, 29(4):775–794.

Beveye, P., and G. Sposito. 1984. The operational significance of the continuum hypothesis in the theory of water movement through soils and aquifers. Water Resources Research, 20:521–530.

Beveye, P., and G. Sposito. 1985. Macroscopic balance equations in soils and aquifers: the case of space and time-dependent instrumental response. Water Resources Research, 21(8):1116–1120.

Billaux, D., J. P. Chiles, K. Hestir, and J. C. S. Long. 1989. Three-dimensional statistical modeling of a fractured rock mass—an example from the Fanay-Augeres Mine. International Journal of Rock Mechanics and Mining Science and Geomechanical Abstracts, 26(3/4):281–299.

Black, J. H., O. Olsson, J. E. Gale, and D. C. Holmes. 1991. Characterization and validation Stage 4: preliminary assessment and detail predictions. TR 91-108, Swedish Nuclear Power and Waste Management Co., Stockholm.

Bodvarrson, G. S., and P. A. Witherspoon. 1989. Geothermal reservoir engineering, Part 1 . Geothermal Science and Technology, 2(1):1–680.

Cacas, M. C., E. Ledoux, G. de Marsily, and B. Tillie. 1990. Modeling fracture flow with a stochastic discrete fracture network: calibration and validation. 1: The flow model. Water Resources Research, 26:479–489.

Carrera, J., J. Heredia, S. Vomvoris, and P. Hufschmied. 1990. Modeling of flow on a small fractured monzonitic gneiss block. Pp. 115–167 in Hydrogeology of Low Permeability Environments,

International Association of Hydrogeologists, Hydrogeology: Selected Papers, vol. 2, S. P. Neuman and I. Neretnieks, eds. Hannover: Heise.

Chang, J., and Y. C. Yortsos. 1990. Pressure transient analysis of fractal reservoirs. SPE Formation Evaluation, p. 631.

Childs, E. C. 1957. The anisotropic hydraulic conductivity of soil. Journal of Soil Science, 8(1):42–47.

Clemo, T. 1994. Dual permeability modeling of fractured media. Ph.D. thesis, University of British Columbia, Vancouver.

Conrad, F., and C. Jacquin. 1975. Representation of a two-dimensional fracture network by a probabilistic model: application to calculation of the geometric magnitudes of matrix blocks. UCRL-TRANS-10814. Translated from Revue de l'Institut Français du Pétrole, 28 (6):843–890.

Cox, S. J. D., and L. Paterson. 1989. Tensile fracture of heterogeneous solids with distributed breaking strengths. Physical Review Board, 40:4690-4695.

Dagan, G. 1987. Theory of solute transport in water. Annual Reviews of Fluid Mechanics, 19:183–215.

Davison, C. C. 1985. URL Drawdown Experiment and comparison with models. TR 375, Atomic Energy of Canada Ltd., Pinawa, Manitoba.

Davison, C. C., T. Chan, and N. W. Scheier. 1987. Experimental activities of the Canadian nuclear fuel waste management program to validate geosphere models. Pp. 401–422 in Proceedings of GEOVAL-87: A Symposium on Verification and Validation of Geosphere Performance Assessment Models. Stockholm: Swedish Nuclear Power Inspectorate.

Davison, C. C., L. H. Frost, E. T. Kozak, N. W. Scheier, and C. D. Martin. 1993. Investigations of the groundwater transport characteristics of a large fracture zone in a granite batholith of different size scales. Pp. 331–338 in Proceedings of the 2d International Workshop on Scale Effects in Rock Masses, Scale Effects in Rock Masses 93, Pinto du Cusha, ed. Rotterdam: A. A. Balkema.

de Marsily, G. 1987. An overview of coupled processes with emphasis on geohydrology. Pp. 27–37 in Coupled Processes Associated with Nuclear Waste Repositories, C. F. Tsang, ed. New York: Academic Press.

Dershowitz, W. S. 1984. Rock joint systems, Ph.D. thesis, Massachusetts Institute of Technology, Cambridge.

Dershowitz, W. S., and H. H. Einstein. 1988. Characterizing rock joint geometry with joint system models. Rock Mechanics and Rock Engineering, 21:21–51.

Dershowitz, W., and I. Miller. 1995. Dual porosity fracture flow and transport. Geophysical Research Letters, 22(11):1441–1444.

Dershowitz, W., P. Wallmann, and S. Kindred. 1991a. Discrete Fracture Modeling for the Stripa Site Characterization and Validation Drift Inflow Predictions. SKB Report 91-16. Swedish Nuclear Power and Waste Management Co., Stockholm.

Dershowitz, W., P. Wallmann, J. E. Geier, and G. Lee. 1991b. Discrete Fracture Network Modeling of Tracer Migration Experiments at the SCV Site. SKB Report 91-23, Swedish Nuclear Power and Waste Management Co., Stockholm.

Doughty, C., J. C. S. Long, K. Hestir, and S. M. Benson. 1994. Hydrologic characterization of heterogeneous geologic media with an inverse method based on iterated function System. Water Resources Research, 30(6):1721-1745.

Duguid, J. O., and P. C. Y. Lee. 1977. Flow in fractured porous media. Water Resources Research, 13(3):558-566.

Dverstrop, B., and J. Anderson. 1989. Application of the discrete fracture network concept with field data: possibilities of model calibration and validation. Water Resources Research, 25 (3):540-550.

Einstein, H. H., G. B. Baecher, and D. Veneziano. 1979. Risk analysis for rock slopes in open pit mines. Series of reports to U.S. Bureau of Mines. Pub. Nos. R80-17 to R80-22, Department of Civil Engineering, Massachusetts Institute of Technology, Cambridge.

Einstein, H. H., G. B. Baecher, and D. Veneziano, et al. 1980. Risk analysis for rock slopes in open pit mines—final technical report, Pub. No. R80-17, Department of Civil Engineering, Massachusetts Institute of Technology, Cambridge.

Einstein, H. H., D. Veneziano, G. B. Baecher, and K. J. O'Reilly. 1983. The effect of discontinuity persistence on rock slope stability. International Journal of Rock Mechanics and Mining Science and Geomechanics Abstracts , 20(5):227-236.

Elsworth, D. 1986. A model to evaluate the transient hydraulic response of three-dimensional, sparsely fractured rock masses. Water Resources Research, 22(13):1809-1819.

Endo, H. K. 1984. Mechanical transport in two-dimensional networks of fractures. Ph.D. thesis, University of California, Berkeley.

Endo, H. K., J. C. S. Long, C. K. Wilson, and P. A. Witherspoon. 1984. A model for investigating mechanical transport in fractured media. Water Resources Research, 20(10):1390-1400.

Evans, D. D., and T. J. Nicholson. 1987. Flow and Transport Through Unsaturated Fractured Rock. Monograph 42. Washington, D.C.: American Geophysical Union.

Freeze, R. A., and J. A. Cherry. 1979. Groundwater. Englewood Cliffs, N.J.: Prentice-Hall.

Freeze, R. A., J. W. Massmann, L. Smith, T. Sperling, and B. James. 1990. Hydrogeological decision analysis. 1: A framework. Groundwater, 28:738–766.

Geier, J. E., K. Lee, and W. S. Dershowitz. 1989. Field validation of conceptual models for fracture geometry. Unpublished monograph, Golder Associates, Redmond, Wash.

Gelhar, L. W., and C. L. Axness. 1983. Three-dimensional stochastic analysis of dispersion in aquifers. Water Resources Research, 19(1):161-1800.

Gilman, J.R., and H. Kazemi. 1983. Improvements in simulation of naturally fractured reservoirs. Society of Petroleum Engineers Journal, Aug.:695-707.

Glass, R. J., M. J. Nicholl, and V. C. Tidwell. 1995. Challenging models for flow in unsaturated, fractured rock through exploration of small scale processes. Geophysical Research Letters, 22(11):1457-1460.

Griffith, A. A. 1920. The phenomena of rupture and flow in solids. Royal Society (London) Philosophical Transactions series A, 221:163-198.

Herbert, A., and G. Lanyon. 1992. Modeling tracer transport in fractured rock at Stripa. SKB Report 92-01, Swedish Nuclear Power and Waste Management Co., Stockholm.

Herbert, A., J. Gale, G. Lanyon, and R. MacLeod. 1991. Modeling for the Stripa site characterization and validation drift inflow: prediction of flow through fractured rock. SKB Report 91-35. Swedish Nuclear Power and Waste Management Co., Stockholm.

Hestir, K., and J. C. S. Long. 1990. Analytical expressions for the permeability of random two-dimensional Poisson fracture networks based on regular lattice percolation and equivalent media theories. Journal of Geophysical Research, 95(B13):21565–21581.

Hirata, T. 1989. Fractal dimension of fault systems in Japan: fractal structure in rock fracture geometry at various scales. Pure and Applied Geophysics, 131:157-170.

Hsieh, P. A., and S. P. Neuman. 1985. Field determination of the three-dimensional hydraulic conductivity tensor of anisotropic media. 1. Theory. Water Resources Research, 21 (11):1655–1666.

Hsieh, P. A., S. P. Neuman, G. K. Stiles, and E. S. Simpson. 1985. Field determination of the three-dimensional hydraulic conductivity tensor of anisotropic media. 2. Methodology and application to fractured rocks. Water Resources Research, 21(11):1667–1676.

Hudson, J. A., and P. R. La Pointe. 1980. Printed circuits for studying rock mass permeability. International Journal of Rock Mechanics and Mining Science and Geomechanics Abstracts, 17:297-301.

Hull, L., and T. Clemo. 1987. Section 4: Dual permeability model: Laboratory and FRACSL validation studies, in Geothermal Injection Technology Program Annual Progress Report Fiscal Year 1986. Idaho Falls, Idaho: Idaho National Engineering Lab.

Huyakorn, P. S., B. H. Lester, and C. R. Faust. 1983a. Finite element techniques for modeling groundwater flow in fractured aquifers. Water Resources Research, 19(4):1019-1035.

Huyakorn, P. S., B. H. Lester, and J. W. Mercer. 1983b. An efficient finite element technique for modeling transport in fractured porous media. 1: Single-species transport. Water Resources Research, 19(3):841-854.

Ibaraki, M. 1994. Colloid-facilitated contaminant transport in discretely-fractured porous media. Ph.D. thesis, University of Waterloo, Waterloo, Ontario, Canada.

Irmay, S. 1955. Flow of liquids through cracked media. Bulletin of the Water Resources Council, Israel, 5A(1):84.

Isaaks, E., and M. Srivastava. 1989. Applied Geostatistics. New York: Oxford University Press.

Iwai, K. 1976. Fundamental studies of fluid flow through a single fracture. Ph.D. dissertation, University of California, Berkeley.

Jones, J. W., E. S. Simpson, S. P. Neuman, and W. S. Keys. 1985. Field and theoretical investigations of fractured crystalline rock near Oracle, Arizona . CR-3736. Washington, D.C.: U.S. Nuclear Regulatory Commission.

Kazemi, H. 1969. Pressure transient analysis of naturally fractured reservoirs with uniform fracture distribution. Society of Petroleum Engineers Journal, 9:451-462.

Kazemi, H., and J. R. Gilman. 1993. Multiphase flow in fractured petroleum reservoirs. Pp. 267–323 in Flow and Contaminant Transport in Fractured Rocks, J. Bear, C. F. Tsang, and G. de Marsily, eds. New York: Academic Press.

Kesten, H. 1987. Percolation theory and first passage percolation. Annals of Probability, 15:1231–1271.

Khaleel, R. 1989. Scale dependence of continuum models for fractured basalts. Water Resources Research, 25(8):1847–1856.

Kirkpatrick, S., D. C. Gelatt, and M. P. Vecchi. 1983. Optimization by simulated annealing. Science, 220:671–680.

Kueper, B. H., and D. B. McWhorter. 1991. The behavior of dense non-aqueous phase liquids in fractured clay and rock. Groundwater, 29(5):716–725.

Kwicklis, E. D., and R. W. Healy. 1993. Numerical investigation of steady liquid water flow in a variably saturated fracture network. Water Resources Research, 29(12):4091–4102.

LaPointe, P. R. 1988. A method to characterize fracture density and connectivity through fractal geometry. International Journal of Rock Mechanics and Mining Science and Geomechanics Abstracts, 25:421–429.

LaPointe, P., and J. A. Hudson. 1985. Characterization and interpretation of rock mass joint patterns. Special Paper 199. Boulder, Colo.: Geological Society of America.

Lawn, B. R., and T. R. Wilshaw. 1975. Fracture of Brittle Solids. Cambridge: Cambridge University Press.

Lee, J. S., D. Veneziano, and H. H. Einstein. 1990. Hierarchical fracture trace model. In Proceedings of the 31st U.S. Symposium on Rock Mechanics. Rotterdam: A. A. Balkema.

Long, J. C. S. 1983a. Construction of equivalent discontinuum models for fracture hydrology. In J. A. Hudson, ed., Rock Testing and Site Characterization, vol. 3, Comprehensive Rock Engineering. New York: Pergamon Press.

Long, J. C. S. 1983b. Investigation of equivalent porous medium permeability in networks of discontinuous fractures. Ph.D. dissertation, University of California, Berkeley.

Long, J. C. S. 1993. Construction of equivalent discontinuum models for fracture hydrology, comprehensive rock engineering. J. Hudson, T. Brown, C. Fairhurst, and E. Hoek, eds. Oxford, N.Y.: Pergamon Press.

Long, J. C. S., and D. M. Billaux. 1987. From field data to fracture network modeling: an example incorporating spatial structure. Water Resources Research, 23(7):1201–1216.

Long, J. C. S., and K. Hestir. 1990. Permeability of random two-dimensional fracture networks. Journal of Geophysical Research, 95(B13):21,256.

Long, J. C. S., and P. A. Witherspoon. 1985. The relationship of the degree of interconnectivity to permeability in fracture networks. Journal of Geophysical Research, 90(B4):3087–3097.

Long, J. C. S., J. S. Remer, C. R. Wilson, and P. A. Witherspoon. 1982. Porous media equivalents for networks of discontinuous fractures. Water Resources Research, 18(3):645–658.

Long, J. C. S., P. Gilmour, and P. A. Witherspoon. 1985. A model for steady state flow in random, three-dimensional networks of disk-shaped fractures. Water Resources Research, 21 (8):1150–1115.

Long, J. C. S., E. Majer, S. Martel, K. Karasaki, J. Peterson, Jr., A. Davey, and K. Hestir, 1990. Hydrologic characterization of fractured rocks—an interdisciplinary methodology. NAGRADOE Cooperative Project Report LBL-27863. Lawrence Berkeley Laboratory, Berkeley, Calif.

Long, J. C. S., C. Doughty, K. Hestir, and S. Martel. 1992a. Modeling heterogeneous and fractured reservoirs with inverse methods based on iterated function system. In Reservoir Characterization III, B. Linville, ed. Tulsa, Okla.: Pennwell Books.

Long, J. C. S., A. Mauldon, K. Nelson, S. Martel, P. Fuller, and K. Karasaki. 1992b. Prediction of flow and drawdown for the site characterization and validation site in the Stripa mine. SKB Report 92-05, Swedish Nuclear Power and Waste Management Co., Stockholm.

Long, J. C. S., O. Olsson, S. Martel, and J. Black. 1996. Effects of excavation on water inflow to a drift. In Fractured and Jointed Rock Masses. Rotterdam: A. A. Balkema.

Mardia, K. V. 1972. Statistics of Directional Data. San Diego: Academic Press.

Martel, S. J. 1992. Geologic characterization of fractures as aid to hydrologic modeling of the SCV block at the Stripa mine. Stripa Project Technical Report 92-24, Swedish Nuclear Power and Waste Management Co., Stockholm.

Martel, S. J., and J. E. Peterson, Jr. 1990. Use of integrated geologic and geophysical information for characterizing the structure of fracture systems at the US/UK site, Grimsel Laboratory, Switzerland. LBL-27912, Lawrence Berkeley Laboratory, Berkeley, Calif.

Martel, S. J., and J. E. Peterson. 1991. Interdisciplinary characterization of fracture systems at the US/BK site, Grimsel Laboratory, Switzerland. International Journal of Rock Mechanics and Mining Science and Geomechanics Abstracts, 28:259–323.

Martel, S. J., and J. E. Peterson. 1993. Techniques for assessing the in situ orientation distribution of fractures from borehole data. Geological Society of America Abstracts with Programs, 25 (114).

Martel, S. J., D. D. Pollard, and P. Segall. 1988. Development of simple strike-slip fault zones in granitic rock, Mount Aboot quadrangle, Sierra Nevada, California. Geological Society of America Bulletin, 100:1451–1465.

Martel, S., K. Hestir, and J. C. S. Long. 1991. Generation of fracture patterns using self-similar iterated function concepts. 1990 Annual report, Earth Sciences Division, Lawrence Berkeley Laboratory, Berkeley, Calif., pp. 52–56.

McKay, L. D., R. W. Gillham, and J. A. Cherry. 1993. Field experiments in a fractured clay till. 2. Solute and colloid transport . Water Resources Research, 29(12):3879–3890.

Moench, A. F. 1984. Double porosity models for a fissured groundwater reservoir with fracture skin. Water Resources Research, 20(7):831–846.

Moreno, L., and I. Neretnieks. 1993. Flow and nuclide transport in fractured media: the importance of the flow-wetted surface for radionuclide migration. Journal of Contaminant Hydrology, 13:49–71.

National Research Council. 1990. Groundwater Models: Scientific and Regulatory Applications. Committee on Groundwater Modeling Assessment, Water Science and Technology Board. Washington, D.C.: National Academy Press.

Neuman, S. P. 1987. Stochastic continuum representation of fractured rock permeability as an alternative to the REV and fracture network concepts. Pp. 533–561 in Rock Mechanics, Proceedings of the 28th U.S. Rock Mechanics Symposium. Rotterdam: A. A. Balkema.

Neuman, S. P. 1990. Universal scaling of hydraulic conductivities and dispersivities in geologic media. Water Resources Research, 26(8):1749–1758.

Neuman, S. P. 1994. Generalized scaling of permeability values: validation and effect of support scale. Geophysical Research Letters, 21(5):349–352.

Neuman, S. P., and J. S. Depner. 1988. Use of variable scale pressure test data to estimate the log hydraulic conductivity covariance and dispersivity of fractured granites near Oracle, Arizona . Journal of Hydrology, 102(1–4):475–501.

Neuman, S. P., and S. Orr. 1993. Prediction of steady-state flow in non uniform geologic media by conditional moments: exact non local formalism, effective conductivities, and weak approximation. Water Resources Research, 29(2):341–364.

Neuman, S. P., E. S. Simpson, P. A. Hsieh, J. W. Jones, and C. L. Winter. 1985. Statistical analysis of hydraulic test data from crystalline rock near Oracle, Arizona. International Association of Hydrogeologists, Memoires, vol. XVII.

Nordqvist, A. W., Y. W. Tsang, C. F. Tsang, B. Dverstrop, and J. Anderson. 1992. A variable aperture fracture network model for flow and transport in fractured rocks. Water Resources Research, 28(6):1703–1714.

Oda, M. 1985. Permeability tensor for discontinuous rock masses. Geotechnique, 35(4):483–495.

Oda, M., Y. Hatsuyama, and Y. Ohnishi. 1987. Numerical experiments on permeability tensor and its application to jointed granite at Stripa mine, Sweden. Journal of Geophysical Research, 92(B8):8037–8048.

Odling, N. E., and I. Webman. 1991. A conductance mesh approach to the permeability of natural and simulated fracture patterns. Water Resources Research, 27:2633–2644.

Okubo, P. G., and K. Aki. 1987. Fractal geometry in the San Andreas fault system. Journal of Geophysical Research, 92:345–355.

Okusu, N. M., K. Karasalai, J. C. S. Long, and G. Bodvarsson. 1989. FMMG: a program for discretizing two-dimensional fracture matrix systems. Theory, design, and user's manual. LBL-26 782, Lawrence Berkeley Laboratory, Berkeley, Calif.

Olson, J. 1991. Fracture mechanics analysis of joints and veins. Ph.D. dissertation, Stanford University, Stanford, Calif.

Olsson, O., ed. 1992. Site characterization and validation. Final Report, Stripa Project, 92-22, Conterra AB, Uppsala, Sweden.

Orbach, R. 1986. Dynamics of fractal networks. Science, 231:814–819.

Parney, R., and L. Smith. 1995. Fluid velocity and path length in fractured media. Geophysical Research Letters, 22(11):1437–1440.

Persoff, P., K. Pruess, and L. Myer. 1991. Two-phase flow visualization and relative permeability measurement in transparent replicas of rough-walled rock fractures . In Proceedings of the 16th Workshop on Geothermal Reservoir Engineering. Stanford, Calif.: Stanford University.

Peters, R. R., and E. A. Klavetter. 1988. A continuum model for water movement in unsaturated fractured rocks. Water Resources Research, 24(3):416–430.

Pollard, D. D., and A. Aydin. 1988. Progress in understanding jointing over the past century. Geological Society of America Bulletin, 100:1181–1204.

Pollek, J. M. 1990. Studies of the hydraulic behavior of hierarchically fractured geometries. LBL-28612, Lawrence Berkeley Laboratory, Berkeley, Calif., 72 pp.

Power, W. L., and T. E. Tullis. 1991. Euclidian and fractal models of surface roughness. Journal of Geophysical Research, 96:415–424.

Power, W. L., T. E. Tullis, S. R. Brown, G. N. Boitnott, and C. H. Scholz. 1987. Roughness of natural fault surfaces. Geophysical Research Letters, 14:29–32.

Priest, S. D., and J. Hudson. 1976. Discontinuity spacings in rock. International Journal of Rock Mechanics and Mining Science, 13:135–148.

Pruess, K., and K. Karasaki. 1982. Proximity functions for modeling fluid and heat flow in reservoirs with stochastic fracture distributions. In Proceedings of the 8th Workshop on Geothermal Reservoir Engineering. Stanford, Calif.: Stanford University.

Pruess, K., and T. N. Narasimhan. 1988. Numerical modeling of multiphase and nonisothermal flows in fractured media. In Proceedings of the Symposium Conference on Fluid Flow in Fractured Rocks, Georgia State University, May 15-18.

Pruess, K., and J. S. Y. Wang. 1987. Numerical modeling of isothermal and nonisothermal flow in unsaturated fractured rock—A review. Pp. 11–21 in Flow and Transport Through Unsaturated

Fractured Rocks, D. D. Evans, and T. J. Nicholson, eds., Monograph 42. Washington, D.C.: American Geophysical Union.

Rasmussen, T. C. 1991. Steady fluid flow and travel times in partially saturated fractures using a discrete air-water interface. Water Resources Research, 27(1):67.

Rasmussen, T. C., and D. P. Evans. 1993. Water infiltration into exposed fractured rock surfaces. Soil Science Society Journal, 57(2):324–329.

Reeves, M., G. A. Freeze, V. A. Kellel, J. F. Pickens, D. T. Upton, and P. B. Davies. 1991. Regional double porosity solute transport in the Culebra dolomite under brine-reservoir-breach release conditions: an analysis of parameter sensitivity and importance. SAND89–7069, Sandia National Laboratories, Albuquerque, N.M.

Robinson, P. 1984. Connectivity, flow and transport in network models of fractured media. Ph.D. thesis, Oxford University.

Rouleau, A. 1984. Statistical characterization and a numerical simulation of a fracture system—application to groundwater flow in the Stripa granite. Ph.D. thesis, University of Waterloo, Waterloo, Ontario, Canada.

Scholz, C. H., and C. A. Aviles. 1986. The fractal geometry of faults and faulting. Pp. 145–155 in Earthquake Source Mechanics, S. Das, J. Boatwright, and C. H. Scholz, eds. Geophysical Monograph Series, vol. 37. Washington, D.C.: American Geophysical Union.

Schwartz, F. W., and L. Smith. 1988. A continuum approach for modeling mass transport in fractured media. Water Resources Research, 24(8):1360–1372.

Segall, P., and D. D. Pollard. 1989. Joint formation in granitic rock of the Sierra Nevada. Geological Society of America Bulletin, 94:563–575.

Segan, S., and K. Karasaki. 1993. TRINET: a flow and transport code for fracture networks—user's manual and tutorial. LBL-34834, Lawrence Berkeley Laboratory, Berkeley, Calif.

Shapiro, A. M., and J. Anderson. 1985. Simulation of steady state flow in three-dimensional fracture networks using the boundary element method. Advances in Water Research, 8(3).

Shimo, M., and J. C. S. Long. 1987. A numerical study of transport parameters in fracture networks. In Flow and Transport Through Unsaturated Fractured Rocks, D. D. Evans and T. J. Nicholson, eds. Monograph 42. Washington, D.C.: American Geophysical Union.

Smith, L., and F. W. Schwartz. 1984. An analysis of the influence of fracture geometry on mass transport in fractured media. Water Resources Research, 20(9):1241–1252.

Smith, L., and F. W. Schwartz. 1993. Solute transport through fracture networks. In Flow and Contaminant Transport in Fractured Rocks, J. Bear, C. F. Tsang, and G. de Marsily, eds. New York: Academic Press.

Smith, L., T. Clemo, and M. Robertson. 1990. New approaches to the simulation of field scale solute transport in fractured rocks. In Proceedings of the 5th Canadian/American Conference on Hydrogeology, S. Bachu, ed. Dublin, Oh.: National Waterwell Association.

Smith, L., C. W. Mase, F. W. Schwartz, and D. Chorley. 1985. Dispersion in three-dimensional fracture networks. In Hydrogeology of Rocks of Low Permeability Symposium. Tucson, Ariz.: International Association of Hydrogeologists.

Snow, D. 1965. A parallel-plate model of fractured permeable media. Ph.D. dissertation, University of California, Berkeley.

Sudicky, E. A., and R. G. McLaren. 1992. The Laplace transform Galerkin technique for large scale simulation of mass transport in discretely fractured porous formations. Water Resources Research, 28(2):499–514.

Takayasu, H. 1985. A deterministic model of fracture. Progress in Theoretical Physics, 74:1343–1345.

Tchalenko, J. S. 1970. Similarities between shear zones of different magnitudes. Geological Society of America Bulletin, 81:1625–1640.

Termonia, Y., and P. Meakin. 1986. Formation of fractal cracks in a kinetic fractal model. Nature, 320:429–431.

Terzaghi, R. 1965. Sources of errors in joint surveys. Geotechnique, 15:287–303.

Teufel, L. W., D. W. Rhett, and H. E. Farrell. 1991. Effects of reservoir depletion and pore pressure drawdown on in-situ stress and deformation in Ekofisk Field, North Sea. Pp. 63–72 in Proceedings of the 32nd U.S. Rock Mechanics Symposium . Rotterdam: A. A. Balkema.

Therrien, R. 1992. Three-dimensional analysis of variably-saturated flow and solute transport in discretely-fractured porous media. Ph.D. dissertation, University of Waterloo, Waterloo, Ontario, Canada.

Vandergraaf, T. T. 1995. Radionuclide migration experiments under laboratory conditions. Geophysical Research Letters, 22(11):1409–1412.

Veneziano, D. 1978. Probabilistic modeling of joints in rock. Unpublished manuscript, Massachusetts Institute of Technology, Cambridge.

Wang, J. S. Y., and T. N. Narasimhan. 1985. Hydrologic mechanisms governing fluid flow in a partially saturated, fractured porous medium. Water Resources Research, 20(12):1861–1874.

Warburton, P. M. 1980a. A stereological interpretation of joint trace data. International Journal of Rock Mechanics and Mining Sciences, 17:181–190.

Warburton, P. M. 1980b. A stereological interpretation of joint trace data: influence of joint shape and implications for geological surveys. International Journal of Rock Mechanics and Mining Sciences, 17:305–316.

Warren, J. E., and P. J. Root. 1963. The behavior of naturally fractured reservoirs. Society of Petroleum Engineers Journal, 3:245–255.

Wels, C., and L. Smith. 1994. Retardation of sorbing solutes in fractured media. Water Resources Research, 30(9):2547–2563.

Zallen, R. 1983. Physics of Amorphous Solids. New York: John Wiley.

7

Induced Changes to Fracture Systems

In this chapter a variety of processes associated with induced changes to fracture systems that involve fluid flow are examined. Fractures are sensitive to changes in temperature, pressure, and fluid chemistry. Indeed, slight perturbations can result in significant alterations in fracture properties. The fundamental mechanisms and the tools to measure or predict these changes are described. Many of the same changes that occur in engineering practice also occur in natural systems, as described in Chapter 2.

This topic is extremely complex, and an exhaustive treatment is well beyond the scope of this report. This chapter provides a brief overview of the types and causes of changes to fracture networks in engineering practice, with some explanation of the approaches used to deal with these changes. In this chapter, these changes are organized first according to the type of change and second according to its cause. Four different ways that fracture systems can be altered are discussed here (Figure 7.1). The first is deformation through changes in stresses in the rock mass. This deformation includes changes in the void geometry of fractures, which in turn changes the ability of fractures to conduct fluids. In the extreme, deformation leads to rock failure. Extensional or shear failure can lead to the creation of new fractures.

The second is modification of the fluids contained in fractures. Fluids with significantly different properties can flow into the fractures, or fluids in the fractures can undergo phase changes or alterations of the distribution of phases or components.

The third is the addition of solid material into fractures. This can occur through the introduction of grout or through fluid injections that transport solid materials.

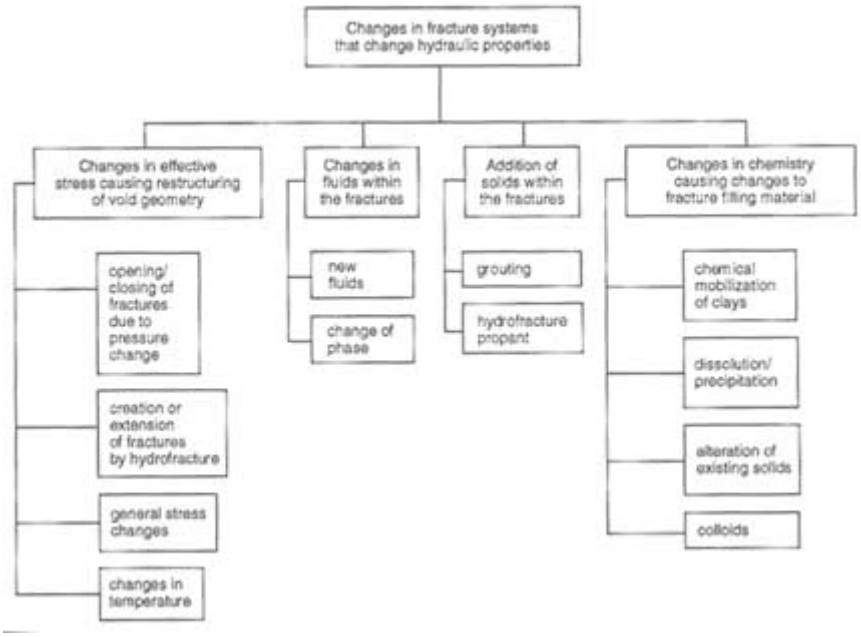

FIGURE 7.1 Changes to fracture systems that change hydraulic properties.

The fourth is a change in the distribution of solid materials in fractures through chemical reactions. Dissolved minerals can precipitate and seal fractures. Leaching fluids can dissolve fracture fillings or fracture walls. In the extreme, precipitates can completely till fractures and form mineral veins, or the rock can dissolve, leading to the development of karst. Most such changes are caused by natural processes, but induced pressure and temperature alterations can produce similar effects.

CHANGES IN FRACTURE VOID GEOMETRY DUE TO CHANGES IN EFFECTIVE STRESS

A variety of engineering activities cause fractured rocks to deform or fail. Changes in fluid pressures, the addition or redistribution of loads, or changes in temperature can lead to changes in the state of stress in the rock. The apertures of fractures depend critically on effective stresses acting normal to the fracture planes. The ability of a fracture to conduct fluid is extremely sensitive to the aperture.

Four kinds of deformation are discussed below: (1) opening or closing of the fracture owing to changes in fluid pressure, (2) the formation and extension of fractures in response to elevated fluid pressures, (3) deformation or failure of

fractures in response to general changes in stress state, and (4) deformation of fractures owing to heating or cooling.

Changes in Fracture Aperture Due to Fluid Pressure Changes

Fluid pressure in fractures can change during many common engineering activities when fluid is withdrawn from or injected into a fractured rock. For fluid injection or withdrawal in a well, radial symmetry results in large fluid pressure changes near the wellbore. For steady-state Darcy flow into or out of a well with a diameter of a few tens of centimeters, most of the pressure change occurs in the first few meters of rock surrounding the well. The flow gradients alter the stresses by changing the pore pressure and by viscous drag on the pore walls. The drag is analogous to a body force acting in the direction of flow. The field of poroelasticity deals with the relationship between pore fluids and matrix stresses. Perkins and Gonzales (1984) provide an example of the use of poroelastic principles for the analysis of stress changes around an injection well.

Any excavation in a rock mass under the groundwater table for tunnels, mines, or foundations tends to drain fluid from the rock. Fluid pressures decrease to near-atmospheric levels in the excavation, which increases the hydraulic gradient. Drainage causes a reduction in water pressure near the excavation. However, this effect can be counteracted by seepage stresses. Reduction of water pressure usually results in a strengthening of the rock mass because of the increase in effective stress. It is possible but rare that this reduction in water pressure can increase the effective stress sufficiently to cause failure and excavation collapse or borehole instability. At the same time, increases in water pressure can produce irreversible changes in fracture network properties, as described in the water well stimulation example illustrated in Appendix 4.C.

Effective Stress and Fluid Flow

Changes in fracture systems owing to variations in pore pressure can be understood by using the concept of effective stress, as discussed in Chapter 3. Fluid pressure in the pore spaces of rock (including the apertures of fractures) works against externally applied compressive stresses. For fractures the effective stress is the difference between the total stress applied on the fracture face and the pore pressure in the fracture (see Chapter 3). Stress-dependent properties such as frictional strength and fluid permeability are governed by the effective stress. An increase in effective stress will close the fractures and reduce their permeability; a decrease in effective stress will have the opposite effect.

A field example of the relationship between flow behavior and effective stress is given in Figure 7.2, for a fractured sandstone gas reservoir at the U.S. Department of Energy's multiwell site in western Colorado (Warpinski, 1991). The matrix permeability of the marine sandstone reservoirs is less that 10^{-18} m^2

(less that one microdarcy; see Chapter 8). The minimum principal stress is normal to the dominant fracture orientation. The fracture network provides an overall in situ permeability that is several orders of magnitude greater than the matrix permeability and a horizontal permeability-anisotropy ratio of about 100:1 (inferred from interference testing with nearby wells). The stress-permeability relationship shown in Figure 7.2 is based on the model presented by Walsh (1981):

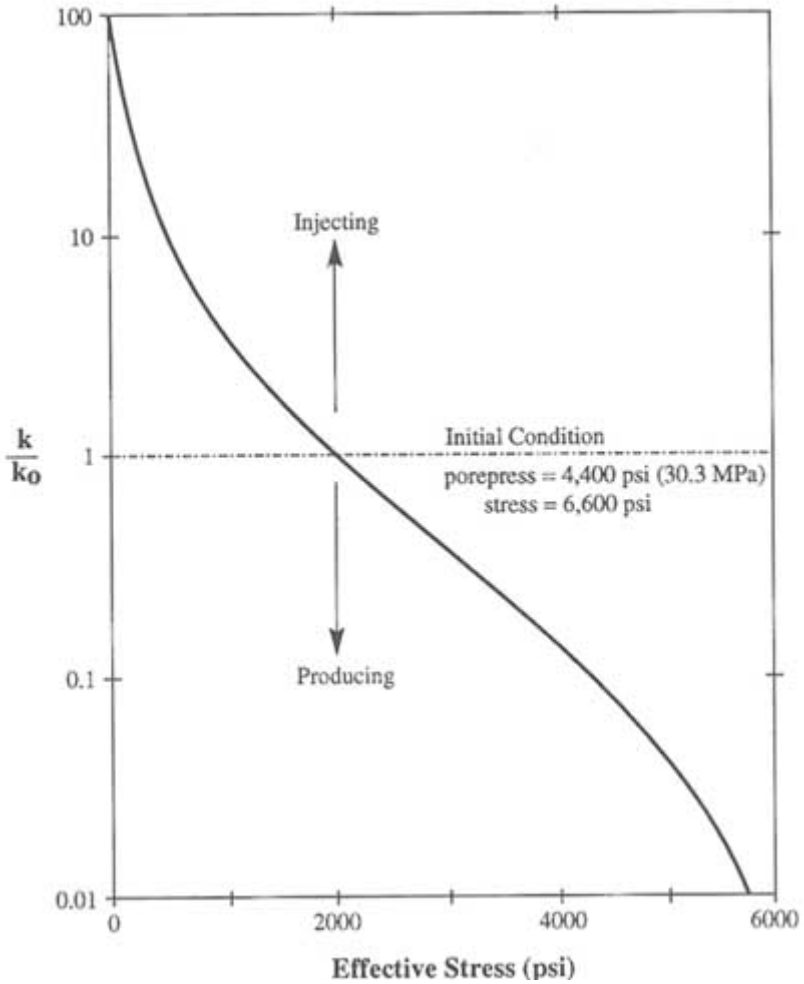

FIGURE 7.2 Permeability vs. stress as determined in the multiwell site. Modified from Warpinski (1991).

$$k = k_o\left(C\ln\frac{\sigma^*}{\sigma - p}\right)^3 \qquad (7.1)$$

where k is permeability, k_o is the reservoir permeability under in situ conditions, σ is the normal stress on the fracture, σ^* is the reference stress state, and C is a constant. The parameters C and σ^* were calibrated by using the results from two different stress conditions. The first was for a low effective stress [<6.89 MPa (<1000 psi)], achieved by injecting nitrogen. Under this condition, the effective reservoir permeability was found to be one to two orders of magnitude greater than that for initial reservoir conditions. The second was for high effective stress [>34.5 MPa (>5000 psi)], achieved by producing the well with a drawdown sufficient to stop all production (i.e., for $k = 0$). During multiple cycles of production, shutin, and injection, the permeability changes in this reservoir were found to be reversible, with no significant changes to the original permeability after reestablishment of the initial reservoir pressure (i.e., after a long shutin period).

The impact of an increase in effective stress on reservoir performance is illustrated in Figure 7.3. This figure shows how the steady-state flow rate is related to steady-state drawdown for a rigid system (dashed line) and calculated for the compliant system (solid line) illustrated in Figure 7.2. In the rigid system, flow into the well is proportional to the drawdown. In the compliant system the increase in flow produced by increasing the drawdown, which increases the effective stress, is offset by the consequent decrease in fracture conductivity. For

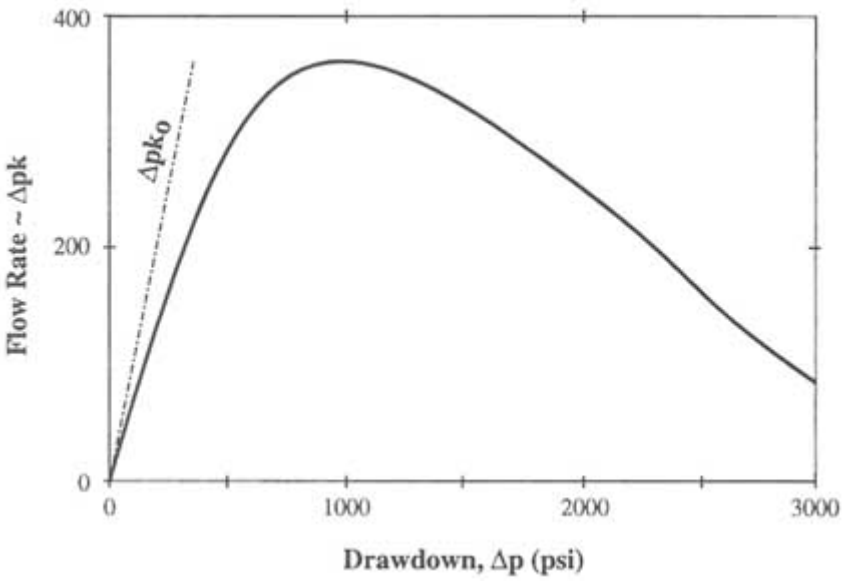

FIGURE 7.3 Change in steady-state flow rate as a function of drawdown based on the permeability reduction relationship given in Figure 7.2.

drawdowns somewhat greater than 6.89 MPa (<1000 psi), production can decline dramatically with increasing drawdown.

Effective Stress and Anisotropy

Changes in pore pressure can affect the degree of permeability anisotropy. For example, in cases with both significant matrix and fracture permeability where there is only one dominant fracture set, an increase in pore pressure will lower the effective stress. This leads to an increase in anisotropy by opening the fractures, thus increasing the permeability parallel to the fracture orientation. The permeability in other directions would be unchanged by comparison because it is controlled by the less stress-sensitive matrix.

Where there is more than one fracture set, the nature of anisotropy change would depend on which of the sets were more deformable. In the case of decreasing pore pressures in a low-permeability rock matrix, the closing of fractures could lead to a situation where the rock mass permeability is equal to the matrix permeability by reducing fracture interconnectivity below the critical limit for percolation (see Chapter 6).

In a poorly connected fracture network, a decrease in pore pressure could theoretically make the rock more isotropic. As some fractures become relatively impermeable, their connectivity is reduced to near the percolation limit. At the percolation limit, the flow in any direction must utilize fractures of all orientations. The flow observed on a large scale then depends on the same few open fractures, and permeability is consequently isotropic.

Determining Effective Stress

Determination of the stress field and pore pressure distributions are prerequisites to determining the effective stress. The state of stress is represented by a symmetric second-order tensor, so there will always exist three mutually perpendicular vectors that define the so-called principal stress directions. In general, the state of stress is anisotropic, and three principal values of stress and their directions are needed for a complete description. Generally, when the stress directions are not altered by nearby faults, the principal stresses are horizontal and vertical, with overburden pressure given by where ρ is the rock density, g is the gravitational acceleration, and z is the depth below the surface. For rock with shear strength in an extensional regime, the vertical stress is usually the major principal stress; the horizontal stresses take on a variety of values. For rock with shear strength in a compressional regime, the maximum principal stress can be horizontal, and the least principal stress can be vertical. Near the surface the maximum principal stress also can be

$$\sigma_{vertical} = \rho g z, \qquad (7.2)$$

where ρ is the rock density, g is the gravitational acceleration, and z is the depth below the surface. For rock with shear strength in an extensional regime, the vertical stress is usually the major principal stress; the horizontal stresses take on a variety of values. For rock with shear strength in a compressional regime, the maximum principal stress can be horizontal, and the least principal stress can be vertical. Near the surface the maximum principal stress also can be

horizontal if the terrain is overconsolidated, that is, if some of the original overburden has been removed by erosion.

Measurement of the magnitude of the minimum principal stresses and their orientation by hydraulic fracturing is well established in the mining, petroleum, and geotechnical industries. Hydrofracturing is discussed more completely below. A number of other methods use measurements of strain to infer the state of stress.

The pore pressure frequently has a hydrostatic gradient, which is given by $p = \rho_w g z^*$, where ρ_w is is the density of water and z^* is the depth below the water table. Under these conditions, the effective vertical stress, σ_v, can easily be estimated [i.e., $\sigma_v = \sigma - p = g \rho z - \rho_w z^*$)]. Both bulk deformation and fluid volume change in response to changes in pressure. When pressure changes in fractures, fluid diffuses at a rate that depends on the permeability distribution in the rock. For fractures in impermeable rock, the matrix has no effect on pressure change. Thus, a change in fluid pressure in the fractures will result in a proportional change in the effective stress acting on the fractures. However, for fractures in a permeable matrix, fluid will diffuse into or out of the surrounding rock, and, consequently, the pressure change introduced into the fractures will be damped. Engelder (1993) gives a recent summary of stress regimes in the lithosphere.

Hydraulic flow models (Chapter 6) are often used to quantify the fluid pressure distribution in places where there are no measurements. Quasi-continuum models or closed form solutions can be used to calculate fluid pressures. To use these models, it is necessary to relate an equivalent quasi-continuum conductivity to the rock mass, either through single- or double-porosity models (see Chapter 6). Most discrete network models such as those described in Chapter 6 are applicable, but the limited knowledge of fracture geometry and fracture flow characteristics in most engineering problems makes their use unlikely. Further, variability in pressure is much smaller than variability in flow. Hence, less sophisticated models may be adequate.

Predicting the Behavior of Stress-Sensitive Flow

Modeling of subsurface flow is usually conducted under the assumption that permeability is independent of the state of stress. Some work has been done, however, on flow through so-called pressure-sensitive media. Because the permeability of fractures usually exhibits some dependence on stress, these models should be applicable to fractured rock masses. One of the earliest treatments of this problem was by Raghavan et al. (1972), who developed type curves for flow in a bounded circular reservoir whose permeability and porosity varied with the pore fluid pressure. Wall et al. (1991) present drawdown curves and pressure profiles for slug tests in pressure-sensitive formations. Dvorkin and Nur (1992) present an approximate analytical solution for a one-dimensional filtration front invading a formation whose permeability changes from zero to k_o as the pressure

changes from $p < p_c$ to $p > p_c$, where p_c is some critical pressure at which an interconnected network of fractures is formed.

In some cases the flow system influences the effective stress enough to significantly change the permeability of the flow system. In these cases it may be necessary to use a coupled stress-flow model to understand the behavior of the fracture flow system. Several coupled models are available (Noorishad et al., 1971, 1982, 1992; Kafritsas, 1987). The hydrogeological simulation models that have been linked to mechanical deformation models originated primarily in geotechnical engineering fields.

Coupled models account for the role of deformation in fluid flow and the stability of the rock mass. Flow is linked to deformation through changes in permeability and storage. Deformation is linked to flow through changes in fluid pressure, which results in changes in effective stress. A critical element in these models is representation of the proper hydrological and material constitutive behaviors for the fracture and solid rock. Models based on a discrete representation of the fracture network assign separate values to the fracture and block stiffnesses.

Fluid flow is also modeled on a fracture-by-fracture basis (e.g., Asgian, 1989). These hydromechanical models have been used to examine the coupling between fluid pressure responses and deformation for idealized settings. Representation of the fractured material in the mechanical model is more complex than the representations described in Chapter 6 for fluid flow. Just as for fluid flow, if the rock is highly fractured and the fractures have a wide range of orientations, it may be possible to use continuum deterministic or stochastic deformation techniques. For heterogeneous fracturing, additional complexity must be built into the model. For example, rock with a series of parallel fractures may be represented as a laminated material. Methods for coupled modeling of flow and deformation have been evaluated by DECOVALEX (1991).

Discrete-element models have been used for coupled fracture flow and deformation problems, such as flow under a dam, rock slope behavior, and flow to or from a well (Noorishad et al., 1971; Kafritsas, 1987). Figure 7.4 provides examples of models of this type. A well is located at the center of a rectangular domain, which contains a much simplified fracture network. The diagram on the left illustrates the computed deformation of the rock mass that occurs with fluid injection. The diagram on the right illustrates the nature of deformation if water is withdrawn from the rock mass through the well.

Assessment of Models of Stress-Sensitive Fluid Flow

In general, the principles governing the relationship between pressure changes and fluid flow are well understood. However, prediction of this behavior through the use of models is problematic. There are few experiments available at field scales that can be used to test these models. The problems are similar to those encountered in defining fracture flow systems (see Chapter 6). There are difficulties

in scaling up point measurements to obtain values that apply to field-scale behavior. There are considerable amounts of laboratory data that establish constitutive relationships between effective stress and fracture permeability for single fractures in rock cores (see Chapter 3), but field-based data are few in number. Boundary conditions are often unknown, yet they may control flow and stress behavior.

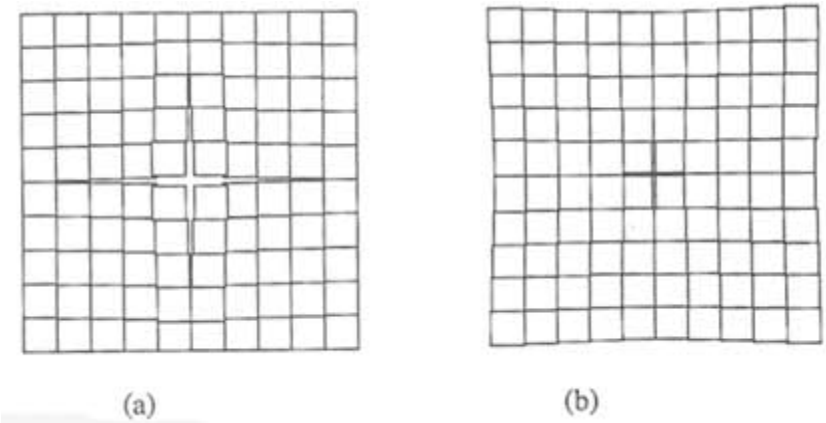

FIGURE 7.4 Deformation computed by a coupled flow and deformation analysis for a well under (a) injection and (b) withdrawal. Computations performed with the Massachusetts Institute of Technology discrete element model. From Kafritsas (1987).

In attempting to fit hydromechanical models to data sets involving single-borehole deformation experiments, it has been observed that there are problems in identifying unique sets of parameters to characterize field responses. Some success has been achieved in duplicating single-fracture experiments (Rutqvist et al., 1992). However, because of the multitude of parameters that determine the nonlinear hydromechanical response of a rock mass containing a network of fractures, site-specific predictive simulation is extremely difficult.

The practical significance of stress-sensitive fluid flow in fractured rock needs to be evaluated for a range of field-scale problems. This can be accomplished by using numerical simulation models that account for stress-dependent flow.

Creation or Extension of Fractures Due to Increases in Fluid Pressures

Hydrofracture is the extensional failure of rock that takes place when fluid pressure increases to the point that effective stresses become negative and exceed the tensile strength of the rock. Hydraulic fracturing occurs intentionally or unintentionally during many activities that provide sources of fluids at high pressures. For fractures to propagate, the fluid must be supplied in sufficient amounts to "fill" the growing volume of opening fractures. There is an extensive literature available on hydrofracture, and only a brief description is given here.

Hydrofracture is used as a stress measurement tool (e.g., Engelder, 1993). In this application a hydrofracture is created in a section of borehole isolated with packers. The pressure in the interval is increased until the borehole ruptures, resulting in the formation of new fractures or the extension of old ones, which causes a sudden decline in pressure. The pressure required to maintain the fracture openings is assumed to be equal to the minimum principal stress. A slightly higher pressure will extend the fracture. (Once it has closed, the pressure required to reopen it can be significantly higher.) For homogeneous isotropic formations, hydrofractures grow in a direction perpendicular to the minimum principal stress.

Hydraulic fracturing is also used to increase conductivities around production wells. A decline in permeability can arise from high effective stresses at the borehole, owing to: (1) stress concentrations around the borehole (which depend on the original stress field) or (2) large pressure drops around the borehole owing to radial flow. A newly formed hydrofracture can increase the conductivity near the well and consequently increase the effective wellbore radius by as much as one-half the fracture penetration (Prats, 1961). Hydraulic fracturing is a common practice in wells used for resource recovery. Typical penetrations (i.e., the propped lengths of the hydrofractures) are greater than 200 m, producing an effective well radius of more than 100 m. Fracturing is a very practical means to achieve a large effective wellbore radius at significant depths.

Hydrofracture can also occur, unintentionally, during injection of fluids. In these cases, studies can be designed to find safe injection pressures that will not cause fractures to open and extend. Control of fracturing during "flooding" operations has been a long-term concern of the petroleum industry. Flooding includes water injection for "secondary recovery" and chemical injection for "tertiary recovery" (e.g., Lake, 1989). The objective of flooding is to provide an effective sweep of the reservoir with the injected fluids. This is achieved by controlling the extent to which hydraulic fractures propagate from the injection well toward a production well in order to prevent a "short-circuit" in the flow pattern of the injected fluid. Mud pressure during drilling can either open or create new fractures. This phenomenon can lead to lost circulation (too little drilling fluid returning to the surface) and, in the extreme, to loss of the hole owing to rock failure and stuck tools.

The control of hydraulic fracturing is also important for waste disposal wells, and much of the petroleum industry's experience and technology are directly applicable. Over time, injection wells are subjected to the cumulative effects of particulates and other contaminants in the injected fluids, which decrease permeabilities. The maintenance of nominal injection rates requires increasing the injection pressure. Eventually, the elevated injection pressures will cause the extension of fractures that create new injection areas beyond the region of significant permeability impairment. Alternatively, the permeability decrease can be ameliorated by chemical treatment (e.g., Economides and Nolte, 1989).

A dam supporting a filled reservoir has large pore and joint water pressure gradients in its abutments and foundations. Such high pressures can reduce the strength of the rock mass and can cause movement of rock blocks, with potentially catastrophic consequences. The pressures can also open fractures and allow significant amounts of fluid to flow around or under the dam. Large pore pressures under the toe or downstream of a dam, in combination with the large shear stresses, can produce foundation failures. Entirely analogous but more serious conditions exist in the dam abutment slopes because the water pressure produces both high pore pressures and high hydraulic thrusts. The 1959 Malpasset Dam failure is an example of such a failure (Londe, 1987).

A related problem is that of reservoir-induced earthquakes or similar seismic events. High water loads and pore pressures can induce slippage along fractures. Earthquakes of magnitudes up to 6.5 have occurred, owing to either injection or withdrawal of fluids (Meade, 1991). Studies indicate that the level of induced seismicity depends strongly on preexisting stress conditions in the upper crust.

Fracture Initiation and Growth

A fracture is initiated when the fluid pressure exceeds the total stress plus the tensile strength of the rock, as discussed earlier. Stress heterogeneity plays a role because it is the total local stress that must be exceeded in order to initiate a fracture. For example, total stress near a well may be elevated above the far-field stress by stress concentrations around the wellbore. If fractures are present, the pressure required to open them is equal to the compressive stresses across the fractures.

The stress intensity factor at the tips of the fractures must exceed a critical value in order for the fractures to be extended. The stress intensity factor is a function of the fluid pressure in the crack and the crack geometry, as described in Chapter 2.

The fracture growth process is governed by the coupling between fracture deformation, fluid flow, and the mechanical properties and stresses in the matrix. For spatially constant properties and stresses, the pressure required to propagate the fracture decreases as the fracture gets longer, because the greater length of the fracture provides greater leverage on the tip (Economides and Nolte, 1989).

Stress variations between different sedimentary layers can enhance lateral fracture extension relative to vertical fracture extension. Such stress variations can produce elongated fractures that will propagate only by increasing pressure (Teufel, 1979). This is a common occurrence for hydraulic fracturing in petroleum reservoirs, as illustrated in Figure 7.5. The figure indicates generally increasing pressure during the injection phase (denoted as "fracture treatment" in the figure). The interval after injection is divided into two time periods. During the first period of "fracture closing," the fluid pressure and fracture aperture decrease as fluid in the fracture infiltrates the surrounding rock (Warpinski, 1985). The period

terminates when the fractures close onto the proppant and fracture deformation essentially ceases. After the fracture closes, the pressure reflects the increased pore pressure in the reservoir because of fluid filtration. This pressure dissipates with time. Gidley et al. (1989) describe various aspects of the hydraulic fracturing propagation process.

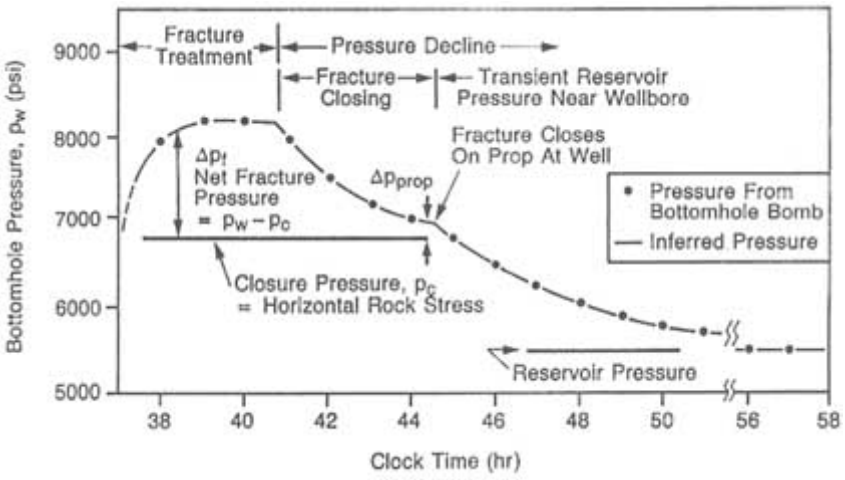

FIGURE 7.5 Example of bottomhole pressure in a well during a hydrofracture operation. After Nolte (1982).

Much is known about hydrofracturing from an engineering perspective (e.g., Gidley et al., 1989), but there are still uncertainties about details of the physical processes. The behavior of hydrofracture in some rock types is not well understood. The effect of heterogeneities (e.g., existing fractures) on hydrofracture geometry also is not well understood (Warpinski and Teufel, 1987).

As a flow rate enhancing tool, hydrofracture may fail if matrix permeability is small and existing fracture orientations are parallel to the current maximum horizontal stress. For this case, the induced fractures will follow the same orientation as the existing fractures, providing little additional connectivity between fractures. To some extent, this problem has been overcome in the petroleum industry with drilling technology that allows wells to be oriented in any direction. Such wells can be drilled normal to the fractures in order to connect them. In a massively fractured formation, hydrofracture can be used to connect the well to a highly productive part of the fracture network.

Stress Sensitivity Tests

The determination of a safe injection pressure can be obtained from a "step-rate" test to infer the conditions to extend a fracture, that is, the "extension

pressure." This test is conducted with a progression of injection flow rates, Q, with each rate generally maintained to reach steady conditions. For each rate the final pressure increase, ΔP, relative to in situ pore pressure, is plotted versus the flow rate, Q. This plot, illustrated on the right side of Figure 7.6, exhibits a characteristic "dogleg" where hydraulic fracturing begins. The dogleg occurs at the extension pressure where the resistance to injection, $\Delta P/Q$, decreases as additional formation area is exposed via an extending fracture, that is, an extending effective well radius.

After prolonged injection, the pore pressure in the formation will change, as will the temperature, if the temperature of the injected fluid is different from the formation temperature (the temperature can either increase or decrease). Consequently, the pressure required to extend the hydrofractures will change with time. Therefore, it is good practice to periodically conduct step-rate tests to rede-line safe injection pressures.

Another way to diagnose and quantify stress sensitivity is to perform several flow or injection tests at substantially different flow rates, Q (as used to obtain the relationship in Figure 7.2), followed by sufficient shut-in periods to perform valid buildup or fall-off analyses. The amount of variation in the values of $Q/\Delta P$ at steady-state for the various tests will indicate the degree of stress-sensitive behavior. If there is no variation in $Q/\Delta P$, the system is rigid. If variation is observed, the data can be used to develop a relationship between pressure and permeability, such as that shown in Figure 7.2. Furthermore, the effects of "skin" (altered near-well permeability) will be evident from the buildup or fall-off analyses, with the far-field (i.e., initial, in situ) permeability reflected by the late-time data. These data provide the required information to diagnose and quantify the stress permeability conditions of the system.

In some cases it is possible to place a strain gauge across a fracture in a borehole. The displacement of the fracture can then be measured as the pressure in the borehole interval is changed. Such measurements using a BoFex strain gauge have been made in the Underground Research Laboratory in Canada

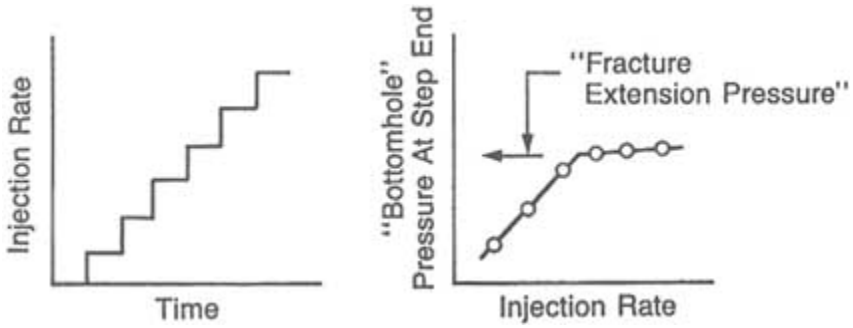

FIGURE 7.6 Step-rate test to determine stress sensitivity of fractured rock. Nolte (1982).

(Martin et al., 1990) and at the Grimsel test facility in Switzerland (Majer et al., 1990; see Chapter 8).

Monitoring of Fracture Location

The extent and orientation of hydraulic fractures created by injecting fluid into a well can be mapped by the resulting seismic activity (Chapter 4). This activity is induced by the infiltration of fluid into a natural fracture network at high pressures, which induces slip. These slippages release seismic energy. The release point can be triangulated in much the same way that an earthquake epicenter is located.

Extremely sensitive tiltmeters can be placed on the surface of the ground to monitor hydrofracturing. These meters can be used to determine the direction and volume of the fractures. Available instruments can measure tilts in the nano-radian range. Strain caused by massive hydrofracture creation at depths of thousands of meters can be detected at the surface with these instruments. See Chapter 4 for a more complete description of tiltmeter technology.

Fracture Propagation Models

Hydraulic fractures were originally modeled as two-dimensional features with constant height. Several types of two-dimensional models were assembled by using analytical solutions (e.g., Khristianovich and Zheltov, 1955; Perkins and Kern, 1961; Geertsma and de Klerk, 1969). More sophisticated pseudo-three-dimensional models have recently been developed to calculate fracture height in layered reservoirs (Nolte, 1982; Settari and Cleary, 1984; Meyer, 1989). The term *pseudo-three-dimensional* (or P3D) is commonly used to describe computationally efficient algorithms the provide some of the desired features of three-dimensional models (e.g., extension and fluid flow in both directions of the vertical fracture plane). However, the desired efficiency of the P3D models is achieved by varying the degrees of constraint on fracture shape and fluid flow or by relaxing the lateral extent of elastic coupling along the fracture plane. One P3D class contains the "lumped-parameter" models and is most applicable to fractures with similar dimensions in all directions of the fracture plane. This shape occurs for formations that are either homogeneous or composed of layers with similar stresses and mechanical properties over the extent of the fracture. The "lumped" models generally constrain the fracture plane and flow field to elliptical shapes and determine the fracture dimensions by parameters averaged over the fracture plane (i.e., lumped parameters). The other popular P3D class contains the "cellular" models and is most applicable to fractures that have a large aspect ratio. This shape occurs for sedimentary sequences that have significant horizontal stress contrasts between the horizontal layers. The higher stress layers limit vertical extension and enhance the desired lateral extension into the petro

leum reservoir. The "cellular" models generally consider fluid pressure gradients only in the long (i.e., lateral) direction and ignore lateral elastic coupling between cells for determining the fracture aperture and vertical height (i.e., the height and aperture for a cell depend only on the fluid pressure in that cell). When conditions do not favor the assumptions for P3D models, fully three-dimensional models using boundary-element and finite-element formulations also are being applied (Clifton and Wang, 1988; Advani et al., 1990). Oil companies predominantly use two-dimensional and P3D codes for fracture design. Warpinski et al. (1994) provide a comparison of results for some of these codes.

Coupled flow and deformation models can be used to model hydrofractures if their propagation directions are known or can be assumed. For the fully three-dimensional and differenced P3D forms, a series of elements in the model are lined up in the direction of the fracture. Elements are either added (fixed mesh) or stretched (moving mesh) as the fracture extends. For the fixed mesh case, as each element is judged to have opened based on the critical stress concentration, the mechanical and hydrological properties of the element are changed from that of rock to that of fracture. Thus, the fracture can be considered to develop in discrete intervals (Rutqvist et al., 1992). Lumped-parameter or integrated models use global parameters, which reflect some averaged properties of the fractures, that are changed as the rock fails.

A new series of models based on boundary elements allow calculation of stress concentrations, including the effects of other fractures. These models calculate the direction and location of fractures that result from the change in loading (Olson, 1990).

The propagation of natural fractures in the earth's crust is discussed in Appendix 7.A.

Deformation or Failure Owing to General Changes in the State of Stress

Previous sections addressed the opening and closing of fractures owing to changes in pore pressure. This section highlights changes to fracture systems (opening, closing, or shear) that are caused by loading factors that affect or are affected by fluid flow. Such loads can occur in slopes, underground openings, reservoirs, or dam foundations.

There are several modes of slope failure, depending on slope material, orientation and type of jointing, and overall geological structure of the formation. In all cases, hydraulic pressure from groundwater is a substantial threat to slope stability. The pressure of groundwater reduces effective stress, as noted previously, which decreases the shearing resistance. Groundwater pressure can also generate a significant force acting toward the slope face that can promote instability. In designing slopes it is essential to consider hydraulic conditions because they determine stable slope geometries. For any specified slope height, the allowable slope angle is a strong function of the degree of saturation (Hoek and Bray,

1981). In some applications there may be a strong economic incentive to achieve high slope angles. For example, in open-pit mining, steep angles minimize the amount of waste rock that must be mined. In such cases, actions can be taken to maintain dry conditions. Options include the drainage measures discussed in Appendix 7.B and reinforcement of the rock mass through bolting or external supports.

Fractures around underground openings represent surfaces of weakness that are potential sources of failure. Significant changes in stress occur around cavities, which usually make instability more likely. In addition, stress effects can play a major role in altering the fracture flow and fluid pressure, which in turn affects the stability of the opening.

Pore pressure reductions caused by fluid production in reservoirs are usually thought to result in subsidence and reduced permeability, as discussed previously. However, in some cases there can be significant subsidence without an associated decline in permeability. Teufel et al. (1991) examined such a case for the Ekofisk field in the North Sea and postulated that the change in stress state could induce the creation of new fractures that offset the permeability decline. This behavior depends on the boundary conditions and Poisson effects in the reservoir.

Changes in fracture systems caused by pore pressure changes associated with dams and reservoirs were discussed previously. A crucial aspect of dam foundation and abutment behavior is the combination of large loads and pore pressures and the abrupt changes in loads and pressures that occur over relatively short distances. The reservoir thrust acts to push the dam downstream and close downstream fractures, which may lead to a pressure buildup near the toe of the dam. This thrust often opens fractures at the upstream (heel) side of the dam, which further promotes pressure increases. The large pore pressures (Figure 7.7) under the toe of the dam or downstream of it, in combination with the large shear stresses acting there, can produce foundation failure. Entirely analogous conditions exist in the dam abutment slopes.

Stress Distribution and Stress-Permeability Relationships

As discussed in Chapter 3, stresses acting on fractures are perturbed by the fractures themselves. Consequently, local stress changes may not be equal to far-field stress changes. Changes in normal stress on the fractures are equivalent to the changes in effective stress (discussed above) for pore pressure changes. Changes in normal stress will cause fractures to open or close, which will change their permeabilities. Changes in shear stress will have little effect unless the fractures displace in shear or fail. Effective stress plays a role in shear because shear strength decreases with decreases in effective stress. The relationship between shear, fracture geometry, and permeability is discussed in Chapter 3. The difference between shear deformation and normal deformation with respect to permeability change is that shear strain can either increase or decrease perme

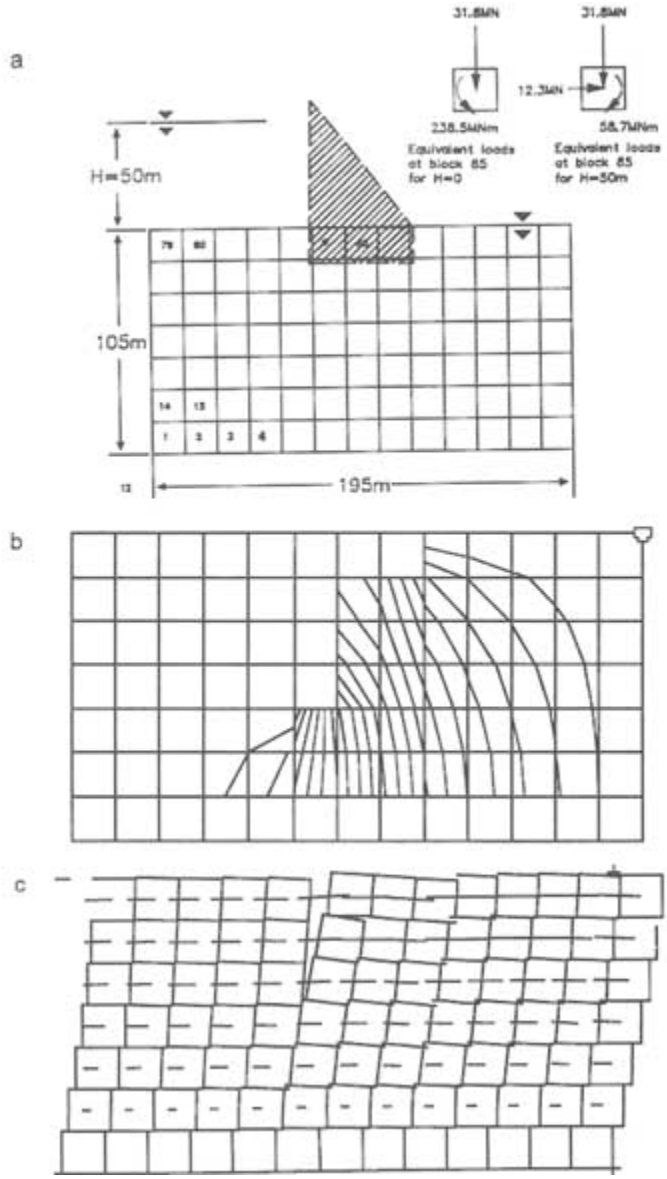

FIGURE 7.7 Flow nets and deformation in fractured rock under a dam. (a) distinct element model; (b) pseudoequipotentials with grout curtain to 60 m below dam foundation; and (c) displacements (magnified) due to dam load and reservoir water pressure. (The term *pseudoequipotentials* is used because the equipotential lines shown here are those seen in a continuum, while the numerical approach used to calculate them is based on discrete elements.) From Kafritsas (1987).

ability. Theoretically, shear can also increase the anisotropy of permeability in the plane of the fracture by creating both channels and barriers perpendicular to the direction of shear.

Modeling Deformation and Failure

Deformation and failure of fractured rock masses can be modeled in three ways: (1) individual block analyses, (2) multiple block analyses, and (3) quasicontinuum analyses. The most common stability analysis methods are rigid-body analyses of individual blocks or wedges. Graphical (e.g., Goodman, 1976) or vector analytical methods (see Wittke, 1965; Hendron et al., 1971; Einstein et al., 1979) are used to determine whether the block or wedge is kinematically unstable and what kind of movement the block or wedge may undergo. Typical movement is translational sliding along one or more (usually two) planes (Figure 7.8a).

Sliding combined with rotation on planes also is possible, as is rotation around edges or corners; the latter movement is called toppling (Figure 7.8b). The vector analytical determination of kinematic instability consists of comparing the resulting driving force and moment to given directions that characterize particular movements. For instance, for movements on a single plane, the driving force must point into this plane and away from other boundary planes (see Figure 7.8c). Other kinematic considerations include the relative inclination of the sliding planes and the slope and various conditions of toppling. A good summary of these conditions is given by Goodman (1976).

Once the kinematic instability and type of movement have been determined, the kinetic stability is analyzed by comparing all driving and resisting forces using limit equilibrium analysis. Driving forces such as gravity, water pressures, and dynamic forces (e.g., earthquakes) are compared to resisting forces, including cohesive- or friction-related forces and artificial stabilizing forces such as bolts or tiebacks. Limit equilibrium analysis, by definition, assumes rigid-body conditions, that is, no deformation and no stress distributions. Some force comparisons require consideration of the size of the block or plane under consideration (e.g., cohesive forces and water pressure), whereas others do not (e.g., weight/friction).

Deformation or Failure of Fractures Owing to Heating or Cooling of the Rock

Significant changes in rock temperature can occur at the earth's surface under natural weather changes or in a nuclear waste repository, a geothermal reservoir, a flooded petroleum reservoir, or an excavation. Natural weather conditions include freezing temperatures that create ice in fractures. Expanding ice extends fractures, and ice can block water flow from fractures, producing pressure buildups.

Nuclear waste stored underground can provide a significant source of heat. Temperature changes in underground repositories can be affected by several

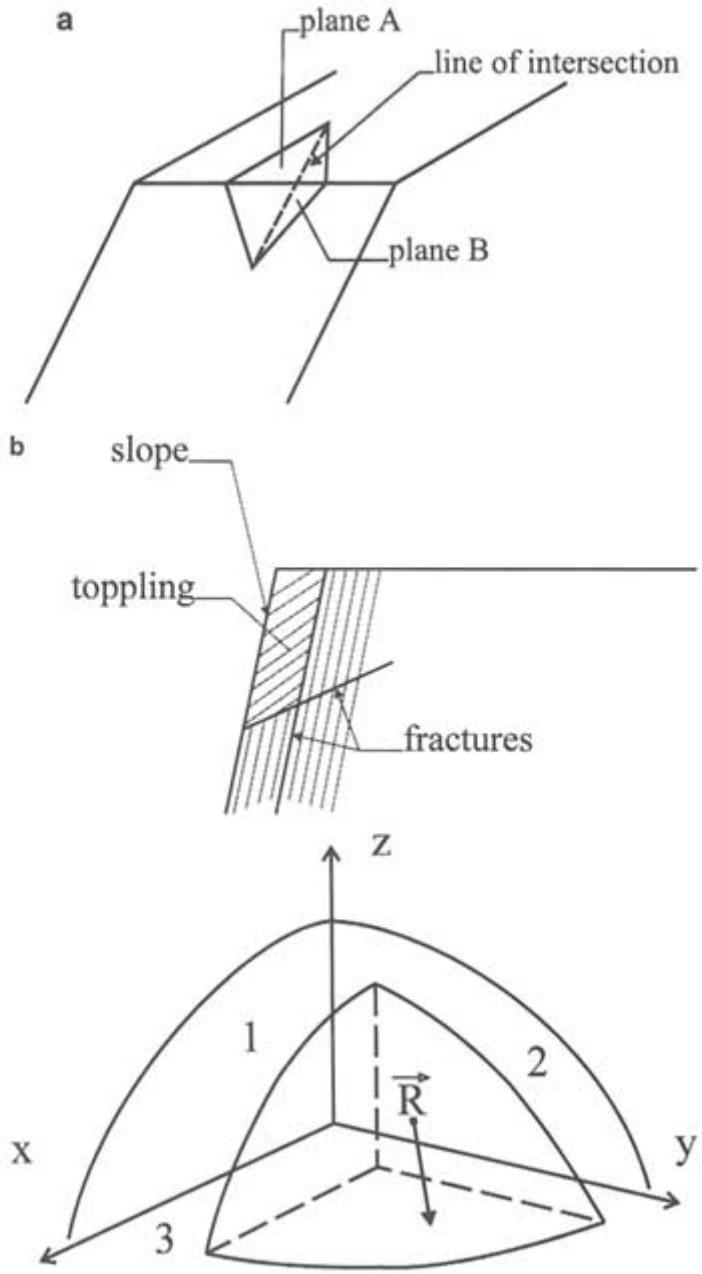

FIGURE 7.8 (a) Failure of a wedge formed by fractures. Sliding occurs, for example, along plane A, plane B, or planes A and B (line of intersection). (b) Toppling failure. (c) Kinematic instability determined with vector analysis.

factors, including the age of the waste before emplacement and the density of waste storage. Repository temperatures over 100°C will create a significantly different environment than temperatures below 100°C because of boiling and steam production (Wang et al., 1981).

Geothermal reservoirs provide many opportunities to observe the effects of temperature changes on fracture systems. As geothermal wells are pumped, they draw heated fluids up from the deeper portions of the reservoir. These fluids heat rocks in the upper part of the reservoir, causing them to expand, which closes fractures and increases fluid pressures. Reinjection of cold fluids cools the rock and may lower fluid pressures.

Prior to 1980, most petroleum flooding projects were in reservoirs with in situ temperatures approximately equal to that of the injected fluids. For these cases, only poroelastic effects were significant, and flooding produced generally increasing pressures. More recently, flooding operations have been undertaken in deeper formations in Alaska and the North Sea, where relatively cool seawater is injected into higher-temperature formations. This can result in undesired hydrofracture owing to thermoelastic effects (e.g., Williams et al., 1989).

Temperature changes can have a significant effect on stresses around a cylindrical cavity such as a wellbore; for example, for rock with typical physical properties, hoop stress can change by 0.1 to 1 MPa/°C (1 to 10 bars/°C), with the precise value primarily dependent on the elastic modulus (Stephens and Voight, 1982). A 20°C decrease in temperature at the cavity face can reduce the total and effective stresses by 2 to 20 MPa (20 to 200 bars) and offset the stress concentration from the far-field stress, with a potential impact on stability. Such reductions in effective stress can be important at the very cold temperatures encountered in underground gas storage. A 20°C increase in temperature can provide an effective stress increase of 2 to 20 MPa (20 to 200 bars), which can lead to local reductions in fracture permeability.

Thermoelasticity and Flow

Thermoelasticity relates the change in temperature to stress through an understanding of thermal expansion coefficients and stress-strain constitutive relationships. Both rock and fluid expand when heated. If expansion is resisted, thermal stresses are created. The amount of thermal stress produced by a change in temperature depends both on the temperature increase and the boundary conditions. For example, if fluid in a rock is heated, its expansion will have little effect on stress if the fluid is unconfined because the resulting fluid pressure can be dissipated. Heating of confined fluids, on the other hand, can increase pore pressures significantly, even to the point of extending fractures. The induced stresses in a confined heated body are roughly on the order of $E \alpha \Delta T$, where E is Young's modulus, α is the thermal expansion coefficient, and ΔT is temperature rise (measured from some reference temperature). The standard treatise on thermal stresses is Boley and Weiner's (1960) text.

A good conceptual model for understanding the effects of temperature on fractured rock is to think of the rock blocks as very stiff compared to the more compliant fractures. As a rock is heated, the blocks expand into the fracture voids. Heating the fluid in the fractures at the same time will cause a net decrease in effective stress as the fluid expands. However, unless the fluid is confined, fluid expansion will be less significant than rock expansion. Consequently, an increase in temperature has the same effect on fractures as an increase in effective stress.

Rapid heating or cooling can lead to failure owing to differential expansion of adjacent rock grains (Stephens and Voight, 1982). Even slow heating can cause extensional regions to form, depending on geometry and boundary conditions (Fredrick and Wong, 1986). Prolonged injection of relatively hot fluids will increase stresses and result in loss of permeability for natural fractures.

Injecting relatively cool fluid (compared to in situ temperatures) can induce a significant reduction in stress by thermoelastic behavior. In the extreme this can lead to a negative effective stress condition and hydraulic fracturing. Consequently, cold water injection results in reduced extension pressures from thermoelastic effects (e.g., Perkins and Gonzalez, 1984, 1985; Williams et al., 1989). When thermal effects are dominant, stresses in the injection zone will decrease, resulting in increased stress contrast between vertical layers. This will retard fracture propagation through the cap rock.

Changes in temperature cause changes in density and viscosity of fluids. In general, both density and viscosity of liquids decrease with increasing temperature; for gases an increase in temperature typically causes a decrease in density but an increase in viscosity. These changes, in turn, cause changes in the flow field.

Coupled Heat, Flow, and Stress Models

One modeling approach for heat and flow problems is to use a thermoelastic continuum model to calculate changes in stress owing to heat conduction alone. These models ignore heat transport by advection of fluids in fractures. Then the stresses are fed into coupled stress-flow models as described above. This approach is inadequate in fractured media if fluid velocities are high enough to result in significant heat transport by advection. Convection cells will form if the Raleigh number, which measures the relative strengths of advective and conductive heat transfer rates, exceeds some critical value (Phillips, 1991).

A more complete approach to the problem is to solve three coupled equations: one each for stress, temperature, and flow. This approach has been applied to the problem of heat production in a nuclear waste repository (Noorishad et al., 1984, 1992), where it was found that extensive regions of increased permeability owing to extension can be formed in rock above the repository.

Kohl et al. (1996) have examined thermoelastic effects that impact the long-term performance of a hot dry rock geothermal system. Extraction of heat from

the subsurface, which typically involves circulating initially cold water through either a natural or an induced fracture network, causes significant stress changes in the rock mass. These stress changes, which are caused by pore pressure changes and thermal shrinkage as heat is extracted, can substantially alter the hydraulic properties of the rock mass.

Figure 7.9 shows a hot dry rock system in its simplest form, a single open fracture embedded in a less permeable rock matrix. Also shown in the figure are the calculated temperature change, fluid pressure, and rock mass displacement 30 years after the system has been in operation. Deformation of fractures owing to thermoelastic effects gives rise to increases in hydraulic apertures that increase flow through the fractures by 25 percent over the 30-year production period. Although the example is very simple, it is representative of the state of the art in modeling the long-term performance of such systems.

The principles governing rock behavior under changes in temperature are fairly well understood (Biot, 1956). However, the effect of heterogeneities and the coupling of temperature with fluid flow can make the consequences of temperature changes very difficult to predict. There is a need for careful laboratory and controlled field experiments in well-characterized fractured rock masses to determine the phenomena that dominate behavior.

CHANGES IN FRACTURE FLUIDS

Many engineering operations lead to changes in the fluids contained in fractures. These include changes in fluid phase or composition or redistribution of phases or components in the rock. The principles governing multiphase flow in fractures were discussed in Chapters 3 and 6 (see also de Marsily, 1987, p. 26). This section gives some examples of these changes, expanding on the discussion in Chapter 6, and addresses the principles that govern such behavior.

Changes in Fluid Phase

When a fracture system is subjected to changes in temperature or pressure, fluids may undergo a change of phase (i.e., from liquid to vapor). An increase in pressure may cause gas to be dissolved in the liquid phase, and, conversely, dissolved gas may evolve from the liquid phase when pressure declines. Chemical or microbiological reactions may also produce gas. Heat can cause vaporization, and cooling can cause condensation.

Dissolved gases can be released from solution as fluid pressure is lowered. This phenomenon occurs in oil wells, where gas comes out of solution as the oil flows toward a well and is pumped upward in the well toward the surface. In some gas reservoirs, pressure declines cause water to enter fractures from the matrix, thus creating a gas/water flow system and reducing the production of gas. Geothermal reservoirs can undergo dramatic phase changes as fluids are

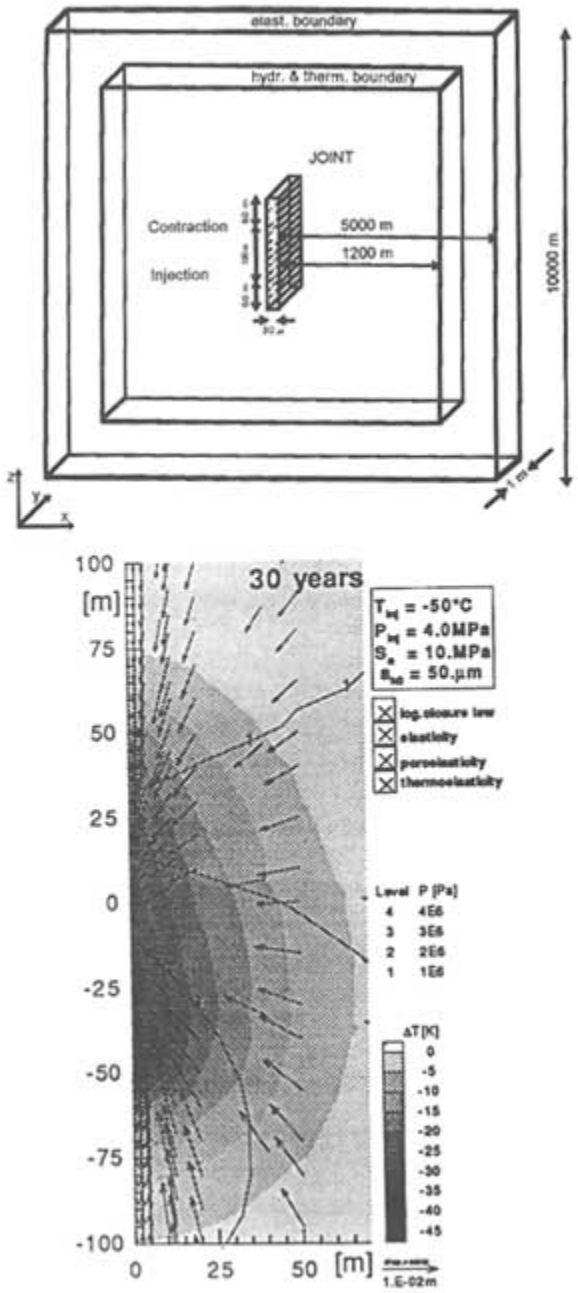

FIGURE 7.9 Simulation of a hot dry rock system in a single open fracture. Modified from Kohl et al. (1996).

produced or injected. These changes may be coupled to chemical changes, as described later in this chapter.

Gas can also evolve from fluids during flow into underground structures. Nitrogen from solution has been hypothesized to explain the dramatic decrease in permeability around a drift in the Stripa mine in Sweden (Long et al., 1992). In this case, inflow to six parallel boreholes was measured when the water pressure head in the holes was held at 17 m above atmospheric. A drift was excavated through the boreholes, but inflow to the drift was almost an order of magnitude lower than that extrapolated from the borehole data. The gas content of the water was about 6 percent nitrogen, and gas bubbles were observed in the outflow. Calculations of stress changes failed to account for this dramatic decrease in flow. One explanation is that two-phase flow conditions decreased the inflow.

The performance of nuclear waste repositories may be affected by phase changes in the fluids of surrounding rock. The repositories can produce significant quantities of heat, which can cause boiling, vapor flow, and condensation. These phase changes may be coupled to other mechanical and chemical changes, as discussed previously. These phenomena are not well understood, particularly for repositories constructed in unsaturated rock. In this case, two types of behavior may occur. The first is called the *hot dry scenario*, where heat from the repository drives all moisture away. The other is the *heat pipe scenario*, where steam is generated and flows upward, where it condenses and flows back to the repository as liquid water under gravity (Doughty and Pruess, 1988). In both cases, heat drives moisture away from the repository and gravity causes downward flow of condensate, which will be reheated and revaporized. The unresolved question is whether downward flow will reach the heat sources (waste packages) or whether there is a superheated region whose upper boundary moves upward some finite distance for significant periods of time. This question cannot be resolved without laboratory and in situ field experiments.

Principles Governing Phase Changes

At any given pressure, there is a maximum amount of gas that can be dissolved in the liquid phase of water. When the concentration of gas is small, a linear relationship exists between the maximum concentration of dissolved gas in the water and the partial pressure of gas in the vapor phase. The constant of proportionality, which depends on the species of gas, is known as Henry's law constant.

The general principles for understanding phase changes and the transfer of mass among phases are the province of chemical thermodynamics. For homogeneous systems in which no chemical reactions occur and external potentials (e.g., gravitational and electrical fields) can be ignored, the thermodynamic state can be specified completely by fixing temperature, pressure, and the number of moles of each component.

The conditions for equilibrium are that the temperature, pressure, and *chemical potential* of each substance are the same in all phases. The chemical potential is equal to the partial molar Gibbs free energy. All of these quantities are intensive variables; that is, they are independent of the total mass (or number of moles) present in the system and are completely determined by specifying temperature, pressure, and composition (e.g., the independent mole fractions of the components) of the phase. The principles governing phase equilibria are well understood, and methods exist for calculating phase properties even for complex multicomponent hydrocarbon mixtures. However, the complexity of the calculations increases rapidly with the number of fluid phases, especially if different parts of the system are not in equilibrium. Disequilibrium may be common in fractured rock because of the large differences in permeability between fractures and the pores in the matrix.

Changes in Fluid Interfaces

Injection or infiltration of miscible and immiscible fluids creates a multicomponent flow system in fractures. An example is contamination of groundwater with nonaqueous-phase liquids, a common problem for both porous and fractured media.

Dynamic large-scale movement of fluid interfaces can occur because of buoyancy effects, which can arise from density differences owing to temperature or compositional changes. For example, gas or water coning in petroleum reservoirs can be exacerbated by natural fractures that enhance vertical permeability. Mobile water, when present, will reside below the petroleum phase because water is more dense. Vertical flow and subsequent production of water is referred to as water coning. Coning begins as a change in the position of the interface between the water and petroleum phases. The boundary change for the dual-density system occurs to equilibrate the pressure gradient caused by producing the petroleum phase.

Water cones upward and gas cones downward. In a gas reservoir, water coning is undesirable and occurs when gas is produced at too high a rate. In an oil reservoir, it usually is not desirable to produce gas because gas production reduces drive energy and, consequently, the ultimate volume of oil recovered.

Water breakthrough by coning has at least three undesirable effects: (1) water is produced in the well and must be disposed of in an environmentally safe manner, (2) the flow height for the petroleum phase in the reservoir is restricted, and (3) the production rate is reduced because of the reduced drawdown at the bottom of the well. A reduced drawdown occurs because of the increase in hydrostatic head of the heavier produced fluids containing the denser water phase. Water coning has had a negative impact on production in many prolific fractured reservoirs. A completely effective countermeasure remains to be developed.

Coning is significant in gas reservoirs because there is a large density difference between gas and water. This difference provides a larger hydrostatic head difference between the water and the well compared to the gas and the well. No gas production can be obtained until the water is pumped off. Pumping is also used in more conventional reservoirs with high water saturations. In either case, fractures may provide the pathways between the two phases and complicate the control of coning.

Saltwater intrusion into coastal aquifers produces large-scale changes in fluid-phase interfaces. Such intrusion is promoted by overpumping fresh water that overlies saltwater. In fracture systems the boundary between fresh water and saltwater can be very complex because it is partly controlled by the connectivity of the fracture system. As measured from the surface, the depth to the interface can vary, depending on which fractures are intersected and how well they are connected to the pumping wells.

The location of an interface is determined by a balance of gravitational and viscous forces. Capillary forces may play a role if more than one phase is present. Gravitational effects arise from differences in fluid density. These density differences may be related to variations in fluid composition, temperature, pressure, or concentration. For example, the change in location of an interface, Δh, after a change in pressure, ΔP, is given by where $\Delta\rho$ is the difference in density between the two fluids. In a fracture network each fracture may have a different ΔP, and therefore a different Δh. Thus, the elevation of the interface may vary significantly from fracture to fracture.

$$\Delta h = \frac{\Delta P}{(\Delta\rho)g}, \qquad (7.3)$$

If the three-dimensional fracture geometry is known, the location of an interface under a given flow regime can be calculated. The problem in calculating interface movement is at least as complicated as that of defining the fracture flow system, as described in Chapter 6.

ADDITION OF SOLIDS

Suspended solids or liquids that solidify may be added to a system deliberately—for grouting or propping of hydraulically induced fractures—or inadvertently during injection of water for aquifer recharge, aqueous waste disposal, well drilling and completion, and water flooding. The introduction of solids into a fractured rock mass will usually decrease its bulk permeability. This permeability decrease is one of the desired results for grouting but is generally undesirable in cases of inadvertent injection of suspended solids.

Proppant

Coarse-grained proppants are suspended in a carrier fluid during hydrofracturing to prevent closure of the fractures after pumping is stopped. If the fractures were allowed to close, there would be little residual change in permeability along their paths. In this application the injection of suspended solid material increases bulk permeability in the vicinity of the well. Most practical applications utilize coarse-grained, well-sorted proppants (e.g., sand or alumina spheres) suspended in the hydrofracture fluid. These proppants fill the fractures, creating a highly permeable flow path to the wellbore. Proppant transport into the fracture is controlled by particle size and concentration, carrier fluid viscosity (which is a function of temperature and chemistry), and carrier fluid velocity (which is a function of pumping rate and leak-off rate). Propping agents and proppant transport are reviewed by Gidley et al. (1989).

Filtration for Proppants and Grouting

The most obvious principle governing the transport of suspended solids through a single fracture or a fracture network is that solid particles will not enter void spaces smaller than their diameters. Hunt et al. (1987) provide a summary of filtration theory for beds of granular material. The critical parameters include the diameters and densities of suspended particles, the diameter of granular filter particles, and the fluid velocity. Although the focus of the Hunt et al. review is on porous media, the general ideas apply to fractures because fractures can be considered two-dimensional porous media, where the pore size distribution can be related to the aperture distribution.

Proppant Engineering

The process of creating a propped fracture must take the following factors into account: the mechanical properties of the rock, the flow of the non-Newtonian slurry of proppant from the injection point out to the leading edge of the fracture, the leak-off of carrier fluid into the surrounding formation, and the settling of proppant owing to gravity segregation in the fracture. The leak-off and settling rates depend on carrier fluid viscosity, among other variables, which in turn depends on temperature. Consequently, it is necessary to account for the rate of heating of the fracturing fluid, which is not in thermal equilibrium with the formation for some time after it is injected. The leak-off rate must be low enough to allow the fracture to be created. Proprietary codes have been developed to model the process of creating propped fractures.

Grouting

Grouting is used in civil engineering, engineering geology, mining engineering, and petroleum engineering to reduce inflow from the rock mass by reducing

its permeability (i.e., impermeabilization grouting) or to reduce deformability or increase the stability of the rock mass. Occasionally, these purposes are satisfied by the same grouting operation. In other cases, as will be shown below, impermeabilization grouting may have detrimental effects on strength and deformability. Depending on the grouting purpose, different grout types and grouting procedures are used, as described in more detail below. Some grouts consist of liquids with suspended solids that correspond in behavior to proppant injections. There are many other grout types, however, that behave differently; some, for instance, are very similar to chemical precipitates (see "Redistribution of Existing Solids by Chemical Processes," later in this chapter).

Grouting Principles

Grouting is usually accomplished by injecting a grout in liquid form into fractures or pores in the rock. The grout solidifies and blocks the water or gas in the rock mass. Depending on the type of grout, it may also increase the resistance and decrease the deformability of the rock mass. Grout is injected from boreholes. The grout type, spacing of holes, injection pressure, and fracture geometry represent an intrinsically coupled system. A successful grouting operation, that is, one that produces an impermeable zone, requires that the components system be balanced. A short description of each component and a summary discussion of how they interact will make this point clear.

Grouts are usually liquids in the form of suspensions, solutions, emulsions, or melts. A grout is injected into fractures in liquid form and solidifies by several processes, including (1) sedimentation of suspended particles, (2) sedimentation and chemical reaction of particles, (3) chemical reaction of solutions or emulsions, (4) phase change of melts, or (5) by chemical reaction of the grout with the rock mass. The particle size of suspensions and the viscosity of solutions in relation to fracture aperture and grout pressure govern their injectability.

Suspensions in water are:

- Cement-mortar[1]
- Cement
- Colloid-cement
- Cement-clay
- Clay

The particle sizes of cements are in the silt range (0.06 mm) and colloid cement has particle sizes of about 0.01mm; the clays are mostly illite and montmorillonite. Fracture openings should be at least $2D_{50}$, where D_{50} is the particle diameter exceeded by 50 percent of the particles.

It is often necessary to add stabilizing agents to suspensions, particularly clay grouts, to prevent premature flocculation. Flocculating agents may be added

to the grout to achieve coagulation at a particular time. Stabilizing and flocculating agents counteract each other. The action of these agents also depends on the clay minerals of the grout. The choice of proper agents and mix proportions is based on laboratory and field tests. It is possible to air entrain the suspensions and thereby improve their fluidity and penetration characteristics. So-called lubricants, mostly fly ash or rock flour, decrease the shearing resistance during flow.

Solutions are either of methatetical precipitation type or polymers. Most methatetical-precipitation-type solutions are silicate solutions or lignin grouts. Polymers can be acrylamides, phenoplasts, and aminoplasts, which are injected in the form of monomers, or epoxys and polyester resins, which are injected in a partially polymerized state. The silicate solutions and the monomers have initial viscosities in the range of one to a few centipoise, that is, the viscosity of water or a bit higher. Epoxys and polyester resins have substantially higher viscosities, which makes them difficult to inject into fractures with small apertures unless grout pressures are very high. Viscosity increases in all cases as the grout solidifies. Ideally, a grout should solidify suddenly, and the point in time at which this occurs should be controllable. A controlled solidification is rarely possible, however, even under laboratory conditions because of the many factors affecting the process.

Solutions can be injected in a single-phase process (also called one-solution process); that is, they are mixed and then injected. Solutions can also be injected in a multiphase (or multisolution) process (usually two phases),[2] where one component is injected first, followed later by the additional component(s).

As mentioned earlier, grouts are injected from grout holes into fractures either under gravity flow or artificial pressure. Grout flow into fractures is governed by the same principles as fluid flow and can be predicted by using the methods discussed in Chapter 6, as well as the coupled methods discussed in this chapter. Complicating factors are the aforementioned characteristics of sedimentation/flocculation of suspensions and the viscosity increase of solutions. Grouts are fluids that are initially Newtonian or can be approximated as such but will deviate from this behavior as they approach solidification. Flow characteristics and the solidification process govern the range in the fracture(s) that can be reached by the grout, in particular, the range that can be grouted from one grout hole. Related to this range is the interference distance, that is, the distance between grout holes at which grouting in one hole reduces the volume that can be grouted from another.

It is often necessary to use a series of grouts in sequence, for example, starting with highly viscous grouts to seal larger fractures and ending with low-viscosity grouts or starting with low-viscosity grouts to seal fractures farther from the grout holes and ending with high-viscosity grouts. This procedure is called multiple-stage grouting.

If grout holes are used, grouting is most commonly performed by one of several basic procedures:

- *Downward* (often called *downward staging*[3] or *stage grouting*), where zones are injected in a downward sequence, necessitating redrilling for each subsequent injection (Figure 7.10a).
- *Upward* (often called *upward staging* or *stop grouting*) is the inverse process, where no redrilling is necessary (Figure 7.10b).
- In the upward and downward procedures, single packers are used to isolate the section of borehole below the packer into which the grout is injected.
- *Tube á Manchetts* or *Sleeve Packers*, is a procedure patented by Solétanche (see Cambeforte, 1964). A perforated tube smaller in diameter than the borehole with rubber sleeves covering the perforations is inserted into the borehole. The space between the tube and the borehole is filled with drilling mud. Inside the tube there is a movable double-packer arrangement and the actual grout tube. This double packer can be placed over any of the perforations, and grout is injected through the drilling mud into the rock fractures. This process can be repeated, possibly with different grouts. Repeatability is the major advantage of this procedure, because it allows regrouting until the desired result is achieved.

In impermeabilization grouting, internal cutoffs are produced by arranging many grout holes in the form of grout curtains, grout blankets, or grouted zones. For instance, curtains can be constructed between a dam foundation and an impermeable or less permeable layer (Figure 7.11a), or flow paths through a grout curtain or grout blanket can be lengthened (Figure 7.11b). Foundation excavations are rendered impermeable by similar arrangements, such as grout curtains to lengthen flow paths (Figure 7.11b) or by implementation of a combination curtain-blanket to form a watertight box around an excavation (Figure 7.11b).

Tunnels are made impermeable through grouting by placing grout holes stepwise in a fanlike pattern from the tunnel (Figure 7.12a) or by placing them from enlarged sections parallel to the tunnel (Figure 7.12b). Radial arrangements (Figure 7.12c) are also possible, as are placements from the surface if the tunnels are shallow (Figure 7.12d). Arrangements as shown in Figure 7.12 can also be applied to waste storage isolation.

In all cases where zones of fractured rock are grouted to form a cutoff, grout holes are usually placed in single (parallel) rows, multiple rows, or radial patterns. The spacing of the grout holes depends on the flow and solidification characteristics of the grout such that continuously grouted zones are produced. Because it is very difficult to predict grout flow and hole spacing, an empirical procedure based on so-called split spacing is used. Grouting starts with a relatively large spacing of primary grout holes and continues by locating new holes midway between existing ones until the desired performance of the grouted zone is achieved. The split-spaced hole may be used to conduct a permeability test before deciding on further grouting. This procedure actually characterizes grouting in general; a grout is injected, and its behavior is observed during injection (flow/pressure behavior) and afterwards (reach, effect on rock mass properties). Based

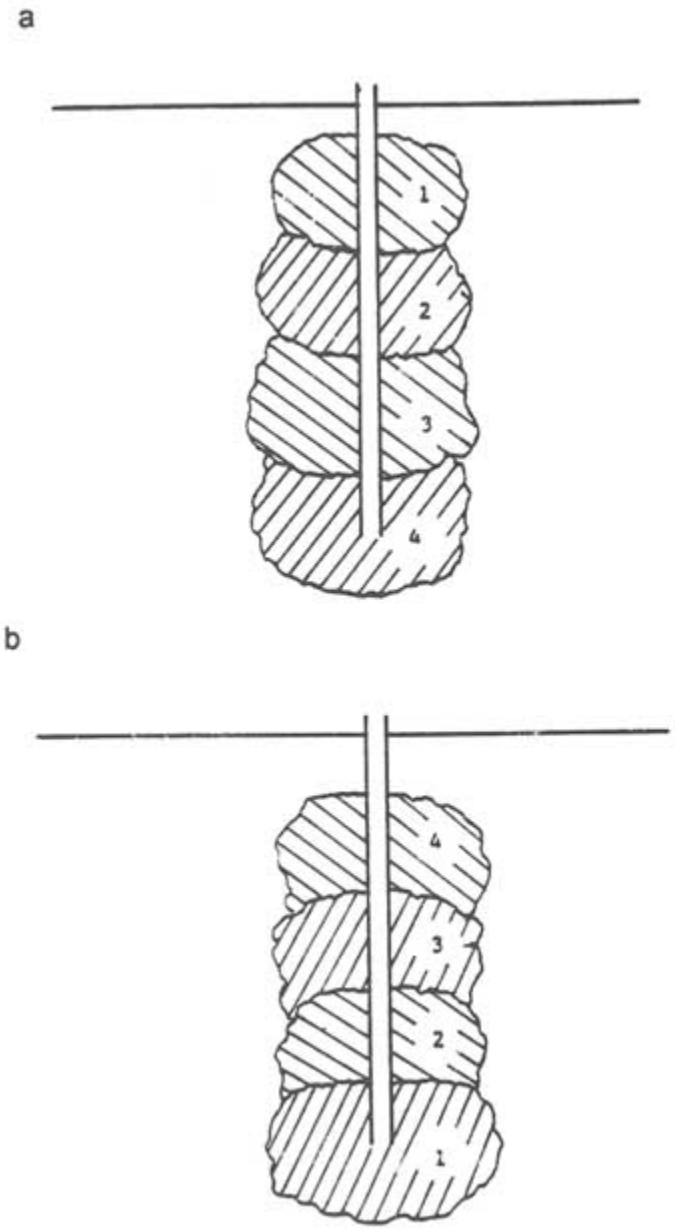

FIGURE 7.10 Procedures for fracture sealing through grout holes. (a) Downward staging or stage grouting. (b) Upward staging or stop grouting.

on this information, more grout is injected through the same hole in one of the procedures mentioned earlier, or grout is injected in new holes, as discussed above. This is a classic application of the adaptable/observational methods (see also "Adaptable/ Observational Methods," later in this chapter). Limited analytical prediction is possible (see below), but much of the grouting procedure is based on experience and on careful application of the adaptable/observational approach. The sequencing of grouting in single and multiple holes is not ad hoc but is a carefully planned engineering process.

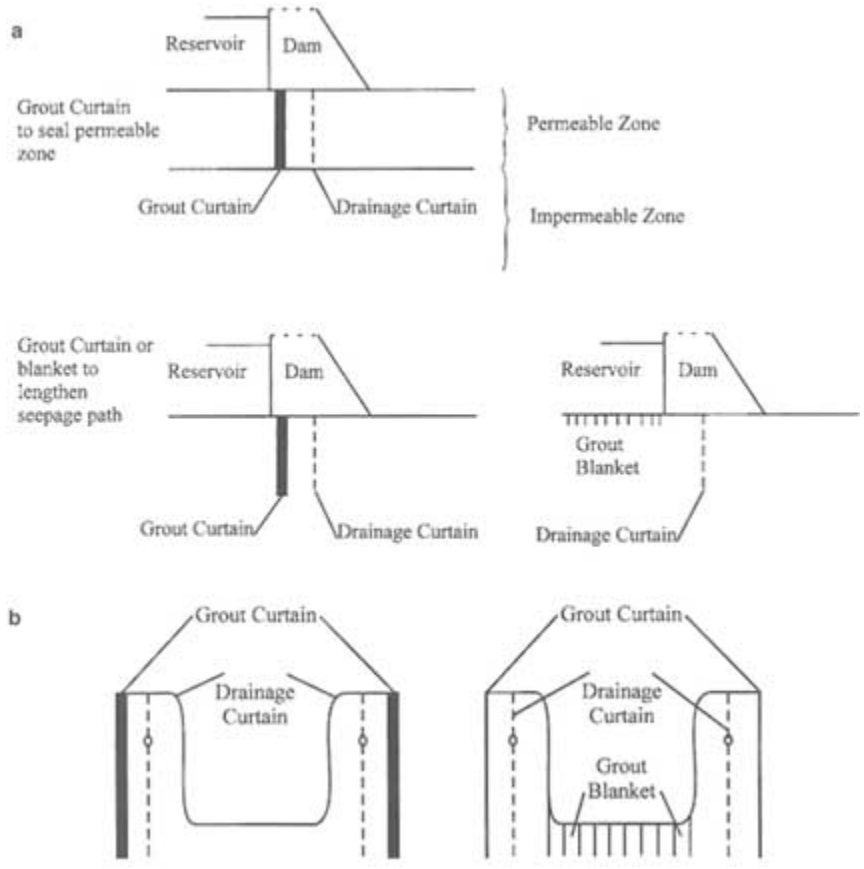

FIGURE 7.11 Grouting to reduce permeability in (a) dams and reservoirs using curtains and blankets and (b) foundation excavations.

From this description of impermeabilization grouting for dams, excavations, and tunnels, it should be evident that the same procedures can be used to strengthen and stiffen weak or deformable fractured rock masses. Most clay-based suspensions and "metathetical precipitation" solutions can only be used for impermeabili

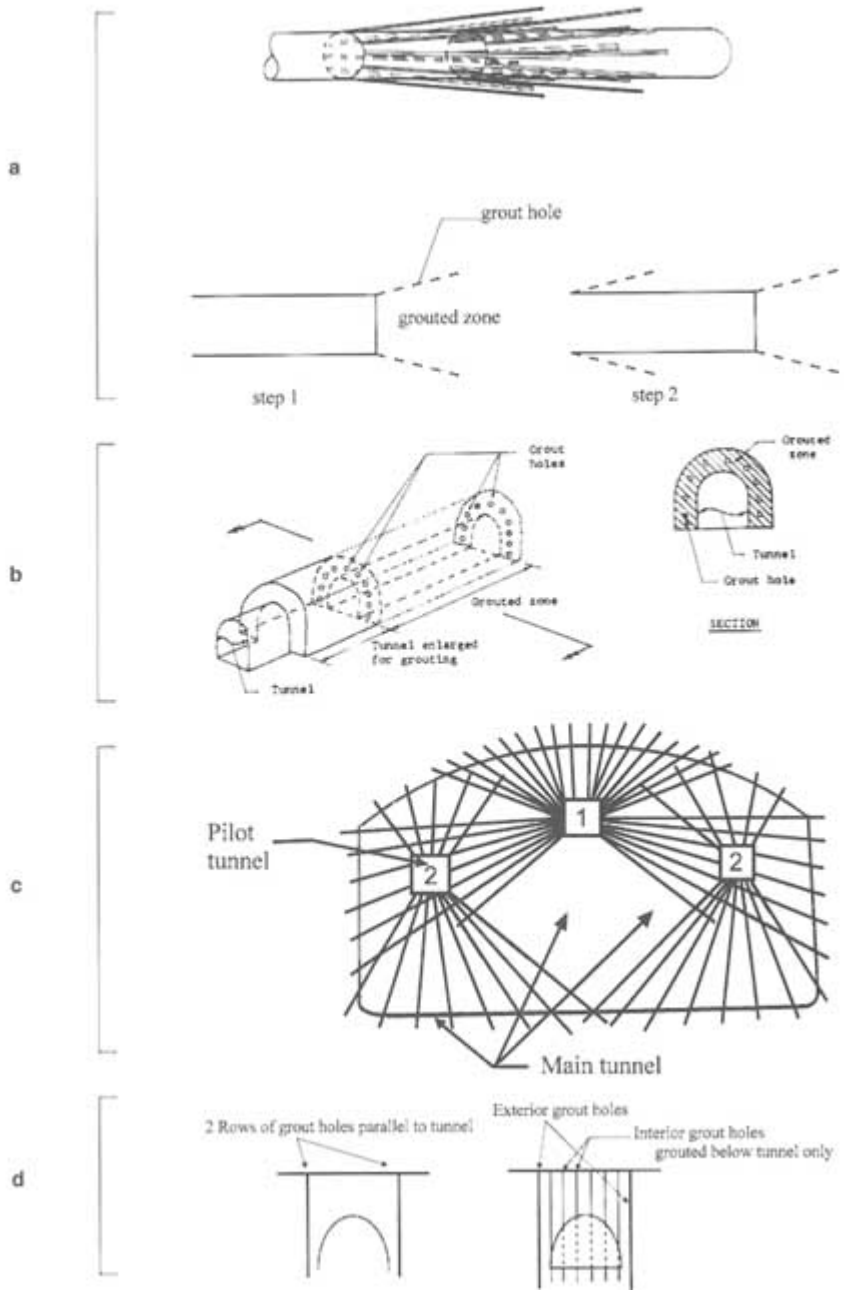

FIGURE 7.12 Tunnel grouting. (a) Grouting in fan pattern. (b) Grouting from an enlarged section. (c) Grouting with radial arrangement of grout holes. (d) Grouting from the surface.

zation. Depending on temperature, some polymers do not have satisfactory resistances and stiffnesses. On the other hand, most other chemical grouts will actually increase the stiffness and strength of rock masses or any ground for that matter.

Grouting, whether for impermeabilization, strengthening, or stiffening, has a number of potentially negative effects. The first is the contaminating effect of grout components. If the grout components do not solidify or are eroded or leached after injection, they may contaminate groundwater. Second, through the creation of an impermeable zone, water pressures will increase upstream. Pressure buildups behind excavation walls (Figure 7.11b) or behind grouted zones under dams and in dam abutments (Figure 7.11a) may endanger their stability (see "Creation or Extension of Fractures Owing to Increases in Fluid Pressures," earlier in this chapter). It is advantageous to combine grouting with drainage, as indicated in Figure 7.11. (In some cases, similar considerations apply in tunneling.) Finally, grouts may not be permanently effective. Grout pressures may hydraulically fracture the rock mass and inadvertently worsen the condition they are intended to improve. Leaching and erosion, particularly if high water pressures exist, may reduce the intended effect of the grout. This is not a problem if grouting is used for construction purposes around foundation excavations or tunnels, but it is a problem in dams and in long-term waste isolation.

Models for Grouting

Analyzing flow through a rock mass containing zones of reduced permeability is usually based on the assumption of a heterogeneous medium, where the grouted rock is modeled by an impermeable/low-permeability layer in a higher-permeability rock mass. In quasi-continuum approaches, flow net distortions (e.g., Cedergren, 1977) can be used to represent different permeabilities, and numerical methods can be applied correspondingly. If discontinuum approaches are used, the permeable rock mass is modeled as a discontinuum; the cutoff is usually modeled as a continuum. This combination is somewhat problematic, but, in principle, is similar to flow through combinations of soil and fractured rock. The usual procedure is to separate the two zones and calculate flow through the fractured medium with the methods described in Chapter 6, under initially assumed boundary conditions at the continuum-discontinuum interface. The process is iterated until the results of the continuum and discontinuum analysis at the interface are within a specified tolerance.

Analyzing flow and solidification of grout is extremely difficult for the reasons explained earlier. Basically, fracture flow models, in which the flow characteristics of the grout change with time, could be used. An alternative is the one by Stille et al. (1992), which models the sequential blocking of fractures as grouting proceeds. Grout is assumed to flow in the channels in joint planes. When grout is injected into a single channel, injection proceeds until the grout

stops, because the shear forces along the wall of the channel balance the driving pressure. The model assumes that the grout behaves as a Bingham fluid (i.e., the model does not account for the particle size distribution in the grout), which means that the shear force per unit area of contact between the grout and the fracture channel wall is constant along the length of the fracture. Grout penetration can be calculated as a function of channel size distribution. This model provides a means of designing an appropriate grouting fluid as determined by the geometry of the fracture network. A drawback of this approach is the uncertainty in knowing the in situ boundary conditions. Consequently, usually only adaptable/observational approaches can be applied in which the grouting procedure is planned based on past experience or some initial laboratory or field tests, which are then adapted on the basis of field observations.

REDISTRIBUTION OF EXISTING SOLIDS BY CHEMICAL PROCESSES

This section addresses changes in the geometry of the void spaces (pores and fractures) resulting from chemical processes. Altering the solid framework can drastically increase or decrease the permeability and porosity of the system, which in turn will modify flow and transport phenomena, possibly leading to more changes in the solid framework.

Chemical Mobilization and Swelling of Clays

Many fractured rocks contain clay in the rock matrix or as fillers in fractures and pores. Clay particles can be mobilized by changes in fluid chemistry and transported in suspension, or the clay can swell. Clays can be mobilized by a change in the nature or concentration of the electrolytes in solution. Clay particles generally have a negative electrical charge, which is neutralized by exchange cations and water dipoles in the form of a so-called double layer. The properties of this double layer are strongly affected by the concentration of the electrolyte solution and the valence and size of its constituent ions.

Smectites and mixed-layer clays have, in addition to this double layer, layers of water molecules that contain exchange cations sandwiched between negatively charged sheets of aluminosilicates. This makes them particularly susceptible to changes in the valence and concentration of surrounding electrolyte solutions. Higher valences or ion concentrations decrease the number of water molecules layers and, consequently, the size of the hydrated clay particle, causing the clays to shrink. A particle stuck in a constriction may shrink enough to become mobile.

If fractures are filled with clay or if the fracture wall rock is argillaceous (i.e., clay rich), exposure of the rock to water may lead to swelling of the clay minerals. In this case there is a time-dependent decrease in the void volume of the fracture. A number of different swelling mechanisms exist in argillaceous

rock. Mechanical swelling is the inverse of consolidation in that a decrease in applied stresses will lead to a reduction in pore pressures. Consequently, pore water will flow into the destressed depressurized zone and cause swelling. Physicochemical swelling can be osmotic interparticle swelling—that is, water being attracted into the double-layer zone surrounding clay particles—or it can be swelling in which water is incorporated into the clay layers, such as occurs in smectite. Other rocks such as anhydrite also swell owing to exposure of fractures to water and stress relief, but the mechanism is different. Swelling of fracture fillings causes clogging, which leads to pore pressure increases that may be detrimental to stability.

Dissolution and Precipitation

Solids can be redistributed by being dissolved, transported in solution, and precipitated in a new location. In general, this process will increase permeability in regions from which material is being removed and decrease it in regions where material is being deposited. The redistribution of solids in fractures can occur with or without changes in the overall mineral assemblage making up the rock mass. A given mineral may be dissolved at one place and precipitated in another, or an existing mineral may be dissolved and a different one precipitated elsewhere (Phillips, 1991). Some geothermal systems are thought to be "self-sealing" through a mechanism involving the dissolution of minerals near the source of the heat and reprecipitation in fractures at some distance from the heat source. These processes are also the basis of "in situ mining," in which economic minerals are leached from the rock by solution mining (U.S. Bureau of Mines, 1989).

Even in mineralogically simple systems, the overall processes of flow, dissolution, transport, and precipitation are coupled in extremely complex ways. Solubility of a given mineral is a function of temperature, pressure, and the composition of the aqueous phase (i.e., the types and concentrations of ionic species in solution). Changes in any of these variables during engineering operations can produce significant large-scale alterations of the spatial permeability distribution. These alterations, in turn, affect flow velocity, which affects dissolution, transport, and precipitation.

Solubility is also a function of other solid minerals present in the system and the conditions of phase equilibrium among different solid phases. Metastable or unstable combinations of minerals are known to persist over geologically significant time periods, presumably because reaction rates are very slow. In such cases the state of the system is controlled by chemical kinetics, rather than thermodynamic equilibrium conditions.

Increased temperature can either increase the solubility of a mineral (e.g., halite) or decrease its solubility (e.g., gypsum, calcite), depending on the chemical species involved. Similar species-specific differences in solubility are observed for fluid pressure changes.

As in other processes involving phase equilibria, dissolution and precipitation reactions depend on chemical potential or partial molar Gibbs free energy. If the chemical potential of a given substance is not the same in all phases in which it is present, the system is not in equilibrium. Mass will be transferred spontaneously from the phase with the higher chemical potential to the phase with the lower chemical potential.

The direction of change induced by perturbations in stress, temperature, fluid pressure, or composition introduced by an engineering operation is easily determined by calculating the changes in chemical potentials. For example, in the case of "pressure solution" an increase in pressure will increase the chemical potential of a species in the solid phase more than in the solution phase. Therefore, there will be a spontaneous transfer of mass from solid to solution, and the void volume of the system will be increased. This volume increase in turn counteracts the increase in pressure. The reverse analysis works equally well for precipitation. If one phase is an aqueous solution and the other a porous or fractured solid, the partial molal quantities can be used to determine the direction of mass transfer, that is, which phase tends to gain mass and which tends to lose.

The example given above is an illustration of Le Chatelier's principle: if a system at equilibrium is disturbed, the resulting changes are always in such a direction as to offset the disturbance and restore equilibrium. Similar results for temperature changes are available in any standard chemical thermodynamics text, with the negative of the partial molal entropy playing the role of the partial molal volume.

The discussion above, has emphasized one of the more powerful principles for analyzing changes involving dissolution or precipitation caused by changes in the temperature or pressure of a system—namely, equilibrium thermodynamics. Similar analyses can be made to determine changes in concentration and the directions of chemical reactions. However, it should be noted that thermodynamics provides no information about the rates of any of the processes involved, whether physical or chemical. To consider these effects, additional theory and experimental measurements are necessary to provide parameters for the rate equations. The rates of chemical reactions may be kinetically controlled or they may be controlled by the flow system, depending on the fluid velocities and the particular reaction. In fact, some parts of the system, with slow fluid movement, may be controlled by equilibrium conditions, and other parts, with more rapid fluid movement, may be controlled by kinetics.

Models

The models used to study dissolution and precipitation are essentially the same as those used to study reactive transport as described in Chapter 6. An example of calculations for the redistribution of silica in a fracture flow system in geothermal applications is given by Lai (1986). In this case the thermodynamic

data base for silica is well understood, and the chemistry is relatively simple. Lai was able to neglect the effect of pressure and model dissolution and precipitation as a function of temperature. However, precipitation and dissolution of other very common fracture fillings, such as calcite, have not been modeled because of the complexity of the chemistry (e.g., buffering and pH dependence in the case of calcite) or the lack of thermodynamic data.

Alteration of Existing Solids

This section is concerned with changes in which a solid is altered by a solid-state phase change that changes the density (and hence the volume) of the solid grains, with accompanying changes in porosity and permeability. For example, the siliceous Monterey formation in California was deposited as an ooze of diatom skeletons composed of amorphous silica. As the depth of burial increased, the amorphous silica was converted to the crystalline-phase cristobalite, which in turn was converted to microcrystalline quartz. This sequence is a key factor in the development of fracture permeability in the Monterey formation and required millions of years because the rate of burial is low and the rates of solid-state reactions are very slow at low-to-moderate temperatures. Other examples of solid-state phase changes include the transformation of aragonite, the crystalline form of calcium carbonate generally produced by biological processes, to calcite, the form generally found in limestones.

At typical engineering time scales, solid-state phase transitions are not usually important because reaction rates are very slow. These effects may be important at the high temperatures generated by in situ combustion methods for enhanced oil recovery, because the rates of most reactions increase rapidly with increasing temperature. Solid-state phase transitions may also be important at the elevated rock temperatures expected around nuclear waste repositories. In this case the time of interest is many thousands of years rather than a few decades, so even a small increase in reaction rate could produce significant effects.

The quantification of the chemical phenomena described in this section can be extremely complex. There are a large number of important parameters. For many reactions the thermodynamic data base is not available. Even if it were, natural mineralogical heterogeneity is rarely if ever quantified. Finally, the flow system itself may not be well understood. There is significant need for research into effective methods of predicting reactive behavior. These should include laboratory and in situ experiments that are designed as analogs to the reactions of interest and that provide an opportunity for heuristic extrapolation.

Colloidal Suspensions

A special class of chemical reactions arises in certain waste disposal applications, including nuclear waste disposal. Under some conditions, chemical reac

tions between the waste and water can produce colloidal suspensions that contain radionuclides. Colloidal suspensions may be capable of transporting much higher concentrations of radionuclides than true solutions. Colloids are generally repelled from the walls of fractures. Consequently, they travel near the centers of the fractures and may be transported more quickly than the average fluid flow velocity.

New information about colloidal behavior has come from recent work by Wan and Wilson (1994a,b) and Wan et al. (1994). Wan and co-workers have shown that colloids are essentially hydrophobic and consequently are attracted to the interfaces between water and air. This phenomenon could have a significant effect on the transport of contaminants under two-phase conditions. In particular, buoyant flow of gas bubbles with entrained colloids may be a possible mechanism for the transport of radionuclides in fractures.

ENGINEERING UNDER UNCERTAIN CONDITIONS

Problems involving changes to fracture systems in engineering and engineering geology involve uncertainty. The basic problem is a lack of data about the heterogeneous medium and an inadequate understanding of the coupled processes involved. The fracture geometry, mechanical properties, water pressure, flow, and chemical conditions in a rock mass are usually ill defined. Design and construction or, more generally, engineering decisions must consider this intrinsic uncertainty. This can be done in several ways, as explained in the following sections.

Reducing Uncertainty

One way to reduce uncertainty is through characterization efforts. A characterization resulting in the complete elimination of uncertainty is, however, not possible. Tradeoffs between the cost of further characterization and the benefits of reducing the uncertainty must be evaluated (Einstein et al., 1976).

Explicit Consideration of Uncertainty in Decision Making

The best-known approach is design with a safety factor or several safety factors. The design parameters are chosen such that design performance has a large margin of safety. Safety factor design does not guarantee safe performance because the distribution of possible performances is not determined. Partial safety factor design is somewhat more robust. In this case each of the major parameters is associated with a safety factor that reflects the uncertainties and importance of the parameter. Another approach is reliability and risk analysis (Ashley et al., 1979). In this approach, probabilities of malperformance are determined on the basis of uncertainties in the parameters. The risk involved in choosing a particular

design is explicitly determined and can be compared to the consequences of mitigation or the consequences (i.e., cost) of choosing a design with a reduced risk.

Adaptable/Observational Methods

As shown in Figure 7.13, a design is chosen on the basis of the most likely expected performance, which can be determined formally or intuitively. Simultaneously, contingency designs are developed to address conditions that deviate from the most likely case. Most importantly, performance criteria and monitoring approaches are included in all designs. The monitored performance is compared with the target performance, and, if deviations are observed, the appropriate contingency design is chosen. Minor adaptations can be made ad hoc. Peck (1969) and Einstein (1978) review many of the applicable methods.

Clearly, combinations of the three approaches discussed here are possible, such as determining the distribution of possible performances, and then using the performances to evaluate the benefits of further exploration before deciding on the most likely performance.

SUMMARY OF DEFICIENCIES AND RESEARCH NEEDS

The preceding discussion of rock-fracture-related problems in civil and mining engineering and engineering geology identified a number of problems:

- It is not possible to completely characterize the geometric, mechanical, and chemical properties of rock masses. Exploration methods often have inadequate ranges of resolution and penetration and are too expensive.
- Even with advances in exploration methods, there will always be uncertainties in rock mass characterization. Further formalization of adaptable analysis-design procedures is required, and, particularly, procedures are needed that allow quick adaptation as observations provide new information.
- Clearly, any progress in knowledge about the geometry, mechanics, and mineralogy of individual fractures and fracture systems is desirable. Most important are relationships between geometry, mechanical behavior, and the creation of new fractures.
- Knowledge of the long-term behavior of most rock mass changes is unreliable.

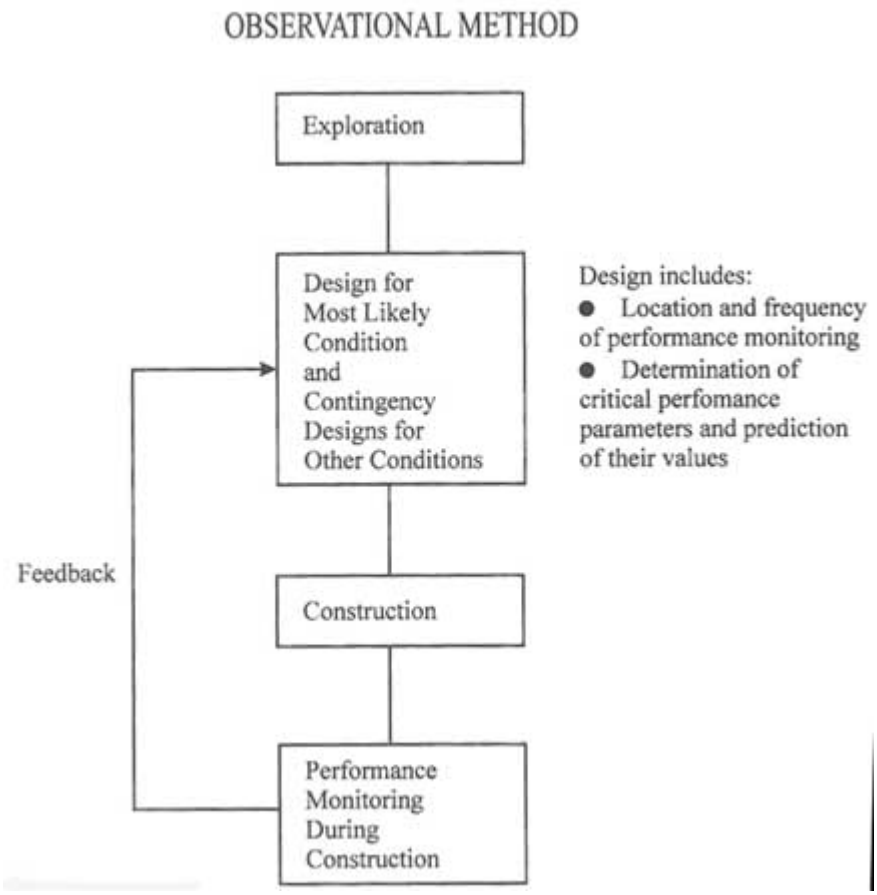

FIGURE 7.13 Knowledge of design parameters is updated through monitoring and feedback.

Appendix 7.A

Natural Fracturing

The basic mechanics of the fracturing process provide insights into natural fracturing deep within the earth's crust. For this case it is appropriate to assume that the formations are massive with continuous field and property gradients. The vertical gradient of stress is proportional to rock density and is larger than the vertical fluid pressure gradients, which means that the effective stress is decreasing in the upward direction. This stress gradient promotes upward propagation of hydrofractures, as illustrated in Figure 7.A1, which shows results from

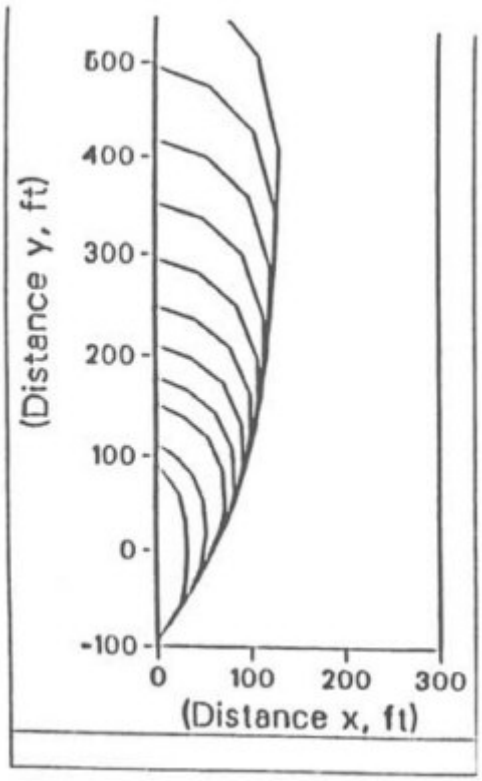

FIGURE 7.A1 Propagation of a vertical hydrofracture. After Clifton (1989).

a numerical simulation of a hydraulic fracture with a fluid source centered at the origin. The fracture front progresses, in time, from a near-radial shape to an elongated shape.

The rate of penetration and degree of vertical preference are governed by the viscous dissipation of the vertical pressure gradient. The preference for vertical growth from a fluid source of massive horizontal dimension will provide parallel sets of fractures.

The interaction of multiple fractures is influenced by the altered stress field around the fractures caused by their deformation. Furthermore, in massive formations the magnitude of the negative effective stress (i.e., pressure) required to propagate a fracture tends to decrease as the fracture dimension increases. The decreasing pressure requirement can be offset by increasing viscosity as the intruding fluid rises and is cooled as it moves away from a heat source.

Because they require less pressure in order to propagate, larger fractures will propagate preferentially when all the fractures are connected by a common pressure source. The existing fractures induce a compressive stress in the direction normal to the fracture plane on a scale proportional to the size of the fracture. The scale-dependent stress increase tends to close neighboring fractures, particularly smaller ones with smaller apertures. The coupling of the scale-dependent stress increase and the preference for growth of larger fractures will define the size distribution and spacing between fractures of various sizes. Additional features of natural hydraulic fracture networks can be illuminated by the comprehensive numerical models used in the petroleum industry (Gidley et al., 1989, Chapters 3, 4, and 5).

Appendix 7.B

Drainage Methods In Construction

Water flow from excavation surfaces may impede construction (operation) or erode fracture fillings or fracture wall rocks. Water flow can be prevented or reduced by applying so-called drainage layers to the excavation walls. These external drainage layers consist of relatively permeable (low cement content) shotcrete or geotextiles (Figure 7.B1a), which are frequently applied in combination with an impermeable seal to form a geomembrane. If drainage occurs from only a few fractures, hoses can be inserted into the fractures to relieve the flow (Figure 7.B1b). Frequently, short holes are drilled into the rock mass to capture the flow before it reaches the surface of the excavation (Figure 7.B1c). This approach may be used in combination with hoses or drainage layers.

External drainage involves the capture of water or gas near an excavated or natural surface. When incorporated into permanent structures, this type of drainage must be a carefully designed system of seals and pipes for the removal of water (Figure 7.B1d). Water pressures should not exceed specified limits to prevent overloading of the seal or the permanent supports. However, a reduction in water pressure may result in the precipitation of calcite in fractures if the water is carrying calcite in solution.

The purpose of internal drainage is to capture water (gas) at a distance from the natural or excavated surface. This type of drainage can be used to induce favorable stress conditions in a zone near the surface and avoid some of the above-mentioned problems when water drains directly at the surface.

Many internal drainage methods make use of boreholes that intercept fractures in the rock mass. Boreholes can be arranged in several geometries as shown in Figure 7.B1e. Possible arrangements include single or multiple rows of vertical or inclined holes to form "drainage curtains"; drainage curtains are also used in conjunction with dams (Figure 7.B1f).

Borehole drainage curtains can be replaced by so-called permeable cutoffs, which are excavated trenches or slots filled with permeable materials (Figure 7.B1 g). The objective of all these methods is to intercept fractures that are under high pore pressures or that are connected to fracture systems under high pore pressures. Depending on the fracture and fracture system geometry, this may require that boreholes be oriented other than in simple vertical or horizontal rows. Figure 7.B1h shows a drainage gallery (tunnel) that can be used alone or in conjunction with drain holes to improve drainage. Internal drainage can also be induced by increasing the permeability of fractured zones in the rock mass. Methods for accomplishing this involve the creation of new fractures by blasting or hydraulic fracturing and increasing fracture conductivity by propping. These methods are discussed earlier in this chapter, under "Creation or Extension of Fractures Owing to Increases in Fluid Pressures."

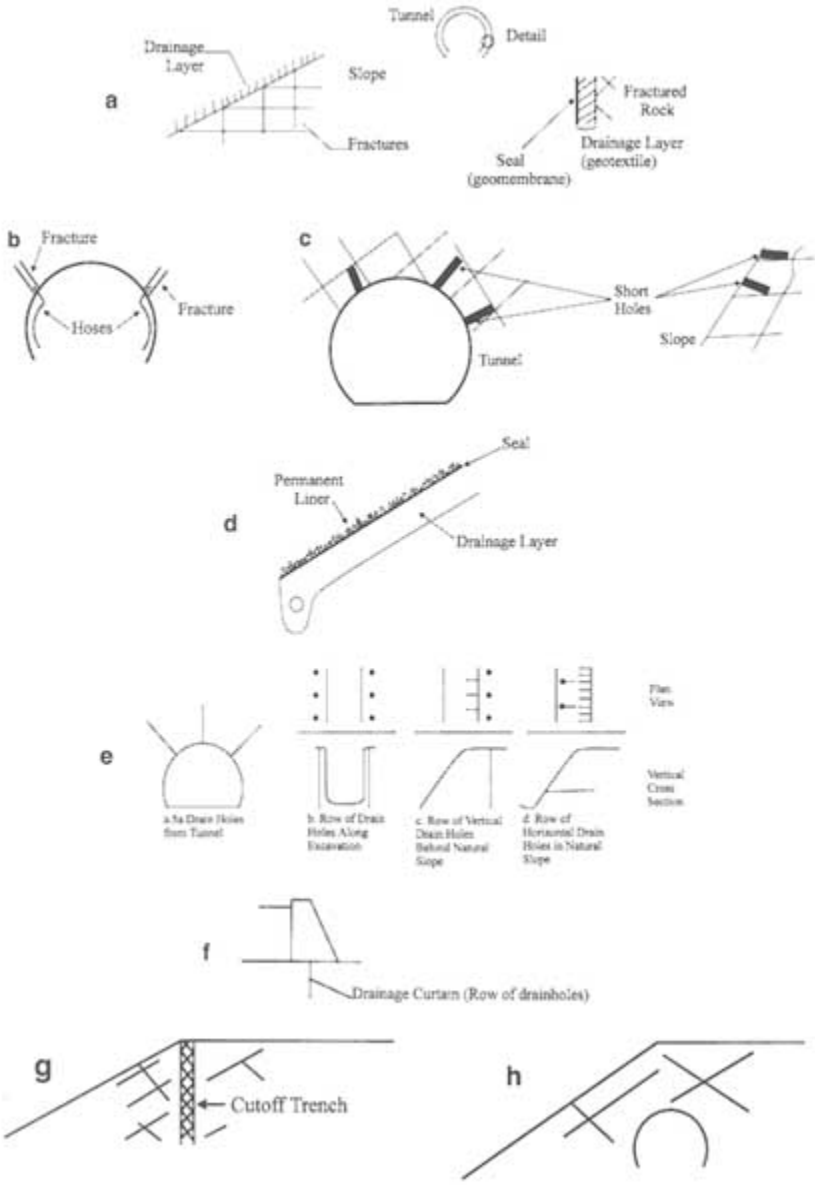

FIGURE 7.B1 Schematic illustration of drainage methods. (a) External drainage layers. (b) Drainage through hoses inserted into fractures. (c) Drainage through short holes drilled into the rock mass. (d) Drainage beneath a permanent liner. (e) Internal drainage through boreholes. (f) Drainage curtain in a dam foundation. (g) Drainage cutoff trench. (h) Drainage tunnel.

Fluids from internal drainage can be removed through gravity flow or pumping. Erosion of fracture fillers or fracture wall rock can be minimized by placing filters and suitably graded materials into the drainage facilities.

REFERENCES

Advani, S. H., T. S. Lee and J. K. Lee. 1990. Three-dimensional modeling of hydraulic fractures in layered media: Part I—finite element formulations. ASME Journal of Energy Research Technology, 112:1–9.

Asgian, M. 1989. A numerical model of fluid flow in deformable naturally fractured rock masses. International Journal of Rock Mechanics and Mining Science and Geomechanics Abstracts, 26:(3/4) 317–328.

Ashley, D. B., H. H. Einstein, and E. Tse. 1979. Advantages and limitations of adaptable tunnel design—construction methods. Pp. 989–1011 in Proceedings of the 4th Rapid Excavation and Tunneling Conference. Richardson, Tex.: American Institute of Mining, Metallurgical and Petroleum Engineers.

Biot, M. A. 1956. Thermoelasticity and irreversible thermodynamics. Journal of Applied Physics, 27:240–253.

Boley, B. A., and J. H. Weiner. 1960. Theory of Thermal Stresses. New York: John Wiley & Sons.

Cambefort, H. 1964. Injection des Sols. Paris: Editions Eyrolles.

Cedergren, H. R. 1977. Seepage, Drainage, and Flownets. New York: John Wiley & Sons.

Clifton, R. J. 1989. Three-dimensional fracture-propagation models. In Recent Advances in Hydraulic Fracturing, J. L. Gidley, S. A. Holditch, D. E. Nierode, and R. W. Veatch, eds. Monograph Series 12. Richardson, Tex.: Society of Petroleum Engineers.

Clifton, R. J., and J. J. Wang. 1988. Multiple fluids, proppant transport and thermal effects in 3-dimensional simulation of hydraulic fracturing. Paper presented at the 63rd Annual Technical Conference, Oct. 2-5, 1988, Houston, Tex. SPE 18198. Richardson, Tex.: Society of Petroleum Engineers.

DECOVALEX. 1991. Bench-mark test 2: multiple fracture model. DECOVALEX Doc 91/104. DECOVALEX Secretariat. Stockholm: Royal Institute of Technology.

De Marsily, G. 1987. An overview of coupled processes with emphasis on geohydrology. In Coupled Processes Associated with Nuclear Waste Repositories, C. F. Tsang, ed. New York: Academic Press.

Doughty, C., and K. Pruess. 1988. A semianalytical solution for heat-pipe effects near high-level nuclear waste packages buried in partially saturated geological media. International Journal of Heat Mass Transfer, 31:79-90.

Dvorkin, J., and A. Nur. 1992. Filtration fronts in pressure compliant reservoirs. Geophysics, 57:1089-1092.

Economides, M. J., and K. G. Nolte. 1989. Reservoir Stimulation, Second Edition. Englewood Cliffs, N.J.: Prentice-Hall.

Einstein, H. H. 1978. Observational Tunnel Design—Construction Methods in the U.S. Shotcrete for Underground Support III. New York: Engineering Foundations.

Einstein, H. H., D. A. Labreche, M. J. Markow, and G. B. Baecher. 1976. Decision analysis applied to rock tunnel exploration. Engineering Geology, 12(2):143–160.

Einstein, H. H., G. B. Baecher, and D. Veneziano. 1979. Risk analysis for rock slopes in open pit mines. MIT report 80–20 to U.S. Bureau of Mines, vol. III, Massachusetts Institute of Technology, Department of Civil Engineering, Cambridge, Mass.

Engelder, T. 1993. Stress Regimes in the Lithosphere. Princeton, N.J.: Princeton University Press, 457 pp.

Fredrick, J. T., and Wong. 1986. Micromechanics of thermally induced cracking in three crustal rocks. Journal of Geophysical Research, 91:12,743–12,764.

Geertsma, J., and F. de Klerk. 1969. A rapid method of predicting width and extent of hydraulic induced fractures. Journal of Petroleum Technology, Dec., pp. 1571–1581.

Gidley, J. L., S. A. Holditch, P. Nierode, and R. Veach, eds. 1989. Recent Advances in Hydraulic Fracturing, vol. 12. Richardson, Tex.: Society of Petroleum Engineers.

Goodman, R. E. 1976. Methods of Geological Engineering. St. Paul, Minn.: West Publishing.

Hendron, A. J., E. J. Cording, and A. K. Aiyer. 1971. Analytical and graphical methods for the analysis of slopes in rock masses. Technical Report No. 36, Nuclear Cratering Group.

Hoek, E., and J. W. Bray: 1981. Rock Slope Engineering, 3d ed. London: The Institute of Mining and Metallurgy.

Hunt, J. R., L. McDowell-Boyer, and N. Sitar. 1987. Colloid migration in porous media: an analysis of mechanisms. Pp. 453–472 in Coupled Processes Associated with Nuclear Waste Repositories, C. F. Tsang, ed. New York: Academic Press.

Kafritsas, J. 1987. Coupled flow/deformation analysis with the distinct element method. Ph.D. thesis, Massachusetts Institute of Technology, Cambridge.

Khristianovich, S. A., and Y. P. Zheltov. 1955. Formation of vertical fractures by means of highly viscous liquids. Pp. 579–586 in Proceedings of the Fourth World Petroleum Congress, section II/T.O.P., paper 3, Rome.

Kohl, T., K. I. Evans, R. J. Hopkirk, and L. Rybach. 1996. Modeling of coupled hydraulic thermal and mechanical processes in the simulation of hot dry rock reservoir behavior. In Fractured and Jointed Rock Masses. Rotterdam: A. A. Balkema.

Lai, C. H. 1986. Mathematical models of thermal and chemical transport in geologic media . Ph.D. thesis, University of California, Berkeley, p. 188.

Lake, L. W. 1989. Enhanced Oil Recovery. Englewood Cliffs, N.J.: Prentice-Hall.

Londe, P. 1987. The Malpasset Dam failure. Engineering Geology, 24(1–4): 295–330.

Long, J. C. S., O. Olsson, S. Martel, and J. Black. 1992. Effects of excavation on water inflow to a drift. In Fractured and Jointed Rock Masses. Rotterdam: A. A. Balkema.

Majer, E. L., L. R. Myer, J. E. Peterson, Jr., K. Karasaki, J. C. S. Long, S.J. Martel, P. Blumling, and S. Vomvoris. 1990. Join Seismic, Hydrogeological, and Geomechanical Investigations of a Fracture Zone in the Grimsel Rock Laboratory. LBL-27913, Lawrence Berkeley Laboratory, Berkeley, Calif., 173 pp.

Martin, C. D., C. C. Davison, and C. T. Kozak. 1990. Characterizing normal stiffness and hydraulic conductivity of a major shear zone in granite. Pp. 549–556 in Rock Joints, Proceedings of the International Symposium on Rock Joints, N. Barton and O. Stephansson, eds. Rotterdam: A. A. Balkema.

Meade, R. B. 1991. Reservoirs and earthquakes. Engineering Geology, 30(314):245–262.

Meyer, B. R. 1989. Three-dimensional hydraulic fracturing simulation of personal computers: theory and comparison studies. SPE 19329. Pp. 213–230 in Proceedings of the Eastern Regional Meeting of Society of Petroleum Engineers, Morgantown, W. Va. Richardson, Tex.: Society of Petroleum Engineers.

Nolte, K. G. 1982. Fracture design considerations based on pressure analysis. SPE 10911. Paper presented at Cotton Valley Symposium of the Society of Petroleum Engineers, Tyler, Tex., May 20. Richardson, Tex.: Society of Petroleum Engineers.

Noorishad, J., P. A. Witherspoon, T. L. Brekke, and T. Maini. 1971. Methods for coupled stress and flow analysis of fractured dam foundations and rock slopes. Geotechnical Engineering Publication 71-6, University of California, Berkeley.

Noorishad, J., M. S. Ayatollahi, and P. A. Witherspoon. 1982. Coupled stress and fluid flow analysis of fractured rocks. International Journal of Rock Mechanics and Mining Sciences and Geomechanics Abstracts, 19:185–193.

Noorishad, J., C. F. Tsang, and P. A. Witherspoon. 1984. A coupled thermal-hydraulic-mechanical finite element model for saturated fractured porous rocks. Journal of Geophysical Research, 89 (B12):10,365–10,373.

Noorishad, J., C. F. Tsang, and P. A. Witherspoon. 1992. Theoretical and field studies of coupled hydromechanical behavior of fractured rocks: I—Development and verification of a numerical simulator. International Journal of Rock Mechanics and Mining Sciences and Geomechanics Abstracts, 29(4):401–409.

Olson, J. 1990. Fracture mechanics of joints and veins. Ph.D. dissertation, Stanford University, Stanford, Calif., p. 174.

Peck, R. B. 1969. Advantages and limitations of the observational method in applied soil mechanics. Geotechnique, 19:171–187.

Perkins, T. K., and J. A. Gonzalez. 1984. Changes in earth stresses around a wellbore caused by radially symmetrical pressure and temperature gradients. Society of Petroleum Engineers Journal, Apr., pp. 129–140.

Perkins, T. K., and J. A. Gonzalez. 1985. The effect of thermoelastic stresses on injection well fracturing. Society of Petroleum Engineers Journal, Feb., pp. 78–88.

Perkins, T. K., and L. R. Kern. 1961. Widths of hydraulic fractures. Journal of Petroleum Technology, Sept., pp. 937–949.

Phillips, O. M. 1991. Flow and Reactions in Permeable Rocks. New York: Cambridge University Press, pp. 57–58.

Prats, M. 1961. Effect of vertical fractures on reservoir behavior incompressible case. Society of Petroleum Engineers Journal, June, pp. 105–118.

Raghavan, R., J. D. T. Scorer, and F. G. Miller. 1972. An investigation by numerical methods of the effect of pressure-dependent rock and fluid properties on well flow tests. Society of Petroleum Engineers Journal, 12:267–275.

Rutqvist, J., J. Noorishad, O. Stephansson, and C. F. Tsang. 1992. Theoretical and field studies of coupled hydromechanical behavior of fractured rocks: 2. Field experiment and numerical modeling. International Journal of Rock Mechanics and Mining Sciences and Geomechanics Abstracts, 29 (4):411–419.

Settari, A., and M. P. Cleary. 1984. Three-dimensional simulation of hydraulic fracturing. Journal of Petroleum Technology, July, pp. 1177–1190.

Stephens, G., and B. Voight. 1982. Hydraulic fracture theory for conditions of thermal stress. International Journal of Rock Mechanics and Mining Science and Geomechanical Abstracts, 19:279–284.

Stille, H. G. Gustafson, V. Hakansson, and P. Olsson. 1992. Passage of water bearing fracture zones —experiences from grouting of the section I-1400 m of the tunnel. SKBPR 25-92-19, Swedish Nuclear Fuel and Waste Management Company, Stockholm.

Teufel, L., D. W. Rhett, and H. E. Farrell. 1991. Effect of Reservoir Depletion and pore pressure drawdown on in-situ stress and deformation in the Ekofisk Field, North Sea. Proceedings of the 32d U.S. Rock Mechanics Symposium. Rotterdam: A. A. Balkema.

Teufel, L. W. 1979. An experimental study of hydraulic fracture propagation in layered rock. Ph.D. thesis, Texas A&M University, College Station.

U.S. Bureau of Mines. 1989. In-situ leach mining. P. 107 in Proceedings: Bureau of Mines Technology Transfer Seminars. IC 9216, Pittsburgh, Pa.

Wall, J., A. Nur, and J. Dvorkin. 1991. A slug test method in reservoirs with pressure sensitive permeability. Pp. 95–105 in Proceedings of the 1991 Coalbed Methane Symposium, May 13-16, University of Alabama, Tuscaloosa.

Walsh, J. B. 1981. Effect of pore pressure and confining stress on fracture permeability. International Journal of Rock Mechanics and Mining Science and Geomechanics Abstracts, 18:429–435.

Wan, J., and J. L. Wilson. 1994a. Visualization of the role of the gas-water interface on the fate and transport of colloids in porous media. Water Resources Research, 30:11–23.

Wan, J., and J. L. Wilson. 1994b. Colloid transport in unsaturated porous media. Water Resources Research, 30:857–864.

Wan, J., J. L. Wilson, and T. L. Kieft. 1994. The effects of the gas-water interface on the fate and transport of microorganisms in unsaturated porous media. Applied and Environmental Microbiology, 60:509–516.

Wang, J. S. Y., C. F. Tsang, N. G. W. Cook, and P. A. Witherspoon. 1981. A study of regional temperature and thermohydrologic effects of an underground repository for nuclear wastes in hard rock. Journal of Geophysical Research, 86:3759–3770.

Warpinski, N. R. 1985. Measurement of width and pressure in a propagating hydraulic fracture. Society of Petroleum Engineers Journal, Feb., pp. 46–54.

Warpinski, N. R. 1991. Hydraulic fracturing in tight, fissured media. Journal of Petroleum Technology, Feb., p. 146.

Warpinski, N. R., and L. W. Teufel. 1987. Influence of geological discontinuities on hydraulic fracture propagation. Journal of Petroleum Technology, Feb., pp. 209–220.

Warpinski, N. R., Z. A. Moschovidia, C. D. Parker, and I. S. Abou-Sayed. 1994. Comparison study of hydraulic fracturing models—test case: GRI staged field experiment no. 3. SPE Production and Facilities, Feb., pp. 7–160.

Williams, D. B., et al. 1989. Impact of inducing fractures at Prudhoe Bay. Journal of Petroleum Technology, Oct., pp. 1096–1101.

Wittke, W. 1965. Verfahren zur Standsicherheitsberechnung starrer, auf ebenen Flächen gelagerter Körper und die Anwendung der Ergebnisse auf die Standsicherheitsberechhung von Felsböschungen, Heft 20. Karlsruhe: Veröffentlichungen des Institutes für Bodenmechanik und Grundbauder Technischen Hochschule Fridericiana.

NOTES

l Other aggregates or fillers can be fly ash, diatomaceous earth, rock flour, sawdust, and gravel.

2 Single-phase injection of silicate solutions containing a gelation retarder is used in several patented processes. Two-phase injection of silicate solutions is the well-known Joosten process, and two-phase injection of a silicate solution followed by an alurninum sulfate solution is the Francois process. The reader is referred to Cambefort (1964) for detailed descriptions of these processes.

3 Note that the term multiple staging has nothing to do with upward or downward staging.

8

Case Histories

The heterogeneity and complexity of flow paths in fractured rocks make field studies very difficult. As a result, there are relatively few field study sites where the distribution and character of fractured rocks have been described in detail. These sites are an extremely valuable scientific resource for a number of reasons. First, field testing and verification of various fracture characterization methods and data analysis techniques require sites where these methods can be developed, applied, and evaluated. Case history studies from such well-documented field sites are useful for demonstrating the application of specific techniques. These studies illustrate how different fracture characterization techniques can be applied to radioactive waste repository siting or water resource development, for example. The careful and thorough documentation of fractures, geomechanical properties of fractured rocks at various scales, and the patterns of tracer dispersal through fractures provide insights into how large-scale geological structure and tectonic history relate to the details of fracture properties and fracture distribution as identified in boreholes, core samples, and outcrops.

A list of some of the better-documented sites where fractured rocks have been studied is provided in Table 8.1. The table lists the locations of the sites, the rock types involved, the depths of investigation, and the primary applications for which the studies were intended. The table does not describe all sites in existence but does provide a representative sample of sites where work has been carried out, and it gives a reasonably complete series of examples of the various fracture characterization techniques that can be applied in the field. The application supporting the majority of the long-term, large-scale fracture studies is high-level radioactive waste repository siting in North American and Europe. Most of

TABLE 8.1 Summary of Fracture Study Sites

Site	Location	Rock Type	Application	Maximum Depth (m)	Reference
Underground Research Laboratory	Southeast Manitoba, Canada	Granite	Radioactive waste disposal	500	Martin (1990); Everitt et al. (1990); Paillet (1991)
Mirror Lake	White Mountains, New Hampshire	Schist	Contaminant transport	200	Shapiro and Hsieh (1994); Paillet and Kapucu (1989); Morganwalp and Aronson (1994)
Hanford	Columbia River Plateau, Central Washington	Basalt	Radioactive waste disposal	1,000	Kim and McCabe (1984); Paillet and Kim (1987)
Oracle	Santa Catalina Mountains, South-Central Arizona	Granite	Radioactive waste disposal	100	Hsieh et al. (1983)
University of Waterloo	Clarkson, Ontario, Canada	Dolomitic shale	Contaminant transport	20	Paillet et al. (1992)
Stripa	Sweden	Granite	Radioactive waste disposal	1,000	Olsson (1992); Nelson et al. (1982)
Grimsel	Crystalline Alps, Switzerland	Granite	Radioactive waste disposal	1,000	Martel and Peterson (1991)
Red Gate Woods	Argonne, Northeast Illinois	Dolomite	Contaminant dispersal	100	Robinson et al. (1993); Nicholas and Healy (1988); Silliman and Robinson (1989)
Fenton Hill	North-Central New Mexico	Granite	Geothermal	1,000	Robinson and Tester (1984); Fehler (1989); Block et al. (1994)

Site	Location	Rock Type	Application	Maximum Depth (m)	Reference
Antrim Shale	Eastern Michigan	Shale	Natural gas resources development	300	Turpening (1984)
Multiwell Experiment	Northwest Colorado	Siltstone	Natural gas resources development	2,000	Lorenz and Finley (1991); Lorenz et al. (1989)
Nevada Test Site	Southwest Nevada	Tuff	Radioactive waste disposal	1,000	Geldon (1993); Nelson (1993)
The Geysers Field	North-Central California	Metamorphic	Geothermal	3,000	Geothermal Resources; Council (1992); Oppenheimer (1986)
Finnsjön	Sweden	Granite	Radioactive waste disposal	500	Andersson et al. (1991); Gustaffson and Andersson (1991)
East Bull Lake	South-Central Ontario, Canada	Gabbro	Radioactive waste disposal	500	Paillet and Hess (1986); Kamineni et al. (1987); Ticknor et al. (1989)
Aitkokan	Southwest Ontario	Granite	Radioactive waste disposal	1,000	Paillet and Hess (1987); Stone and Kamineni (1982); Kamineni and Bonardi (1983)
Niagara Falls	Northwest New York	Dolomite	Contaminant dispersal	200	Yager (1993)
Pierre Shale	Central South Dakota	Shale	Waste disposal	100	Bredehoeft et al. (1983); Neuzil (1993)
Travis Peak	Southeast Texas	Sandstone	Gas production	3,000	Laubach (1988); Laubach et al. (1988)
Waste Isolation Pilot Project	Southeastern New Mexico	Dolomite and anhydrite	Radioactive waste disposal	1,000	Davies et al. (1991); Beauheim (1988)

Site	Location	Rock Type	Application	Maximum Depth (m)	Reference
Apache Leap	Central Arizona	Tuff	Radioactive waste disposal	800	Basset et al. (1994, 1996)
Wake/Chatham	Central North Carolina	Sandstone and shale	Radioactive waste disposal	120	Chem-Nuclear Systems (1993)
Sellafield	Northwestern Coast of England	Basalt and sediments	Radioactive waste disposal	2,000	Michie (1992)

these studies deal with crystalline rocks. The sites listed in Table 8.1 are too numerous to be described in detail in this report. Each entry is associated with one or two key references to provide the most efficient introduction to the literature. A few representative sites are discussed in detail in the following sections.

CASE HISTORY I. U.S. GEOLOGICAL SURVEY FRACTURED ROCK RESEARCH SITE NEAR MIRROR LAKE, NEW HAMPSHIRE

The U.S. Geological Survey is conducting research on fluid flow and solute transport in fractured rock at a site near Mirror Lake in central New Hampshire (Winter, 1984; Shapiro and Hsieh, 1991). Started in 1990, this study aims to (1) develop and assess field methods for characterizing fluid flow and solute transport in fractured rocks; (2) develop a multidisciplinary approach that uses geological, geophysical, geochemical, and hydrological information for data interpretation and model building; and (3) establish a site for long-term monitoring. The discussion below summarizes the preliminary results of this ongoing study. Additional information can be found in an overview paper by Shapiro and Hsieh (1995) and in a series of papers edited by Morganwalp and Aronson (1995).

Mirror Lake lies at the lower end of the Hubbard Brook valley in the southern White Mountains of New Hampshire. The surface area that drains into Mirror Lake occupies 0.85 km^2 of mountainous terrain, which varies in altitude from 213 m at the lakes surface to 481 m at the top of the drainage divide. The bedrock is a sillimanite-grade schist extensively intruded by granite, pegmatite, and lesser amounts of lamprophyre. It is covered by 0 to 55 m of glacial drift. Outcrops are few; the largest exposure of bedrock occurs where a highway cuts through a small hill. Here, four subvertical surfaces, exposed by road construction, and one subhorizontal surface, cleared by glaciation, provide approximately 8,000 m^2 of exposed rock for mapping and studying fractures and geology. The roadcut shows a complex distribution of rock types. The schist is multiply folded. The granitic intrusions occur as dikes, irregular pods, and anastomosing fingers, ranging in width from centimeters to meters. Pegmatite and basalt dikes cross-cut both the schist and granite.

Investigations at the Mirror Lake site are proceeding at two scales: the 100-m scale and the kilometer scale. The 100-m-scale investigations focus on several subregions, each occupying an area of approximately 100 × 100 m. The goal is to characterize in detail the fracture geometry and the hydraulic and transport properties to a depth of about 80 m. The kilometer-scale investigations cover approximately 1 km^2 (Figure 8.1), including the entire surface area that drains into Mirror Lake. The site investigations are proceeding outward from the vicinity of the lake in a systematic fashion, and some of the most recently drilled bedrock boreholes are located in areas beyond the actual surface watershed. The goal is to characterize the large-scale movement of groundwater to a depth of about 250 m.

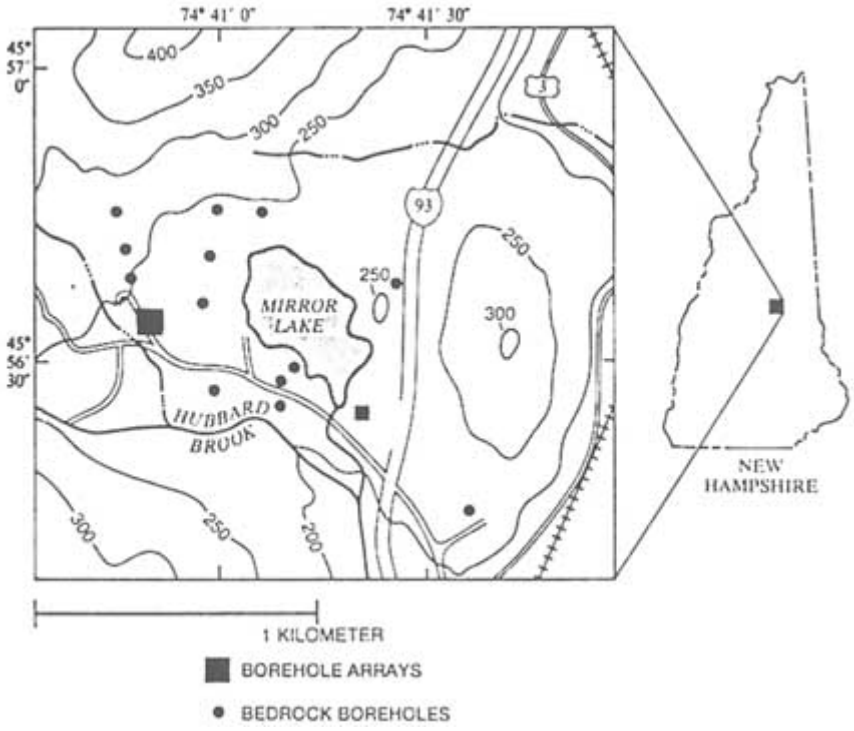

FIGURE 8.1 The Mirror Lake, New Hampshire, study area, showing the location of individual bedrock well and the two well fields. The larger of the two squares represents the FSE borehole array, and the smaller represents the CO array. From Paillet and Kapucu (1989).

100-m-Scale Investigation

The 100-m-scale investigations use many of the tools described in Chapter 2 (fracture mapping), Chapter 4 (fracture detection by geophysical methods), and Chapter 5 (hydraulic and tracer tests). Surficial mapping of fractures is carried out at the highway roadcut. For subsurface investigations, two well fields (Forest Service East, or FSE, and Camp Osceloa, or CO) have been established (Figure 8.1). In the following discussion of characterization techniques used at the Mirror Lake site, the reader can find a detailed description of the fracture mapping, geophysical method, and hydraulic tracer test methods in Chapters 2, 4, and 5.

At the highway roadcut, fractures were mapped by the "pavement method" developed by Barton and Larson (1985) and described by Barton and Hsieh (1989). This method consists of (1) making a detailed map of the fractures on an exposed rock surface (pavement); (2) measuring the orientation, surface roughness, aperture, mineralization, and trace length of each fracture; and

(3) measuring the connectivity, density, and scaling characteristics of the fracture network. Results suggest a correlation between fracturing and rock type. The granite is more densely fractured with shorter and more planar fractures. The schist has fewer and less planar fractures. Connectivity of the fracture network at Mirror Lake is low compared to fractures mapped in volcanic tuff, quartz diorite, limestone, and sandstone at other sites. The low connectivity at the Mirror Lake site suggests that fluid moves through highly tortuous paths in the bedrock.

In a 100 × 100 m area adjacent to the CO well field, directional soundings using direct current electricity and refracted seismic waves were carried out to determine the predominant strikes of near-vertical fractures in the bedrock, which underlies 3 to 10 m of glacial drift. Analyses yield predominant strikes of N 30° E from the electrical sounding and N 22° E from the seismic survey. These orientations agree closely with the predominant strike of 30° determined from fractures mapped at the highway roadcut. The agreement suggests that, where overburden is thin (e.g., less than 10 m), directional sounding can be an effective method for determining the predominant strikes of near-vertical fractures.

At the FSE well field west of Mirror Lake, 13 wells were drilled in a 120 × 80 m area (Figure 8.2). Drill cuttings and downhole video camera images show that the wells penetrate varying thicknesses of schist, granite, and pegmatite but that there is little to no apparent correlation in the distribution of rock types in neighboring wells. Borehole televiewer logs show that, between depths of 20 m (bedrock surface) and 80 m, each well intersects 20 to 60 fractures. With a few exceptions, these fractures do not project from one well to another (Hardin et al., 1987; Paillet, 1993). In each well, water-producing fractures were determined by single-borehole flowmeter surveys and single-borehole packer tests. The results show that one to three fractures in each well together produce more than 90 percent of the water when the well is pumped. The remaining fractures are less transmissive by two to five orders of magnitude. These findings suggest that bedrock underlying the FSE well field contains a small number of highly transmissive fractures within a larger network of less transmissive fractures.

The geometry and interconnectivity of the highly transmissive fractures were examined by cross-hole flowmeter survey (pumping one well and measuring vertical velocity in an observation well), vertical seismic profiling, seismic and electromagnetic tomography, multiple-borehole hydraulic tests, and converging-flow tracer tests. These field data are still under analysis, but a conceptual picture of the fracture network is emerging. The highly transmissive fractures appear to form local clusters; each fracture cluster occupies a near-horizontal, tabular-shaped volume several meters thick and extends laterally a distance of 10 to 40 meters. These clusters are connected to each other via a network of less transmissive fractures. Figure 8.3 illustrates the inferred locations of four highly transmissive fracture clusters, marked A through D, in the vertical section between wells FSE1 and FSE6.

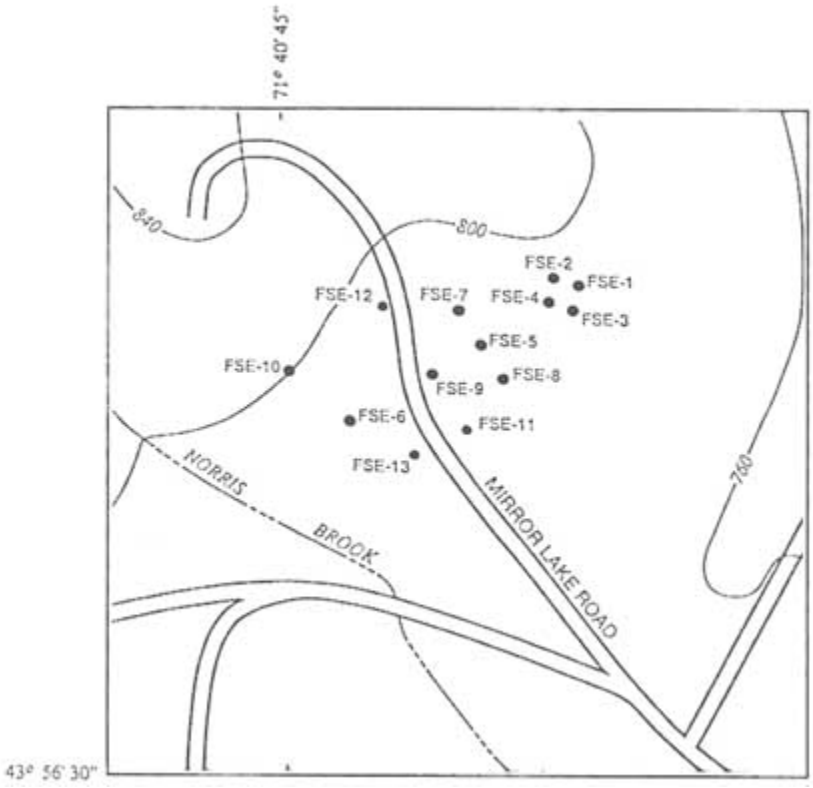

FIGURE 8.2 Locations of the 13 boreholes in the Forest Service East (FSE) well field at the Mirror Lake site. See Figure 8.1 for location of the FSE well field in the Mirror Lake area. From Hsieh and Shapiro (1994).

Preliminary analyses of the geophysical tomography results suggest that these techniques are extremely valuable for tracing the high-transmissivity zones between wells. For example, in the vertical section between wells FSE1 and FSE4 (14 m apart), fracture cluster B was detected by seismic and electromagnetic tomography and also by vertical seismic profiling. The low-velocity region in the electromagnetic tomogram (Figure 8.4) agrees closely with the highly transmissive fractures identified by flowmeter survey and hydraulic testing. At greater separation distances between wells, however, the tomogram becomes more fuzzy, owing to decreasing signal strength at the receivers. There are also instances in which a low-velocity zone in a tomogram does not correlate with a high-transmissivity fracture zone, possibly because of heterogeneities in rock properties. Therefore, hydraulic tests are needed to interpret the tomography results. Difference tomography (comparing tomographs made before and after injecting

electrically conductive fluid into a fracture zone; Andersson et al., 1989) could also help in resolving ambiguities.

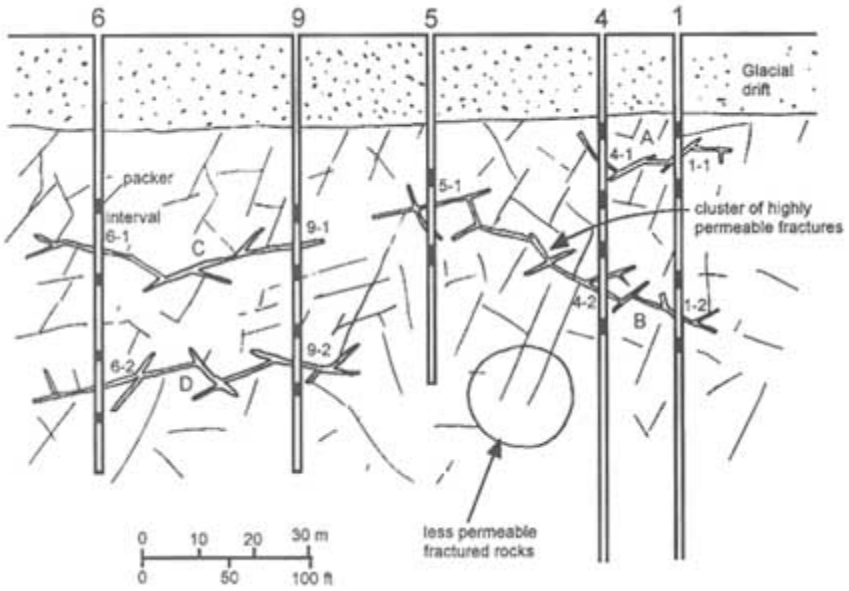

FIGURE 8.3 Vertical cross section between wells FSE1 and FSE6 at the Forest Service East well field. Four clusters of highly permeable fractures labeled A, B, C, and D occur in the less permeable fractured rocks. Borehole packers are shown in black. Modified from Shapiro and Hsieh (1994).

The highly transmissive fracture clusters in the FSE well field exert a strong influence on multiple-borehole hydraulic tests. To prevent hydraulic communication through the wells, fracture clusters in each well are isolated from one another by packers, as illustrated by Figure 8.3. During pumping, the drawdown behavior is different from that in a homogeneous aquifer. If two packer-isolated intervals straddle the same fracture cluster, the drawdowns in the two intervals tend to be nearly identical. In contrast, if two packer-isolated intervals straddle different fracture clusters, the drawdowns are significantly different.

To analyze these tests, analytical methods are generally not suitable because they are based on oversimplified assumptions. Instead, a conventional porousmedium type numerical model is used to simulate the highly transmissive fracture clusters as high-permeability zones and the surrounding network of less transmissive fractures as low-permeability zones. Preliminary analyses yield transmissivities in the range of 10^{-5} to 10^{-4} m^2/s for the highly transmissive fracture clusters, and an equivalent hydraulic conductivity of about 10^{-7} m/s for the surrounding rock mass.

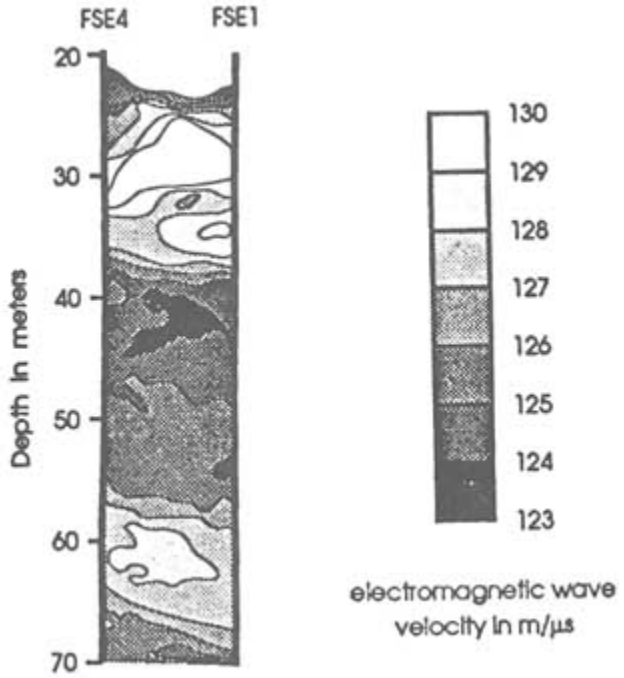

FIGURE 8.4 Electromagnetic velocity tomogram in vertical section between wells FSE1 and FSE4. From Hsieh et al. (1993).

Kilometer-Scale Investigations

Compared to the 100-m scale investigation, kilometer-scale investigations are less detailed for practical reasons. Drilling a dense network of wells (e.g., on a square grid of 50-m spacing) throughout the entire 1-km^2 study area is too expensive. In fact, such a dense network of wells might be undesirable. If left open, the wells could alter the natural flow of groundwater by connecting previously unconnected fractures. Another constraint on the kilometer-scale investigation is that many of the tools described in Chapters 4 and 5 provide information on small volumes of rock. Fracture detection methods (such as borehole logging and cross-hole tomography) are typically limited to less than 100 m of penetration. Hydraulic and tracer tests also are impractical. Response to pumping becomes undetectable beyond a few hundred meters from the pumping well, and tracer movement over a kilometer may take many years. Therefore, kilometer-scale investigations aim to characterize the large-scale flow of groundwater while neglecting small-scale details.

The kilometer-scale investigation monitors the response of the groundwater system to natural perturbations and long-term human disturbances. For example,

seasonal and long-term variations in infiltration to the groundwater system cause fluctuations in hydraulic heads. By monitoring the recharge and discharge of groundwater and the temporal and spatial variations in hydraulic head, it may be possible to infer hydraulic properties on the kilometer scale. Collection of groundwater samples for chemical analysis is another method for kilometer-scale investigations. Recent advances in the detection of human-made chemicals such as chlorofluorocarbons (used as refrigerants and aerosol propellants) and the parent-daughter isotopes tritium and helium-3 (produced from atmospheric testing of thermonuclear devices) have made it possible to determine the ages of shallow groundwaters (Busenberg and Plummer, 1992; Solomon et al., 1992). Knowledge of the spatial distribution of groundwater ages can help identify flow paths. As groundwater flows from recharge to discharge areas, its chemical composition evolves as the water reacts with the rock. Understanding this chemical evolution can help determine groundwater velocity.

Hydrological monitoring in the study area includes precipitation measurements at two locations, streamflow and lake discharge measurements using flumes, various meteorological measurements for evaporation calculations, and the construction of 14 well sites for hydraulic head monitoring and groundwater sampling. Each site consists of a well drilled into bedrock with packers and piezometers installed at different depths. Multiple packers are installed in the bedrock portions of the wells to allow hydraulic head measurements at different depths. The packers also prevent hydraulic communication between fractures through the wellbore. Over 30 piezometers, screened at the water table, are installed throughout the study area to monitor the position of the water table in the glacial drift.

Hydrological properties on the kilometer scale are inferred from modeling studies. As a base case, the bedrock and glacial drift are each represented as a layer of porous medium. Each layer has a homogeneous and isotropic hydraulic conductivity. Calibration of this model to match observed hydraulic heads and stream discharges yields a bedrock hydraulic conductivity of 4×10^{-7} m/s. This value is close to the average hydraulic conductivity of 3×10^{-7} m/s determined from over 100 single-borehole packer tests conducted at the 14 well sites. The near agreement suggests that, at the Mirror Lake site, large-scale hydraulic conductivity can be inferred from a statistical average of many small-scale measurements.

The chlorofluorocarbon and tritium-helium-3 methods were used to determine the ages of water samples collected from packer-isolated intervals in bedrock wells and from a select number of piezometers in the glacial drift. For this purpose, groundwater age is defined as the time between water infiltration into the saturated groundwater system and water collection for analysis. Both methods yield similar ages. Most of the samples are less than 45 years old. However, the spatial distribution of groundwater ages suggests that flow paths are highly complex. Figure 8.5 shows the distribution of groundwater ages in a vertical section on a hillslope through wells R1, TR2, and T1. If the land has a uniform

slope and the subsurface has a uniform hydraulic conductivity, the flow lines should be similar to those illustrated in Figure 8.6. In the vertical direction, ages should increase with depth. Along any flow line, groundwater should be younger near the recharge area (at higher elevations) and older near the discharge area (at lower elevations). In contrast, the observed age distribution in Figure 8.5 is more complex. Younger water is found at several deeper locations and close to

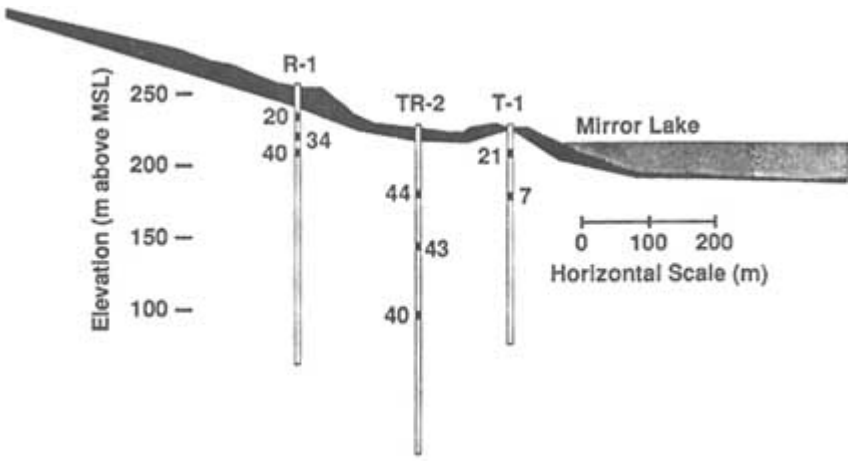

FIGURE 8.5 Groundwater ages (in years) determined from CFC-12 concentrations at the Mirror Lake study site. From Shapiro and Hsieh (1994).

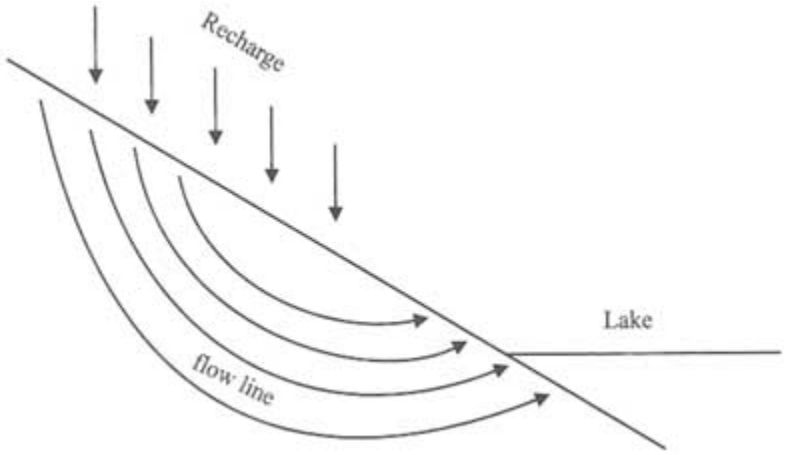

FIGURE 8.6 Expected flow lines for the cross section shown in Figure 8.5, assuming a uniform hillslope and uniform hydraulic conductivity.

an anticipated discharge area. These findings suggest that hillslope topography and bedrock heterogeneity at this site strongly influence groundwater flow paths.

Groundwater samples were also analyzed for major ions, dissolved gases, and a variety of stable and radioactive isotopes. An interesting finding from these analyses is an apparent correlation between alkalinity and groundwater age. Figure 8.7 shows that alkalinity appears to increase with age. That is, water in the glacial till is younger and has a lower alkalinity, whereas water in the bedrock is older and has a higher alkalinity. The higher alkalinity of bedrock water is almost entirely due to the presence of bicarbonate ions (HCO_3^-). Carbon isotope analyses suggest that bicarbonate ions are derived from the dissolution of carbonate minerals such as calcite. However, there is no evidence of calcite on fracture surfaces. Instead, samples of granite from outcrops and cores were found to contain small amounts (approximately one weight percent) of calcite in the rock matrix. This finding suggests that calcite dissolution occurs inside the rock matrix, releasing bicarbonate ions. The bicarbonate ions diffuse from the rock matrix into the fractures, causing an increase in groundwater alkalinity. Because older groundwater has been flowing through fractures for a longer time, it should be higher in alkalinity. This relationship should hold until the alkalinity reaches equilibrium with respect to calcite in the groundwater.

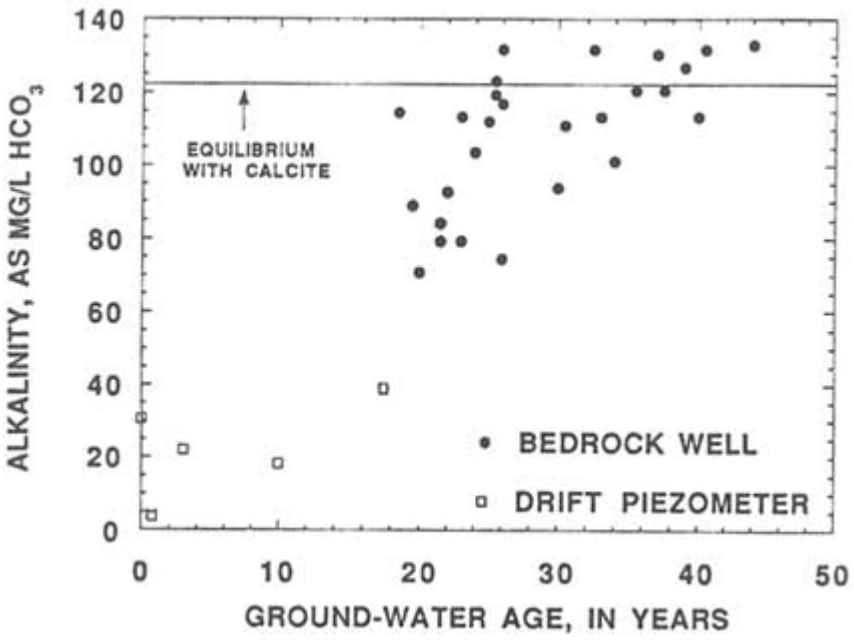

FIGURE 8.7 Plot of groundwater age versus alkalinity of groundwater samples from the Mirror Lake site. From Shapiro and Hsieh (1994).

The importance of matrix diffusion in the evolution of groundwater chemistry is supported by laboratory measurements of rock porosity and diffusion coefficients. Porosities of 32 intact granite samples average 1.5 percent. To measure diffusion in the matrix, a granite sample was soaked in a solution of cesium-137. After 101 days, the cesium-137 was found to have penetrated the granite to a depth of approximately 7 mm. This suggests that over tens of years matrix diffusion is an important mechanism for chemical transport between a fracture and the rock matrix. The calculated effective diffusion coefficient for cesium-137 in the granite matrix is approximately 6×10^{-13} m^2/s.

To explore the relationships between alkalinity, groundwater age, and groundwater velocity, a simple model was developed to simulate bicarbonate transport. In the model a flow path in the bedrock is represented by a fracture bounded by intact rock. Groundwater enters the fracture with low alkalinity, characteristic of water in the glacial drift. As the water moves along the fracture, its alkalinity increases because of the incoming flux of bicarbonate ions from the rock matrix (Figure 8.8). The relationship between alkalinity and age is controlled by dissolution of calcite and diffusion of bicarbonate ions in the matrix and the velocity of groundwater in the fracture. Assuming the diffusion coefficient is known from laboratory measurements, the groundwater velocity can be estimated by adjusting its value until the modeled bicarbonate concentration and groundwater age match the measured values for groundwater samples (Figure 8.7). Based on this approach, preliminary analysis suggests that groundwater velocities in the bedrock vary between 10^{-3} and 10^{-2} m/day.

Discussion

Research at the Mirror Lake site clearly demonstrates the need for an interdisciplinary approach to fractured rock characterization. At the same time, multiple

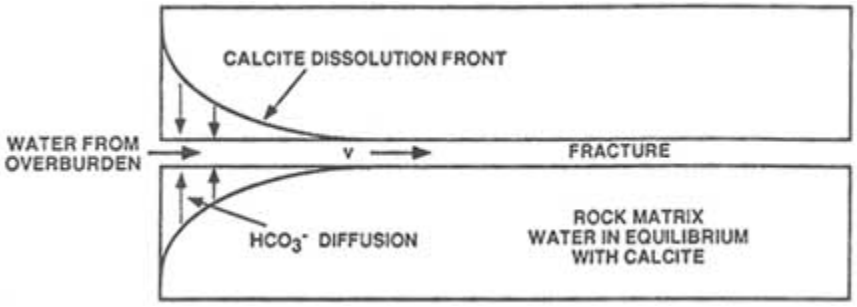

FIGURE 8.8 Schematic illustration of a simple flow model used to estimate fluid velocities at the Mirror Lake site. The flow path is from left to right in the fracture. Bicarbonate (HCO3/-) ions diffuse into the fracture from the surrounding rock matrix. From Shapiro and Hsieh (1994).

investigation efforts must be coordinated. Detailed studies on the 100-m scale may require the explicit identification and characterization of major (highly transmissive) fractures. Combining fracture detection methods with hydraulic and tracer testing yields a promising approach to accomplishing this objective. Knowledge gained from fracture mapping provides a sound basis for making inferences and for data interpretation. For kilometer-scale investigations, long-term monitoring, groundwater age dating, and geochemical analyses are useful and deserve greater exploitation. The identification of flow paths through a heterogeneous rock environment remains a challenge.

CASE HISTORY II. THE SITE CHARACTERIZATION AND VALIDATION PROJECT: STRIPA MINE, SWEDEN

The Site Characterization and Validation (SCV) Project was performed as a part of the Organization for Economic Cooperation and Development/Nuclear Energy Association's International Stripa Project from 1986 to 1992. The objectives of the project were to test the predictive capabilities of newly developed radar and seismic characterization methods and numerical groundwater models. A basic experiment was designed to predict the distribution of water flow and tracer transport through a volume of granitic rock before and after excavation of a subhorizontal drift (the validation drift) and to compare these predictions with actual field measurements.

A multidisciplinary characterization program was implemented at the SCV site. Because the site was located several hundred meters below the ground surface, all investigations were performed from drifts and boreholes drilled from drifts. The dimensions of the investigated volume were approximately $150 \times 150 \times 50$ m.

The fractures in the drifts adjacent to the SCV site were mapped along scanlines. Maps of the drift walls were made in selected locations. Detailed maps were also made to study the variability in fracturing in fracture zones intersected by several drifts. All boreholes were mapped and oriented by identifying reference fractures from TV logging. The fracture mapping program provided data on fracture orientations, trace lengths, termination modes, and spacing.

Cross-hole and single-hole radar measurements were made to determine the orientation and extent of fracture zones at the site. The directional borehole radar system developed for the project proved particularly useful because it provided data on the orientation of fracture zones based on measurements in a single borehole (see Chapter 4). Radar difference tomography also was used to show how saline tracer injected in a borehole became distributed in the rock mass as it traversed three survey planes.

Seismic techniques were used successfully to determine the orientation and extent of fracture zones. The seismic program included both cross-hole reflection and tomography measurements. The reflection measurements provided the best

data for characterization of the fracture zones. The success of the seismic method was largely due to the application of the Image Space Transform, a novel processing technique developed for the project (Cosma et al., 1991).

To obtain in situ data on the physical properties of the rock in the vicinity of the boreholes, the following logs were run: borehole deviation, sonic velocity, single-point resistance, normal resistivity, caliper, temperature, borehole fluid conductivity, natural gamma radiation, and neutron porosity. The sonic velocity, single-point resistance, and normal resistivity were found to be useful in identifying fractures and fracture zones.

Initially, single-borehole testing was done to provide data on transmissivity and head along the boreholes. Equipment was developed to ensure that reliable information could be collected in the mine environment in reasonable times. The system was built around a multiple-packer probe that allowed rapid testing of permeable features with high spatial resolution. Single-borehole testing was followed by cross-hole testing to define hydraulic properties of the fracture zones on the scale of the site (» 100 m). An important aspect of the cross-hole testing was that it provided a check on the hydraulic properties of the fracture zones identified by using other geophysical techniques. The hydraulic program also included monitoring of head in more than 50 locations across the site. This monitoring provided data on the hydraulic responses to various activities in the mine that could be used to characterize hydraulic connections across the site.

Groundwater samples were taken during hydraulic testing and analyzed for major constituents. The analysis showed that there were three types of groundwater present. These were classified as shallow, mixed, and deep. The groundwater was also found to contain about 3 percent of dissolved gas by volume (at standard temperature and pressure), mainly nitrogen.

An important aspect of groundwater flow through fractures is the effect of stress on fracture transmissivity. Flow through fractures under different stress loads was studied on several samples and in one in situ test. This yielded stress-permeability relationships that were used for modeling studies. Measurements were made, using the overcoring method with a tool called the CSRIO Hollow Inclusion Cell, to determine in situ stresses. At the level of the validation drift, the maximum principal stress was oriented parallel to the drift (i.e., NNW-SSE). It is interesting to note that almost all of the water inflow to the drift was through a single fracture perpendicular to the maximum principal stress.

Characterization of the SCV site was made in several stages. Initial data collection was followed by data interpretation and predictive modeling. Additional boreholes were then drilled to check the predictions based on the initial data set. These new data were then used to refine the conceptual model of the site and groundwater flow predictions. Finally, the predictions were checked by a series of dedicated experiments.

To provide for an adequate description of groundwater flow through the site, the key issue for the characterization work was to identify important flow paths.

In fractured rock environments, fracture zones are normally identified as important permeable hydraulic units; this was the working assumption at the onset of the SCV Project. However, the locations, widths, and extents of fracture zones are commonly defined by expert judgment. This can, in many cases, impose a number of problems, as the opinions of experts may vary, and the facts behind a given opinion may be obscure or poorly documented.

An attempt to circumvent this problem and to arrive at a more objective definition of what constitutes a fracture zone was made during the project (Olsson, 1992). A fracture zone index was defined in order to address the following issues:

- Is a binary division of the rock mass into "fracture zones" and "average-fractured rock" appropriate?
- Is there an objective method of identifying a fracture zone, and can it be used to define the boundaries of a zone?
- Is the arrived-at procedure for fracture zone identifications appropriate for a hydraulic description of the site?

For characterization of a rock volume deep below the ground surface, it is common to base a binary representation of the rock mass on physical properties measured in the vicinity of the boreholes. Hence, the location and width of "fracture zones" can be defined where they intersect boreholes. The extent and geometry of the zones at larger distances from the boreholes can then be probed by using remote sensing methods.

A subset of the data, including normal resistivity, sonic velocity, hydraulic conductivity, coated (and presumably open) fractures, and single-hole radar reflections, was selected for identification of the fracture zones using principal component analysis. First, logarithms were taken of the normal resistivity, sonic velocity, and hydraulic conductivity data. The data were then normalized by subtracting the mean value and dividing by the standard deviation for each parameter. A matrix of correlation coefficients was formed, and the eigenvectors were found for that matrix. Each eigenvector represents a weighting of the data, and new parameters (principal components) were produced by multiplying an eigenvector by the normalized data values. The parameter associated with the largest eigenvalue should represent the most important characteristic of the rock.

For the SCV site the parameter associated with the largest eigenvalue was expected to represent fracturing of the rock. This parameter is referred to as the fracture zone index (FZI). There is essentially only one rock type at the site. Consequently, all observed anomalies in rock properties are caused by fracturing or faulting.

The usefulness of a binary representation of the rock mass can be determined from the frequency distribution of the FZI. Based on the skewed frequency

distribution of the FZI (Figure 8.9), it is justifiable to use a binary description of the rock mass, where average-fractured rock is represented by FZI less than 2 and fracture zones are represented by FZI greater than 2. Using this index, the points in the boreholes that were considered to represent the occurrence of fracture zones could be defined.

The FZI compresses the information from single-hole investigations into a single parameter that describes the most significant properties of the rock (see Figure 8.10). It simplifies interpretation because it allows a single parameter to be used for identification of the anomalous sections in boreholes. Because FZI has been obtained through a quantitative and well-defined procedure, it provides an objective means of classifying the rock into the two classes, averagely fractured rock and fracture zones.

The FZI is also considered to be better for identifying hydraulically significant features than single-hole hydraulic conductivity data alone. The basic reason is that single-hole hydraulic tests yield parameters that are applicable only in a very small volume surrounding the borehole. In the fractured rock at Stripa, hydraulic properties vary by more than an order of magnitude over small distances. Hence, a weighted parameter that incorporates several types of data should be less

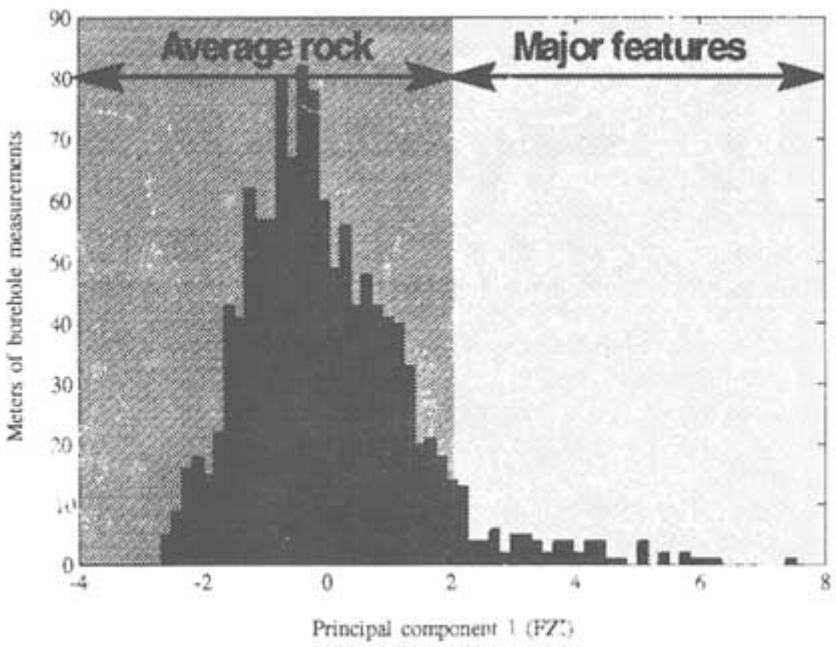

FIGURE 8.9 Frequency distribution of FZI (principal component 1). Values for the tail of the distribution (FZI > 2) are designated as "fracture zones," while values less than 2 are designated as "average rock." From Olsson (1992).

sensitive to small-scale variations in the rock mass and better for defining the hydraulically important features. In the definition of the FZI, hydraulic conductivity is included as just one of several measurements, and the weighting is determined by the data set itself.

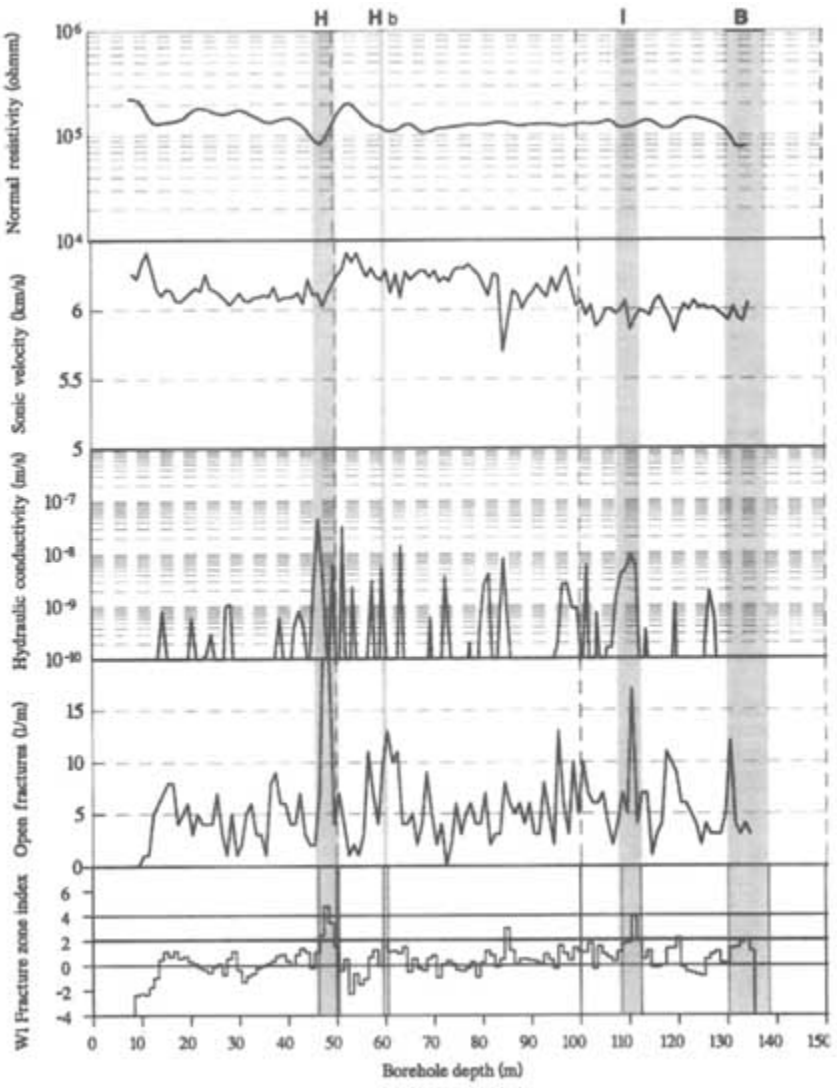

FIGURE 8.10 Composite log of the FZI and the single-hole logs used to construct it. The letters at top (H_1, H_b, I, and B) indicate major zones correlated between the boreholes. From Olsson (1992).

Based on this concept of a binary representation of the rock mass, a procedure was defined for constructing a conceptual model of the site. The procedure is based on identification of fracture zone locations in the boreholes using the FZI and finding the extent of the zones through the use of remote sensing techniques (i.e., radar and seismic techniques). The hydrogeological significance of the geometric model thus obtained was then determined by cross-hole hydraulic testing, which also yielded data on the hydraulic properties of the zones. Further checking of the consistency of the conceptual model was made by comparison with geological and geochemical data. This procedure is iterative and produces lists of identified features, as well as lists of inconsistencies and unexplained anomalies. The procedure is outlined graphically in Figure 8.11.

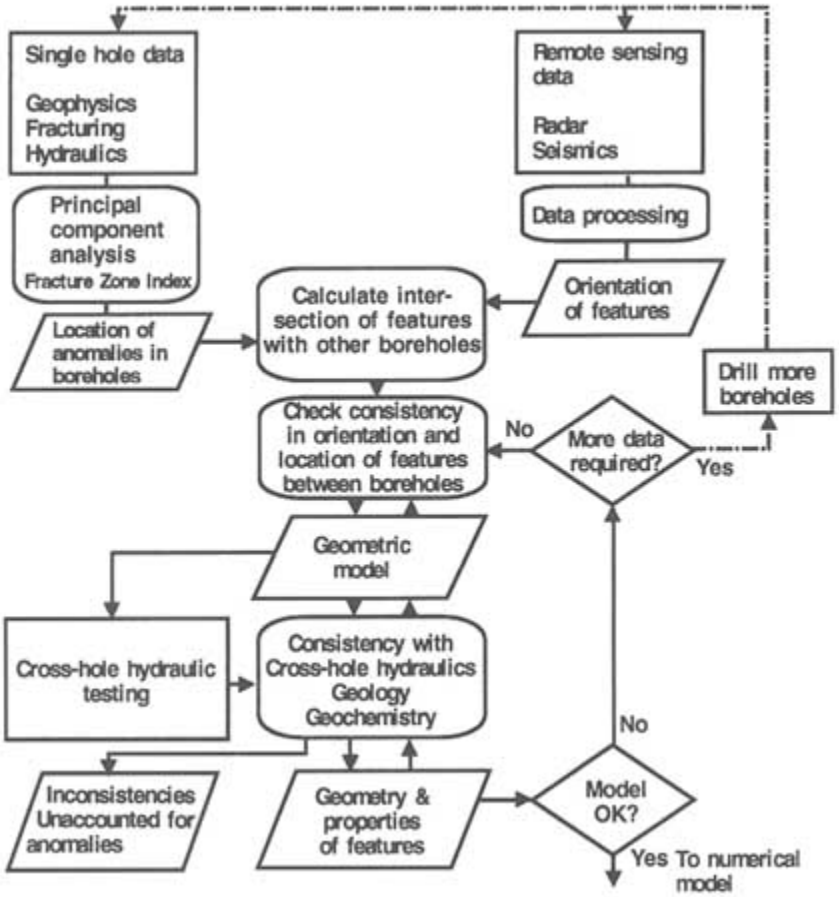

FIGURE 8.11 Outline of procedure used for construction of the conceptual model of the SCV site. From Olsson (1992).

The conceptual model for the SCV site was found to be consistent with field and test data. Major hydraulic responses were confined to the identified fracture zones, and there were few anomalies in the data that could not be explained. At the site, 80 to 90 percent of the flow was through these fracture zones, as evidenced both by single-hole and cross-hole hydraulic tests. Flow in the fractured rock was dominated by a small fraction of the identified features. Flow in the fracture zones was concentrated in one or two fractures in the zones, and the transmissivity distribution in these fractures was heterogeneous. The hydraulic transmissivity in the fracture zones varied by one to two orders of magnitude over a distance of a meter. Of the fractures in the averagely fractured rock, only a few were found to be transmissive.

Much effort went toward on numerical modeling of groundwater flow and solute transport at the site. Several different models were used. Most included stochastic representations of the permeable features in the rock mass. The conceptual model described above, which provides a deterministic representation of major flow paths, cannot adequately represent the heterogeneity of flow through a fractured rock mass. To achieve more realistic descriptions of the flow system, discrete fracture models were developed and tested. However, to achieve reasonable agreement between predicted and observed flow distributions, it was necessary to include the fracture zones explicitly in the stochastic fracture models.

The SCV Project demonstrated that fracture zones are the dominant groundwater pathways at Stripa and suggested that this may be a common situation in fractured crystalline rock. This finding is consistent with investigations at many other sites in crystalline rock. Work at this site also demonstrated that fracture zones need to be included explicitly in groundwater flow and transport models in crystalline rock. In the SCV Project, procedures were outlined for a quantitative and objective definition of fracture zones. The project demonstrated the capability of radar and seismic techniques to correctly describe the geometry of these zones. It is also evident that the application of these techniques is a prerequisite for constructing a reliable conceptual model for a site. Cross-hole tests should be used to verify the hydraulic significance of geophysically identified fracture zones and to quantify their hydraulic properties. The refined representation of flow heterogeneity requires stochastic modeling techniques. This project demonstrated that data required for stochastic modeling could be collected with a reasonable effort and that discrete fracture network models provide predictions of flow and transport that are in good agreement with observations.

CASE HISTORY III. HYDROCARBON PRODUCTION FROM FRACTURED SEDIMENTARY ROCKS: MULTIWELL EXPERIMENT SITE

The U.S. Department of Energy developed the Multiwell Experiment (MWX) site in order to perform detailed experiments on all aspects of low-permeability

natural gas reservoir evaluation, stimulation, and production (Spencer and Keighin, 1984; Finley and Lorenz, 1987; Lorenz and Finley, 1991). Natural and stimulated fractures are expected to be the primary source of production in these relatively "tight" formations. The MWX site is located in the Piceance Basin of Colorado, about 14 km west-southwest of the town of Rifle. The rocks of interest are primarily sandstones, siltstones, shales, mudstones, and coals of the upper Cretaceous Mesaverde group. At MWX, these strata occur at depths between 1,200 and 2,500 m. The reservoirs in the bottom 250 m of the section consist of marine strandplain sandstones (fossil beach sediments); the overlying rocks are deltaic and fluvial in origin.

The MWX site consists of three closely spaced wells (spacings of 30 to 67 m), from which over 1,200 m of core has been taken; about one-third of the core is oriented (Lorenz, 1990). Testing at the site consisted of detailed in situ stress measurements, single-well drawdown and buildup tests, multiwell interference tests, tracer injections, stimulation experiments, and poststimulation production tests. Detailed core analyses and multiple log runs also were performed. Subsequent to MWX, the Department of Energy conducted a follow-up test, named the Slant-Hole Completion Test (SHCT), with the objective of using directional drilling technology to intercept the natural fractures and enhance production. Several hundred feet of core provided additional valuable information about the natural fractures at this site. Primary information about the natural fractures has been derived from the abundant core at this site (Lorenz et al., 1989; Lorenz and Finley, 1991). Two basic types of fractures have been found at the MWX site: extensional fractures in the sandstone and siltstones and shear-type features in the mudstones and shales. Many of the shear-type fractures in the mudstones appear to be dewatering features or other planes of weakness that have accommodated some shear offset and thus display slickenlines. These fractures do not appear to be important for gas production.

The extensional fractures are part of a regional fracture pattern, with essentially all of the fractures being vertical and oriented about N 70° W. The extensional fractures, some of which are incompletely cemented, are the primary production sites from these tight sands; the matrix rocks have submicrodarcy permeability, and gas flow from the matrix is not economic. The degree of fracturing is highly depth dependent. There are one to two orders of magnitude more fractures present in core at depths of 1,675 to 1,890 m than from depths greater than 1,980 m. Televiewers were run in these wells to identify fractures, but the high mud weights required to control abnormal formation pressures made them useless for fracture identification. Formation microscanners and televiewers with variable-frequency and focused transducers were not available in the early 1980s when these wells were drilled and cased.

Extensive outcrops of correlative strata exist on the east and west sides of the Piceance Basin, and these have provided ancillary information on the fracture

systems. Figure 8.12 shows a plan view of fractures found in outcrop sandstone and the projection of those fractures into the subsurface, where they would be intersected by boreholes. Clearly, the small orthogonal fractures, which are not seen in core, are relief fractures. The predominant regional extensional fractures are unidirectional, subparallel, and poorly interconnected. Outcrops have also provided data on fracture spacing, length, and height, although these data are possibly affected by relief. The SHCT directional core, however, provides direct evidence of fracture spacings in the subsurface, yielding two populations of fractures, one widely spaced population (1.2 to 2.1 m) and a second population with a spacing of a few centimeters. Spacing is not related to bed thickness in any obvious way.

Field testing of the productive capacity of the fracture systems was performed in eight different intervals of the section (Lorenz, 1989). In the marine sandstones, single-well drawdown/buildup tests yielded permeabilities of 0.15 md and 400 md in two separate intervals. For comparison, in situ matrix permeabilities in

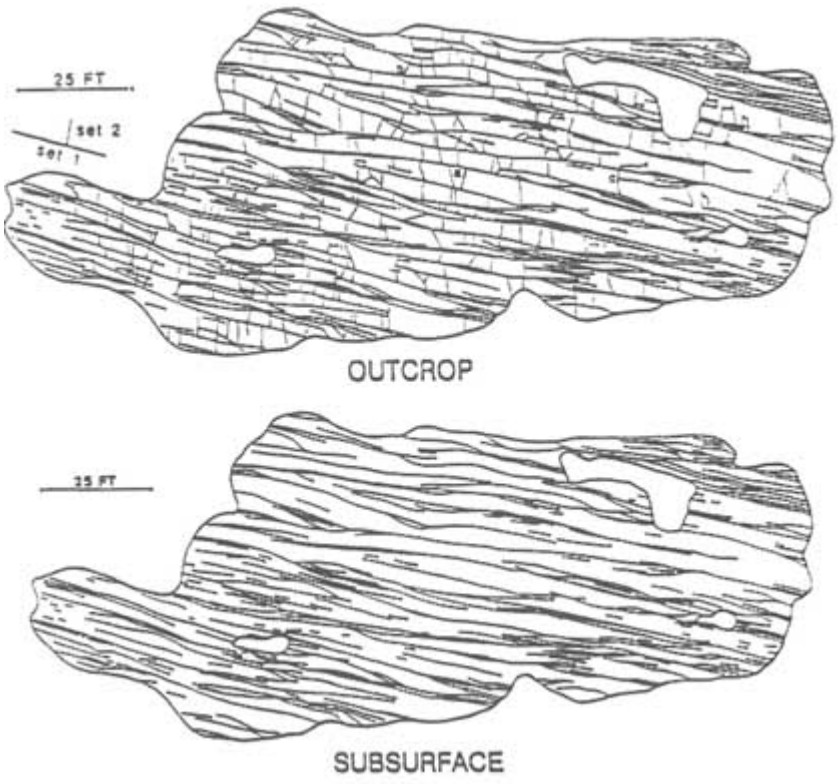

FIGURE 8.12 Plan view illustration of fractures from a sandstone outcrop at the Multi-well Experiment site. The subsurface view shows real data. From Lorenz and Finley (1991).

these zones were only about 0.2 μd. Interference tests showed that horizontal permeability anisotropies were on the order of 100:1 owing to the unidirectional nature of the fracture system. Production tests showed that the natural fracture systems are highly stress sensitive. By decreasing the reservoir pressure below a critical value (typically about 6.9 MPa at this site), the production from the well could be almost totally stopped because the decrease in pressure created higher effective confining stresses that physically closed the fractures.

In the fluvial/deltaic sandstones, tests were conducted in six different lenticular reservoirs. Single-well drawdown/buildup tests yielded system total permeabilities of 12 to 50 μd; matrix permeabilities measured in core were 0.1 to 2 μd. Figure 8.13 shows a comparison of system permeabilities for various intervals compared to rock matrix permeabilities. Interference tests were conducted in five nonmarine reservoirs, but interference was detected in only one. Tracer injections were conducted in two reservoirs, but only minimal amounts of the tracers were detected in the offset wells, and they were detected in an almost random pattern relative to the pump cycles. The interference patterns suggested permeability anisotropies of 30:1 to 50:1 for most of these reservoirs. Fracture systems in these reservoirs were also stress sensitive, and stimulation experiments showed that they were easily damaged by fracturing fluids. Studies of outcrops of these reservoirs showed that the fractures were limited by lithological variations in the sand bodies, resulting in compartmentalized fracture systems of limited extent, with minimal connections across compartments.

Laboratory experiments on plugs containing fractures were performed for several samples. Mudstone fractures (mostly unmineralized planes of weakness) showed a rapidly decreasing, irreversible loss in conductivity with increasing

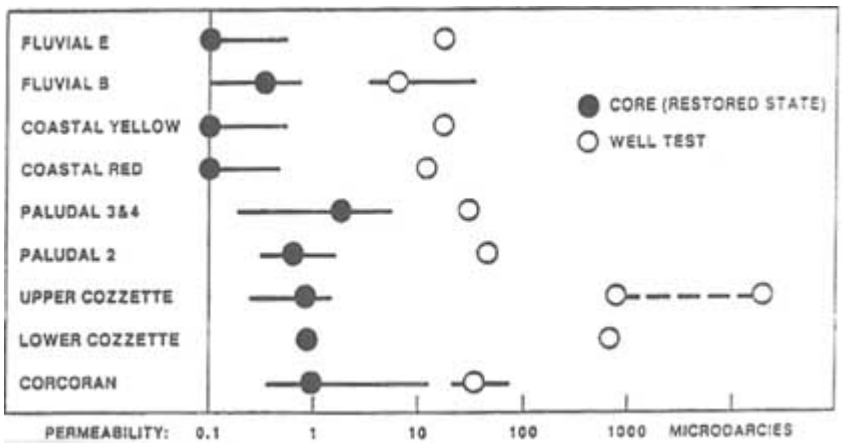

FIGURE 8.13 Comparison of system permeabilities to rock matrix permabilities from various intervals in the Multiwell Experiment site. Modified from Lorenz et al. (1989).

stress. Conductivities of fractures in sandstone were also sensitive to changes in stress, but conductivity loss was reversible. One sandstone fracture, however, showed no stress sensitivity whatsoever.

In summary, the natural fractures were found to be the gas production sites in tight sandstone reservoirs. The fractures are unidirectional, of limited extent, and stress sensitive. They are also easily damaged by drilling and completion fluids. Correlation of fracture data from core, outcrop, and various well tests was necessary to define the fracture system and its response to drilling, completion, and production activities.

CASE HISTORY IV. INVESTIGATING THE ANATOMY OF A LOW-DIPPING FRACTURE ZONE IN CRYSTALLINE ROCKS: UNDERGROUND RESEARCH LABORATORY, MANITOBA

In-depth studies of a single large-scale fracture zone are very rare in the literature, and there are relatively few such studies where the results show precisely how groundwater flow through individual fractures relates to the geometry and movement of a fracture zone. One of the most complete studies is the investigation of a fracture zone intersected by a shaft constructed at an Atomic Energy of Canada Limited (AECL) research site on the Canadian Shield. Investigations pertaining to the safety and feasibility of the concept of spent nuclear fuel disposal in plutonic rocks are being conducted at this site at AECL's Underground Research Laboratory (URL). The main working levels of the URL are at depths of 240 and 420 m (240 and 420 levels) with shaft stations at 130 and 300 m (Figure 8.14). Access to the 240-m level is provided by a 2.8 × 4.9 m timber-framed shaft and to the 420-m level by a 4.6-m-diameter circular shaft. Bored (1.83-m-diameter) raises between the surface and the 240 level and between the 240 and 420 levels provide ventilation and alternative access. This section discusses the results obtained from the intensive study of a fracture zone intersected by the URL shaft at about 250 m in depth.

The URL is excavated in the Archean granite of the Lac Du Bonnet Batholith, approximately 120 km northeast of Winnipeg, Manitoba, at the western edge of the Canadian Shield (Figure 8.14). The rocks of the batholith crystallized at a depth 10 to 16 km, approximately 2,670 million years ago, near the close of the regional deformation, which affected the surrounding metavolcanics, metasediments, and gneisses (Everitt et al., 1990). Apart from autointrusive dikes and foliations, there are no significant deformational features in the batholith. The existing fracture network was largely created in the early Proterozoic during cooling and crystallization of the batholith roof zone and in response to ambient regional stresses. Portions of this fracture network were open (reactivated) during regional peneplanation, deposition and then removal of phanerozoic sediments, and subsequent glaciation and deglaciation. However, no new fracture systems are believed to have been formed by these processes (Everitt et al., 1990).

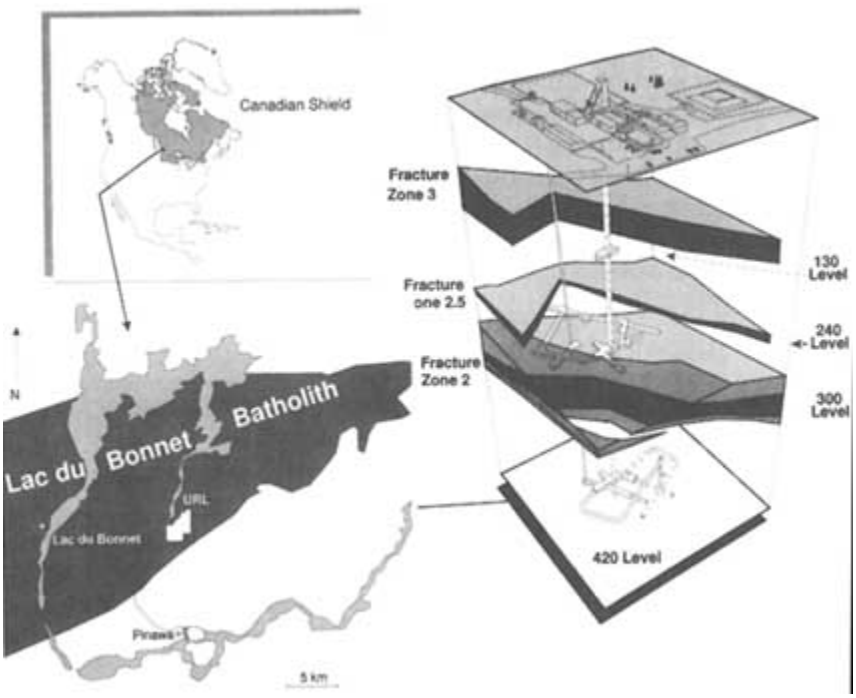

FIGURE 8.14 Location and layout of the Underground Research Laboratory. The location of the Lac Du Bonnet batholith is shaded on the map. On the right are fracture zones 3, 2.5, and 2.

The URL is located near the southern contact of the batholith with the surrounding gneiss. The distribution of xenoliths and deuteric alteration indicates that the present topographic surface is close to the original roof zone of the batholith. The roof zone is marked by shallow-dipping compositional layering (Everitt et al., 1990). The URL access shafts (Figure 8.15) provide a cross section of the roof zone. The geology and fracture distributions in the vicinity of the URL site were extensively investigated by surface and borehole geophysical techniques (Soonawala, 1983, 1984; Wong et al., 1983; Paillet, 1991). These studies showed that the structural geology and hydrogeology of the portion of the batholith surrounding the URL is dominated by a series of southeastward dipping fracture zones (Davison, 1984). Three major low-dipping fracture zones and associated splays were identified at the URL during surface-based drilling and shaft construction. These fracture zones are parallel the shallow-dipping layering of the batholith roof and are generally confined to xenolithic zones or their margins.

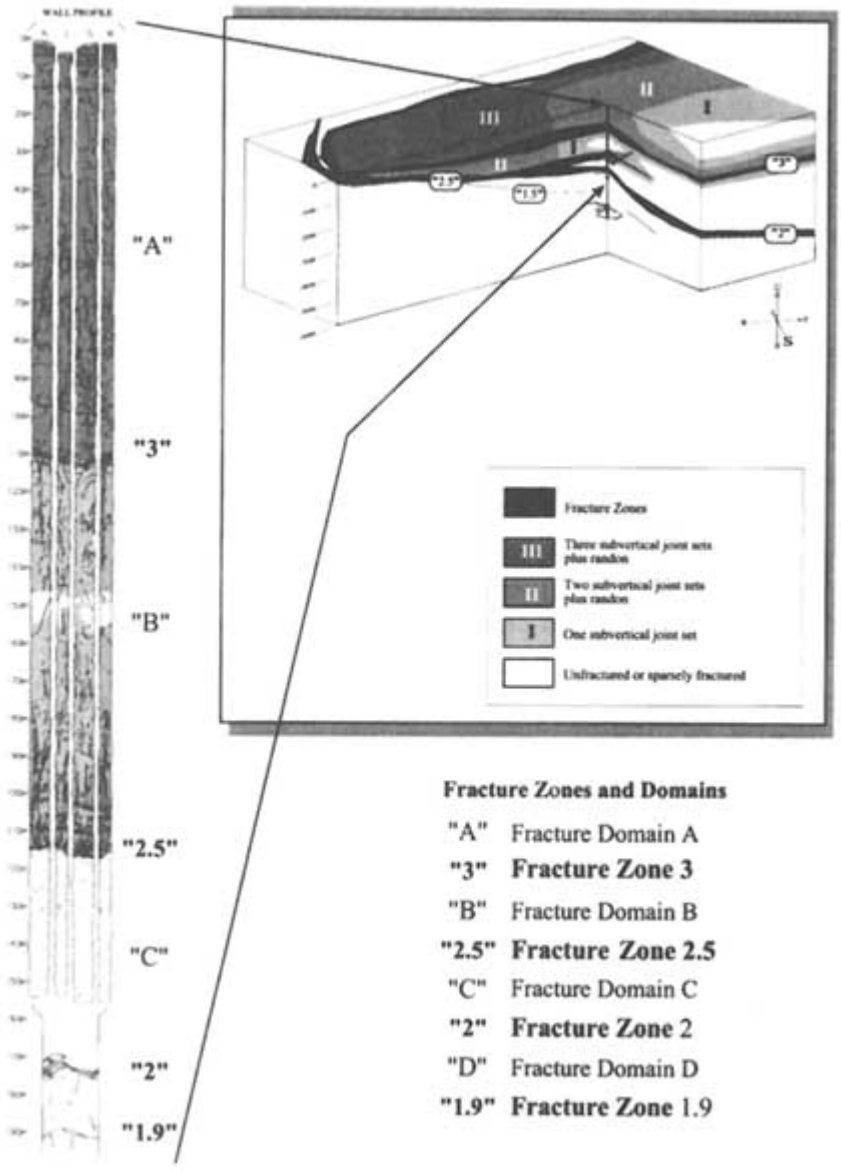

FIGURE 8.15 Fracture zones encountered by the URL shaft and their relationship to large-scale distribution of fractures at the URL site. Adapted from Everitt and Brown (1996).

Fracture Zone 2 (FZ2, the primary fracture zone discussed here; Figure 8.15) is the dominant member of the low-dipping fault group. Fracture Zone 3 (FZ3) is similar but has less displacement, whereas Fracture Zone 2.5 (FZ2.5) is a splay between these two large fracture zones. A fourth fracture zone (FZ1) is not encountered in the excavations and most boreholes and is not described here. Subvertical fractures are ubiquitous above FZ2.5. Between FZ2.5 and FZ2 they are confined to the fault margins, and they are absent below FZ2 (Everitt et al., 1990; Everitt and Brown, 1996). In general, the fracture zones comprise several chloritic slip surfaces, cataclasite horizon(s), and a variety of smaller-scale fractures and associated alterations extending into the hanging wall and, to a lesser extent, the footwall. The cataclasites consist of recrystallized fault rubble cemented by a fine-grained chlorite-carbonate matrix and are cross-cut by the chloritic slip surfaces, minor fractures, and seams of soft clay-goethite gouge. This assemblage is in varying degrees of groundwater-induced decomposition.

FZ2, FZ2.5, and FZ3 differ in the degree of complexity of their internal fracture patterns, and the extent of fracturing alteration into the adjacent rock. Fracture patterns become simpler, and the extent of fracturing and of alteration is more restricted, with increasing depth. FZ2, the deepest fracture zone intersected by the excavations, comprises a relatively simple system of conjugate shear and extension fractures (the cataclasite zone/chloritic fractures and the antithetic hematite-filled fractures, respectively). Displacement appears to have been dipslip only, with the overlying block moving 7.3 m to the northwest.

The fracture patterns for FZ2.5 and FZ3 are dominated by the same general arrangement of the major slip surfaces, but additional low-dipping and subvertical fracture sets are present. Overall, their geometry suggests two conjugate systems, superimposed to give orthorhombic symmetry, as described by Davis (1984). Reverse dip-slip (up to 1-m throws) dominates in these zones, but strike-slip and oblique-slip lineations also are present. The fracture zones divide the rock mass into a number of tabular-to-wedge-shaped blocks. These blocks are cross-cut by one or more sets of subvertical fractures, the pattern and frequency of which vary from one block (or fracture domain) to the next. The factors influencing the pattern of intrablock fracturing include overall distance from the ground surface, proximity to the bounding faults, and local rock type. The subvertical fractures become less frequent, less continuous, and simpler in pattern with increasing depth. They also become increasingly confined to the immediate margins of the fault zones or to lithological heterogeneities such as dikes. The most prominent set of subvertical fractures parallels the strike of the thrust faults. However, fracture sets oblique or perpendicular to this direction are common above FZ3. Variations in the structure of the fracture zones, and in the fracture domains between them, are illustrated by using the model depicted in Figure 8.15. The northeast face of the model is normal to the strike of the fracture zones as seen in the area of the excavations. FZ2 forms an arcuate outcrop pattern along the south and west sides of the model.

In the block above FZ2, the present-day maximum principal stress is oriented northeast-southwest, parallel to the dominant fracture set and the strike of FZ2. In the shaded area below FZ2, subvertical fracturing is rare or absent, and the maximum principal stress is oriented northwest-southeast, perpendicular to the strike of the thrust fault. The geometry of the thrust faults suggests they were formed when the regional stress field was oriented such that the plane containing the maximum and intermediate principal stresses was subhorizontal, with the former aligned in the northwest-southeast direction. This stress field is believed to be associated with plate accretion on the margins of the Superior craton during the late Archean/early Proterozoic (Everitt et al., 1990). In the case of FZ2, the simple conjugate system of fractures suggests that strain accommodated by fracturing was largely two dimensional. In the case of FZ2.5 and FZ3, however, the orthorhombic pattern of low-dipping major and minor fractures suggests that brittle strain was three dimensional (Davis, 1984). This difference is seen as a consequence of FZ2.5 and FZ3 being "piggybacked" on FZ2. As such, strike and oblique slip in FZ2.5 and FZ3 are seen as a natural accommodation to displacement on the underlying and dominant thrust fault (FZ2). The subvertical fracture sets are seen as extensional intrablock fracturing that was initiated by geometric flexing and general expansion of the thrust plates in the late Archean to early Proterozoic. The plane containing the maximum and intermediate principal stresses was still subhorizontal, but the local maximum principal stress axis was reoriented and is now aligned northeast-southwest. Reactivation and extension of some fractures likely occurred during Paleozoic transgression, during subsequent removal of the Paleozoic cover, and during repeated continental glaciations. The decreasing frequency, extent, and complexity of subvertical fracturing with depth from the surface are seen as a consequence of both the stacking of the thrust plates and the distance from the surface. The greatest and most varied "flexing" and fracturing would occur in the uppermost blocks. In a single fracture domain the pattern and frequency of subvertical fracturing reflect the distance from, and configuration of, the underlying thrust fault. Between FZ2 and FZ2.5, for example, the pattern of subvertical fractures varies from unimodal to bimodal (orthogonal) as the wedge of rock between FZ2 and FZ2.5 thins to the south. Similar variations are seen in the complexity and preferred orientations of fracturing above FZ2.5, as the plane of FZ3 curves from northeast to north striking.

Hydrogeological studies including single-hole straddle-packer tests and large-scale multiple-borehole hydraulic pressure interference tests conducted before, during, and after shaft construction revealed complex local and regional-scale patterns of permeability in the fracture zones (e.g., Davison and Kozak, 1988; Everitt et al., 1990). In FZ2, permeabilities range over six orders of magnitude, with high and low permeabilities appearing to form distinctive channels at the site scale (Figure 8.16). The prominent northeast-trending transmissivity channel is believed to coincide with the intersection of this fault with FZ2.5. The other channels apparently result from other factors, some of which include

structural controls and hydrogeochemical phenomena, such as the precipitation of different minerals in fillings owing to the mixing of groundwaters with dissimilar chemistries in the fault. In the area of the 240 level, a well-defined isolated region of high transmissivity and low storage is located in the fault immediately northwest of the shaft (Figure 8.17). This region is surrounded entirely by extremely low permeability conditions and has very limited hydraulic communication, with a much more extensive region of high permeability and high storage to the north and west.

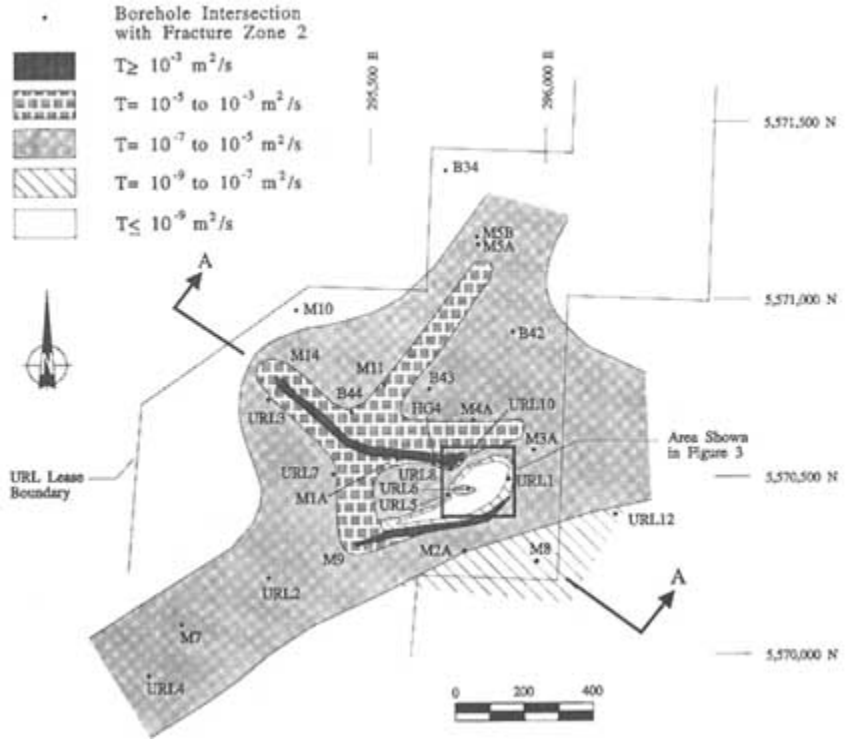

FIGURE 8.16 Hydraulic conductivity variations in FZ2. Modified from Davison and Kozak (1988).

These variations in permeability are accompanied by:

- Flexures in the fault zone, generalized here by structure contours representing the "middle" of the central cataclasite horizon.
- "Anomalies" in the rock-type map of the fault (Figure 8.18); the fracture zone is largely confined to a xenolithic horizon (area 1 in Figure 8.18), but to the west and northwest the zone changes in orientation such that it cross-cuts the layering to intersect the neighboring or gneiss granites.

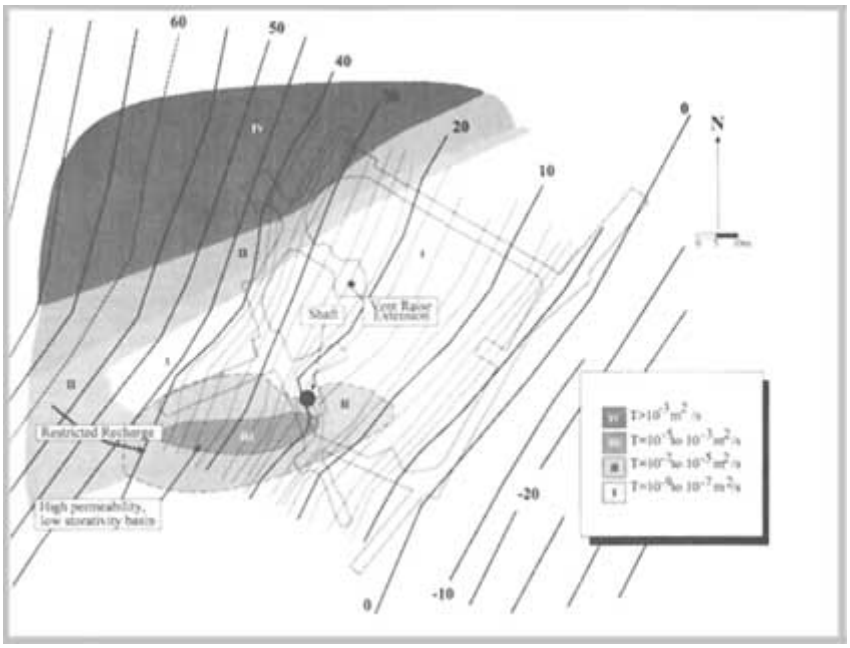

FIGURE 8.17 Hydraulic conductivity variations in FZ2 in the area of 240 Level. Modified from Davison and Kozak (1988).

- Occurrence of core disking in this area that represents locally high in situ stresses adjacent to the fault zone and by variations in the in situ stress normal to the fault zone (Figure 8.19) (in situ stress data from Martin et al., 1990).

It is concluded that the variations in the character and permeability of FZ2, and the variations in the stress magnitudes, are the direct result of undulations in the fault surface. As shown in Figure 8.20, movement on any undulating surface can be expected to result in dilational gaps, restraining bends, fault-bounded structural wedges (such as that between FZ2 and FZ1.9) and secondary subvertical fractures in the fault-bounded blocks. Variations in relative permeability in the fracture zone are reflected by corresponding variations in the thickness of the alteration halo. This correlation is a useful one because it serves as a qualitative indicator of historic flow variation, which in turn has practical application in the layout of characterization drilling.

The subvertical fracture shown in Figure 8.20 is a wedge-shaped zone of fractures that begins at the base of FZ2.5 and narrows downward until it terminates at the 240 level, about 35 m above FZ2. It parallels the strike of FZ2 and is known to extend 35 m vertically and at least 105 m horizontally. This fracture is interpreted as having formed in response to flexing of the fault block owing

to the change in dip angle of the fault directly beneath it. Such flexing would have led, at least locally, to a reorientation of the principal stresses. The maximum principal stresses below and above the fault zone are perpendicular and parallel, respectively, to the strike of the thrust fault (Everitt et al., 1990). The stress field above the thrust fault is oriented such that the subvertical fractures in this area are open and conductive. Extensive efforts to characterize the geology, hydrogeology, and geomechanical characteristics of this major thrust fault have led to the following conclusions:

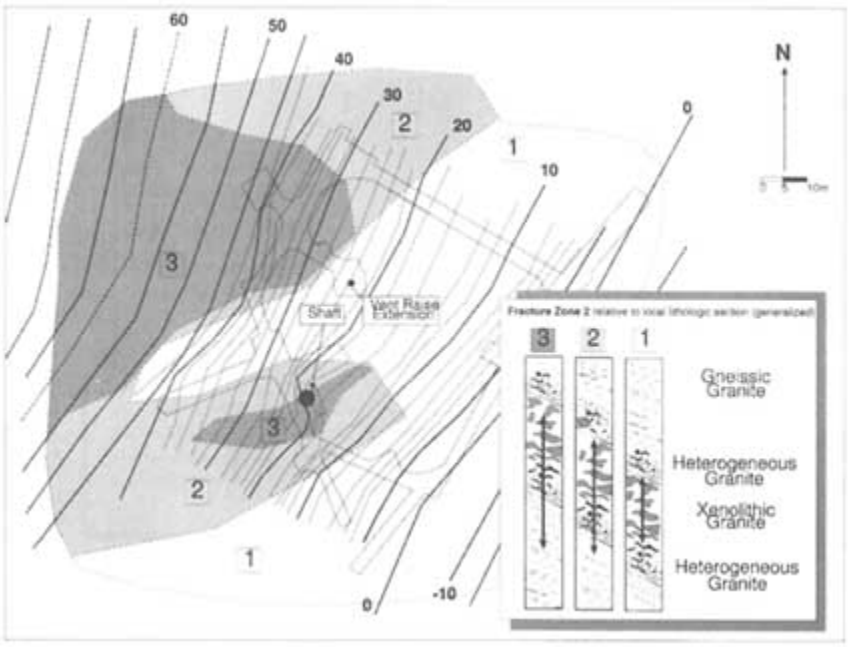

FIGURE 8.18 Map of litho-structural domains crossed by FZ2.

- Complex patterns of permeability exist in FZ2 at the scale of the site and at the scale of the excavations. These patterns include channels of high or low permeability that alternate along the strike of the fault.
- The variations in permeability appear to correlate with undulations in the plane of the fracture zone, which in turn correlate with dilational gaps (the high-conductivity channels), restraining bends (the areas of core disking and high normal stresses), and fault-bounded structural wedges and secondary fractures in the fault-bounded blocks.

These interpretations are based on the compilation of geological, hydrogeological, and geomechanical data and emphasize the need for an integrated multi

disciplinary approach to characterizing permeability variations in a fractured medium.

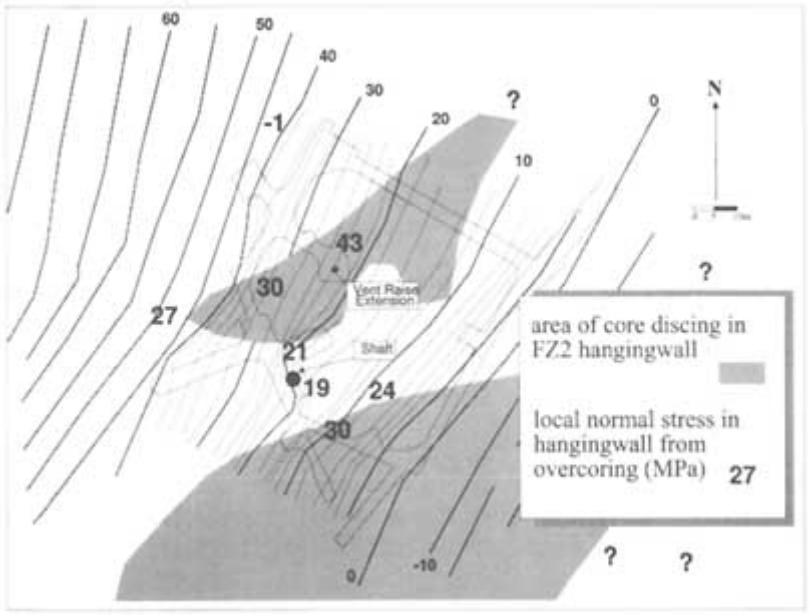

FIGURE 8.19 Areas of disking and measured normal stresses. From Martin et al. (1990).

CASE HISTORY V. FRACTURE STUDIES IN A GEOTHERMAL RESERVOIR: THE GEYSERS GEOTHERMAL FIELD, CALIFORNIA

The Geysers geothermal field in central California (Figure 8.21) is one of the best-known geothermal reservoirs in North America and one where steam production is associated with fractures and faults in otherwise low-permeability metasedimentary and hypabyssal plutonic rocks. This field is one of the most thoroughly studied geothermal reservoirs in the world. However, the characteristics and hydraulic properties of fractures are only partially understood at even this well-studied site for a variety of reasons common to most geothermal study sites: (1) complexity of the local geology; (2) difficulty of geological mapping and geophysical soundings in a deeply weathered and rugged terrain; (3) problems in obtaining well logs and other measurements in hostile borehole environments; and (4) difficulties in modeling two-phase flow in heterogeneous, dual-porosity reservoirs. Despite these difficulties, the results from ongoing studies at The Geysers provide examples of how geological, geochemical, geophysical, and reservoir modeling techniques can be applied to one of the most difficult problems in fracture hydrology.

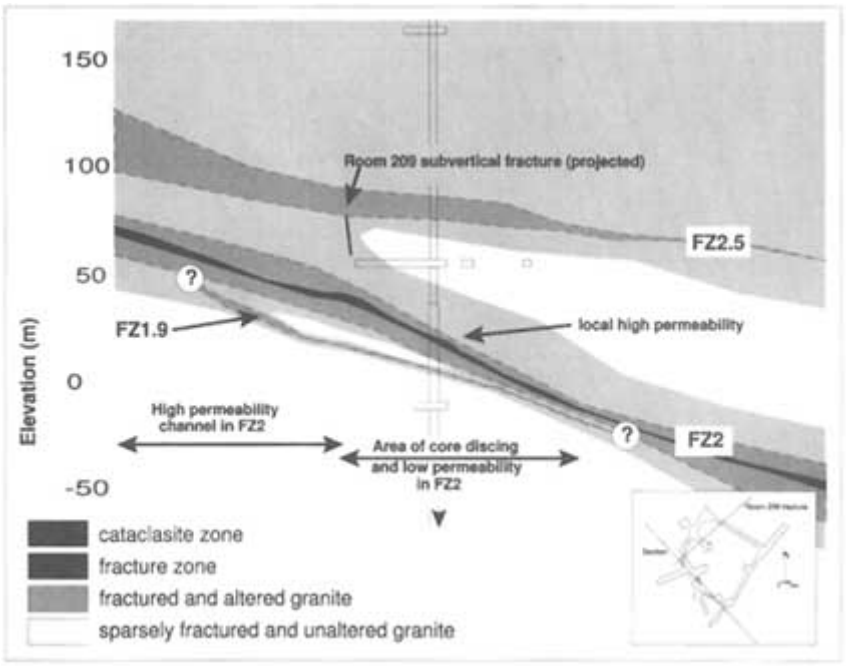

FIGURE 8.20 Cross section through fracture zones 2 and 2.5, with the subvertical "room 209 fracture."

The Geysers geothermal field is located in the Coast Ranges province of central California. Because of the difficulty in obtaining geophysical soundings in this rugged and geologically complex terrain, models of The Geysers geothermal reservoir have been developed mostly from surface geological and structural investigations and from detailed study of borehole cuttings and cores. Surface investigations reveal a series of northwest-trending, steeply dipping, strike-slip faults superimposed on previously faulted and folded terrain. Reservoir rocks consist of blueshist- and greenshist-grade metasedimentary rocks of the Franciscan assemblage intruded by a large felsic pluton that appears genetically related to late Tertiary and Quaternary surficial rhyolites of the Clear Lake volcanic field, which lies just northeast of the geothermal reservoir (McLaughlin and Donnelly-Nolan, 1981). The reservoir itself is located beneath relatively impermeable caprocks and is developed in both the pluton and overlying Franciscan metagraywackes and argillites (Figure 8.21). The intrusive "felsite" is at least 1.3 million years ago (Schriener and Suemnicht, 1981; Dalrymple, 1992). The reservoir is believed to have developed in the graywacke because of its intrinsic brittleness and high susceptibility to fracturing and because of hydrothermal dissolution of Franciscan calcite, aragonite, and other minerals that were only

partially filled by late-stage secondary phases (Gunderson, 1990; Hulen et al., 1992). The heat source for the geothermal system is believed to be from felsite intrusions beneath the reservoir (Hebein, 1985; Walters et al., 1988).

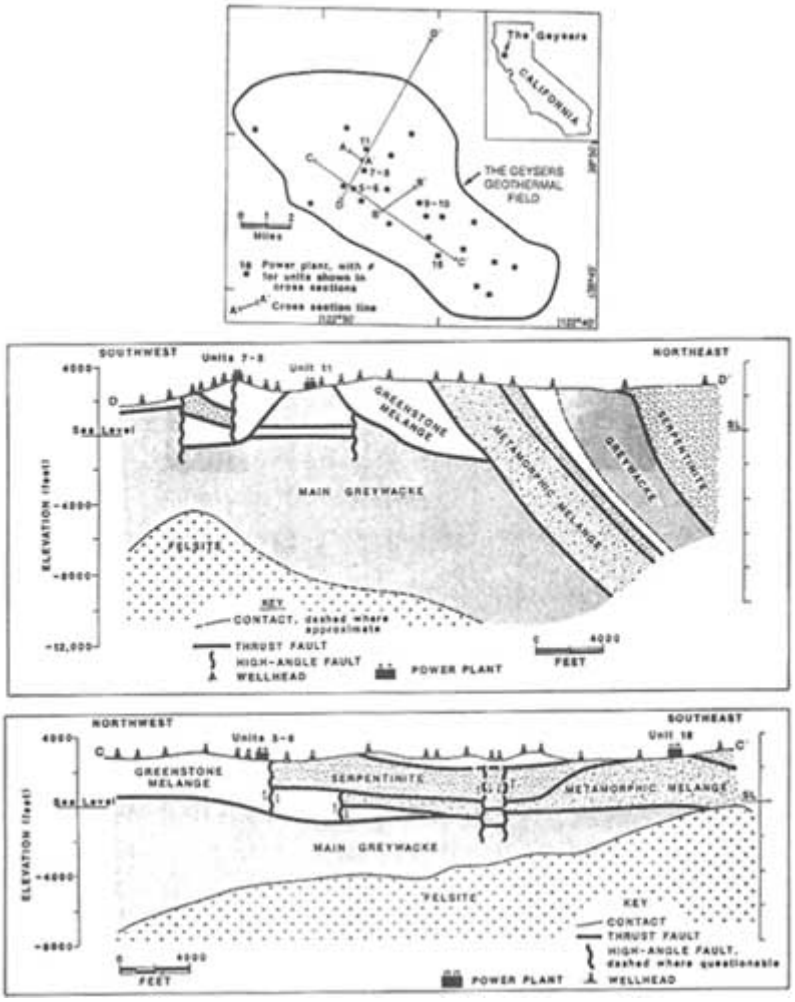

FIGURE 8.21 Sketch map (top) and schematic cross sections (middle and bottom) of the geothermal reservoir at The Geysers geothermal field. From Thompson (1992).

Surface geophysical measurements yield some information about the nature of the geothermal reservoir and underlying rocks, but the complexity of the terrain and geological environment have made these measurements very difficult to interpret. Gravity measurements indicate a pair of negative anomalies associ

ated with the reservoir (Chapman, 1978; Chapman et al., 1981; Isherwood, 1981). The larger and presumably deeper anomaly is centered northeast of the field and is believed to be associated with a magmatic body at depth below the Clear Lake volcanic field. A smaller, shallower gravity low (the "production low") is apparently associated with the geothermal reservoir itself. The local density deficiency is attributed to a combination of effects, including fluid withdrawal, the presence of steam in the reservoir, geochemical dissolution of minerals, and the presence of relatively less dense minerals in reservoir rocks (Denlinger, 1979; Denlinger and Kovach, 1981). Aeromagnetic surveys generally confirm the structure indicated by the gravity data and help further define the lateral limits of the reservoir. Surface resistivity measurements have done little more than confirm the separation of the subsurface environment into three layers: basement, reservoir, and cap rock (Keller and Jacobson, 1983; Keller et al., 1984).

Passive seismic surveys have been especially useful in defining reservoir properties, based on both identification of source areas for microseismic events and characterization of reservoir volumes through which such seismic waves pass (Iyer et al., 1979; Majer and McEvilly, 1979). The seismic source area maps indicate the location of a magma chamber at a depth of several kilometers to the northeast. The elevated level of seismic activity may be associated with fluid withdrawal from the reservoir (Young and Ward, 1981). Seismic activity in the reservoir provides an important constraint on geomechanical models of the reservoir. The most frequently cited mechanism for the generation of this activity is the response of the fractured rock to compression as steam is withdrawn (Hamilton and Muffler, 1972; Majer and McEvilly, 1979). Most recent studies indicate that microseismic activity is closely associated with both injection and withdrawal of fluids (Majer et al., 1988; Stark, 1990).

Active seismic surveys have been very difficult to carry out and have done little more than confirm the stratigraphy and faults inferred from drilling. Coupling of source energy to the ground surface has been a continuing problem. Most effective surface seismic surveys have used the Vibroseis method, which was designed to improve seismic sounding in such terrains (Denlinger and Kovach, 1981). Even with this method, most energy is apparently scattered in the reservoir volume. The few weak deep reflections probably represent the top of the basement. However, the microseismic monitoring technique has been much more effective in delineating the properties of reservoir rocks in part because the energy source is well coupled to the rock mass. These surveys indicate that the developed reservoir volume is associated with relatively low Vp/Vs ratios (ratios of compressional to shear velocity). This implies a reduced value for Poisson's ratio of reservoir rocks from which fluids have been withdrawn (O'Connell and Johnson, 1991). A similar result was obtained in vertical seismic profile studies reported by Majer et al. (1988).

Geochemical investigations generally form a major part of geothermal reservoir studies, and this is certainly true of The Geysers. Patterns of geochemical

alteration of reservoir rocks and minerals deposited in fracture fillings indicate that the reservoir has evolved from a liquid-dominated to a vapor-dominated system (Sternfeld, 1989). This has apparently occurred in part because the relatively impermeable caprock and sealed margins of the system inhibited recharge of the reservoir (White et al., 1971). Much of the geochemical and thermal history of the reservoir and caprock is based on interpretation of fluid inclusions in core samples and the compositions, textures, and paragenesis of minerals deposited in fractures, breccias, and dissolution cavities (Walters et al., 1988; Hulen et al., 1991). This result has important consequences for fracture studies. The complex evolution of a geothermal reservoir is important in evaluating the coupling between flow, temperature, stress, and fluid chemistry. Depending on location, the caprock is also a consequence of stratigraphy and the interaction of stress, temperature, and mineral deposition.

Geomechanical investigations have also contributed to the study of the reservoir. Much of this work centers on definition of the geomechanical nature of the reservoir and is concerned with questions about the effects of structural control on the lateral continuity of permeable zones and the flow of steam toward production wells. Fault and fracture orientation may be the primary determinant of flow in the reservoir (Thompson and Gunderson, 1989; Beall and Box, 1992). Several models have been proposed for the generation of open fractures in the reservoir, including wrench faulting of blocks and opening of near-vertical fractures and faults in the direction of minimum horizontal stress (Oppenheimer, 1986; Thompson and Gunderson, 1989; Nielson and Brown, 1990). At least some oriented cores indicate that the strike of fractures is perpendicular to the present direction of the least principal stress (Nielson and Brown, 1990). Other data indicate a strong lithological control on fracture generation or preservation; in some cores, graywacke beds are fractured, but intervening argillite beds are not (Sternfeld, 1989; Hulen et al., 1991). Production data indicate that there is horizontal continuity between producing wells. Fracture generation and opening mechanisms need to account for this horizontal continuity as well as the presence of conduits for the upward convection of fluids.

Observations of fractures, veins, and the texture of core samples have further contributed to an understanding of the source and movement of fluids in the reservoir. A double-porosity framework has been applied to the reservoir (Williamson, 1990). Major flow conduits are assumed to be fractures, faults, and brecciated zones, although only a single example of a major steam conduit has been recovered from core (Gunderson, 1990). The bulk of fluid reserves in the reservoir is stored in "matrix" porosity, where the matrix refers to everything besides the main fluid conduits. Detailed core examination reveals that the matrix porosity consists of open microfractures, dissolution voids from leaching of calcite and aragonite, and vuggy hydrothermal veinlets (Gunderson, 1990; Hulen et al., 1992). Much of the reservoir production apparently comes from water

adsorbed on the surfaces of minerals lining pore spaces and veins (Barker et al., 1992).

One of the most effective methods for investigating the flow of water and steam along fractures in the reservoir is production testing and tracer studies. Fluids injected into the reservoir appear to preferentially follow planes perpendicular to the direction of the least principal stress (Thompson and Gunderson, 1989). In the past, tritium and deuterium from power plant injectate have been used as tracers in attempting to follow the path of injected water from injection to production wells (Gulati et al., 1978). These tracers are difficult to interpret because relatively high detection limits are required and the effects of vapor fractionation on the tracers in the reservoir are unknown. Recent studies have used halogenated alkenes, which fractionate almost exclusively into steam and have extremely low detection limits (Adams et al., 1991a,b). Vapor-phase tracers have been detected in production wells within days of injection, indicating horizontal velocities in the reservoir as large as 1 km/day (Adams et al., 1991a,b). The path traveled by the first few percent of steam generated from injection water appears to be the same as that indicated for the injection water using deuterium tracers. The extremely short travel times indicate that flow takes place along major fractures and faults, rather than through the "matrix" porosity of the bulk of the reservoir rock.

These results demonstrate the way in which various lines of investigation can be used to constrain one of the most complicated problems related to fracture flow—delineation and modeling of flow in geothermal reservoirs. The difficulty in obtaining measurements in a complex geological environment, the hostile environment of boreholes, and the multivariate nature of two-phase flow in fractured media combine to make such studies extremely difficult to carry out. One of the most interesting aspects of fracture studies in geothermal reservoirs is the interaction of temperature, stress, and geochemistry in controlling flow. Stress and temperature determine mechanical properties, and temperature and geochemistry determine where mineral dissolution and growth occur. These interrelationships allow for many possible kinds of behavior. One of the most important examples is the generation of a caprock. If these zones of sealed fractures were in fact formed during the evolution of geothermal systems, the fracture infilling clearly influences the distribution of temperature in the reservoir as well as the geometry of convective flow.

The number of independent variables in such geomechanical investigations requires that the full array of potential measurements be applied. This overview of investigations at The Geysers geothermal area provides an example of the techniques that can be applied to these difficult investigations and the various models that can be developed in attempting to constrain a multivariate, two-phase, dual-porosity fracture flow problem where reservoir porosity and permeability are a time-varying function of temperature, pressure, and in situ stress conditions.

REFERENCES

Adams, M. C., J. M. Moore, and P. Hirtz. 1991a. Preliminary assessment of halogenated alkanes as vapor-phase tracers. Paper presented at the Sixteenth Annual Workshop on Geothermal Reservoir Engineering, Stanford University, Stanford, Calif., pp. 57–62.

Adams, M. C., J. J. Beall, S. L. Enedy, and P. Hirtz. 1991b. The application of halogenated alkanes as vapor-phase tracers: a field test in the southeast Geysers. Geothermal Resources Council Transactions, 15:457–463.

Andersson, J. E., P. Andersson, and E. Gustafsson. 1991. Effects of gas-lift pumping on borehole hydraulic conditions at Finnsjön, Sweden. Journal of Hydrology, 126(1–2):113–127.

Andersson, K. P., P. M. Andersson, E. Gustafsson, and O. Olsson. 1989. Mapping ground water flow paths in crystalline bedrock using differential radar crosshole tomography measurements utilizing saline tracers. In Proceedings of the Third International Symposium on Borehole Geophysics for Minerals, Geotechnical, and Groundwater Applications. Tulsa, Okla.: Society of Professional Well Log Analysts.

Barker, B. J., M. S. Gulati, M. A. Bryan, and K. L. Reidel. 1992. Geysers reservoir performance. Monograph on The Geysers Geothermal Field. Special report no. 17, Geothermal Resource Council, Davis, Calif., pp. 167–178.

Barton, C. C., and P. A. Hsieh. 1989. Physical and hydrologic-flow properties of fractures. Field Guide Book T385, American Geophysical Union, Washington, D.C., 36 pp.

Barton, C. C., and E. Larsen. 1985. Fractal geometry of two-dimensional fracture networks at Yucca Mountain, southwest Nevada. Pp. 77–84 in Fundamentals of Rock Joints, O. Stephansson, ed. Lulea, Sweden: Centek Publishers.

Bassett, R. L., S. P. Neumann, T. C. Rasmussen, A. Guzman, G. R. Davidson, and C. F. Lohrstorfer. 1994. Validation studies for assessing unsaturated flow and transport through fractured rock. Report NUREG/CR-6203, prepared by the University of Arizona, Tucson, for the U.S. Nuclear Regulatory Commission.

Bassett, R. L., E. L. Fitzmaurice, and A. Guzman. 1996. Rapid and long-distance transport of water and solute through networks in variably saturated tuff. Submitted to Water Resources Research.

Beall, J. J., and W. T. Box, Jr. 1992. The nature of steam-bearing fractures in the South Geysers Reservoir. Pp. 69–75 in Monograph on The Geysers Geothermal Field. Special report no. 17, Geothermal Resource Council, Davis, Calif.

Beauheim, R. L. 1988. Scale effects in well testing in fractured media. Pp. 152–161 in Proceedings of the 4th Canadian/American Conference on Hydrogeology, B. Hitchon and S. Bachu, eds. Dublin, Oh.: National Water Well Association.

Block, L., C. H. Cheng, M. Fehler, and W. S. Phillips. 1994. Seismic imaging using microearthquakes induced by hydraulic fracturing. Geophysics, 59:102–112.

Bredehoeft, J. D., C. E. Neuzil, and P. C. D. Milly. 1983. Regional flow in the Dakota aquifer: a study of the role of confining layers . Water Supply Paper 2237, U.S. Geological Survey, Reston, Va.

Busenberg, E., and L. N. Plummer. 1992. Use of chlorofluorocarbons (CC13F and CC12F2) as hydrologic tracers and age-dating tools: the alluvium and terrace system of central Oklahoma. Water Resources Research, 28 (9):2257–2283.

Chapman, R.H. 1978. Gravity anomalies in The Geysers-Clear Lake Area, Northern California, Field Trip Guidebook 45, Castle Steam Field, Great Valley Sequence. Pp. 89–98 in 53rd Annual Meeting, Pacific Section, American Association of Petroleum Geologists, Society of Economic Paleontologists and Mineralogists, and Society of Exploration Geophysicists, Sacramento, Calif.

Chapman, R. H., R. P. Thomas, H. Dykstra, and L. D. Stockton. 1981. A reservoir assessment of The Geysers geothermal field. Publication TR 27, California Division of Oil and Gas, Sacramento, Calif., pp. 21–33.

Chem-Nuclear Systems, Inc. 1993. Site characterization report for the Wake/Chatham County potentially suitable site, North Carolina. Raleigh, N.C.: Chem-Nuclear Systems, 85 pp.

Cosma, C., P. Heikkinen, and S. Pekonen. 1991. Improvement of high resolution borehole seismics. Stripa Project TR 913, Swedish Nuclear Fuel and Waste Management Co., Stockholm.

Dalrymple, G. B. 1992. Preliminary report on 40Ar/39Ar incremental heating experiments on feldspar samples from the telsite unit, Geysers geothermal field, California. USGS Open-File Report 92–407, U.S. Geological Survey, Reston, Va., 15 pp.

Davies, P. B., L. H. Brush, and F. T. Mendenhall. 1991. Assessing the impact of waste-generated gas from the degradation of transuranic waste at the Waste Isolation Pilot Plant. In Proceedings of the Workshop on Gas Generation and Release from Radioactive Waste Repositories, Aixen-Provence, France, September 23-26. Washington, D.C.: Nuclear Regulatory Commission.

Davis, G. H. 1984. Structural Geology of Rocks and Regions. New York: John Wiley & Sons.

Davison, C. C. 1984. Monitoring hydrogeological conditions in fractured rock at the site of Canada's Underground Research Laboratory. Groundwater Monitoring Review, 3(4):95–102.

Davison, C. C., and E. T. Kozak. 1988. Hydrogeological characteristics of fracture zones in a granite batholith of the Canadian Shield. Pp. 53–59 in Proceedings of the 4th Canadian/ American Conference on Hydrogeology. B. Hitchon and S. Bachu, eds. Dublin, Oh.: National Water Well Association.

Denlinger, R. P. 1979. Geophysics of The Geysers geothermal field, northern California. Ph.D. thesis, Stanford University, Stanford, Calif., 87 pp.

Denlinger, R. P., and R. L. Kovach. 1981. Three-dimensional gravity modeling of The Geysers hydrothermal system and vicinity, northern California: Geological Society of American Bulletin, Pt. 1, 92(6):404–410.

Everitt, R. A., and A. Brown. 1996. Geological mapping of the AECL Research's Underground Research Laboratory—A cross section of thrust faults and associated fractures in the roof zone of an Archean batholith. In Fractured and Jointed Rock Masses. Rotterdam: A. A. Balkema.

Everitt, R. A., A. Brown, C. C. Davison, M. Gascoyne, and C. D. Martin. 1990. Regional and local setting of the Underground Research Laboratory. Pp. 64-1–64-23 in Proceedings of the International Symposium on Unique Underground Structures. Golden, Colo.: Colorado School of Mines.

Fehler, M. 1989. Stress control of seismicity patterns observed during hydraulic fracturing experiments at the Fenton Hill hot dry rock geothermal energy site, New Mexico. International Journal of Rock Mechanics and Mining Science and Geomechanics Abstracts, 26:211–219.

Finley, S. J., and J. C. Lorenz. 1987. Significance of drilling and coring-induced fractures in Mesaverde core, northwestern Colorado. Sandia National Laboratories, AAPG Bulletin, 71 (5):556.

Geldon, A. L. 1993. Preliminary hydrogeologic assessment of boreholdes UE-25 C-1, UE-25 C-2, UE-25 C-3, Yucca Mountain, Nye City, Nevada. USGS Water Resources Investigations Report 92-4016, U.S. Geological Survey, Reston, Va.

Geothermal Resources Council. 1992. Monograph on The Geysers geothermal field. Special Report No. 17, Geothermal Resources Council, Davis, Calif., 325 pp.

Gulati, M. S., S. C. Lipman, and C. J. Strobel. 1978. Tritium tracer survey at The Geysers. Geothermal Resources Council Transactions, 13:487-490.

Gunderson, R.P. 1990. Reservoir matrix porosity at The Geysers from core measurements. Geothermal Resources Council Transactions, 14:449–454.

Gustafsson, E., and P. Andersson. 1991. Groundwater flow conditions in a low-angle fracture zone at Finnsjön, Sweden. Journal of Hydrology, 126(1–2):79–11.

Hamilton, R. M., and L. M. P. Muffler. 1972. Microearthquakes at The Geysers geothermal area, California. Journal of Geophysical Research, 77(11):2081–2086.

Hardin, E. L., C. H. Cheng, F. L. Paillet, and J. D. Mendelson. 1987. Fracture characterization by means of attenuation and generation of tube waves in fractured crystalline rock at Mirror Lake, New Hampshire. Journal of Geophysical Research, 92(B8):7989–8006.

Hebein, J. J. 1985. Historical hydrothermal evolutionary facets revealed within the exploited Geysers steam field. Geothermal Resources Council Bulletin, 14(6):13–16.

Hsieh, P. A., and A. M. Shapiro. 1994. Hydraulic characteristics of fractured bedrock underlying the FSE well field at the Mirror Lake site, Grafton County, New Hampshire. In U.S. Geological Survey Toxics Substance Hydrology Program, D. W. Morganwalp and D. A. Aronson, eds., Proceedings of the technical meeting, Colorado Springs, Colorado, Sept. 20–24, 1993. USGS Water-Resources Investigations Report, U.S. Geological Survey, Reston, Va.

Hsieh, P. A., S. P. Neuman, and E. S. Simpson. 1983. Pressure testing of fractured rocks—a methodology employing three-dimensional hole test. NUREG/CR-3213, U.S. Nuclear Regulatory Commission, Washington, D.C., 176 pp.

Hsieh, P. A., A. M. Shapiro, C. C. Barton, F. P. Haeni, C. D. Johnson, C. W. Martin, F. L. Paillet, T. C. Winter, and D. L. Wright. 1993. Methods of characterizing fluid movement and chemical transport in fractured rock. In Field Trip Guide Book for Northeastern United States, J. T. Chaney and J. C. Hepburn, eds. Boulder, Colo.: Geological Society of America.

Hulen, J. B., D. L. Nielson, and W. Martin. 1992. Early calcite dissolution as a major control on porosity development in The Geysers steam field, California—additional evidence in core from Unocal well NEGU-17. Geothermal Resources Council Transactions, 16:167–174.

Hulen, J. B., M. A. Walters, and D. L. Nielson. 1991. Comparison of reservoir and caprock core from the northwest Geysers steam field, California—implications for development of reservoir porosity. Geothermal Resources Council Transactions, 15:11–18.

Isherwood, W. F. 1981. Geophysical overview of The Geysers. Pp. 83–95 in Research in the Geysers-Clear Lake area, northern California, R. J. McLaughlin and J. M. Donnelly-Nolan, eds., USGS Professional Paper 1141, U.S. Geological Survey, Reston, Va.

Iyer, H. M., D. H. Oppenheimer, and T. Hitchcock. 1981. Abnormal *P*-wave delays in The Geysers-Clear Lake geothermal area. Science, 204:495–497.

Kamineni, D. C., and M. Bonardi. 1983. Bastnaesite in fractures of the Eye-Dashwa lakes pluton, Atikokan, Ontario, Canada. Chemical Geology, 39:263.

Kamineni, D. C., G. F. McCrank, and D. Stone. 1987. Multiple alteration events in the East Bull Lake anorthosite-gabbro layered complex, NE Ontario, Canada: evidence from fracture mineralogy and 40AR-39AR dating. Applied Geochemistry, 2:73–80.

Keller, G. V., and J. J. Jacobson. 1983. Deep electromagnetic soundings northeast of The Geysers steam field. Geothermal Resources Council Transactions, 7:497–603.

Keller, G. V., J. I. Pritchard, J. J. Jacobson, and N. Harthill. 1984. Megasource time-domain electromagnetic sounding methods. Geophysics, 49:993–1009.

Kim, K., and W. M. McCabe. 1984. Geomechanics characterization of a candidate nuclear waste repository site in basalt. Proceedings of the 25th Symposium on Rock Mechanics, Northwestern University, pp. 1126–1135.

Lapcevic, P. A., K. W. Novakowski, and F. L. Paillet. 1993. Analysis of transient flow in an observation well intersecting a single fracture. Journal of Hydrology, 151:227–239.

Laubach, S. E. 1988. Subsurface fractures and their relationship to stress history in East Texas Basin sandstone. Techtonophysics, 156(1-2):37–49.

Laubach, S. E., R. W. Baumgardner, Jr., E. R. Monson, E. Hunt, and K. J. Meador. 1988. Fracture detection in low-permeability reservoir sandstone; a comparison of BHTV and FMS logs to core. SPE-18119, Society of Petroleum Engineers of AIME, Richardson, Tex., pp. 129–139.

Lorenz, J. C. 1989. Difference in fracture characteristics and related production, Mesaverde formation, northwestern Colorado. Sandia National Laboratories, SPE Formation Evaluation, 4(1):11-16.

Lorenz, J. C. 1990. Significance of coring-induced fractures in Mesaverde core, northwestern Colorado. Sandia National Laboratories, AAPG Bulletin, 74(7):1017–1029.

Lorenz, J. C., and S. J. Finley. 1991. Regional fractures. II. Fracturing of Mesaverde reservoirs in the Piceance Basin, Colorado. Sandia National Laboratories, AAPG Bulletin, 75(11):1738–1757.

Lorenz, J. C., N. R. Warpinski, P. T. Branagan, and A. R. Sattler. 1989. Fracture characteristics and reservoir behavior of stress-sensitive fracture systems in flat-lying lenticular formations. Journal of Petroleum Technology, 41:615–622.

Majer, E. L., and T. V. McEvilly. 1979. Seismological investigations at The Geysers geothermal field. Geophysics, 44:246–269.

Majer, E. L., T. V. McEvilly, F. S. Eastwood, and L. R. Myer. 1988. Fracture detection using *P*-wave and *S*-wave vertical seismic profiles at The Geysers geothermal field. Geophysics, 53:76–84.

Martel, S. J., and J. E. Peterson, Jr. 1991. Interdisciplinary characterization of fracture systems at the US/BK site, Grimsel Laboratory, Switzerland. International Journal of Rock Mechanics and Mining Science and Geomechanics Abstracts, 28(4):295–323.

Martin, C. D. 1990. Characterizing in-situ stress domains at the AECL Underground Research Laboratory. Canadian Geotechnical Journal, 27(5):631–646.

Martin, C. D., C. C. Davison, and E. T. Kozak. 1990. Characterizing normal stiffness and hydraulic conductivity of a major shear zone in granite. Pp. 549–556 in Rock Joints, N. E. Barton and O. E. Stephansson, eds. Rotterdam: A. A. Balkema.

McLaughlin, R. J., and J. M. Donnelly-Nolan, eds. 1981. Research in The Geysers-Clear Lake Geothermal Area, Northern California. USGS Professional Paper 1141, U.S. Geological Survey, Reston, Va., 259 pp.

Michie, U. McL. 1992. The geology and hydrogeology of Sellafield, United Kingdom. Technical Report No. 263. Harwell, Oxfordshire, U.K.: NIREX, Inc.

Morganwalp, D. W., and D. A. Aronson, eds. 1995. U.S. Geological Survey Toxic Substances Hydrology Program—Proceedings of the technical meeting, Colorado Springs, Colorado, September 20-24, 1993. USGS Water Resources Investigation Report 94-4015, U.S. Geological Survey, Reston, Va.

NAGRA. 1985. Grimsel Test Site—Overview and test programs. Technical Report 85-46, Baden, Switzerland, 118 pp.

Nelson, P. H. 1993. Geological and mineralogical controls on physical properties of tuffs at Yucca Mountain. The Log Analyst, 34(1):58–68.

Nelson, P. H., K. A. Magnusson, and R. Rachiele. 1982. Application of borehole geophysics at an experimental waste disposal site. Geophysical Prospecting, 30(6):910–934.

Neuzil, C. E. 1993. Low fluid pressure within the Pierre Shale: a transient response to erosion . Water Resources Research, 29:2007–2020.

Nicholas, J. R., and R. W. Healy. 1988. Tritium migration from a low-level radioactive-waste disposal site near Chicago, Illinois. USGS Water Supply Paper 2333, U.S. Geological Survey, Reston, Va.

Nielson, D. L., and D. Brown. 1990. Thoughts on stress around The Geysers geothermal field. Geothermal Resources Council Transactions, 14:1685–1690.

O'Connell, D. R., and L. R. Johnson. 1991. Progressive inversion for hypocenters and *P*-wave and *S*-wave velocity structure: application to The Geysers, California, geothermal field. Journal of Geophysical Research, 96:6223–6236.

Olsson, O., ed. 1992. Site characterization and validation—final report: Stripa Project TR 92-22, Swedish Nuclear Fuel and Waste Management Co., Stockholm.

Oppenheimer, D. H. 1986. Extensional tectonics at The Geysers geothermal area, California. Journal of Geophysical Research, 91:463–476.

Paillet, F. L. 1991. The 1st core hole at Mirror Lake, New Hampshire—comparing geophysical logs to core and cross-hole flow logging. Pp. 162–171 in U.S. Geological Survey Toxic Substances Hydrology Program—Proceedings of the technical meeting, Monterey, Calif., March 11-15, G. E. Mallard and D. A. Aronson, eds. USGS Water Resources Investigations Report 91-4034, U.S. Geological Survey, Reston, Va.

Paillet, F. L. 1993. Using borehole geophysics and cross-borehole flow testing to define hydraulic connections between fracture zones in bedrock aquifers. Journal of Applied Geophysics, 30:261–279.

Paillet, F. L., and A. E. Hess. 1986. Geophysical well-log analysis of fractured crystalline rocks at East Bull Lake, Ontario, Canada. USGS Water Resources Investigation Report 86-4052, U.S. Geological Survey, Reston, Va., 37 pp.

Paillet, F. L., and A. E. Hess. 1987. Geophysical well log analysis of fractured granitic rocks at Atikokan, Ontario, Canada. USGS Water Resources Investigation Report 87-4154, U.S. Geological Survey, Reston, Va., 36 pp.

Paillet, F. L., and K. Kapucu. 1989. Characterization of fracture permeability and fracture flow modeling at Mirror Lake, New Hampshire. USGS Water Resources Investigation Report 89-4058, U.S. Geological Survey, Reston, Va., 49 pp.

Paillet, F. L., and K. Kim. 1987. Character and distribution of borehole wall breakouts and their relationship to in-situ stresses in deep Columbia River basalts. Journal of Geophysical Research, 92:6223-6234.

Paillet, F. L., K. Novakowski, and P. Lapcevic. 1992. Analysis of transient flows in boreholes during pumping in fractured formations. Pp. S1-S21 in Society of Professional Well Log Analysts 33rd Annual Logging Symposium Transactions. Tulsa, Okla.: Society of Professional Well Log Analysts.

Robinson, B., and J. Tester. 1984. Dispersed flow in fractured reservoirs: an analysis of tracer-determined residence time distributions. Journal of Geophysical Research, 89:10374-10384.

Robinson, R., S. Silliman, and C. Cady. 1993. Identifying fracture interconnections between boreholes using natural temperature profiling. II. Application to a fractured dolomite. The Log Analyst, 34(1):69-77.

Schriener, A., Jr., and G. A. Suemnicht. 1981. Subsurface intrusive rocks at The Geysers geothermal area, California. Pp. 295-302 in USGS Open-File Report 81-355, U.S. Geological Survey, Reston, Va.

Shapiro, A. M., and P. A. Hsieh. 1991. Research in fractured-rock hydrogeology: characterizing fluid movement and chemical transport in fractured rock at the Mirror Lake drainage basin, Pp. 155-161 in Proceedings of the Technical Meeting of U.S. Geological Survey Toxic Substances Hydrology Program, Monterey, Calif., March 11-15, G.E. Mallard and D.A. Aronson, eds. USGS Water Resources Investigation Report 91-4034, U.S. Geological Survey, Reston, Va.

Shapiro, A. M., and P. A. Hsieh. 1994. Overview of research at the Mirror Lake site: use of hydrologic, geophysical and geochemical methods to characterize flow and transport in fractured rock. In U.S. Geological Survey Toxic Substances Hydrology Program—Proceedings of the Technical Meeting, Colorado Springs, Colorado, September 20-24, 1993, D.W. Morganwalp and D.A. eds. USGS Water Resources Investigation Report 94-4015, U.S. Geological Survey, Reston, Va.

Silliman, S., and R. Robinson. 1989. Identifying fracture interconnections between boreholes using natural temperature profiling: I. Conceptual basis. Groundwater, 27(3):393-402.

Solomon, D. K., R. J. Poreda, S. L. Schiff, and J. A. Cherry. 1992. Tritium and helium-3 as groundwater age tracers in the Borden aquifer. Water Resources Research, 28(3):741-755.

Soonawala, N. M. 1983. Geophysical logging in granites. Geoexploration, 21:221-230.

Soonawala, N. M. 1984. An overview of the geophysics activity with the Canadian Nuclear Fuel Waste Management program. Geoexploration, 21:149-168.

Spencer, C. W., and C. W. Keighin. 1984. Geologic studies in support of the U.S. Department of Energy Multiwell Experiment, Garfield County, Colorado. USGS Open File Report 84-0757, U.S. Geological Survey, Reston, Va.

Stark, M. A. 1990. Imaging injected water in The Geysers reservoir using microearthquake data. Geothermal Research Council Transactions, 14:1697-1704.

Sternfeld, J. N. 1989. Lithologic influences on fracture permeability and the distribution of steam in the northwest Geysers steam field, Sonoma County, California. Geothermal Resources Council Transactions, 13:473-479.

Stone, D., and D. C. Kamineni. 1982. Fractures and fracture infillings of the Eye-Dashwa Lakes pluton, Atikokan, Ontario. Canadian Journal of Earth Science, 19(4):789.

Thompson, R. C. 1992. Structural stratigraphy and intrusive rocks at The Geysers geothermal fields.Monograph on the Geyser Geothermal Field, Special Report No. 17, Geothermal Resource Council, Davis, Calif.

Thompson, R. C., and R. P. Gunderson. 1989. The orientation of steam-bearing fractures at The Geysers geothermal field. Geothermal Resources Council Transactions, 13:487-490.

Ticknor, K. V., T. T. Vandegraaf, and D. C. Kamineni. 1989. Radionuclide sorption on primary and fracture-filling minerals from the East Bull Lake Pluton, Massey, Ontario, Canada. Applied Geochemistry, 4:163-176.

Turpening, R. 1984. Differential vertical seismic profiling: fracture volume assessment. Pp. 307-360 in Vertical Seismic Profiling: Techniques, Applications and Case Histories, A. H. Balch and M. W. Lee, eds. Boston, Mass.: International Human Resources Development Corp.

Walters, M. A., J. N. Stemfeld, J. R. Haizlip, A. F. Drenick, and J. Combs. 1988. A vapor-dominated geothermal reservoir exceeding 600 F at The Geysers, Sonoma County, California. Pp. 73-81 in Proceedings of the 13th Annual Workshop on Geothermal Research Engineering, Stanford University, Stanford, Calif.

White, D. E., L. J. P. Muffler, and A. H. Truesdell. 1971. Vapor-dominated hydrothermal systems compared with hot water systems. Economic Geology, 66:75-96.

Williamson, K. H. 1990. Reservoir simulation at The Geysers geothermal field. P. 11 in Stanford University, 15th Annual Workshop on Geothermal Reservoir Engineering, Proceedings Volume. Davis, Calif.: Geothermal Resource Council.

Winter, T. C. 1984. Geohydrologic setting of Mirror Lake, West Thornton, New Hampshire. USGS Water Resources Investigations Report 84-4266, U.S. Geological Survey, Reston, Va., 61 pp.

Wong, J., P. Hurley, and G. F. West. 1983. Crosshole seismology and seismic imaging in crystalline rocks. Geophysical Research Letters, 10(8):686-689.

Yager, R. M. 1993. Simulated three-dimensional groundwater flow in the Lockport Group, a fractured dolomite aquifer near Niagara Falls, New York. USGS Water Resources Investigation Report 92-4189, U.S. Geological Survey, Reston, Va., 43 pp.

Young, C. Y., and R. W. Ward. 1981. Attenuation of teleseismic P-waves in The Geysers-Clear Lake region. USGS Professional Paper 1141, U.S. Geological Survey, Reston, Va. , pp. 149-160.

9

Technical Summary

This report describes the tools that are currently available for characterizing fracture systems and for understanding, predicting, and controlling fluid flow and chemical transport in fractures. In many applications, fractures have been problematic. Their locations are often a mystery, but their effects on flow can be dramatic. Practitioners frequently ignore fractures or do not account for them adequately because the tools for dealing with them are too expensive, not widely available, or poorly understood. However, in the past few decades, researchers have made many advances in analyzing and characterizing fracture systems, in understanding fluid flow in fractured media, and in accounting for the importance of fracture systems in engineering design. New conceptual, physical, and numerical tools are now available to solve many problems associated with fracture systems.

In this report the committee describes these tools and the scientific theories behind them, gives the essential components of application, assesses their utility and limitations, and suggests topics for further work. This report is for students, educators, researchers, practitioners, and public officials.

Chapter 1 reviews fracture problems encountered in a variety of applications. Subsequent chapters address three key issues that are commonly encountered in these applications:

- How can fractures that are significant hydraulic conductors be identified, located, and characterized? (Chapters 2, 3, 4, and 5)
- How do fluid flow and chemical transport occur in fracture systems? (Chapters 3, 5, and 6)
- How can changes to fracture systems be predicted and controlled? (Chapter 7)

Fractures that are significant for fluid flow are open and connected to other fractures over distances comparable to the spatial and temporal scales of the problem of interest. In some cases there may be myriad fractures that are not significant and only a few that dominate flow behavior. In other cases only fractures having certain orientations (e.g., normal to the least principal stress) may be important. Fractures that conduct a significant amount of fluid may be a particular component of a fracture network, but it may be necessary to understand the entire fracture system to understand why that component is important (e.g., extension features that connect segments of a fault).

Fluid flow and transport take place in the void space created by these hydraulically conductive fractures. The geometry of the void space and the relationship between fracture permeability and matrix permeability determine how flow takes place. If the fractures are poorly interconnected and the matrix rock is relatively impermeable, an analysis of flow may need to account for the network of discrete fractures and could well ignore the matrix. On the other hand, if the matrix is permeable and the fractures are regular and highly interconnected, an analysis of flow could treat the fracture network as an equivalent continuum with fluid storage provided by the matrix. A major factor in analysis of flow and transport is the appropriate representation of the features that control flow.

Understanding and controlling changes to the fracture system are tantamount to understanding and controlling changes in fracture void space. Any combination of changes in stress, fluid pressure, temperature, fluid composition, or chemical conditions that commonly occur in engineering activities can change the geometry of the void space. For example, a decrease in fluid pressure increases the effective stress, which decreases the void space and the permeability of the fratures. Similarly, precipitation of minerals in a fracture (e.g., vein formation) decreases void space and, therefore, permeability.

What are the conceptual, physical, and numerical tools that help address these three key questions? Tools from geology, geomechanics, geophysics, geochemistry, and hydrogeology were primarily developed to solve fracture problems related to petroleum reservoirs, mines, and nuclear waste isolation. They have further application in a variety of reservoir, environmental, and construction endeavors. The tools are in various stages of development and use. This report collects and evaluates the scattered information about them.

In bringing these tools together to study fractures, the power of an interdisciplinary approach is evident. The fundamental reason that fracture problems are difficult to solve is that fracture systems tend to be extremely complex and heterogeneous. In any one discipline there are excellent, well-developed tools for handling homogeneous systems and some tools for handling anisotropic or simple composite systems, but each of these tools has severe limitations when applied to complex heterogeneous systems. The most effective way to solve problems in heterogeneous media is to apply a variety of tools so that the particular

strength of each method compensates for the weaknesses of the other methods. This approach may have applications in other endeavors involving analysis of behavior in the earth.

This chapter summarizes the key tools and shows how they address the three key questions given previously. A number of recommendations that follow from the discussion are given here for completeness. These are italicized. These recommendations are summarized in the Executive Summary of this report.

HOW CAN FRACTURES THAT ARE SIGNIFICANT HYDRAULIC CONDUCTORS BE IDENTIFIED, LOCATED, AND CHARACTERIZED?

The tools to address this first key question come primarily from:

- Geology and fracture mechanics (Chapter 2)
- Laboratory and field studies of fracture properties (Chapters 2 and 3)
- Geophysics (Chapters 3 and 4)
- Hydraulic and tracer testing (Chapter 5)

Tools from geology and geomechanics can help address the following questions: What kinds of fractures tend to form in a given environment? What patterns do they commonly assume? Which fractures are more likely to conduct fluid? Understanding of fracture properties and tools from geophysics can help answer the question: How can hydraulically conductive fractures be detected at depths where they are not visible? Hydraulic and tracer testing can provide proof that a feature is hydrologically important by measuring flow and transport properties directly.

Each of these methods has limitations. The genesis of many fracture systems and the resulting fracture geometries are extremely complex and difficult to understand, especially at depths where fractures are not directly accessible. Geophysical methods can detect the mechanical or electrical anomalies produced by fractures, but these geophysical properties do not have a one-to-one correlation with hydrological properties. Well tests measure hydrological properties, but many different distributions of heterogeneity can give the same hydrological response. Moreover, well tests may not be practical, especially on very large scales, when producing wells must be shut down, or in contaminant environments. Used together, these tools can provide an understanding of the likely locations and the hydrological properties of major flow paths.

Geology and Fracture Mechanics

Quantitative calculations of fracturing based on principles of fracture mechanics (i.e., the study of the mechanics of fracture formation) explain many

fracture patterns observed in the field. Central to the use of fracture mechanics is an understanding of the role of heterogeneities in both stress and material properties. Flaws and other heterogeneities in the rock mass concentrate stress, so fractures begin to propagate. The new fractures perturb the local state of stress and enhance material property heterogeneity, which, in turn, affects the propagation of other fractures. This process creates fracture systems on every scale of observation. The fracture systems that result sometimes have recurrent, recognizable patterns or "themes." These recognizable patterns can be used to infer the nature of subsurface fracture systems and their control on fluid flow.

Examples of fracture patterns that result in hydraulically significant flow paths include:

- Highly connected, regionally extensive networks of open fractures, such as cooling fractures that form polygonal networks.
- Clusters of open joints or fracture zones.
- Open fractures that occur as parts of faults, such as extension fractures that occur between steps in shear zones.

In the absence of subsequent fracture closure or filling, equivalent porous medium behavior (see Chapter 6) might be more likely in a system of regular cooling joints than in a concentrated system of joint clusters, fracture zones, or tension fractures. Such inferences can form the framework for characterization and modeling of flow behavior. However, many (if not most) fracture system patterns cannot yet be explained or categorized. Furthermore, the nature of fluid flow has not yet been confirmed in many of the patterns that have been described. *Knowledge of the processes responsible for producing distinctive fracture patterns that are likely in various lithological and tectonic environments can help us understand systems of fracture flow. These relationships can guide hydrological investigations and should be a focus for further research.*

The relationships between fractures at different scales are not yet understood. Although the mechanisms of fracture formation are similar at different scales, lithological and structural heterogeneities may be dissimilar over large ranges of scale. *Scale effects in fracture patterns warrant more thorough investigation. This should entail an analysis of scaling relationships as a function of stress history, structure, and lithology at a number of different sites*.

The formation of shear zones is usually studied in the plane of the maximum and minimum principal stresses. However, important hydrological features associated with tension fractures and openings tend to be parallel to an intermediate principal stress. Little is known about the extent and interconnection of fractures in the direction of intermediate principal stress. This is also true for joint clusters. Joints are usually studied in the plane of the maximum and minimum principal stresses, but critical interconnections between these joints can take place in the third dimension or in areas where the orientations of the principal stresses rotate.

Fracture genesis and geometry should be considered a fully three-dimensional problem in order to infer the flow properties in three dimensions.

Fracture Properties

Geology and fracture mechanics can be applied to help understand fracture patterns and to predict and assess their importance for subsurface flow, but it may be difficult to use these tools to identify the locations of fractures at depth. By understanding the properties of fractures (Chapter 3), it is possible to design tools that detect these fractures remotely. Fractures have relatively more porosity than adjacent rock. Consequently, at least three distinct properties are useful for detection:

- Unfilled fractures are less stiff than surrounding rock, so they represent an elastic anomaly, especially in shear.
- Fluids in fractures can be more or less electrically conductive than the rock matrix, so they represent resistive and electromagnetic anomalies.
- Unfilled fractures are usually more permeable than the surrounding rock matrix, so they concentrate flow.

Rock type and stress history control the geometry of a fracture system, which in turn controls the properties of the fractures. Although stress history may be difficult to determine quantitatively, even a qualitative understanding can be important in understanding the fracture void geometry that is likely to be present. Fractures that have formed because of contractive cooling have distinctive surface patterns and consequently should have distinctive void geometry patterns that are different from fractures that have undergone shear, for example. *Small-scale laboratory and large-scale in situ research should be undertaken to determine how the character of the fracture void geometry depends on lithology and stress history*.

A large number of tools have been developed to quantify fracture surface and pore space geometry. These include profilometer and optical scanning instruments and a variety of casting techniques. It is now possible to quantify the spatial relationships of asperity height and aperture distributions and to relate these geometric properties to a variety of fracture flow, mechanical, and geophysical properties.

A number of recent studies have quantified the geometry of laboratory fracture samples as well as their hydrological and geophysical properties. These studies greatly benefit the design of methods for detecting conductive fractures and the interpretation of field data. It is not always easy to extrapolate such measurements to field scales, but laboratory studies can provide an understanding of trends in behavior and a framework for interpretating of field data.

Some theoretical analyses suggest a correlation between the elastic properties of fractures and permeability. Fractures that are less stiff may also tend to be more

permeable. The elastic properties of a fracture are a function of the distribution of contact areas in the fracture. More open and permeable fractures have smaller contact areas and are less stiff. Because fractures tend to be less stiff than surrounding rock, they concentrate strain. Fractures thus create a "displacement discontinuity." The displacement discontinuity concept has been used to analyze the propagation of seismic waves across fractures. This has led to a model that provides quantitative relationships between fracture spacing and stiffness and between velocity and attenuation of seismic waves. This model has opened significant new possibilities for the design and interpretation of seismic surveys for detecting fractures. There is also a correlation between electrical and hydraulic conductance, although electrical conductance is not as sensitive to fracture opening as permeability is. Electrical conductance is proportional to the cross-sectional area of the fracture opening (i.e., the local aperture), whereas fluid conductance is locally proportional to the aperture cubed. Thus, fluid flow is much more sensitive to aperture variation than electrical conductivity. Consequently, electrical conductivity measurements cannot be used alone to quantify hydraulic conductivity, either for single fractures or the bulk medium.

An important area of research impacting the interpretation of geophysical surveys is the relationship between seismic and electrical properties of fractures and hydraulic conductance (volumetric flow per unit gradient). *More theoretical work should be done to reduce the description of each phenomenon to a minimum number of free parameters, in order to identify quantitative relationships among the various properties. Additionally, the properties of fractures in a network should be related to the bulk properties of the rock.*

The relationship between fracture stiffness and wave propagation is particularly interesting for shear waves (*S* waves). A shear wave propagating through a fracture set splits into two modes. The component vibrating normal to the fracture planes is significantly delayed compared to the component vibrating parallel to the planes. This phenomenon is called shear-wave splitting. Attenuation is larger for waves polarized subnormal to the fracture compared to waves polarized subparallel to the fracture. *Research to determine how the properties of fractures affect shear-wave propagation in fractured rock should be undertaken to improve fracture detection.*

Theoretical and laboratory studies of the correlation between hydrological and geophysical properties are useful, but it is essential to examine whether these relationships hold in situ. Two approaches hold promise: one is to make in situ measurements of elastic stiffness and electrical and hydraulic conductances of fractures and to use these measurements to develop empirical relationships. However, unique relationships would only be expected to hold under comparable geological conditions. Isolating significant numbers of fractures in a given geological setting might be extremely difficult. Alternatively, one could examine the hydrologic and geophysical properties of a single isolated fracture under different stress regimes (e.g., by changing the fluid pressure). Significant changes in pres

sure should change void space volumes and contact areas in the fracture and, consequently, stiffness and electrical and fluid conductivities. *In situ studies of the geophysical and hydrological properties of fractures should be undertaken to relate the results of seismic and electromagnetic surveys to the hydrological behavior of rocks*.

Geophysical Methods

Geophysical methods utilize the anomalous properties of fractures to locate and characterize them remotely. For example, single fractures have different elastic and electrical properties than the rock matrix. Fracture sets cause anisotropic behavior in the rock. Either of these conditions can be detected with geophysical methods. However, the line between detecting a fracture as a heterogeneity or as an anisotropy can become somewhat blurred, especially when the matrix rock is inherently anisotropic. This distinction also depends on the resolving power of the measurement technique used.

Surface reflection surveys utilizing polarized *S* waves can identify highly fractured rocks at depth by locating regions of high horizontal anisotropy. Similar surveys utilizing *P* waves fail to detect rocks with vertical fractures because at significant depths the waves propagate nearly parallel to the fractures and thus are largely unaffected by them. *Acquisition and interpretation techniques should be more fully developed to take advantage of shear-wave properties of fractures*.

Cross-hole and surface-to-borehole tomographic surveys use either seismic or electromagnetic waves to image the velocity and attenuation properties of rock. These methods can be used to identify hydrologically important features with sizes over several hundred meters if the rock is not highly attenuating. Inversion of travel time or attenuation data can resolve anomalous features on the order of a meter or less. The results depend significantly on survey geometry and wavelength. For example, two-sided tomography (e.g., between two parallel boreholes) is much less accurate than three-sided tomography. *Efforts should be made to develop borehole shear-wave sources for tomographic imaging*.

One of the important practical limitations of tomographic techniques for characterizing fracture hydrology is that tomography requires at least two boreholes that lie in the same plane. In many cases only one borehole is available for imaging the rock. *Work should be undertaken to develop borehole seismic reflection methods that can map fractures at an appreciable distance from a single borehole, similar to what can now be achieved with borehole radar*.

Tomography is practically limited to two dimensions, whereas hydrological flow paths in fractured rock are rarely confined to two dimensions. Surface reflection seismic methods that can create three-dimensional images are now relatively common in the petroleum industry. The technique is very useful but expensive because it requires a large number of source-receiver pairs. *Efforts*

should be made to reduce the cost of three-dimensional seismic methods and to adapt them to shallower and smaller-scale applications.

Images produced by geophysical tomography reflect variations in seismic or electrical properties, not hydrological properties. In some cases it is possible to qualitatively deduce the density and orientation of fractures from these geophysical properties. Quantitative interpretations of hydrological properties from these geophysical properties are extremely difficult, but not impossible, to develop. These interpretations will always be site specific. The primary difficulty is that interconnection of void space controls the hydrological-conductance properties of the rock, whereas interconnection has little effect on most geophysical properties. In fractured rock the relationship between interconnected porosity and total porosity is complex.

Probably the most useful approach for detecting hydrologically important fractures is to identify the particular geophysical signatures of particular geological settings. Case studies can be used to calibrate the methods and identify appropriate signatures. Application of several methods at one site greatly improves the possibility of identifying the signatures of hydrologically important fractures. Once the signatures are identified, the locations of similar features at other sites may be easier to detect.

An example discussed in Chapter 4 involved the laboratory analysis of core samples. It was shown that the matrix rock near a hydrologically active shear zone had a higher seismic velocity than the surrounding rock, possibly caused by deformation or alteration by circulating fluids. The fractures in the shear zone delayed the seismic waves, but the higher velocity of the rock near the shear zone nearly offset this delay. The result was a weak-velocity anomaly. However, fractures in the shear zone increased attenuation. The geophysical signature of this hydrologically important shear zone was a weak-velocity anomaly coupled with a high attenuation anomaly.

Another example discussed in Chapter 4 showed that the radar velocity anomaly was displaced in space with respect to the attenuation anomaly. The velocity anomaly may have been due to fluid-filled porosity, whereas the attenuation anomaly may have been due to clay minerals in the alteration zone around the fractures.

Field studies based on multiple measurements that identify the geophysical signatures of known, hydrologically significant fractures should be undertaken. Learning to interpret and catalog such signatures will greatly improve the use of geophysics in locating hydrologically important fracture systems.

Geophysical methods are very good at detecting changes, so one of the more promising approaches for locating hydrologically active fractures is to image the rock mass before and after changing some aspect of the flow system. The images produced before and after the change are differenced, which cancels out the natural heterogeneities, leaving only the anomalies caused by the hydrologically activated part of the system. A very successful example of this approach, discussed

in Chapter 4, used radar tomography before and after the injection of a highly conductive saline solution. The difference image showed the location of saline water in the rock, not unlike a barium x-ray used in medical applications. The analogy for seismic tomography might be measurements before and after the injection of gas, because a small-percentage decrease in saturation has a large effect on seismic properties. This type of imaging also has important application in remote monitoring of underground processes. *Difference tomography is an important and promising area of research. Efforts should be made to develop these techniques for investigation of fracture systems.*

Borehole logging techniques used in conjunction with other types of information have been very successful in characterizing fracture flow systems. A large variety of borehole logs are specifically designed for fracture systems. These are readily available and can provide multiple measurements of physical properties along the borehole. However, these logs usually sample only a small volume of the drilling-disturbed rock surrounding the borehole. Most logs are, at best, indirect measures of hydrological properties.

Borehole logging devices to map fractures and detect the rather discrete inflow (or outflow) zones that occur in fracture-dominated systems include a variety of imaging devices and extremely sensitive flowmeters. *Development and commercialization of borehole logging devices and techniques for fractured rock should continue because they hold promise for relatively inexpensive, quick, and effective characterization tools*.

In many cases the state of the art in geophysical imaging is far more advanced than the state of practice. *Efforts should be made to develop and promote state-of-the-art geophysical technologies for routine use in the field. These should include radar, electromagnetic, and seismic methods.*

Hydraulic and Tracer Testing

Geophysical investigations can help locate hydrologically important fractures. These investigations are vital for designing well testing programs. In classical porous medium hydrology, stratigraphy determines the location and geometry of permeable units (i.e., "hydrostratigraphic units"). In fracture systems the permeable units (i.e., fracture zones or swarms) may have extremely complex geometries. Effective testing strategies must account for these geometries a priori. For example, to measure the properties of a fracture zone, it is very helpful to know its location, thickness, and orientation. Packers set above and below the fracture zone in both the pumping and monitoring wells isolate the hydraulic response of the zone.

The identification of hydraulically significant fracture zones in boreholes is not necessarily straightforward. Two fractures (or fracture zones) encountered in a borehole may have nearly identical geophysical signatures, but only one may conduct fluid. A single-hole hydraulic test that indicates a large hydraulic

conductivity may be bracketing an important fracture zone, or it may simply be testing a spurious single fracture that is connected to a fracture zone at some distance from the borehole. If the test indicates a small hydraulic conductivity, the test may not bracket the fracture zone, or it may simply be testing a low-conductivity part of the zone. Consequently, the identification of major fracture features from borehole data can be problematic.

A combination of borehole measurements (e.g., transmissivity, fracture frequency, electrical conductivity, acoustic velocity) can be used to identify important fracture zones. At Stripa, for example, a fracture zone index (FZI) was defined as a weighted combination of borehole measurements (see Chapter 4). The weights were a function of the correlation matrix of all the measured variables. The FZI was a much better indicator of hydrologically important fracture zones than single measurements. *Fracture zone indices based on multiple geological, geophysical, and hydrological measurements should be developed and tested at several sites in order to determine the general utility of this approach.*

Hydraulic tests are valuable tools for diagnosing certain aspects of fracture geometry. Test data are usually interpreted by specifying a conceptual model for the hydrological system in the vicinity of the well and then determining the parameters (e.g., size permeability or storativity of the specific features) that give the best match to the observed hydraulic data. A good match between the data and the model results (arrived at with realistic parameters) lends support to the underlying conceptual model. For example, model solutions exist for the case of a single fracture of large areal extent intersecting a well. Flow geometries in fractured rocks are usually more complex than this simple case; consequently, interpretation of hydraulic tests in fractured systems can be challenging. In addition, fluid flow is described by the diffusion equation, which means that the signal decays rapidly and may not be affected by heterogeneities. Further, large-scale tests can take a long time to complete. Diffusive behavior limits the ability of hydraulic tests to diagnose flow system geometry.

Hydraulic tests permit inferences about the geometry of the fracture network beyond the wellbore by comparing the test results to specific model geometries. For example, a well that intersects a large, highly conductive fracture has a test response like a constant-head boundary. If the rock has a fracture or if other fractures intersect the fracture being tested, the test results will match the mathematical solution for leakage into a high-transmissivity "aquifer." Likewise, a fracture termination will match the solution for an impermeable boundary. Such solutions are widely available and well known. Application of these solutions to fracture systems only requires relating the geometry underlying the previously derived mathematical expressions to the geometry of the fracture system.

It may be valuable to compare hydraulic test results to solutions for flow systems that are one, two, and three dimensional. One-dimensional, or linear, flow occurs in an open fracture where the borehole lies in the plane of the fracture (e.g., a vertical fracture intersecting a vertical well). One-dimensional flow can

also occur in a one-dimensional fracture channel. Two-dimensional, or radial, flow occurs in open fractures that are not parallel to the borehole, in highly interconnected networks of fractures confined to a relatively thin stratum, or in two-dimensional fracture zones. Three-dimensional flow occurs in networks of fractures that are highly interconnected throughout a three-dimensional volume of rock or when matrix permeability is comparable to the fracture permeability.

Well test solutions now exist that allow the dimension of flow to take on a range of noninteger flow values between 1 and 3. For example, a two-dimensional fracture zone consisting of poorly interconnected fractures might have a flow dimension between 1 and 2. A flow dimension between 2 and 3 could indicate a poorly connected three-dimensional network. Comparing test data to these solutions can be a powerful diagnostic for system geometry when some additional information about geometry is available. In the absence of any constraints, however, it may be difficult to distinguish between different system geometries. There is a need to relate geometric fractal dimensions for fracture systems to flow dimensions determined by matching noninteger dimension solutions to the well test equation. In this way it may be possible to determine something about the fractal dimension of the fracture system from the well test solution.

The cointerpretation of multiple well tests is a good way to determine critical aspects of fracture flow systems. Cointerpretation forces the system response to be consistent with all the observations simultaneously. Two approaches are useful. In the first, observations are analyzed statistically to find the best-fitting permeability tensor for the medium. In the second, inverse techniques are used to find patterns of heterogeneity that fit the data. *Cointerpretation of multiple well tests and well test observations is a promising research area that may provide a practical characterization for many sites. Research in this area should be expanded.*

Tracer tests are powerful tools for confirming the existence of connected flow paths. However, meaningful interpretation of the transport properties of the medium require that the geometry and boundary conditions of the flow system be extremely well understood. The only examples of successful tracer test interpretation are for simple fracture geometries, for instance, in cases in which there are dominant fracture zones. *The detailed characterization, flow modeling, and subsequent tracer testing of complex fracture systems should have a high research priority. Such tracer tests should include natural gradient tracer tests where possible. This research will allow the development of appropriate tracer testing methodologies and interpretations. There is a need to determine successful testing strategies, including borehole configurations and injection and withdrawal rates*.

Summary

Tools have been identified that address the first key question—How can fractures that are significant hydraulic conductors be identified, located, and

characterized? Geological investigations can indicate which features are likely to conduct fluid and their likely spatial relationships. Geophysical techniques can detect these features, and well tests can confirm their hydrological role and allow inferences to be made about the fracture network geometry. In crystalline rocks it is now possible to identify important fracture features over scales of several hundred meters. For larger scales of interest, other geological media, or limited resources, it is more difficult. However, it is increasingly possible to make educated hypotheses about the nature of fracture systems.

The ability to identify hydrologically important fractures in crystalline rocks is a result of the number of excellent in situ research facilities in this medium (Chapter 8). Recently, the petroleum industry has begun to develop in situ research facilities in fractured sedimentary units. Characterization research consists of repeated sequences of characterization, prediction, and comparison. In situ research facilities are important because they provide the opportunity to move freely between these stages. Progress in fracture characterization depends to a great extent on the availability of appropriate in situ research sites. These sites are especially useful when a large number of characterization methods can be applied to assess the utility and advantages of each method. *Additional in situ facilities should be developed in fractured rocks in a variety of geological environments in order to improve the ability to identify, locate, and characterize hydraulically conductive fractures.*

HOW DO FLUID FLOW AND CHEMICAL TRANSPORT OCCUR IN FRACTURE SYSTEMS?

There are three key tools used to understand how flow and transport occur in fracture systems:

- Conceptual modeling (Chapters 2, 3, 4, 5, and 6)
- Mathematical modeling (Chapter 6)
- In situ flow and transport experiments (Chapters 5 and 8)

Conceptual Modeling

A conceptual model is a simplified representation of the real system based on a cointerpretation of all the observations. A conceptual model is a hypothesis describing the main features of the geology, hydrology, and site-specific relationships between geological structure and patterns of fluid flow and transport. The conceptual model serves as the basis for mathematical models of flow and transport. There are no standard parameters for these models; each conceptual model defines its own appropriate parameters. Consequently, it is necessary to alternate between in situ testing, interpretation, and definition of a model. Predictions made with the model are compared to measurements, and the model is updated

accordingly. Then the process begins again. Each cycle of prediction, measurement, interpretation, and model update should bring the system representation closer to reality. If the iterative process does not improve the predictions, it is appropriate to question the underlying assumptions. Such an elaborate process is not always possible in practical situations, but it is a fundamental and critical part of successful characterization and predictive modeling.

Building the conceptual model is the most important part of the modeling process. Consider a system with an in situ measurement of transmissivity. The predicted transport velocity for this system will vary by many orders of magnitude depending on whether a three-dimensional porous medium model, two-dimensional parallel-plate model, or one-dimensional channel model is used. The error associated with the choice of conceptual models is much more significant than any measurement error or numerical errors involved in the mathematical simulation.

The amount of detail required in a conceptual model depends on the phenomenon of interest. A simple prediction of flow rate as a function of time is not highly dependent on a detailed representation of the heterogeneity. Thus, problems involving reservoir yield may not require detailed conceptual modeling. Protecting a water supply well from contamination or optimizing a fluid recovery system, on the other hand, requires a more complete understanding of geology and hydrology.

Understanding the geometry of fracture system and how that geometry controls flow is central to conceptual modeling. In the laboratory it is possible to measure the geometry of a portion of a single fracture and quantify the void space that controls flow with a variety of methods. It is possible to control the boundary conditions that produce flow in a fracture and make measurements of flow and transport phenomena. However, if a sample can be brought to the laboratory for study, it usually is not highly fractured. Highly fractured samples do not maintain their integrity and are consequently difficult to collect and study. In many, but not all, cases this is tantamount to saying that only those fractures that are not the primary conduits for flow can be studied in the laboratory. Further, laboratory samples are necessarily small. Consequently, they are not representative, and in most cases it is difficult if not impossible to scale up results obtained in the laboratory to applications in the field.

For these reasons, laboratory studies of fracture flow may be difficult to apply to field cases from a quantitative point of view; in the worst cases, their application may lead to misconceptions about the natural flow systems. Nevertheless, these studies are extremely valuable from the qualitative point of view because they reveal the relationships between fracture geometry and flow and transport properties. Although in situ values of permeability cannot be determined from laboratory studies, such studies do reveal how fracture geometry controls the flow. Laboratory studies are also the primary source of information to link geophysical and hydrological properties.

Recent work has demonstrated that an appropriate conceptual model for flow in a single fracture is that of a two-dimensional porous medium that is sensitive

to stress. This key concept has almost entirely replaced the parallel-plate analogy for fractures. The parallel-plate analogy is useful for predicting changes in permeability that occur as a fracture is opened, such as in hydrofracture operations. However, when fractures have a significant contact area, the parallel-plate analogy is applicable only on the local scale and is not particularly useful for understanding flow and transport on the macroscale. The concept of identifying a single aperture for a fracture (i.e., the parallel-plate analogy) is far too simple for many applications. However, it is impractical to completely define fracture void geometry in most cases. *Consequently, simple methods should be developed to describe the geometry of fracture openings to provide sufficient information to determine flow and transport properties*.

Following the two-dimensional porous medium analogy, it is not surprising that flow in fractures occurs along the paths of least resistance, which are formed by the most efficient connections between large pores. Fluid flow through these pores is effectively "channelized." The necks in these "channels" control flow. During transport of solutes, the large pores, which contain relatively large volumes of water, dilute the solute and thus delay its movement. *Research is needed to determine how the geometry of a fracture gives rise to preferential flow paths and determines the amount of rock surface area that will affect matrix diffusion and reactive transport*.

The two-dimensional porous medium model for flow in a fracture is particularly important for two-phase and multicomponent immiscible flow. Theoretical and laboratory studies indicate significant phase interference (the presence of one phase that blocks the flow of other phases) in fractures when the matrix rock is impermeable. Conceptualization of the fracture as a two-dimensional porous medium provides a basis for understanding this phenomenon because the blocked phase does not have the third dimension to use as an alternate route.

In multicomponent flow the nonwetting phases tend to occupy the larger pores. If the fracture surfaces become sealed with impermeable minerals or if the matrix rock is near saturation, transport of the wetting phase in the fracture may be even more channelized than in single-phase flow. Increased channelization implies short fluid flow paths. If the matrix is permeable, however, the wetting fluid, which initially enters the system through fractures, migrates into the smaller pores of the matrix. In this case the matrix controls the flow and the fractures act as barriers. These two conceptual models give radically different values of travel time: the channelized flow model will conduct fluids much more quickly than the permeable matrix flow model. More work is needed to determine which of these mechanisms is dominant under realistic conditions.

Many analyses of two-phase flow in fractures assume that the flowing phase is continuous. However, observations have shown that isolated "blobs" of either phase may move. For example, air bubbles can be entrained in water flow. Another mechanism that may be important is phase displacement. As pressure in the wetting phase increases, isolated portions of the wetting phase may displace

the nonwetting phase occupying the larger, more permeable pores in the fractures. Subsequently, the nonwetting phase displaces the wetting phase again. This suggests that two-phase flow in fractures may be oscillatory in nature. Researchers have observed oscillatory two-phase flow in the laboratory. *Additional work should be undertaken to determine if the period of oscillatory behavior increases with the scale of the flow system*. Further, the behavior of two-phase flow in fractures may be truly chaotic.

Development of appropriate conceptual models for multiphase flow in fractures is a critical research problem, with applications to many problems of societal interest, for example, the siting of nuclear waste repositories above or even below the water table, predicting the effects of corrosive gas releases from the corrosion of nuclear waste containers, for nonaqueous-phase liquid contamination, and for enhanced oil recovery. *New theoretical and laboratory work should be undertaken to relate multiphase flow in fractures to aperture distribution, matrix properties, and stress. There is a critical need for experimentation and observation of two-phase flow in natural systems.*

Given insights gained from laboratory tests, field observations provide the basis for developing conceptual models appropriate to the site and problem at hand. All the tools described above under the first key question are brought into play. The identification of fracture patterns, inferences about which fractures are open and connected, characterization of fractures through geophysical imaging, and well testing are used as discussed above. The analyst interprets the data to develop a working description of the fluid flow system. The process should be flexible and interactive. Uncertainties in the model indicate the need for further data collection.

The characterization of fracture systems and the development of conceptual models require access to the field. *Conceptual modeling studies should be pursued in a variety of geological settings in order to define the relationships between lithology, stress, structure, fracture style, and permeability. Researchers should integrate these studies for presentation to the earth sciences community in the form of review articles as well as detailed, narrowly focused technical articles*.

The best way to develop conceptual models is through examination of case studies; Chapter 8 gives some recent examples. Good case studies are available for fractures in crystalline rocks. The Stripa Project, for example, stands out for its use of geophysics in conceptual modeling. Here, researchers made an integrated interpretation of the flow system from a comprehensive set of geophysical and hydrological measurements. The project documented the process and thus serves as a significant resource. The Underground Research Laboratory case study is a good example of the application of geological understanding to hydrology. Researchers correlated the structure of a major shear zone to measured hydrological properties. This correlation provides a basis for extrapolating hydrological properties through geological analysis. Work at the Grimsel site in Switzerland is a good example of integrating geological mapping and geophysical imaging.

The Mirror Lake example shows that various geophysical and hydrological measurements are needed to characterize flow and transport in fractured rock. The Geysers case study shows how to use the relationship between hydrological activity and monitored acoustic emissions to define a reservoir.

In crystalline rock sites, fracture zones dominate the hydrology. Many of these zones have undergone significant shear deformation, and they are not uniformly permeable. Hydrology dominated by flow in fracture zones may not be a universal property of crystalline rocks, but there is certainly enough evidence to suggest that this is a common occurrence. Case studies for fracture systems in stratified rocks indicate that the hydraulically significant fractures are the classic strata-bound joint systems, with joint clusters forming regions of significant permeability. Compared to the number of research facilities in massive crystalline rocks constructed mainly for nuclear waste storage research, there is a dearth of multidisciplinary experimental facilities in bedded rocks, which are important for many resource and structural problems. *Experimental facilities in bedded rocks should be developed*. Conceptual models developed at such facilities will aid conceptual modeling process at other sites with similar geological conditions.

Numerical Models

Given an appropriate conceptual model, the analyst can choose from a large suite of numerical modeling tools. It is important to note that all of these models use similar mathematical constructs. They differ mainly in their representation of physical heterogeneity. The nature of the geometry that controls flow, the scale of the problem of interest, and the phenomena being modeled dictate the choice of how to discretize the system, that is, the choice of modeling approach.

Numerical model types comprise a spectrum ranging from equivalent continuum models to discrete fracture models. Equivalent continuum models have the advantage of being well known and commonly applied. They tend to be more useful for well-connected fracture systems, for relatively large scales of interest, and where information is needed on average behavior rather than details of the flow paths. These models treat large portions of a flow region as having uniform properties. Such a treatment may fail to adequately represent the flow field if the fractures have highly variable properties or are poorly interconnected. The approach of using a stochastic continuum may overcome many of these problems. In this approach the continuum is discretized into elements and a stochastic process determines the properties of each element. This approach is likely to be useful when fracture connectivity is high, but there is still a significant variability in fracture conductance.

Multiple-continuum models have been used extensively in cases where fractures form the dominant flow paths and the matrix porosities are high enough to provide significant storage. The literature on this topic is extensive, especially the petroleum literature. The interested reader may consult any of several good

reviews of this literature (e.g., Kazemi and Gilman, 1993). These models work best when the fracture network is well connected, for relatively large scales of interest, and where information is needed on average behavior rather than details of the flow path.

At the other end of the spectrum are those discrete fracture models that attempt to include every conductive fracture as an explicit feature in the model. Discrete fracture codes assign continuum properties to subdomains and prescribe how these subdomains interact. The subdomains may represent a single fracture, a channel in a fracture, or a fracture zone, for example. These models are suitable for calculating complex flow paths resulting from the geometry of the interconnected fracture network. A stochastic process places the fractures in the model according to specified statistical distributions describing the location, orientation, extent, and conductive properties of fractures, as well as any spatial relationships between fractures.

The discrete approach may require significant data collection efforts. Data requirements can be difficult to meet, particularly if individual fracture conductances are required. Conductance distribution measurements have been attempted with hydraulic tests using short test intervals to isolate single fractures. However, it is not usually possible to isolate single fractures in situ or to determine how the conductance measurement is affected by other fractures that are connected to the fractures being measured. Consequently, different fracture conductance distributions can be inferred from a single set of flow test data.

If a fracture can be isolated in a well test, it is not usually exposed in an excavation or outcrop where the trace length can be measured. Consequently, it is extremely difficult to find statistical correlations between fracture size and conductivity. One way to overcome this difficulty is to generate a random series of fracture systems that match the observed distributions of fracture trace length, orientation, and transmissivity. These, in turn, provide for a range of possible models.

In the past, the discrete approach was limited by the amount of computational power required to account for every fracture. However, this limitation is disappearing rapidly; presently available computers now have the necessary computing power for practical problems. Models with hundreds of thousands of fracture elements have been run in workstation environments. Further advances are anticipated with parallel computers. Research into efficient numerical methods continues to be important for practical application of fracture models.

One way to reduce the computational requirements is to change the way in which a "discrete" feature is interpreted. For example, on a scale of tens of meters, the model may include every fracture that is larger than about 10 cm. On a scale of hundreds or thousands of meters, however, fractures can be lumped into discrete zones that are interpreted as single features. This "lumping" or "equivalencing" produces a model that has both discrete and continuum properties. The more features that are lumped together and described in terms of average

properties, the closer the model is to an equivalent continuum model. *A rationale for lumping features of the fracture network when modeling either fluid flow or the transport of reactive solutes should be developed.*

An attractive approach to fracture system modeling incorporates the hierarchical nature of fracture systems. This involves the generation of fractures according to stochastic rules inferred from observations made at outcrops. For example, some methods describe the geometry of the random smaller fractures with respect to larger fractures that are either random or deterministic. The construction of the model network can mimic the inferred genesis of the natural fracture system. This involves the creation of random flaws that grow at each iteration according to rules inferred from fracture mechanics and calibrated by observations from outcrops. The generation of fracture models based on fracture genesis incorporates physical processes into the fracture pattern. Consequently, these methods provide a physical basis for extrapolating fracture patterns to locations where there are no measurements. Mathematical descriptions that are based on physical properties of fracture genesis provide an additional level of confidence in model predictions. *The development of hierarchical fracture models based on physical processes should be a priority for research.*

It is also possible to create hierarchical fracture systems through inverse methods. In this approach a general arrangement of fluid conductors is first defined based on a conceptual model. Then the particular arrangement and strength of the fracture conductors are optimized such that the model's results match certain observations, for example, interference or tracer test results. These methods are particularly useful when the pattern of conductors determines the hydraulic behavior. For example, fracture systems can be modeled as simple, partially filled lattices that lie on planes representing major fracture zones. These are called equivalent discontinuum models. The system is fully described by specifying the presence or absence of each lattice element. However, a rather large number of parameters must be optimized in this process. Consequently, another issue that arises from the use of inverse analysis is the nonuniqueness of resulting models. A large number of inverse solutions can be found, and these can be examined to identify common elements.

Recently, iterated function systems (IFSs) have been used to represent networks of conductors. IFSs use a small number of parameters to control an iterative process that determines a geometric object called an attractor or a fractal. If the attractor defines the variations in hydraulic conductance, the parameters of the iterated function system can be optimized so that the system reproduces the observed test results. Using an IFS, a complex fracture flow system can be fully described by using tens of parameters rather than thousands. *Research to find simple but sufficient mathematical descriptions of fracture networks and to determine what constraints the data actually place on the model should be a priority for inverse modeling research.*

Little work has been done to understand the relationship between fracture connectivity and matrix permeability. When matrix permeability is low, fracture connectivity controls flow. When matrix permeability is comparable to fracture permeability, flow can pass from one fracture to the next through the matrix and fracture connectivity is not important. As long as fracture connectivity is an important factor in the models, continuum assumptions are suspect. *Parameter studies should be conducted to see how the relationship between fracture connectivity and fracture network permeability is affected by matrix permeability*.

On large (regional) scales it may be more difficult to locate the hydrological features and to test the hydraulic behavior of the fractured rocks. One of the most promising methods for inferring hydrological behavior at large scales is to use natural geochemical tracers. The use of natural geochemical tracers to constrain large-scale flow models in fracture systems deserves more attention. *These efforts should include research to understand geochemical processes and boundary conditions*.

Discrete or hierarchical models are useful when it is necessary to model the locations of flow paths and transport velocities. In many fracture systems, flow paths are highly irregular compared to those predicted by continuum models; consequently, models that account for heterogeneity are at a distinct advantage. However, the development of appropriate conceptual models for transport in fractured rock is not yet complete. It is difficult to characterize solute distribution, especially when transport occurs in narrow pathways in fracture planes. It is also difficult to design and run effective tracer tests in fractured rocks. Such research is ongoing at a number of sites, including the Mirror Lake site operated by the U.S. Geological Survey in New Hampshire and the Underground Research Laboratory operated by Atomic Energy of Canada Limited in Manitoba. Similar work is planned at the Hard Rock Laboratory, operated by the Swedish Nuclear Fuel and Waste Management Company in Sweden.

The modeling of two-phase flow, heat transfer, and chemical transport in fracture networks is almost completely confined to single- and dual-porosity continuum models. These modeling efforts are hampered by a poor understanding of two-phase flow parameters as well as the mechanisms governing flow behavior. Recently, fracture network approaches have been used to investigate the behavior of networks under two-phase conditions. These studies utilized what are essentially theoretical percolation models. As mentioned above, these modeling efforts are hampered by a poor understanding of the appropriate physics to use in the conceptual model. Models of two-phase flow in fracture networks can help reveal how the geometry of a network controls flow. *Such theoretical research on the nature of two-phase flow in fracture network should be continued*.

One of the key problems in the prediction of reactive solute transport is a poor understanding of the geometry that controls reactions between the rock and the transported species. The problem of reactive transport in fracture systems is largely unsolved. *Theoretical investigations and experimental work should be*

supported to link hydrogeological and geochemical processes in a transport model for reactive solutes that accounts for the unique properties of fluid pathways in fractured rocks. Efforts should also be directed toward determining the effective contact area between a reactive solute and the network of fractures forming connected pathways.

In Situ Experimentation

In situ experimentation is important for determining how flow and transport occur in a fracture system. *Field-based flow and solute migration experiments should be carried out at a variety of scales, ranging from several tens of meters to hundreds of meters in a variety of host media with a range of styles in fracturing*. Field experiments can test the appropriateness of conceptual models. *The design of these field-based experiments should address data requirements for evaluating modeling approaches and capabilities for both flow and transport. This effort should also address the practicality of collecting appropriate data in routine hydrogeological practice*.

It is not straightforward to compare the results of flow and transport experiments to stochastic model predictions. The stochastic model produces multiple predictions and a distribution of results that can be quite broad. Field experiments are usually very expensive; frequently, only one experiment is carried out, producing only a single realization of the flow system. It is difficult to evaluate the model prediction using this single realization. Measurement on a small scale exacerbates the problem. For example, at Stripa, prediction of total inflow to six parallel boreholes in a 1-m radius was much better than prediction of flow into a single borehole because the six-borehole measurements represented an average over a larger scale. In addition, it is not always possible to measure the quantities predicted by the model. Conversely, the measurements frequently do not constrain those critical aspects of the model that affect the predictions. In other words, it is very difficult to "validate" a model.

Improved methodologies for formulating conceptual models of flow and transport in fractured media are under development. Efforts to translate these models into quantitative simulation tools should include estimates of the uncertainties in the predictions. Modelers and experimentalists should devise useful, appropriate alternatives, such as the process of "confidence building," to strict model validation. Where possible, field investigations should be designed for multiple repetitions of the same simple experiment, as this may serve to build confidence better than one complex, all-encompassing experiment. Efforts should be made to focus model and field comparisons on predicted quantities that have small variances.

Summary

Conceptual modeling, numerical modeling, and in situ testing can be used to address the question: How do fluid flow and chemical transport occur in

fracture systems? Several conceptual models have now been developed for crystalline rocks, and several examples are available. *However, additional work should be undertaken to develop appropriate conceptual models for transport and multiphase flow. Conceptual models should have a strong physical basis to provide a reasonable rationale for extrapolation and scaling up. More investigations should be undertaken in bedded sedimentary units.* A wide variety of numerical models are available, and progress with these is noteworthy. *Fracture flow and transport models should be developed and made more practical and usable. A poor understanding of the physical basis for complex phenomena in fractured rock is primarily responsible for inhibiting their modeling, and research should be directed at this problem. As with the first key question, progress depends on the availability of experimental facilities, and such facilities should be supported.*

HOW CAN CHANGES TO FRACTURE SYSTEMS BE PREDICTED AND CONTROLLED?

The role that fractures play in fluid flow and transport can change quickly and dramatically. Changes in effective stress, shear deformation, or temperature gradients, as well as fracture leaching or filling, can change the void space that controls fluid flow. Relatively small changes in void space can be significant because fractures behave like two-dimensional porous media: when the fluid flow in the fracture is blocked, the third dimension is not available as an alternate pathway. Conversely, opening a constriction can dramatically increase flow. Predicting and attempting to control changes in fracture systems are often the most critical parts of an endeavor involving fracture flow.

Change occurs through physical or chemical processes that alter the pore space of a fracture. For example, a fracture may deform in response to changes in effective stress caused by changes in boundary conditions, fluid pressure, loading, or temperature. Fluids may undergo phase or component changes, where one phase or component blocks the flow of the other. Solids may be added to the fractures by injection of hydrofracture proppant or grout. Mineral precipitates may fill the void spaces. Leaching of the fracture walls by corrosive fluids may occur. These processes are further complicated by coupling between mechanical, hydraulic, chemical, and temperature effects.

Problems involving changes to fracture systems are usually addressed through:

- Laboratory studies of coupled behavior in single fractures (Chapter 3)
- In situ testing and procedures (Chapter 7)
- Mathematical models of coupled phenomena (Chapter 7)

Laboratory Studies of Coupled Behavior in Single Fractures

There have been relatively extensive laboratory studies of the interaction of effective stress and flow. The same is not true for the relationship between shear stress and flow. Very little laboratory work has been done to study the way in which fractures become filled or leached.

The parallel-plate analogy traditionally used to describe fracture geometry implies that fracture conductance is proportional to the "hydraulic" aperture cubed (the cubic law). The cubic law works well for fractures whose sides are not in contact. However, it breaks down as the fracture sides come into contact. In this case the amount and distribution of the contact area control the flow. As the contact area increases, the aperture available for flow decreases faster than predicted by the cubic law. Numerical models that relate fracture void geometry, deformation, and flow are available and are generally good at matching experimental results. However, generalized relationships between fracture stress, closure, and flow properties are not yet available. *Research should be undertaken to relate specific changes in flow properties and stress to different lithologies and fracture histories. Understanding gained in the laboratory should be correlated to behavior observed in the field. Part of this work should be focused on studies relating the local stress heterogeneities to fracture permeability and flow*.

The relationship between shearing and fracture conductance is poorly understood. It must be considered in three spatial directions: (1) in the plane of the fracture in the direction of the shear, (2) in the plane of the fracture perpendicular to the shear; and (3) perpendicular to the plane of the fracture.

Conductance in the direction of shear could increase owing to dilation accompanying deformation, but continued shear or high normal stresses can produce an impermeable gouge in the fracture plane. In the plane of the fracture and in the direction perpendicular to shear, permeability can increase for two reasons. First, dilation of the fracture may create channels perpendicular to the direction of shear. Second, small fractures may form parallel to the intermediate principal stress. The direction perpendicular to the plane of the fracture is important if fluid storage in the rock matrix is of interest. Here, dilation should have little effect, but gouge would cause a significant decrease in communication between the fracture and the matrix. The effect of secondary fracturing may offset the effect of gouge production. Our understanding of these phenomena is incomplete. *A better understanding of the effect of shear on fracture permeability should be the focus for new research because of its significance for engineering projects, as well as for understanding the nature of fracture conductance in natural shear zones*.

Little laboratory work has focused on precipitation, sedimentation, and leaching in fractures. Fluid velocities in large pore spaces of fractures are likely to be lower, which may encourage precipitation. On the other hand, dissolution may occur preferentially at the asperity contacts, owing to higher contact pressures.

Precipitation that takes place preferentially in the large pores would tend to even out the aperture size. Thus, filling the large pores would have little effect on the conductance and a large effect on storage. Consequently, precipitate-laden fluids could continue to flow through and fill the fractures. If precipitation occurs evenly throughout the fractures, the necks will be closed first, reducing fracture permeability and leaving isolated void spaces. These fractures may appear as geophysical anomalies but would not be significant fluid conductors. In general, the opening of fractures increases fluid conductance and lowers the pressure, which tends to encourage precipitation, thus closing the fractures, decreasing the conductance and increasing the pressure. Further study of vein formation may provide insight into problems involving chemical precipitation in fractures as well as the nature of relict flow systems. *Laboratory and theoretical studies should determine how and when fractures become filled or leached and how these changes affect fluid flow and transport. Part of this effort should involve examination of the rheology of grouts and their flow behavior in complex fractures.*

In Situ Testing And Procedures

The importance of couplings between mechanical, hydraulic, chemical, and temperature effects in fracture systems should be evaluated in the field, and techniques should be developed to predict their effects on fractures. It is especially important to understand the couplings between these processes for projects with long design lives because the effects of changes in fracture systems may be hard to predict based on short-term testing and evaluation schemes.

There is considerable laboratory data to establish constitutive relationships between effective stress and fracture permeability for single fractures in rock cores (Chapter 3), but field-based data are few in number. Wellbore operations cause stress-related changes in fracture systems. Under fluid extraction, formation pressures decrease and fracture conductances can decline. However, stress changes do not always affect fracture permeability. Stress sensitivity may be absent in diagenetically altered fractures with stiff mineral "bridges" that prop open the fracture. For shallow flow systems, fracture permeability can be entirely independent of the state of stress or flow. At the other extreme, hydraulic fracture studies indicate a strong relationship between permeability, stress, and flow. The borderline between these two regimes seems rather poorly explored. *Work should evaluate the practical significance of stress-sensitive fluid flow in fractured rock for a range of field-scale problems. Work should also identify the threshold and scale where the stress regime affects fluid flow.*

Pressure decreases near an extraction well, leading to a decline in permeability. It may be possible to overcome these pressure effects through hydrofracture. Hydrofracture creates new fractures to augment the existing permeability. Hydrofracturing increases the permeability by creating fluid conductors that intersect the well. In a sense the hydrofracture simply increases the effective radius of

the well. If the hydrofracture connects the well to an existing fracture system, a significant increase in hydraulic communication will result. However, if the present stress orientation is responsible for the existing fractures, the hydrofractures will likely be parallel to the existing fractures. In this case, hydrofracturing is unlikely to increase fracture connectivity and permeability. *Better methods should be developed to predict hydrofracture geometry in complex geologies, especially when the rocks exhibit nonelastic behavior, in order to predict the effect of the hydrofracture on the local fluid flow regime*.

Water well drillers are now commonly using hydrofracture technology. Typically, water well drillers do not use proppants and could benefit from proppant technology developed in the petroleum industry. *Hydrofracture technology developed in the petroleum industry should be transferred to water supply hydrofracture practice*.

Fluid injection is more complex than extraction because chemical reactions between the injected fluid or particulates and the formation can plug the fractures. Consequently, the pressure needed to inject fluid increases, possibly to the point of hydrofracturing the formation. In general, such hydrofractures propagate upward as well as outward. A vertical hydrofracture may be particularly problematic for disposal wells because it can breach the strata chosen to isolate the waste.

Temperature changes create thermal stresses that affect hydraulic conductance. Cold fluids injected into hot rock produce thermal stresses that decrease effective stresses. Placing a heat source in rock (e.g., nuclear waste) may close some fractures and open others. These stress changes, which are caused by pore pressure changes and thermal volume changes, can substantially alter the hydraulic properties of the rock mass. *Work should be undertaken to relate temperature changes to effective stress changes and change in flow properties through in situ experiments conducted where fracture systems have been extensively characterized*.

Injection of grout into fracture systems from boreholes is a technology that is receiving increasing attention. Grouting helps prevent fluid flow into underground openings and around dams. This technology has been used to isolate previously emplaced toxic waste. The success of a grouting program depends on the characterization of the fracture system. Grouting programs are more likely to be successful if the flow paths are well-characterized beforehand. Discrete fracture flow models developed for a site may be very useful in planning an isolation system, especially if the model can simulate the fluid properties of the grout. Geophysical monitoring of the grouting process provides important information about the progress of the operation and its success. *Given the vast amount of waste in the underground and the extreme difficulty associated with its remediation, as well as the large number of landfills situated over fractured rock, grouting as an isolation technique in fractured rock deserves much more attention. Research should couple grouting techniques with the characterization and flow modeling of the fracture system*.

Corrosive waste materials or in situ mining operations can leach fracture walls or fillings. Withdrawal of geothermal fluids can leave precipitates in fractures. The coupling between flow and chemistry is very difficult to understand and predict. *Fracture characterization and monitoring of fracture systems should be linked to the chemical processes in controlled in situ experiments*.

The effects of stress, precipitation, and temperature are coupled. For example, hot, mineral-rich fluids precipitate minerals as they cool. As the fractures become filled with minerals, resistance to flow increases. If there is a constant driving force, an increase in fluid pressure and a consequent decrease in effective stress will result. The increased pressure causes fractures to open or hydrofracture, increasing the conductance, which, in turn, increases the amount of fluid circulation and precipitation. This cyclic behavior has been observed in nature. For example, accretionary wedges associated with plate subduction are the source of "book quartz," which consists of fractures filled with quartz laminations representing multiple cycles of filling and opening. Further work in understanding how natural coupled processes affect fracture patterns would be useful in applications such as in situ mining and geothermal energy production. *Studies of fracture filling should be keyed to fracture characterization as a way of advancing an understanding of large-scale coupled processes*.

Mathematical Modeling of Coupled Behavior

A fully coupled model of fracture behavior links hydrological, stress, temperature, and chemical effects. It may be possible to link all four of these effects when the geometry and boundary conditions are very simple. For more complex situations it is difficult to incorporate even two of these phenomena in a coupled model.

Hydrogeological simulation models that are linked to mechanical deformation models originate primarily in the field of geotechnical engineering. The models generally use a discrete representation for the fracture network, with separate values assigned to fracture and matrix stiffnesses. These hydromechanical models have been used to examine the nature of the coupling between fluid pressure response and deformation in idealized settings. Workers attempting to fit hydromechanical models to data sets from single-borehole deformation experiments have great difficulty in identifying unique sets of parameters that adequately characterize the field data. Some success has been achieved in duplicating single-fracture experiments. However, because of the multitude of parameters that determine the nonlinear hydromechanical response of a rock mass containing a network of fractures, the prospect of site-specific predictive simulations is not promising in the near future. *Field-scale experiments should be conducted to test models that calculate the deformation of a fractured rock mass during fluid injection or withdrawal. Efforts should be made to construct simplified hydromechanical models that predict changes in flow conditions from changes in stress*.

Numerical models for calculating the effects of temperature changes relate temperature gradients to changes in stress. Models exist to calculate the opening of a single fracture caused by thermoelastic effects. However, existing coupled stress, flow, and temperature models may not predict long-term behavior, particularly for two-phase flow, because they may not include the right physics or account for complex fracture geometry. *In situ experiments, particularly at large scales, should be conducted to develop reliable models for the effects of coupled stress, flow, and temperature*.

Numerical models that couple fracture flow, stress, and fracture filling are used to address the deformation of fractured rock masses. For example, deformation of a rock mass caused by well drawdown, or the effects of grouting and drainage on a fractured rock mass underlying a dam, can be calculated with these models. Models that address coupling between flow and leaching or precipitation in fractures are not generally available. *Such models should be developed, as they may be necessary for certain contaminant transport or in situ mining problems*.

The factors controlling chemical precipitation during reinjection of fluids are incompletely understood. Researchers have modeled silica redistribution for geothermal reinjection problems. Simulation of more complex chemistries, such as carbonate precipitation, is very difficult because of buffering effects. *Better methods for predicting permeability reduction owing to chemical precipitation (scaling) in fracture networks should be developed*.

Summary

Answers to the third key question—How can changes to fracture systems be predicted and controlled?—are critical in a variety of endeavors of societal importance. The effects of changes in effective stress are better understood than changes in shear stress; the effects of temperature changes are better understood than chemical changes. Predicting and controlling these changes requires thorough characterization of the fracture systems. There is much practical experience with coupled fracture problems, but there are few controlled sites where the various processes can be sorted out from the effects of the fracture geometry. *Again, research facilities in a variety of rock types should be established. These facilities should be used to develop technology to control and predict changes to fracture systems*.

REFERENCE

Kazemi, H., and J. R. Gilman. 1993. Multiphase flows in fractured petroleum reservoirs. In Flow and Contaminant Transport in Fractured Rocks, J. Bear, C. F. Tsang, and G. de Marsily, eds. New York: Academic Press.

Appendix A

Committee's Statement of Task

The principal objective of this study is to review, synthesize and integrate recent research concerning techniques and approaches to fracture characterization and fluid flow in rock fractures.

Subordinate objectives of the study are:

(1) to identify and review the status of current research in fracture characterization and fluid flow,
(2) to identify federal and other governmental activities and problem areas in the field,
(3) to explore mechanisms to advance the field, and
(4) to offer guidance on recent progress in the field to government agencies responsible for sponsoring or performing research, regulation and environmental restoration.

The committee will prepare a report that will cover research in fracture origin, morphology, geophysical imaging, and flow and transport analysis and modeling. The report will address applications such as toxic and nuclear waste transport in fractured rocks; fractured petroleum gas, geothermal, and water reservoirs; and construction of dams and tunnels (including the Superconducting Super Collider) in fractured rocks. The report will identify the tools and methods of locating and predicting fractures, describe the essential fundamentals behind the use and interpretation of the tools and methods, assess these methods and provide illustrative examples of their use. The report will identify areas of cross-fertilization between various disciplines and between applications.

Index

G